FINAL REPORT

DTPH56-14-H-00008
"Definition of Geotechnical and Operational Load Effects on Pipeline Anomalies"

SUBMITTED BY: **Team Project Manager**
Abdelfettah Fredj
BMT Fleet Technology
311 Legget Drive
Ottawa, Ontario K2K 1Z8 Canada
Telephone: (613) 592-2830
E-mail: afredj@fleetech.com

TEAM TECHNICAL COORDINATOR: **Team Technical Coordinators**
Aaron Dinovitzer
BMT Fleet Technology
311 Legget Drive
Ottawa, Ontario K2K 1Z8 Canada
Telephone: (613) 592-2830
E-mail: adinovitzer@fleetech.com

TEAM PARTICIPANTS: BMT Fleet Technology Limited
Fredj, A., Dinovitzer, A. and Hassannejadasl,A.

SUBMITTED TO: U. S. Department of Transportation
Pipeline and Hazardous Materials Safety Administration
Mr. Warren D. Osterberg
Agreement Officer
warren.osterberg@dot.gov

REPORTING PERIOD:

SUBMITTED ON: 22 Sept 2017

BMT Fleet Technology Limited accepts no liability for any errors or omissions or for any loss, damage, claim or other demand in connection with the usage of this report, insofar as those errors and omissions, claims or other demands are due to any incomplete or inaccurate information supplied to BMT Fleet Technology Limited for the purpose of preparing this report.

BMT DOCUMENT QUALITY CONTROL DATA SHEET

REPORT: DTPH56-14-H-00008 - "Definition of Geotechnical and Operational Load Effects on Pipeline Anomalies"

DATE: 22 Sept 2017

PREPARED BY:

A. Fredj, PhD
Senior Structures Specialist

REVIEWED BY:

A. Dinovitzer, MASc, MBA, PEng
Vice President, Engineering & Technology

APPROVED BY:

A. Dinovitzer, MASc, MBA, PEng
Vice President, Engineering & Technology

PROJECT TEAM:
Abdelfettah Fredj
Aaron Dinovitzer
Amir Hassannejadasl

REVISION HISTORY RECORD

Revision No.	Date of Issue	Description of Change
00	16 June 2017	Initial submission.
01	28 June 2017	Minor editorial changes.
02	22 Sept 2017	Feedback from final report review and presentation.

TABLE OF CONTENTS

1 INTRODUCTION 1
1.1 Project Objective 2

2 MODEL & VALIDATION 3
2.1 Task 2: Scope of Work 3
2.2 Finite Element Model Description 3
2.2.1 Introduction 3
2.2.2 Continuum Multi-Material ALE Model 3
2.2.3 Continuum SPH Mode 4
2.2.4 Soil Material 4
2.3 Validation of the SPH Model 6
2.3.1 Introduction 6
2.3.2 Finite Element Model Validation – Pipeline Subjected to Axial Ground Movement 6
2.4 Finite Element Model Validation – Pipeline Subjected to Surface Faulting 13
2.4.1 Finite Element Analysis of Experimental Split-Box Tests – Buried HDPE Pipeline 13
2.5 Finite Element Model Validation – Pipeline Subjected to Lateral Movement 16
2.5.1 Large-Scale Experimental Model 16
2.5.2 Finite Element Model 17
2.5.3 Analytical and Experimental Results 18
2.6 Validation of the Multi-Material-ALE Model 21
2.6.1 Introduction 21
2.7 Finite Element Model Validation – Pipeline Subjected to Lateral Ground Movement 21
2.7.1 Finite Element Analysis of Experimental Tank Test – Flexible Pipe 21
2.7.2 Analytical and Experimental Results 25
2.7.3 Finite Element Analysis of Experimental Tank Test – Rigid Pipe 30
2.7.4 Analytical and Experimental Results 32
2.7.5 Sensitivity Analyses 36
2.8 Finite Element Analysis of Soil-Pipe Interaction for Slope Movements 41
2.8.1 Finite Element Model Validation: PGD Effects on Buried Pipelines with Elbows 42
2.9 Validation of DEM Model in LS-DYNA 48
2.9.1 Soil Restraint on Pipe Buried in Road Mulch 48
2.9.2 Soil Restraint on NPS 16 (406 mm) Pipe Buried in Moist Sand 49
2.9.3 Soil Restraint on NPS 18 (457mm) Pipe Buried in Moist Sand 51
2.9.4 Soil Restraint on Pipe Buried in Road Mulch 52
2.9.5 Pipe-Soil Interaction Model Parameter Calibration 54
2.9.6 Conclusion: Validation of DEM Model in LS-DYNA 56
2.10 Conclusion of Model Validation Studies 57

3 PIPE LIMIT STATES 59
3.1 Pipeline Compressive Strain Capacity CSA Z662 -2011 59
3.2 PRCI 2004 and University of Alberta Critical Buckling Strain Formula 60
3.3 Tensile Strain Limit 62

4 ILLUSTRATIVE SAMPLE GEOTECHNICAL HAZARD ASSESSMENT APPLICATIONS 64
4.1 Modeling of Landslide Hazard 64
4.1.1 Summary of Inputs Required and Processes Modelled 64
4.1.2 Structural Analyses for a 30-inch Pipeline 70
4.1.3 Structural Analyses for the 40-inch Pipeline 80
4.2 Modeling of Subsidence 88
4.2.1 Mining Subsidence Phenomena and Terminology 88
4.2.2 Finite Element Analyses 92
4.2.3 Application of Finite Element Model to Predict Pit Subsidence and Effects on Pipelines 102

5 MODELING OF PIPELINE SUBSIDENCE HAZARDS 105
5.1 Finite Element Model Description 105
5.1.1 DEM Model 106
5.1.2 Loading Sequence 106
5.1.3 Pipe Properties 106
5.2 Structural Analyses for the 24-inch Pipeline 107
5.3 Results Base Case 109
5.3.1 Effect of the Mining Width to Depth Ratio 112
5.3.2 Comparison with Strain Capacity and Strain Demand Envelopes 118
5.3.3 Effect of the Width of the Subsidence 120
5.3.4 Comparison with Strain Capacity and Strain Demand Envelopes 123
5.4 Effect of Pipe Wall Thickness and D/t 131
5.4.1 Effect of the Width of Ground Movement 135
5.4.2 Comparison with Strain Criteria and Safety Envelopes 142
5.5 Effect of Temperature 154
5.6 Effect of Operating Pressure 156
5.7 Structural Analyses for the 12-inch Pipeline 158
5.7.1 12 Inch Pipeline Results 158
5.8 Structural Analyses for an 18-inch Pipeline 162
5.8.1 Results 163
5.9 Pipeline Subsidence Modelling Observations 169

6 MODELING OF LANDSLIDE HAZARD 171
6.1 Introduction 171
6.2 Finite Element Model Description 171
6.3 Structural Analyses for the 24-inch Pipeline 172
6.4 Results Base Case 174
6.4.1 Effect of the Width of Ground Movement 175
6.4.2 Comparison with Strain Capacity and Strain Demand Envelopes 180
6.5 Effect of Pipe Wall Thickness and D/t 185
6.5.1 Effect of the Width of Ground Movement 187
6.5.2 Comparison with Strain Criteria and Safety Envelopes 191
6.6 Effect of Material Grade: 195
6.6.1 Effect of the Width of Ground Movement 197
6.6.2 Comparison with Strain Capacity and Strain Demand Envelopes 200

6.7 Effect of Temperature 204
6.8 Effect of Operating Pressure 206
6.8.1 Comparison with Strain Capacity and Strain Demand Envelopes 210
6.9 Effect of Ground Movement Pattern 215
6.9.1 Comparison with Strain Capacity and Strain Demand Envelopes 219
6.10 Effect of Burial Depth 224
6.11 Effect of Slope 226
6.11.1 Comparison with Strain Capacity and Strain Demand Envelopes 230
6.12 Effect of Soil Properties 234
6.13 Effect of Soil to Pipe Friction 238
6.14 Structural Analyses for a 12-Inch Pipeline 240
6.14.1 12-Inch Pipeline Results 240
6.15 Structural Analyses for an 18-Inch Pipeline 243
6.15.1 18 Inch Pipeline Results 243
6.16 Structural Analyses for a 30-Inch Pipeline 244
6.16.1 30 Inch Pipeline Results 245
6.17 Pipeline Lateral Ground Movement Modelling Observations 247

7 CONCLUDING REMARKS 250

8 REFERENCES 253

9 CONCLUDING REMARKS 257

LIST OF FIGURES

Figure 1.1: Pipe soil interaction Model Application Sample Results 2
Figure 2.1: Pressure vs. Volumetric Strain 5
Figure 2.2: UBC Experimental Sand Compartment – Karimian et al., 2006 7
Figure 2.3: Illustration of the FE Model including the Pipe 9
Figure 2.4: Comparison between Numerical Model and Test Results – Dense Sand 10
Figure 2.5: Comparison between Numerical Model and Test Results – Loose Sand..... 10
Figure 2.6: Illustration of the FE Model including the Pipe 12
Figure 2.7: Comparison between Numerical Model and Test Results – Undisturbed Soil Fill.. 13
Figure 2.8: Large-Scale Split-Box Test Basin at Cornell University NEES Equipment Site (O'Rourke et al., 2007)..... 14
Figure 2.9: Illustration of the FE Model Including the Pipe 14
Figure 2.10: Illustration of the FE Model including the Pipe 15
Figure 2.11: Deformed Pipe in Soil – FE Results 16
Figure 2.12: Pipe Deformation: Comparison between Numerical Model and Test Results..... 16
Figure 2.13: UBC Experimental Sand Compartment – Karimian et al., 2006 [4]..... 18
Figure 2.14: Illustration of the FE Model including the Pipe 18
Figure 2.15: SPH-FEM Simulation – Vector Velocity 19
Figure 2.16: SPH-FEM Simulation – Vertical Displacement..... 19
Figure 2.17: SPH-FEM Simulation – Shear Failure Surface 20
Figure 2.18: Comparison between Numerical Model and Test Results 20
Figure 2.19: Experimental Setup Test (GS01) – Profile View 21
Figure 2.20: Plan View 22
Figure 2.21: Stress-Strain Curve (1010 Steel) 22
Figure 2.22: Estimated Pressure vs. Volumetric Strain – GSC Trial..... 23
Figure 2.23: Illustration of the Finite Element Model for the GSC Trials Including the Pipe 25
Figure 2.24: Comparison of Experimental and Finite Element GSC Trial Load Displacement Results 26
Figure 2.25: Deformed Pipe – Experimental Results 26
Figure 2.26: Deformed Pipe – Finite Element Result..... 27
Figure 2.27: Deformed Pipe in Soil – Finite Element Results..... 27
Figure 2.28: Illustration of Soil Movement around the Pipe 28
Figure 2.29: Bending Moment at the Plastic Hinge..... 29
Figure 2.30: Pipeline Node 49426 Displacement Trace (at the Plastic Hinge) 29
Figure 2.31: Pipe Node Displacement Trace (Node 49426 at the Plastic Hinge and at the Pipe End Node 49606)..... 30
Figure 2.32: UBC Experimental Sand Compartment – Karimian et al., 2006 [4]..... 31
Figure 2.33: Illustration of the FE Model Including the Pipe..... 32
Figure 2.34: Displacement Patten (FE Analysis)..... 33
Figure 2.35: FEM Simulation of the UBC Trial Results 33
Figure 2.36: Comparison between Numerical Model Results and Test Results..... 34
Figure 2.37: Comparison between Numerical Model and Test Results 35
Figure 2.38: Displacement Trace Illustrating Pipe and Soil Displacements..... 35

Figure 2.39: Comparison between Numerical Model and Test Results: Mesh Size 50 mm to 100 mm 36
Figure 2.40: Effects of Pipe Self-Weight on Force-Displacement Curves 37
Figure 2.41: Hydrostatic Compression vs. Volumetric Strain 38
Figure 2.42: Effects of Saturation on Force-Displacement Curves 39
Figure 2.43: Effective Plastic Strain and Velocity Vectors at Pipe Displacement = 296 mm – Drained Sand with 17% Moisture Content 40
Figure 2.44: Effective Plastic Strain and Velocity Vectors at Pipe Displacement = 296 mm – Undrained Sand with 13% Moisture Content 40
Figure 2.45: Effective Plastic Strain and Velocity Vectors at Pipe Displacement = 296 mm – Undrained Sand with 17% Moisture Content 41
Figure 2.46: Permanent Ground Movement, Observed and Schematic Response of Landslide .. 41
Figure 2.47: Experimental Concept for PGD Effect on Buried Pipelines with Elbow (O'Rourke et al., 2004 [13]) 42
Figure 2.48: Plan View of the Experimental Setup (O'Rourke et al., 2004 [13]) 43
Figure 2.49: True Stress-Strain Curves (Yoshisaki et al., 2004 [17]) 43
Figure 2.50: Illustration of the FE Model including the Pipe 44
Figure 2.51: Overhead View of Test Compartment Before (Left) and After (Right) the Experiment. (Yoshisaki et al., 2004 [17]) 45
Figure 2.52: Deformed Experimental Pipeline (Yoshizaki et al., 2004 [17]) 45
Figure 2.53: Deformed Pipeline – Finite Element Analysis Results 46
Figure 2.54: Pipeline Deformation: Comparison between the Numerical Model and Test Results 46
Figure 2.55: Strain Distribution at the Cross-section of the Connection between the Elbow and the Straight Pipe Segment (Section A-A) – Comparison between the Numerical Model and Test Results 47
Figure 2.56: Strain Distribution at the Cross-Section of the Elbow (Section B-B) – Comparison between the Numerical Model and Test Results 47
Figure 2.57: Soil Deformation of Moist Sand (Experimental Results – Y=0.9 D) [41] 50
Figure 2.58: Soil Deformation of Moist Sand (FE Results – Y=0.9 D) 50
Figure 2.59: Comparison between Numerical Model Results and Test Results – (NPS 16 -Moist Sand Soil) 51
Figure 2.60: Comparison between Numerical Model Results and Test Results – (NPS 18 -Moist Sand Soil) 52
Figure 2.61: Soil Deformation of Road Mulch (Experimental Results – Y=0.75 D) [41] 53
Figure 2.62: Soil Deformation of Road Mulch (FE Results – Y=0.9 D) 53
Figure 2.63: Comparison between Numerical Model Results and Test Results – Road Mulch Soil 54
Figure 2.64: Pipe Movement and Soil Displacement 55
Figure 2.65: Axial Soil Force – Comparison between FEA (DEM) and ASCE 1984 / ALA 2001 56
Figure 2.66: Lateral Soil Force – Comparison between FEA (DEM) and ASCE / ALA 56
Figure 2.67: Soil Deformation of Wet Clay Soil 57
Figure 4.1: Illustration of the SPH FE Model Including the Pipe-Side View 65
Figure 4.2: Illustration of the SPH FE Model: Lateral Ground Movement 66
Figure 4.3: Illustration of the SPH FE Model: Ground Movement at Crossing Angle of 45° .. 66

Figure 4.4: True Stress-Strain Curves for X70 (483 MPa) Materials 67
Figure 4.5: Photo of Carson Sink Soil (NASA 2008) 69
Figure 4.6: Volume Strain vs. Mean Stress (NASA 2008) 69
Figure 4.7: Line 1 - Pipe Deformation & Axial Strain (Blue Compressive and Red is Tensile) For Case1: Soil Movement of 4.9 m & Width=10 m 71
Figure 4.8: Line 1 - Pipe Deformation & Axial Strain (Blue Compressive and Red is Tensile) For Case2: Soil Movement of 4.9 m & Width=20 m 71
Figure 4.9: Line 1 - Pipe Deformation & Axial Strain (Blue Compressive and Red is Tensile) For Case3: Soil Movement of 4.9 m & Width=40 m 72
Figure 4.10: Line 1 - Ground Movement Profiles at Different Levels of Soil Movement for Case2: W=20 m 72
Figure 4.11: Line 1 - Pipe Movement Profiles at Different Levels of Soil Movement for Case2: W=20 m 73
Figure 4.12: Line 1 - Axial Strain & Pipe and Ground Movement Profiles for Case1: W=10 m Considering Soil Movement of 1.93 m 73
Figure 4.13: Line 1 - Axial Strain & Pipe and Ground Movement Profiles for Case2: W=20 m Considering Soil Movement of 1.93 m 74
Figure 4.14: Line 1 - Axial Strain & Pipe and Ground Movement Profiles for Case3: W=40 m Considering Soil Movement of 1.93 m 74
Figure 4.15: Line 1 - Maximum Tensile in the Pipe vs. Ground Movement Widths: [5 - 50m] .. 77
Figure 4.16: Maximum Compressive Strain in the Pipe vs. Ground Movement: Widths [5-50 m] 78
Figure 4.17: Line 1 - Safety Envelopes: Tensile Strain Limit 79
Figure 4.18: Line 1 - Safety Envelopes: Compressive Strain Limit 80
Figure 4.19: Line 2 - Ground Movement Profiles at Different Levels of Soil Movement for Case2: W=20 m 81
Figure 4.20: Line 2 - Pipe Movement Profiles at Different Levels of Soil Movement for Case2: W=20 m 82
Figure 4.21: Line 2 - Axial Strain & Pipe and Ground Movement Profiles for Case3: W=15 m Considering Soil Movement of 1.93 m 82
Figure 4.22: Line 2 - Maximum Tensile in the Pipe vs. Ground Movement Widths: [5-50 m] ... 85
Figure 4.23: Line 2 - Maximum Compressive Strain in the Pipe vs. Ground Movement: Widths [5-50 m] 85
Figure 4.24: Line 2 - Safety Envelopes: Tensile Strain Limit 87
Figure 4.25: Line 2 - Safety Envelopes: Compressive Strain Limit 87
Figure 4.26: Typical type of Subsidence Associated with Underground Coal Mining (Bauer and Hunt, 1982; USGS 2008) 89
Figure 4.27: Longwall Mining Subsidence Parameters (New South Wales Coal Association) ... 90
Figure 4.28: Graph for Subsidence Factor (NCB-1975) 91
Figure 4.30: Illustration of the FE Model: Subsidence 93
Figure 4.31: Illustration of the Model Including the Pipe-Side View and Backfill Trench 93
Figure 4.31: Predicted Subsidence Profile from the Maximum Deflection Point and Longitudinal Soil Displacement and Tensile Strain in the Soil 96
Figure 4.32: Comparison of Subsidence Profiles Predicted by FE Model and Empirical Method (NCB Method, Appalachian Method) for Subcritical Panel Extraction Width..... 96

Figure 4.33: Comparison of Subsidence Profiles Predicted by FE Model and Empirical Method (NCB Method, Appalachian Method) for Critical Panel Extraction Width 97
Figure 4.34: Comparison of Subsidence Profiles Predicted by FE Model and Empirical Method (NCB Method), for Super-Critical Extraction Width 97
Figure 4.35: Surface Subsidence and Pipeline Deformation, for Case2: Subcritical Extraction Width, W/H=0.75 98
Figure 4.36: Soil Subsidence and Pipeline Deformation, for Case2: Critical Extraction Width, W/H=1.5 98
Figure 4.37: Soil Subsidence and Pipeline Deformation, for Case3: Super-Critical Extraction Width, W/H=3 99
Figure 4.38: Surface Subsidence, Pipeline Profile and Axial Strains Distribution, for Subcritical Extraction Width (W/H=0.75) – Case1a (D/T= 120) 99
Figure 4.39: Surface Subsidence, Pipeline Profile and Axial Strains Distribution, for Subcritical Extraction Width (W/H=0.75) – Case1a (D/T= 96) 100
Figure 4.40: Surface Subsidence, Pipeline Profile and Axial Strains Distribution, for Critical Extraction Width (W/H=1.5) - Case2a (D/T=120) 100
Figure 4.41: Surface Subsidence, Pipeline Profile and Axial Strains Distribution, for Critical Extraction Width (W/H=1.5) - Case2b (D/T=96) 101
Figure 4.42: Surface Subsidence Pipeline Profile and Axial Strains Distribution, for Super Critical Extraction Width (W/H=3) - Case3a (D/T=120) 101
Figure 4.43: Surface Subsidence Pipeline Profile and Axial Strains Distribution, for Super Critical Extraction Width (W/H=3) - Case3b (D/T=96) 102
Figure 4.44: Pit Subsidence – Pipe Deflection 103
Figure 4.45: Predicted Pipeline Profile and Maximum Tensile Strains in the Pipe for Pit Subsidence of 2.05 M 103
Figure 4.46: Peak Pipe Displacement in Relation to Pit Subsidence 104
Figure 4.47: Maximum Tensile Strains in the Pipe in Relation to Pit Subsidence (Left) and Vertical Pipe Deflection (Right) 104
Figure 5.1: (a) Penalty-Based Particle-Particle Interaction in LS-DYNA and (b) Possible Collision States for Mechanical Contact [43, 45] 106
Figure 5.2: True Stress-Strain Curves for X52 and X70 (359 and 483 MPa) Materials 107
Figure 5.3: Subsidence Profile Pattern, W =200 ft (61 m) - H/W = 0.5, 1.5 and 3 108
Figure 5.4: Subsidence Profile Pattern, W = 400 ft (122 m) - H/W = 0.5, 1.5 and 3 108
Figure 5.5: Subsidence Profile Pattern, W = 600 ft (182 m) - H/W = 0.5, 1.5 and 3 109
Figure 5.6: Pipe Deformation and Axial Strains for W = 61m (200 Ft) and Ground Subsidence of 4 M (13 Ft) (Top View –Soil Above the Pipe is Hidden) 110
Figure 5.7: Pipe Deformation and Axial Strains for W = 61 m (200 Ft) and Ground Subsidence of 4 M (13 Ft) (Top View – Soil Above the Pipe is Hidden) 111
Figure 5.8: Total Axial Strains in NPS 24 (D/t=96) for W = 200 ft (61 m), W/H = 0.5 and Soil Settlement of 4 m 111
Figure 5.9: NPS 24 (D/t=64) - Maximum Tensile in the Pipe vs. Ground Subsidence W =61 m (200 ft); W/h Ratio 0.5, 1.5 and 3 113
Figure 5.10: NPS 24 (D/t=64) - Maximum Local Compressive Strains in the Pipe vs. Ground Subsidence W =61 m (200 ft); W/h Ratio 0.5, 1.5 and 3 113
Figure 5.11: NPS 24 (D/t=64) - Maximum Nominal Compressive Strains in the Pipe vs. Ground Subsidence W =61 m (200 ft); W/h Ratio 0.5, 1.5 and 3 114

Figure 5.12: Pipe Deformation and Total Axial Strains in NPS 24 (D/t=96) for W = 200 ft (61 m), W/H = 0.5, 1.5 and 3 for Surface Settlement of 4 m 114
Figure 5.13: Pipe Deformation and Total Axial Strains in NPS 24 (D/t=96) for W = 200 ft (61m), W/h = 0.5, 1.5 and 3 for Surface Settlement of 4 m (Top View – Soil above the pipe is hidden) 115
Figure 5.14: NPS 24 (D/t=96) - Pipe Displacing vs. Soil Settlement of 4m 116
Figure 5.15: Total Axial Strains in NPS 24 (D/t=96) for W = 200 ft (61 m), W/H = 0.5 and Soil Settlement of 4 m..... 116
Figure 5.16: Total Axial Strains in NPS 24 (D/t=96) for W = 200 ft (61 m), W/H = 1.5 and Soil Settlement of 4 m..... 117
Figure 5.17: Total Axial Strains in NPS 24 (D/t=96) for W = 200 ft (61 m), W/H = 3 and Soil Settlement of 4 m..... 117
Figure 5.9: Pipe Axial Tensile Strains Envelopes versus Width to Depth Ratio (W =61 m, 200 ft) for Ground Settlement of 0.5, 1, 1.5, 2.0, 2.5, 3.0, 3.5 and 4.0 m 119
Figure 5.10: Pipe Axial Compressive Strains Envelopes versus Width to Depth Ratio (W =61 m, 200 ft) for Ground Settlement of 0.5, 1, 1.5, 2.0, 2.5, 3.0, 3.5 and 4.0 m 119
Figure 5.11: NPS 24 (D/t=96) - Maximum Tensile and Local Compressive Strains in the Pipe vs. Ground Settlement: [W/h= 0.5] 120
Figure 5.12: NPS 24 (D/t=96) - Maximum Tensile and Local Compressive Strains in the Pipe vs. Ground Settlement: [W/h= 1.5] 121
Figure 5.13: NPS 24 (D/t=96) - Maximum Tensile and Local Compressive Strains in the Pipe vs. Ground Settlement: [W/h= 3] 121
Figure 5.14: NPS 24 (D/t=96) – Sum of Maximum Tensile (Positive) and Local Compressive Strains (Negative) vs. Ground Settlement: [W/h= 0.5] 122
Figure 5.15: NPS 24 (D/t=96) – Sum of Maximum Tensile (Positive) and Local Compressive Strains (Negative) vs. Ground Settlement: [W/h= 1.5] 122
Figure 5.16: NPS 24 (D/t=96) – Sum of Maximum Tensile (Positive) and Local Compressive Strains (Negative) vs. Ground Settlement: [W/h= 3] 123
Figure 5.17: NPS 24 (D/t=64) - Maximum Tensile in the Pipe vs. Ground Subsidence W = 61 m (200 ft); W/h Ratio 0.5, 1.5 and 3..... 124
Figure 5.18: NPS 24 (D/t=64) - Maximum Tensile in the Pipe vs. Ground Subsidence W = 122 m (400 ft); W/h Ratio 0.5, 1.5 and 3..... 125
Figure 5.19: NPS 24 (D/t=96) - Maximum Tensile in the Pipe vs. Ground Subsidence W = 183 m (600 ft); W/h Ratio 0.5, 1.5 and 3..... 125
Figure 5.20: NPS 24 (D/t=96) - Maximum Nominal Compressive Strains in the Pipe vs. Ground Subsidence W = 61 m (200 ft); W/h Ratio 0.5, 1.5 and 3 126
Figure 5.21: NPS 24 (D/t=96) - Maximum Nominal Compressive Strains in the Pipe vs. Ground Subsidence W = 122 m (400 ft); W/h Ratio 0.5, 1.5 and 3 126
Figure 5.22: NPS 24 (D/t=96) - Maximum Nominal Compressive Strains in the Pipe vs. Ground Subsidence W = 183 m (600 ft); W/h Ratio 0.5, 1.5 and 3 127
Figure 5.23: Pipe Axial Tensile Strains Envelopes versus Width to Depth Ratio (W = 61 m, 200 ft) for Ground Settlement of 0.5, 1, 1.5, 2.0, 2.5, 3.0, 3.5 and 4.0 m 128
Figure 5.24: Pipe Axial Tensile Strains Envelopes versus Width to Depth Ratio (W = 122 m, 400 ft) for Ground Settlement of 0.5, 1, 1.5, 2.0, 2.5, 3.0, 3.5 and 4.0 m 128
Figure 5.25: Pipe Axial Tensile Strains Envelopes versus Width to Depth Ratio (W = 183 m, 600 ft) for Ground Settlement of 0.5, 1, 1.5, 2.0, 2.5, 3.0, 3.5 and 4.0 m 129

Figure 5.26: Pipe Axial Compressive Strains Envelopes versus Width to Depth Ratio (W =61 m, 200 ft) for Ground Settlement of 0.5, 1, 1.5, 2.0, 2.5, 3.0, 3.5 and 4.0 m 130
Figure 5.27: Pipe Axial Compressive Strains Envelopes versus Width to Depth Ratio (W = 122 m, 400 ft) for Ground Settlement of 0.5, 1, 1.5, 2.0, 2.5, 3.0, 3.5 and 4.0 m 130
Figure 5.28: Pipe Axial Compressive Strains Envelopes versus Width to Depth Ratio (W = 183 m, 600 ft) for Ground Settlement of 0.5, 1, 1.5, 2.0, 2.5, 3.0, 3.5 and 4.0 m 131
Figure 5.29: NPS 24 – Maximum Axial Strain versus Ground Settlement for Ground Subsidence Width of 200 ft (61 m) and W/h= 0.5 133
Figure 5.30: NPS 24 – Maximum Axial Strain versus Ground Settlement for Ground Subsidence Width of 200 ft (61 m) and W/h= 1.5 133
Figure 5.31: NPS 24 – Maximum Axial Strain versus Ground Settlement for Ground Subsidence Width of 200 ft (61 m) and W/h= 3 134
Figure 5.32: Total Axial Strains in NPS 24 at 6 o'clock Position for W = 200 ft (61 m), W/H = 0.5 and Soil Settlement of 4 m 134
Figure 5.33: Total Axial Strains in NPS 24 at 12 o'clock Position for W = 200 ft (61 m), W/H = 0.5 and Soil Settlement of 4 m 135
Figure 5.34: NPS 24 (D/t=64) - Maximum Tensile and Local Compressive Strains in the Pipe vs. Ground Settlement: [W/h= 0.5] 136
Figure 5.35: NPS 24 (D/t=48) - Maximum Tensile and Local Compressive Strains in the Pipe vs. Ground Settlement: [W/h= 0.5] 136
Figure 5.36: NPS 24 (D/t=64) - Maximum Tensile and Local Compressive Strains in the Pipe vs. Ground Settlement: [W/h= 1.5] 137
Figure 5.37: NPS 24 (D/t=48) - Maximum Tensile and Local Compressive Strains in the Pipe vs. Ground Settlement: [W/h= 1.5] 137
Figure 5.38: NPS 24 (D/t=64) - Maximum Tensile and Local Compressive Strains in the Pipe vs. Ground Settlement: [W/h= 3] 138
Figure 5.39: NPS 24 (D/t=48) – Sum of Maximum Tensile (Positive) and Local Compressive Strains (negative) vs. Ground Settlement: [W/h= 3] 138
Figure 5.40: NPS 24 (D/t=64) – Sum of Maximum Tensile (Positive) and Local Compressive Strains (negative) vs. Ground Settlement: [W/h= 0.5] 139
Figure 5.41: NPS 24 (D/t=48) – Sum of Maximum Tensile (Positive) and Local Compressive Strains (negative) vs. Ground Settlement: [W/h= 0.5] 139
Figure 5.42: NPS 24 (D/t=64) – Sum of Maximum Tensile (Positive) and Local Compressive Strains (negative) vs. Ground Settlement: [W/h= 1.5] 140
Figure 5.43: NPS 24 (D/t=48) – Sum of Maximum Tensile (Positive) and Local Compressive Strains (negative) vs. Ground Settlement: [W/h= 1.5] 140
Figure 5.44: NPS 24 (D/t=64) – Sum of Maximum Tensile (Positive) and Local Compressive Strains (negative) vs. Ground Settlement: [W/h= 3] 141
Figure 5.45: NPS 24 (D/t=48) – Sum of Maximum Tensile (Positive) and Local Compressive Strains (negative) vs. Ground Settlement: [W/h= 3] 141
Figure 5.46: NPS 24 (D/t=64) - Maximum Tensile Strain in the Pipe vs. Ground Subsidence W =61 m (200 ft); W/h Ratio 0.5, 1.5 and 3 143
Figure 5.47: NPS 24 (D/t=48) - Maximum Tensile Strain in the Pipe vs. Ground Subsidence W =61 m (200 ft); W/h Ratio 0.5, 1.5 and 3 143
Figure 5.48: NPS 24 (D/t=64) - Maximum Tensile Strain in the Pipe vs. Ground Subsidence W =122 m (400 ft); W/h Ratio 0.5, 1.5 and 3 144

Figure 5.49: NPS 24 (D/t=48) - Maximum Tensile Strain in the Pipe vs. Ground Subsidence W =122 m (400 ft); W/h Ratio 0.5, 1.5 and 3 144
Figure 5.50: NPS 24 (D/t=64) - Maximum Tensile Strain in the Pipe vs. Ground Subsidence W =183 m (600 ft); W/h Ratio 0.5, 1.5 and 3 145
Figure 5.51: NPS 24 (D/t=48) - Maximum Tensile Strain in the Pipe vs. Ground Subsidence W =183 m (600 ft); W/h Ratio 0.5, 1.5 and 3 145
Figure 5.52: NPS 24 (D/t=64) - Maximum Nominal Compressive Strains in the Pipe vs. Ground Subsidence W =61 m (200 ft); W/h Ratio 0.5, 1.5 and 3 146
Figure 5.53: NPS 24 (D/t=48) - Maximum Nominal Compressive Strains in the Pipe vs. Ground Subsidence W =61 m (200 ft); W/h Ratio 0.5, 1.5 and 3 146
Figure 5.54: NPS 24 (D/t=64) - Maximum Nominal Compressive Strains in the Pipe vs. Ground Subsidence W =122 m (400 ft); W/h Ratio 0.5, 1.5 and 3 147
Figure 5.55: NPS 24 (D/t=48) - Maximum Nominal Compressive Strains in the Pipe vs. Ground Subsidence W =122 m (400 ft); W/h Ratio 0.5, 1.5 and 3 147
Figure 5.56: NPS 24 (D/t=64) - Maximum Nominal Compressive Strains in the Pipe vs. Ground Subsidence W =183 m (600 ft); W/h Ratio 0.5, 1.5 and 3 148
Figure 5.57: NPS 24 (D/t=48) - Maximum Nominal Compressive Strains in the Pipe vs. Ground Subsidence W =183 m (600 ft); W/h Ratio 0.5, 1.5 and 3 148
Figure 5.58: NPS 24 (D/t=64) - Pipe Axial Tensile Strains Envelopes versus Width to Depth Ratio (W =61 m, 200 ft) for Ground Settlement of 0.5, 1, 1.5, 2.0, 2.5, 3.0, 3.5 and 4.0 149
Figure 5.59: NPS 24 (D/t=48) - Pipe Axial Tensile Strains Envelopes versus Width to Depth Ratio (W =61 m, 200 ft) for Ground Settlement of 0.5, 1, 1.5, 2.0, 2.5, 3.0, 3.5 and 4.0 m 149
Figure 5.60: NPS 24 (D/t=64) - Pipe Axial Tensile Strains Envelopes versus Width to Depth Ratio (W =122 m, 400 ft) for Ground Settlement of 0.5, 1, 1.5, 2.0, 2.5, 3.0, 3.5 and 4.0 m 150
Figure 5.61: NPS 24 (D/t=48) - Pipe Axial Tensile Strains Envelopes versus Width to Depth Ratio (W =122 m, 400 ft) for Ground Settlement of 0.5, 1, 1.5, 2.0, 2.5, 3.0, 3.5 and 4.0 m 150
Figure 5.62: NPS 24 (D/t=64) - Pipe Axial Tensile Strains Envelopes versus Width to Depth Ratio (W =183 m, 600 ft) for Ground Settlement of 0.5, 1, 1.5, 2.0, 2.5, 3.0, 3.5 and 4.0 m 151
Figure 5.63: NPS 24 (D/t=48) - Pipe Axial Tensile Strains Envelopes versus Width to Depth Ratio (W =183 m, 600 ft) for Ground Settlement of 0.5, 1, 1.5, 2.0, 2.5, 3.0, 3.5 and 4.0 m 151
Figure 5.64: NPS 24 (D/t=64) - Pipe Axial Compressive Strains Envelopes versus Width to Depth Ratio (W =61 m, 200 ft) for Ground Settlement of 0.5, 1, 1.5, 2.0, 2.5, 3.0, 3.5 and 4.0 m 152
Figure 5.65: NPS 24 (D/t=48) - Pipe Axial Compressive Strains Envelopes versus Width to Depth Ratio (W =61 m, 200 ft) for Ground settlement of 0.5, 1, 1.5, 2.0, 2.5, 3.0, 3.5 and 4.0 m 152
Figure 5.66: NPS 24 (D/t=64) - Pipe Axial Compressive Strains Envelopes versus Width to Depth Ratio (W =122 m, 400 ft) for Ground Settlement of 0.5, 1, 1.5, 2.0, 2.5, 3.0, 3.5 and 4.0 m 153

Figure 5.67: NPS 24 (D/t=48) - Pipe Axial Compressive Strains Envelopes versus Width to Depth Ratio (W =61 m, 200 ft) for Ground settlement of 0.5, 1, 1.5, 2.0, 2.5, 3.0, 3.5 and 4.0 m 153
Figure 5.68: NPS 24 (D/t=64) - Pipe Axial Compressive Strains Envelopes versus Width to Depth Ratio (W = 183 m, 600 ft) for Ground Settlement of 0.5, 1, 1.5, 2.0, 2.5, 3.0, 3.5 and 4.0 m 154
Figure 5.69: NPS 24 (D/t=48) - Pipe Axial Compressive Strains Envelopes versus Width to Depth Ratio (W =183 m, 600 ft) for Ground Settlement of 0.5, 1, 1.5, 2.0, 2.5, 3.0, 3.5 and 4.0 m 154
Figure 5.70: NPS 24 (D/t=96) – Maximum Axial Strain Versus Ground Settlement for Ground Subsidence Width of 61 m (200 ft) –Temperature Effect 155
Figure 5.71: NPS 24 (D/t=96) – Sum of the Maximum Tensile and Compressive Strain versus Ground Settlement for Ground Subsidence Width of 61 m (200 ft) – Pressure Effect 156
Figure 5.72: NPS 24 (D/t=64) – Maximum Pipe Axial Strain Due to Ground Settlement for Ground Subsidence Width of 61 m (200 ft) – Pressure Effect 157
Figure 5.73: NPS 24 (D/t=64) – Sum of the Maximum Tensile and Compressive Strain versus Ground Settlement for Ground Subsidence Width of 61 m (200 ft) – Pressure Effect 157
Figure 5.83: NPS 12 – Maximum Axial Strain Versus Ground Settlement for Ground Subsidence Width of 200 ft (61 m) and W/h = 0.5 159
Figure 5.84: NPS 12 – Maximum Axial Strain Versus Ground Settlement for Ground Subsidence Width of 200 ft (61 m) and W/h = 1.5 160
Figure 5.85: NPS 12 – Maximum Axial Strain versus Ground Settlement for Ground subsidence Width of 200 ft (61 m) and W/h = 3 160
Figure 5.86: Total Axial Strains in NPS 12 at 6 o'clock position for W = 200 ft (61m), W/H = 0.5 and Soil Settlement of 4 m 161
Figure 5.87: Total Axial Strains in NPS 12 at 12 o'clock Position for W = 200 ft (61m), W/H = 0.5 and Soil Settlement of 4 m 161
Figure 5.88: Total Axial Strains in NPS 12 at 12 o'clock Position for W = 200 ft (61m), W/H = 0.5 and Soil Settlement of 4 m 162
Figure 5.89: NPS 18 – Maximum Axial Strain versus Ground Settlement for Ground Subsidence Width of 200 ft (61 m) and W/h = 0.5 164
Figure 5.90: NPS 18 – Maximum Axial Strain versus Ground Settlement for Ground Subsidence Width of 200 ft (61 m) and W/h = 1.5 165
Figure 5.91: NPS 18 – Maximum Axial Strain versus Ground Settlement for Ground Subsidence Width of 200 ft (61 m) and W/h = 3 165
Figure 5.92: NPS 18 – Sum of Tensile and Compressive Axial Strain versus Ground Settlement for Ground Subsidence Width of 200 ft (61 m) and W/h = 0.5 166
Figure 5.93: NPS 18 – Sum of Tensile and Compressive Axial Strain versus Ground Settlement for Ground Subsidence Width of 200 ft (61 m) and W/h = 1.5 166
Figure 5.94: NPS 18 – Sum of Tensile and Compressive Axial Strain versus Ground Settlement for Ground Subsidence Width of 200 ft (61 m) and W/h = 3 167
Figure 5.95: Total Axial Strains in NPS 18 at 6 o'clock Position for W = 200 ft (61 m), W/H = 0.5 and Soil Settlement of 4m 167

Figure 5.96: Total Axial Strains in NPS 18 at 12 o'clock Position for W = 200 ft (61 m), W/H = 0.5 and Soil Settlement of 4 m 168
Figure 5.97: Total Axial Strains in NPS 18 at 12 o'clock Position for W = 200 ft (61 m), W/H = 0.5 and Soil Settlement of 4 m 168
Figure 6.1: Ground Movement Pattern n=2 173
Figure 6.2: Ground Movement Pattern n=0.1 173
Figure 6.3: Pipe Deformation and Axial Strains for W= 20 m and Soil Movement of 3 m (Top View – Soil above the pipe is hidden) 175
Figure 6.4: Total Axial Strains in NPS 24 (D/t=96) for W= 20 m and Soil Movement of 3 m . 175
Figure 6.5: NPS 24 (D/t=64) - Maximum Tensile in the Pipe vs. Ground Movement Widths: [10-100 m] 176
Figure 6.6: NPS 24 (D/t=64) - Maximum local Compressive Strain vs. Ground Movement Widths: [10-100 m] 177
Figure 6.7: NPS 24 (D/t=64) - Maximum Nominal Compressive Strain vs. Ground Movement Widths: [10-100 m] 177
Figure 6.8: NPS 24 (D/t=64) – Pipe Displacement versus Ground Displacement 178
Figure 6.9: NPS 24(D/t=64) – Maximum Axial Strain vs. Ground Movement for the Critical Widths of 20 m (66 ft) 179
Figure 6.10: Pipe Deformation and Axial Strains for given Soil Movement of 1m, 2 m and 3 m (Top View) 180
Figure 6.11: Pipe Axial Tensile Strains Envelopes versus Width (W) for Soil Movements of 0.5, 1, 1.5, 2.0 and 2.5 m 182
Figure 6.12: Tensile Strain Capacity Envelopes versus Ground Width (W) Movements 182
Figure 6.13: Pipe Axial Compressive Strains Envelopes versus Width (W) (for Soil Movement of 0.5, 1, 1.5, 2.0 and 2.5 m). 183
Figure 6.14: Compressive Strain Capacity Envelopes versus Ground Width (W) Movements . 184
Figure 6.15: Tensile Strain Demand versus Width (W) 185
Figure 6.16: Compressive Strain Demand Envelopes versus Width (W) 185
Figure 6.17: NPS 24 – Maximum Axial Strain versus Ground Movement for the Critical Widths of 20 m (66 ft) 187
Figure 6.18: NPS 24 (D/t=64) - Maximum Tensile in the Pipe Versus Ground Movement Widths: [10-100 m] 188
Figure 6.19: NPS 24 (D/t=64) - Maximum Local Compressive Strains in the Pipe versus Ground Movement Widths: [10-100 m] 188
Figure 6.20: NPS 24 (D/t=64) - Maximum Nominal Compressive Strains in the Pipe versus Ground Movement Widths: [10-100 m] 189
Figure 6.21: NPS 24 – Maximum Axial Strain versus Ground Movement for the Critical Widths of 20 m (33 ft) 189
Figure 6.22: Pipe Deformation and Axial Strains for given Soil Movement of 1 m, 2 m and 3 m (Top View) 190
Figure 6.23: NPS 24 (D/t=64) - Maximum Pipe Displacement versus Ground Displacement .. 191
Figure 6.24: Pipe Axial Tensile Strains Envelopes versus Width (W) for Soil Movements of 0.5, 1, 1.5, 2.0 and 2.5 m. 192
Figure 6.25: Tensile Strain Capacity Envelopes versus Ground Width (W) Movements 192
Figure 6.26: Pipe Axial Compressive Strains Envelopes versus Width (W) (for Soil Movement of 0.5, 1, 1.5, 2.0 and 2.5 m) 193

Figure 6.27: Compressive Strain Capacity Envelopes versus Ground Width (W) Movements. 194
Figure 6.28: Tensile Strain Demand versus Width (W) 195
Figure 6.29: Compressive Strain Demand Envelopes versus Width (W)..... 195
Figure 6.30: NPS 24 (D/t=64) – Maximum Axial Strain versus Ground Movement for the Critical Widths of 20 m (66 ft) 196
Figure 6.31: NPS 24 (D/t=64) – Maximum Pipe Displacement versus Ground Movement for the Critical Widths of 20 m (66 ft) 197
Figure 6.32: NPS 24 (D/t=64, X70) - Maximum Tensile in the Pipe vs. Ground Movement Widths: [10-100 m] 198
Figure 6.33: NPS 24 (D/t=64, X70) - Maximum local Compressive Strain vs. Ground Movement Widths: [10-100 m] 198
Figure 6.34: NPS 24 (D/t=64, X70) - Maximum Nominal Compressive Strain vs. Ground Movement Widths: [10-100 m] 199
Figure 6.35: NPS 24 (D/t=64, X70) – Pipe Displacement versus Ground Displacement 199
Figure 6.36: Pipe Axial Tensile Strains Envelopes versus Width (W) for Soil Movements of 0.5, 1, 1.5, 2.0 and 2.5 m, Material Grade X70 201
Figure 6.37: Tensile Strain Capacity Envelopes versus Ground Width (W) Movements Material Grade X70 201
Figure 6.38: Pipe Axial Compressive Strains Envelopes (X70) versus Width (W) (for Soil Movement of 0.5, 1, 1.5, 2.0 and 2.5 m), Grade X70..... 202
Figure 6.39: Compressive Strain Capacity Envelopes versus Ground Width (W) Movements. Grade X70 203
Figure 6.40: Tensile Strain Demand versus Width (W), Grade X70..... 204
Figure 6.41: Compressive Strain Demand Envelopes versus Width (W), Grade X70..... 204
Figure 6.42: NPS 24 (D/t=64) – Maximum Axial Strain versus Ground Movement for the Critical Widths of 20 m (66 ft) –Temperature Effect..... 205
Figure 6.43: NPS 24 (D/t=64) – Maximum Pipe Displacement vs. Ground Movement for the Critical Widths of 20 m (66 ft) –Temperature Effect, Grade X52 206
Figure 6.44: NPS 24 (D/t=64) – Maximum Axial Strain versus Ground Movement for the Critical Widths of 20 m (66 ft) –Pressure Effect..... 207
Figure 6.45: NPS 24 (D/t=64) – Sum of the Maximum Tensile and Compressive Strain versus Ground Movement for the Critical Widths of 20 m (66 ft) – Pressure Effect..... 208
Figure 6.46: NPS 24 (D/t=64) – Maximum Pipe Displacement vs. Ground Movement for the Critical Widths of 20 m (66 ft) – Temperature Effect, Grade X52 208
Figure 6.47: Pipe Deformation and Axial Strains for given Soil Movement of 2.5 m (Top View) – 0.72 SMYS Pressure (No Wrinkle observed)..... 209
Figure 6.48: Pipe Deformation and Axial Strains for given Soil Movement of 2.5 m (Top View) – 0.50 SMYS Pressure (Wrinkle observed, Amplitude = 8 mm)..... 209
Figure 6.49: Pipe Deformation and Axial Strains for given Soil Movement of 2.5 m (Top View) –0.36 SMYS Pressure (Wrinkle observed, Amplitude = 28 mm)..... 210
Figure 6.50: NPS 24 (D/t=64, X52) - Maximum Tensile in the Pipe vs. Ground Movement Widths: [10-100m] 211
Figure 6.51: NPS 24 (D/t=64, X52) - Maximum Local Compressive Strain in the Pipe vs. Ground Movement Widths: [10-100 m]..... 212
Figure 6.52: NPS 24 (D/t=64, X52) - Maximum Nominal Compressive Strain in the Pipe vs. Ground Movement Widths: [10-100 m]..... 212

Figure 6.53: Pipe Axial Tensile Strains Envelopes versus Width (W) for Soil Movements of 0.5, 1, 1.5, 2.0 and 2.5 m Operating Pressure 36% SMYS 213
Figure 6.54: Tensile Strain Capacity Envelopes versus Ground Width (W) Movements 213
Figure 6.55: Pipe Axial Compressive Strains Envelopes versus Width (W) for Soil Movements of 0.5, 1, 1.5, 2.0 and 2.5 m Operating Pressure 36% SMYS 214
Figure 6.56: Compressive Strain Capacity Envelopes versus Ground Width (W) Movements . 214
Figure 6.57: Tensile Strain Demand versus Width (W), (Pressure is 36% SMYS) 215
Figure 6.58: Compressive Strain Demand versus Width (W), (Pressure is 36% SMYS) 215
Figure 6.59: Soil Movement Patterns, Width W=10m, and 20 m 216
Figure 6.60: Pipe Deformation and Axial Strains for given Soil Movement of 2 m and W=20 m (Top View), n=2 216
Figure 6.61: Pipe Deformation and Axial Strains for given Soil Movement of 2 m and W=20 m (Top View), n=0.1 217
Figure 6.62: NPS 24 (D/t=64) – Maximum Axial Strain vs. Ground Movement for the Critical Widths of 20 m (66 ft) 218
Figure 6.63: NPS 24 (D/t=64) –Maximum Axial Strain vs. Ground Movement for the Critical Widths of 20 m (66 ft) and 10 m (33ft) 218
Figure 6.64: NPS 24 (D/t=64, X52) - Maximum Tensile in the Pipe vs. Ground Movement Widths: [10-100 m], n = 0.1 220
Figure 6.65: NPS 24 (D/t=64, X52) - Maximum Local Compressive Strain in the Pipe vs. Ground Movement Widths: [10-100 m], n = 0.1 220
Figure 6.66: NPS 24 (D/t=64, X52) - Maximum Nominal Compressive Strain in the Pipe vs. Ground Movement Widths: [10-100 m], n = 0.1 221
Figure 6.67: Pipe Axial Tensile Strains Envelopes versus Width (W) for Soil Movements of 0.5, 1, 1.5, 2.0 and 2.5 m, n = 0.1 221
Figure 6.68: Tensile Strain Capacity Envelopes versus Ground Width (W) Movements, n = 0.1 222
Figure 6.69: Pipe Axial Compressive Strains Envelopes versus Width (W) for Soil Movements of 0.5, 1, 1.5, 2.0 and 2.5 m, n = 0.1 222
Figure 6.70: Compressive Strain Capacity Envelopes versus Ground Width (W) Movements, n = 0.1 223
Figure 6.71: Tensile Strain Demand versus Width (W), n = 0.1 223
Figure 6.72: Compressive Strain Demand versus Width (W), (n = 0.1) 224
Figure 6.73: NPS 24 (D/t=64) – Maximum Axial Strain vs. Ground Movement for the Critical Widths of 20 m (66 ft) 225
Figure 6.74: NPS 24 (D/t=64) – Sum of the Maximum Tensile and Compressive Strain versus Ground Movement for the Critical Widths of 20 m (66 ft) –Burial Depth Effect . 225
Figure 6.75: NPS 24 (D/t=64) – Maximum Pipe Displacement vs. Ground Movement for the Critical Widths of 20 m (66 ft) – Temperature Effect, Grade X52 226
Figure 6.76: Pipe and Soil Deformation for Maximum Soil Movement of 3 m 227
Figure 6.77 Pipe and Soil Deformation for Maximum Soil Movement of 3 m Considering Slope of 16 Deg. 227
Figure 6.78: NPS 24 (D/t=64) - Maximum Tensile in the Pipe versus Ground Movement Widths: [10-100 m] 228
Figure 6.79: NPS 24 (D/t=64) - Maximum Tensile in the Pipe versus Ground Movement Widths: [10-100 m] 228

Figure 6.80: NPS 24 (D/t=64) – Maximum Axial Strain versus Ground Movement for the Critical Widths of 20 m (66 ft) 229
Figure 6.81: NPS 24 (D/t=64) –Maximum Pipe Displacement versus Ground Movement for the Critical Widths of 20 m (66 ft) 229
Figure 6.82: Pipe Axial Tensile Strains Envelopes versus Width (W) for Soil Movements of 0.5, 1, 1.5, 2.0 and 2.5 m, Material Grade X70 230
Figure 6.83: Tensile Strain Capacity Envelopes versus Ground Width (W) Movements, Grade X52 231
Figure 6.84: Pipe Axial Compressive Strains Envelopes (X70) versus Width (W) (for Soil Movement of 0.5, 1, 1.5, 2.0 and 2.5 m), Grade X70 232
Figure 6.85: Compressive Strain Capacity Envelopes versus Ground Width (W) Movements, Grade X52 233
Figure 6.86: Tensile Strain Demand versus Width (W), Grade X52 234
Figure 6.87: Compressive Strain Demand Envelopes versus Width (W), Grade X52 234
Figure 6.88: NPS 24 (D/t=64) – Maximum Axial Strain versus Ground Movement for the Critical Widths of 20 m (66 ft) – Soil 1 and 2 235
Figure 6.89: NPS 24 (D/t=64) – Sum of Maximum Axial Compressive and Tensile Strains versus Ground Movement for the Critical Widths of 20 m (66 ft) – Soil 1 and 2 236
Figure 6.90: Pipe Soil Deformation Left (sand), Right clay (soil displacement 1.5, 2, 2.5 and 3 m) 237
Figure 6.91: NPS 24 (D/t=64) – Maximum Axial Strain versus Ground Movement for the Critical Widths of 20 m (66 ft) – Friction 0.32, 0.56 and 0.72 239
Figure 6.92: NPS 24 (D/t=64) – Sum of the Maximum Axial Tensile and Compressive Strains versus Ground Movement for the Critical Widths of 20 m (66 ft) – Friction 0.32, 0.56 and 0.72 239
Figure 6.93: NPS 12 (D/t =71, 51 and 34) – Maximum Axial Strain versus Ground Movement for the Critical Widths of 10 m (33 ft) 241
Figure 6.94: NPS 12 (D/t =71, 51 and 34) – Sum of Maximum Axial Tensile and Compressive Strain versus Ground Movement for the Critical Widths of 10 m (33 ft) 242
Figure 6.95: NPS 12 (D/t =71, 51 and 34) – Maximum Pipe Displacement versus Ground Movement for the Critical Widths of 10 m (33 ft) 242
Figure 6.96: Pipe Deformation and Axial Strains for given Soil Movement of 3 m and W=10 m (Top View) 244
Figure 6.97: NPS 30 (D/t = 96) - Maximum Tensile Strains in the Pipe versus Ground Movement Widths: [10-100 m] 246
Figure 6.98: NPS 30 (D/t = 96) - Maximum Compressive Strains in the Pipe versus Ground Movement Widths: [10-100 m] 246
Figure 6.99: NPS 30 (D/t = 80) - Maximum Tensile Strains in the Pipe versus Ground Movement Widths: [10-100m] 247
Figure 6.100: NPS 30 (D/t = 80) - Maximum Compressive Strains in the Pipe versus Ground Movement Widths: [10-100 m] 247

LIST OF TABLES

Table 2.1: Summary of Axial Pullout Tests (UBC Test) ... 7
Table 2.2: Soil Parameters (UBC Test) ... 8
Table 2.3: Summary of Axial Pullout Tests 24-inch Polyethylene Wrapped Pipe ... 11
Table 2.4: Natural Soil Parameters ... 12
Table 2.5: Soil Parameters (UBC Test) ... 17
Table 2.6: Soil Parameters (UBC Test) ... 30
Table 2.7: Material Properties of "Lebanon Sand" ... 38
Table 2.8: Summary Parameters for Pipe-Soil Test Cases [41] ... 49
Table 2.9: Summary Parameters for DEM Model ... 57
Table 3.1: Maximum Allowable Compressive Strain Calculated According to CSA Z662-11 60
Table 3.2: Compressive Strain Limits Calculated According to PRCI ... 62
Table 3.3: Compressive Strain Limits for Plain Pipe Calculated According to PRCI ... 62
Table 3.4: Tensile Strain Limits: (a=0.5, 1 and 2 mm, 2c=50 mm, CTOD=0.05 mm) ... 63
Table 4.1: Input Parameters ... 64
Table 4.2: Input Parameters Used for the Analyses ... 67
Table 4.3: Soil Material Model Properties Used in the Continuum Model ... 68
Table 4.4: Line 1 - Required Ground Displacement to Cause Tensile Strain Capacity ... 78
Table 4.5: Line 1 - Required Ground Displacement to Cause Compressive Strain Capacity - CS-Z662 ... 78
Table 4.6: Line 1 - Required Ground Displacement to Cause Compressive Strain Capacity - PRCI -2004 ... 79
Table 4.7: Line 2 - Required Ground Displacement to Cause Tensile Strain Capacity ... 86
Table 4.8: Line 2 - Required Ground Displacement to Cause Compressive Strain Capacity - CS-Z662 ... 86
Table 4.9: Line 2 - Required Ground Displacement to Cause Compressive Strain Capacity - PRCI-2004 ... 86
Table 5.1: Maximum Allowable Tensile and Compressive Strain for NPS 24, Wt=6.35mm, D/t=96, Grade X52 ... 118
Table 5.2: Maximum Tensile and Compressive Strain [%] for NPS 24, W =200 ft (61 m) –Effect of D/t (Settlement of 4m) ... 132
Table 5.3: Maximum Allowable Tensile and Compressive Strain for NPS 24, Wt=12.7 mm, D/t=48, Grade X52 ... 142
Table 5.4: Maximum Allowable Tensile/Compressive Strain for NPS 24, Wt=9.52 mm, D/t=64, Grade X52 ... 142
Table 5.5: Maximum Tensile and Compressive Strain [%] for NPS 12, W =200 ft (61 m) –Effect of D/t ... 159
Table 5.6: Maximum Tensile/Compressive Strain [%] for NPS 18, W =200 ft (61 m) – Effect of D/t ... 164
Table 6.1: Maximum Allowable Tensile/Compressive Strain for NPS 24, Wt=9.52 mm, D/t=64, Grade X52 ... 181
Table 6.2: Maximum Allowable Tensile/Compressive Strain for NPS 24, Wt=6.35mm, D/t=96, Grade X52 ... 191
Table 6.3: Maximum Allowable Tensile/Compressive Strain for NPS 24, Wt=9.52mm, D/t=64, Grade X70 ... 200

ACRONYMS AND ABBREVIATIONS

ALA	American Lifelines Alliance
ARA	Applied Research Associates
BMT	BMT Fleet Technology
ASPIReTM	Advanced Soil-Pipe Interaction Research
CEV	Crew Exploration Vehicle
CSC	Compressive Strain Capacity
CSCE	Compressive Strain Capacity Envelopes
DEM	Discrete Element Method
FE	Finite Element
GSC	Geological Survey of Canada
HDPE	High Density Polyethylene
MM-ALE	Multi-material Arbitrary Lagrangian Eulerian
MOP	Maximum Operation Pressure
NCB	National Coal Board
NCS	Natural Clayed Soil
NPS	Nominal Pipe Size
PGD	Permanent Ground Deformation
PRCI	Pipeline Research Council International
RF	Resistance Factor
SDE	Strain Demand Envelopes
SPH	Smooth Particle Hydrodynamic
TSCE	Tensile Strain Capacity Envelopes
UBC	University of British Columbia
UofA	University of Alberta
USCS	Unified Soil Classification System
W/h	Width to depth ratio
Y/T	Yield to Tensile

1 INTRODUCTION

This submission serves as the Project Final Report to DOT PHMSA for Project DTPH56-14-H-00008, "Definition of Geotechnical and Operational Load Effects on Pipeline Anomalies". This report covers the completion of the project consolidating the result of the preceding tasks.

The project results were previously reported in several interim reports describing the modelling tools, data, process and results for pipeline subsidence and soil movements across the pipeline.

The project developed engineering data or a tool for government, operators and technology providers to consider the effects of operational and geotechnical loads on liquid and gas pipeline systems to support decision making regarding threat severity or repair scheduling. This work employed the BMT Fleet Technology (BMT) pipe soil interaction model that has been developed to consider operational conditions in the presence of the loads and restraint applied to a pipeline system by surrounding soil and geotechnical factors. The BMT LS-DYNA based 3D continuum pipe soil interaction model was developed and validated [33] and been shown to be capable of simulating small- and full-scale lab trials as well as operational incidents [23, 24, 25]. The improved predictive capability of this modeling approach over traditional soil spring based modeling has been demonstrated in the validation process [21, 24, 25]. Based upon these results, strains developed for various ground movements, in the presence of thermal and pressure loads, have been defined and initial work towards the development of empirical engineering tools for geotechnical strain based design and assessment tools has commenced [34]. Figure 1.1 illustrates an application considering the localized movement of light colored soil down the slope along the pipe axis resulting in soil mounding and pipe deformation. As illustrated, the model can consider a range of soil movements including a traditional rotational slip and the planar soil movement. By simultaneously considering the soil and pipeline the BMT model can define the relationship between interrelating parameters including pipe-to-wall-thickness ratio, D/t; operating conditions (e.g., operating pressure and temperature); material grade; and, geotechnical loading (e.g., soil displacements and restraint) to peak tensile and compression strains. This, in turn, is used to identify the soil displacement associated with onset of buckling/wrinkling or girth weld fault tensile failure. The results below and others demonstrate that the soil displacement and pipe strain relationship is affected by pipe geometry, soil type and condition (drained, undrained), pipe coating (friction), internal pressure (pipe stiffness), pipe burial depth, slope inclination and the movement scenario.

The information contained herein is the copyright of and proprietary to BMT Fleet Technology Limited. Use of this information is governed by the legend on the cover page of this document."

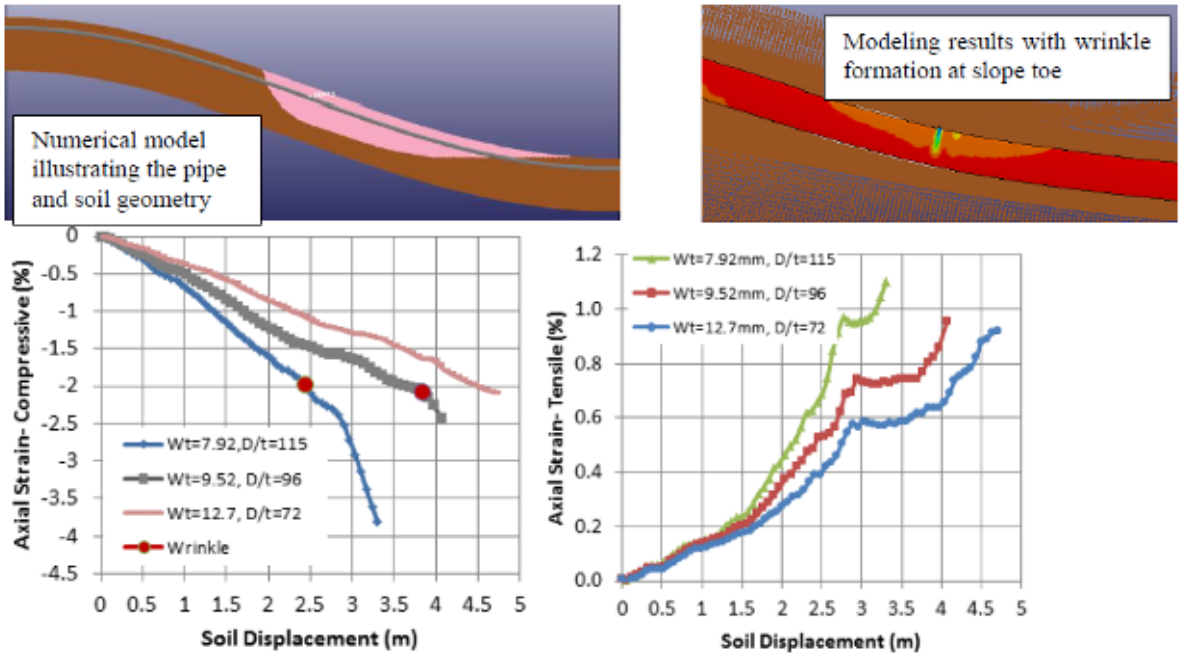

Figure 1.1: Pipe soil interaction Model Application Sample Results

These results, being generated in an ongoing project, relate the geotechnical event, soil, pipe and pipeline operating conditions to tensile and compressive strains produced for soil movements along the axis of the pipe. The BMT pipe-soil interaction model has been used for individual evaluations of soil displacements lateral to the pipe and subsidence, but trends in these behaviors have not been explored. Work by others, using large elements or soil spring representations, have explored lateral soil movements [35] and subsidence [36]; however, their results have been limited by their formulations to uniaxial soil response and small displacements.

1.1 Project Objective

The objective of this project was to use BMT's previously validated pipe soil interaction model to develop an engineering tool to define the effects of operational and geotechnical loads on liquid and gas pipeline systems to support decision making regarding threat severity or repair scheduling. This tool could be incorporated in strain based design and assessment to facilitate the consideration of complex loading scenarios inducing significant flexural loads, including pipeline subsidence and ground movements inducing lateral pipeline movements. The results of this project will define the local nominal strain state that can be used to assess localized anomalies / defects (e.g., corrosion, cracks, dents, weld faults, gouges, etc.) or the potential for the formation of a wrinkle or buckle.

This project will support the development of pipeline standards and best practice guides by helping them take a step forward in rapid assessment of the combination of geotechnical and operational loads for a range of pipe materials and geometries. Previous work related to geotechnical design has focused primarily on qualitative issues and assessments [37, 38], while this approach will permit geotechnical hazard assessment to be unified with existing anomaly assessments employed across the pipeline industry. The results generated will support pipeline integrity and thus prevent environmental damage that can be associated with pipeline failures.

The information contained herein is the copyright of and proprietary to BMT Fleet Technology Limited. Use of this information is governed by the legend on the cover page of this document."

2 MODEL & VALIDATION

2.1 Task 2: Scope of Work

The task objective, approach and results were outlined in the project proposal, and are repeated here for reference.

The objective of this task was to document the existing model validation to assure confidence in the simulation tool. To this end, finite element based modeling techniques and tools, previously developed at BMT were to be documented, including descriptions of the validations completed. The validation cases to be presented were to include comparison with full-scale lab trials for pipe loading in the axial and transverse directions. The validations consider the effects of pipe geometry, coating type, soil type, moisture and compaction and loading direction relative to the pipe, amongst other factors in the prediction of pipe displacements, loads and strains. Further, comparative analysis results illustrating the ability of the model to simulate observed pipeline responses to ground movements were to be presented. This task was to draw from previously completed work to provide the Client with access to the details of the tools that will be used in this project and their ability to simulate reality. No new validation work was planned. This task was to focus on assembling and documenting the BMT work previously completed.

The expected result of this task was the production of a model validation report describing the numerical model that will support this project and its capabilities as a simulation tool. This report represents the task deliverable.

2.2 Finite Element Model Description

2.2.1 Introduction

Soil-pipe interaction numerical simulation requires large deformation analysis capability; this requirement is difficult to meet for Lagrangian-based codes. LS-DYNA [1] offers the possibility to use continuum Multi-material Arbitrary Lagrangian Eulerian (MM-ALE) finite element model and continuum Smooth Particle Hydrodynamic (SPH) capabilities for modeling materials that undergo large deformations.

In this study, the soil-pipe interaction under soil movement is investigated with particular attention to both the soil constitutive model and the use of the LS-DYNA MM-ALE and SPH modeling technique. The results are compared with published experimental data of large-scale tests to verify the numerical analysis method adopted.

2.2.2 Continuum Multi-Material ALE Model

LS-DYNA 971[1] explicit, was used to produce a 3D Continuum model using the MM-ALE method. The MM-ALE formulation is an improved formulation of the basic ALE technique, which allows multiple materials to exist within each solid element and permits the material flow from one element to another. The Eulerian method first performs a purely Lagrangian step avection that must occur between adjacent elements to restore the mesh to its initial Eulerian configuration. The Lagrangian coupling allows structural elements to be placed within the Eulerian mesh. Interaction between the Eulerian elements (i.e. fluid, soil) and structural elements

The information contained herein is the copyright of and proprietary to BMT Fleet Technology Limited. Use of this information is governed by the legend on the cover page of this document."

Lagrangian (i.e. pipe) is handled via constraint formulation referred to as "Constrained Lagrange in Solid", Souli, et al.,[2].

2.2.3 Continuum SPH Mode

LS-DYNA 971[1] explicit, was used to produce a 3D continuum model using the SPH method. The SPH method utilizes a meshless Lagrangian method to represent soils. The method does not require element meshing (mesh-less) and can handle extreme material distortion. In the SPH method, the soil material is treated as particles that have their masses smoothed in space. The coupling between the SPH grid points (soil) and the pipe is accomplished through a normal Lagrangian contact definition.

2.2.4 Soil Material

Soil materials have pronounced non-linear behavior and correct numerical simulation requires sophisticated constitutive models. In this study, a soil and foam constitutive model was used.

2.2.4.1 Soil and Foam Model

One of the classical geomaterial models is that attributed to Drucker and Prager (1952) and has the stress invariant for:

$$\sqrt{J_2} = \alpha J_1 + k = 3\alpha P + k$$

in which α and k are material constants related to friction and cohesion of the material, respectively. J_1 is the first invariant (J_1 = 3P) and for triaxial loading, i.e. $\sigma_3 = \sigma_2$ and all shear stresses are zero, then the second invariant of the deviatoric stress tensor is defined as:

$$J_2^{'} = \frac{1}{6}\left[(\sigma_{11} - \sigma_{22})^2 + (\sigma_{22} - \sigma_{33})^2 + (\sigma_{33} - \sigma_{11})^2\right] + \sigma_{23}^2 + \sigma_{31}^2 + \sigma_{12}^2$$
$$= \frac{1}{3}(\sigma_1 - \sigma_3)^2$$
$$\sqrt{3J_2^{'}} = (\sigma_1 - \sigma_3) = SD$$

Where SD is the stress difference, σ_1 is the axial stress, σ_3 the lateral stress and $\sigma_{i,j}$ are the shear stresses.

The Soil and Foam Model is the most basic of the geomaterial models available in LS-DYNA. It is also the oldest and therefore, has had a considerable amount of user experience and feedback, and is thus quite robust (Schewer, 2002-[3]). The shear failure criterion for the soil and foam model has a mean stress (pressure) dependent strength, typical of geomaterials, in the form:

$$J_2 = a_0 + a_1 P + a_2 P^2$$

The information contained herein is the copyright of and proprietary to BMT Fleet Technology Limited. Use of this information is governed by the legend on the cover page of this document."

where P is the mean stress and coefficients a_0, a_1 and a_2 are determined by calibrating (fitting) the model to tri-axial compression data. The relative values of the coefficients a_0, a_1 and a_2 determine the shape of the shear failure envelope, elliptical for a_2 less than zero, parabolic for a_2 equal to zero, and hyperbolic for a_2 greater than zero.

The Soil and Foam Model will be identical to the Drucker-Prager Model with the following parameters:

$$a_2 = 9\alpha^2$$
$$a_1 = 6\alpha k$$
$$a_0 = k^2$$

The Soil and Foam Model requires the volumetric strains to be presented in the form of a natural log of the relative volume, as in Figure 2.1, which is negative in compression. The other input parameters required for the Soil and Foam Model are:

- Elastic Shear Modulus (G);
- Bulk Unloading Modulus (K); and
- Pressure Cutoff for Tensile Failure-specify a minimum (negative) value for the mean stress for which values more negative (more tensile) indicate the material has failed in tension; all the stress components are set to zero.

In the Soil and Foam Model, the volumetric strain must be input in the form of the natural log of the relative volumetric strain. Since the laboratory data is reported as volumetric strain, the user must convert the volumetric strain data to the requested natural log format. Figure 2.1 illustrates the pressure versus volumetric strain relationship used in the model and the laboratory hydrostatic data.

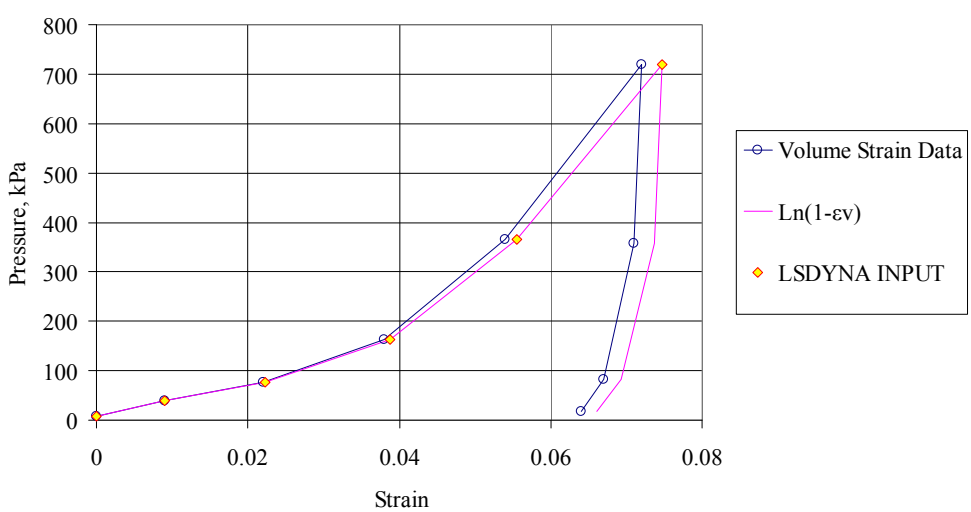

Figure 2.1: Pressure vs. Volumetric Strain

The information contained herein is the copyright of and proprietary to BMT Fleet Technology Limited. Use of this information is governed by the legend on the cover page of this document."

2.3 Validation of the SPH Model

2.3.1 Introduction

The objective of this section is to demonstrate that the response of the pipeline subjected to abrupt ground deformation (surface faulting, lateral spreading, slope failure or landslide) can be simulated using SPH techniques within the non-linear explicit code, LS-DYNA [1]. The soil-pipe interaction models are validated and calibrated based on available published full-scale experimental data including pipeline subjected to:

1. Axial ground movement
2. Abrupt ground deformations similar to surface faulting
3. Lateral ground movement

2.3.2 Finite Element Model Validation – Pipeline Subjected to Axial Ground Movement

2.3.2.1 Finite Element Analysis of Experimental Axial Pullout of Pipe Buried in Dry Sand

Karimian et al. (2009-[4]) performed large-scale tank experiments to investigate pipeline behaviors when subjected to axial soil movements. The test program consisted of four axial tests; the pipe loading tests were performed in a large soil chamber of 3.8 to 5.0 m (length) x 2.50 m (width) x 2.5 m (height) at the University of British Columbia. A perspective view of the soil chamber (box) used for the axial pullout is shown in Figure 2.2. The length of the pipeline test specimen was longer than the length of the box so that the pipe extended through both ends of the chamber walls. This ensured a constant soil-pipe test length and also avoided soil disturbance at the back of the soil box during pullout. The soil parameters in Table 2.1 were derived from tri-axial testing and reported.

The information contained herein is the copyright of and proprietary to BMT Fleet Technology Limited. Use of this information is governed by the legend on the cover page of this document."

Figure 2.2: UBC Experimental Sand Compartment – Karimian et al., 2006

The four axial pipe pullouts were performed as summarized in Table 2.1 and 2.2. Three of the tests (AB-3, AB-4, and AB-6) were performed in dense sand, with an average density of 1600 kg/m^3 and a relative density of 75%, and one test (AB-5) was performed in medium loose sand with an average density of 1430 kg/m^3 and a relative density of 20%.

The UBC pipe (Grade A524) had an outside diameter of 457 mm (18 in) and a wall thickness of 12.7 mm (0.5 in). The pipe was buried at the overburden ratio (H/D) of 2.5 for dense sand and (H/D) of 2.7 for medium loose sand to provide nearly the same vertical effective stress at the pipe level for all tests. The test with dense sand was performed three times; all tests were conducted within 24 hours after filling the box; only one test (AB-6) was performed 45 days after preparation in order to evaluate any effect of aging (compaction) of the soil on pipe response.

In all the test configurations, the pipe was loaded in a displacement-controlled manner. The displacement rate varied between 2 and 50 mm/s (.08 and 2 in). Test results as reported by Karimian et al. (2009 [8]) indicated that the loading rates had no noticeable effect on the results.

Table 2.1: Summary of Axial Pullout Tests (UBC Test)

Test No.	H/D Ratio	Soil Density (Relative Density Dr %)	Time of Axial Loading After Soil Placement	Soil Chamber Length (m)
AB-3	2.5	Dense (Dr=75%)	Within 24 hours	5.0
AB-4	2.5	Dense (Dr=75%)	Within 24 hours	3.8
AB-5	2.7	Loose (Dr= 20%)	Within 24 hours	3.8
AB-6	2.5	Dense (Dr=75%)	45 days after	3.8

The information contained herein is the copyright of and proprietary to BMT Fleet Technology Limited. Use of this information is governed by the legend on the cover page of this document."

Table 2.2: Soil Parameters (UBC Test)

Soil Type	Fraser River Sand
Average Density	1600 kg/m^3 – dense sand "compacted" 1430 kg/m^3 – loose sand
Relative Density	Dr = 75% – dense sand "compacted" Dr = 20% – loose sand
Internal Friction Angle	Peak: 46^0 – 43^0 for σ_3 of 10 to 50 kPa, respectively, for dense sand
Soil-Pipe Friction Angle (shear test)	Dense sand: Peak = 36^0, Constant volume friction = 31^0 Loose sand: Peak = 33^0, Constant volume friction = 31^0

In the absence of soil laboratory test data appropriate for the proposed FE work, a soil and foam model using a two-surface plasticity model with constant shear failure surface and pressure-volume strain (compaction) independence is used. The soil shear parameters were derived from the available critical friction (ϕ_{crit} = 36º for dense sand, ϕ_{crit} = 33º for loose sand) and constant cohesion, c = 0 kPa. More complex material models for soil such as a Cap model were also considered. However, the coefficients and parameters needed for the Cap model could not be determined given the available data.

The FE mesh used for the analysis is shown in Figure 2.3, with the same geometry as the experimental setup. The distance between the bottom boundary and the pipe is the same for both numerical and mesh and the tank experiment. A 3D analysis using LS-DYNA Smooth Particle Hydrodynamic (SPH) technique was performed. The model (Figure 2.3) consists of soil particles and pipe shell elements. The soil mass in the tank is taken to be stress free and have uniform properties in the initial state. The load is imposed in two steps. In the first step, gravitational acceleration is applied; sufficient time is allowed to ensure that the soil stresses reach a stationary state. In the second step, the pipe was pulled in the axial direction by imposing displacement boundary conditions to all nodes of the end of the pipes, hence the pipe is assumed to be rigid. The interaction between the pipeline and the surrounding soil is modeled by Lagrangian contact, in which slip and separation is allowed. The interface friction angle (δ) between the sand and the steel was directly available from direct shear tests conducted by Karimian et al. (2009-[8]). The peak δ values of 33º (tan(δ) = 0.65) and 36º (tan(δ) = 0.73) were obtained for loose and dense sand, respectively, and a large strain value of 31º (tan(δ) = 0.6) was obtained for both loose and dense sands.

The information contained herein is the copyright of and proprietary to BMT Fleet Technology Limited. Use of this information is governed by the legend on the cover page of this document."

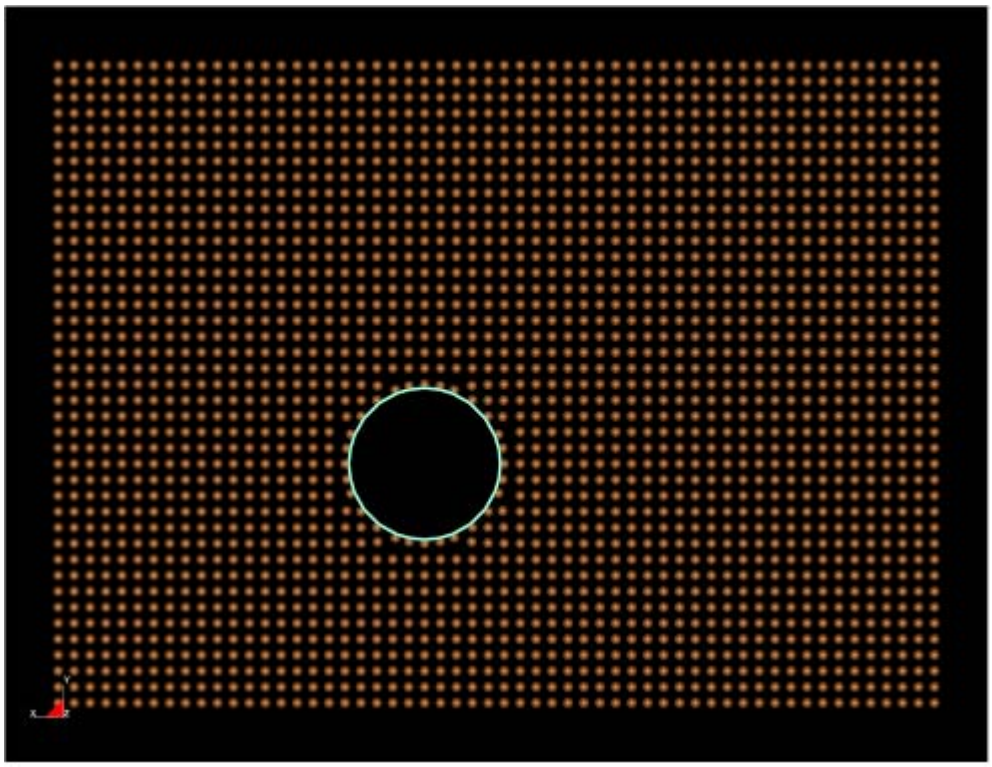

Figure 2.3: Illustration of the FE Model including the Pipe

Figure 2.4 presents a comparison of numerical and experimental force resistance versus displacement responses for tests conducted on dense sand (AB-3 and AB-4). Note that test AB-4 was conducted with pipe length of 3.8 m (12.5 ft), whereas test AB-3 was conducted with pipe length of 5.0 m (16.5 ft), because significant trends were not noted with respect to pipe length by Karimian et al. (2006) [4], the test results of both pipe lengths were grouped together here.

In the experimental force displacement results, the force increased with the axial displacement, a peak resistance load of approximately 26 kN/m was achieved at an axial displacement of 7 to 10 mm (0.3 to 0.4 in). The post-peak load approached a constant value of 20 kN/m after axial displacement of 200 mm (8 in). The results are presented in terms of the force applied to the pipe divided by the length of the pipe in contact with the soil (e.g., force per unit length).

The numerical modeling has a lower initial stiffness than the physical experiment. As a result, the simulated pullout peak load occurs at approximately 25 kN/m for a pipe displacement of 10 mm (0.4 in). The load resistance dropped to 21 kN/m after an axial displacement of 200 mm (8 in). With this said, the LS-DYNA model results appear to provide a quite reasonable simulation of the trial loads and displacements for this application.

Figure 2.5 presents a comparison of numerical and experimental force resistance versus displacement responses for tests conducted on loose sand (AB-5). A peak load of 9.7 kN/m was reached in the experiment after a displacement of 10 mm (0.4 in) and this value dropped to a constant value of 8.5 kN/m after an axial displacement of 150 mm (6 in). The peak and post peak

The information contained herein is the copyright of and proprietary to BMT Fleet Technology Limited. Use of this information is governed by the legend on the cover page of this document."

forces predicted by the numerical model were 8.5 kN/m and 8.1 kN/m, respectively. These results are in good agreement with the measured forces.

As may be noted, both measured and predicted peak loads for the loose sand test are less than half of the peak load for dense sand tests.

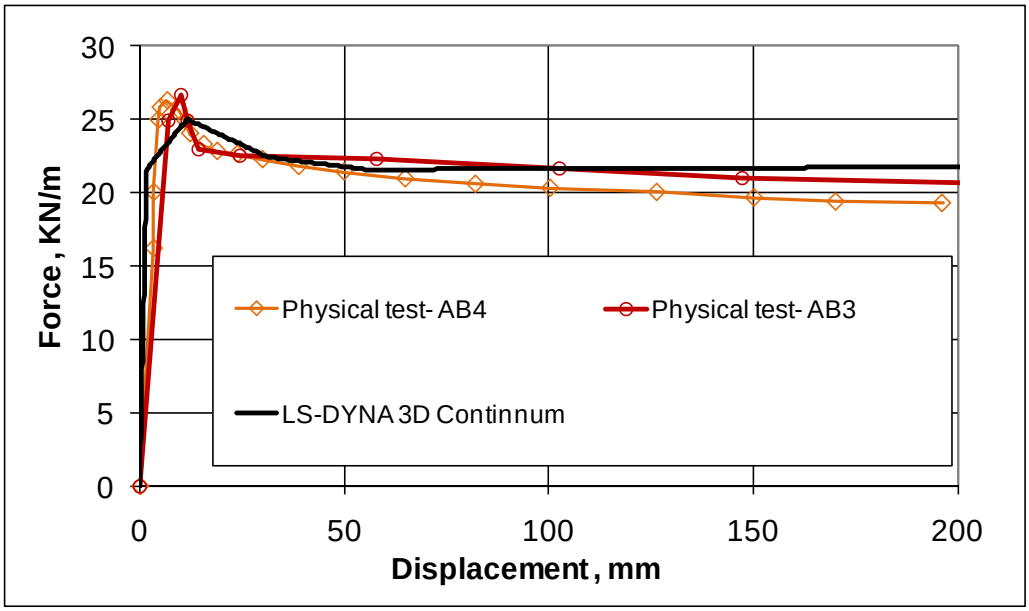

Figure 2.4: Comparison between Numerical Model and Test Results – Dense Sand

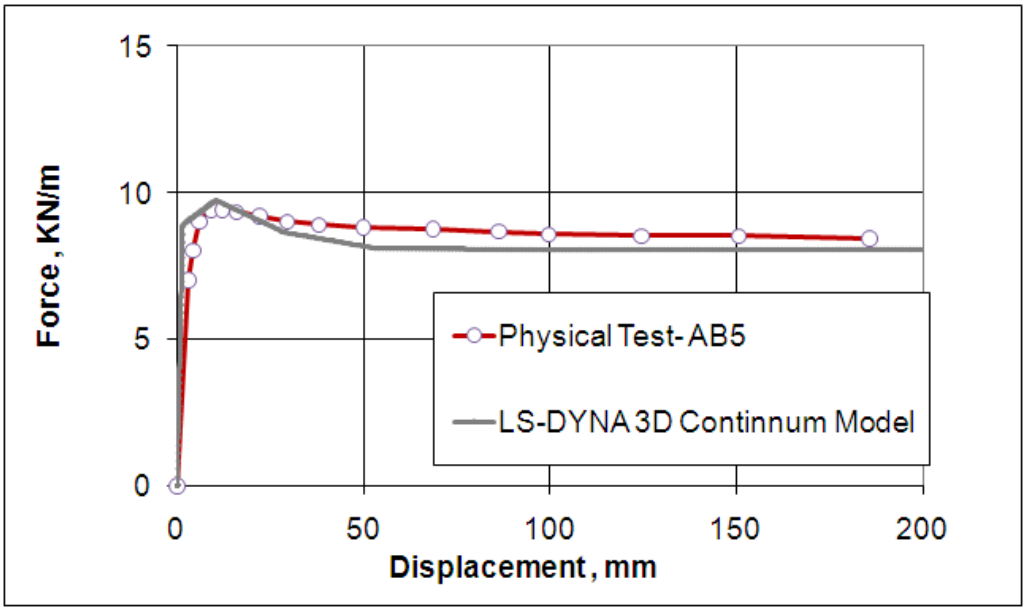

Figure 2.5: Comparison between Numerical Model and Test Results – Loose Sand

The information contained herein is the copyright of and proprietary to BMT Fleet Technology Limited. Use of this information is governed by the legend on the cover page of this document."

2.3.2.2 Finite Element Analysis of Full-Scale Axial Pullout – Field Trial for Pipe Embedded in the Clay Backfill

Scarpelli et al. (1998 & 2003-[5] & [6]) performed in situ full-scale pullout tests to investigate the behaviors of pipeline subjected to axial soil movements. These tests were conducted at two sites with out-of-service pipelines, located in northern and central Italy. The pipes tested were an 8-inch coal tar coated pipe and a 24-inch polyethylene wrapped pipe. A series of four tests were performed as follows:

1. One test performed in the original consolidated backfill (mostly silty clay), not distributed since the pipeline's construction more than 20 years prior to the test.

2. One test performed with the same soil excavated and loosely backfilled without compaction.

3. One test performed with the soil around the pipe replaced by artificial granulate (frictional material with low specific weight) for about 30-50 cm (11.8-19.7 in) above the pipe, then covered with excavated soil.

4. One test performed in granular backfill material (gravelly soil) for about 50 cm (19.7 in) around the pipe and covered by the original soil up to ground level.

The four axial pullouts performed for the 24-inch polyethylene wrapped pipe are summarized in Table 2.3. In all of the test configurations, the pipes were loaded in a displacement-controlled manner.

Table 2.3: Summary of Axial Pullout Tests 24-inch Polyethylene Wrapped Pipe

Test No.	Pipe Length (m)	Axis Depth (m)	Pipe Length (m)	Coating Thickness
G1	Gravelly soil	2.05	18.2	1 mm PE
G2	Undisturbed natural soil fill	1.95	19.6	1 mm PE
G3	Loosely backfill natural soil	1.95	19.6	1 mm PE
G4	Artificial granulate around the pipe and loosely backfilled silt and clay above	1.95	19.6	1 mm PE

In the absence of soil laboratory test data appropriate for the proposed FE work, a soil and foam model using a two-surface plasticity model with constant shear failure surface and pressure-volume strain (compaction) independence is used. The soil shear parameters were derived from the available critical friction ϕ_{crit} = 30º and the average undrained shear strength cu = 38 kPa.

Key soil parameters are presented in Table 2.4.

The information contained herein is the copyright of and proprietary to BMT Fleet Technology Limited. Use of this information is governed by the legend on the cover page of this document."

Table 2.4: Natural Soil Parameters

Soil Type	Natural Soil Fill
Unit Weight	19.4 kN/m^3
Undrained Strength	35 - 40 kPa
Internal Friction Angle	30^0 - 36^0
Soil-Pipe (polyethylene) Friction Coefficient (shear box test)	Peak: tanδ = 0.312 Ultimate: tanδ = 0.2383 Average: tanδ = 0.275

A 3D analysis using LS-DYNA Smooth Particle Hydrodynamic (SPH) technique was performed. The modeling only simulated the G2 test conducted for the 24-inch polyethylene wrapped pipe embedded in the natural soil (undisturbed clay). The FE mesh used for the analysis is shown in Figure 2.6; the model (Figure 2.6) consists of soil particles and pipe shell elements. The soil mass in the tank is taken to be stress free and have uniform properties in the initial state. The load is imposed in two steps. In the first step, gravitational acceleration is applied; sufficient time is allowed to ensure that the soil stresses reach a stationary state. In the second step, the pipe was pulled in the axial direction by imposing displacement boundary conditions to all nodes at the end of the pipes, hence the pipe is assumed to be rigid. The interaction between the pipeline and the surrounding soil is modeled by Lagrangian contact, in which slip and separation is allowed. The interface friction angle (δ) between natural clay soil and the polyethylene coating was directly available from direct shear tests conducted by Scarpelli et al. (2003) [6]. A peak δ value of 18º (tan(δ) = 0.312) and a large strain value of 13.4º (tan(δ) = 0.238).

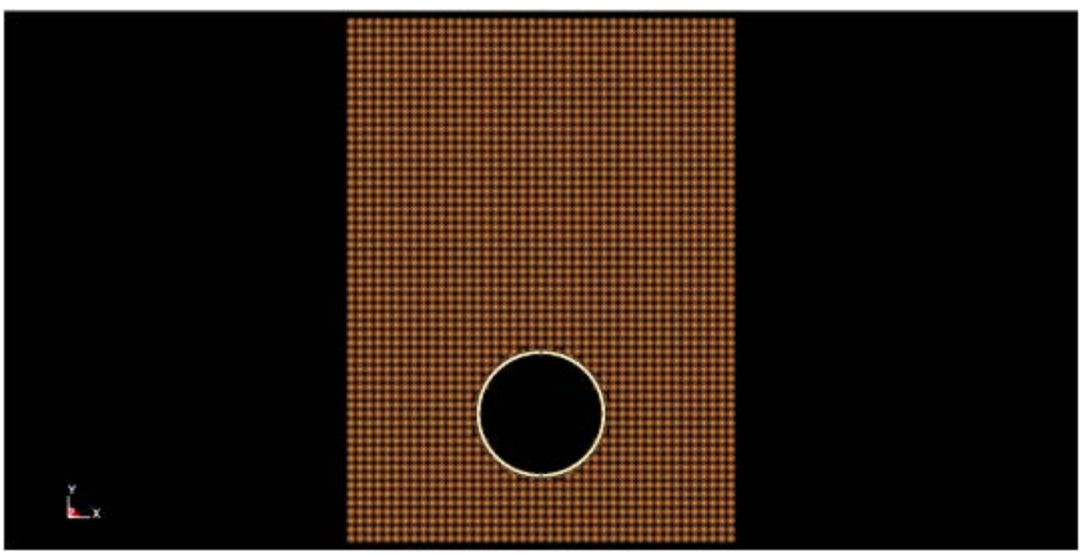

Figure 2.6: Illustration of the FE Model including the Pipe

Figure 2.7 presents a comparison of numerical and experimental force resistance versus displacement response for tests conducted on natural clayed soil (NCS). A peak load of 30.2 kN/m was reached in the experiment after a displacement of 3.6 mm (0.1 in) and this value drops to a constant value of 18 kN/m after the axial displacement of 100 mm (4 in). The peak and post

The information contained herein is the copyright of and proprietary to BMT Fleet Technology Limited. Use of this information is governed by the legend on the cover page of this document."

peak forces predicted by the numerical model were 31kN/m and 21 kN/m, respectively. These results are in good agreement with the measured forces.

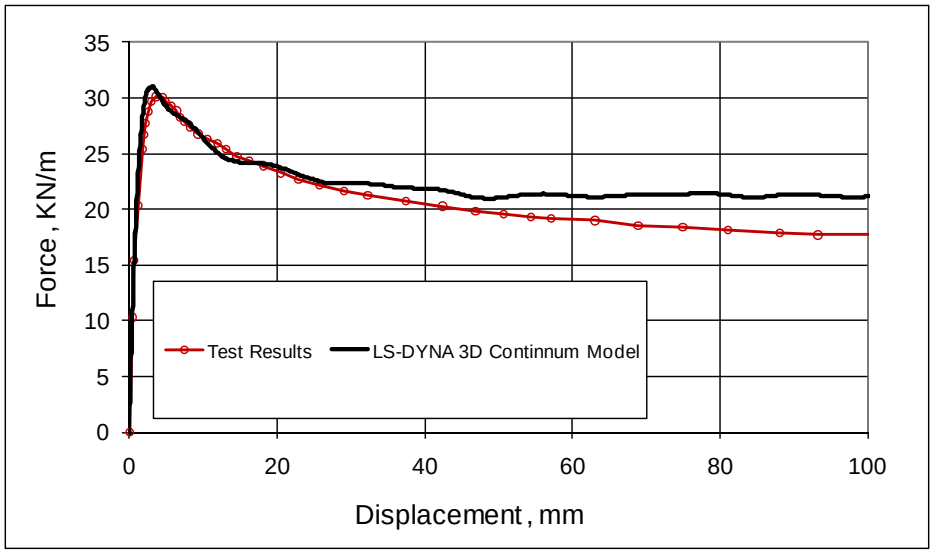

Figure 2.7: Comparison between Numerical Model and Test Results – Undisturbed Soil Fill

2.4 Finite Element Model Validation – Pipeline Subjected to Surface Faulting

2.4.1 Finite Element Analysis of Experimental Split-Box Tests – Buried HDPE Pipeline

2.4.1.1 Large Scale Experimental Model

Large full-scale permanent ground deformations (PGD) on high density polyethylene (HDPE) pipes were conducted by Cornell University; O'Rourke, 2008 [7]. Their results are used here to examine the capability of the current FE analysis. The pipe loading tests were performed in two movable basins of 6.6 m (21.65 ft) long by 3.2 m (10.5 ft) wide by 2.3 m (7.5 ft) deep. The experimental basin of a total of 90 metric tons of partially saturated sand was displaced 1.22 relative to each other at a crossing angle of 65º as illustrated in Figure 2.8. The pipe had an outside diameter of 407 mm (16 inch) and a wall thickness of 24 mm. The pipeline was installed at a 0.9-m depth to the top of the pipe. The soil is partially saturated sand with 4% water content, a dry unit weight of 15.5 KN/m^3 and an average friction angle of 39 to 40 degrees. The value of the friction angle is reported in terms of total stress because suction in moist sand (effective stress conditions) is not measured directly. The purpose of the tests was to investigate the performance of highly ductile pipelines subjected to abrupt ground deformations similar to surface faulting; O'Rourke[7].

2.4.1.2 Finite Element Model

An example of the FE mesh used for the analysis is shown in Figure 2.9 with the geometry exactly similar to the experimental setup (Figure 2.8). The distance between the bottom boundary and the pipe is the same for both numerical and mesh and the tank experiment. A 3D analysis using LS-DYNA SPH technique was performed to simulate the laboratory setup.

The information contained herein is the copyright of and proprietary to BMT Fleet Technology Limited. Use of this information is governed by the legend on the cover page of this document."

The finite element model consists of soil and pipe shell elements (Figure 2.9). The soil material is treated as particles that have their masses smoothed in space. The pipe is modeled using Belyschko-Tasy shell elements. The soil mass in the tank is taken to be stress free and has uniform properties in the initial state. The load is imposed in two steps. In the first step, gravitational acceleration is applied and sufficient time is allowed to ensure that the soil stress reaches a stationary state. In the second step, the mobile soil box movement is applied. The interaction between the pipe and the surrounding soil is modeled by contact in which slip and separation are allowed. The interface friction between the pipe and soil ϕ_μ is assumed equal to 0.6ϕ ($\mu = \tan(0.6\phi)$).

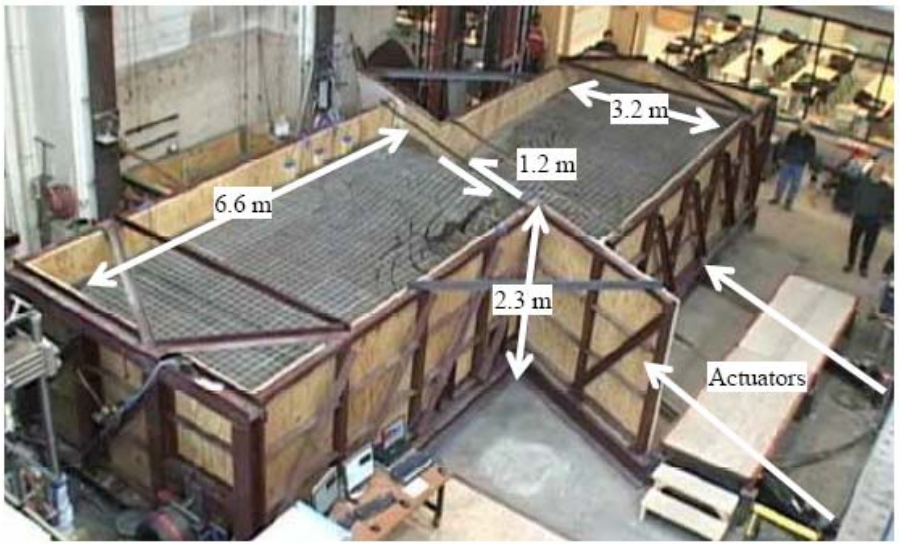

Figure 2.8: Large-Scale Split-Box Test Basin at Cornell University NEES Equipment Site (O'Rourke et al., 2007)

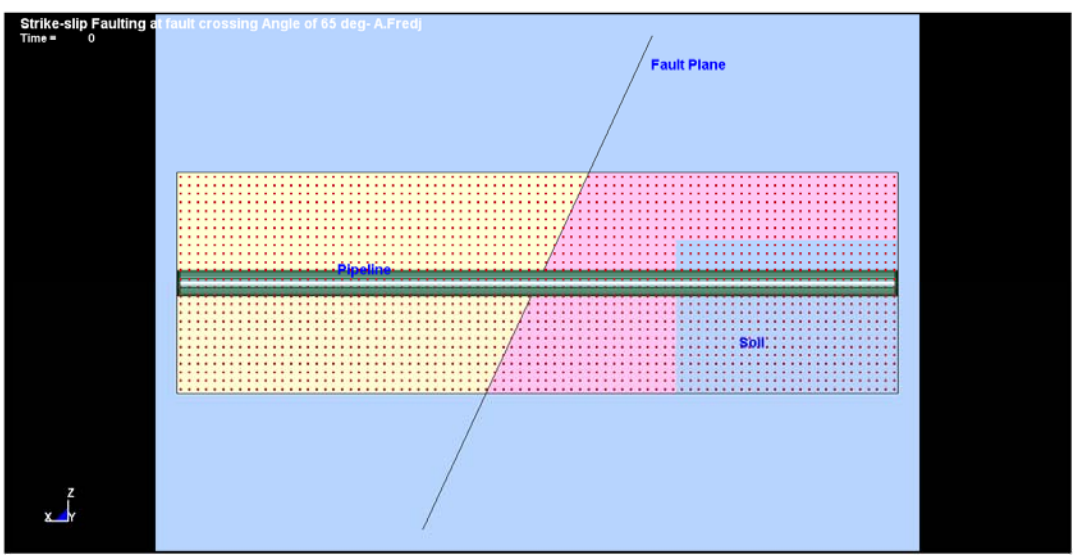

Figure 2.9: Illustration of the FE Model Including the Pipe

The information contained herein is the copyright of and proprietary to BMT Fleet Technology Limited. Use of this information is governed by the legend on the cover page of this document."

2.4.1.3 Analytical and Experimental Results

Figure 2.8 and Figure 2.10 show an overhead view of the test compartment; O'Rourke et al., [7]. Typical graphical output from the model is illustrated in Figure 2.11. The figure illustrates the response of pipeline subjected to ground movement similar to the laboratory shear box test. Figure 2.12 compares the deformed pipeline shape of the finite element model and the full-scale experimental pipe. Comparison between the numerical prediction and the full-scale test results showed that the SPH model was able to closely predict the pipe deformation.

Figure 2.10: Illustration of the FE Model including the Pipe

The information contained herein is the copyright of and proprietary to BMT Fleet Technology Limited. Use of this information is governed by the legend on the cover page of this document."

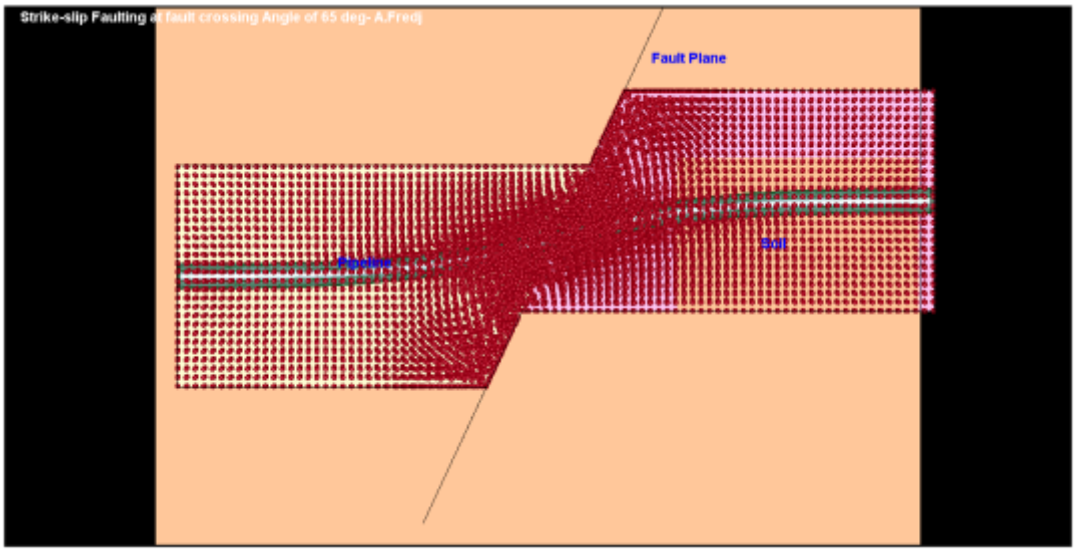

Figure 2.11: Deformed Pipe in Soil – FE Results

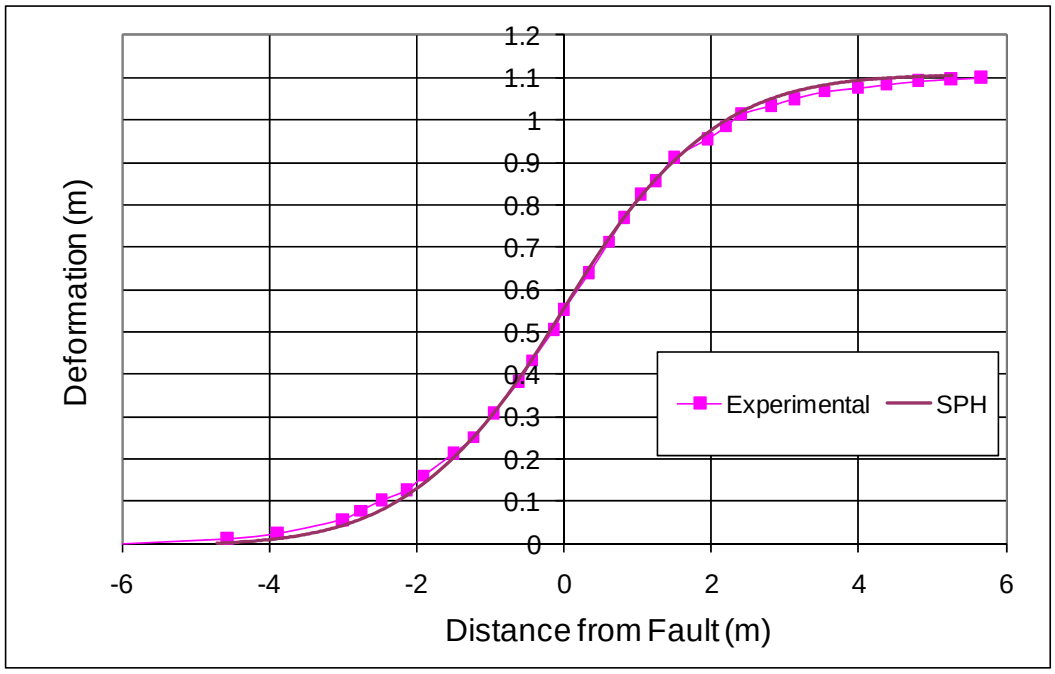

Figure 2.12: Pipe Deformation: Comparison between Numerical Model and Test Results

2.5 Finite Element Model Validation – Pipeline Subjected to Lateral Movement

2.5.1 Large-Scale Experimental Model

Karimian et al. (2006), [4] performed large-scale tank experiments to investigate pipe behaviors when subjected to lateral soil movements. Their results are used here to examine the capability of the current FE analysis. The pipe loading tests were performed in a large sand chamber of 2.50 m (8.2 ft) x 3.8 m (12.5 ft) x 2.5 m (8.2 ft) at the University of British Columbia. Figure 2.13 shows the experimental setup. The UBC pipe had an outside diameter of 457 mm (18 in) and a wall

The information contained herein is the copyright of and proprietary to BMT Fleet Technology Limited. Use of this information is governed by the legend on the cover page of this document."

thickness of 13.0 mm (0.5 in). The pipe was buried at the overburden ratio (H/D) of 1.92. The test was performed twice. The soil parameters in Table 2.5 were derived from tri-axial testing and reported.

Table 2.5: Soil Parameters (UBC Test)

Parameter	Units	Value
Internal Friction Angle	Deg.	45.5 to 43.3
Constant Volume Friction ϕ_{crit}	Deg.	32 to 34
Interface Friction	Deg.	36 to 30.5
Shear Modulus	MPa	3 to 12

In the absence of soil laboratory test data appropriate for the proposed FE work, a soil and foam model using a two-surface plasticity model with a constant shear failure surface and pressure-volume strain (compaction) independence is used. The soil shear parameters were derived from the available critical friction (ϕ_{crit} = 32º) and constant cohesion, c=0 kPa. More complex material models for soil such as a Cap model were also considered. However, the coefficients and parameters needed for the Cap model could not be determined given the available data.

2.5.2 Finite Element Model

The FE mesh used for the analysis is shown in Figure 2.14, with the same geometry as the experimental setup. The distance between the bottom boundary and the pipe is the same for both numerical and mesh and the tank experiment. A 3D analysis using LS-DYNA SPH technique was performed. The soil mass in the tank is taken to be stress free and have uniform properties in the initial state. The load is imposed in two steps. In the first step, gravitational acceleration is applied; sufficient time is allowed to ensure that the soil stresses reach a stationary state. In the second step, the pipe was pulled in the lateral direction by imposing displacement boundary conditions to all nodes of the pipes, hence the pipe is assumed to be rigid. The interaction between the pipe and the surrounding soil is modeled by constraint Lagarangian contact, in which slip and separation are allowed.

The information contained herein is the copyright of and proprietary to BMT Fleet Technology Limited. Use of this information is governed by the legend on the cover page of this document."

Figure 2.13: UBC Experimental Sand Compartment – Karimian et al., 2006 [4]

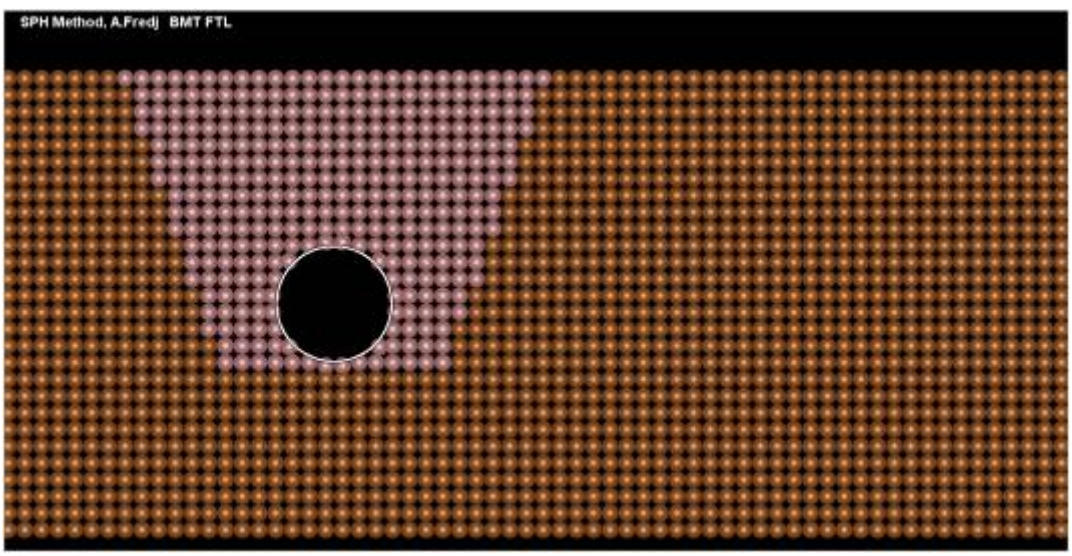

Figure 2.14: Illustration of the FE Model including the Pipe

2.5.3 Analytical and Experimental Results

Typical graphical output from the SPH model is illustrated in Figure 2.15, Figure 2.16 and Figure 2.17. Figure 2.15 and Figure 2.16 illustrate the simulated displaced position of the pipe and the soil. The figures include soil particle velocity vectors describing the trajectory and

The information contained herein is the copyright of and proprietary to BMT Fleet Technology Limited. Use of this information is governed by the legend on the cover page of this document."

relative speed of movement of soil particles. Qualitatively, the displaced soil profile and flow history make intuitive sense and match the observed behaviors.

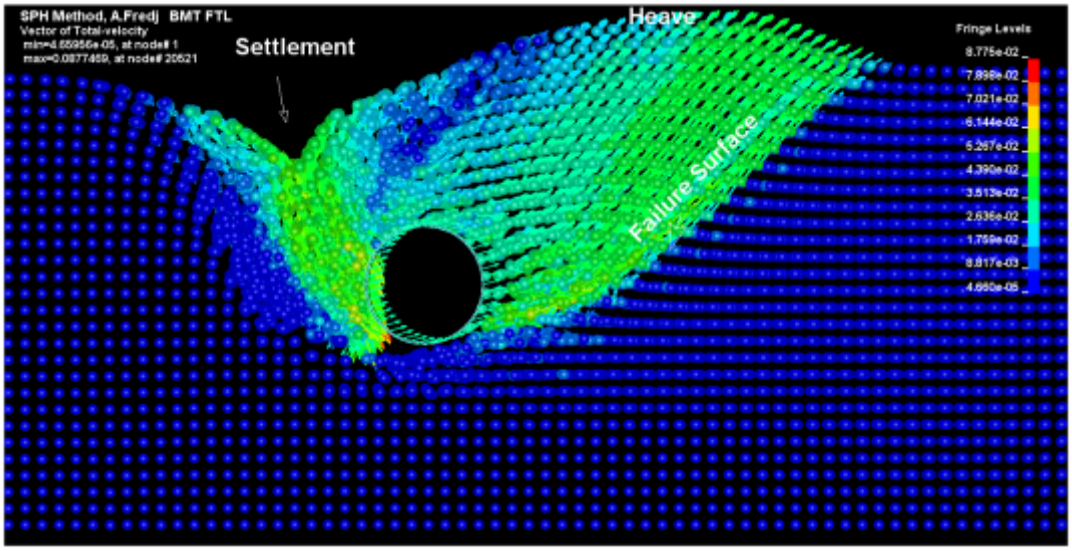

Figure 2.15: SPH-FEM Simulation – Vector Velocity

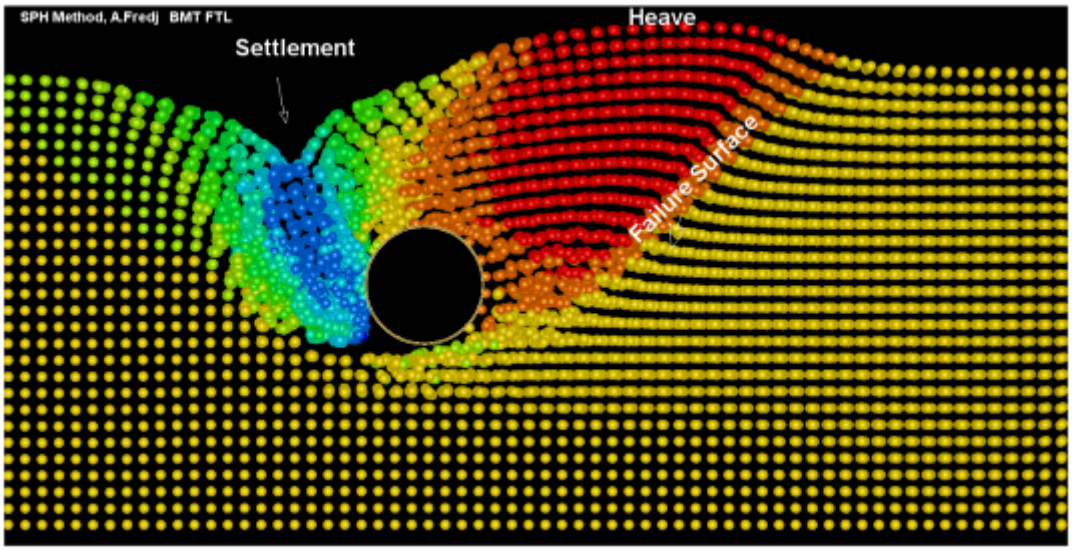

Figure 2.16: SPH-FEM Simulation – Vertical Displacement

Figure 2.17 shows the shear strains with rupture or slip surface through soil in the front of the pipe and the tensile failure zone above the pipe modeled using the SPH method. The slip and tensile failure modes were better explained by the SPH model.

The information contained herein is the copyright of and proprietary to BMT Fleet Technology Limited. Use of this information is governed by the legend on the cover page of this document."

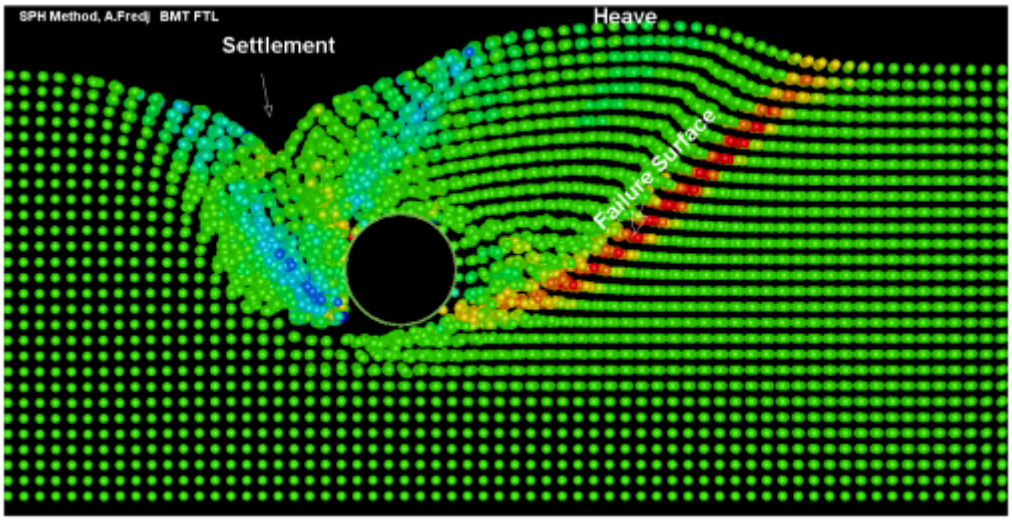

Figure 2.17: SPH-FEM Simulation – Shear Failure Surface

Figure 2.18 presents the comparison of experimental and numerical force-displacement curves. For lateral pipe movement, at H/D of 1.92, the results match the experimental data well. For both experimental and numerical force displacement using ALE and SPH methods, the failure load is about 50 kN/m obtained at the pipe displacement of 75 mm.

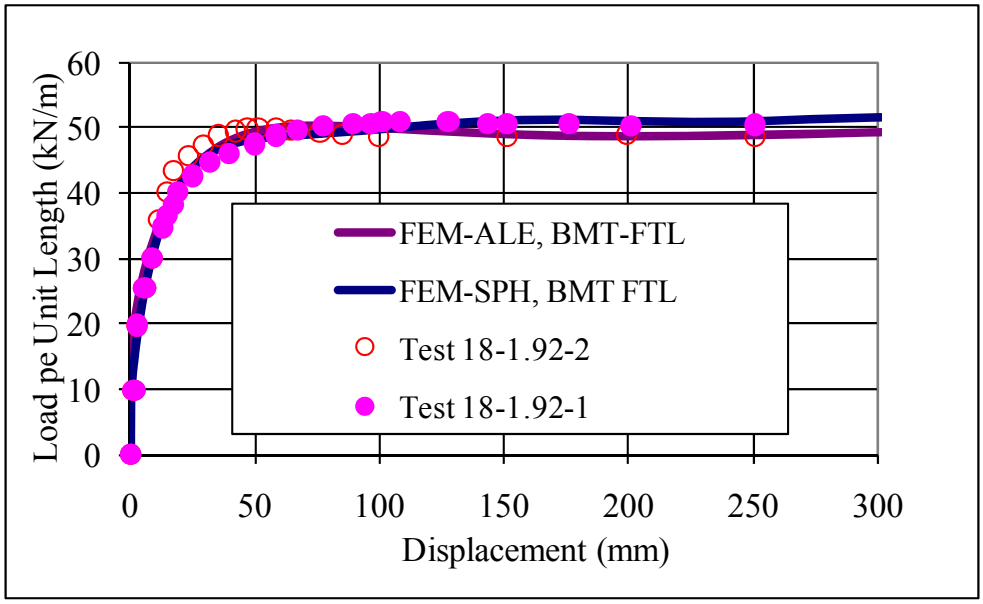

Figure 2.18: Comparison between Numerical Model and Test Results

The information contained herein is the copyright of and proprietary to BMT Fleet Technology Limited. Use of this information is governed by the legend on the cover page of this document."

2.6 Validation of the Multi-Material-ALE Model

2.6.1 Introduction

The objective of this section is to demonstrate that the response of the pipeline subjected to abrupt ground deformation (surface faulting, lateral spreading, slope failure or landslide) can be simulated using MM-ALE techniques within the non-linear explicit code, LS-DYNA [1]. The soil-pipe interaction models are validated and calibrated based on available published full-scale experimental data, including pipeline subjected to:

1. Lateral ground movement; and
2. Abrupt ground deformations similar to slope failure or landslide.

2.7 Finite Element Model Validation – Pipeline Subjected to Lateral Ground Movement

2.7.1 Finite Element Analysis of Experimental Tank Test – Flexible Pipe

2.7.1.1 Large-Scale Experimental Model

Large full-scale lateral pullout tests on steel pipe were conducted by C-CORE 1999 [9], Paulin et al. (1998) [10]; and Popescu et al. (2002 & 2003[11], [12] for the Geological Survey of Canada (GSC). Their results are used here to examine the capability of the current FE analysis. The pipe loading tests were performed in a test compartment of 2.950 m (10 ft) (W) x 6.170 m (20 ft) (L) x1.3 m (4.3 ft) (H). Figure 2.19 and Figure 2.20 show the experimental setup profile and plan views. The GSC pipe had an outside diameter of 203.2 mm (8 in) and a wall thickness of 3.175 mm (0.125 in) and was made from 1010 steel. The yield strength of the pipe is 260 MPa, and the ultimate strength is about 370 MPa. The measured stress-strain behavior of the pipe steel is presented in Figure 2.21.

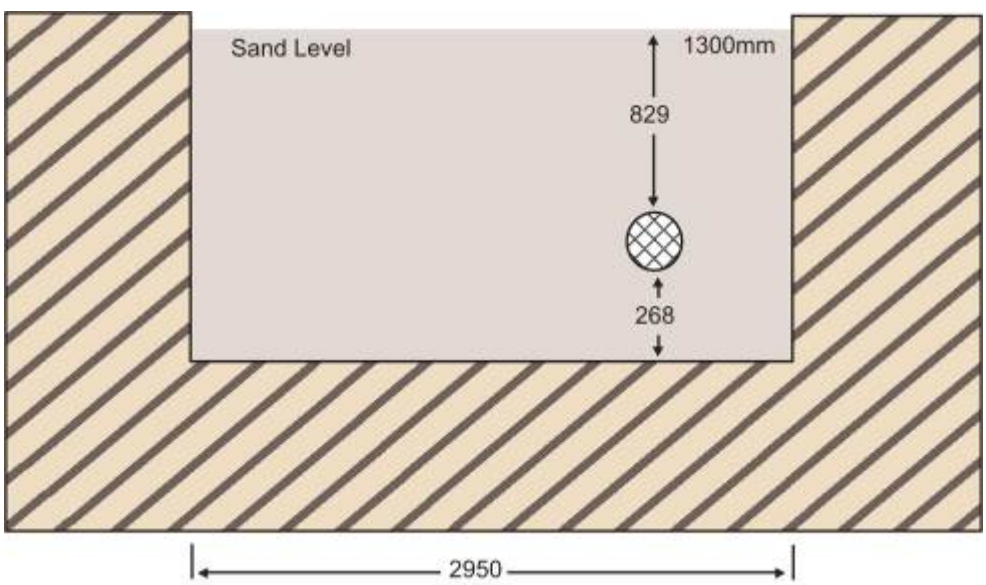

Figure 2.19: Experimental Setup Test (GS01) – Profile View

The information contained herein is the copyright of and proprietary to BMT Fleet Technology Limited. Use of this information is governed by the legend on the cover page of this document."

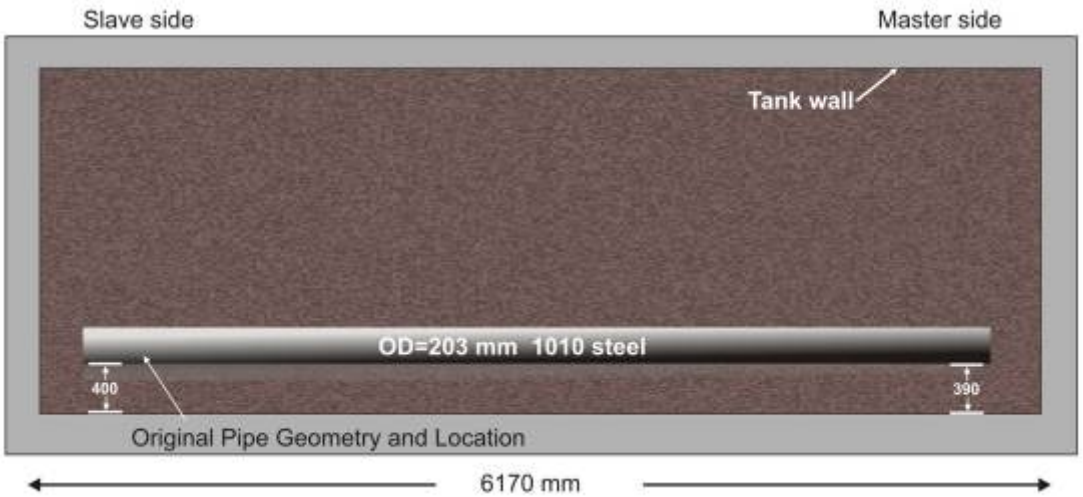

Figure 2.20: Plan View

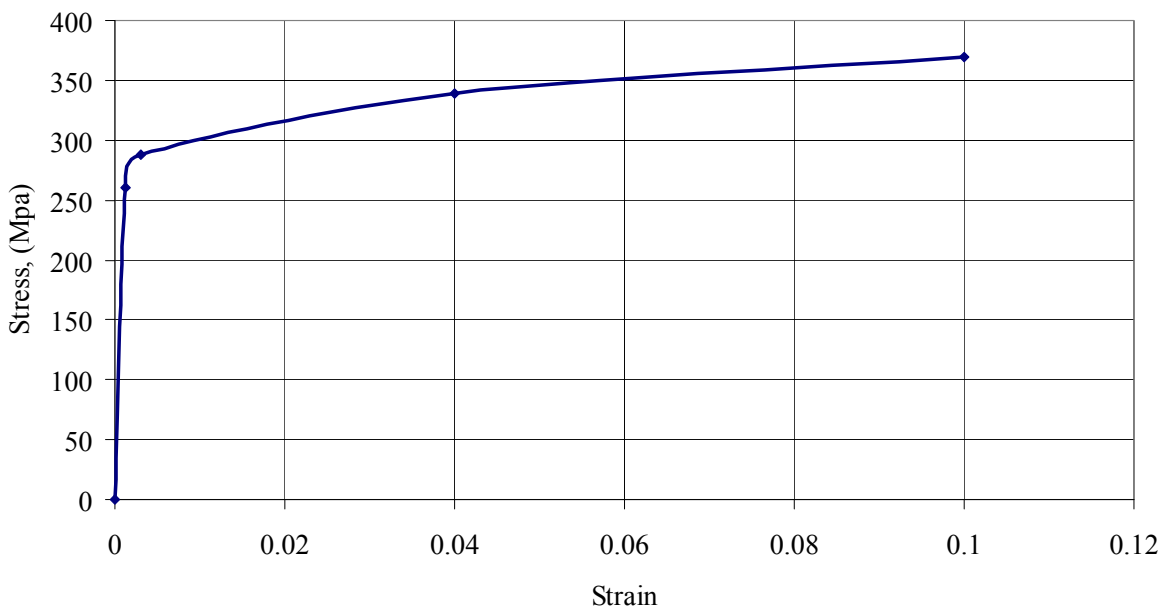

Figure 2.21: Stress-Strain Curve (1010 Steel)

The GSC01 test was carried out using 6 m long pipe buried in dense sand, loaded laterally at its ends, approximately 0.3 m (0.98 ft) from each end. Figure 2.25 shows the observed deformed pipe geometry, which includes localized buckling or plastic hinges. These hinge locations were observed to be located 1.3 m (4.26 ft) from the Master and 1.2 m (3.93 ft) from the Slave ends of the pipe. (The “Master” and “Slave” designations are used to describe the experimental apparatus loading control system and repeated in this report to maintain consistency with the experimental program reporting.)

The information contained herein is the copyright of and proprietary to BMT Fleet Technology Limited. Use of this information is governed by the legend on the cover page of this document."

The soil depth at the pipe spring line was 932 mm (36.69 in). The sand had a unit weight of 17.3 KN/m^3. Due to the large quantity of sand required to fill the tank, three different soil shipments were obtained from local supplier (C-CORE [9] and Paulin et al., 1998[10]). An average friction angle of 53 degrees was reported. As reported in (Popescu et al., 2003[12]), friction angles larger than 44-45 degrees are often not trusted and can be attributed to apparent cohesion and interlocking. Therefore, the friction angle of 44 degrees and equivalent cohesion was used for the soil. In conclusion, the following parameters where used by (C-CORE 1999 [9] and Paulin et al., 1998 [10]).

- Peak friction angle; ϕ_{max} = 44°and $\phi_{residual}$ = 35º
- Constant cohesion; c = 7.5 kPa
- Elastic modulus; 9 to 25 MPa
- Friction coefficient at soil/pipe interface; $\mu = \tan(0.6\phi) = 0.5$
- Soil unit weight; 17.3 KN/m^3

In the absence of soil laboratory test data appropriate for FE work, a Soil and Foam Model was employed using a two-surface plasticity models where the shear failure surface and pressure-volume strain (compaction) surfaces are independent. The shear parameters were derived from the available critical friction (ϕ_{crit} = 35º) and constant cohesion, c = 7.5 kPa. In the absence of laboratory data, the pressure-volumetric strain for similar critical friction angle was used. The elastic parameters are the shear modulus of 25 MPa and Poisson ratio, 0.3. The pressure versus volumetric strain (ε_v) relationship developed for this material, based upon these assumptions, is presented in Figure 2.22.

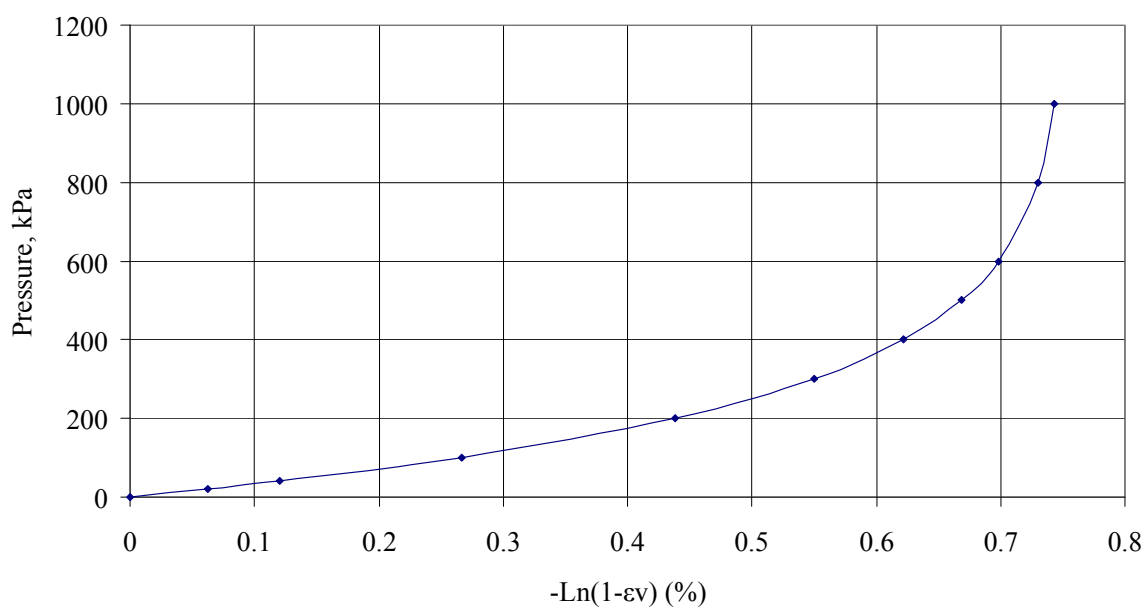

Figure 2.22: Estimated Pressure vs. Volumetric Strain – GSC Trial

The information contained herein is the copyright of and proprietary to BMT Fleet Technology Limited. Use of this information is governed by the legend on the cover page of this document."

More complex material models for the soil, such as a Cap model, were also considered. However, the coefficients and parameters needed for the Cap model could not be determined given the available data.

2.7.1.2 Finite Element Model

An example of the FE mesh used for the analysis is shown in Figure 2.23 with the geometry exactly similar to the experimental setup (Figure 2.19 and Figure 2.20). The distance between the bottom boundary and the pipe is the same for both numerical model and the tank experiment. A 3D analysis using LS-DYNA Multi-Material Eulerian technique was performed to simulate the laboratory experiment.

The finite element model consists of soil and air (Figure 2.23), and the soil is modeled using an 8-node constant stress (one point integration) model formulation. In LS-DYNA, the void elements were used to represent the air, which can accept material from other neighboring elements. The pipe is modeled using Belyschko-Tasy shell elements. The soil mass in the tank is taken to be stress free and have uniform properties in the initial state. The load is imposed in two steps. In the first step, gravitational acceleration is applied and sufficient time is allowed to ensure the soil stress reaches a stationary state. In the second step, the pipe was pulled 0.3 m (1 ft) in the lateral direction by the pipe ends. The interaction between the pipe and the surrounding soil is modeled by constraint Lagarangian contact in which slip and separation are allowed. The interface friction between the pipe and soil ϕ_μ is assumed equal to 0.6ϕ ($\mu = \tan(0.6\phi) = 0.55$).

This parameter is difficult to evaluate (Yimsiri et al., 2004 [13]), as it depends on the interface characteristic and degree of relative movement (slip) between the pipe and soil. In general, the pipe surface friction angle ϕ_μ ranges from about 20º to the friction angle of the soil (Yusima and Kishida, 1981 [14]). The surface friction angle depends on the pipe surface; a large value could be used for rusty or corroded pipe and a lower value for pipe with a smooth coating.

The information contained herein is the copyright of and proprietary to BMT Fleet Technology Limited. Use of this information is governed by the legend on the cover page of this document."

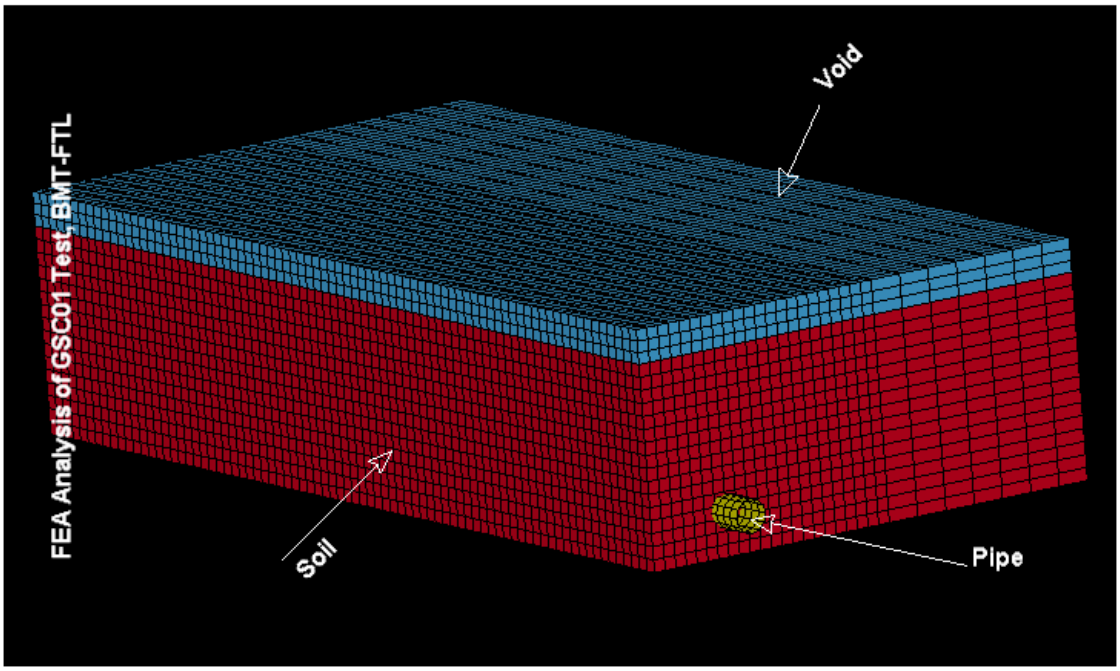

Figure 2.23: Illustration of the Finite Element Model for the GSC Trials Including the Pipe

2.7.2 Analytical and Experimental Results

Figure 2.24 presents a comparison of experimental and numerical force-displacement curves. In the experimental force displacement, a failure load (maximum load) of approximately 101 kN was obtained at a pipe displacement of 30.6 mm (1.20 in). The numerical modeling has a lower initial stiffness than the physical experiment; therefore, the simulated failure load occurs at approximately 105 kN at a predicted pipe end displacement of 80 mm (3.14 in). With this said the LS-DYNA model results appear to provide a quite reasonable simulation of the trial loads and displacements for this application.

The information contained herein is the copyright of and proprietary to BMT Fleet Technology Limited. Use of this information is governed by the legend on the cover page of this document."

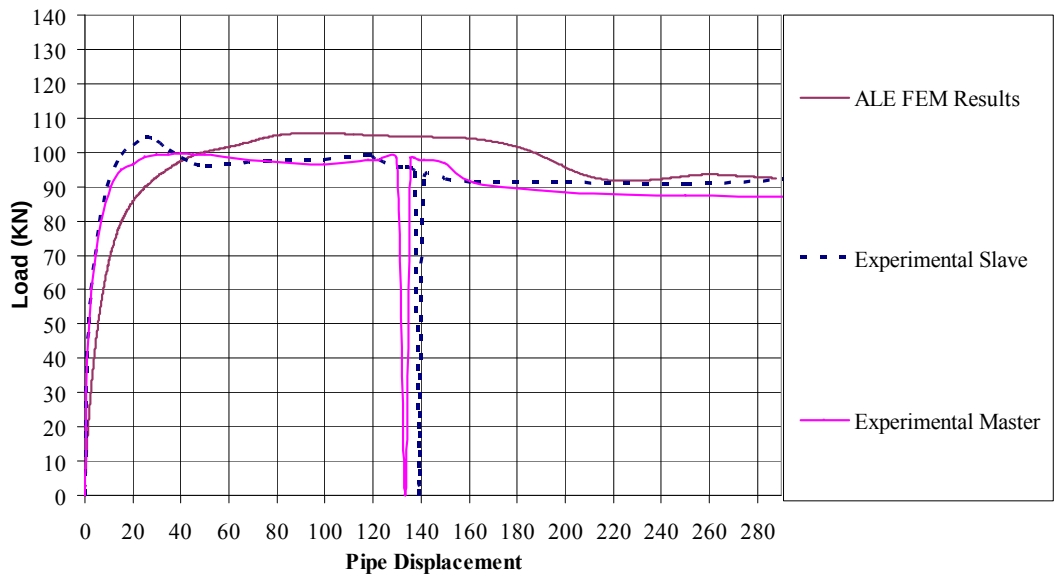

Figure 2.24: Comparison of Experimental and Finite Element GSC Trial Load Displacement Results

Figure 2.25 illustrates the pipe plastic hinges observed in the experimental results. A hinge is observed to form (1.3 m (4.26 ft) from the Master and 1.2 m (3.93 ft) from the Slave end. Figure 2.26 through Figure 2.28 show the finite element model pattern of pipe deformation; the plastic hinge develops about 1 to 1.1 m (3-3.5 ft) from the pipe end. The small difference in results could easily be attributed to minor disagreements between the experimental and numerical pipe or soil properties and the results illustrate the ability of the LS-DYNA model to simulate pipe deformations in the presence of soil restraints.

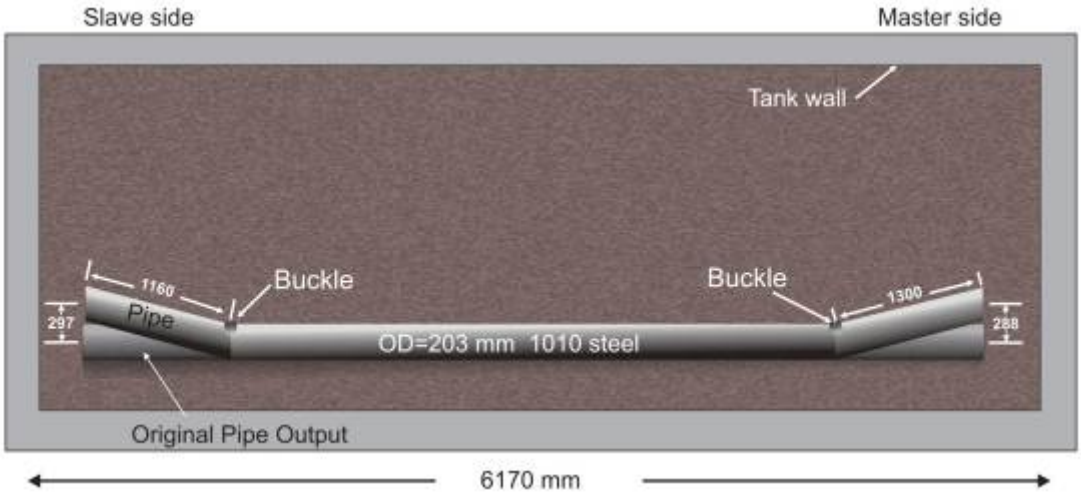

Figure 2.25: Deformed Pipe – Experimental Results

The information contained herein is the copyright of and proprietary to BMT Fleet Technology Limited. Use of this information is governed by the legend on the cover page of this document."

Figure 2.26: Deformed Pipe – Finite Element Result

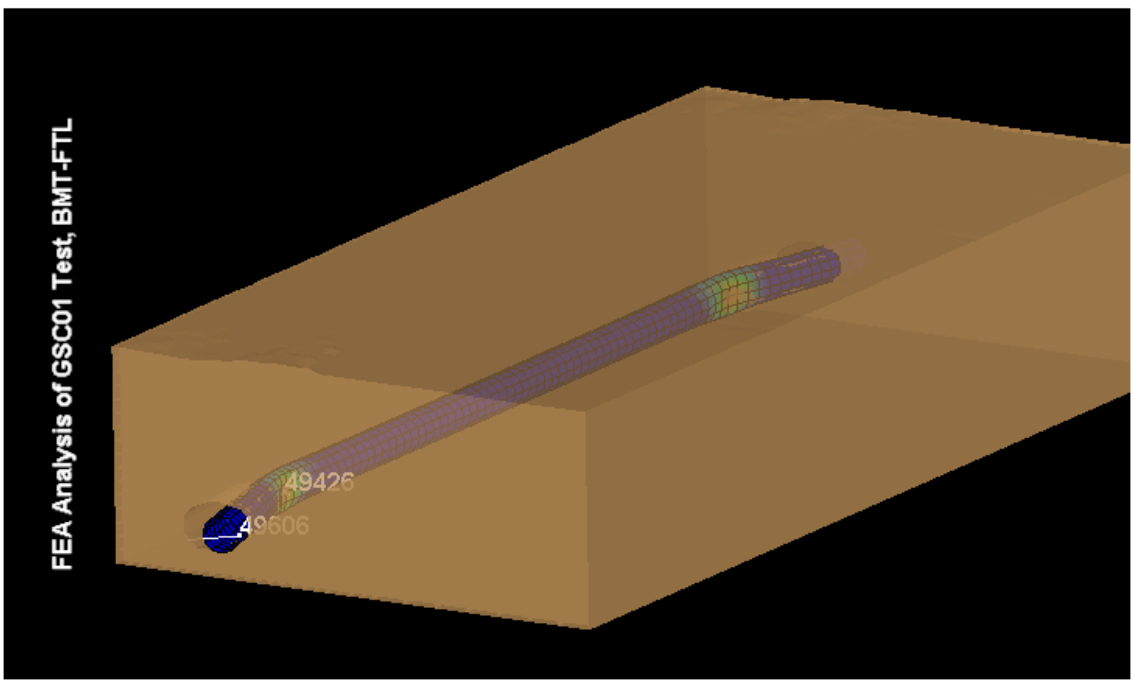

Figure 2.27: Deformed Pipe in Soil – Finite Element Results

Figure 2.27 and Figure 2.28 provide illustrations of the simulated pipe and soil displacements. While the pipe ends beyond the buckle/plastic hinge locations see significant displacements, the surrounding soil accommodates this through a combination of soil compaction, flow around the pipe, and the development of an air void in the pipe wake. Qualitatively, this behavior makes intuitive sense and replicates the observed experimental behavior.

The information contained herein is the copyright of and proprietary to BMT Fleet Technology Limited. Use of this information is governed by the legend on the cover page of this document."

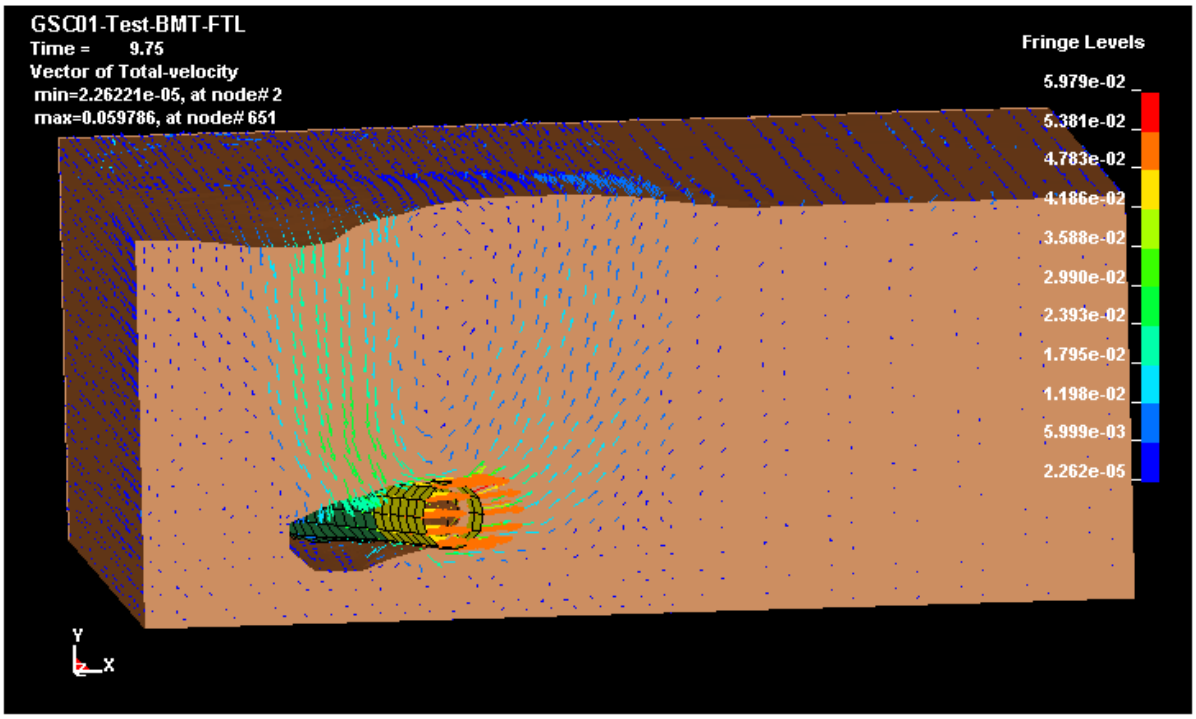

Figure 2.28: Illustration of Soil Movement around the Pipe

Figure 2.29 shows the bending moment versus end pipe displacement at 1 m from the end pipe location where the buckling occurred in the numerical simulation. The figure also illustrates the deformed cross-section of the pipe at discrete stages in the loading process. This illustrates the ability of the shell finite element model to explicitly simulate the onset and growth of pipe buckles or wrinkles, which cannot be demonstrated explicitly using beam or pipe elements.

Figure 2.30 traces the pipe displacement at 1 m from the pipe end (node 49426, see Figure 2.27), the location where the buckling occurred in the numerical simulation. As the pipe is pulled in the lateral direction, since no restriction is applied on the vertical movement of the pipe, it moves forward and upward. After a certain displacement, the lateral trajectory of the pipe reverses and the pipe appears to reverse its direction of movement. The displacement being plotted is the lateral displacement of a pipe surface node on the compression face of the pipe (see Figure 2.27). The reduction in the rate of lateral displacement and eventual reversal are due to the pipe ovalization, buckling and post buckling collapse deformation process.

Figure 2.31 traces the pipe displacement at the pipe end (node 49606, see Figure 2.27) and the displacements simulated at the plastic hinge (pipe buckle) discussed in Figure 2.30 for comparison. The pipe end moves forward and upwards, and the sand tends to flow downward to fill the forming void at the back of the pipe, accompanied by mounding at the free surface, Figure 2.28.

The information contained herein is the copyright of and proprietary to BMT Fleet Technology Limited. Use of this information is governed by the legend on the cover page of this document."

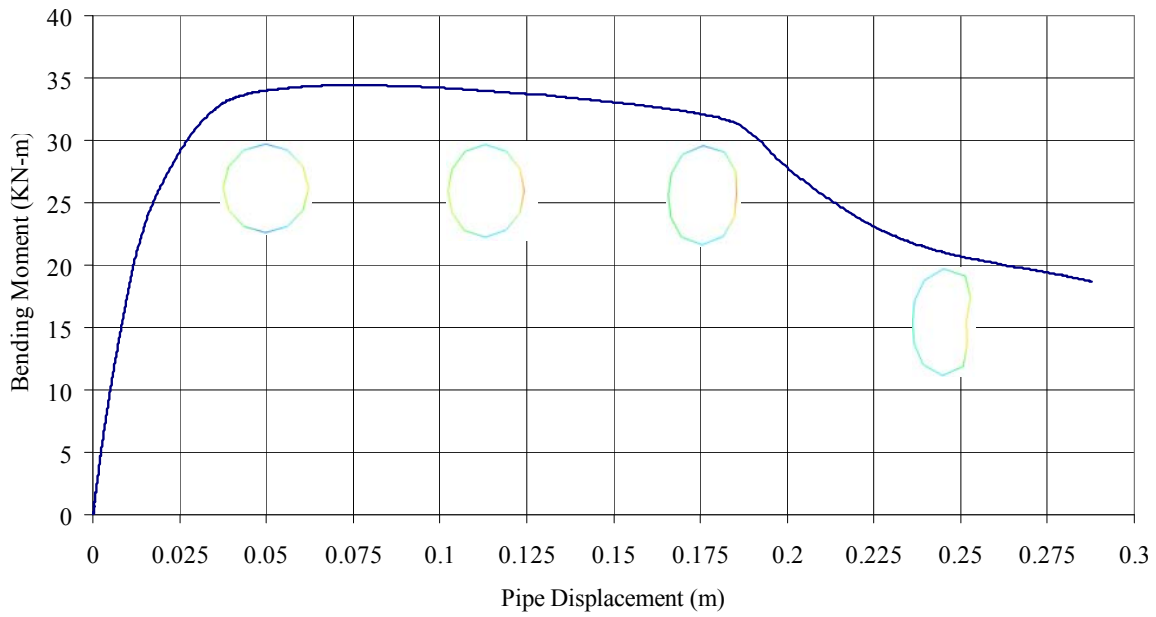

Figure 2.29: Bending Moment at the Plastic Hinge

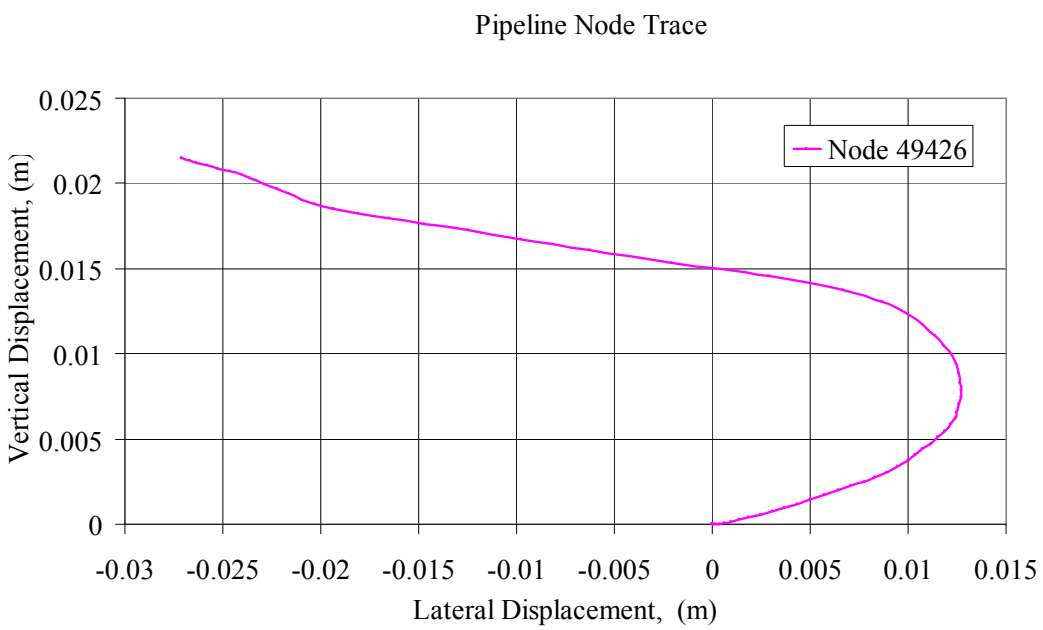

Figure 2.30: Pipeline Node 49426 Displacement Trace (at the Plastic Hinge)

The information contained herein is the copyright of and proprietary to BMT Fleet Technology Limited. Use of this information is governed by the legend on the cover page of this document."

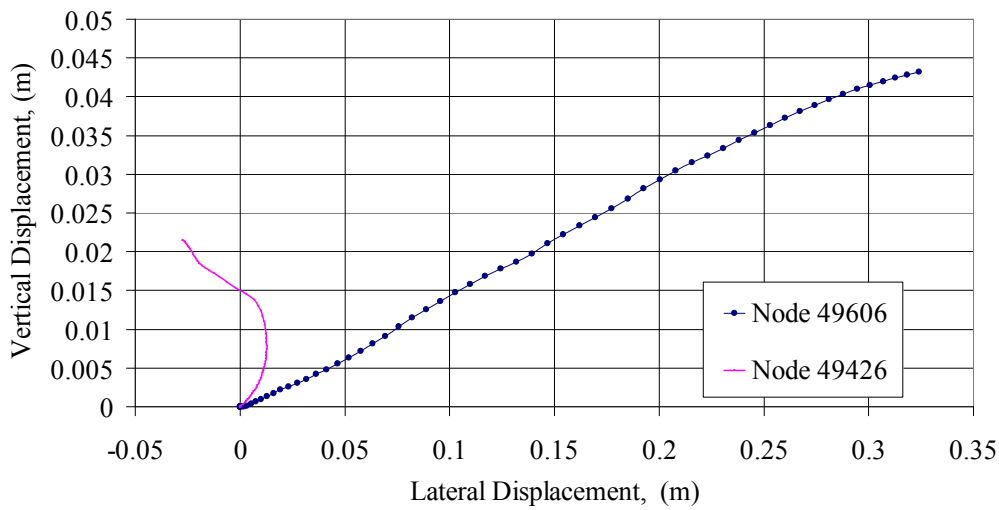

Figure 2.31: Pipe Node Displacement Trace (Node 49426 at the Plastic Hinge and at the Pipe End Node 49606)

2.7.3 Finite Element Analysis of Experimental Tank Test – Rigid Pipe

2.7.3.1 Large-Scale Experimental Model

Karimian et al. (2006) [4] performed large-scale tank experiments to investigate the pipeline behaviors when subjected to lateral soil movements. Their results are used here to examine the capability of the current FE analysis. The pipe loading tests were performed in a large sand chamber of 2.50 m (8.2 ft) x 3.8 m (12.5 ft) x 2.5 m (8.2 ft) at the University of British Columbia. Figure 2.32 shows the experimental setup. The UBC pipe had an outside diameter of 457 mm (18 in) and a wall thickness of 13.0 mm (0.5 in). The pipe was buried at the overburden ratio (H/D) of 1.92. The test was performed twice. The soil parameters in Table 2.6 were derived from tri-axial testing and reported.

Table 2.6: Soil Parameters (UBC Test)

Parameter	Units	Value
Internal Friction Angle	Deg.	45.5 to 43.3
Constant Volume Friction ϕ_{crit}	Deg.	32 to 34
Interface Friction	Deg.	36 to 30.5
Shear Modulus	MPa	3 to 12

The information contained herein is the copyright of and proprietary to BMT Fleet Technology Limited. Use of this information is governed by the legend on the cover page of this document."

Figure 2.32: UBC Experimental Sand Compartment – Karimian et al., 2006 [4]

In the absence of soil laboratory test data appropriate for the proposed FE work, a soil and foam model using a two-surface plasticity model with constant shear failure surface and pressure-volume strain (compaction) independence is used. The soil shear parameters were derived from the available critical friction (ϕ_{crit} = 32º) and constant cohesion, c = 0 kPa. More complex material models for soil such as a Cap model were also considered. However, the coefficients and parameters needed for the Cap model could not be determined given the available data.

2.7.3.2 Finite Element Model

The FE mesh used for the analysis is shown in Figure 2.33, with the same geometry as the experimental setup. The distance between the bottom boundary and the pipe is the same for both numerical model and the tank experiment. A 3D analysis using LS-DYNA Multi-Material Eulerian technique was performed. The model (Figure 2.33 consists of soil, air and pipe shell elements. The soil is modeled using 8-noded constant stress (one point integration) elements. In LS-DYNA the void elements were used to represent the air, which can accept material from other neighboring elements/material volumes. The soil mass in the tank is taken to be stress free and have uniform properties in the initial state. The load is imposed on two steps. In the first step, gravitational acceleration is applied; sufficient time is allowed to ensure that the soil stresses reach a stationary state. In the second step, the pipe was pulled in the lateral direction by imposing displacement boundary conditions to all nodes of the pipes, hence the pipe is assumed to be rigid. The interaction between the pipeline and the surrounding soil is modeled by constraint Lagarangian contact, in which slip and separation are allowed.

The information contained herein is the copyright of and proprietary to BMT Fleet Technology Limited. Use of this information is governed by the legend on the cover page of this document."

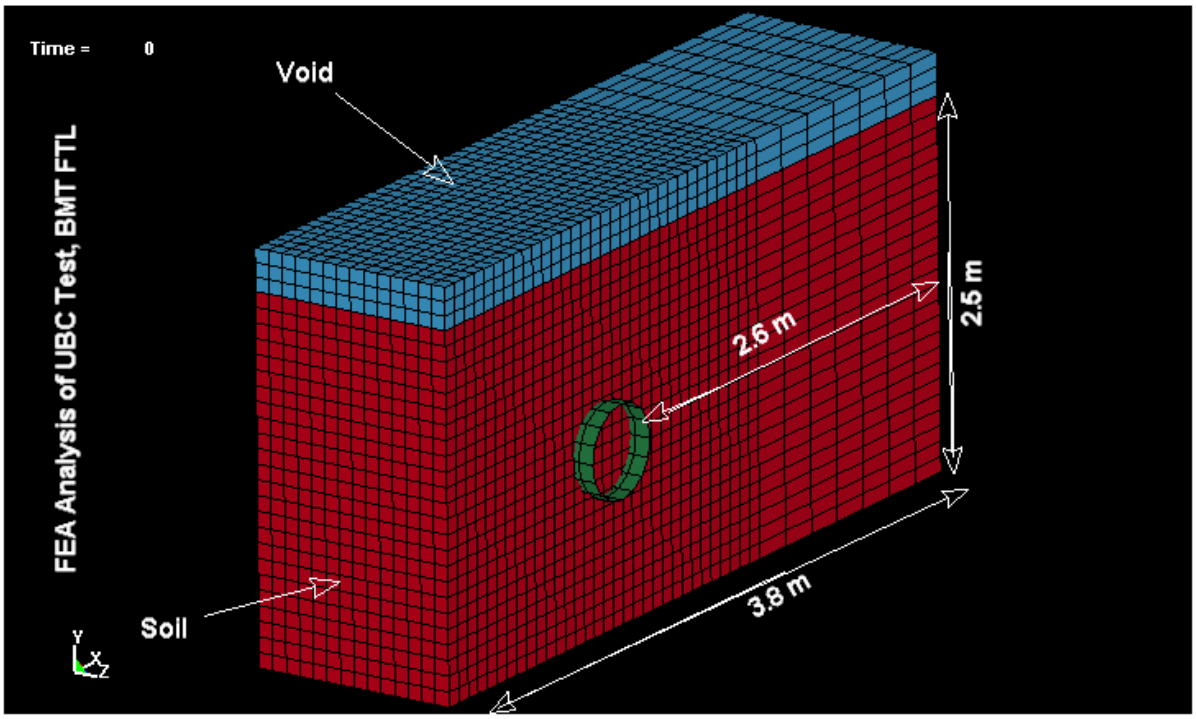

Figure 2.33: Illustration of the FE Model Including the Pipe

2.7.4 Analytical and Experimental Results

Figure 2.34 traces the simulated pipe displacement through the trial. At the beginning, the pipe moves slightly downwards and the sand tends to flow downward to fill the forming void at the back of the pipe; after certain displacement, this tendency is inverted, and the pipe moves upwards. The pipe displacement is accompanied by large formation heaps on the free surface. This phenomenon is observed in both the experimental and FE results (Figure 2.32 and Figure 2.35).

Figure 2.35 illustrates the simulated displaced position of the pipe and soil at the end of the trial. The figure includes soil particle velocity vectors describing the trajectory and relative speed of movement of soil particles. Qualitatively, the displaced soil profile and flow history make intuitive sense and match the observed behaviors. The primary difference between the simulated final soil profile and the experimental profile lies in the absence of the experimentally observed surface soil cracking (see Figure 2.32). This tensile failure mode has not been explained by the model. Perhaps the use of a more advanced (e.g., Cap) soil constitutive model would have replicated this behavior.

The information contained herein is the copyright of and proprietary to BMT Fleet Technology Limited. Use of this information is governed by the legend on the cover page of this document."

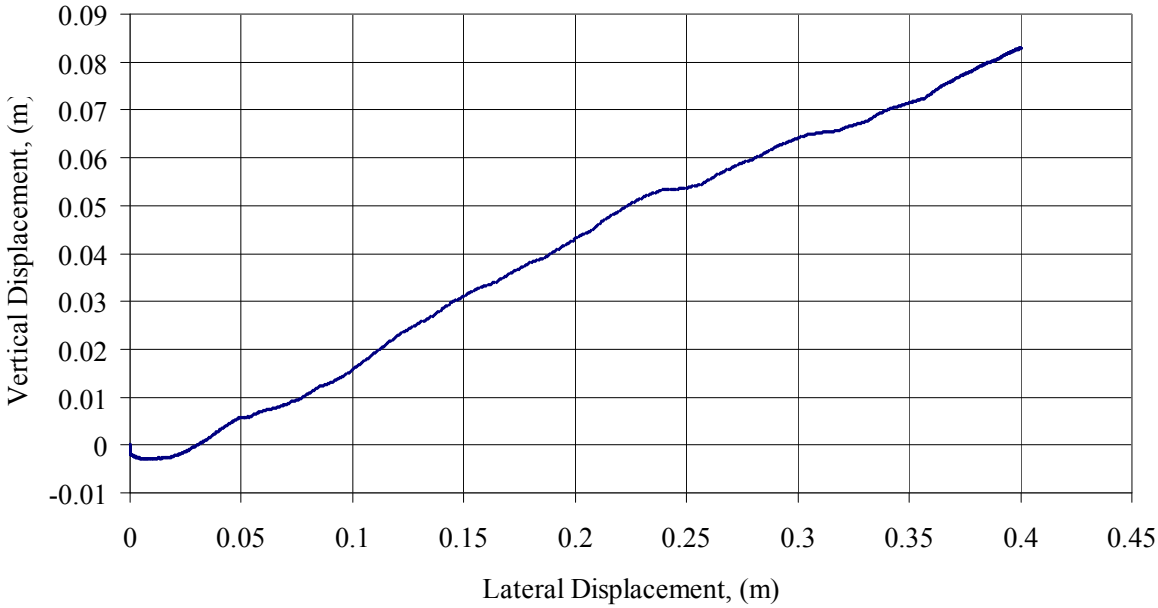

Figure 2.34: Displacement Patten (FE Analysis)

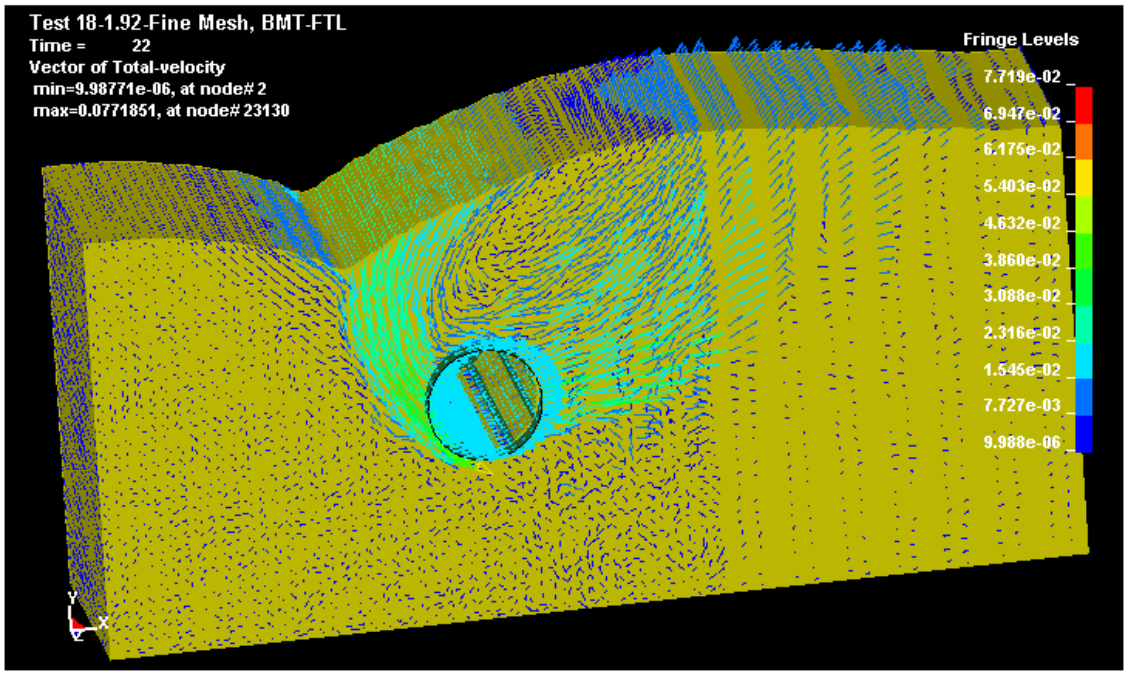

Figure 2.35: FEM Simulation of the UBC Trial Results

Figure 2.36 presents the comparison of experimental and numerical force-displacement curves. For lateral pipe movement, at H/D of 1.92, the results match the experimental data well. For both experimental and numerical force displacement, the failure load is about 50 KN/m obtained at the pipe displacement of 75 mm (2.9 in). Figure 2.37 presents the same results in terms of

The information contained herein is the copyright of and proprietary to BMT Fleet Technology Limited. Use of this information is governed by the legend on the cover page of this document."

dimensionless load (FL') and dimensionless displacement (Y') as defined in the following equations:

$$F_L^{'} = \frac{F}{(\gamma.H.D.L)}$$

$$Y^{'} = \frac{Y}{D}$$

where

F = Pullout load

γ = Soil density

H = Height of soil over pipe springline

D = Pipe diameter

Y = Pipe displacement

L = Pipe length

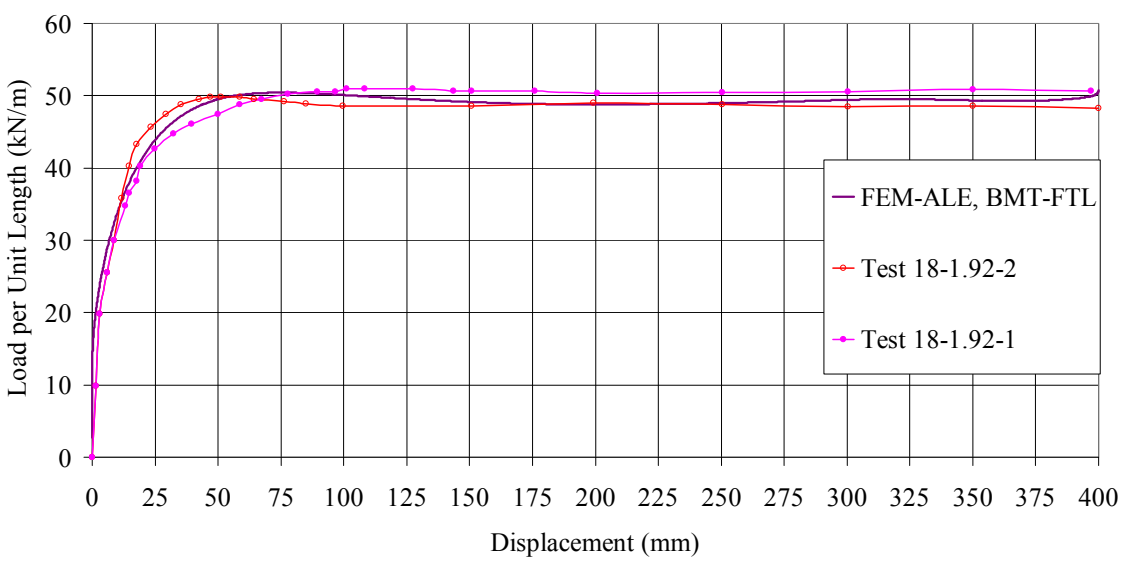

Figure 2.36: Comparison between Numerical Model Results and Test Results

The information contained herein is the copyright of and proprietary to BMT Fleet Technology Limited. Use of this information is governed by the legend on the cover page of this document."

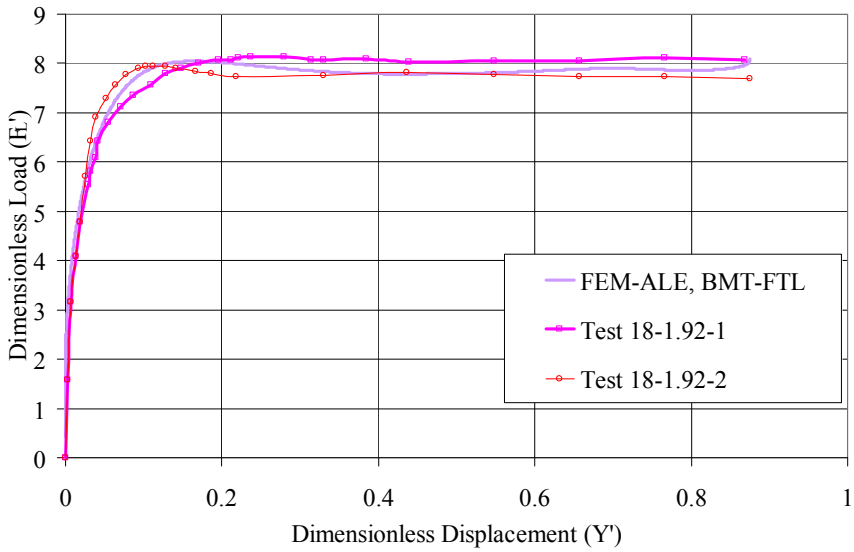

Figure 2.37: Comparison between Numerical Model and Test Results

The results presented in Figure 2.38 describe the trajectory of the pipe and soil particles through the simulated trial process. This result illustrates the stability of the soil below the pipe and the rotation of the soil mass from the pipe bottom to the pipe surface about a point located approximately half the burial depth above the pipe. This soil movement pattern describes the process that forms the experimentally-observed soil surface profile.

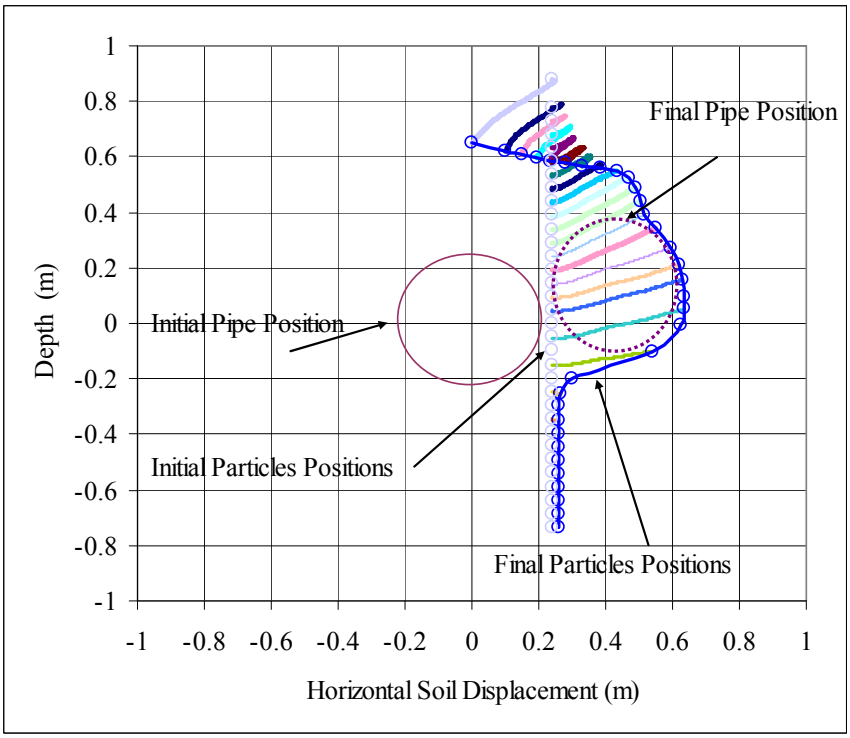

Figure 2.38: Displacement Trace Illustrating Pipe and Soil Displacements

The information contained herein is the copyright of and proprietary to BMT Fleet Technology Limited. Use of this information is governed by the legend on the cover page of this document."

The simulated results of the UBC trial differ from those developed in the previous section for the GSC trials, Section 2.7.1, in that the pipe is shorter and much stiffer, being essentially rigid. The simulation results in both cases appear to match the experimental observations.

2.7.5 Sensitivity Analyses

The finite element model of UBC experimental tank test with a rigid pipe (described in Section 2.8.1) was used to investigate the effects of the finite element model mesh size, pipe weight and soil water content. These sensitivity studies are not explicitly supported by experimental trial results. They are, however, presented to illustrate effects of modelling parameters on the simulation results or the ability of the model to differentiate between differing trial conditions.

2.7.5.1 Finite Element Mesh Size Effects

The effects of the mesh size in soil-pipe interaction were investigated by considering three different element sizes: 50, 75 and 100 mm (2 in, 3 in and 4 in). The results of the three analyses are compared in Figure 2.39. The predicted force displacement results (Figure 2.39) show that element size in the range of 50 to 100 mm (2 to 4 in) has little effect on the predicted force and displacement. It is expected, however, that significantly larger soil elements will result in simulation solution errors and/or cause model convergence problems.

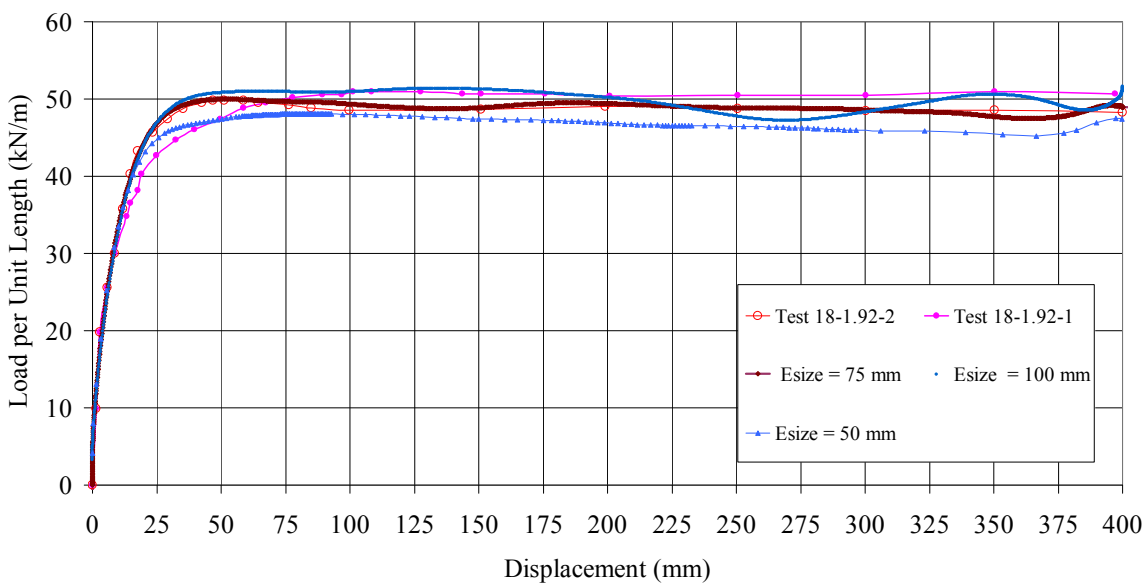

Figure 2.39: Comparison between Numerical Model and Test Results: Mesh Size 50 mm to 100 mm

2.7.5.2 Pipe Self-Weight Effects

The effects of the pipeline self-weight effects on the soil-pipe interaction were investigated by considering three different cases – a first case with self-weight, second without self-weight and the third case doubling the self-weight. The predicted force displacement results for the three cases are compared to the experimental results in Figure 2.40. The results show good agreement

The information contained herein is the copyright of and proprietary to BMT Fleet Technology Limited. Use of this information is governed by the legend on the cover page of this document."

between predicted force displacement using pipe self-weight and the experimental results. The weightless case under-predicts the maximum force, yet on the other hand the double self-weight scenario over-predicts the peak force. These results illustrate the sensitivity of the pipe force displacement behavior to pipe weight, indicating that weight (including fluid) should be considered an important modelling parameter.

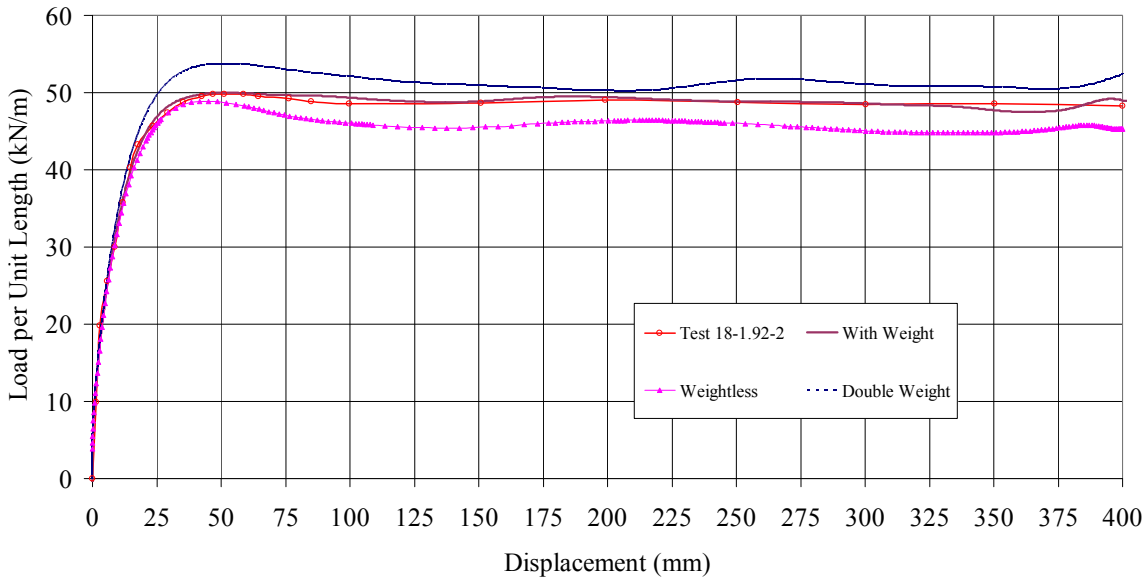

Figure 2.40: Effects of Pipe Self-Weight on Force-Displacement Curves

2.7.5.3 Effects of Soil Water Content

The objective of this section is to analyze the effects of the soil moisture content and drainage condition on the soil-pipe interaction forces, assuming perfectly drained and undrained conditions.

2.7.5.4 Finite Element Model

The finite element model of the UBC experimental test with a rigid pipe in a soil box (described in Section 2.7.1) was used to investigate the effects of the soil saturation on the soil-pipe interaction using sandy soil, referred to as "Lebanon Sand" by Shoop et al., 2005 [15].

2.7.5.5 Material Properties

Shop et al., 2005 performed tri-axial compression tests on "Lebanon Sand". Using the Mohr Coulomb approach, the angle of internal friction for these tests is 36º and 17º for saturated (17% moisture content) drained and undrained tests, respectively, and 33º for the undrained test at 13% moisture content. The water content of the specimen at saturation was reported to range from 17.5 to 17.8%.

The drained saturated sand behavior shows essentially no cohesion as would be expected for a sandy soil. The undrained sand tested at 13% moisture content shows a small amount of apparent

The information contained herein is the copyright of and proprietary to BMT Fleet Technology Limited. Use of this information is governed by the legend on the cover page of this document."

cohesion, as is typical in unsaturated soils because of the moisture tension, (Shoop et al., 2005,[15]. A brief summary of the measured soil material properties is presented in Table 2.7.

Table 2.7: Material Properties of "Lebanon Sand"

"Lebanon Sand" Test Condition	Cohesion, c (kPa)	Friction Angle, Ø (Deg.)
Drained, 17% mc (saturated)	0	36
Undrained, 17% mc (saturated)	4.8	17
Undrained, 13% mc	9	33

Figure 2.41 illustrates the pressure versus volumetric strain relationship used in the model, and the laboratory hydrostatic data. In the Soil and Foam Model, the volumetric strain must be input in the form of the natural log of the relative volumetric strain. Since the laboratory data are reported as volumetric strain, the user must convert the volumetric strain data to the requested natural log format required by the numerical model (LS DYNA). The diamond data points presented in Figure 2.41 are used as input data in LS DYNA.

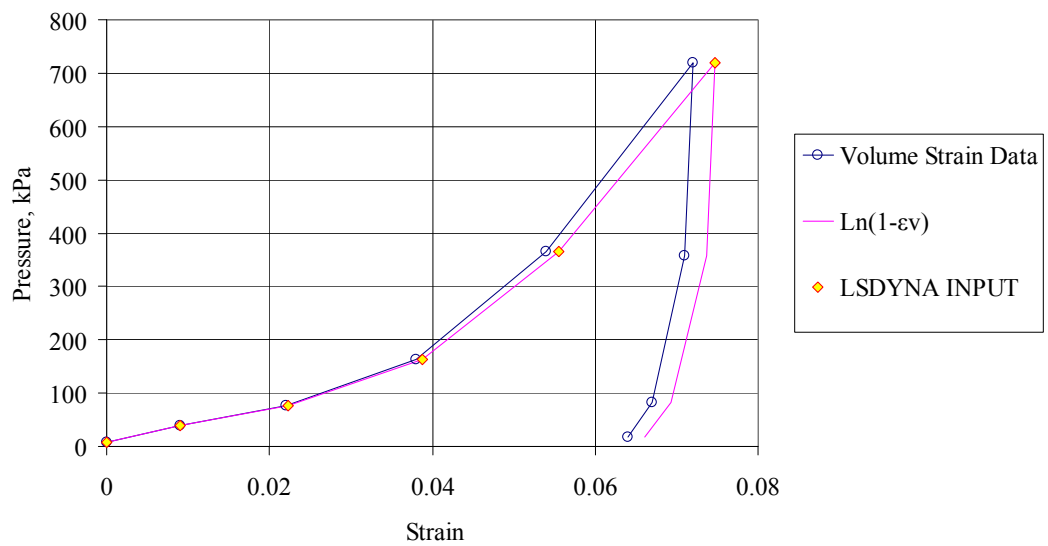

Figure 2.41: Hydrostatic Compression vs. Volumetric Strain

2.7.5.6 Finite Element Results

Predicted force displacement curves are shown in Figure 2.42 for the pipe movement simulation trials for the three soil conditions being investigated. These results illustrate that the finite element model is capable of producing simulation results that agree at least qualitatively with the observed effects of moisture content for the sand in an undrained condition. The undrained sand with the higher moisture content (17%) has a lower strength due to the pore water pressure preventing intergranular friction/contact. The model also provides a sensible demonstration of the effects of soil drainage by demonstrating the increased strength of the drained sand condition, which maximizes intergranular friction.

The information contained herein is the copyright of and proprietary to BMT Fleet Technology Limited. Use of this information is governed by the legend on the cover page of this document."

The observed changes in soil forces agree with expected behaviors since both the friction strength and apparent cohesion are affected by soil saturation. Similar results to those produced here are predicted by Popescu et al., 2003 [12].

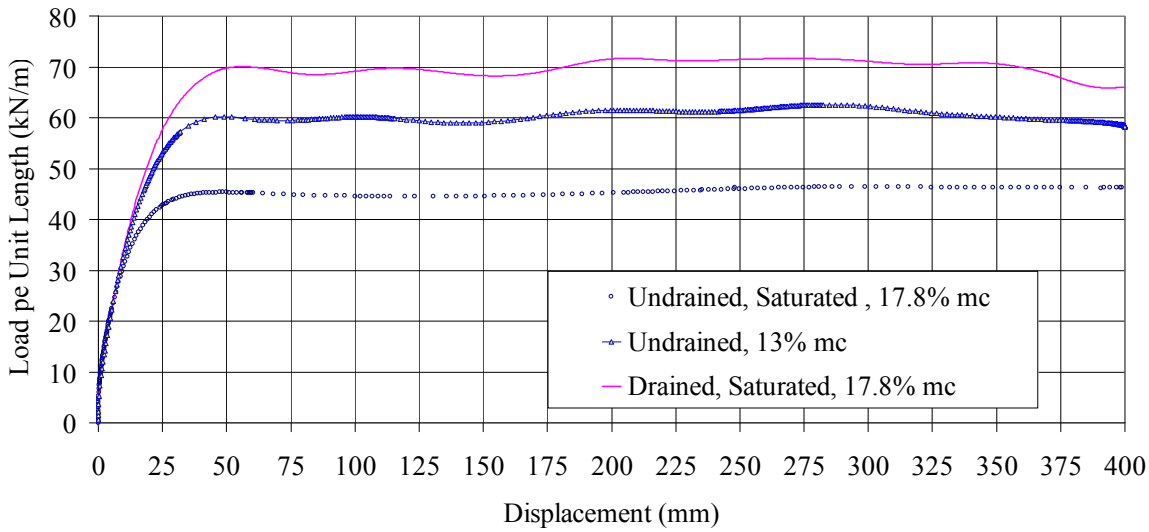

Figure 2.42: Effects of Saturation on Force-Displacement Curves

Figure 2.43 to Figure 2.45 show the predicted plastic strain contours for the three cases. The finite element analysis plots were developed for the three trial simulations at the same pipe displacement representing the intercept of the curves in Figure 2.42 with a vertical line. These plots also illustrate the soil particle velocity vectors describing the movement of the soil. The plots relate the soil displacement to the pipe soil interaction loads described in Figure 2.42. It is observed that soil load on the pipe is directly related to the volume of soil that is displaced in the trial. The displacement vectors also illustrate the center of rotation for the soil flow around the pipe.

The information contained herein is the copyright of and proprietary to BMT Fleet Technology Limited. Use of this information is governed by the legend on the cover page of this document."

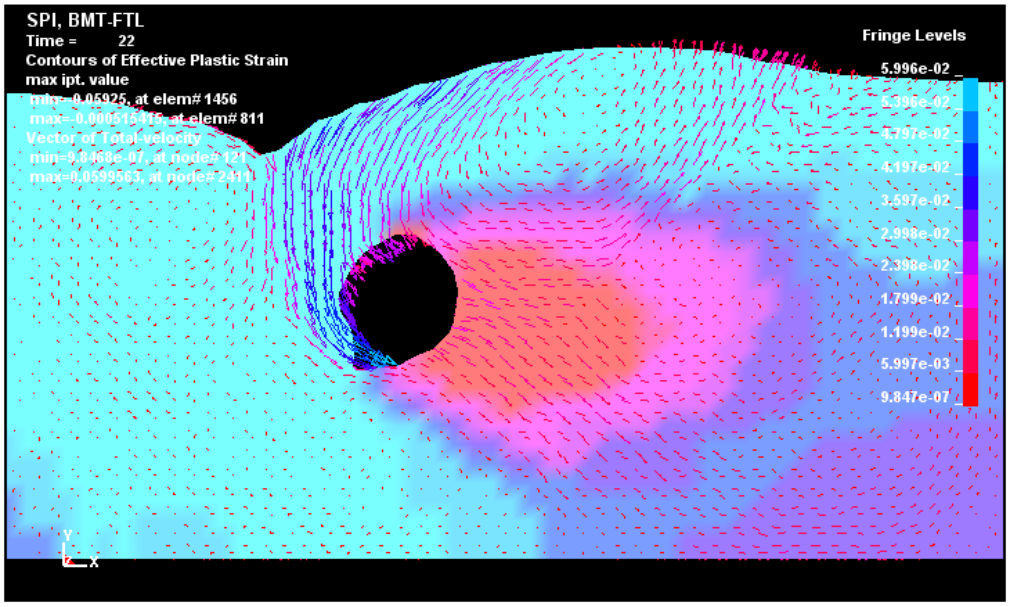

Figure 2.43: Effective Plastic Strain and Velocity Vectors at Pipe Displacement = 296 mm – Drained Sand with 17% Moisture Content

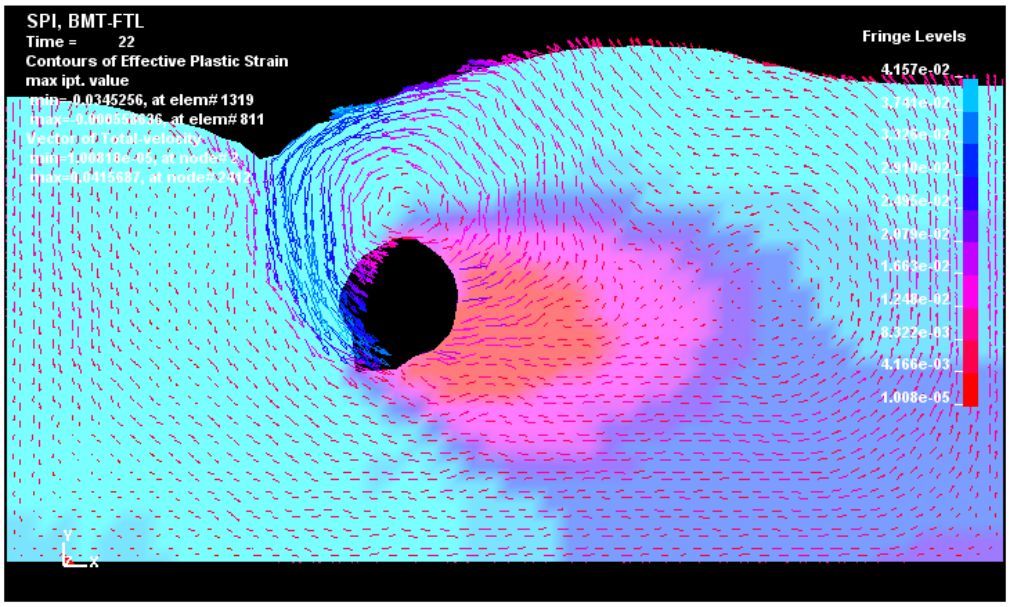

Figure 2.44: Effective Plastic Strain and Velocity Vectors at Pipe Displacement = 296 mm – Undrained Sand with 13% Moisture Content

The information contained herein is the copyright of and proprietary to BMT Fleet Technology Limited. Use of this information is governed by the legend on the cover page of this document."

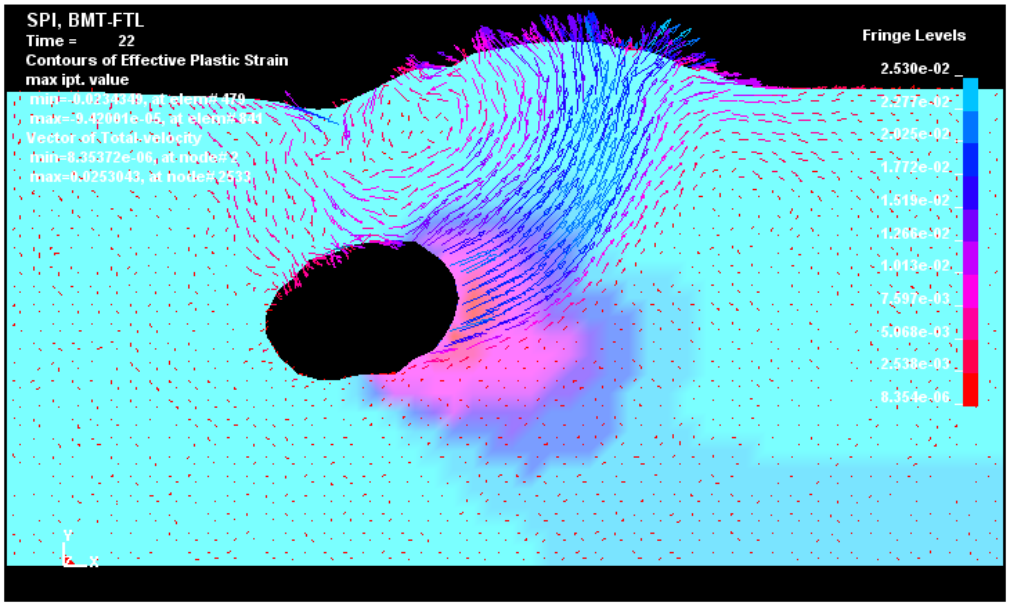

Figure 2.45: Effective Plastic Strain and Velocity Vectors at Pipe Displacement = 296 mm – Undrained Sand with 17% Moisture Content

2.8 Finite Element Analysis of Soil-Pipe Interaction for Slope Movements

The response of oil and gas pipelines to permanent ground movement is an important consideration in pipeline design and route selection. Permanent ground movements may be initiated by various forms of instabilities on sloping ground caused by heavy rain, seismic events or other causes. Permanent ground deformations can occur as surface faulting, liquefaction, lateral spreading due to liquefaction, or landslide. The responses of pipelines subjected to permanent ground deformation have been studied in literature using experimental, empirical and numerical methods.

The objective of this section is to show that the response of pipelines subjected to permanent ground deformation can be simulated by applying the ALE method to continuum mechanics, avoiding the limitations of some of the other numerical methods. One of the deformation conditions of interest is illustrated in Figure 2.46, showing the pipe subjected to lateral spreading or landslides.

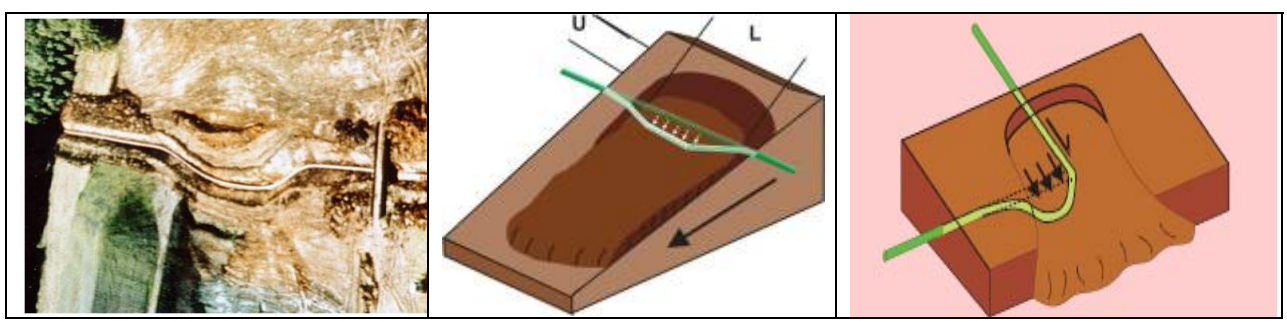

Figure 2.46: Permanent Ground Movement, Observed and Schematic Response of Landslide

The information contained herein is the copyright of and proprietary to BMT Fleet Technology Limited. Use of this information is governed by the legend on the cover page of this document."

2.8.1 Finite Element Model Validation: PGD Effects on Buried Pipelines with Elbows

2.8.1.1 Large-Scale Experimental Model:

Large full-scale permanent ground deformation (PGD) on steel pipe with elbows was conducted by Cornell University. The work was performed for Tokyo Gas, MCEER and NFS through its program for US-Japan Cooperative Research in Urban Earthquake Disaster Mitigation Yoshisaki et al. (2001, 2004) [16],[17] & [18]. Their results are used here to examine the capability of the current FE analysis. The pipe loading tests were performed in a test L-shape movable box 4.2 m (13.7 ft) long by 6 m (19.68 ft) wide by 1.5 m (4.9 ft) deep. Figure 2.47 and Figure 2.48 show the experimental concept setup for PGD effects on buried pipelines and plan view of the experimental setup. The pipe had an outside diameter of 100 mm (4 in) and a wall thickness of 4.1 mm (0.16 in). The pipe had an L-shape of 5.4 m (17.7 ft) by 9.3 m (30.5 ft) welded to a 90-degree elbow. The measured pipe and elbow material stress-strain curves used in the analysis are presented in Figure 2.49. The pipe was installed at a 0.9 m (3 ft) burial depth to the top of the pipe. The sand had a unit weight of 18.4 KN/m^3 and an average friction angle of 50 degrees. The pipe internal pressure during the trial was 0.1MPa (14.5 psi).

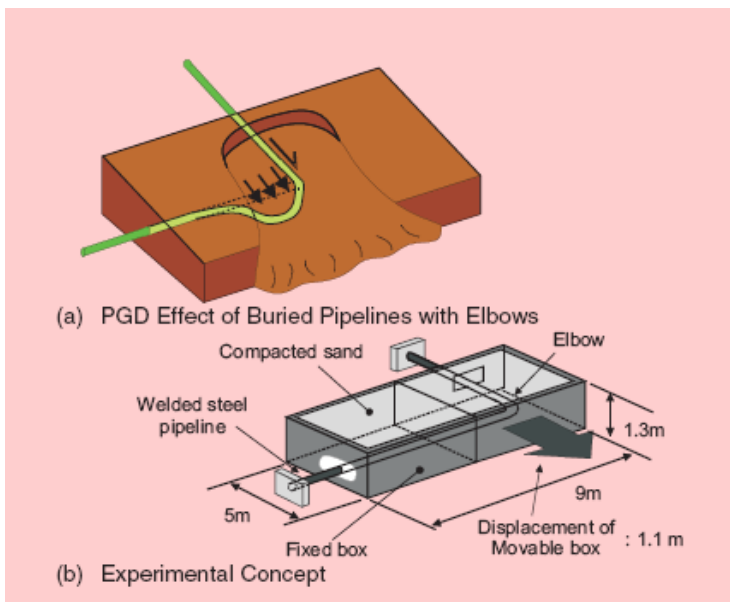

Figure 2.47: Experimental Concept for PGD Effect on Buried Pipelines with Elbow (O'Rourke et al., 2004 [13])

The information contained herein is the copyright of and proprietary to BMT Fleet Technology Limited. Use of this information is governed by the legend on the cover page of this document."

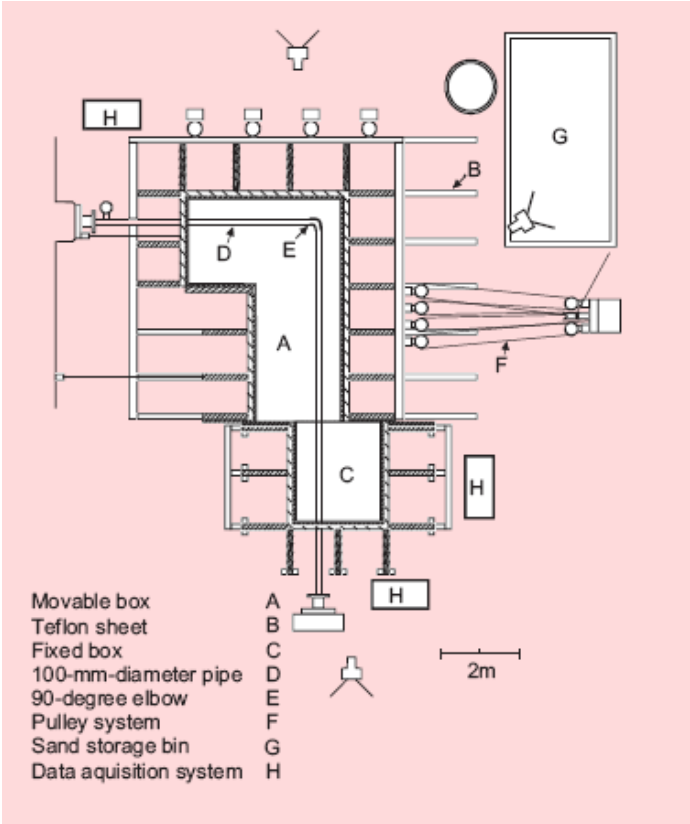

Figure 2.48: Plan View of the Experimental Setup (O'Rourke et al., 2004 [13])

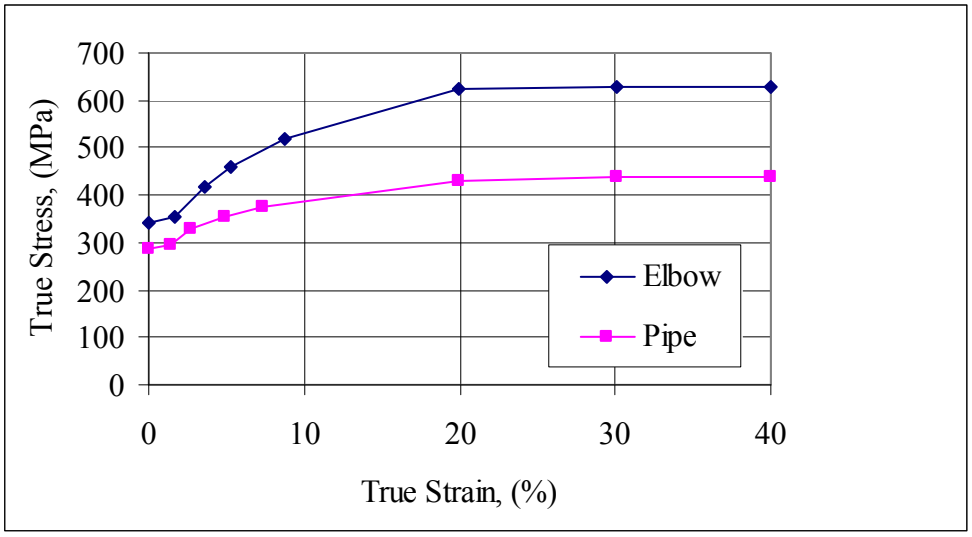

Figure 2.49: True Stress-Strain Curves (Yoshisaki et al., 2004 [17])

2.8.1.2 Finite Element Model:

An example of the FE mesh used for the analysis is shown in Figure 2.50 with the geometry exactly similar to the experimental setup (Figure 2.47 and Figure 2.48). The distance between the

The information contained herein is the copyright of and proprietary to BMT Fleet Technology Limited. Use of this information is governed by the legend on the cover page of this document."

bottom boundary and the pipe is the same for both numerical model and soil box experiment. A 3D analysis using LS-DYNA Multi-Material Eulerian technique was performed to simulate the laboratory experiment.

The finite element model consists of soil, air and pipe shell elements (Figure 2.50). The soil is modeled using an 8-node constant stress (one point integration) model formulation. In LS-DYNA, the void elements were used to represent the air, which can accept material from other neighboring elements. The pipe is modeled using Belyschko-Tasy shell elements. The soil mass in the tank is taken to be stress free and have uniform properties in the initial state. The load is imposed in two steps. In the first step, gravitational acceleration and the pipe internal pressure are applied and sufficient time is allowed to ensure that the soil stress reaches a stationary state. In the second step, the mobile soil box movement is applied. The interaction between the pipeline and the surrounding soil is modeled by constraint Lagarangian contact in which slip and separation are allowed. The interface friction between the pipe and soil ϕ_μ is assumed equal to 0.6ϕ ($\mu = \tan(0.6\phi) = 0.55$).

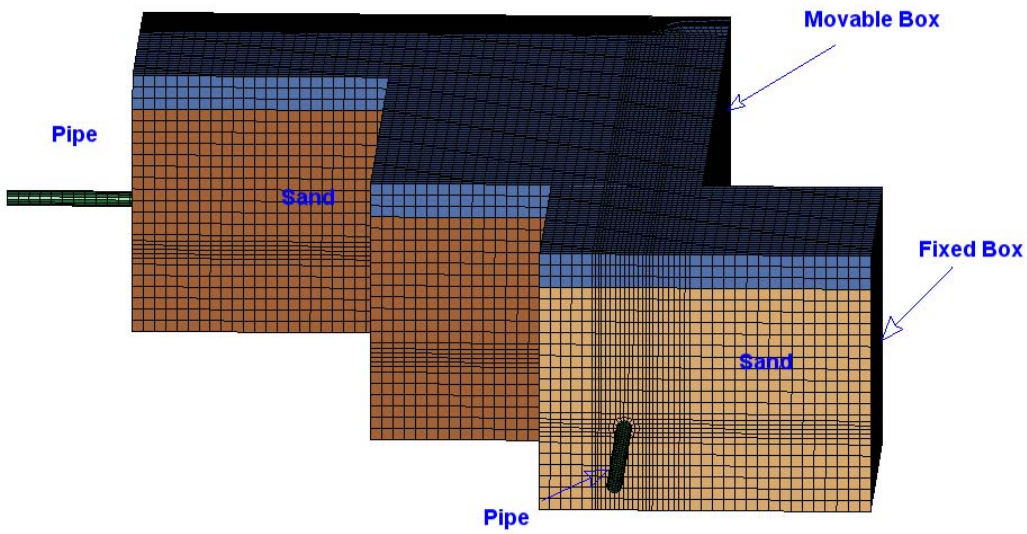

Figure 2.50: Illustration of the FE Model including the Pipe

2.8.1.3 Analytical and Experimental Results:

Figure 2.51 shows the experimental test compartment before and after the experiment; Yoshisaki et al., 2004 [17]. Figure 2.52 shows an overhead view of the test compartment after excavation. Typical graphical output from the model is illustrated in Figure 2.53. The figure illustrates the response of pipeline subjected to ground movement similar to the laboratory shear box test. In this figure, the color fringes indicate the pipe lateral displacement. Figure 2.54 compares the deformed pipe shape of the finite element model and the full-scale experimental pipeline. Comparison between the numerical prediction and the full-scale test results showed that the ALE finite element model was able to closely predict the pipe deformation.

The information contained herein is the copyright of and proprietary to BMT Fleet Technology Limited. Use of this information is governed by the legend on the cover page of this document."

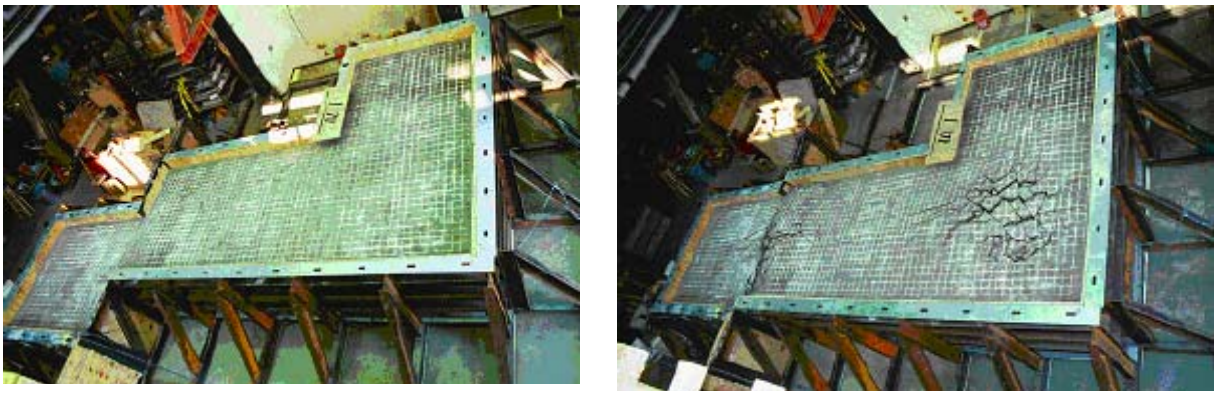

Figure 2.51: Overhead View of Test Compartment Before (Left) and After (Right) the Experiment. (Yoshisaki et al., 2004 [17])

Figure 2.52: Deformed Experimental Pipeline (Yoshizaki et al., 2004 [17])

The information contained herein is the copyright of and proprietary to BMT Fleet Technology Limited. Use of this information is governed by the legend on the cover page of this document."

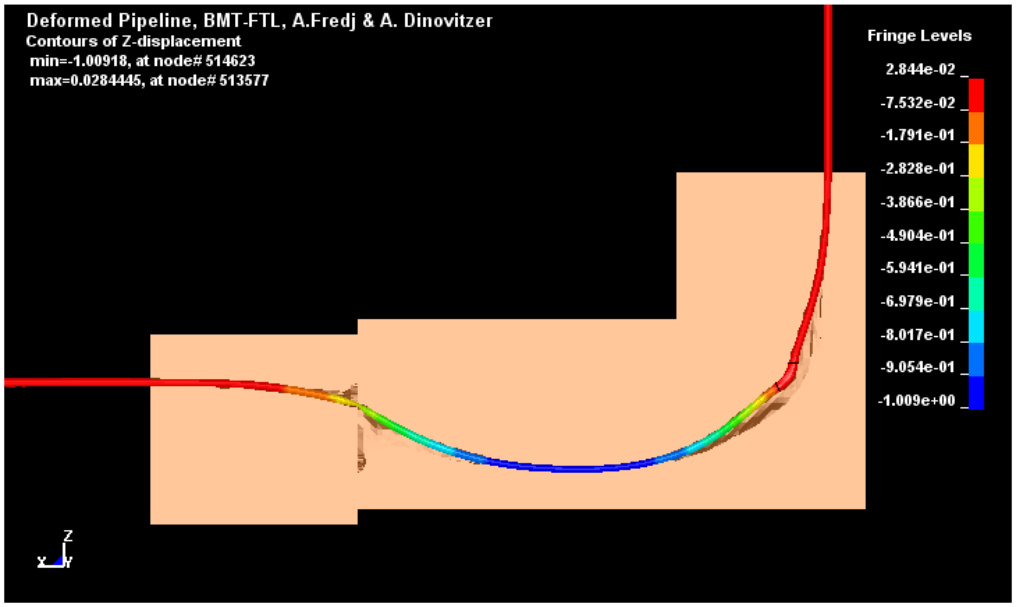

Figure 2.53: Deformed Pipeline – Finite Element Analysis Results

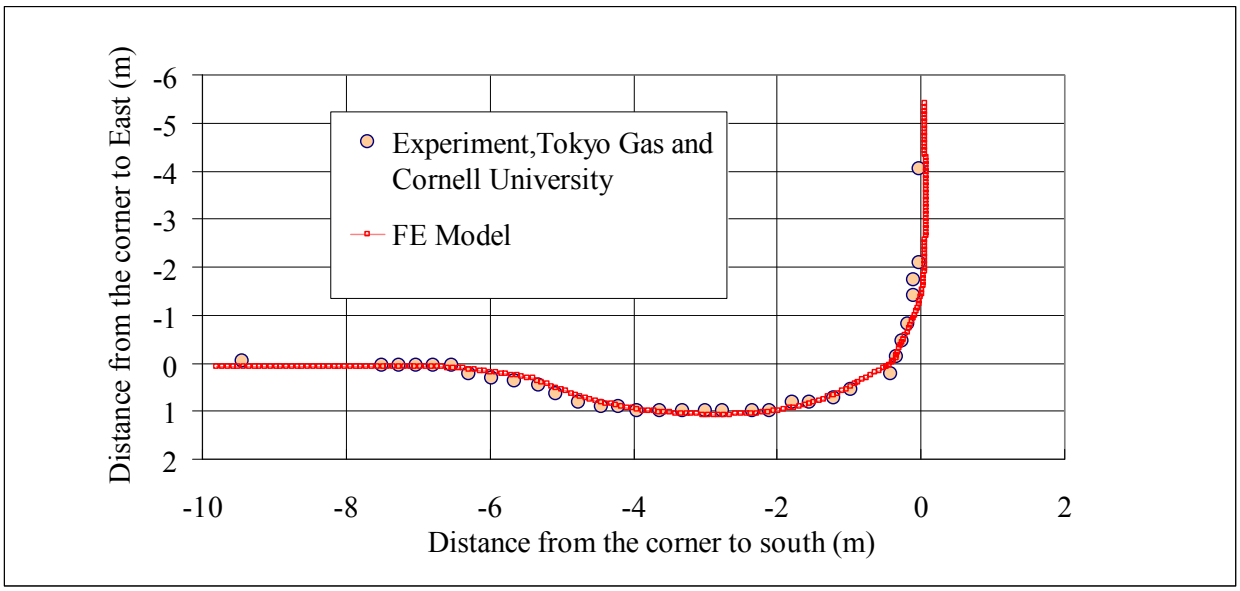

Figure 2.54: Pipeline Deformation: Comparison between the Numerical Model and Test Results

Figure 2.55 compares the measured and simulated longitudinal and circumferential strains at the junction of the pipe elbow and the pipeline short leg (Section A-A) at the end of the loading process. These results illustrate the ability of the FE model to replicate the measured pipe strain, at various points around the pipe circumference since the finite element model simulated strains compare well with the measured strains.

The information contained herein is the copyright of and proprietary to BMT Fleet Technology Limited. Use of this information is governed by the legend on the cover page of this document."

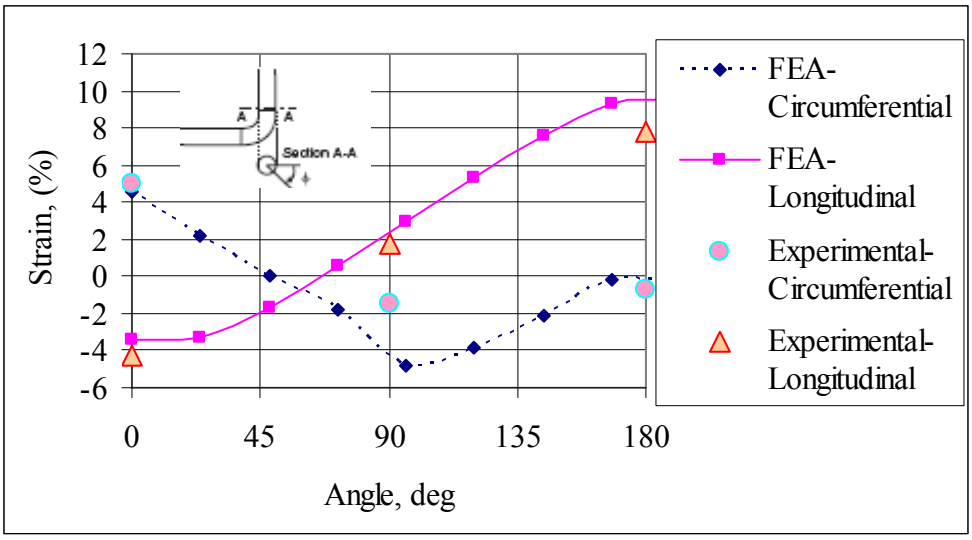

Figure 2.55: Strain Distribution at the Cross-section of the Connection between the Elbow and the Straight Pipe Segment (Section A-A) – Comparison between the Numerical Model and Test Results

Figure 2.56 shows the measured and predicted longitudinal and circumferential strains at the cross-section of the elbow (Section B-B). The finite element model was able to closely predict the circumferential strain but over-estimate the longitudinal strain. The difference in the predicted longitudinal strain could easily be attributed to the disconnection of the strain gauges during the experiment as reported by Yoshisaki et al., 2004 [17]. Regardless of this source of uncertainty in the experimental results, the trend in the measured strains and those derived from the finite element model is similar.

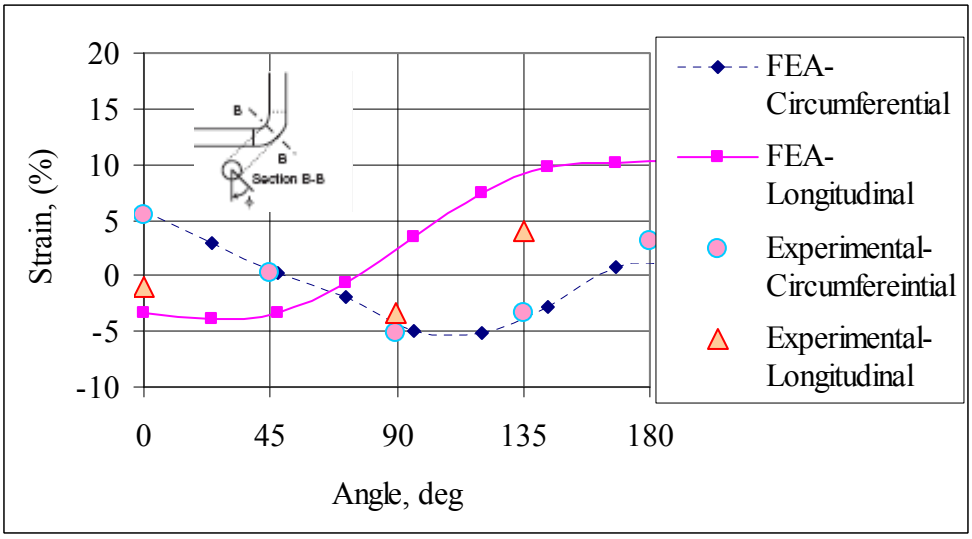

Figure 2.56: Strain Distribution at the Cross-Section of the Elbow (Section B-B) – Comparison between the Numerical Model and Test Results

The information contained herein is the copyright of and proprietary to BMT Fleet Technology Limited. Use of this information is governed by the legend on the cover page of this document."

Overall, the comparison between the analytic prediction and full-scale experimental results show that the ALE model was able to closely predict the pipe response and the magnitude and distribution of the pipe strains.

2.9 Validation of DEM Model in LS-DYNA

The LS DYNA implementation of a discrete element model (DEM) to represent soils was found to be efficient in assessing geotechnical hazards and as such further validation studies were completed to demonstrate the abilities of this modelling technique. Pipe-soil interaction using the DEM models within the non-linear explicit code, LS-DYNA [1], are validated and calibrated based on available published full-scale experimental data including pipelines subjected to lateral and axial soil movements. The models are further calibrated for nominal soil types to replicate the pipe-soil load displacement properties outlined in ASCE guideline recommendations [39].

2.9.1 Soil Restraint on Pipe Buried in Road Mulch

Monroy [40] and Wijewickreme et al., [41] performed a series of full-scale lateral soil restraint tests considering three types of soil: (i) sand, (ii) crushed sand and gravel (referred to as road mulch), and crushed limestone. The steel pipes tested were NPS 16 and NPS 18. The pipe loading tests were performed in a large soil chamber of 3.8 to 5.0 m (length) x 2.50 m (width) x 2.5 m (height) at the Advanced Soil-Pipe Interaction Research (ASPIReTM) chamber at the University of British Columbia (UBC), Vancouver, Canada. As shown in Figure 5.1, one outside wall of the chamber is fitted with a Plexiglas sheet to allow visual observation of the pipe-soil deformation during the test. In all the test configurations, the pipe was loaded in a displacement-controlled manner. The displacement rate varied from 2 to 50 mm/s.

1. The UBC NPS 16 (406 mm diameter) tests were in moist sand with an overburden-to-pipe diameter ratio (H/D) of 1.6. The test was performed one time (referred to as Test No. 1).

2. The UBC NPS 18 (457 mm diameter) tests were in moist sand with an overburden-to-pipe diameter ratio (H/D) of 1.9. The test was performed twice (referred to as Test No. 2 and Test No. 3).

3. The UBC NPS 18 (457 mm diameter) tests were in road mulch with an overburden-to-pipe diameter ratio (H/D) of 1.9. The test was performed twice (referred to as Test No. 4 and Test No. 5).

The key parameters for the soil used in the test cases are summarized in Table 2.8. The test results are presented in terms of normalized values of lateral soil restraint (N_{qh}) and normalized pipe displacement (Y') defined as follow:

$$N_{qh} = \frac{P}{(\gamma HDL)}$$

$$Y' = \frac{Y}{D}$$

The information contained herein is the copyright of and proprietary to BMT Fleet Technology Limited. Use of this information is governed by the legend on the cover page of this document."

Where, P is the measured load, and is γ the dry unit weight of the soil.

Table 2.8: Summary Parameters for Pipe-Soil Test Cases [41]

	Moist Sand		Crushed Gravel and Sand (Road Mulch)
Average density (kg/m3)	1600	1600	1800
Average moisture (%)	4	4	3 to 4
Internal peak friction angle, deg.	43	43	49
Dilation angle, ψ	12 to 14	12 to 14	16
Pipe diameter, D (in)	NPS 16 (406 mm)	NPS 18 (457 mm)	NPS 18 (457 mm)
Pipe length (m)	2.4	2.4	2.4

A 3D analysis was performed using the LS-DYNA DEM method to simulate the UBC full-scale lateral soil restraint trials considering the two different types of soils (road mulch and moist sand).

2.9.2 Soil Restraint on NPS 16 (406 mm) Pipe Buried in Moist Sand

A 3D analysis was performed to simulate UBC lateral soil restraint on NPS 16 (406 mm) buried in moist sand with an overburden ratio H/D of 1.6 (test No. 1), test was simulated.

Figure 2.57 and 2.58 compare the observed and simulated displaced position of the pipe and soil. The pipe moves forward and upwards, and the soil tends to flow downward to fill the void that forms at the back of the pipe. The pipe movement results in soil mounding at the free surface. Qualitatively, the displaced soil profile and flow history make intuitive sense and match the observed behaviors.

Figure 2.59 presents a comparison of numerical and experimental lateral soil resistance (N_{qh}) to pipe movement as a function of normalized pipe displacement (Y') ratio. A peak soil load of 34 kN/m (for N_{qh} = 7.8) was reached at pipe displacements 0.25D. The peak soil load of 34 kN/m was reached (for an N_{qh} value of 7.8) at pipe displacement 0.2D is in good agreement with the measured lateral soil restraint. Minor variations in the numerical simulation response may be attributed to the size of the discrete elements (soil particles).

This result is an illustration of the ability of the DEM simulation technique to accurately reproduce measured forces and displacements. The validation process for a numerical simulation process, such as the DEM, requires that the model agreement with physical trials or operational experience be demonstrated across a variety of scenarios and this is just one element of the validation process.

The information contained herein is the copyright of and proprietary to BMT Fleet Technology Limited. Use of this information is governed by the legend on the cover page of this document."

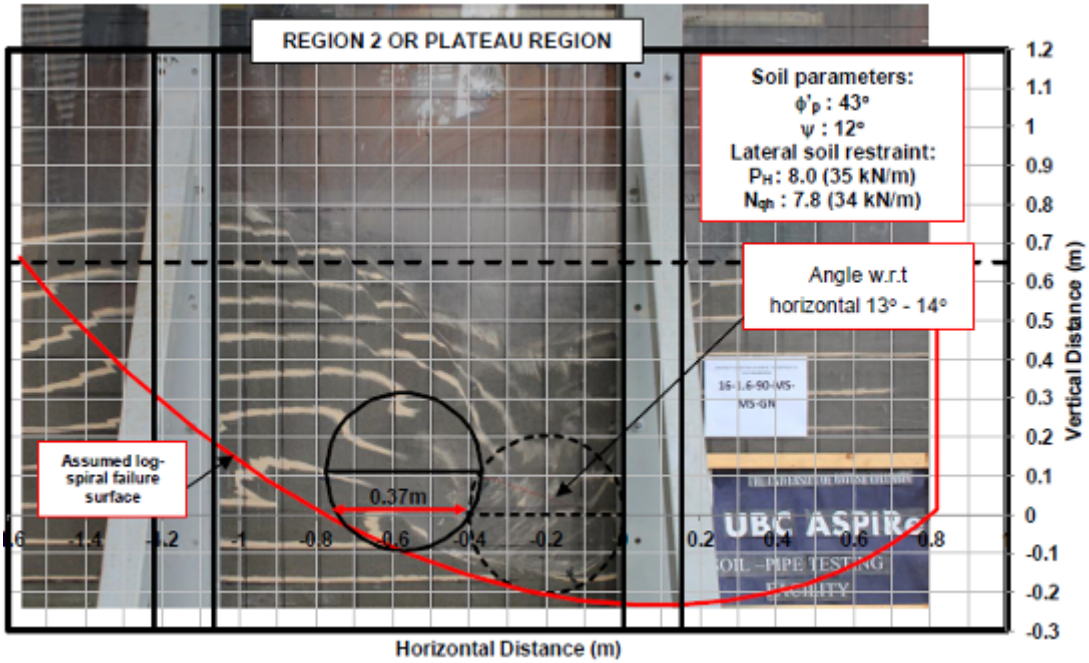

Figure 2.57: Soil Deformation of Moist Sand (Experimental Results – Y=0.9 D) [41]

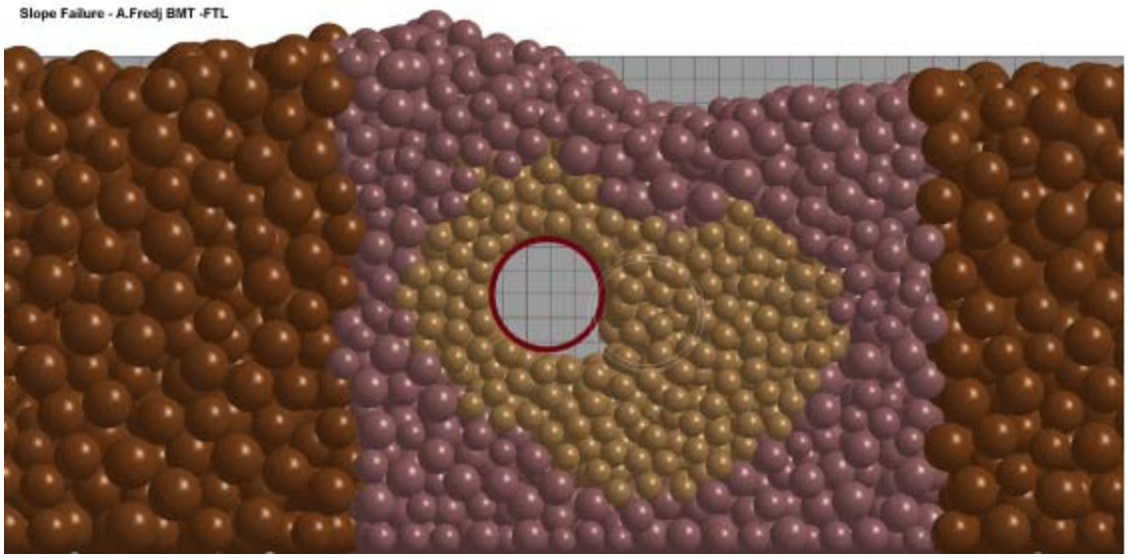

Figure 2.58: Soil Deformation of Moist Sand (FE Results – Y=0.9 D)

The information contained herein is the copyright of and proprietary to BMT Fleet Technology Limited. Use of this information is governed by the legend on the cover page of this document."

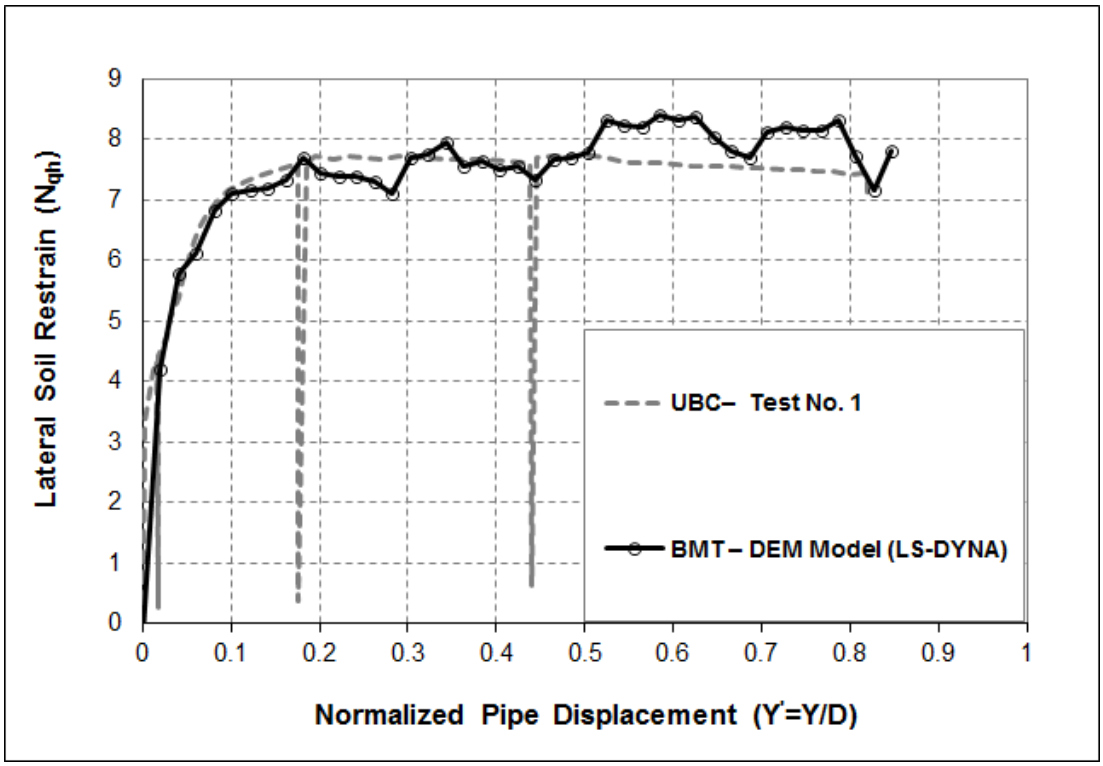

Figure 2.59: Comparison between Numerical Model Results and Test Results – (NPS 16 - Moist Sand Soil)

2.9.3 Soil Restraint on NPS 18 (457mm) Pipe Buried in Moist Sand

A 3D analysis was performed to simulate UBC lateral soil restraint on NPS 18 (457 mm) buried in moist sand with an overburden ratio H/D of 1.9 (test No. 2 and No. 3), test was simulated.

Figure 2.60 presents a comparison of numerical and experimental lateral soil resistance (N_{qh}) to pipe movement as a function of normalized pipe displacement (Y') ratio. A peak soil load of 34 kN/m (for N_{qh} = 7.8) was reached at pipe displacements 0.05D for test 3 and 0.15D for Test 2. The peak soil load of 35 kN/m was reached (for an N_{qh} value of 8) at pipe displacement 0.2D is in good agreement with the measured lateral soil restraint.

The information contained herein is the copyright of and proprietary to BMT Fleet Technology Limited. Use of this information is governed by the legend on the cover page of this document."

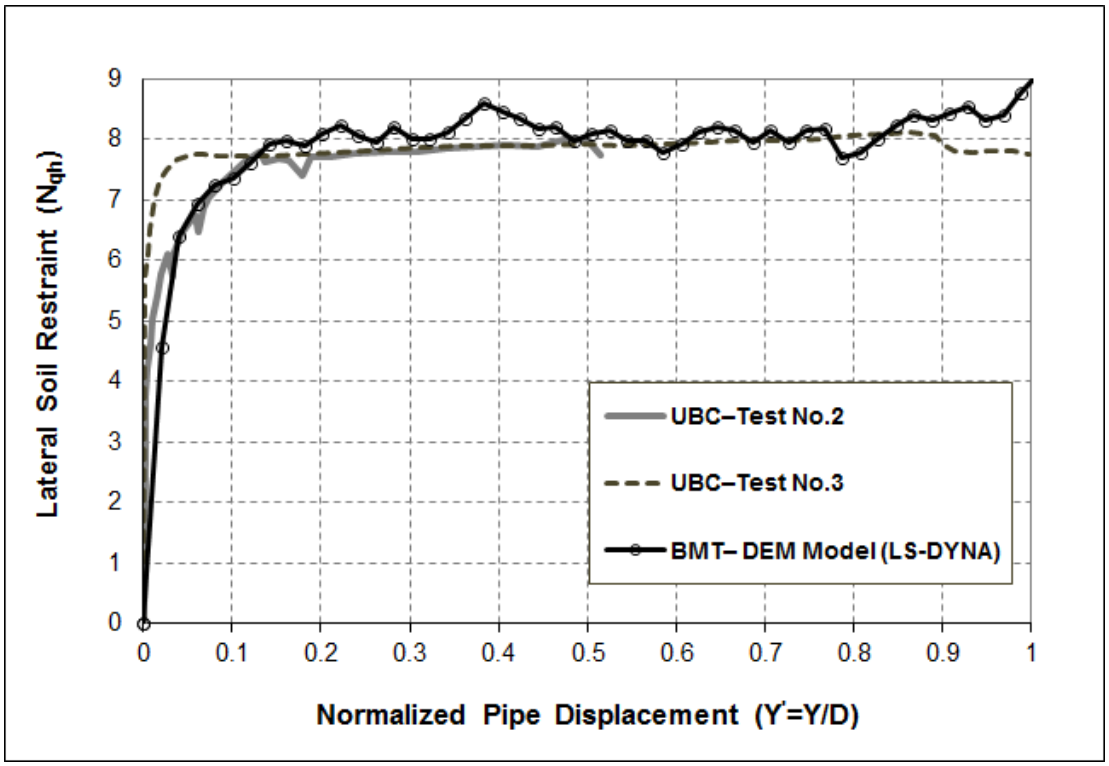

Figure 2.60: Comparison between Numerical Model Results and Test Results – (NPS 18 - Moist Sand Soil)

2.9.4 Soil Restraint on Pipe Buried in Road Mulch

A 3D analysis was performed to simulate UBC lateral soil restraint on NPS 18 (457 mm) buried in road mulch with an overburden ratio H/D of 1.9 (test No. 4 and No. 5), test was simulated.

Figure 2.61 and Figure 2.62 compare the observed and simulated displaced position of the pipe and soil. The pipe moves forward and upwards, and the soil tends to flow downward to fill the void that forms at the back of the pipe. The pipe movement results in soil mounding at the free surface. Qualitatively, the displaced soil profile and flow history make intuitive sense and match the observed behaviors.

Figure 2.63 presents a comparison of numerical and experimental lateral soil resistance (N_{qh}) to pipe movement as a function of normalized pipe displacement (Y') ratio. A peak soil load of 75.8 kN/m (for N_{qh} = 10.2) and 82 kN/m (for N_{qh} = 11) for tests 4 and 5 were reached at pipe displacements 0.45D and 0.35D, respectively. The peak soil load of 82.75 kN/m was reached (for an N_{qh} value of 11.1) at pipe displacement 0.35D is in good agreement with the measured lateral soil restraint. This result is an illustration of the ability of the DEM simulation technique to accurately reproduce measured forces and displacements.

The information contained herein is the copyright of and proprietary to BMT Fleet Technology Limited. Use of this information is governed by the legend on the cover page of this document."

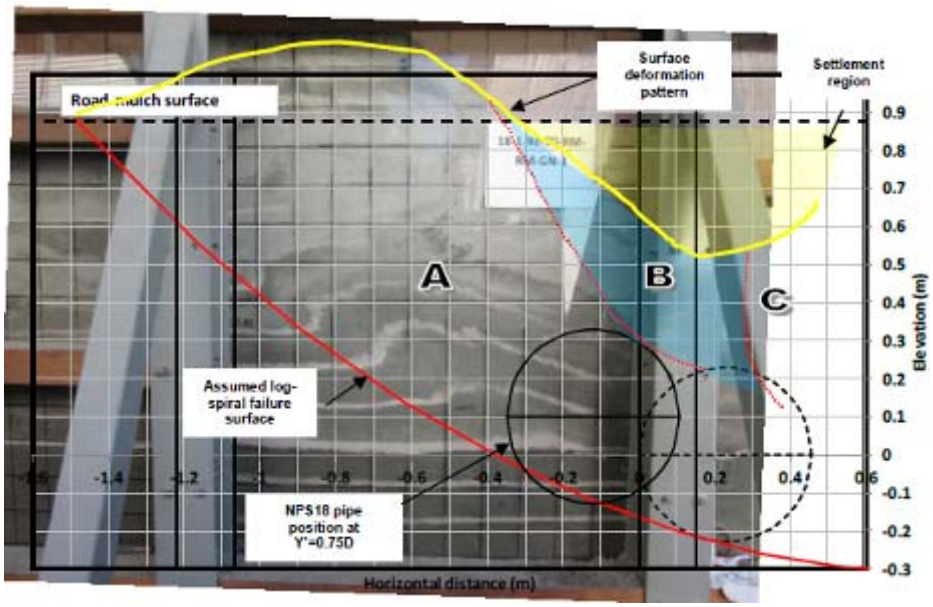

Figure 2.61: Soil Deformation of Road Mulch (Experimental Results – Y=0.75 D) [41]

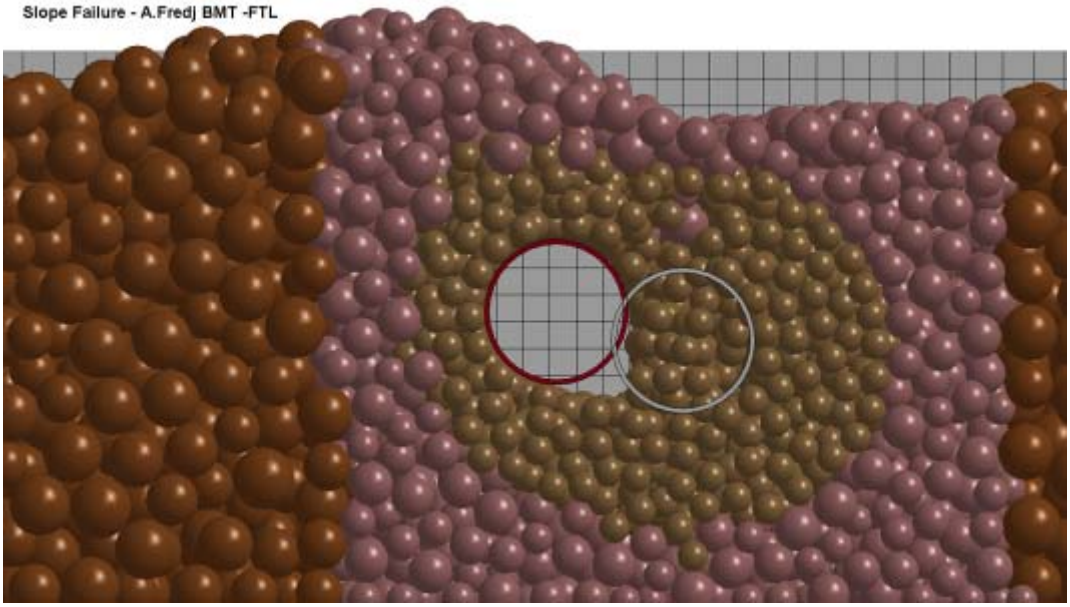

Figure 2.62: Soil Deformation of Road Mulch (FE Results – Y=0.9 D)

The information contained herein is the copyright of and proprietary to BMT Fleet Technology Limited. Use of this information is governed by the legend on the cover page of this document."

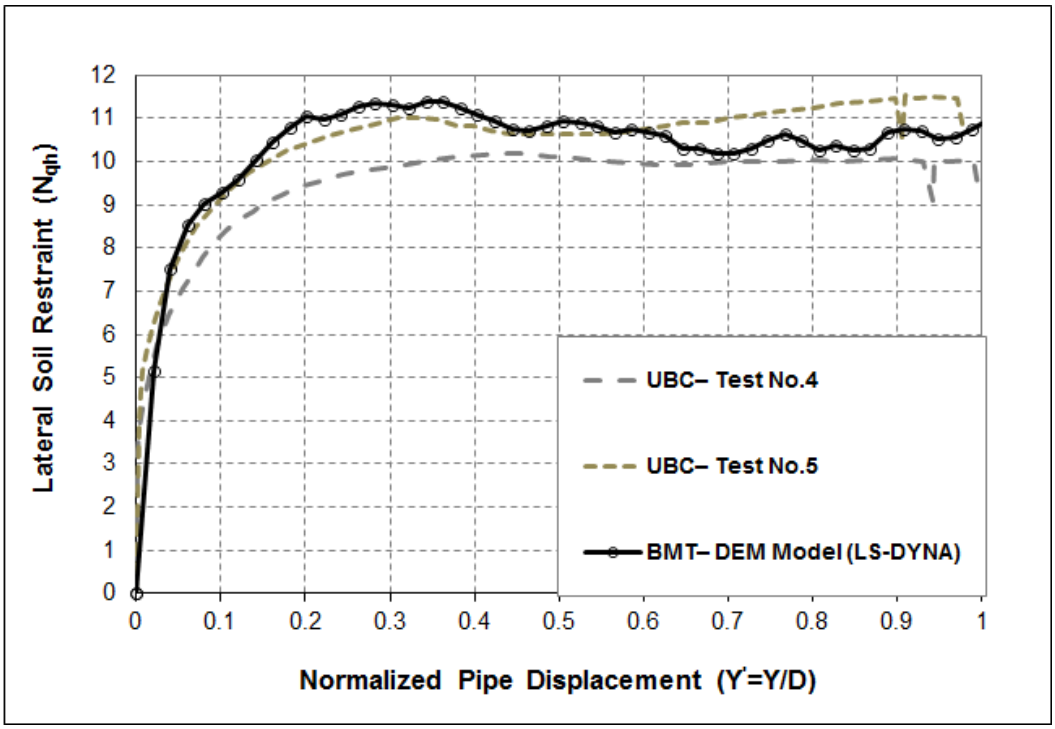

Figure 2.63: Comparison between Numerical Model Results and Test Results – Road Mulch Soil

2.9.5 Pipe-Soil Interaction Model Parameter Calibration

In the absence of site-specific soil properties, the pipe-soil force-displacement responses used in the DEM in LS-DYNA pipe-soil interaction model can be calibrated based on ASCE 1984, which are consistent with American Lifelines Alliance (ALA) 2001 [42] soil properties. These soil properties have been developed through experimentation and engineering judgment for typical soil types and, in many cases, are reasonable engineering representations for this type of geotechnical hazard assessment.

An NPS 24 (610 mm diameter) pipeline subjected to axial and lateral soil displacements were simulated in a large soil box measuring 4.0 m long by 4.0 m wide by 2.5 m high to predict the pipe-soil interaction forces. The simulations consisted of one axial pullout test and one lateral displacement test. The 24-inch pipe has a wall thickness of 0.375 inch (9.52 mm). The pipe was buried at the overburden ratio (H/D) of 2.46 in sand/clay till (ϕ'=30o and C'=5 kPa).

A 3D analysis of the experimental trial using LS-DYNA DEM was performed. The model (Figure 2.64) consists of soil particles and pipe shell elements reproducing the geometry of the physical trial. The soil mass in the tank is taken to be stress-free and have uniform properties in its initial state. The simulation loading is imposed in two steps. In the first step, gravitational acceleration is applied and sufficient time is allowed to ensure the soil stresses reach a steady state. In the second step, the pipe is pulled in along the pipe longitudinal axis for the axial load case and perpendicular to the pipe axis for the lateral loading case by imposing displacement boundary conditions to all nodes at the end of the pipe. Due to the loading and the relatively

The information contained herein is the copyright of and proprietary to BMT Fleet Technology Limited. Use of this information is governed by the legend on the cover page of this document."

short length of pipe modeled, the pipe can be assumed to be rigid. The interaction between the pipeline and the surrounding soil is modeled by Lagrangian contact in which slip and separation are allowed. The interface friction coefficient between the soil and pipe was estimated at 0.4.

Figure 2.65 illustrates the simulated displaced position of the pipe and the soil as the trial lateral displacement is applied to the pipe. Qualitatively, the displaced soil profile and flow history make intuitive sense and match the observed behaviors of experimental tests. The predicted soil restraint on a buried pipeline was compared to those estimated using the formulations presented in ASCE 1984/ALA 2001 [39, 42]. Figure 2.66 presents the comparison of ASCE/ALA and numerical force-displacement curves. For axial pipe movement, the results match the ASCE data well. For both ASCE and numerical force displacement, the failure load is about 18 kN/m obtained at the pipe displacement of about 5 mm to 7.5 mm.

Figure 2.67 presents the comparison of ASCE /ALA and numerical force-displacement curves. For lateral pipe movement, the maximum lateral soil resistance predicted by ASCE/ALA was 118 kN/m, at a pipe displacement of 72 mm. The ALA 2001 guidelines reported that although tests have indicated the maximum soil force on the pipeline decreases at large relative displacements, the guideline is based on the assumption that the soil force is constant once it reaches the maximum value. The maximum soil resistance predicted by the numerical model was 125 kN/m, at a soil displacement of 90 mm. The predicted force gradually decreases to 100 kN for relatively large deformations of 300 mm, This behavior was observed in the experimental results conducted by Trautmann and O'Rourke [43] and this large displacement behavior is not captured in the ALA simplified engineering idealization.

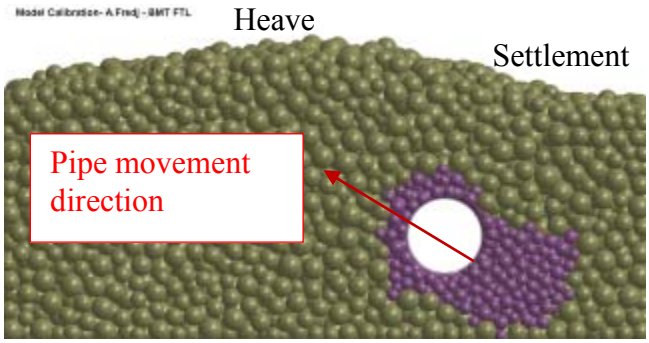

Figure 2.64: Pipe Movement and Soil Displacement

The information contained herein is the copyright of and proprietary to BMT Fleet Technology Limited. Use of this information is governed by the legend on the cover page of this document."

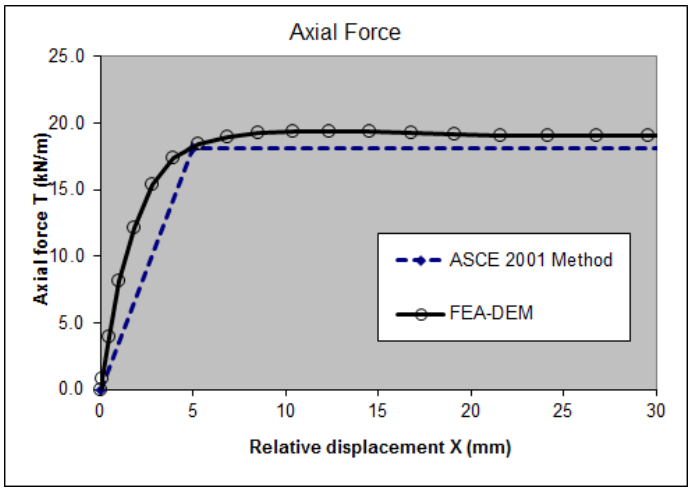

Figure 2.65: Axial Soil Force – Comparison between FEA (DEM) and ASCE 1984 / ALA 2001

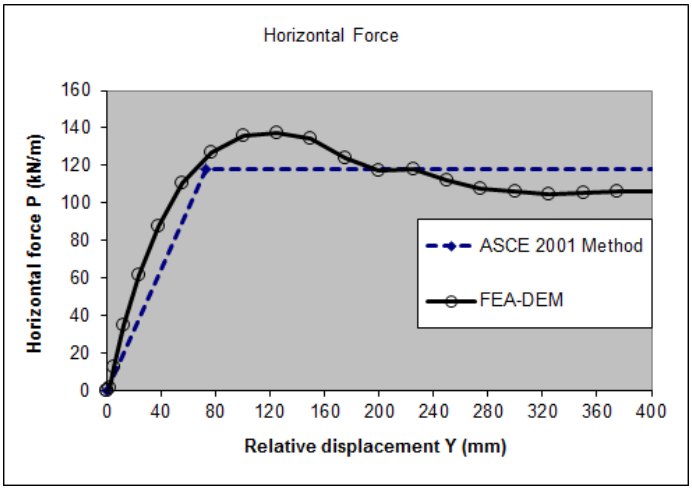

Figure 2.66: Lateral Soil Force – Comparison between FEA (DEM) and ASCE / ALA

2.9.6 Conclusion: Validation of DEM Model in LS-DYNA

This section has described the development and validation of a Discrete Element Method (DEM) modeling technique for assessing the performance of a pipeline subjected to large soil displacements. This analytic process made use of the LS-DYNA DEM Modeling Capabilities and considered a range of soil types (sand, clay, and gravel), dry and wet conditions and different soil movement scenarios. Figure 2.67 shows the pipe movement and soil deformation of pipeline load in wet clay soil using capillary forces. The pipe moves forward and upwards, and the soil behind the pipe did not deform with the pipe, so a void (cave) forms. The response differs from the example presented earlier in this report when the soil was less cohesive and as a result the soil tends to flow downward, around the pipe, to fill the void that forms at the back of the pipe. A summary of DEM input used in this cohesive soil example is listed in Table 2.9 for comparison with those used in the previous examples. This result illustrates the flexibility of the model in that it can simulate the differing soil and pipe responses, such as that exhibited in this case by the

The information contained herein is the copyright of and proprietary to BMT Fleet Technology Limited. Use of this information is governed by the legend on the cover page of this document."

soil void left in the wake of the pipe. The differing soil movement response has been shown to correlate with differences in pipe response (strain accumulation).

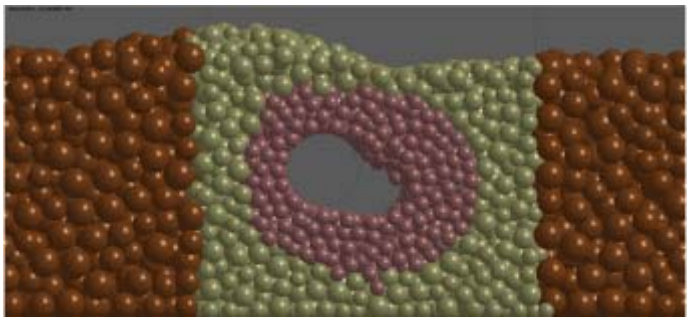

Figure 2.67: Soil Deformation of Wet Clay Soil

Table 2.9: Summary Parameters for DEM Model

DEM Parameters	Value
Radius (mm)	30 to 60
Friction Coefficient	0.3 to 0.5
Mass Density (kg/m3)	3000
Elastic Modulus (MPa)	200 to 300
Poison's Ratio	0.33

The ability of pipe-soil interaction modelling techniques to simulate the behavior and responses of numerous full-scale laboratory tests conducted at the University of British Columbia and others has been demonstrated. Given the positive outcome of the numeric predictions and experimental test comparisons, it has been concluded that the validated soil-structure interaction models are well suited for predicting pipeline response to various ground movements and could serve as an essential decision tool for geotechnical hazards.

2.10 Conclusion of Model Validation Studies

This report has described the development and validation of a 3D continuum modeling technique for assessing the performance of a pipeline system subjected to large soil displacements. This analytic process made use of the LS-DYNA SPH, ALE and DEM modeling capabilities and considered a range of soil types and soil movement scenarios.

The BMT numeric modelling results and the results from numerous full-scale laboratory tests conducted at Cornell University, the University of British Columbia and others compare very well overall. Only in one comparison case did the numeric modeling over-estimate the pipe longitudinal strain. This, however, is likely due to the disconnection of the strain gages during the experiment. Given the positive outcome of the numeric predictions and experimental tests comparisons, it can be concluded that the validated BMT soil-structure interaction model is well suited for predicting pipeline response to various ground movements and could serve as an essential decision tool for geotechnical hazards.

The information contained herein is the copyright of and proprietary to BMT Fleet Technology Limited. Use of this information is governed by the legend on the cover page of this document."

The SPH, ALE and DEM simulation processes continue to be developed by BMT. As such, further validation and engineering applications have been completed and documented. The model has proven useful in the design of slope remediation and maintenance activities for pipelines. The simulated pipeline behaviors have been used to assess interactions with active slope movement and evaluate pipeline strain demand and strain limit capacity (A, Fredj et al; 2008, 2010, 2011, 2012, 2014 capacity (A, Fredj et al; 2008, 2010, 2011, 2012, 2014 [19], [21], [22], [23], [24], [25], [26] and A. Dinovitzer et al; 2014 [20]). These engineering applications have further demonstrated the ability and utility of the pipe soil interaction tool to predict pipe response, support engineering decision making and contribute to geotechnical hazard mitigation.

The information contained herein is the copyright of and proprietary to BMT Fleet Technology Limited. Use of this information is governed by the legend on the cover page of this document."

3 PIPE LIMIT STATES

The slope movement will result in axial strain in the pipe. These strains are generally compressive at the toe of the slope and tensile at the top of the slope. Compressive strains may results in local buckling/wrinkling of the pipe in the compressive zone. The tensile strains may result in girth weld failure in the tensile strain zone.

The onset of local buckling is considered a serviceability limit state and can be evaluated using a number of limit state equations including those found in CSA Z662 [27]. In this standard, the limit state is considered when the load is secondary, such as displacement controlled ground movement. Although local buckling or wrinkling does not immediately result in loss of the integrity of the pressure boundary (leakage), the buckles/wrinkles make the pipe line segment prone to subsequent fatigue damage.

The sections that follow provide several approaches to evaluating the compressive strain limit, maximum allowable compressive strains. The objective of this project was to define the strain accumulation due to geotechnical hazards, the strain demand. In practice the strain demand is compared to the strain capacity (or resistance) of the pipeline segment as evaluated using any one of various limit state formulations. The strain capacity (limit states) presented in this report are used as reference points to illustrate the application of the project strain demand results. Other pipeline strain capacity (resistance) formulations are available and may be used in conjunction with the strain accumulation data developed in this project. To limit the scope of pipeline strain limit definition, not all of the limit state equations are reviewed in this this project.

3.1 Pipeline Compressive Strain Capacity CSA Z662 -2011

The ultimate longitudinal compressive strains may be determined based on empirical equations available in CSA Z662 standard [27].

$$\varepsilon_c^{crit} = 0.5\frac{t}{D} - 0.0025 + 3000\left[\frac{(P_i - P_e)D}{2tE_s}\right]^2 \qquad for\ \frac{(P_i - P_e)D}{2tF_y} < 0.4 \qquad \text{[Eq. 3.1]}$$

$$\varepsilon_c^{crit} = 0.5\frac{t}{D} - 0.0025 + 3000\left[\frac{0.4F_y}{E_s}\right]^2 \qquad for\ \frac{(P_i - P_e)D}{2tF_y} \geq 0.4 \qquad \text{[Eq. 3.2]}$$

Where:

ε_c^{crit} = ultimate compressive strain capacity of the pipe wall
t = pipe wall thickness (mm)
D = outside diameter (mm)
P_i = maximum internal design pressure (MPa)
P_e = minimum external hydrostatic pressure (MPa)
E_s = 207 000 MPa
F_y = effective specified minimum yield strength (MPa)

The critical strain is dependent on diameter-to-thickness ratio and internal pressure. The internal pressure or hoop stress increases pipe resistance to local buckling. The hoop stress is normalized by the elastic modulus in the proposed formulation.

The information contained herein is the copyright of and proprietary to BMT Fleet Technology Limited. Use of this information is governed by the legend on the cover page of this document."

It is recognized that it is not only the D/t ratio and internal pressure that influences wrinkling. The shape of the stress-strain curve and weld-induced imperfections are also very important. The CSA formulation does not consider all of these factors.

The maximum allowable compressive strains calculated according to CSA Z662-11 are shown in Table 3.1.

Table 3.1: Maximum Allowable Compressive Strain Calculated According to CSA Z662-11

Line #	OD inch (mm)	T inch (mm)	D/t	MOP ksi (MPa)	SMYS ksi (MPa)	Design factor	ε_{cr} (%)		
							Pressurized to MOP	Pressurised to 0.5 MOP	Unpressurised
1	30 (762)	0.31 (7.92)	96	1.02 (7.0)	70 (483)	0.7	0.58	0.39	0.27
2	40 (1016)	0.35 (9.52)	106	0.94 (6.5)			0.53	0.37	0.22

3.2 PRCI 2004 and University of Alberta Critical Buckling Strain Formula

Pipeline Research Council International (PRCI 2004) Guidelines [28] provides recommended allowable compressive strains for gas and liquid hydrocarbon pipelines. The PRCI 2004 compressive strains limit empirical equations (3.3 through 3.6) were originally developed by Researchers in the University of Alberta (U of A) (Das et al., 2000, 2006) [29] to determine the critical buckling strain based on extensive full scale pipe laboratory tests. The PRCI or U of A relations are provided for two types of typical pipeline stress-strain curves:

1. Exhibiting rounded shapes at yield.

2. Exhibiting yield plateau.

These empirical equations account for the yield to tensile ratio (Y/T), girth weld misalignment, D/t ratio and the effect of internal pressure, as shown below.

The compressive strain capacity based on the PRCI formula is judged to be realistic yet somewhat conservative.

1. For plain pipes with typical rounded material property curves

$$\varepsilon_c = 5.6 * \left(\frac{t}{D}\right)^{1.59} * \left(\frac{1}{1 - 0.868\left(\frac{P}{P_y}\right)}\right) * \left(\frac{E}{F_y}\right)^{0.854} * \left(1.27 - \left(\frac{imp}{t}\right)^{0.15}\right) \qquad [3.3]$$

The information contained herein is the copyright of and proprietary to BMT Fleet Technology Limited. Use of this information is governed by the legend on the cover page of this document."

2. For girth-welded pipes with typical rounded material property curves

$$\varepsilon_c = 43.7 * \left(\frac{t}{D}\right)^{1.72} * \left(\frac{1}{1 - 0.892\left(\frac{P}{P_y}\right)}\right) * \left(\frac{E}{F_y}\right)^{0.7} * \left(1.09 - \left(\frac{offset}{t}\right)^{0.0863}\right) \quad [3.4]$$

3. For plain pipes with a distinct yield plateau

$$\varepsilon_c = 40.4 * \left(\frac{t}{D}\right)^{2} * \left(\frac{1}{1 - 0.906\left(\frac{P}{P_y}\right)}\right) * \left(\frac{E}{F_y}\right)^{0.8} * \left(1.12 - \left(\frac{imp}{t}\right)^{0.15}\right) \quad [3.5]$$

4. For girth-welded pipes with a distinct yield plateau

$$\varepsilon_c = 106 * \left(\frac{t}{D}\right)^{2} * \left(\frac{1}{1 - 0.5\left(\frac{P}{P_y}\right)}\right) * \left(\frac{E}{F_y}\right)^{0.7} * \left(1.1 - \left(\frac{offset}{t}\right)^{0.09}\right) \quad [3.6]$$

Where

ε_c =critical buckling strain
t = nominal wall thickness
Offset = weld offset (assumed)
D = outside diameter (nominal value)
P_i = internal pressure
Py = yield pressure
E = young modulus

The PRCI equation includes girth weld factor defined as the weld offset normalized by the pipe wall thickness. The level of weld offset was based on actual measured data during full scale pipe laboratory tests, which had a range from 3% to 9.7% of the pipe wall thickness. Table 3.2 shows the allowable compressive strain limits calculated for the 30 inch (Line 1) and 40 inch (Line 2) using the PRCI 2004 equation for two offset/t ratios of 3% and 9.7% using equation 3.4. Table 3.3 shows the compressive strains limit calculated for plain pipe using equation 3.5 developed by PRCI.

The information contained herein is the copyright of and proprietary to BMT Fleet Technology Limited. Use of this information is governed by the legend on the cover page of this document."

Table 3.2: Compressive Strain Limits Calculated According to PRCI

OD mm (in)	T mm (in)	D/t	P (MPa)	Fy (MPa)	PY (MPa)	P/PY	ε (%) for offset/t	
							0.03	0.097
762 (30)	7.92	96	0	483	10	0	0.39	0.3
			3.93			0.35	0.57	0.44
			7.0			0.7	1.03	0.81
1016 (40)	9.52	106	0	483	9	0	0.33	0.25
			3.25			0.36	0.48	0.37
			6.5			0.72	0.91	0.71

Table 3.3: Compressive Strain Limits for Plain Pipe Calculated According to PRCI

OD (in)	T (in)	D/t	P (Mpa)	Fy (Mpa)	PY (Mpa)	P/PY	ε (%) for Imp (%)	
							2	3
762 (30)	7.92 (0.31)	96	0	483	10	0	0.46	0.44
			3.93			0.35	0.66	0.62
			7.86			0.7	1.16	1.1
1016 (40)	9.52 (0.35)	106	0	4.83	9	0	0.39	0.37
			3.25			0.36	0.56	0.54
			6.5			0.7	1.03	0.98

3.3 Tensile Strain Limit

The maximum allowable tensile strains are considered to be governed by the failure stress or strain state for a circumferential defect. This assessment was completed using a British Standard 7190 Level 2A failure assessment approach [30]. These strain limits were estimated by considering the axial pipe wall membrane strain that would cause a reference flaw to extend. The BS7910 failure assessment approach considering the potential for both ductile and brittle crack extension was used to define the membrane stress/strain state that would cause crack extension.

In developing the tensile strain limit, the following data and assumptions were considered:

- The pipe was assumed to have the minimum specified strength properties outlined in Table 3.4;
- The welds were assumed to overmatch the base material. Conservatively, the weld metal properties were assumed to be the same as the base material;

The information contained herein is the copyright of and proprietary to BMT Fleet Technology Limited. Use of this information is governed by the legend on the cover page of this document."

- The design flaw that was adopted was 0.5 mm, 1 mm and 2 mm deep, 50 mm long semi-elliptical surface flaw;

- The design flaw was assumed to be located at the weld toe. The stress concentrating effects of the weld toe defined in BS 7910 were applied considering a maximum weld width of 25 mm; and

- The pipe CTOD fracture toughness was assumed to be 0.05 mm. Based upon experience this represents low toughness (brittle) behavior.

The FlawCheck software was used to apply the BS7910 Level 2A assessment procedure to each pipe geometry and material combination (see Table 3.4) to define the pipe wall local membrane stress and strain state that would result in crack extension. The results of this assessment are listed in Table 3.4 below. The results presented below are consistent with the girth weld defect acceptance techniques adopted by API 579 and CSA Z662, as both of these standards have incorporated the BS 7910 procedure.

Table 3.4: Tensile Strain Limits: (a=0.5, 1 and 2 mm, 2c=50 mm, CTOD=0.05 mm)

Line	OD mm (in)	t mm (in)	D/t	Grade	Flaw Size mm (in)	Tensile Stress Limit σ_t MPa (ksi)	Tensile Strain Limit $\varepsilon_{t\,(\%)}$
1	762 (30)	7.92 (0.31)	96	X70	0.5	498	0.62
					1	473	0.43
					2	455	0.33
2	1016 (40)	9.52 (0.35)	106		0.5	504	0.7
					1	484	0.49
					2	464	0.38

The tensile strain limit was estimated from the tensile stress limit based upon the engineering stress-strain relationship developed for the minimum specified material properties presented in Table 4.1.

The information contained herein is the copyright of and proprietary to BMT Fleet Technology Limited. Use of this information is governed by the legend on the cover page of this document."

4 ILLUSTRATIVE SAMPLE GEOTECHNICAL HAZARD ASSESSMENT APPLICATIONS

4.1 Modeling of Landslide Hazard

The objective of this section is to complete three (3) lateral soil movement simulations considering three potential slope failures width to illustrate the impact of the problem parameters on the analysis results as part of Task 3, then complete a sensitivity study to define the relationship between problem parameters and the pipe strains developed in lateral soil movements and identify the trends.

Analyses were completed for the 30 and 40-inch diameter pipes to assess its response to lateral ground movement and to determine the structural integrity significance of ground movement induced strain demands. The analyses considered a total of seven (7) potential slope failures with a total estimated width of failure along the pipeline approximately 5 m, 10 m, 15 m, 20 m, 30 m, 40 m and 50 m.

The strain demand determined from the analysis was compared with the calculated strain limits defined in Sections 3 and 4 of CSA Z662, PRCI 2004 and BS 7910.

4.1.1 Summary of Inputs Required and Processes Modelled

The input parameters used in the modeling are summarized in Table 4.1 and Table 4.2.

Table 4.1: Input Parameters

Pipeline Parameters	Value(s)
Outside Diameter (mm)	762, 1016 (30 and 40- inch)
Wall Thickness (mm)	7.92, 952
D/t Ratio	96, 106
Material Grade	X70
Yield Strength, SMYS (MPa)	483
Ultimate Strength, SMTS (MPa)	565
Operating Pressure (0.6SMYS) (MPa)	7,6.5
Temperature Differential (^{0}C)	30
Soil	
C' (kPa)	7.8
Φ' (deg) for Clay Fill	28.8
Interface Friction angle (undrained/drained)	28
Soil Unit Weight (kN/m^3)	19
Average depth to pipe centerline (m)	1.85 m

The information contained herein is the copyright of and proprietary to BMT Fleet Technology Limited. Use of this information is governed by the legend on the cover page of this document."

4.1.1.1 Landslide Hazard Finite Element Model Description

4.1.1.2 Introduction

Soil-pipe interaction numerical simulation requires large deformation analysis capability; this requirement is difficult to meet for Lagrangian-based codes. LS-DYNA offers the possibility to use continuum Multi-material Arbitrary Lagrangian Eulerian (MM-ALE) finite element model and continuum Smooth Particle Hydrodynamic (SPH) capabilities for modeling materials that undergo large deformations.

In this study, the soil-pipe interaction under soil movement is investigated with particular attention to both the soil constitutive model and the use of the LS-DYNA SPH modeling technique.

4.1.1.3 Continuum SPH Model

LS-DYNA 971 explicit was used to produce a 3D continuum model using the SPH method. The SPH method utilizes a meshless Lagrangian method to represent soils. The method does not require element meshing (mesh-less) and can handle extreme material distortion. In the SPH method, the soil material is treated as particles that have their masses smoothed in space. The coupling between the SPH grid points (soil) and the pipe is accomplished through a normal Lagrangian contact definition.

The analyses use the displacement control method similar to the shear box test where the pipe is embedded into three adjacent boxes, where the middle of the three soil boxes is displaced relative to the others as shown in Figures 4.1 and 4.2. Figures 4.2 and 4.3 show an example of the middle box movement relative to the others at crossing angle of 90° and 45° to simulate lateral ground movement (perpendicular to the pipeline) and ground movement at crossing angle of 45°.

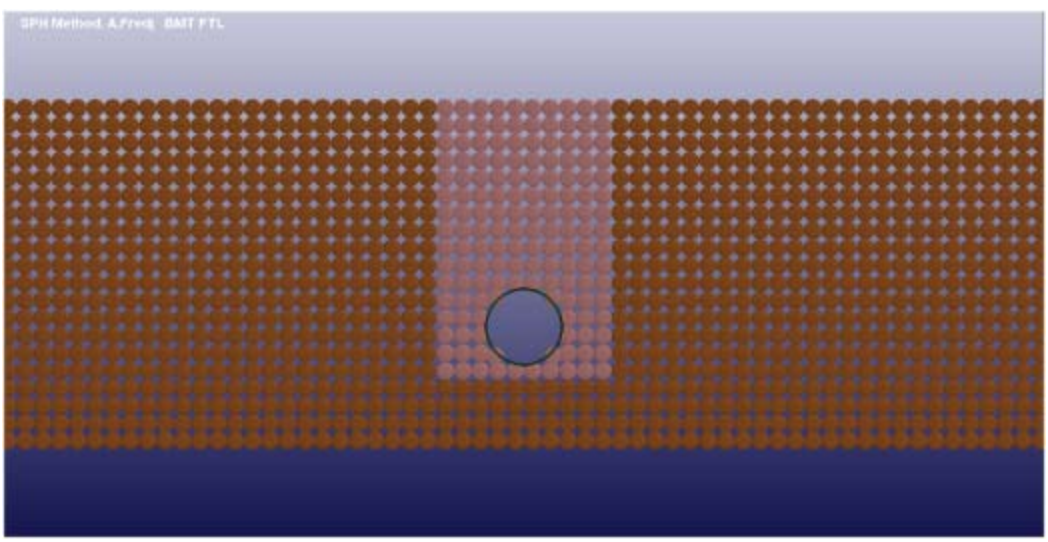

Figure 4.1: Illustration of the SPH FE Model Including the Pipe-Side View

The information contained herein is the copyright of and proprietary to BMT Fleet Technology Limited. Use of this information is governed by the legend on the cover page of this document."

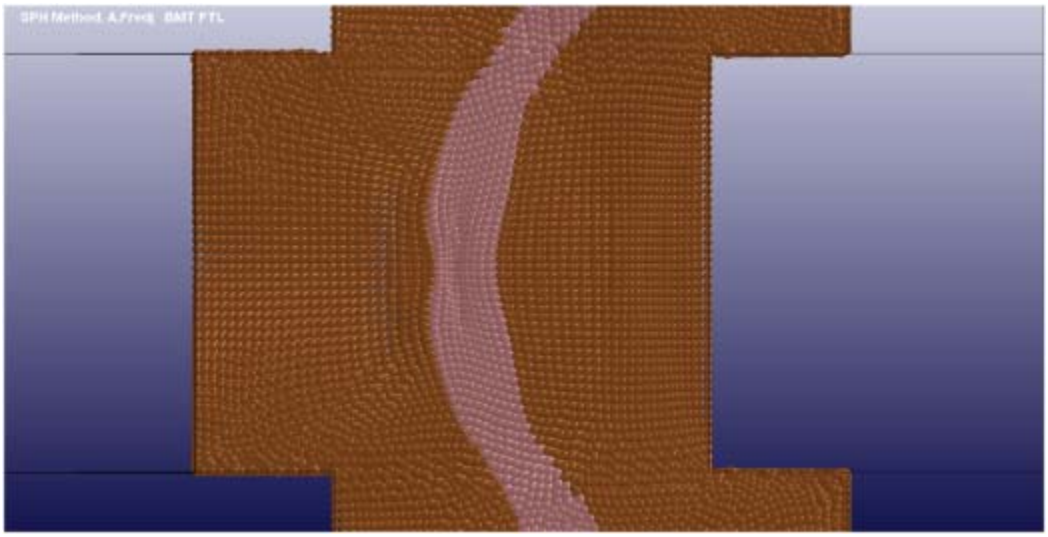

Figure 4.2: Illustration of the SPH FE Model: Lateral Ground Movement

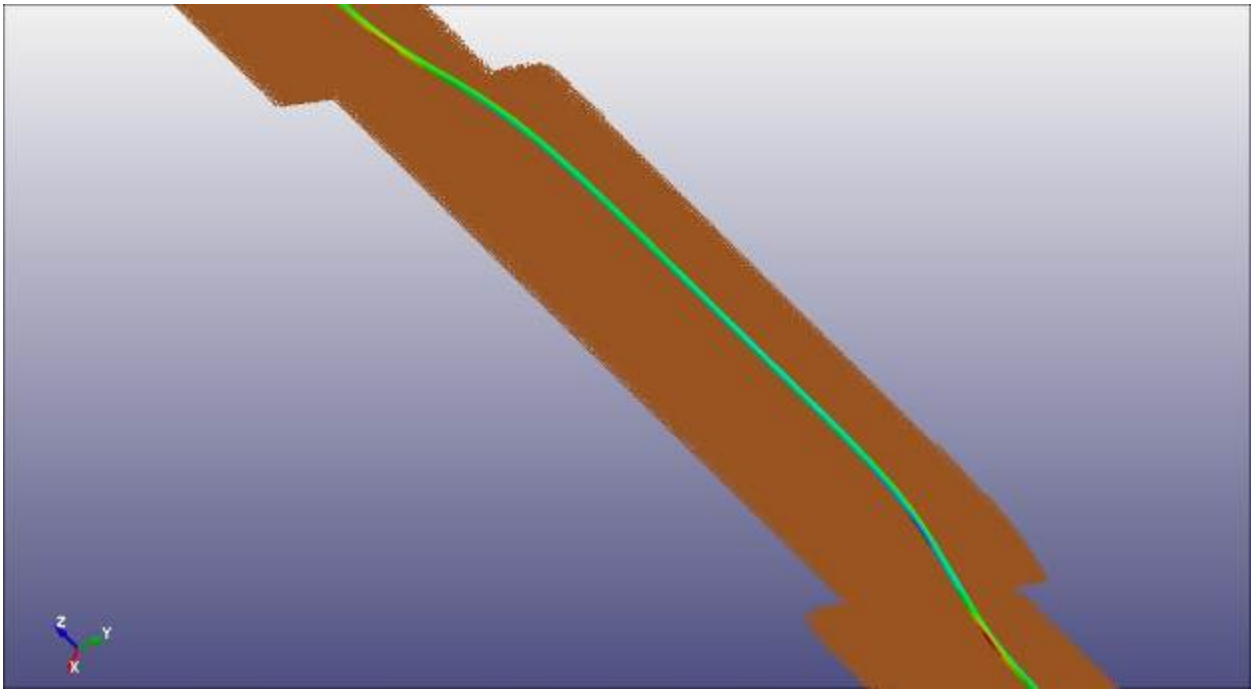

Figure 4.3: Illustration of the SPH FE Model: Ground Movement at Crossing Angle of 45°

The information contained herein is the copyright of and proprietary to BMT Fleet Technology Limited. Use of this information is governed by the legend on the cover page of this document."

Loading Sequence

The soil mass in the simulation is taken to be stress free prior to the simulation and the simulation loading is imposed in three steps. In the first step, the gravitational acceleration is applied and sufficient time is allowed to ensure that the soil stress reaches a stationary state. In the second load step, an operating pressure equal to the MOP (see Table 4.2) and a temperature differential of 30°C were applied. In the third load step, the moving (unstable) soil mass was moved at a desired crossing angle.

4.1.1.4 Pipe Properties

Table 4.2 lists the material properties used. The full stress-strain curves of the pipe materials were incorporated in the finite element modeling. Figure 4.4 shows the stress for X70 materials. This curve was developed based upon the minimum specified material properties from API X70 material.

Table 4.2: Input Parameters Used for the Analyses

Line	OD inch (mm)	t (mm)	D/t	MOP ksi (MPa)	Grade	SMYS(1) ksi (MPa)	SMTS(1) ksi (MPa)	(Y/T) Ratio
1	30 (762)	0.31 (7.92)	96	1.02 (7.0)	X70	70 (483)	81.9 (565)	0.85
1	40 (1016)	0.35 (9.52)	106	0.94 (6.5)				

Note1: Tensile Requirements per minimum specified values from Grade X70

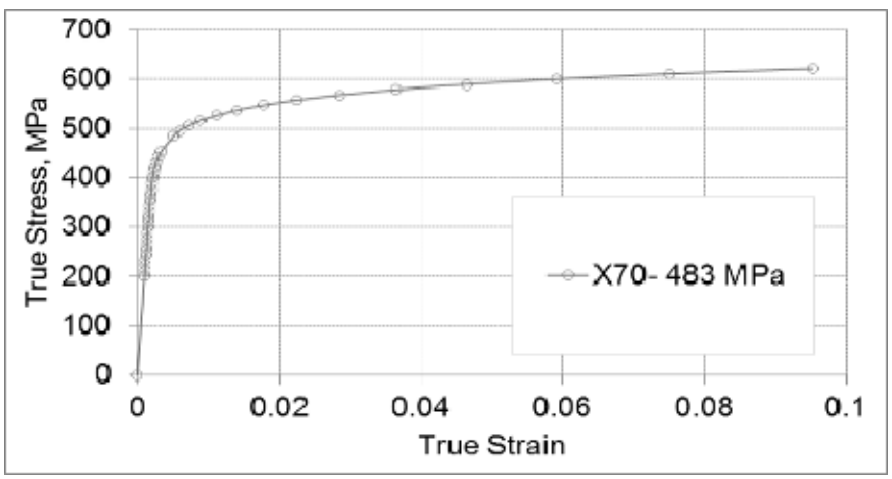

Figure 4.4: True Stress-Strain Curves for X70 (483 MPa) Materials

4.1.1.5 Soil Material Model

LS-DYNA offers the possibility to use a large range of material types that can be applied to objects within the simulation. For the present analyses, the soil is modelled using a two surface plasticity model, where the shear failure surface and pressure-volume strain (compaction) surface are independent. In LS-DYNA, this constitutive model is known as material model 5, or the "soil and foam model". The soil and foam model is the most basic of the geo-material models available in

The information contained herein is the copyright of and proprietary to BMT Fleet Technology Limited. Use of this information is governed by the legend on the cover page of this document."

LS-DYNA. It is also the oldest and, therefore, has had a considerable amount of user experience, and feedback. It is also considered to be quite robust. The shear failure criterion for the soil and foam model has a mean stress (pressure) dependent strength, typical of geo-materials, of the form:

$$J_2 = a_0 + a_1 P + a_2 P^2 \qquad \text{[Eq. 4.1]}$$

where P is the mean stress and coefficients, a_0, a_1 and a_2, are determined by calibrating (fitting) the model to tri-axial compression data. The relative value of the coefficients a_0, a_1, and a_2 determine the shape of the shear failure envelope, elliptical for a_2 less than zero, parabolic for a_2 equal zero and hyperbolic for a_2 greater than zero.

The effects of the excess pore water pressures were not considered in this modeling exercise. The simulations were also limited to a single phase material response.

The soil material model properties used in the continuum model are summarized in Table 4.3. This data was developed based upon soil properties obtained from soil study performed by Applied Research Associates, Inc. (ARA) under contract to NASA Langley Research Center's [44], charged with evaluating Crew Exploration Vehicle (CEV) terrain landing Design. The soil types considered are CSW or Carson Sink wet clay of Nevada, classified as clay of low to medium plasticity. The Unified Soil Classification System Symbol (USCS) is CL. The softness of the soil is attributed to fat clay and moisture content. Figure 4.5 shows a picture of Carson Sink soil and Figure 4.6 shows the soil volume strain versus mean stress.

Table 4.3: Soil Material Model Properties Used in the Continuum Model

Soil Property	Value
C' (kPa)	7.8 [1.16 psi]
Φ' (deg)	28.8
Soil unit weight (kN/m^3)	18
Shear Modulus (MPa)	3.58 [520 psi]
Yield surface Coefficient, a_0 (kPa)^2	93 [1.97 psi^2]
Yield surface Coefficient, a_1 (kPa)	12.8 [1.86 psi]
Yield surface Coefficient, a_2	0.43
Moisture content	12%

The information contained herein is the copyright of and proprietary to BMT Fleet Technology Limited. Use of this information is governed by the legend on the cover page of this document."

Figure 4.5: Photo of Carson Sink Soil (NASA 2008)

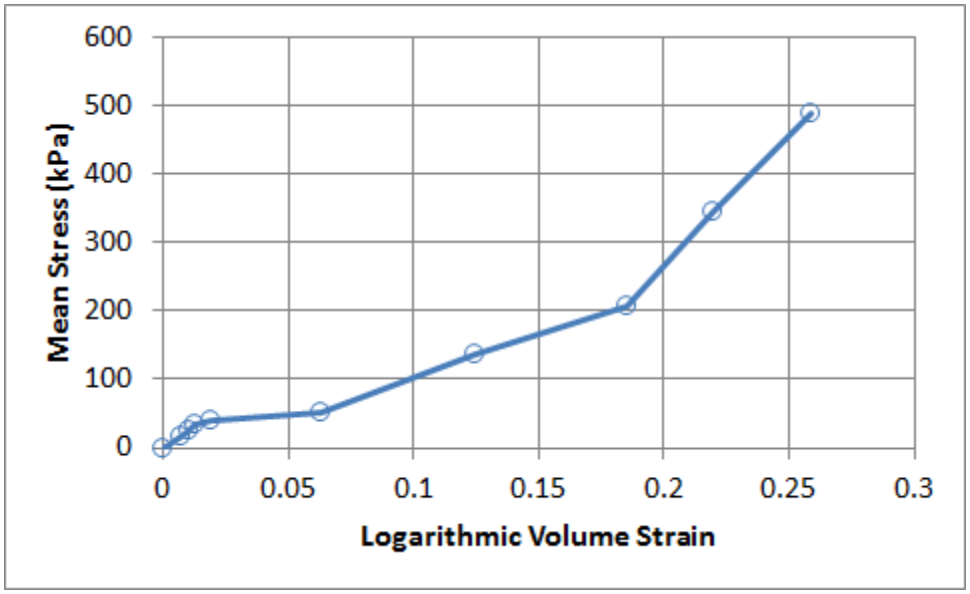

Figure 4.6: Volume Strain vs. Mean Stress (NASA 2008)

The information contained herein is the copyright of and proprietary to BMT Fleet Technology Limited. Use of this information is governed by the legend on the cover page of this document."

4.1.2 Structural Analyses for a 30-inch Pipeline

Analyses were completed for the 30-inch pipe (Line 1) to assess its response to lateral ground movement and to determine the structural integrity significance of ground movement induced strain demands. The analyses considered seven potential ground movement failures with a total estimated width of failure perpendicular to the pipeline including:

- Case1: W=5 m
- Case2: W=10 m
- Case3: W=15 m
- Case4: W=20 m
- Case5: W=30 m
- Case6: W=40 m
- Case7: W=50 m

4.1.2.1 30-Inch Diameter Line Results

The following Figures illustrate the SPH Finite element model and snapshots of the finite element model output.

- Figure 4.7 illustrates the response of pressurized pipeline subjected to ground movement for Case1 (W=10 m). Figure 4.7 shows also the axial strains distribution (blue color is compressive and red is tensile strain); in this Figure, the soil above the pipe is hidden so the pipe deformation can be visualized.
- Figure 4.8 illustrates the response of pressurized pipeline subjected to ground movement for Case2 (W=20 m). Figure 4.8 shows also the axial strains distribution (blue color is compressive and red is tensile strain); in this Figure, the soil above the pipe is hidden so the pipe deformation can be visualized.
- Figure 4.9 illustrates the response of pressurized pipeline subjected to ground movement for Case3 (W=40 m). Figure 4.9 shows also the axial strains distribution (blue color is compressive and red is tensile strain); in this Figure, the soil above the pipe is hidden so the pipe deformation can be visualized
- Figure 4.10 illustrates an example of ground movement profile at different levels of movements considering movement width of 20 m (Case2). The soil displacements illustrated in this Figure illustrate that the soil moves uniformly up to a shear zone at the limits of the displacement zone.
- Figure 4.11 illustrates an example of pipeline deformation profile at different levels of ground movement considering ground movement width of 20 m (Case2). These results, compared with those in Figure 4.10, illustrate that the pipe does not follow the same profile since some of the soil flows around the pipe.
- Figure 4.12 shows the true axial strain at 3'oclock and 9 o'clock position along the pipeline for Case1 (W=10 m) considering soil movement of 1.93 m
- Figure 4.13 shows the true axial strain at 3'oclock and 9 o'clock position along the pipeline for Case2 (W=20 m) considering soil movement of 1.93 m
- Figure 4.14 shows the true axial strain at 3'oclock and 9 o'clock position along the pipeline for Case3 (W=40 m) considering soil movement of 1.93 m

The information contained herein is the copyright of and proprietary to BMT Fleet Technology Limited. Use of this information is governed by the legend on the cover page of this document."

The analysis has demonstrated that pipeline parameters and operating loading have a significant effect on the pipeline response and integrity. For a given pipe geometry and operating conditions, there is a critical lateral soil movement width that maximizes pipe bending moments and strains. The critical soil movement width is about 10 m for the 30 inch pipeline.

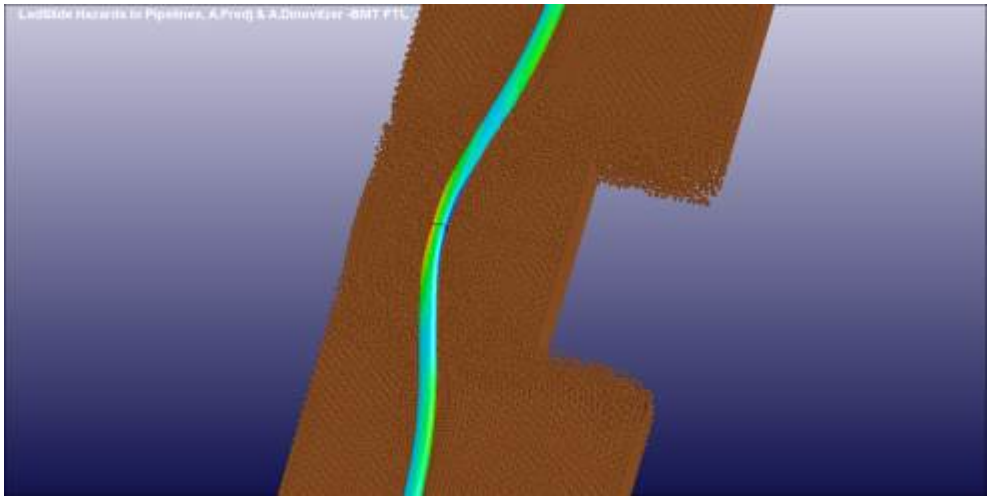

Figure 4.7: Line 1 - Pipe Deformation & Axial Strain (Blue Compressive and Red is Tensile) For Case1: Soil Movement of 4.9 m & Width=10 m

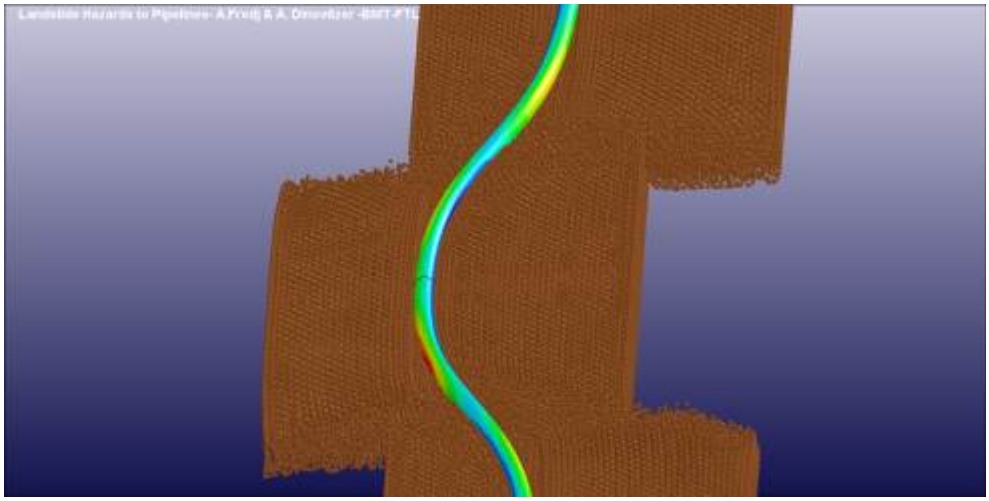

Figure 4.8: Line 1 - Pipe Deformation & Axial Strain (Blue Compressive and Red is Tensile) For Case2: Soil Movement of 4.9 m & Width=20 m

The information contained herein is the copyright of and proprietary to BMT Fleet Technology Limited. Use of this information is governed by the legend on the cover page of this document."

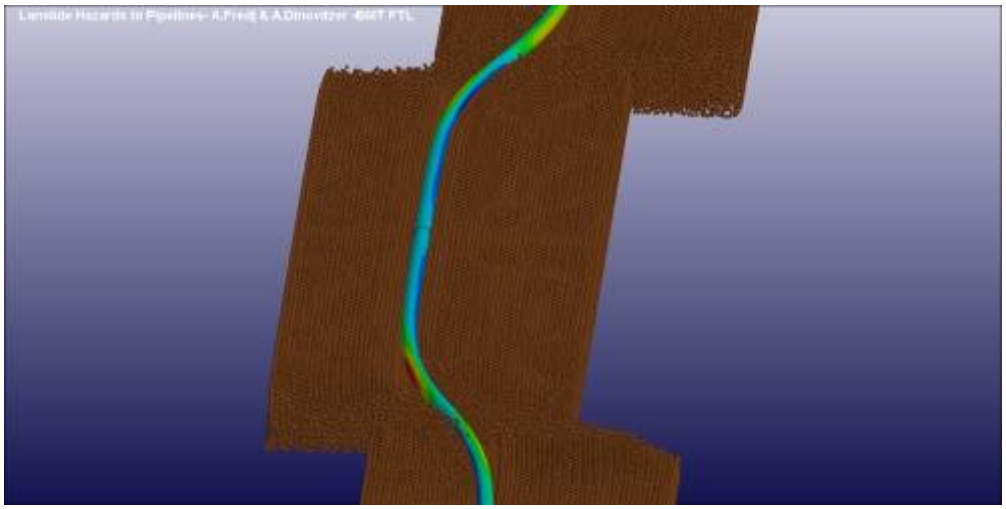

Figure 4.9: Line 1 - Pipe Deformation & Axial Strain (Blue Compressive and Red is Tensile) For Case3: Soil Movement of 4.9 m & Width=40 m

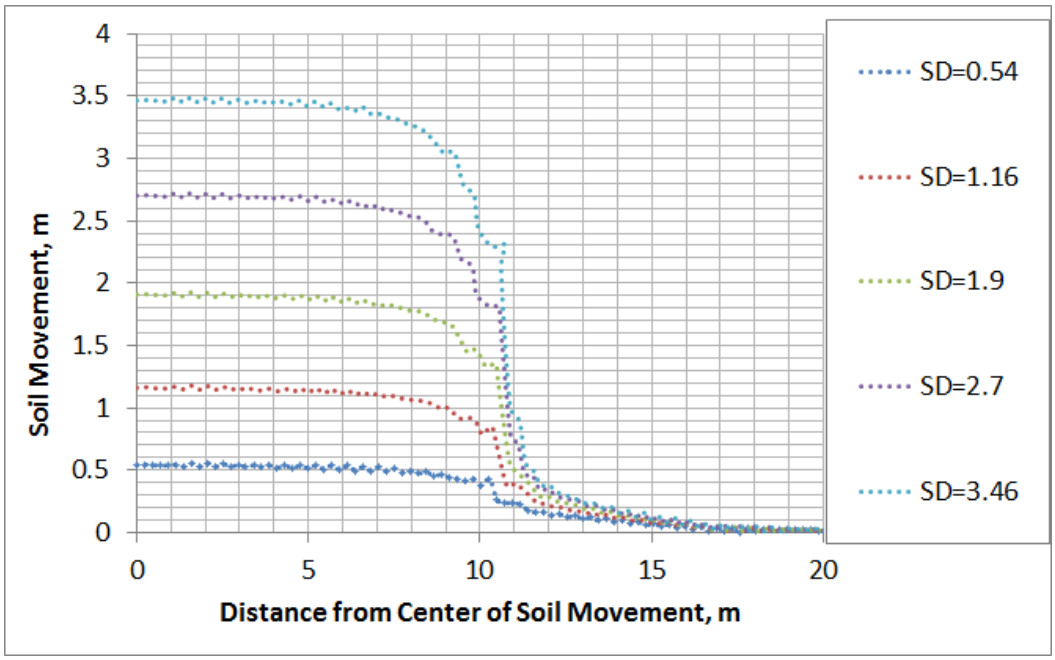

Figure 4.10: Line 1 - Ground Movement Profiles at Different Levels of Soil Movement for Case2: W=20 m

The information contained herein is the copyright of and proprietary to BMT Fleet Technology Limited. Use of this information is governed by the legend on the cover page of this document."

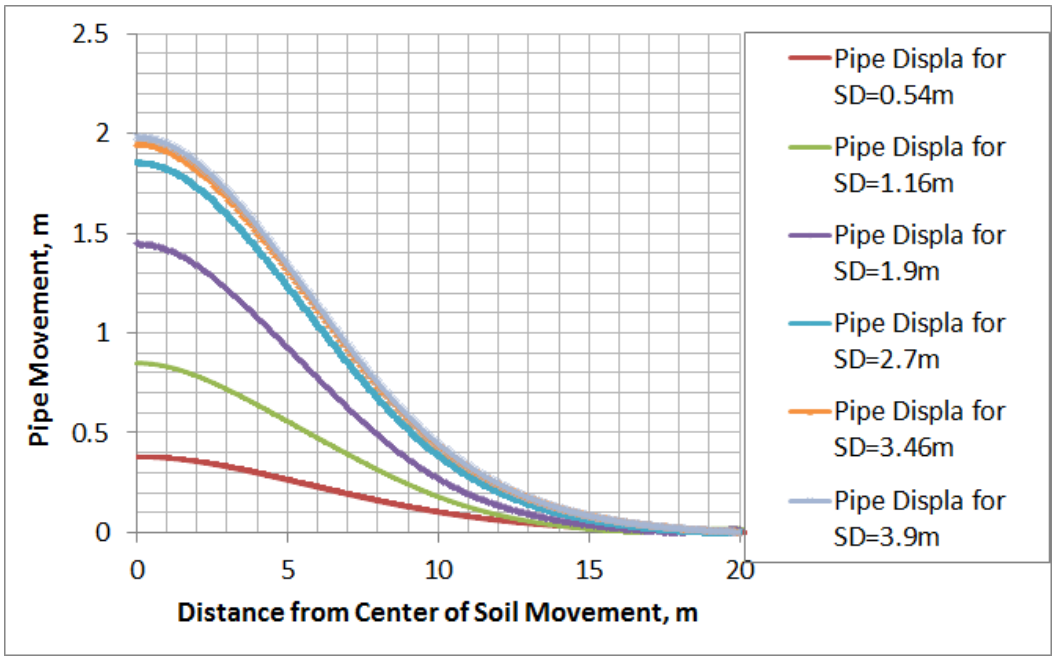

Figure 4.11: Line 1 - Pipe Movement Profiles at Different Levels of Soil Movement for Case2: W=20 m

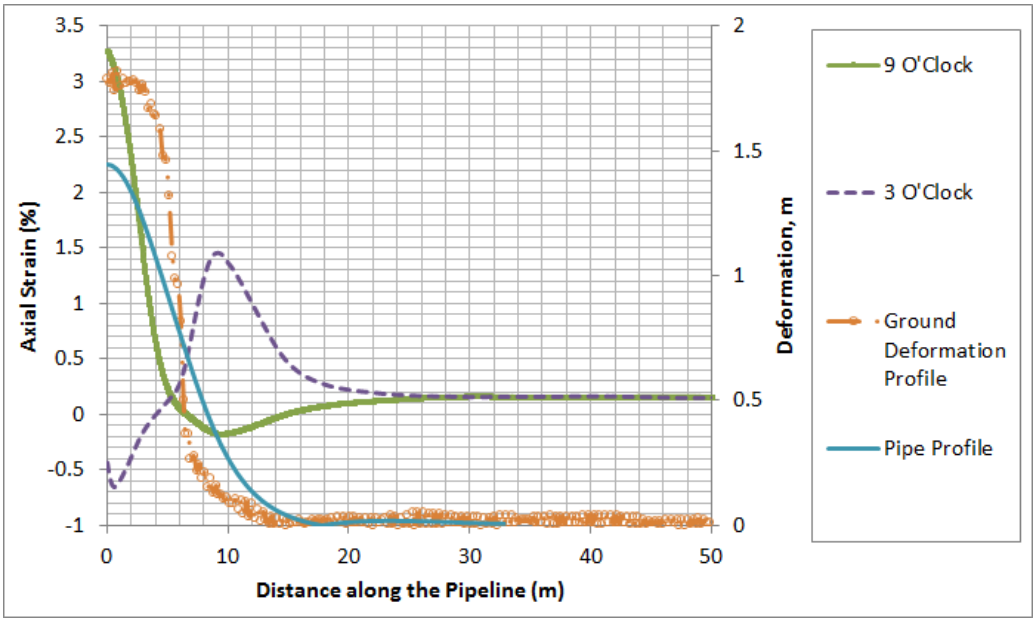

Figure 4.12: Line 1 - Axial Strain & Pipe and Ground Movement Profiles for Case1: W=10 m Considering Soil Movement of 1.93 m

The information contained herein is the copyright of and proprietary to BMT Fleet Technology Limited. Use of this information is governed by the legend on the cover page of this document."

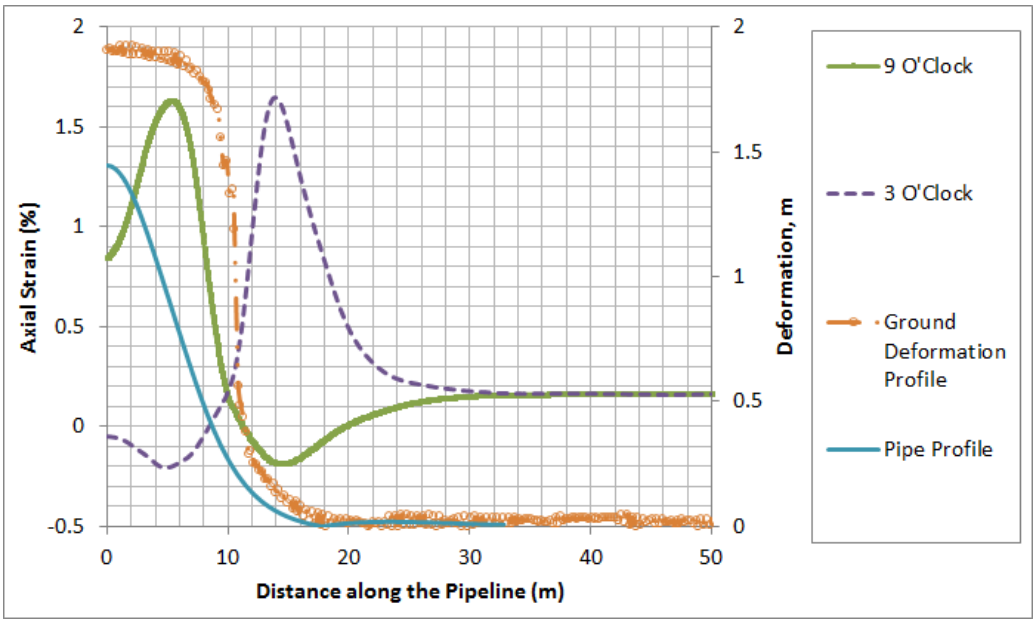

Figure 4.13: Line 1 - Axial Strain & Pipe and Ground Movement Profiles for Case2: W=20 m Considering Soil Movement of 1.93 m

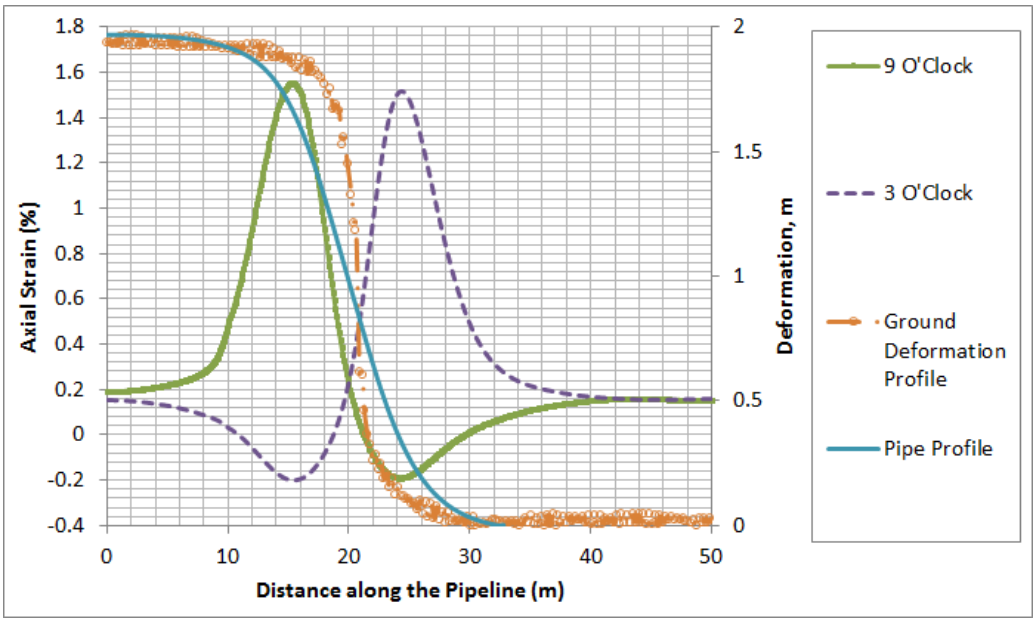

Figure 4.14: Line 1 - Axial Strain & Pipe and Ground Movement Profiles for Case3: W=40 m Considering Soil Movement of 1.93 m

4.1.2.2 Comparison with Strain Criteria and Safety Envelopes

The objective was to develop a simple method to define the effects of operational and geotechnical loads on liquid and gas pipeline systems to support decision making regarding

The information contained herein is the copyright of and proprietary to BMT Fleet Technology Limited. Use of this information is governed by the legend on the cover page of this document."

threat severity or repair scheduling. This tool incorporated in strain based design and assessment to facilitate the consideration of complex loading scenarios inducing significant flexural loads, including pipeline subsidence or lowering, and ground movements inducing lateral pipeline movements.

The results of the finite element analyses were interpolated, to produce an envelope defining the combinations of ground displacement and width where the pipe was safe and not safe. Failure or "not safe Pipe" was presumed to occur if the axial strains (tensile and/or compressive strains) at any location exceeded strain limits defined from BS 7910, CSA-Z662 and PRCI 2004.

4.1.2.2.1 Tensile Strain Criteria and Safety Envelopes

The strain demand determined from the analysis was compared with the calculated strain limits defined from the guidance provided by Sections 4 and 5 of BS 7910 for tensile strain, CSA-Z662 and PRCI 2004 for compressive strain.

Figures 4.15 and 4.16 show the axial tensile and compressive strains in the 30-inch pipe as a function of the centerline of lateral soil displacement for various lateral soil widths [5–50 m]. The results were presented in Table 4.4 through Table 4.6. It was found that:

- Case1: W=5 m
  - the tensile strain related failure limits were reached for ground displacement ranging from 0.3 m to 0.44 m considering flaw size of 2 mm, 1 mm and 0.5 mm, respectively;
  - CSA-Z662 and PRCI 2014 compressive strain related failure limits were reached for ground displacement ranging from 1.5 m to 1.6 m for pipeline operating at 0.5 maximum operation pressure (MOP). The allowable soil displacement range increases to 2 to 2.9 m when the pipe is pressurized to MOP.
- Case2: W=10 m
  - the tensile strain related failure limits were reached for ground displacement ranging from 0.3 m to 0.44 m considering flaw size of 2 mm, 1 mm and 0.5 mm, respectively;
  - CSA-Z662 and PRCI 2014 compressive strain related failure limits were reached for ground displacement ranging from 1.39 m to 1.5 m for pipeline operating at 0.5 maximum operation pressure (MOP). The allowable soil displacement range increases to 1.65 to 1.98 m when the pipe is pressurized to MOP.
- Case3: W=15 m
  - the tensile strain related failure limits were reached for ground displacement ranging from 0.36 m to 0.57 m considering flaw size of 2 mm, 1 mm and 0.5 mm, respectively;

The information contained herein is the copyright of and proprietary to BMT Fleet Technology Limited. Use of this information is governed by the legend on the cover page of this document."

- CSA-Z662 and PRCI 2014 compressive strain related failure limits were reached for ground displacement ranging from 2.09 m to 2.25 m for pipeline operating at 0.5 maximum operation pressure (MOP). The allowable soil displacement range is higher than 2.9m when the pipe is pressurized to MOP.

- Case4: W=20 m
  - the tensile strain related failure limits were reached for ground displacement ranging from 0.4 m to 0.67 m considering flaw size of 2 mm, 1 mm and 0.5 mm, respectively;
  - CSA-Z662 and PRCI 2014 compressive strain related failure limits were reached for ground displacement ranging from 2.09 m to 2.25 m for pipeline operating at 0.5 maximum operation pressure (MOP). The allowable soil displacement range is higher than 3 m when the pipe is pressurized to MOP.

- Case5: W=30 m
  - the tensile strain related failure limits were reached for ground displacement ranging from 0.4 m to 0.71 m considering flaw size of 2 mm, 1 mm and 0.5 mm, respectively;
  - CSA-Z662 and PRCI 2014 compressive strain related failure limits were reached for ground displacement ranging from 2.09 m to 2.25 m for pipeline operating at 0.5 maximum operation pressure (MOP). The allowable soil displacement range is higher than 3 m when the pipe is pressurized to MOP.

- Case6: W=40 m
  - the tensile strain related failure limits were reached for ground displacement ranging from 0.46 m to 0.72 m considering flaw size of 2 mm, 1 mm and 0.5 mm, respectively;
  - CSA-Z662 and PRCI 2014 compressive strain related failure limits were reached for ground displacement ranging from 2.09 m to 2.25 m for pipeline operating at 0.5 maximum operation pressure (MOP). The allowable soil displacement range is higher than 3 m when the pipe is pressurized to MOP.

- Case7: W=50 m
  - the tensile strain related failure limits were reached for ground displacement ranging from 0.5 m to 0.72 m considering flaw size of 2 mm, 1 mm and 0.5 mm, respectively;
  - CSA-Z662 and PRCI 2014 compressive strain related failure limits were reached for ground displacement ranging from 2.09 m to 2.25 m for pipeline operating at 0.5 maximum operation pressure (MOP). The allowable soil displacement range is higher than 3 m when the pipe is pressurized to MOP.

The results were interpolated, to produce an envelope defining the combinations of ground displacement and width where the pipe was safe and not safe. Failure “not safe pipe” was presumed to occur if the tensile strain at any location exceeded strain limits.

The information contained herein is the copyright of and proprietary to BMT Fleet Technology Limited. Use of this information is governed by the legend on the cover page of this document."

Figure 4.17 shows a set of pipe safety envelopes for BS7910 tensile strain limits, considering a flaw size of 0.5mm, 1mm and 2mm. Figure 4.18 shows a set of pipe safety envelopes for CSA-Z662 and PRCI compressive strain limits. The results show the importance of ground soil movement width. It shows that the critical soil movement width that maximizes pipe bending moments and strains are about 5 m to 10 m for the 30 inch pipe.

The results are very sensitive to the assumption made regarding the key analysis parameters. A sensitivity analysis is being carried to define "safety envelopes" for the case where pipe is loaded by lateral ground movement. Safety envelopes were defined with respect to the combination of ground displacement width for various soil strengths, pipe geometry (D/t), steel grade and pipe to soil coefficient of friction.

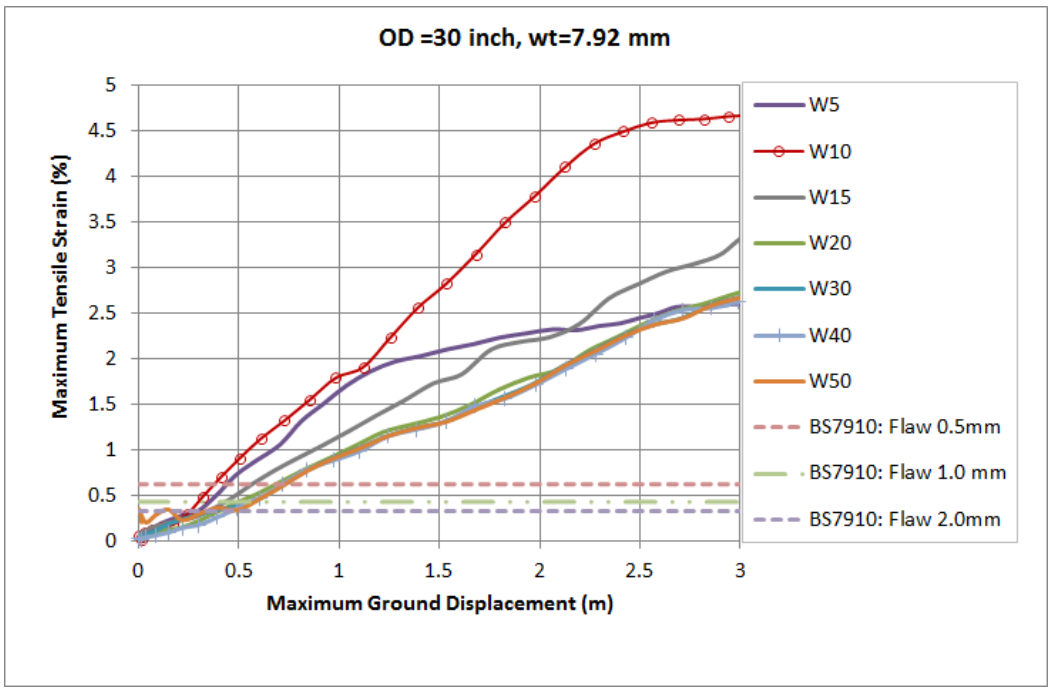

Figure 4.15: Line 1 - Maximum Tensile in the Pipe vs. Ground Movement Widths: [5 - 50m]

The information contained herein is the copyright of and proprietary to BMT Fleet Technology Limited. Use of this information is governed by the legend on the cover page of this document."

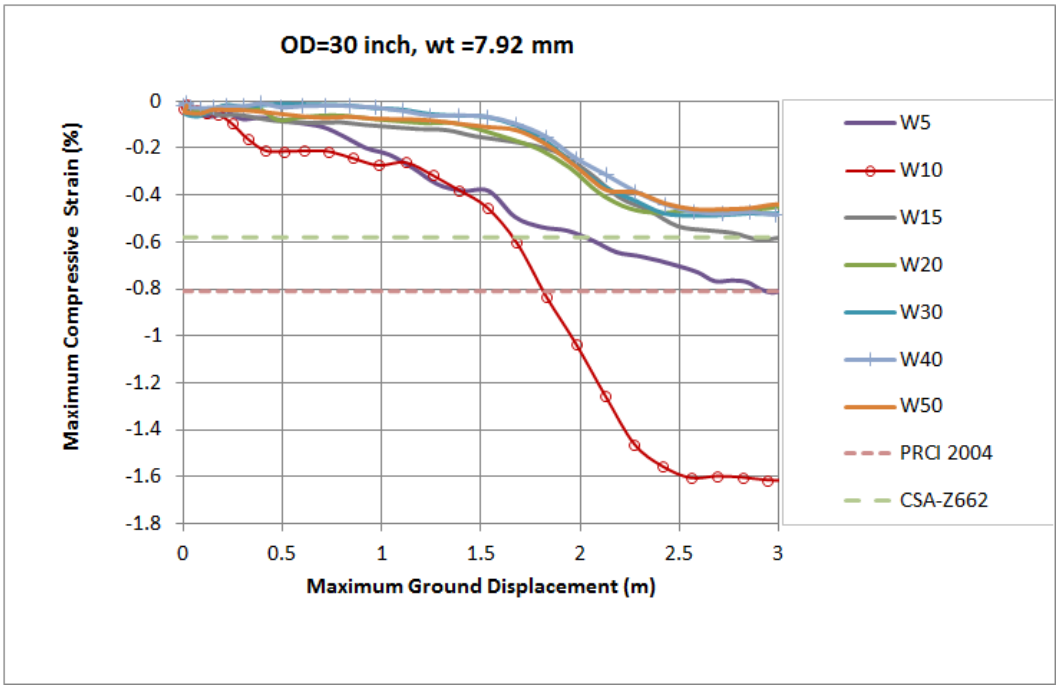

Figure 4.16: Maximum Compressive Strain in the Pipe vs. Ground Movement: Widths [5-50 m]

Table 4.4: Line 1 - Required Ground Displacement to Cause Tensile Strain Capacity

Flaw Size	Strain Limit BS7910	Required Ground Displacement						
		Ground Movement Width (m)						
mm	%	W5	W10	W15	W20	W30	W40	W50
0.5	0.62	0.44	0.42	0.57	0.67	0.71	0.72	0.72
1	0.43	0.34	0.32	0.42	0.5	0.54	0.56	0.6
2	0.33	0.3	0.26	0.36	0.4	0.42	0.46	0.5

Table 4.5: Line 1 - Required Ground Displacement to Cause Compressive Strain Capacity - CS-Z662

Pressure	Strain Limit CSA-Z662	Required Ground Displacement						
		Ground Movement Width (m)						
	%	W5	W10	W15	W20	W30	W40	W50
0.5 MOP	0.39	1.54	1.39	2.09	2.1	2.2	2.28	2.3
MOP	0.57	2	1.65	2.9	3	3.2	3.3	3.36

The information contained herein is the copyright of and proprietary to BMT Fleet Technology Limited. Use of this information is governed by the legend on the cover page of this document."

Table 4.6: Line 1 - Required Ground Displacement to Cause Compressive Strain Capacity - PRCI -2004

Pressure	Strain Limit PRCI-2004 (offset/t=0.097)	Required Ground Displacement						
		Ground Movement Width (m)						
	%	W5	W10	W15	W20	W30	W40	W50
0.5 MOP	0.44	1.6	1.5	2.25	2.25	2.34	2.42	2.5
MOP	0.81	2.9	1.98	>3.5	>3.5	>3.5	>3.5	>3.5

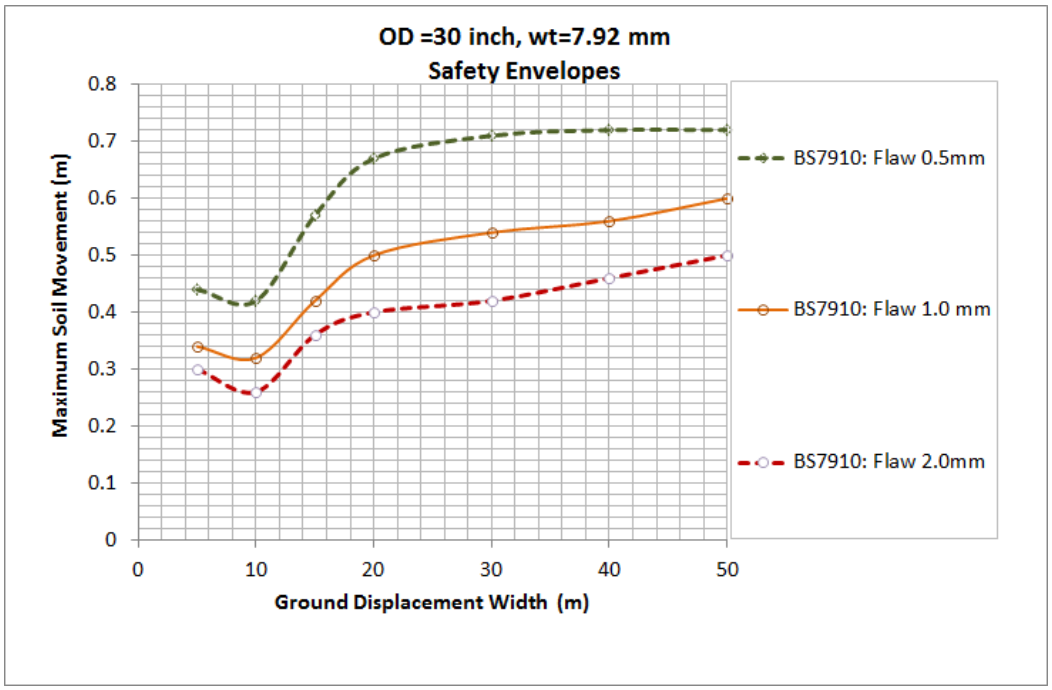

Figure 4.17: Line 1 - Safety Envelopes: Tensile Strain Limit

The information contained herein is the copyright of and proprietary to BMT Fleet Technology Limited. Use of this information is governed by the legend on the cover page of this document."

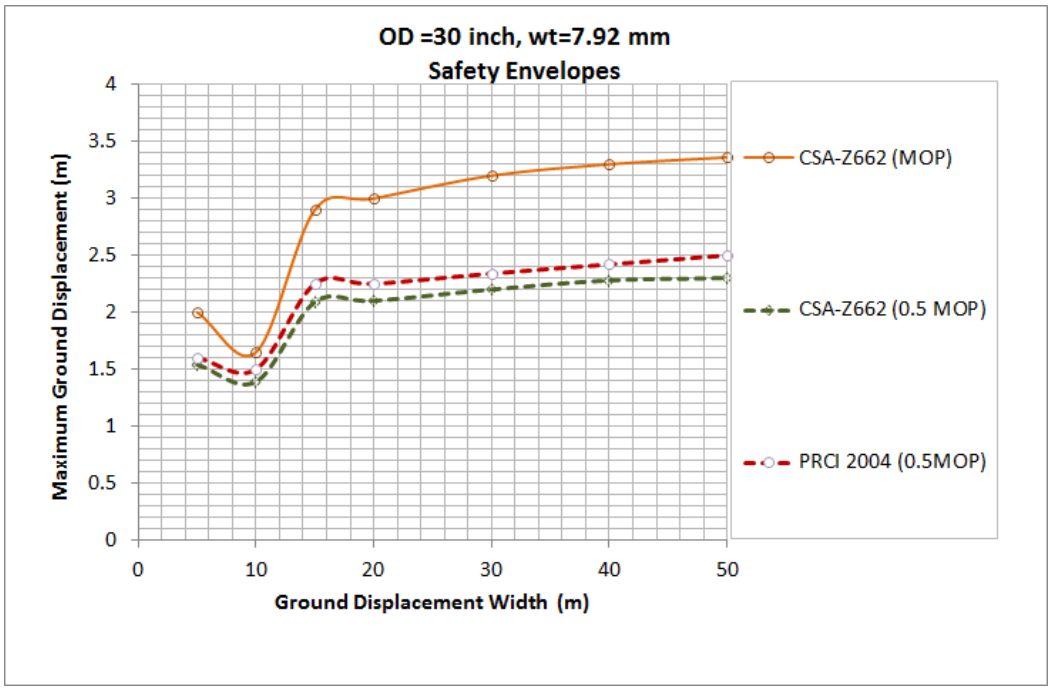

Figure 4.18: Line 1 - Safety Envelopes: Compressive Strain Limit

4.1.3 Structural Analyses for the 40-inch Pipeline

Analyses were completed for the 40-inch pipe (Line 2) to assess its response to lateral ground movement and to determine the structural integrity significance of ground movement induced strain demands. The analyses considered seven potential ground movement failures with a total estimated width of failure perpendicular to the pipeline including:

- Case1: W=5 m
- Case2: W=10 m
- Case3: W=15 m
- Case4: W=20 m
- Case5: W=30 m
- Case6: W=40 m
- Case7: W=50 m

The strain demand determined from the analysis was compared with the calculated strain limits defined from the guidance provided in Section 3 the CSA Z662, PRCI 2014 and BS 7910 limit states.

4.1.3.1 40-Inch Diameter Line Results

The following Figures illustrate the SPH Finite element model and snapshots of the finite element model output.

The information contained herein is the copyright of and proprietary to BMT Fleet Technology Limited. Use of this information is governed by the legend on the cover page of this document."

- Figure 4.19 illustrates an example of ground movement profile at different levels of movements considering movement width of 20 m (Case2). The soil displacements illustrated in this Figure illustrate that the soil moves uniformly up to a shear zone at the limits of the displacement zone.

- Figure 4.20 illustrates an example of pipeline deformation profile at different levels of ground movement considering ground movement width of 20 m (Case2). These results compared with those in Figure 5. 19 illustrate that the pipe does not follow the same profile since some of the soil flows around the pipe.

- Figure 4.21 shows the true axial strain at 3'oclock and 9 o'clock position along the pipeline for Case3 (W=15 m) considering soil movement of 1.93 m.

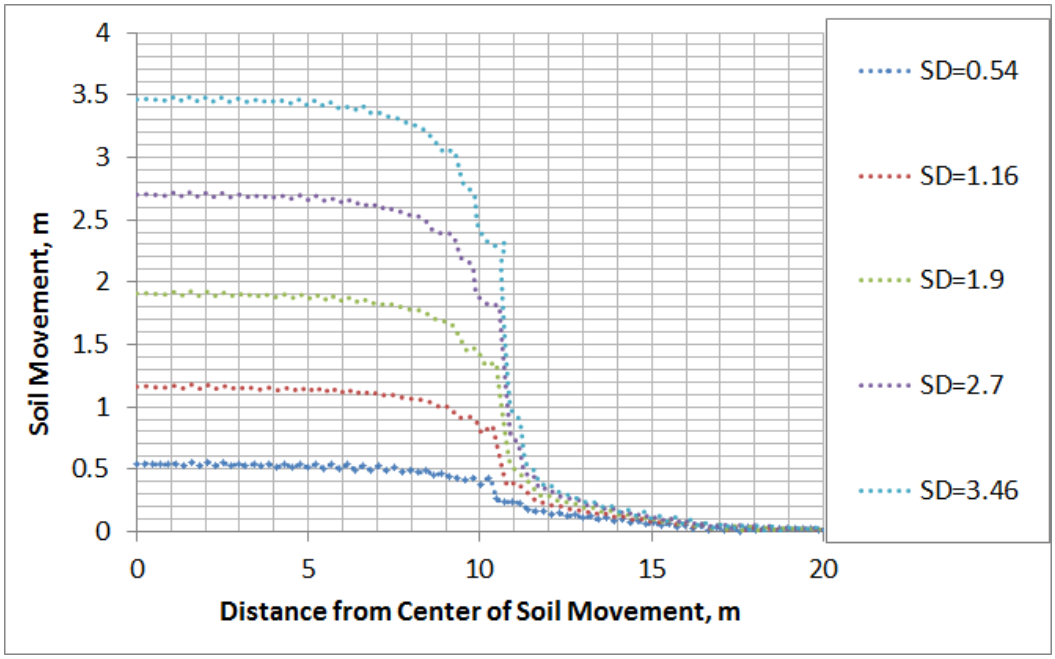

Figure 4.19: Line 2 - Ground Movement Profiles at Different Levels of Soil Movement for Case2: W=20 m

The information contained herein is the copyright of and proprietary to BMT Fleet Technology Limited. Use of this information is governed by the legend on the cover page of this document."

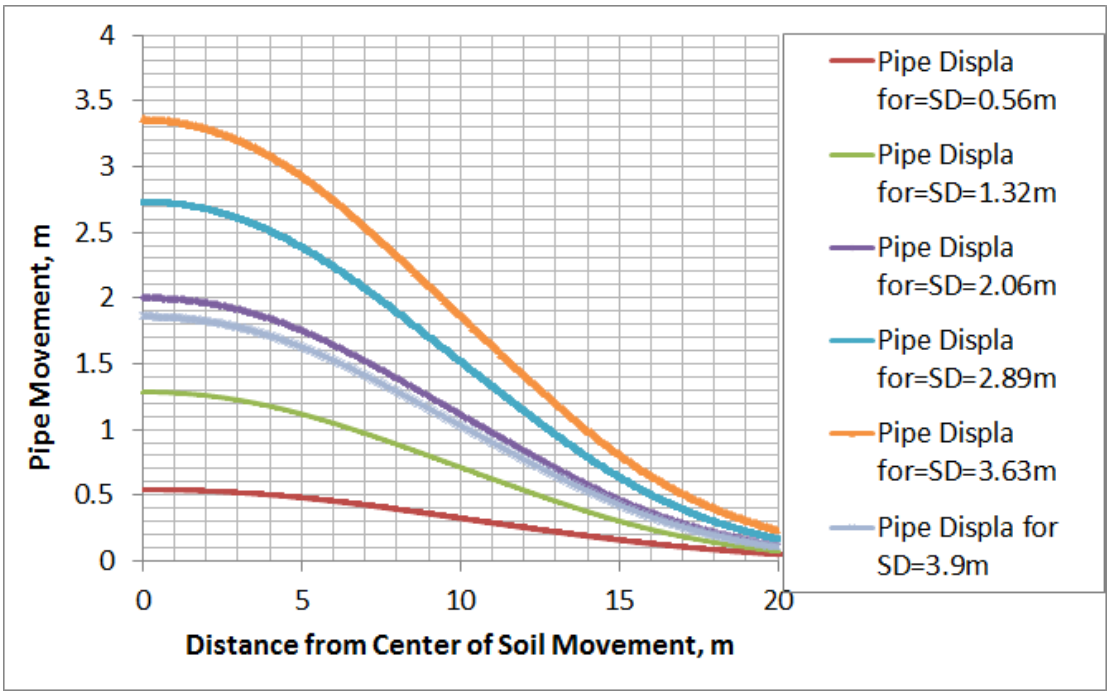

Figure 4.20: Line 2 - Pipe Movement Profiles at Different Levels of Soil Movement for Case2: W=20 m

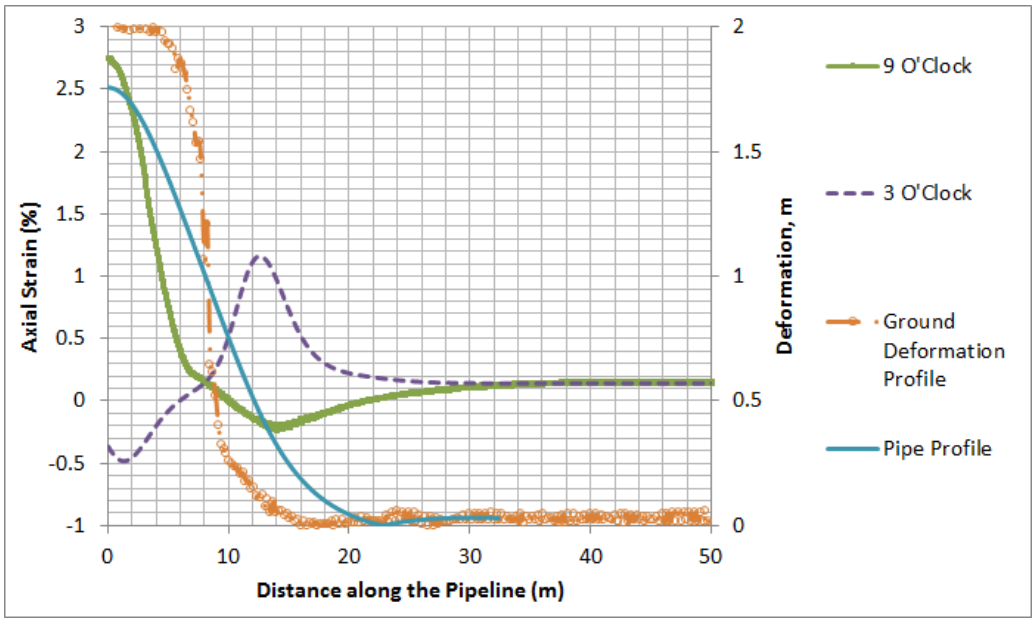

Figure 4.21: Line 2 - Axial Strain & Pipe and Ground Movement Profiles for Case3: W=15 m Considering Soil Movement of 1.93 m

The information contained herein is the copyright of and proprietary to BMT Fleet Technology Limited. Use of this information is governed by the legend on the cover page of this document."

4.1.3.1.1 Comparison with Strain Criteria and Safety Envelopes

The objective was to develop a simple method to define the effects of operational and geotechnical loads on liquid and gas pipeline systems to support decision making regarding threat severity or repair scheduling. This tool incorporated in strain based design and assessment to facilitate the consideration of complex loading scenarios inducing significant flexural loads, including pipeline subsidence or lowering, and ground movements inducing lateral pipeline movements.

The results of the finite element analyses were interpolated, to produce an envelope defining the combinations of ground displacement and width where the pipe was safe and not safe. Failure or "not safe pipe" was presumed to occur if the axial strains (tensile and/or compressive strains) at any location exceeded strain limits.

4.1.3.1.2 Tensile Strain Criteria and Safety Envelopes

The strain demand determined from the analysis was compared with the calculated strain limits defined from the guidance provided by Sections 3 and 4.

Figures 4.24 and 4.25 show the axial tensile and compressive strains in the 40-inch pipe as a function of the centerline of lateral soil displacement for various lateral soil widths [5–50 m]. The results were presented in Tables 4.7 through 4.9. It was found that:

- Case1: W=5 m
  - the tensile strain related failure limits were reached for ground displacement ranging from 0.6 m to 1.12 m considering flaw size of 2 mm, 1 mm and 0.5 mm, respectively;
  - CSA-Z662 and PRCI 2014 compressive strain related failure limits were reached for ground displacement of 2.76 m for pipeline operating at 0.5 maximum operation pressure (MOP). The allowable soil displacement range increases to 3.6 to 4.0 m when the pipe is pressurized to MOP.
- Case2: W=10 m
  - the tensile strain related failure limits were reached for ground displacement ranging from 0.26 m to 0.62 m considering flaw size of 2 mm, 1 mm and 0.5 mm, respectively;
  - CSA-Z662 and PRCI 2014 compressive strain related failure limits were reached for ground displacement of 0.96 m for pipeline operating at 0.5 maximum operation pressure (MOP). The allowable soil displacement range increases to 1.22 and 1.5 m when the pipe is pressurized to MOP.
- Case3: W=15 m
  - the tensile strain related failure limits were reached for ground displacement ranging from 0.4 m to 0.62 m considering flaw size of 2 mm, 1 mm and 0.5 mm, respectively;
  - CSA-Z662 and PRCI 2014 compressive strain related failure limits were reached for ground displacement to 0.96 m for pipeline operating at 0.5 maximum operation

The information contained herein is the copyright of and proprietary to BMT Fleet Technology Limited. Use of this information is governed by the legend on the cover page of this document."

pressure (MOP). The allowable soil displacement range increases to 1.56 m and 2.5 m when the pipe is pressurized to MOP.

- Case4: W=20 m
  - the tensile strain related failure limits were reached for ground displacement ranging from 0.55 m to 0.82 m considering flaw size of 2 mm, 1 mm and 0.5 mm, respectively;
  - CSA-Z662 and PRCI 2014 compressive strain related failure limits were reached for ground displacement ranging from 2.09 m to 2.25 m for pipeline operating at 0.5 maximum operation pressure (MOP). The allowable soil displacement range is higher than 3 m when the pipe is pressurized to MOP.
- Case5: W=30 m
  - the tensile strain related failure limits were reached for ground displacement ranging from 0.76 m to 1.25 m considering flaw size of 2 mm, 1 mm and 0.5 mm, respectively;
  - CSA-Z662 and PRCI 2014 compressive strain related failure limits were reached for ground displacement higher than 3.8 m for pipeline operating at 0.5 and maximum operation pressure (MOP).
- Case6: W=40 m
  - the tensile strain related failure limits were reached for ground displacement ranging from 0.77 m to 1.3 m considering flaw size of 2 mm, 1 mm and 0.5 mm, respectively;
  - CSA-Z662 and PRCI 2014 compressive strain related failure limits were reached for ground displacement ranging higher than 3.8 m for pipeline operating at 0.5 and maximum operation pressure (MOP).
- Case7: W=50 m
  - the tensile strain related failure limits were reached for ground displacement ranging from 0.78 m to 1.3 m considering flaw size of 2 mm, 1 mm and 0.5 mm, respectively;
  - CSA-Z662 and PRCI 2014 compressive strain related failure limits were reached for ground displacement higher than 3.8 m for pipeline operating at 0.5 and maximum operation pressure (MOP).

The results were interpolated, to produce an envelope defining the combinations of ground displacement and width where the pipe was safe and not safe. Failure “not safe pipe” was presumed to occur if the tensile strain at any location exceeded strain limits defined from BS 7910, CSA-Z662 and PRCI 2004.

Figure 4.17 shows a set of pipe safety envelopes for BS7910 tensile strain limits, considering a flaw size of 0.5 mm, 1 mm and 2 mm. Figure 4.18 shows a set of pipe safety envelopes for CSA-Z662 and PRCI compressive strain limits. The results show the importance of ground soil movement width. It shows that the critical soil movement width that maximizes pipe bending moments and strains are about 10 m to 15 m for the 40-inch pipe with D/t ratio of 106.

The information contained herein is the copyright of and proprietary to BMT Fleet Technology Limited. Use of this information is governed by the legend on the cover page of this document."

The results are very sensitive to the assumption made regarding the key analysis parameters. A sensitivity analysis is being carried to define "safety envelopes" for the case where pipe is loaded by lateral ground movement. Safety envelopes were defined with respect to the combination of ground displacement width for various soil strengths, pipe geometry (D/t), steel grade and pipe to soil coefficient of friction.

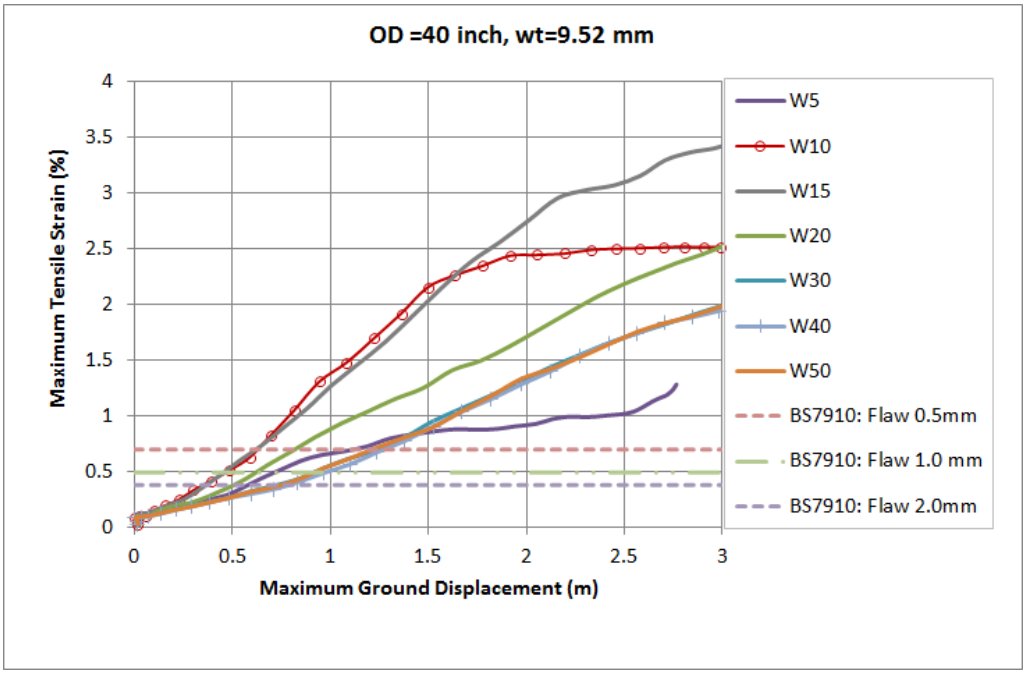

Figure 4.22: Line 2 - Maximum Tensile in the Pipe vs. Ground Movement Widths: [5-50 m]

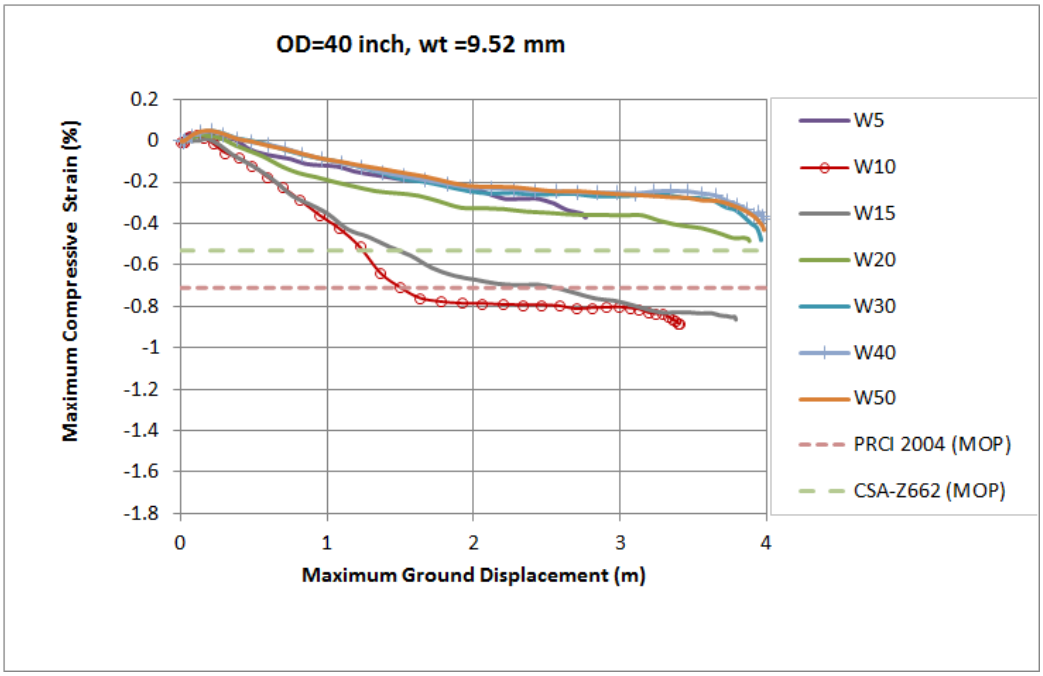

Figure 4.23: Line 2 - Maximum Compressive Strain in the Pipe vs. Ground Movement: Widths [5-50 m]

The information contained herein is the copyright of and proprietary to BMT Fleet Technology Limited. Use of this information is governed by the legend on the cover page of this document."

Table 4.7: Line 2 - Required Ground Displacement to Cause Tensile Strain Capacity

Flaw Size	Strain Limit BS7910	Required Slope Movement						
		Ground Movement Width (m)						
mm	%	W5	W10	W15	W20	W30	W40	W50
0.5	0.70	1.12	0.62	0.62	0.82	1.25	1.3	1.3
1	0.49	0.7	0.45	0.45	0.62	0.95	1	1
2	0.38	0.6	0.26	0.4	0.55	0.76	0.77	0.78

Table 4.8: Line 2 - Required Ground Displacement to Cause Compressive Strain Capacity - CS-Z662

Pressure	Strain Limit CSA-Z662	Required Ground Displacement						
		Ground Movement Width (m)						
	%	W5	W10	W15	W20	W30	W40	W50
0.5 MOP	0.37	2.76	0.96	0.96	3.1	3.8	3.8	3.8
MOP	0.53	3.6	1.22	1.56	3.8	4	4.1	4.1

Table 4.9: Line 2 - Required Ground Displacement to Cause Compressive Strain Capacity - PRCI-2004

Pressure	Strain Limit PRCI-2004 (offset/t=0.097)	Required Ground Displacement						
		Ground Movement Width (m)						
	%	W5	W10	W15	W20	W30	W40	W50
0.5 MOP	0.37	2.76	0.96	0.96	3.1	3.8	3.8	3.8
MOP	0.71	>3.8	1.5	2.5	3.8	>3.8	>3.8	>3.8

The information contained herein is the copyright of and proprietary to BMT Fleet Technology Limited. Use of this information is governed by the legend on the cover page of this document."

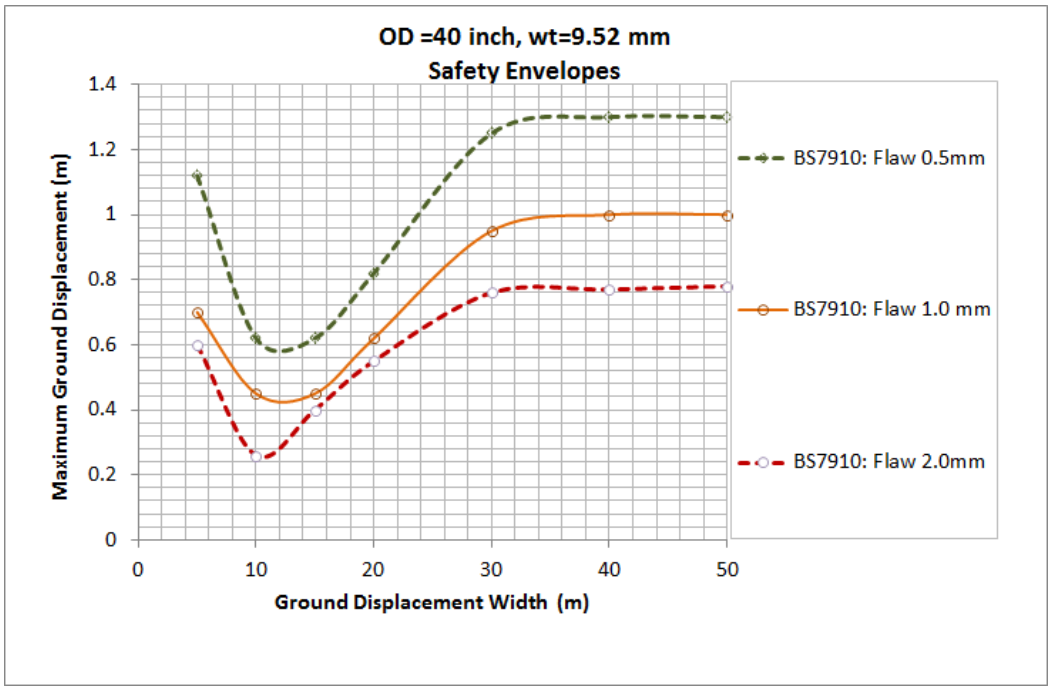

Figure 4.24: Line 2 - Safety Envelopes: Tensile Strain Limit

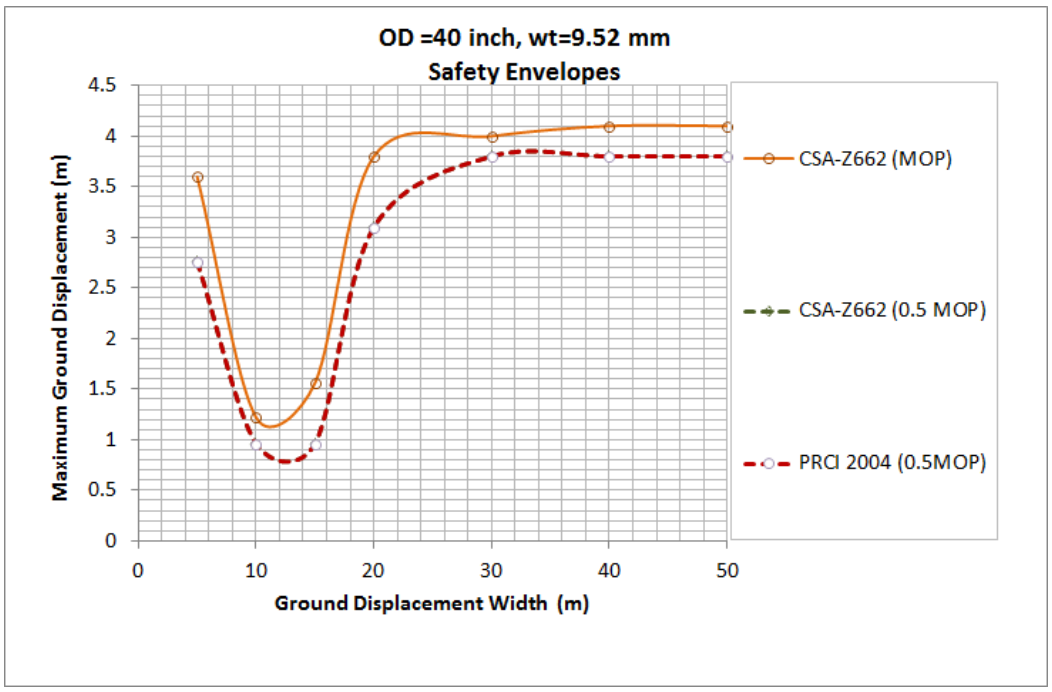

Figure 4.25: Line 2 - Safety Envelopes: Compressive Strain Limit

The information contained herein is the copyright of and proprietary to BMT Fleet Technology Limited. Use of this information is governed by the legend on the cover page of this document."

4.2 Modeling of Subsidence

The objective of the analyses presented in this section is to simulate surface subsidence and evaluate the effects on pipeline. The goal was to develop a simple method to define the effects of operational and geotechnical loads on liquid and gas pipeline systems to support decision making regarding threat severity or repair scheduling. This tool incorporated strain based design and assessment to facilitate the consideration of complex loading scenarios inducing significant flexural loads, including pipeline subsidence or lowering.

This section focuses on the analysis of surface subsidence associated with underground mining and its effects on pipelines. The analyses were completed for the 30-inch pipe (D/t =96) to assess its response to longwall mining subsidence and to determine the structural integrity significance of ground subsidence induced strain demands. The analyses considered a total of three (3) potential panel extraction widths that influence surface subsidence, including:

1. Sub-critical panel extraction width.

2. Critical panel extraction width.

3. Super- critical panel extraction width.

The strain demand determined from the analysis was compared with the calculated strain limits defined from the guidance provided in Section 3 outlining the CSA Z662, PRCI 2004 and BS 7910 limit states.

4.2.1 Mining Subsidence Phenomena and Terminology

Ground subsidence pose hazards to pipelines, the principal causes are subsurface fluid withdrawal, drainage of organic soil, sinkholes, underground mining, hydrocompaction, thawing permafrost, and natural consolidation (USGS-2008). This section focuses on the analyses of subsidence associated with underground mining. Surface subsidence due to underground coal mining is generally classified as (USGS-2008):

1. Pit subsidence: is a circular hole in the ground with a diameter ranging from 1 to 12 m, generally occurs over shallow mines, depth less than 50 m.

2. Sag/trough subsidence is a rectangular depression with large subsidence depth and area typically occurs in conjunction with longwall mining.

These classifications are illustrated in Figure 4.26.

The information contained herein is the copyright of and proprietary to BMT Fleet Technology Limited. Use of this information is governed by the legend on the cover page of this document."

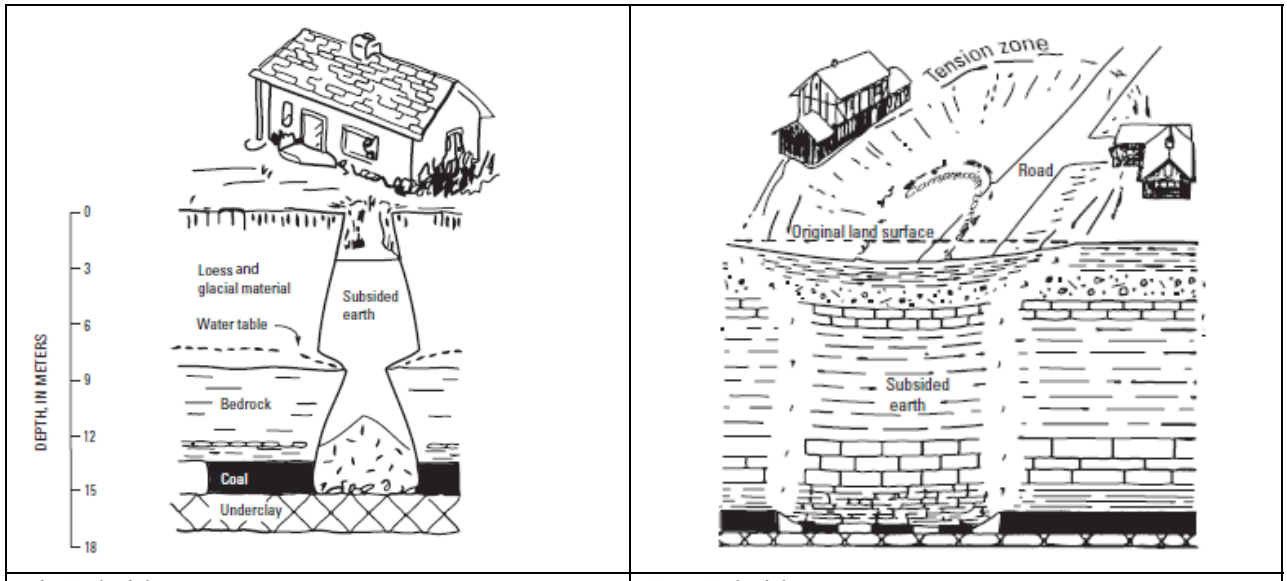

Pit Subsidence	Sag Subsidence

Figure 4.26: Typical type of Subsidence Associated with Underground Coal Mining (Bauer and Hunt, 1982; USGS 2008)

In general, underground mining and in particular longwall mining can cause significant surface subsidence displacement, which is usually about 25 to 95 percent of the mined thickness of coal (PRCI 1986).

There are three classifications of extraction area that influence the characteristic of subsidence sag/trough.

Figure 4.27 illustrates the three panel extraction areas that influence surface subsidence. The panel extraction areas are defined based on panel width to mining depth ratio (W/H) as follows:

- Sub-critical panel extraction width – occurs when the extraction width is narrow, having a W/H ratio less than 1.4, and causes less than the maximum possible subsidence at the ground surface;

- Critical panel extraction width –is slightly wider than sub-critical and is defined as an extraction that has a W/H ratio of approximately 1.5 to 2;

- Super-critical panel extraction width- is defined as an extraction that has a W/H ratio larger than 2.0. Super-critical extraction is large enough to potentially cause the maximum possible subsidence at the ground surface. It causes a flat area of maximum subsidence in the center of the flat surface.

The information contained herein is the copyright of and proprietary to BMT Fleet Technology Limited. Use of this information is governed by the legend on the cover page of this document."

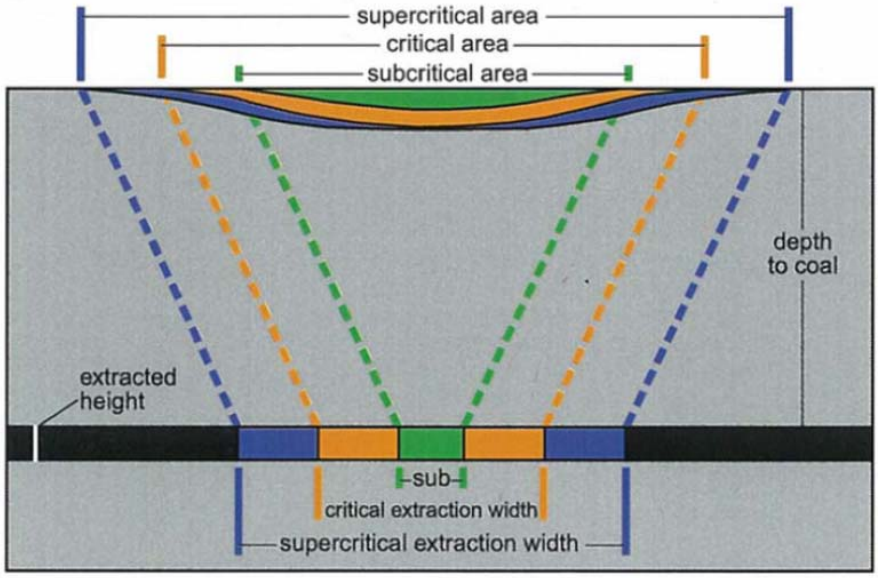

Figure 4.27: Longwall Mining Subsidence Parameters (New South Wales Coal Association)

Various empirical (e.g., National Coal Board (NCB) 1966, Appalachian method 1985) models have been used to predict ground surface subsidence for given mining operation described above. These empirical methods were based on large number of field measurements. The profile functions are based on a curve fitting.

The NCB method uses different graphs and tables for different conitions to predict the subsidence profile. For example, a graph for prediction of subsidence factor and profile are presented in Figure 4.28 and Figure 4.29.

The information contained herein is the copyright of and proprietary to BMT Fleet Technology Limited. Use of this information is governed by the legend on the cover page of this document."

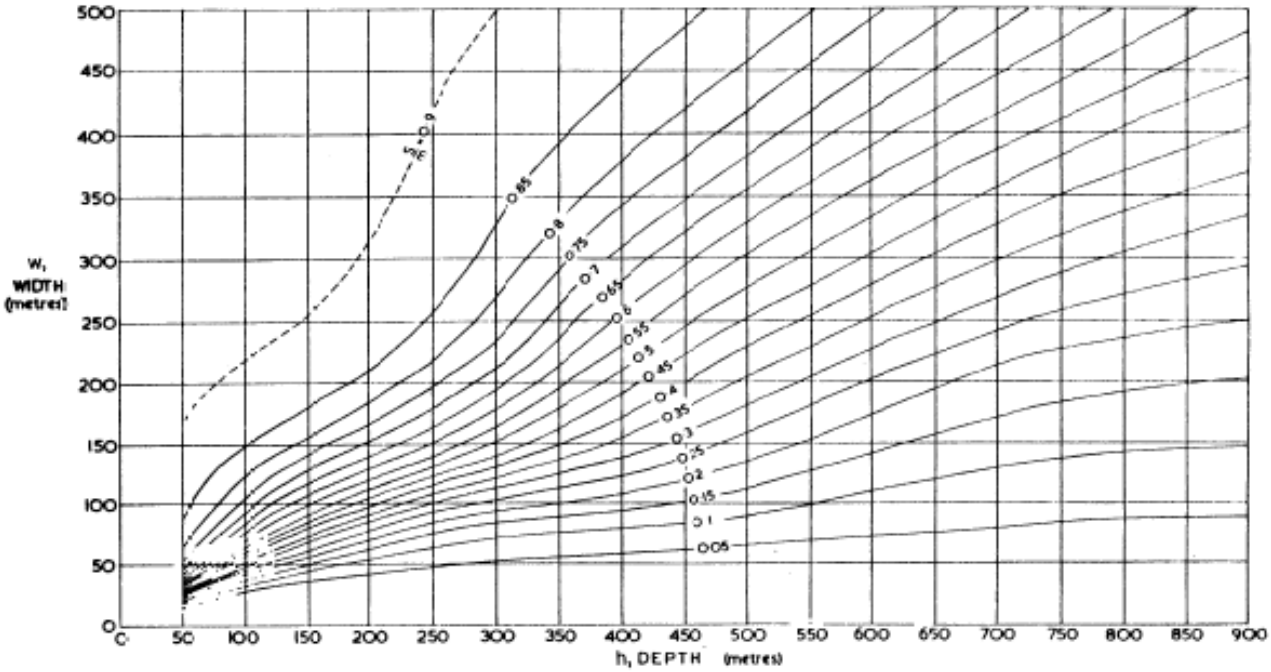

FIGURE 3. SUBSIDENCE FACTORS (NATIONAL COAL BOARD, SUBSIDENCE ENGINEERS' HANDBOOK-1975)

Figure 4.28: Graph for Subsidence Factor (NCB-1975)

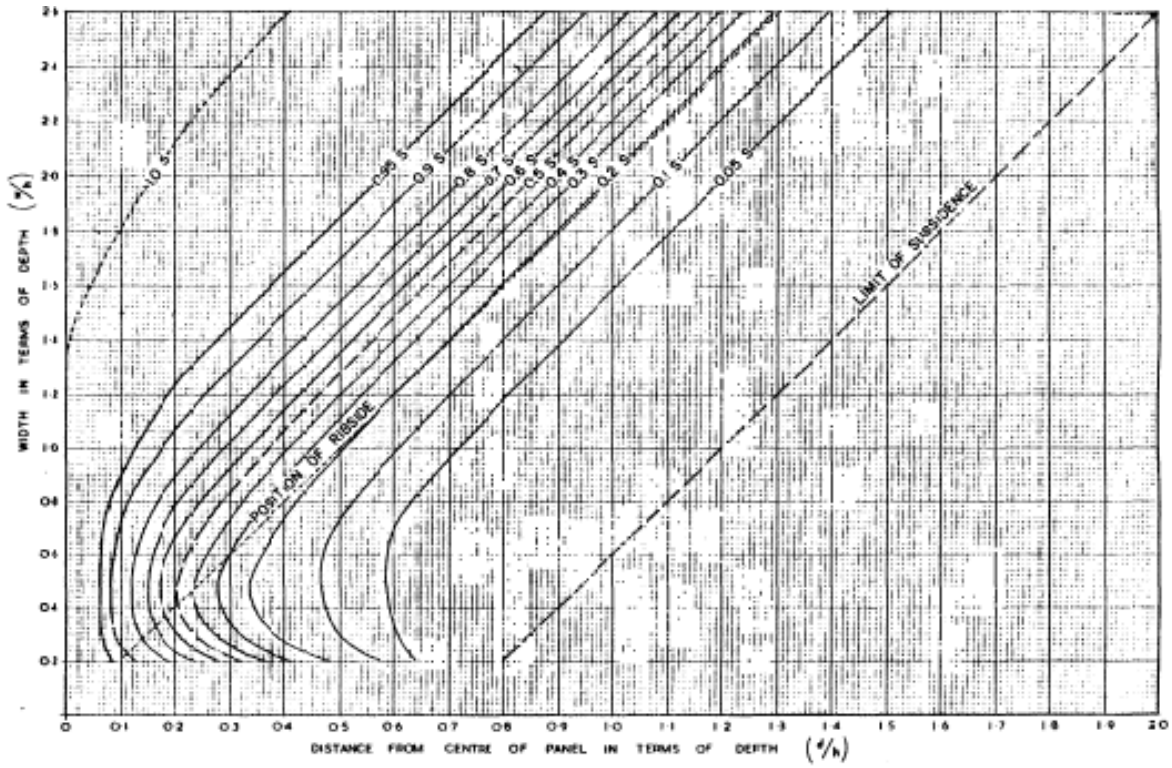

FIGURE 4. GRAPH FOR PREDICTING SUBSIDENCE PROFILES (NATIONAL COAL BOARD, SUBSIDENCE ENGINEERS' HANDBOOK-1975)

Figure 4.29: Graph for Prediction Subsidence Profile (NCB-1975)

The information contained herein is the copyright of and proprietary to BMT Fleet Technology Limited. Use of this information is governed by the legend on the cover page of this document."

An alternative method based upon Appalachian mining experience was used to predict subsidence profile in Appalachian coalfield in the USA. The subsidence profile for this method can be represented by mathematical model as follows:

$$S(x) = \frac{S_0}{2}\left(1 - \tanh\left(\frac{cx}{B}\right)\right)$$

Where:

S_0 is the maximum subsidence
X is the horizontal distance from the origin point of deflection (center of the subsidence)
B is the distance from the influence point to the center of the profile
c is a site-specific coeficient

The site specific coefficient (c) is developed based upon local observations at the site of interest or similar sites to calibrate the empirical model. As such, the ground movement mechanism is somewhat predetermined based upon past geotechnical event historical experience.

Finite element models can be used as an alternative to estimate the subsidence profile, the modeling approach can account for the characteristic of various rock strata, as well as the orientation of the bedding planes. However, the FE method requires more input data and iterations to calibrate to case history than the empirical methods.

4.2.2 Finite Element Analyses

4.2.2.1 Model Description

The following section summarizes the development of the finite element models used to assess the effect of longwall mining subsidence on pipelines. To understand the effect of numerous variables on the estimated pipeline behavior, two (2) 3-Dimensional pipe-soil interaction models were developed using LS-DYNA.

The first model, using a coupled Smooth Particle Hydrodynamic (SPH) and Lagragian method was developed to explicitly estimate the ground subsidence profile, soil strain and the effects of the of the subsidence on pipelines. The coupled model, shown in Figures 4.30 and 4.31 consist of the pipeline, trench backfill, ground surface, overburden strata, coal seam and panel width extraction. A sample application of the coupled finite element model is presented and discussed in the next section.

The second model is also 3 dimensional pipe-soil interaction model, using the discrete-elements method (DEM) where the ground subsidence was initiated using empirical method. This model was used to complete a sensitivity study to define the problem parameters and the pipe strains developed in ground events and identify trends. The results are presented in the sectons tht follow. This method was found to be more computationally efficient. Both the SPH and DEM methods were validated by demonstrating their ability to simulate full-scale lab trials. These results were presented in previous project reports.

The information contained herein is the copyright of and proprietary to BMT Fleet Technology Limited. Use of this information is governed by the legend on the cover page of this document."

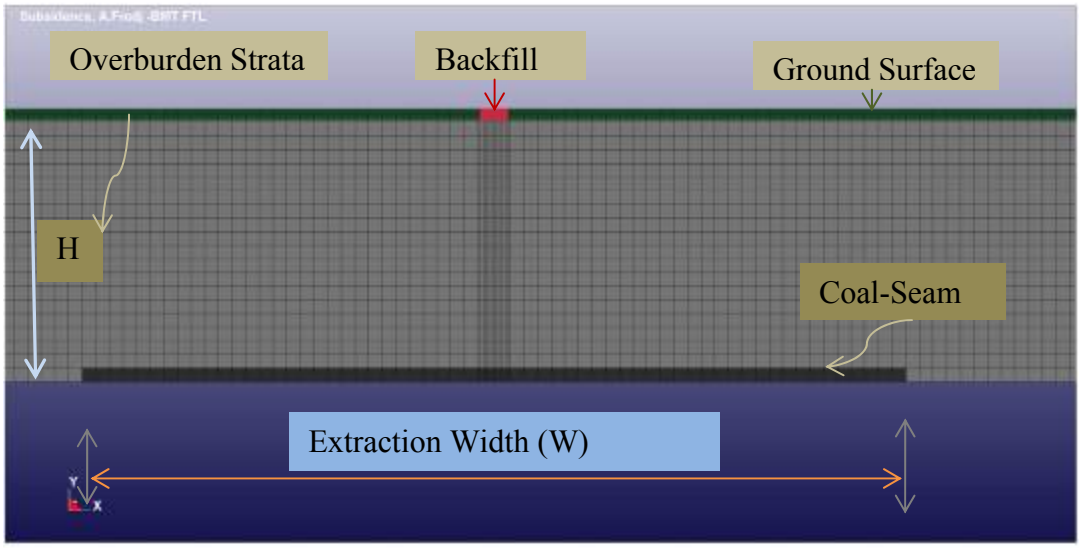

Figure 4.30: Illustration of the FE Model: Subsidence

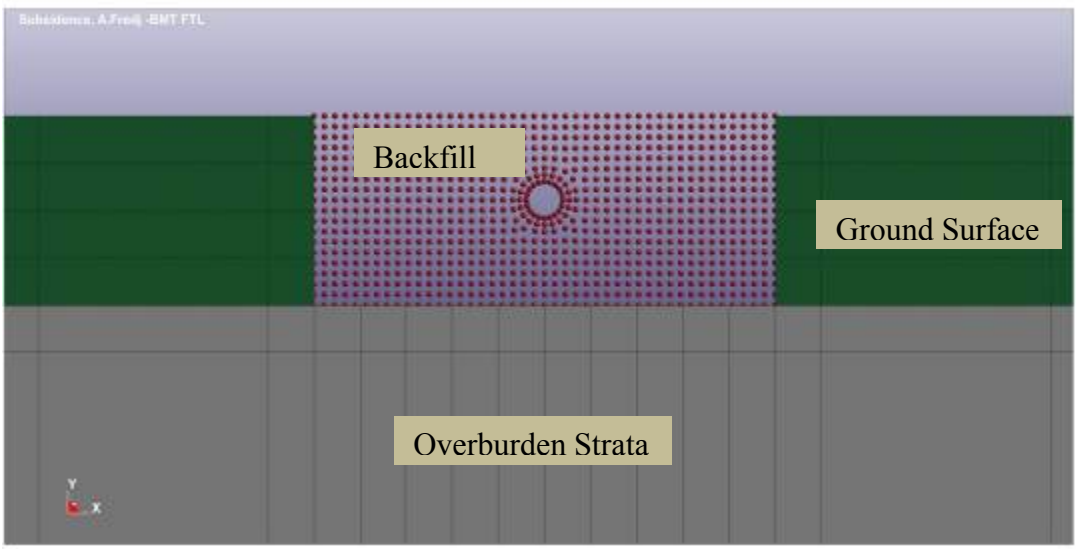

Figure 4.31: Illustration of the Model Including the Pipe-Side View and Backfill Trench

4.2.2.2 Summary of Inputs Required and Processes Modelled

Finite element analyses using a 3D continuum model developed for this project were carried out to predict to predict both surface subsidence due to coal-seam mining and its effects on pipelines. The model is a coupled 3D continuum model that can consider the effects of layered soils, trench geometries, operating conditions, and pipe materials stress-strain behavior including differences in tensile and compressive material behaviors.

The information contained herein is the copyright of and proprietary to BMT Fleet Technology Limited. Use of this information is governed by the legend on the cover page of this document."

The analyses were completed for a 30 inch dimeter pipeline with 6.35 mm (D/t=120) and 7.92 mm (D/t=96) wall thickness and Grade X52, considering the subsidence resulting from a longwall mine face length of 300 m, seam depth of 100 m, extraction height of 5 m and three different extraction widths including:

- Case1: Sub-critical panel extraction width of W=75 m that has a W/H ratio of 0.75
- Case2: Critical panel extraction width of 150 m with a W/H ratio of 1.5
- Case3: Super-critical panel extraction width of 300 m with W/H ratio of 3

The maximum possible subsidence at the ground surface was estimated using NCB subsidence factor presented in Figure 4.31. A subsidence factor of 0.74, 0.87 and 0.96 are assumed for super critical, critical and subcritical panel extraction widths, respectively.

Figure 4.32 shows an example of predicted subsidence basin along the pipeline for critical subsidence width. The mining subsidence results in ground surface subsidence, axial soil movement and strain in the soil. This demonstrates the capability of the model to predict bot the subsidence profile and soil strains.

The subsidence profiles predicted by finite element analyses were compared with the best known empirical methods, NCB method and Appalachian methods. Figures 4.32, 4.33 and 4.34 compare the subsidence profiles predicted by the FE model and best known empirical methods, NCB Method and Appalachian method. Note, that while there is a difference in the subsidence profile from one empirical method to the other, the FEA model prediction is closer to the NCB method. The FE model results predicted a less abrupt curvature than the NCB method for these cases. The results are sensitive to input parameters including soil properties which are not explicitly considered in the NCB and Appalachian empirical models. The advantage of the FE model, demonstrated to generally agree with the empirical subsidence predictors, is that it is coupled analysis technique that can report the impact of the subsidence event on the response of the pipeline. The strains experienced by the pipeline due to the subsidence event can be evaluated.

Detailed results are presented as follow:

- Figure 4.35 shows an example of predicted ground subsidence and pipe deformation for Case1 considering subcritical extraction width (W/H=0.75). In this figure, the pipe backfill trench continuum is hidden so that the displaced pipeline can be visualized.

- Figure 4.36 shows an example of the predicted ground subsidence and pipe deformation for Case2 considering critical extraction width (W/H=1.5). In this figure, the pipe backfill trench continuum is hidden so that the displaced pipeline can be visualized.

- Figure 4.37 shows an example of the predicted ground subsidence and pipe deformation for Case3 considering critical extraction width (W/H=3). In this figure, the pipe backfill trench continuum is hidden so that the displaced pipeline can be visualized.

The information contained herein is the copyright of and proprietary to BMT Fleet Technology Limited. Use of this information is governed by the legend on the cover page of this document."

- Figure 4.38 and 4.39 plots the surface subsidence profile, pipeline profile and pipeline axial strains distribution at different clock positions (3, 6 and 12 o'clock) along the length of the pipeline for D/t of 120 and 96. The results presented in this figure are for Case1 considering a sub-critical extraction width (W/H ratio of 0.75).

- Figure 4.40 and 4.41 plots the surface subsidence profile, pipeline profile and pipeline axial strains distribution at different clock positions (3, 6 and 12 o'clock) along the length of the pipeline for D/t of 120 and 96. The results presented in this figure are for Case2 considering a critical extraction width (W/H ratio of 1.5).

- Figure 4.42 and 4.43 plots the surface subsidence profile, pipeline profile and pipeline axial strains distribution at different clock positions (3, 6 and 12 o'clock) along the length of the pipeline for D/t of 120 and 96. The results presented in this figure are for Case3 considering a Super-critical extraction width (W/H ratio of 3).

Figures 4.35 to 4.43 plot the surface subsidence profile, pipeline profile and axial strains distribution at different clock positions (6 and 12 o'clock) along the length of the pipeline. The results presented in these figures are for the three (3) analyzed cases for D/t of 120 and 96. The results demonstrate that the pipeline strain distribution response is significantly affected by the panel width to mining depth ratio (W/H). Also, the super-critical panel extraction width results in the largest tensile strain in the pipe for the six (6) analyzed cases. General observations on the trends in pipe response to the subsidence hazard include:

- For sub-critical panel extraction width (W/h=0.5); the peak tensile of 0.4% and 0.36% at the maximum deflection point for D/t 120 and 96, respectively.

- For critical panel extraction width; and (W/h=1.5), the peak tensile strain of 0.67% and 0.36% for D/t of 120 and 96, respectively. The maximum strains occurred at in the curved portion with two bending zones at 45 m and 65 meters from the deflection point.

- For super- critical panel extraction width (W/h=3), the peak tensile strain of 0.75% and 0.51% for D/t of 120 and 96, respectively. The maximum strains occurred at in the curved portion with two bending zones at 130 m and 150 meters from the deflection point.

The information contained herein is the copyright of and proprietary to BMT Fleet Technology Limited. Use of this information is governed by the legend on the cover page of this document."

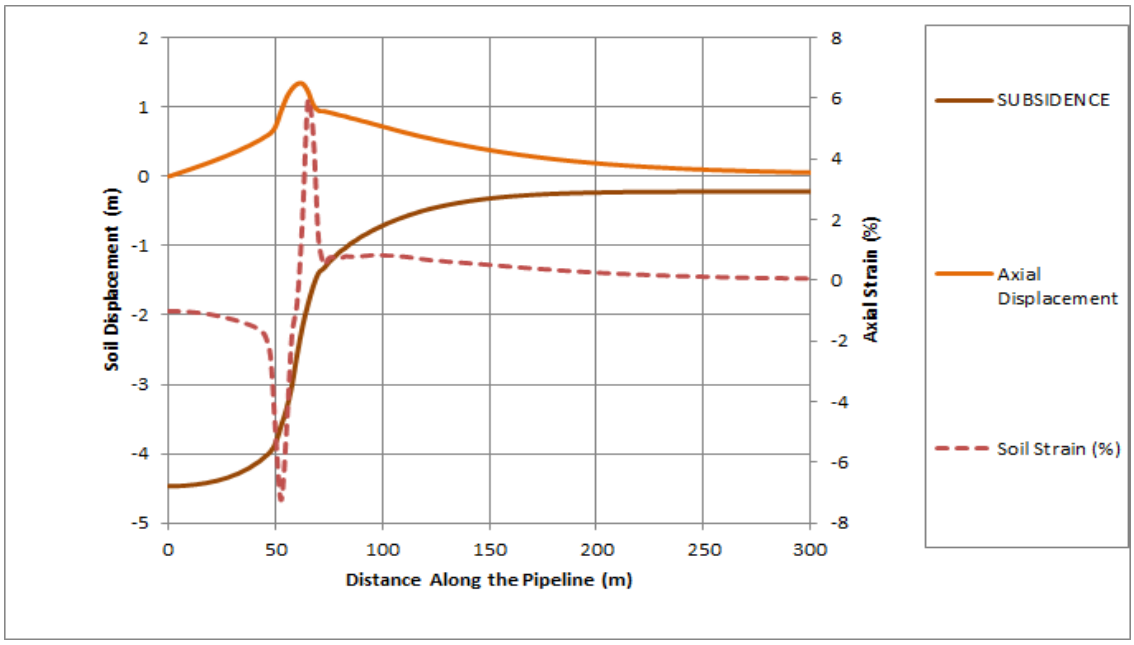

Figure 4.31: Predicted Subsidence Profile from the Maximum Deflection Point and Longitudinal Soil Displacement and Tensile Strain in the Soil

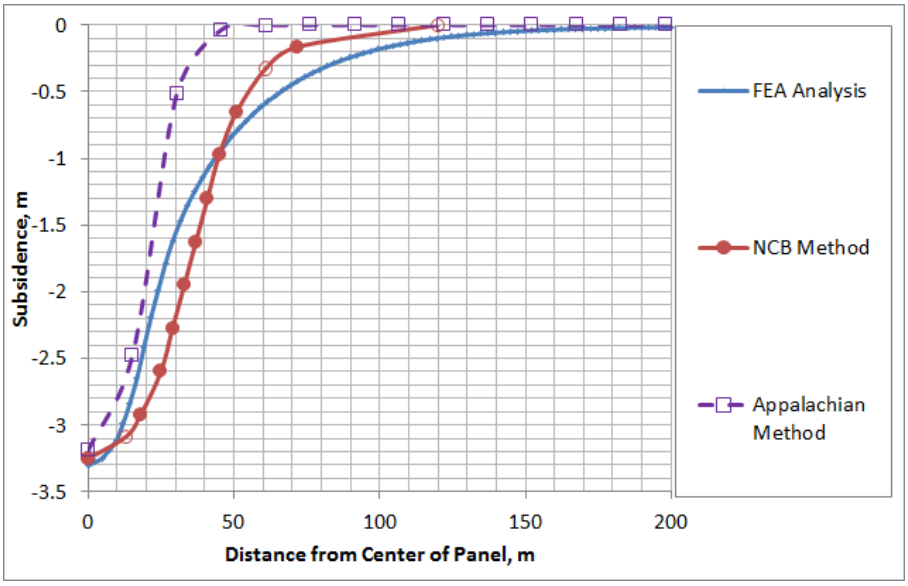

Figure 4.32: Comparison of Subsidence Profiles Predicted by FE Model and Empirical Method (NCB Method, Appalachian Method) for Subcritical Panel Extraction Width

The information contained herein is the copyright of and proprietary to BMT Fleet Technology Limited. Use of this information is governed by the legend on the cover page of this document."

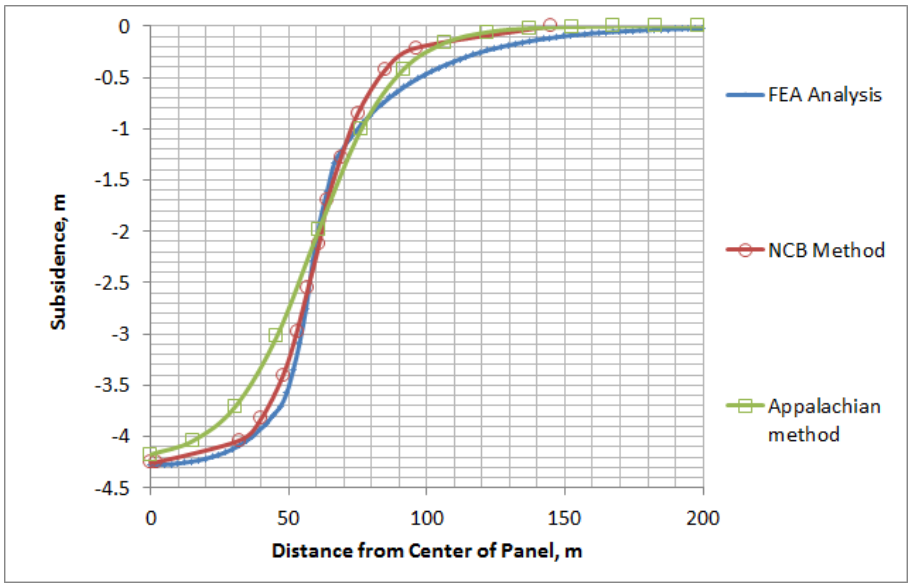

Figure 4.33: Comparison of Subsidence Profiles Predicted by FE Model and Empirical Method (NCB Method, Appalachian Method) for Critical Panel Extraction Width

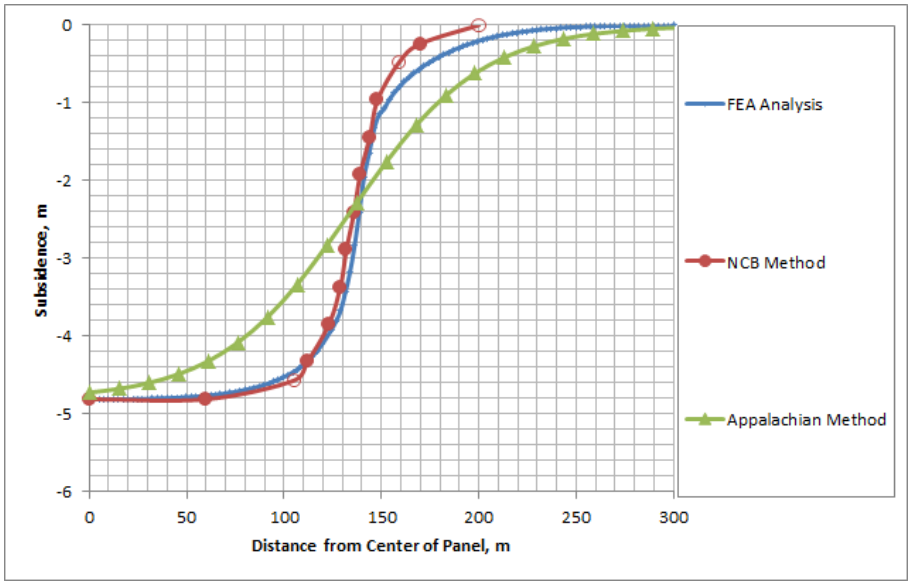

Figure 4.34: Comparison of Subsidence Profiles Predicted by FE Model and Empirical Method (NCB Method), for Super-Critical Extraction Width

The information contained herein is the copyright of and proprietary to BMT Fleet Technology Limited. Use of this information is governed by the legend on the cover page of this document."

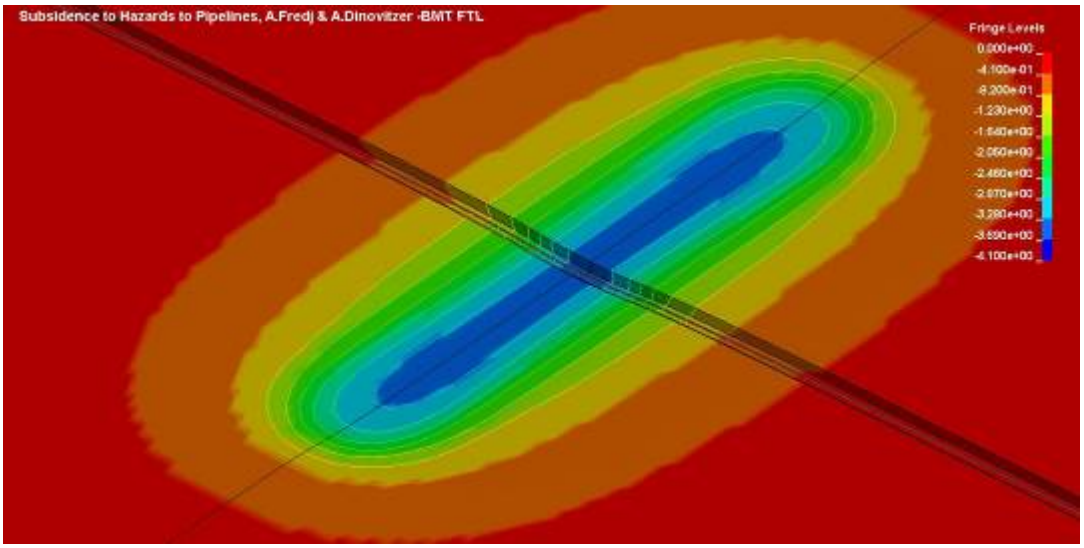

Figure 4.35: Surface Subsidence and Pipeline Deformation, for Case2: Subcritical Extraction Width, W/H=0.75

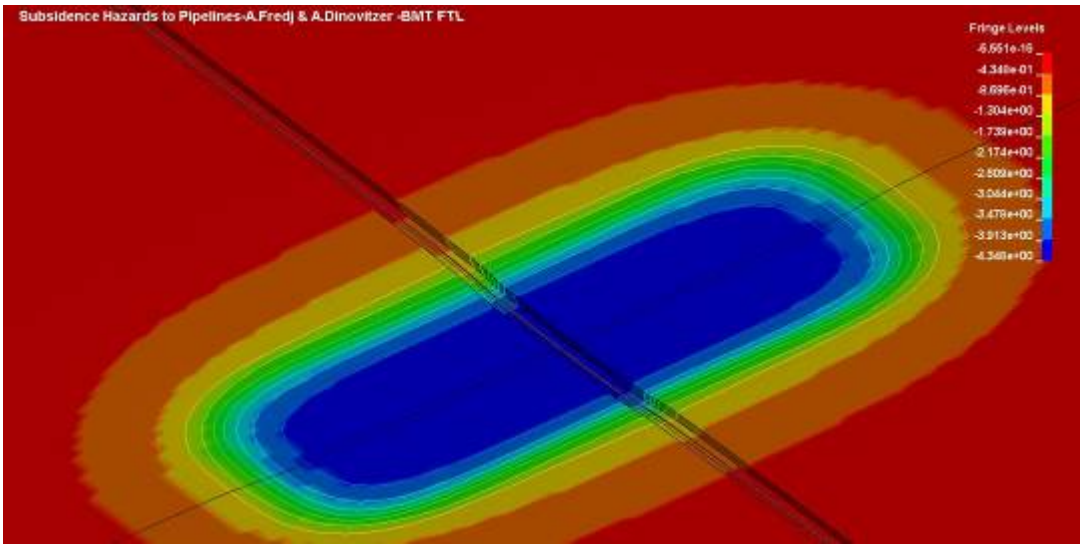

Figure 4.36: Soil Subsidence and Pipeline Deformation, for Case2: Critical Extraction Width, W/H=1.5

The information contained herein is the copyright of and proprietary to BMT Fleet Technology Limited. Use of this information is governed by the legend on the cover page of this document."

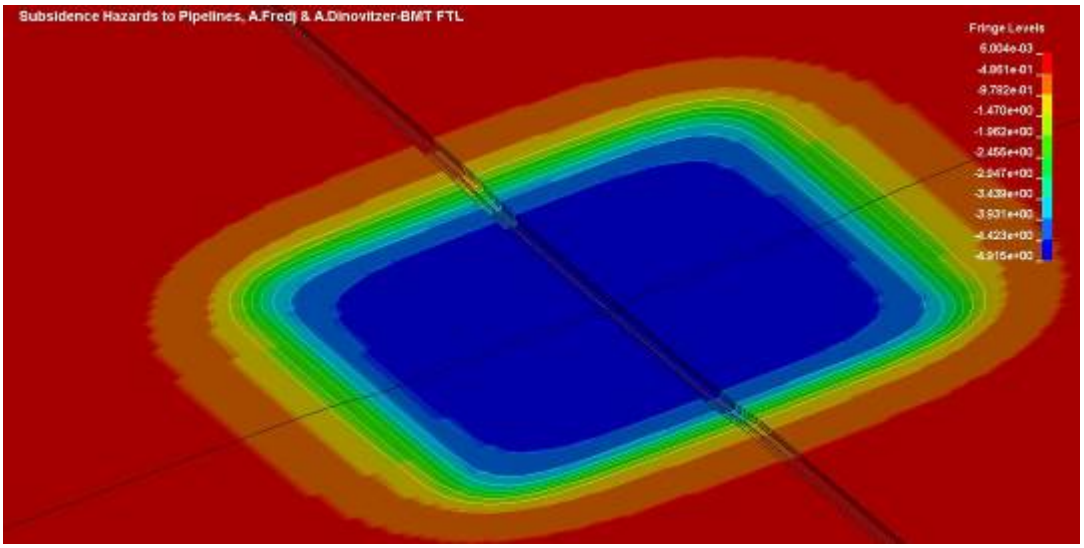

Figure 4.37: Soil Subsidence and Pipeline Deformation, for Case3: Super-Critical Extraction Width, W/H=3

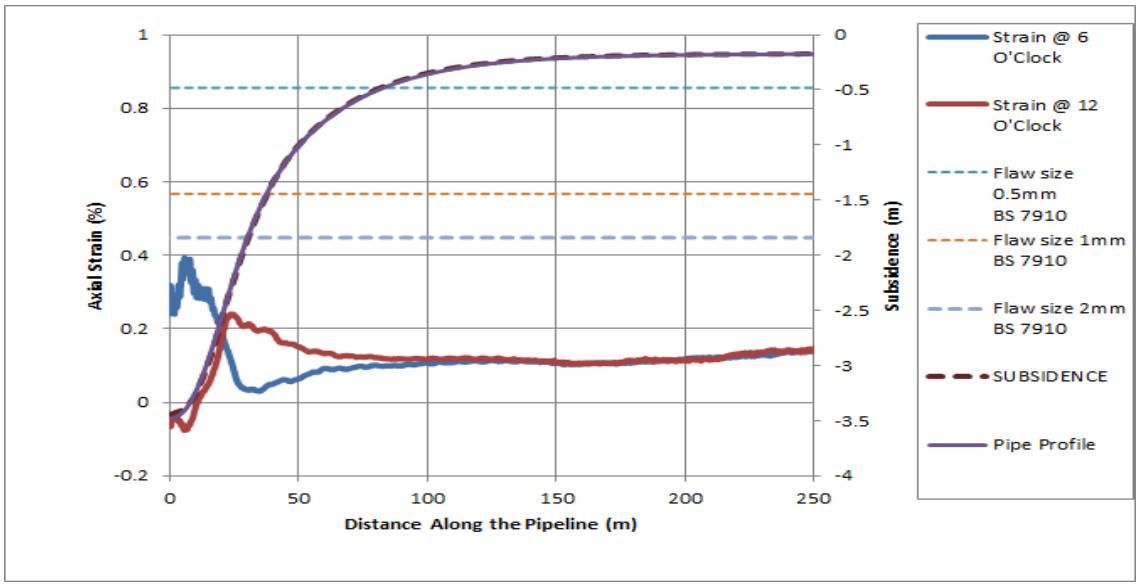

Figure 4.38: Surface Subsidence, Pipeline Profile and Axial Strains Distribution, for Subcritical Extraction Width (W/H=0.75) – Case1a (D/T= 120)

The information contained herein is the copyright of and proprietary to BMT Fleet Technology Limited. Use of this information is governed by the legend on the cover page of this document."

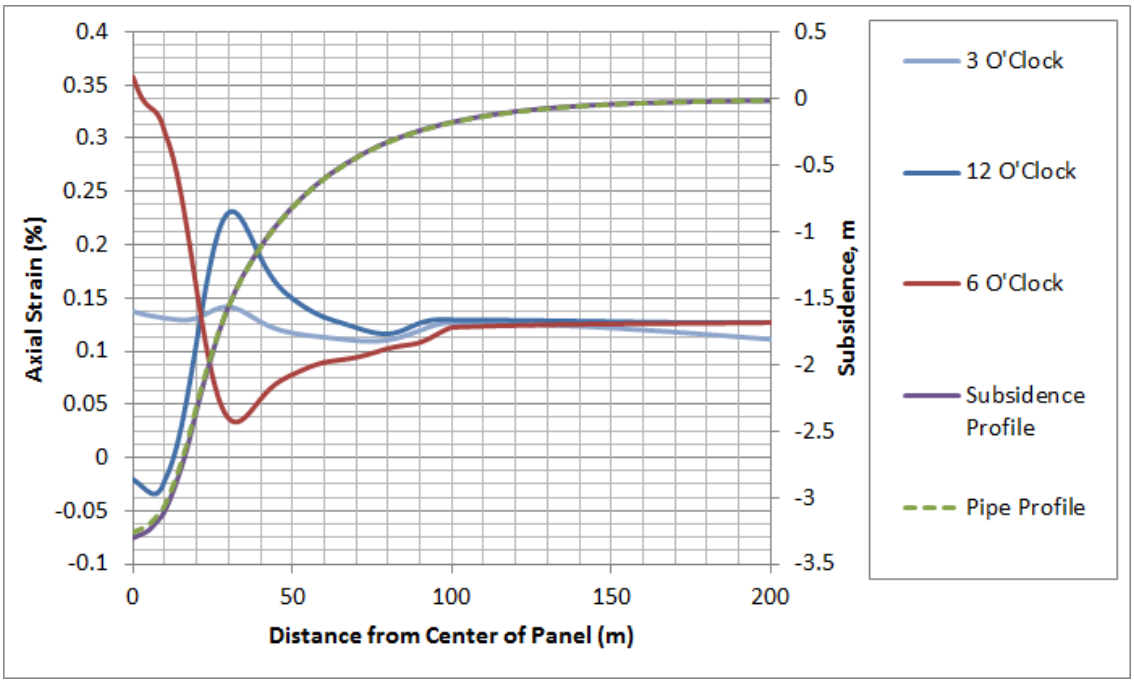

Figure 4.39: Surface Subsidence, Pipeline Profile and Axial Strains Distribution, for Subcritical Extraction Width (W/H=0.75) – Case1a (D/T= 96)

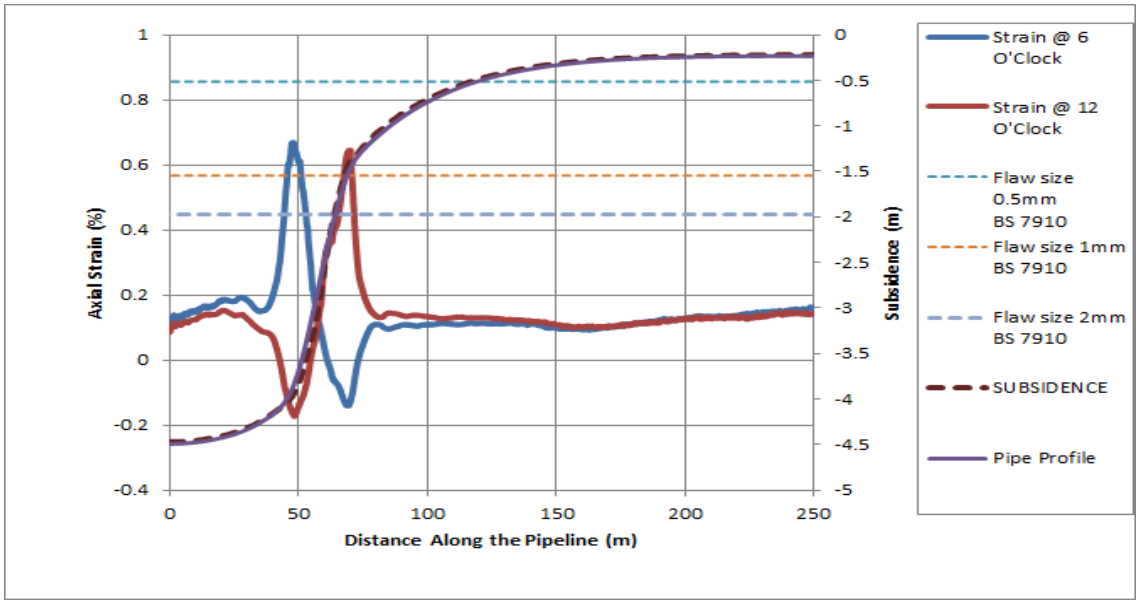

Figure 4.40: Surface Subsidence, Pipeline Profile and Axial Strains Distribution, for Critical Extraction Width (W/H=1.5) - Case2a (D/T=120)

The information contained herein is the copyright of and proprietary to BMT Fleet Technology Limited. Use of this information is governed by the legend on the cover page of this document."

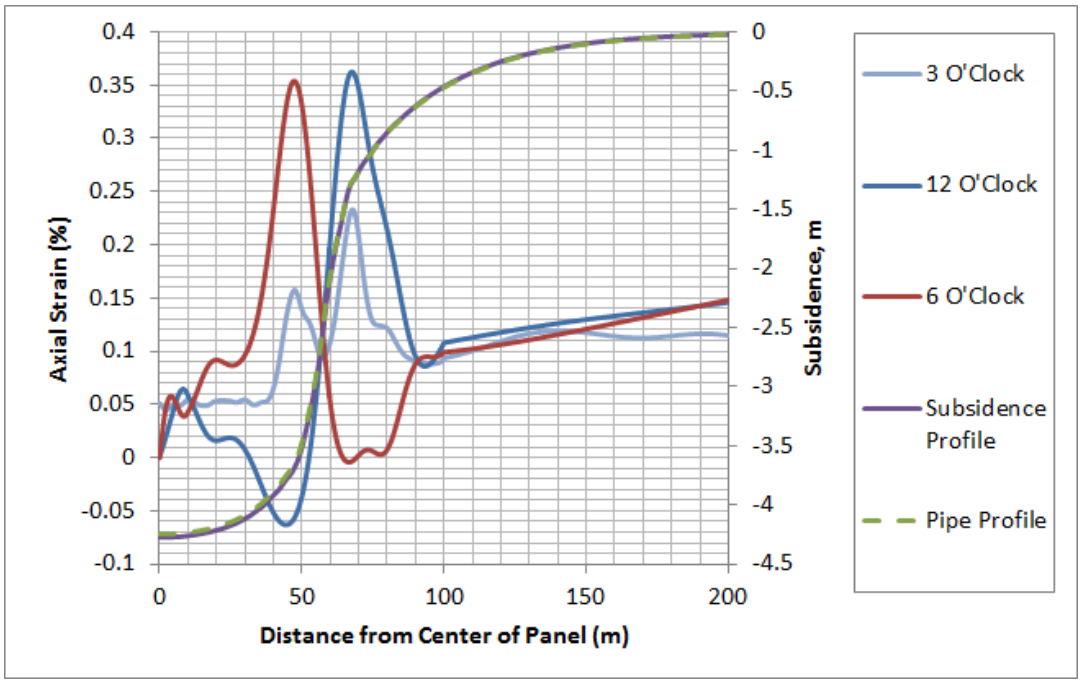

Figure 4.41: Surface Subsidence, Pipeline Profile and Axial Strains Distribution, for Critical Extraction Width (W/H=1.5) - Case2b (D/T=96)

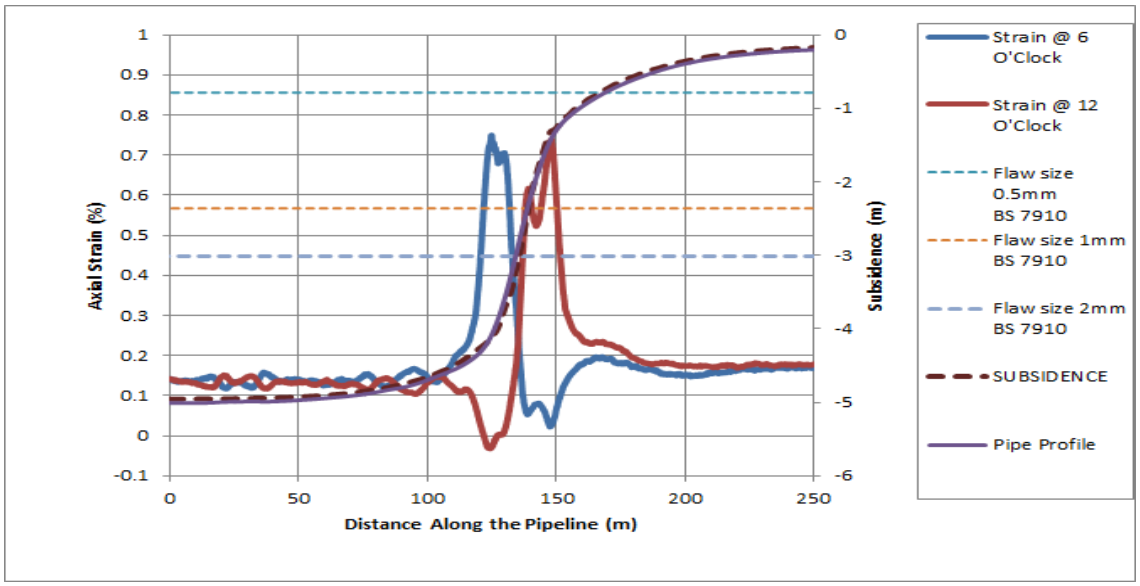

Figure 4.42: Surface Subsidence Pipeline Profile and Axial Strains Distribution, for Super Critical Extraction Width (W/H=3) - Case3a (D/T=120)

The information contained herein is the copyright of and proprietary to BMT Fleet Technology Limited. Use of this information is governed by the legend on the cover page of this document."

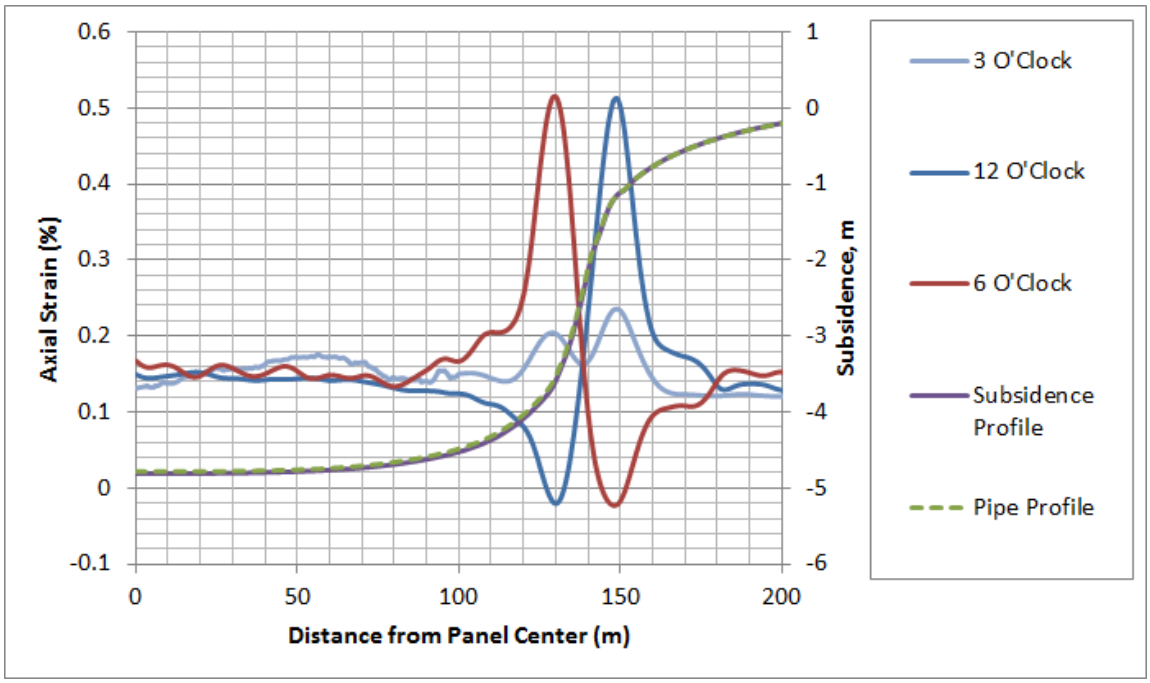

Figure 4.43: Surface Subsidence Pipeline Profile and Axial Strains Distribution, for Super Critical Extraction Width (W/H=3) - Case3b (D/T=96)

4.2.3 Application of Finite Element Model to Predict Pit Subsidence and Effects on Pipelines

The developed model was applied to predict pit subsidence and the effects on pipelines. The analysis was completed for the 30-inch with D/t ratio of 96 to assess its response to pit subsidence considering a large pit diameter of 20 m. Note that the focus of the project is sag subsidence. This example was completed to demonstrate the significance of the pit subsidence geotechnical hazard events.

Detailed results are presented as follows:

- Figure 4.44 shows an example of predicted pit subsidence, where the pipeline experiences the adhesive resistance from the surrounding soil in addition to the weight of the soil above.

- Figure 4.45 plots pipeline profile and axial strains distribution at different clock positions (6 and 12 o'clock) along the length of the pipeline. The results indicated that the tensile strains increase to levels higher than 2% while the peak compressive strains were on the order of 0.5% for this analyzed case.

- Figure 4.46 and 4.47 plot the pipe vertical displacement and peak tensile in pipe in relation to subsidence. The results clearly indicate that the pipeline response to pit subsidence is fairly complex and cyclic. The pipe in the mid plane settles to transfer the load from weight of the soil above and the soil resistance from the surrounding soil. However, as the soil surrounding start to move, "fall" around the pipe, the pipe

The information contained herein is the copyright of and proprietary to BMT Fleet Technology Limited. Use of this information is governed by the legend on the cover page of this document."

starts to rebound and covers about 17% of its vertical deflection, for the analyzed case.

These results suggest that while the response of the pipe included bending (curvature) effects, a significant component of the pipe strains are derived from pipe axial extension.

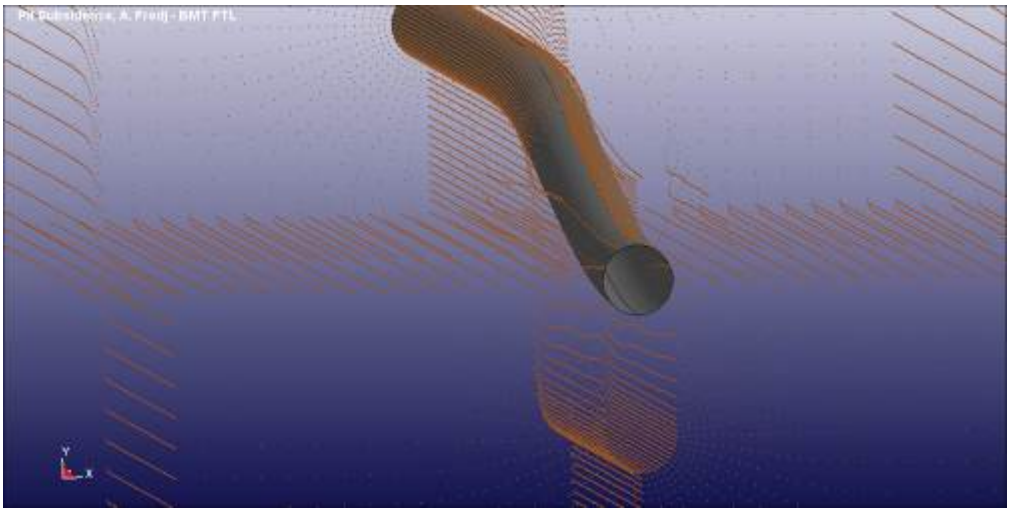

Figure 4.44: Pit Subsidence – Pipe Deflection

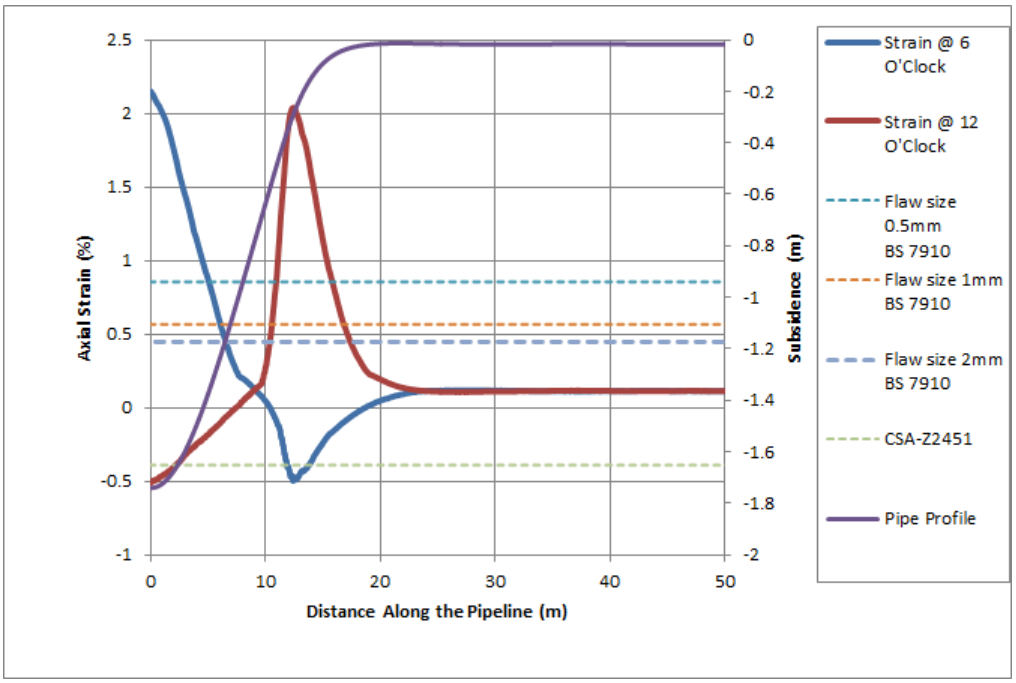

Figure 4.45: Predicted Pipeline Profile and Maximum Tensile Strains in the Pipe for Pit Subsidence of 2.05 M

The information contained herein is the copyright of and proprietary to BMT Fleet Technology Limited. Use of this information is governed by the legend on the cover page of this document."

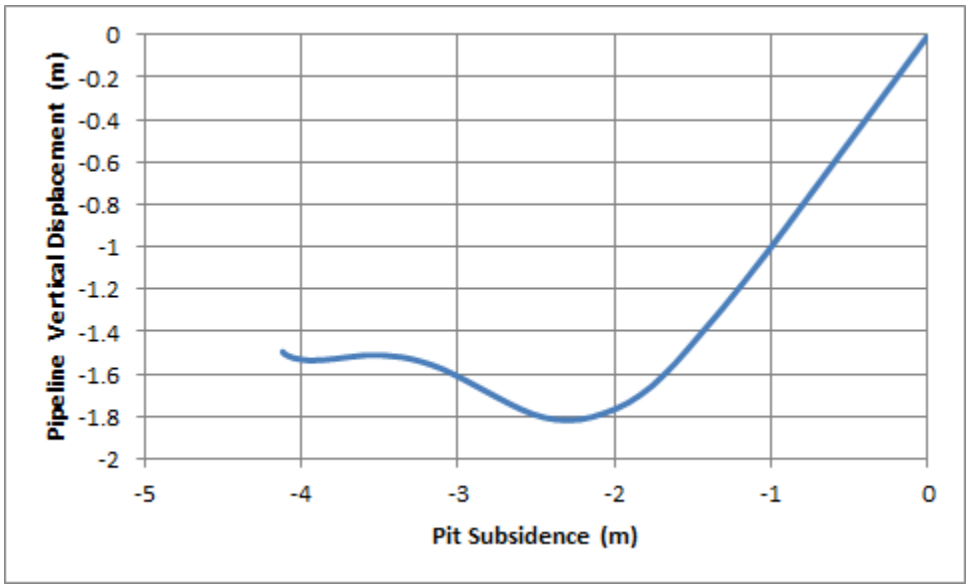

Figure 4.46: Peak Pipe Displacement in Relation to Pit Subsidence

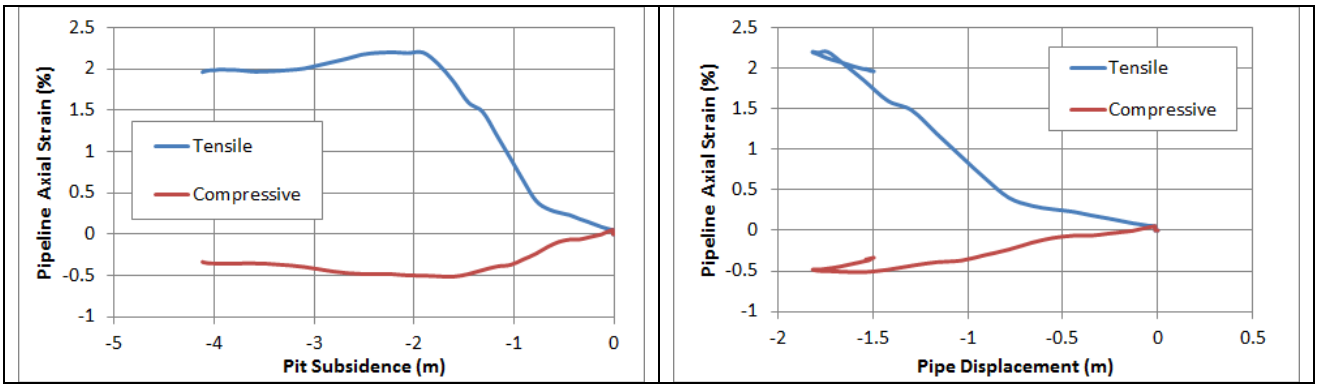

Figure 4.47: Maximum Tensile Strains in the Pipe in Relation to Pit Subsidence (Left) and Vertical Pipe Deflection (Right)

The information contained herein is the copyright of and proprietary to BMT Fleet Technology Limited. Use of this information is governed by the legend on the cover page of this document."

5 MODELING OF PIPELINE SUBSIDENCE HAZARDS

The objective of this section is to complete a sensitivity study to define the problem parameters and the pipe strains developed in pipeline subsidence events and identify trends.

The analyses considered 90 ground subsidence scenarios. The scenarios included the following:

- Pipe geometry: four pipe diameter NPS 12 (324 mm OD), NPS 18 (457 mm OD), NPS 24 (610 mm OD) and NPS 30 (762 mm OD);
- Pipe wall thickness: three wall thicknesses: 6.35 mm (0.25 inch), 9.52 mm (0.375) and 12.7 mm (0.5 in); corresponding to D/t ratio of 96, 64 and 48, respectively;
- Ground displacement direction: Subsidence, vertical to the pipeline axis;
- Panel widths: three panel widths of 61 m (200 ft), 122 m (400 ft) and 183 m (600 ft)
- Mining depths: three different mining depth for each panel width
- Panel extraction areas defined based on panel width to mining depth ratio (W/H): three W/H ratio of 0.5, 1.5 and 3.0 for each panel width;
- Shape of ground displacement: three ground subsidence patterns;
- One soil conditions with soil properties consistent with sand/clay till; and
- Pipeline burial depth: One burial depth of 1.2m (4 ft) to top pipe, corresponding to 1.5 m (5 ft) depth to pipe center line.

The assumptions for the analyses included in the sensitivity study considering pipeline response to soil displacement pattern were as follows:

- 72%, 50% and 36 % SMYS internal pressure were considered;
- 45°C thermal differential (installation -20°C, max operating temperature 25°C) for the base case. Temperature differentials between construction and operation (ΔT) of 0 °C and 65°C were considered for the sensitivity analysis to evaluate the effect of the temperature differential; and
- Generic stress strain curves for Grade X-52 (359), and X-70 (483) pipe according to the API 5L.

5.1 Finite Element Model Description

LS-DYNA 971 was used to undertake 3D pipe-soil interaction modeling using a Discrete Element Method (DEM). In the DEM model considered in this report the soil is represented by discrete particles and the pipe is modeled using shell element with five (5) integration points through the thickness. The LS-DYNA MAT24 isotropic hardening material model incorporating a Von Mises yield response was calibrated based upon a full true stress strain curve for the pipe material allowing the non-linear bi-axial stress state in the pipe to be considered.

The interaction between the pipeline and the surrounding soil is modeled by a robust penalty-based contact in which slip and separation are allowed between soil particles and the pipe. The

The information contained herein is the copyright of and proprietary to BMT Fleet Technology Limited. Use of this information is governed by the legend on the cover page of this document."

DEM has been applied because it offers the ability to represent the soil as a continuous volume that appropriately permits large displacements while respecting the soil constitutive response and has proven to be a computationally efficient modeling technique.

5.1.1 DEM Model

The LS-DYNA discrete element method used in this report was originally developed by Cundall et al. [45] for rock and soil applications. In the DEM, the granular material is idealized using rigid spherical particles. Each particle may have three displacements and three rotation degrees of freedom. The motion of each particle is computed using Newton's law of motion. A robust penalty-based contact is used to capture the particle-to-particle and particle-structure interaction of dry and wet particles, as shown in Figure 5.1. Penalty-based particle contact is used to capture the inter-particle response and its ability to capture the additional moments introduced by spherical particles through its rolling contact parameter. The motions of the particles are considered in LS-DYNA such that the motions and interactions of individual particles are resolved into normal and tangential components and the total force on a particle is summed. By defining the inter-particle response parameters the volumetric response of the soil can be calibrated to simulate a range of soil types. More detailed information about DEM in LS-DYNA can be found in the LS-DYNA manual and Karajan et al. [46].

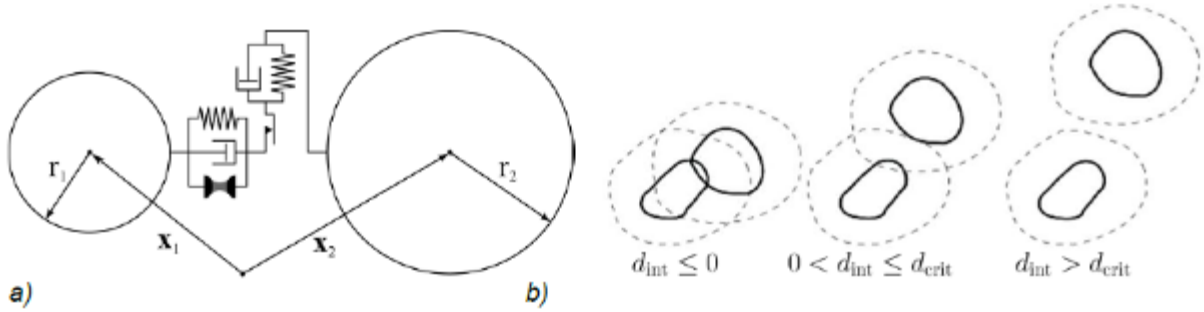

Figure 5.1: (a) Penalty-Based Particle-Particle Interaction in LS-DYNA and (b) Possible Collision States for Mechanical Contact [43, 45]

5.1.2 Loading Sequence

The soil mass in the simulation is taken to be stress free prior to the simulation and the simulation loading is imposed in three steps. In the first step, the gravitational acceleration is applied and sufficient time is allowed to ensure that the soil stress reaches a stationary state. In the second load step, an operating pressure equal to the MOP (72% SMYS) and a temperature differential of 45°C were applied. In the third load step, the surface subsidence was initiated using Appalachian method developed based upon Appalacian mining experince in the USA.

5.1.3 Pipe Properties

The full stress-strain curves of the pipe materials were incorporated in the finite element modeling. Figure 5.2 shows the stress for X70 and X52 materials. This curve was developed based upon the minimum specified material properties from API X52 and X70 material.

The information contained herein is the copyright of and proprietary to BMT Fleet Technology Limited. Use of this information is governed by the legend on the cover page of this document."

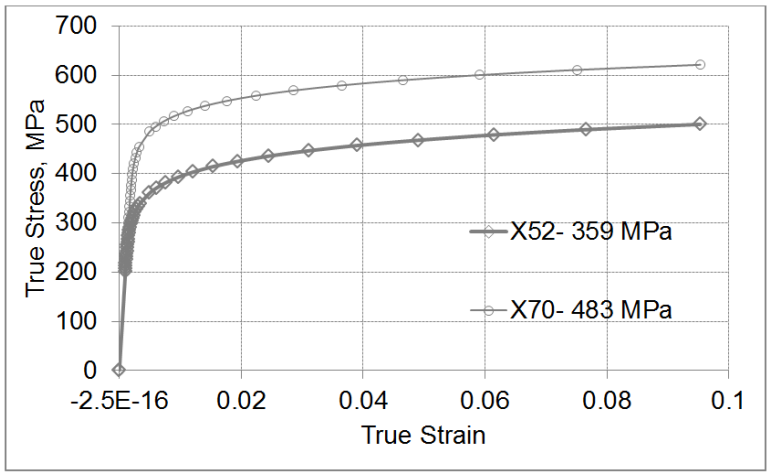

Figure 5.2: True Stress-Strain Curves for X52 and X70 (359 and 483 MPa) Materials

5.2 Structural Analyses for the 24-inch Pipeline

Analyses were completed for the NPS 24 (609 mm outside diameter) pipeline to assess its response to surface subsidence and to determine the structural integrity significance of ground movement induced strain demands. The analyses considered 30 ground subsidence scenarios. The scenarios included the following:

- Pipe wall thickness: three wall thicknesses: 6.35 mm (0.25 inch), 9.52 mm (0.375) and 12.7 mm (0.5 in); corresponding to D/t ratio of 96, 64 and 48, respectively;
- Ground displacement direction: Subsidence, vertical to the pipeline axis;
- Panel widths: three panel widths of 61 m (200 ft), 122 m (400 ft) and 183 m (600 ft)
- Mining depths: three different mining depth for each panel width
- Panel extraction areas defined based on panel width to mining depth ratio (W/H): three W/H ratio of 0.5, 1.5 and 3.0 for each panel width;
- Shape of ground displacement: three ground subsidence patterns;
- One soil conditions with soil properties consistent with sand/clay till; and
- Pipeline burial depth: One burial depth of 1.2m (4 ft) to top pipe, corresponding to 1.5 m (5 ft) depth to pipe center line.

The surface subsidence profile was initiated using Appalachian method developed based upon Applachian mining experience in The USA.

Figures 5.3, 5.4 and 5.5 show the assumed patterns for different widths considering sub-critical, critical and super-critical panel width extraction.

The information contained herein is the copyright of and proprietary to BMT Fleet Technology Limited. Use of this information is governed by the legend on the cover page of this document."

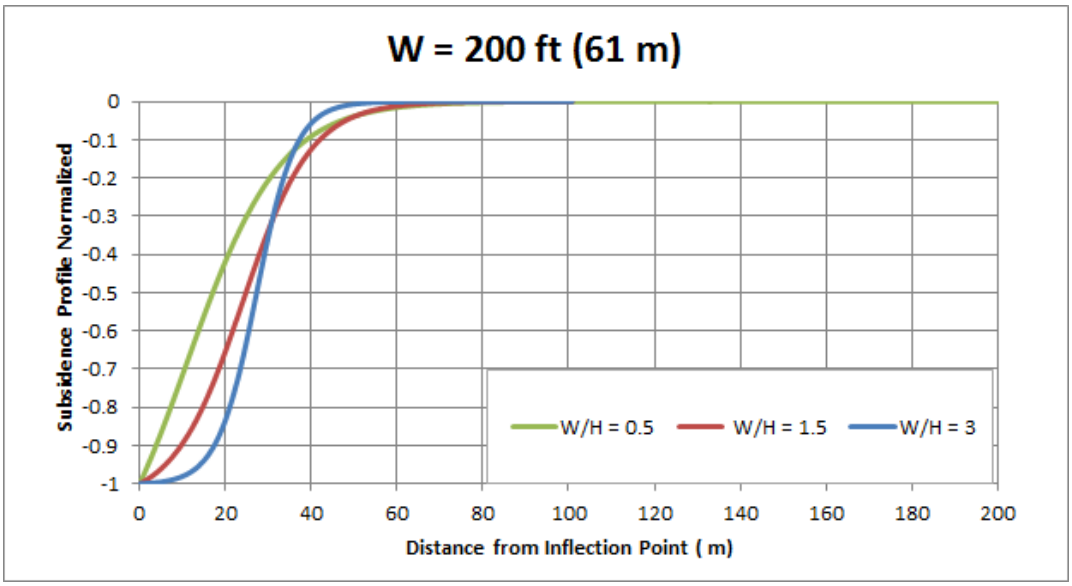

Figure 5.3: Subsidence Profile Pattern, W =200 ft (61 m) - H/W = 0.5, 1.5 and 3

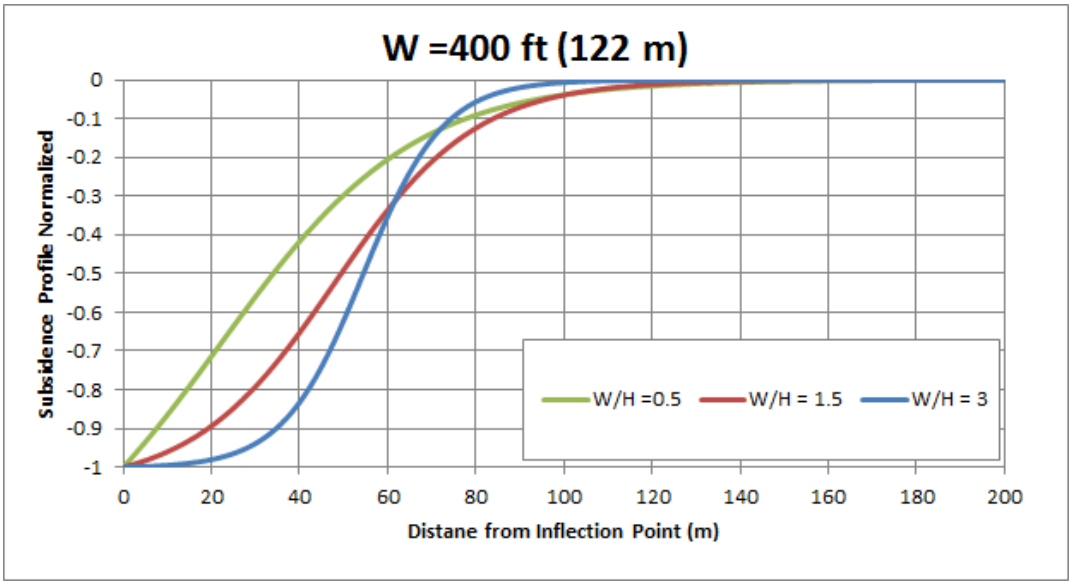

Figure 5.4: Subsidence Profile Pattern, W = 400 ft (122 m) - H/W = 0.5, 1.5 and 3

The information contained herein is the copyright of and proprietary to BMT Fleet Technology Limited. Use of this information is governed by the legend on the cover page of this document."

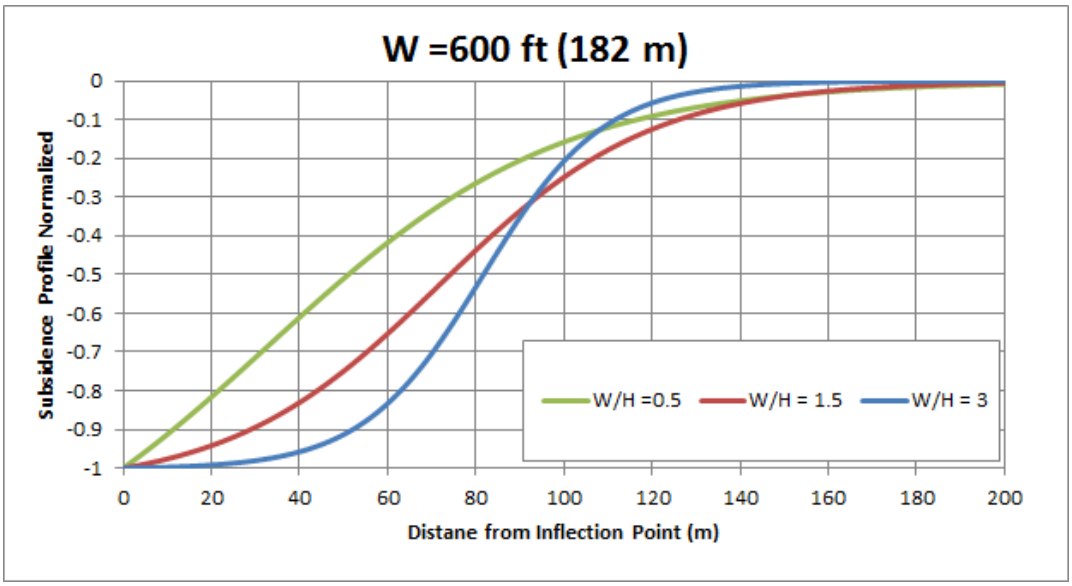

Figure 5.5: Subsidence Profile Pattern, W = 600 ft (182 m) - H/W = 0.5, 1.5 and 3

The assumptions for the analyses included in the sensitivity study considering pipeline response to soil displacement pattern were as follows:

- 72%, 50% and 36 % SMYS internal pressure were considered;
- 45°C thermal differential (installation -20°C, max operating temperature 25°C) for the base case. Temperature differentials between construction and operation (ΔT) of 0°C and 65°C were considered for the sensitivity analysis to evaluate the effect of the temperature differential;
- Generic stress strain curves for Grade X-52 (359), and X-70 (483) pipe according to the API 5L.

5.3 Results Base Case

The following section represents the summary results for the NPS 24 (609 mm outside diameter) for the base case with:

- 6.35 mm (0.25 inch) wall thickness (D/t =96);
- Grade 359 (X-52) pipes;
- 72% SMYS internal pressure, 5.4 MPa;
- 45°C thermal differential (installation -20°C, max operating temperature 25°C);
- Burial depth H=1.2 m (4 ft), corresponding to 1.5 m (5 ft) depth to pipe center line, overburden ratio (H/D) of 2.46;
- Soil: sand/clay till with (ϕ'=30° and C'=5 kPa);

Typical graphical output from finite element model is illustrated in Figure 5.6 and 5.7. These figures illustrate the response of the pressurized NPS 24 pipeline subjected to ground settlement

The information contained herein is the copyright of and proprietary to BMT Fleet Technology Limited. Use of this information is governed by the legend on the cover page of this document."

for mine subsidence width of W= 61 m (200 ft) considering panel width to depth ratio of 0.5. The figures also show the axial strain distribution (blue color is compressive and red is tensile strain). In these figures, the soil above the pipe is hidden so the pipe deformation can be visualized.

Figure 5.8 shows the pipeline longitudinal strains at the 3 o'clock and 9 o'clock positions for peak soil displacement of 3 m. The peak tensile strain is about 1.8 % and is higher than the compressive strain which is approximately 0.79%. This differential in peak tensile and compressive strains indicates that there is a significant uniform axial strain in the pipe due to a large catenary effect.

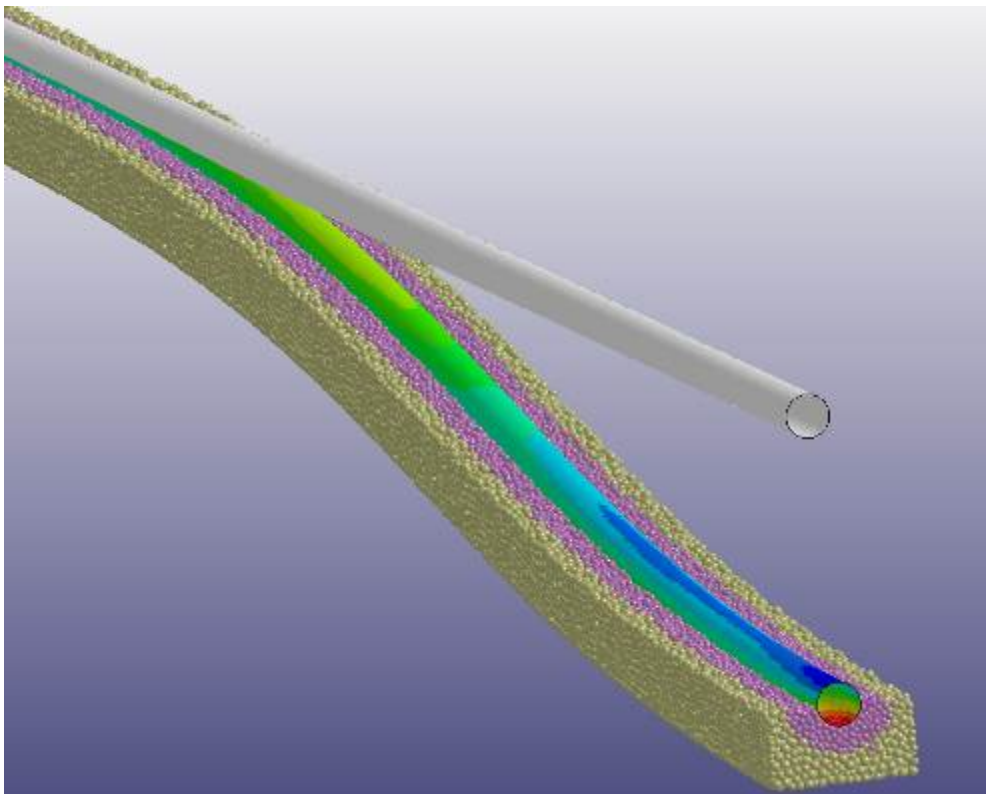

Figure 5.6: Pipe Deformation and Axial Strains for W = 61m (200 Ft) and Ground Subsidence of 4 M (13 Ft) (Top View –Soil Above the Pipe is Hidden)

The information contained herein is the copyright of and proprietary to BMT Fleet Technology Limited. Use of this information is governed by the legend on the cover page of this document."

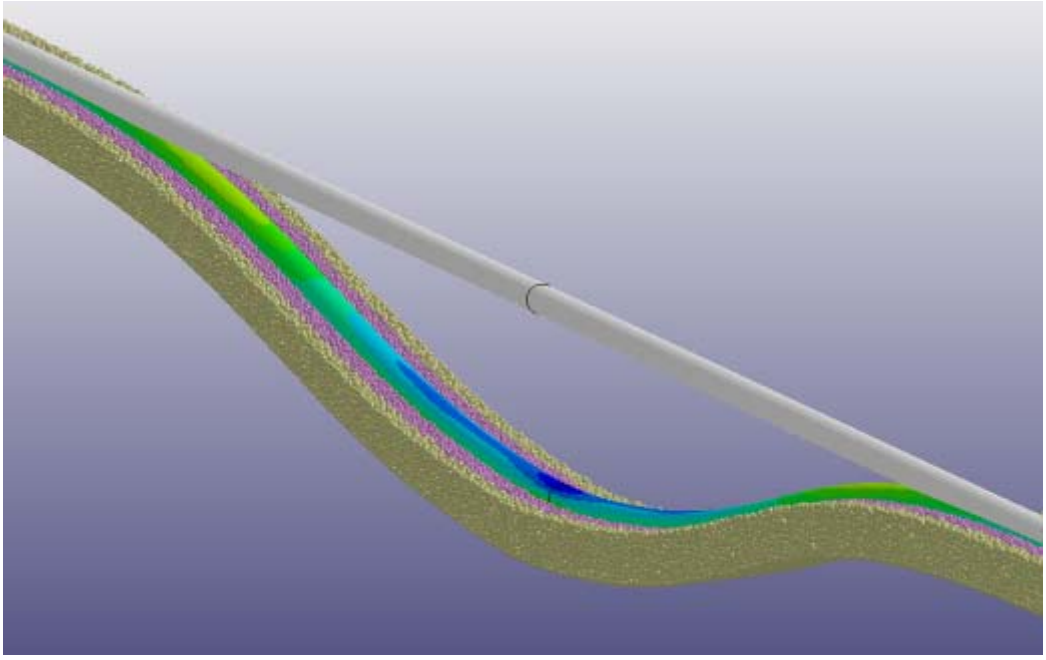

Figure 5.7: Pipe Deformation and Axial Strains for W = 61 m (200 Ft) and Ground Subsidence of 4 M (13 Ft) (Top View – Soil Above the Pipe is Hidden)

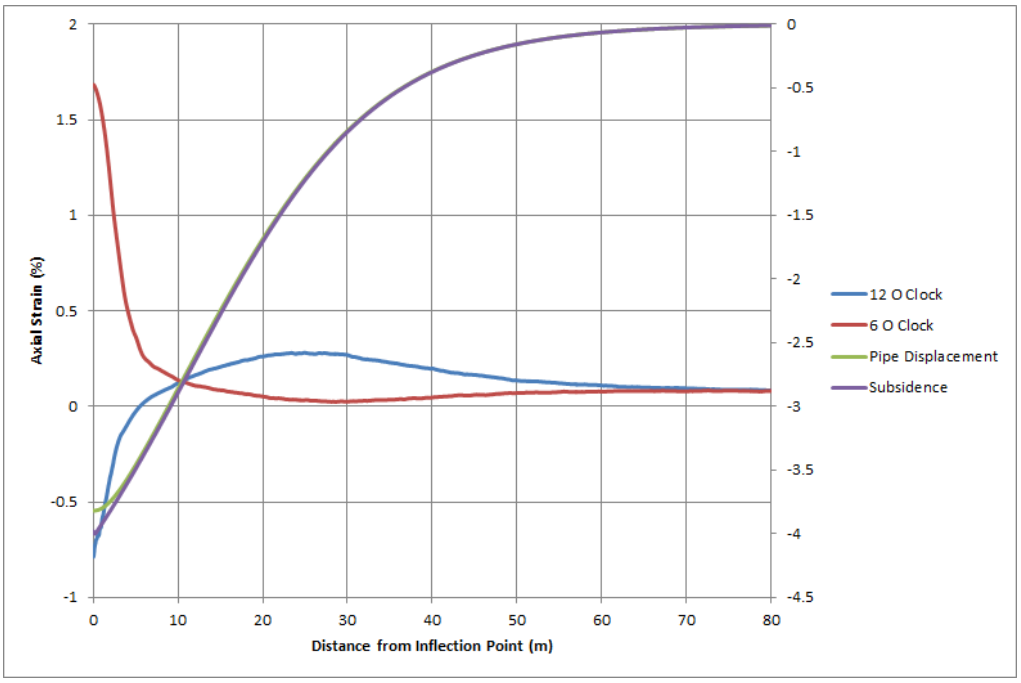

Figure 5.8: Total Axial Strains in NPS 24 (D/t=96) for W = 200 ft (61 m), W/H = 0.5 and Soil Settlement of 4 m

The information contained herein is the copyright of and proprietary to BMT Fleet Technology Limited. Use of this information is governed by the legend on the cover page of this document."

5.3.1 Effect of the Mining Width to Depth Ratio

Figure 5.9 presents the maximum tensile strains in the longitudinal direction of the pipeline versus the maximum ground subsidence for panel extraction width of 61 m (200 ft) considering three (3) potential panel depth that influence surface subsidence, including:

1) sub-critical panel extraction width (W/h=0.5);
2) critical panel extraction width; and (W/h=1.5);
3) super-critical panel extraction width (W/h=3).

Figures 5.10 and 5.11 present the maximum local and nominal compressive strains in the longitudinal direction of the pipeline versus the maximum ground subsidence for various ground subsidence widths to depth ratio considered in the analyses. The nominal compressive strain is defined as the average compressive strain measured over a gauge length of 2D (D is the pipe outside diameter). This large stain gauge length is used to permit the analyses to be compared directly to codified permissible strain formulations which are reported over this gauge length.

The results indicate that for the three (3) cases considered, the sub-critical panel extraction width (W/h=0.5) results in the largest tensile and compressive strain in the pipe for any given value of ground subsidence for analyzed cases.

Figures 5.12 and 5.13 plot the pipe deformation for panel extraction width of 61 m considering a three (3) potential panel width to depth ratio 0.5, 1.5 and 3. The results demonstrate that the pipe deformation is significantly affected by the by the panel width to mining depth ratio (W/H).

- For W/h ratio equal to 0.5 (sub-critical) the width of pipe deformation is narrow and results in higher bending strain. The maximum pipe displacement follows the ground settlement up to a certain soil settlement then the pipe displacement increase more slowly with ground settlement (Figure).
- For W/h ratio equal to 1.5 (critical) the width of pipe deformation is slightly wider than sub-critical strain but large enough to cause the pipe to follow the ground settlement as shown in (Figure).
- For W/h ratio equal to 3 (super - critical) the width of pipe deformation is large enough to potentially cause the maximum possible pipe settlement. It causes a flat area of maximum pipe deformation in the center of the flat surface and causes the pipe to follow the ground settlement as shown in (Figure).

Figures 5.16 through Figures 5.17 plot the surface subsidence profile, pipeline profile and axial strains distribution at different clock positions (6 and 12 o'clock) along the length of the pipeline. The results presented in these figures are for the three (3) analyzed cases. The results demonstrate that the pipeline strain distribution response is significantly affected by the panel width to mining depth ratio (W/H).

The information contained herein is the copyright of and proprietary to BMT Fleet Technology Limited. Use of this information is governed by the legend on the cover page of this document."

1. For sub-critical panel extraction width (W/h =0.5); the peak tensile (1.7%) and compressive (0.8%) strains are at the maximum deflection point.

2. For critical panel extraction width; and (W/h =1.5), the peak tensile strain (0.6%) and compressive strain (0.15%) are at the maximum deflection with 2 additional bending zones at 15 m and 35 meters from the deflection point.

3. For super-critical panel extraction width (W/h =3), the peak tensile strain (0.91%) and compressive strain (0.35%) are at 20 m and 35 m from the deflection point.

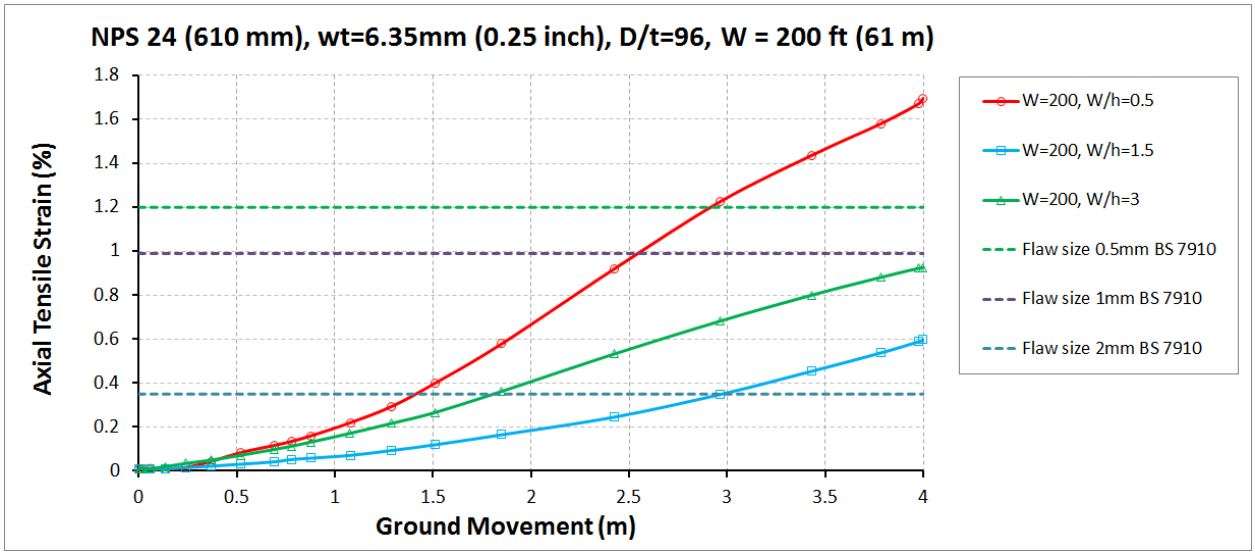

Figure 5.9: NPS 24 (D/t=64) - Maximum Tensile in the Pipe vs. Ground Subsidence W =61 m (200 ft); W/h Ratio 0.5, 1.5 and 3

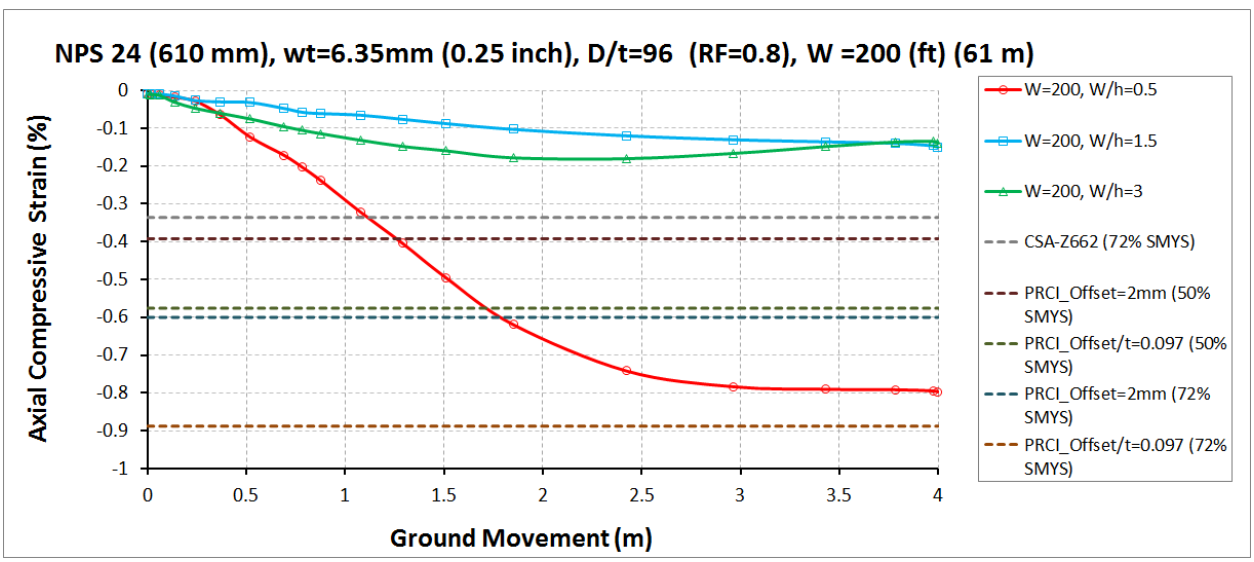

Figure 5.10: NPS 24 (D/t=64) - Maximum Local Compressive Strains in the Pipe vs. Ground Subsidence W =61 m (200 ft); W/h Ratio 0.5, 1.5 and 3

The information contained herein is the copyright of and proprietary to BMT Fleet Technology Limited. Use of this information is governed by the legend on the cover page of this document."

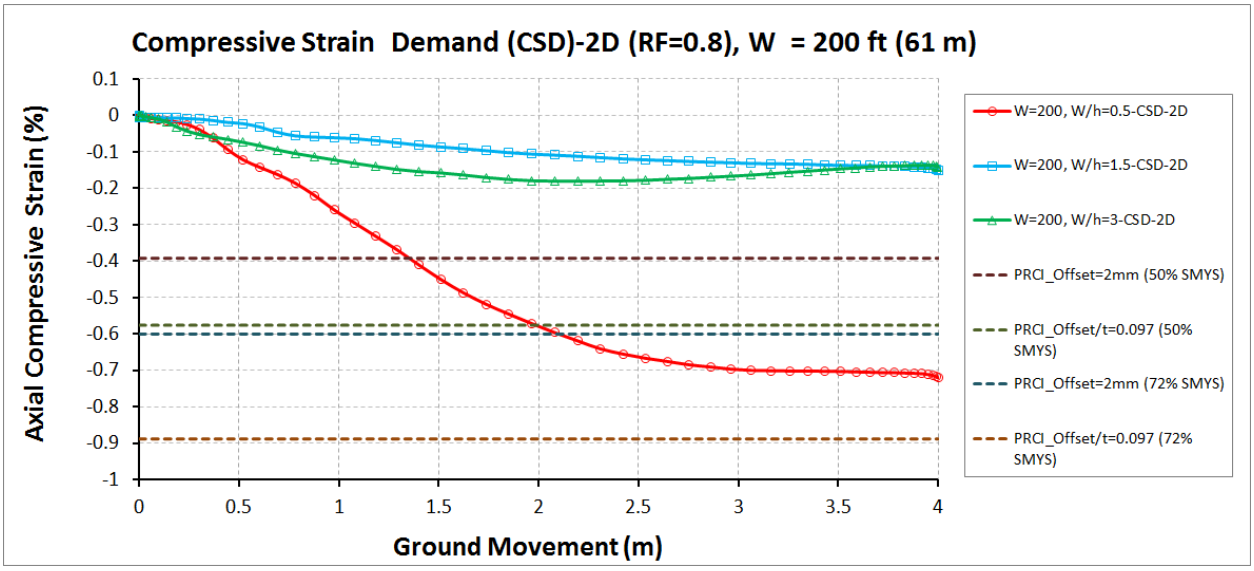

Figure 5.11: NPS 24 (D/t=64) - Maximum Nominal Compressive Strains in the Pipe vs. Ground Subsidence W =61 m (200 ft); W/h Ratio 0.5, 1.5 and 3

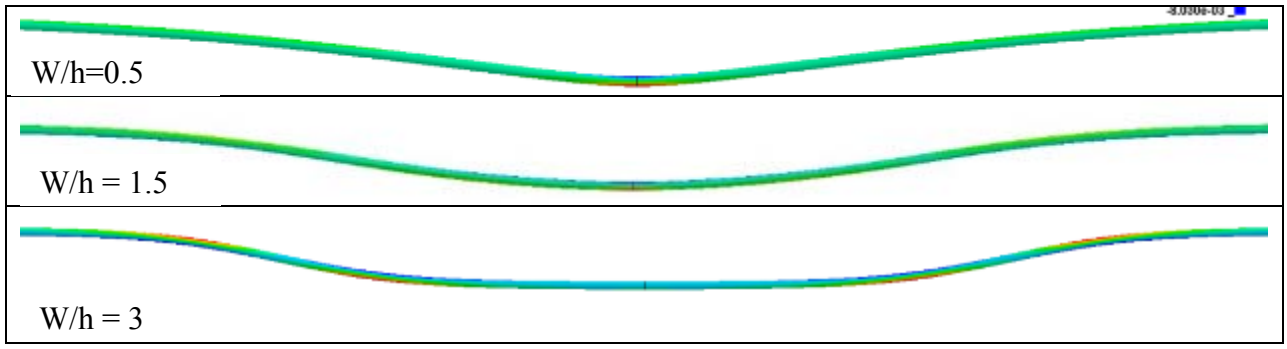

Figure 5.12: Pipe Deformation and Total Axial Strains in NPS 24 (D/t=96) for W = 200 ft (61 m), W/H = 0.5, 1.5 and 3 for Surface Settlement of 4 m

The information contained herein is the copyright of and proprietary to BMT Fleet Technology Limited. Use of this information is governed by the legend on the cover page of this document."

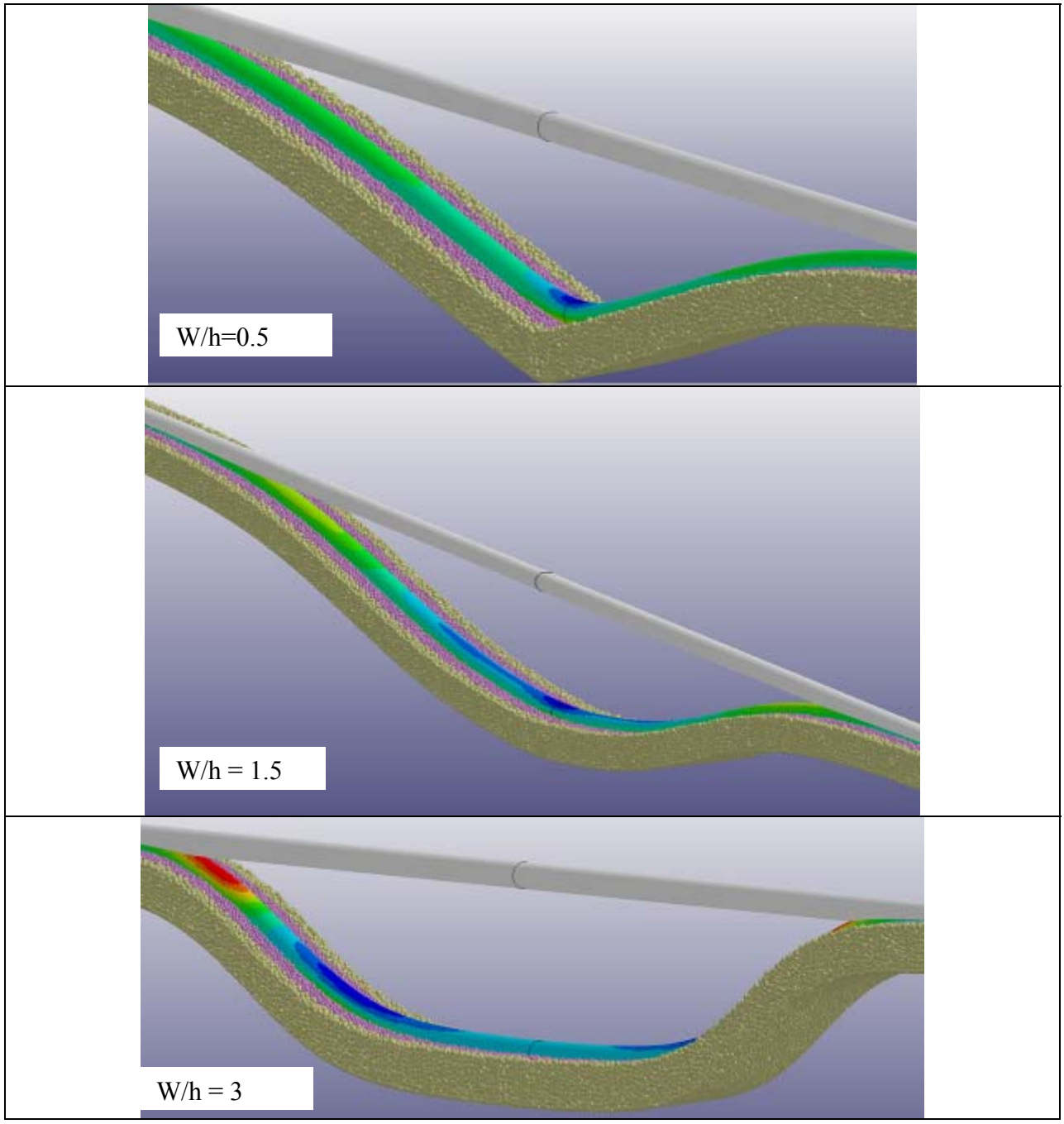

Figure 5.13: Pipe Deformation and Total Axial Strains in NPS 24 (D/t=96) for W = 200 ft (61m), W/h = 0.5, 1.5 and 3 for Surface Settlement of 4 m (Top View – Soil above the pipe is hidden)

The information contained herein is the copyright of and proprietary to BMT Fleet Technology Limited. Use of this information is governed by the legend on the cover page of this document."

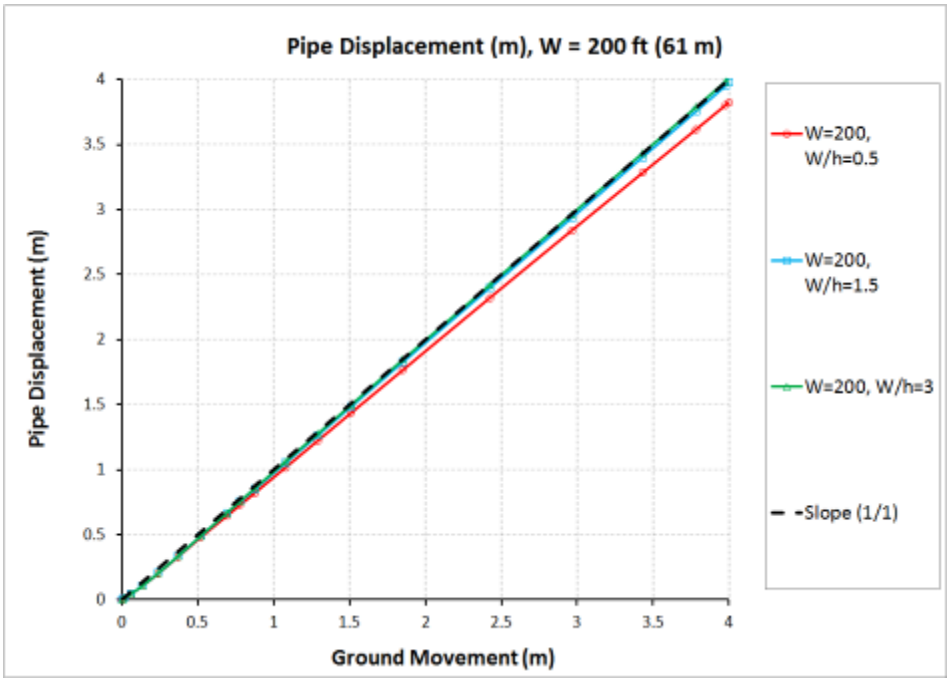

Figure 5.14: NPS 24 (D/t=96) - Pipe Displacing vs. Soil Settlement of 4m

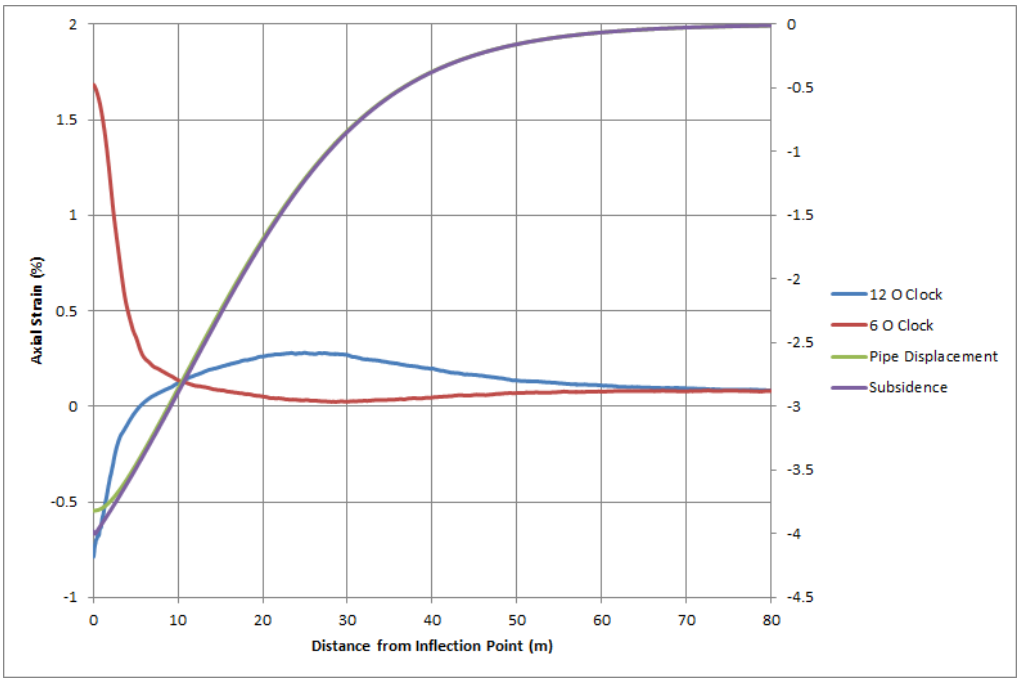

Figure 5.15: Total Axial Strains in NPS 24 (D/t=96) for W = 200 ft (61 m), W/H = 0.5 and Soil Settlement of 4 m

The information contained herein is the copyright of and proprietary to BMT Fleet Technology Limited. Use of this information is governed by the legend on the cover page of this document."

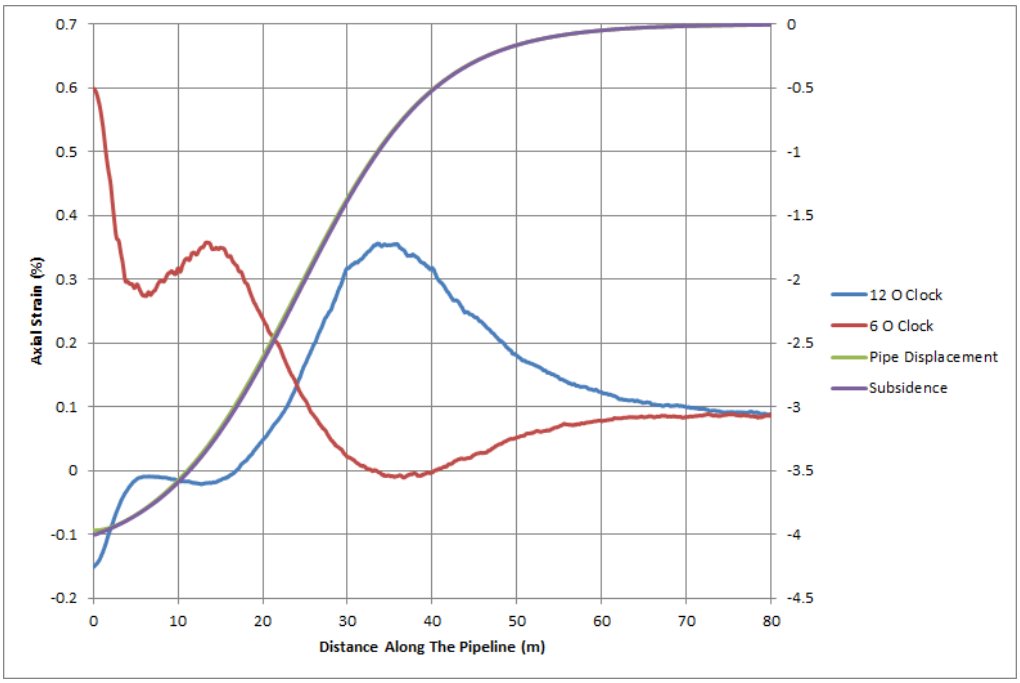

Figure 5.16: Total Axial Strains in NPS 24 (D/t=96) for W = 200 ft (61 m), W/H = 1.5 and Soil Settlement of 4 m

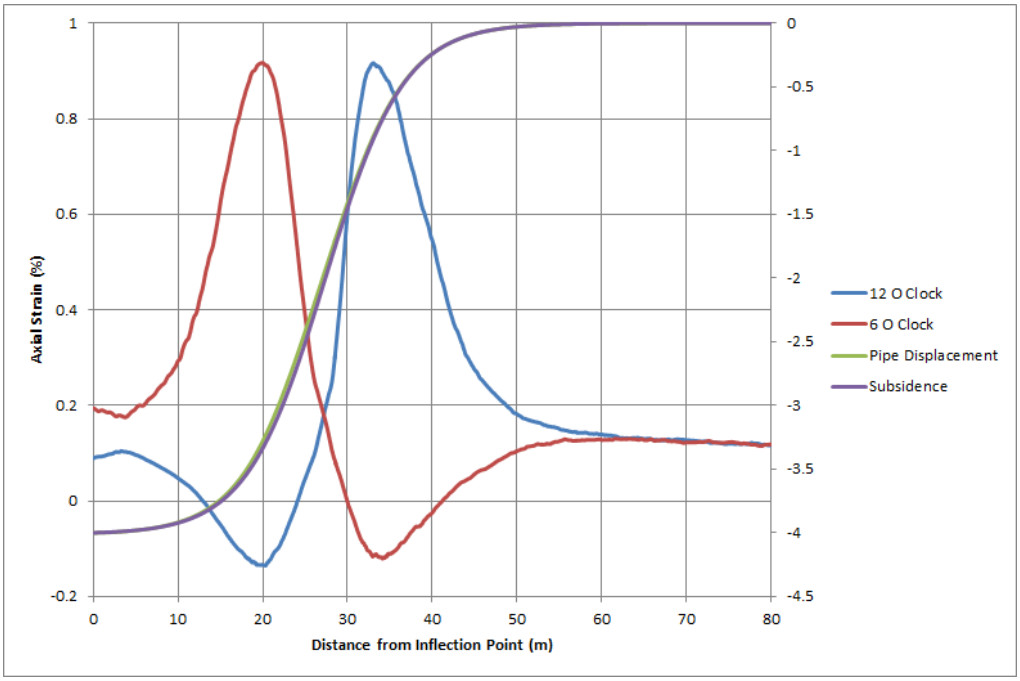

Figure 5.17: Total Axial Strains in NPS 24 (D/t=96) for W = 200 ft (61 m), W/H = 3 and Soil Settlement of 4 m

The information contained herein is the copyright of and proprietary to BMT Fleet Technology Limited. Use of this information is governed by the legend on the cover page of this document."

5.3.2 Comparison with Strain Capacity and Strain Demand Envelopes

5.3.2.1 Comparison with Strain Capacity of the 24 inch pipeline (D/t = 96)

The strain demand determined from the analysis was compared with the calculated strain capacity defined from the guidance; BS 7910 for tensile strain, and CSA Z662 and PRCI 2004 for compressive strain. In the final report, other strain capacity formulations will be considered. The strain capacities calculated in this example and described in Sections 3.0 and 4.0 are provided in Table 5.1 and presented with dashed horizontal line in Figure 5.9 and Figure 5.10. The compressive strain capacity (CSC) given in Table 5.1 is the value after applying a resistance factor (RF) of 0.8 to the computed CSC directly from CSA and UOA/PRCI equations. The tensile strain limit considers the presence of several 50-mm long surface-breaking, semi-elliptical girth weld flaws and all of the strain limits consider the pipeline to be operating at an internal pressure that induces a pipe wall stress of 72% of its SMYS.

Table 5.1: Maximum Allowable Tensile and Compressive Strain for NPS 24, Wt=6.35mm, D/t=96, Grade X52

Tensile Strain Limit (%)			Compressive Strain (%) –Resistance Factor =0.8		
BS 7910 Flaw Depth (mm)			CSA Z662	PRCI	
0.5	1	2	(72% SMYS)	(50% SMYS)	(72% SMYS)
1.2	0.99	0.35	-0.34	-0.39	-0.6

5.3.2.1.1 Tensile Strain Capacity Envelopes (TSCE)

Figure 5.9 presents the maximum tensile strains in pipe versus the ground subsidence width (W) to panel depth for given ground displacement of 0.5, 1.0, 1.5, 2.5, 3.0, 3.0 and 4.0. In this figure, the BS-7910 tensile strain capacity is presented with dash horizontal line. Any tensile strain above the horizontal line is strain-related failure limit.

In Figure , Figure , Figure 5.9 and Figure 5.10 the strain demands from the analysis were used to relate the geotechnical event (subsidence), soil, pipe and pipeline operating conditions to tensile and compressive strains produced ground settlement.

The results indicate that for this pipe and operating condition combination, panel width to depth ratio of 0.5 can be considered critical. This result suggests that the pipeline is forced to follow the ground subsidence pattern and more sharp subsidence profiles promotes higher curvature along with pipe axial extension. The tensile strain-related failure limit for the critical width is reached for ground displacement from 1.5 to 3 m considering a flaw size of 2, 1 and 0.5 mm, respectively. Strains are minimized when the panel width to depth ratio is at a value of approximately 1.75.

The information contained herein is the copyright of and proprietary to BMT Fleet Technology Limited. Use of this information is governed by the legend on the cover page of this document."

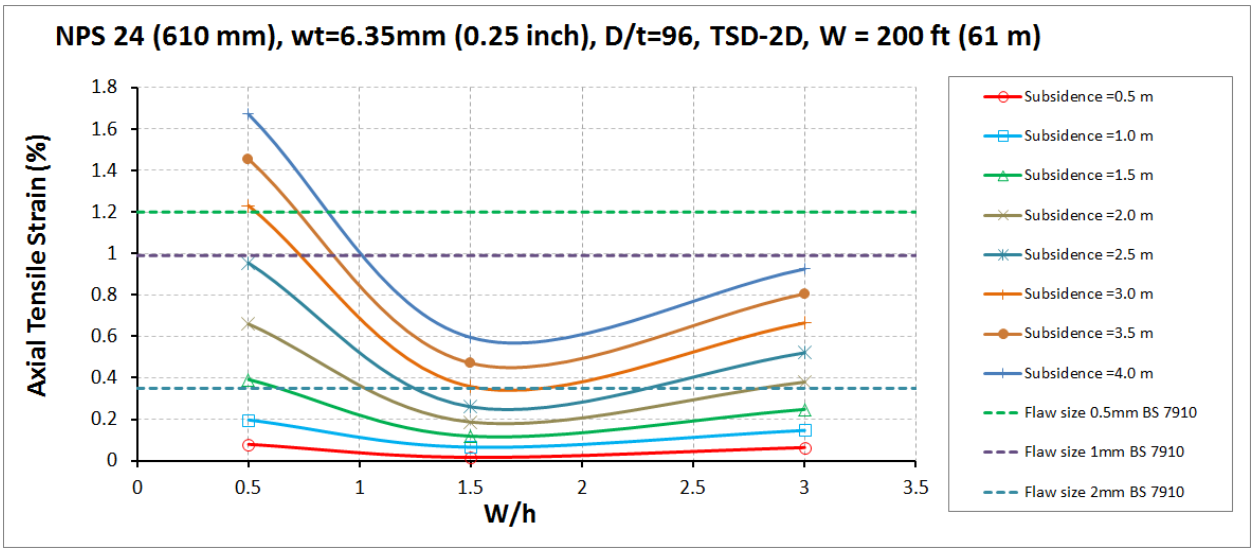

Figure 5.9: Pipe Axial Tensile Strains Envelopes versus Width to Depth Ratio (W =61 m, 200 ft) for Ground Settlement of 0.5, 1, 1.5, 2.0, 2.5, 3.0, 3.5 and 4.0 m

5.3.2.1.2 Compressive Strain Capacity Envelopes (CSCE)

Figure 5.10 presents the maximum nominal compressive strain in the pipe versus the panel width to depth ratio (W/h) for given ground settlement of 0.5, 1.0, 1.5, 2.0, 2.5, 3.0, 3.5 and 4.0. The nominal compressive strain is defined as the average compressive strain measured over a gauge length of 2D (D is the pipe outside diameter). In this figure, the CSA and PRCI compressive strain capacity is presented with dash horizontal line. The compressive strains are maximized for lower panel width ratios.

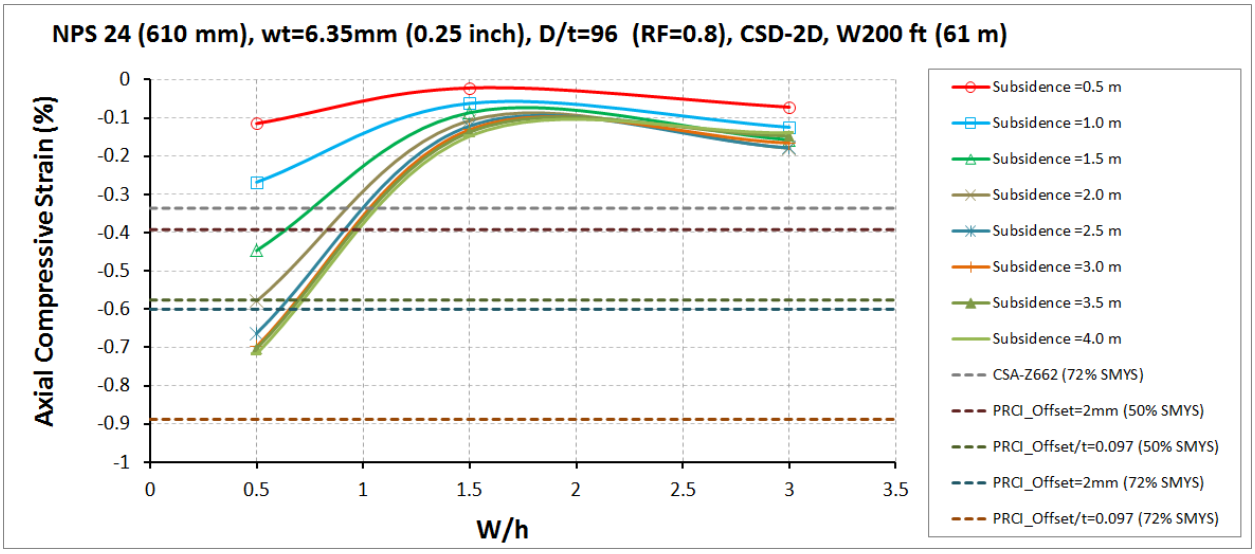

Figure 5.10: Pipe Axial Compressive Strains Envelopes versus Width to Depth Ratio (W =61 m, 200 ft) for Ground Settlement of 0.5, 1, 1.5, 2.0, 2.5, 3.0, 3.5 and 4.0 m

The information contained herein is the copyright of and proprietary to BMT Fleet Technology Limited. Use of this information is governed by the legend on the cover page of this document."

5.3.3 Effect of the Width of the Subsidence

Figure 5.11 through Figure 5.13 present the maximum tensile and compressive strains in the pipe versus the maximum ground settlement for three (3) panel widths analyzed; 200 ft (61 m), 400 ft (122 m) and 600 ft (183m) considering panel width to depth ratio of 0.5, 1.5 and 3.0 for each case (width). The results indicate that for the three (3) widths considered, the width of 200 ft (61m) results in the largest tensile and compressive strain in the pipe for any given value of ground settlement. Also, the panel width to depth ratio of 0.5 results in the largest tensile and compressive strain in the pipe for the three (3) analyzed widths.

Figure 5.14 through Figure 5.16 presents the sum of tensile (positive) and compressive (negative) strains in the pipe. The results indicated that for subsidence width of 200 ft (61 m) the calculated compressive strains are slightly higher at ground displacement less than 0.5 m; this is mainly due to compressive strain induced by thermal loading. At large ground displacement, tensile strains are higher than compressive strain. This differential in peak tensile and compressive strains indicates that there is a significant uniform axial strain in the pipe due to larger catenary effect. Also, the results indicated that for subsidence higher that 400 ft (122 m) the sum of tensile (positive) and compressive (negative) strains in the pipe is negligible that indicate that the pipe is subjected to pure bending.

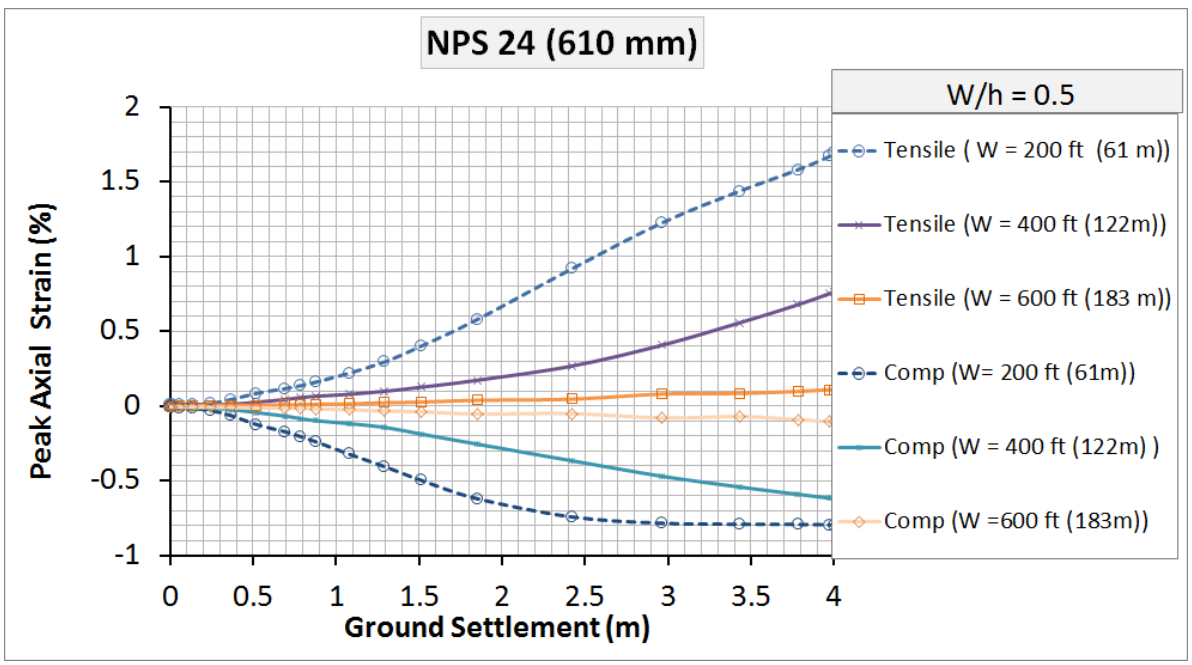

Figure 5.11: NPS 24 (D/t=96) - Maximum Tensile and Local Compressive Strains in the Pipe vs. Ground Settlement: [W/h= 0.5]

The information contained herein is the copyright of and proprietary to BMT Fleet Technology Limited. Use of this information is governed by the legend on the cover page of this document."

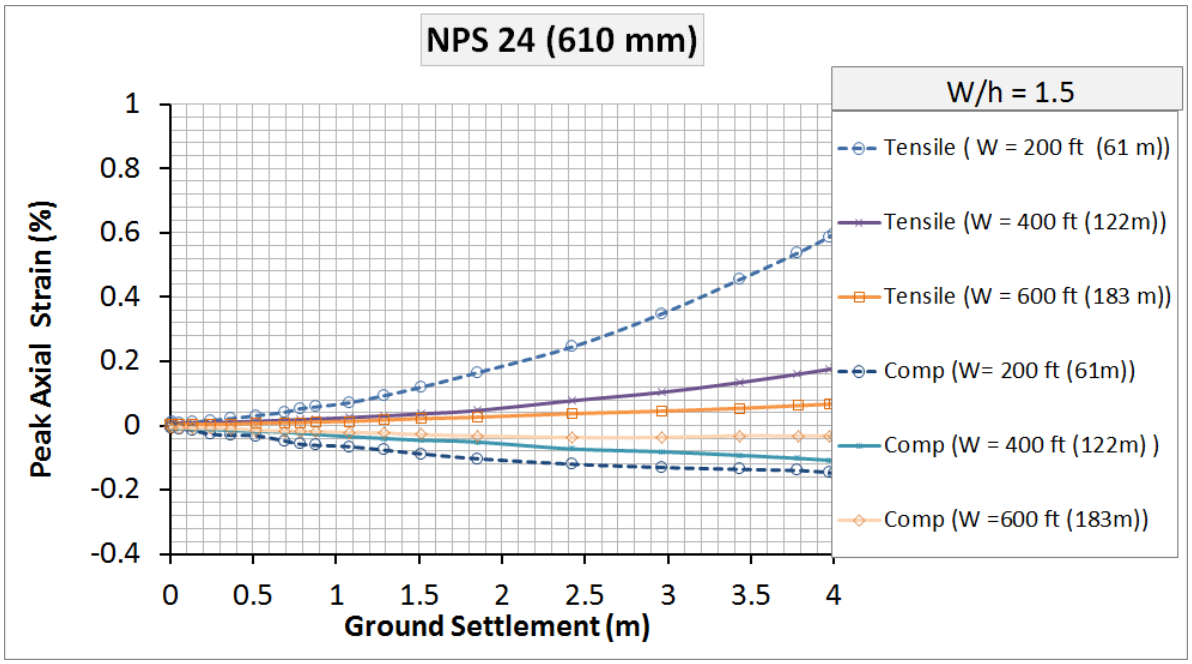

Figure 5.12: NPS 24 (D/t=96) - Maximum Tensile and Local Compressive Strains in the Pipe vs. Ground Settlement: [W/h= 1.5]

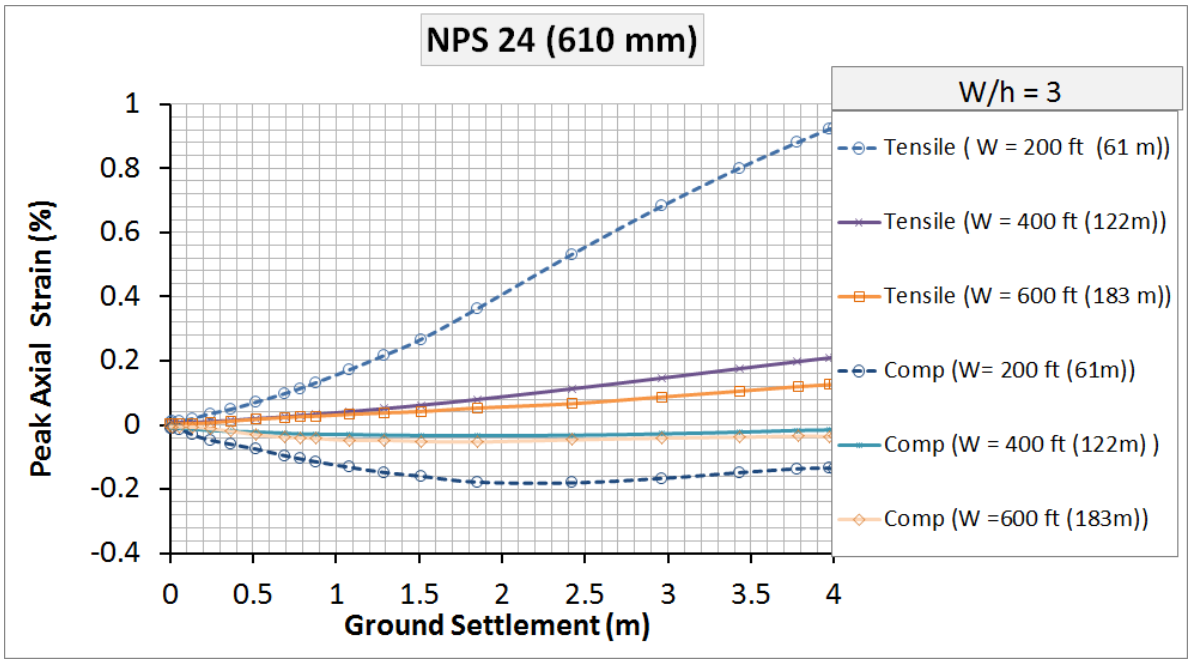

Figure 5.13: NPS 24 (D/t=96) - Maximum Tensile and Local Compressive Strains in the Pipe vs. Ground Settlement: [W/h= 3]

The information contained herein is the copyright of and proprietary to BMT Fleet Technology Limited. Use of this information is governed by the legend on the cover page of this document."

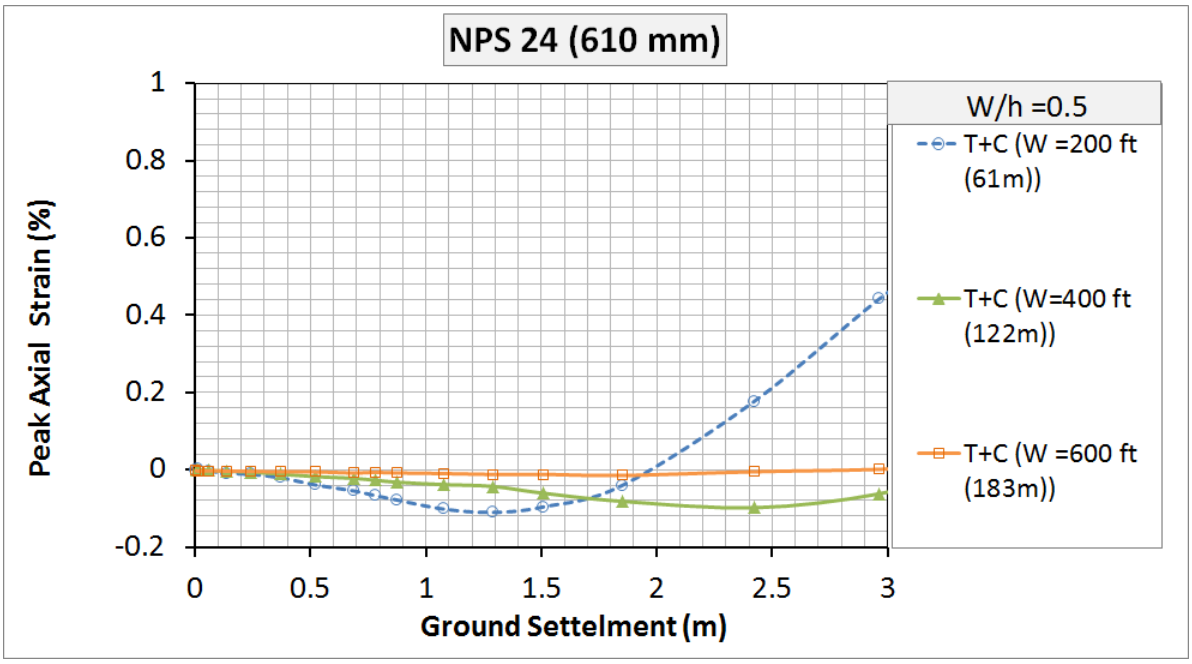

Figure 5.14: NPS 24 (D/t=96) – Sum of Maximum Tensile (Positive) and Local Compressive Strains (Negative) vs. Ground Settlement: [W/h= 0.5]

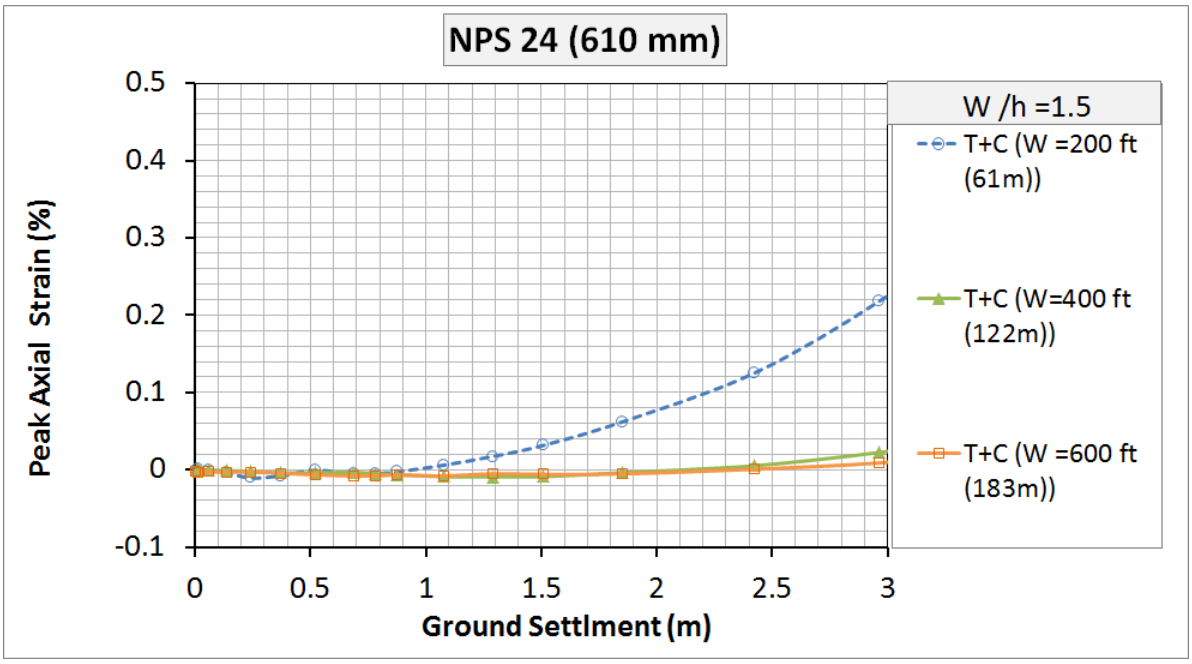

Figure 5.15: NPS 24 (D/t=96) – Sum of Maximum Tensile (Positive) and Local Compressive Strains (Negative) vs. Ground Settlement: [W/h= 1.5]

The information contained herein is the copyright of and proprietary to BMT Fleet Technology Limited. Use of this information is governed by the legend on the cover page of this document."

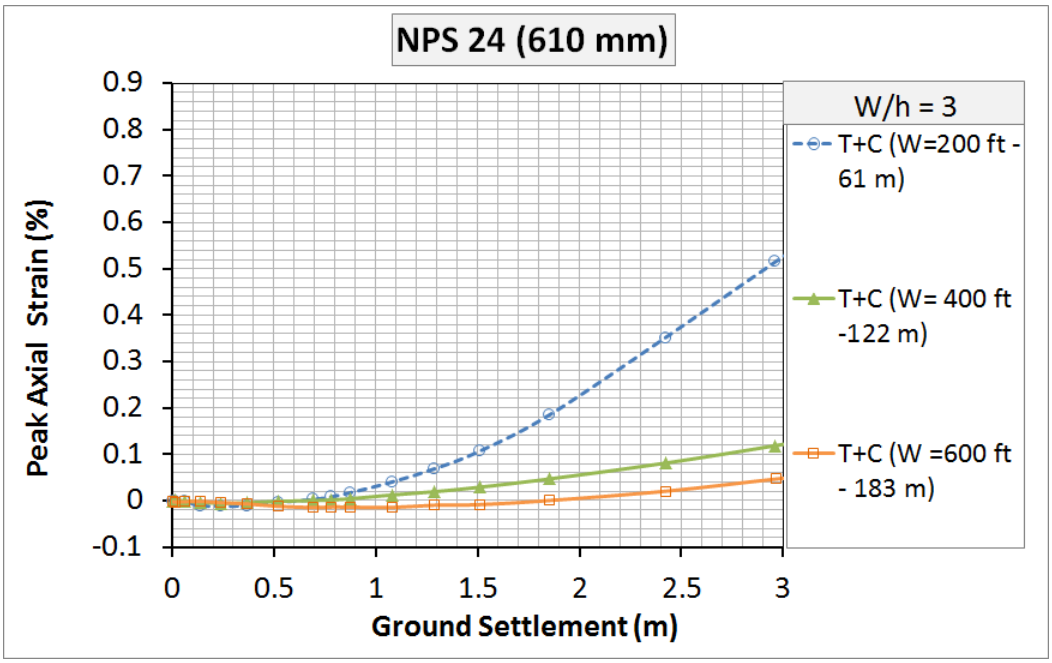

Figure 5.16: NPS 24 (D/t=96) – Sum of Maximum Tensile (Positive) and Local Compressive Strains (Negative) vs. Ground Settlement: [W/h= 3]

5.3.4 Comparison with Strain Capacity and Strain Demand Envelopes

5.3.4.1 Comparison with Strain Capacity of the 24 inch Pipeline (D/t=96)

The strain demand determined from the analysis was compared with the calculated strain capacity defined from the guidance; BS 7910 for tensile strain, and CSA Z662 and PRCI 2004 for compressive strain. In the final report, other strain capacity formulations will be considered. The strain capacities calculated in this example and described in Sections 3.0 and 4.0 are provided in Table 5.1 and presented with dash horizontal line in Figure 5.13 and Figure 5.15. The compressive strain capacity (CSC) given in Table 5.1 is the value after applying a resistance factor (RF) of 0.8 to the computed CSC directly from CSA and UOA/PRCI equations. The tensile strain limit considers the presence of several 50-mm long surface-breaking, semi-elliptical girth weld flaws and all of the strain limits consider the pipeline to be operating at an internal pressure that induces a pipe wall stress of 72% of its SMYS.

Figure 5.17 through Figure 5.19 presents the maximum tensile strains in the longitudinal direction of the pipeline versus the maximum ground settlement for various ground subsidence widths and width to depth ratio considered in the analyses. In this figure, the BS-7910 tensile strain capacity is presented with dash horizontal line. Any tensile strain above the horizontal line is strain-related failure limit. The results indicated that subsidence width of 61 m (200 ft) with width to depth ratio of 0.5 results in the largest tensile and compressive strain

Figure 5.20 through Figure 5.22 present the maximum nominal compressive strains in the longitudinal direction of the pipeline versus the maximum ground subsidence for various ground subsidence widths considered in the analyses. The nominal compressive strain is defined as the

The information contained herein is the copyright of and proprietary to BMT Fleet Technology Limited. Use of this information is governed by the legend on the cover page of this document."

average compressive strain measured over a gauge length of 2D (D is the pipe outside diameter). This large stain gauge length is used to permit the analyses to be compared directly to codified permissible strain formulations which are reported over this gauge length. In this figure, the PRCI compressive strain capacity is presented with dash horizontal line. Any compressive strain above the horizontal line is strain-related failure limit.

The results indicate that for the three (3) widths considered, the width of 61 m (200 ft) results in the largest tensile and compressive strain in the pipe for any given value of ground displacement.

The results indicated that subsidence width of 61 m (200 ft) with width to depth ratio of 0.5 results in the largest tensile and compressive strain. For large width of 183 m (600 ft) the strain demand do not exceed the tensile and compressive strain limit for ground subsidence up to 4 m (13 ft).

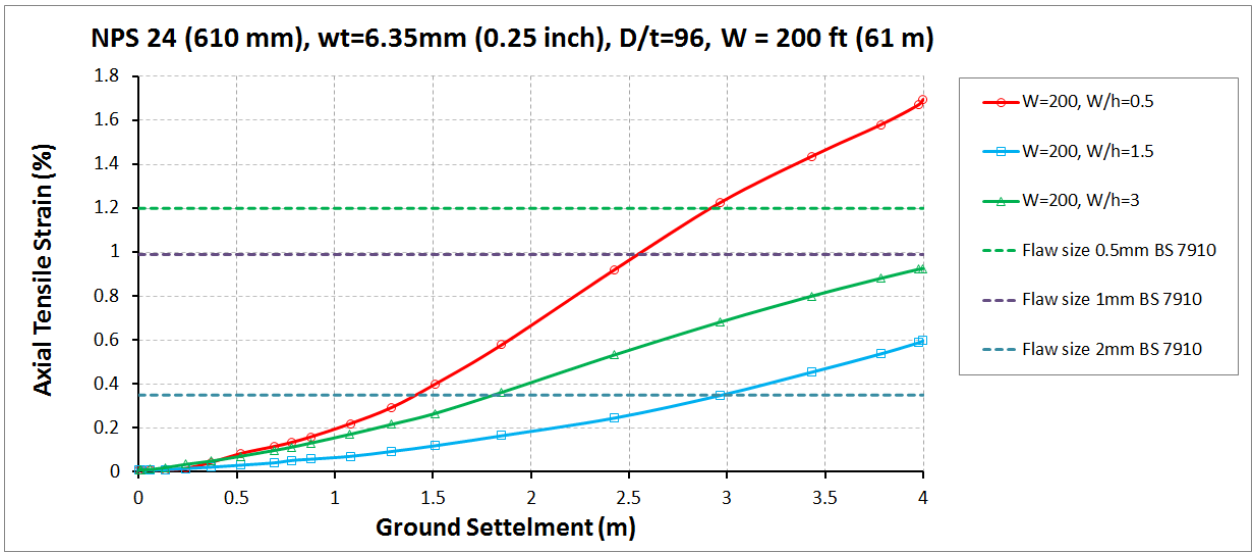

Figure 5.17: NPS 24 (D/t=64) - Maximum Tensile in the Pipe vs. Ground Subsidence W = 61 m (200 ft); W/h Ratio 0.5, 1.5 and 3

The information contained herein is the copyright of and proprietary to BMT Fleet Technology Limited. Use of this information is governed by the legend on the cover page of this document."

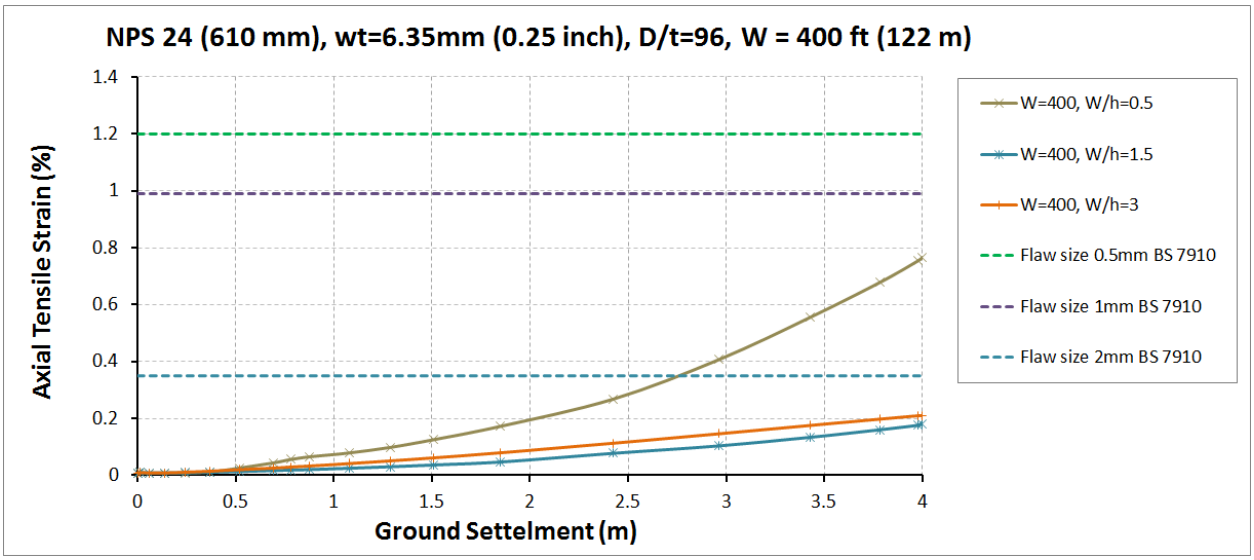

Figure 5.18: NPS 24 (D/t=64) - Maximum Tensile in the Pipe vs. Ground Subsidence W = 122 m (400 ft); W/h Ratio 0.5, 1.5 and 3

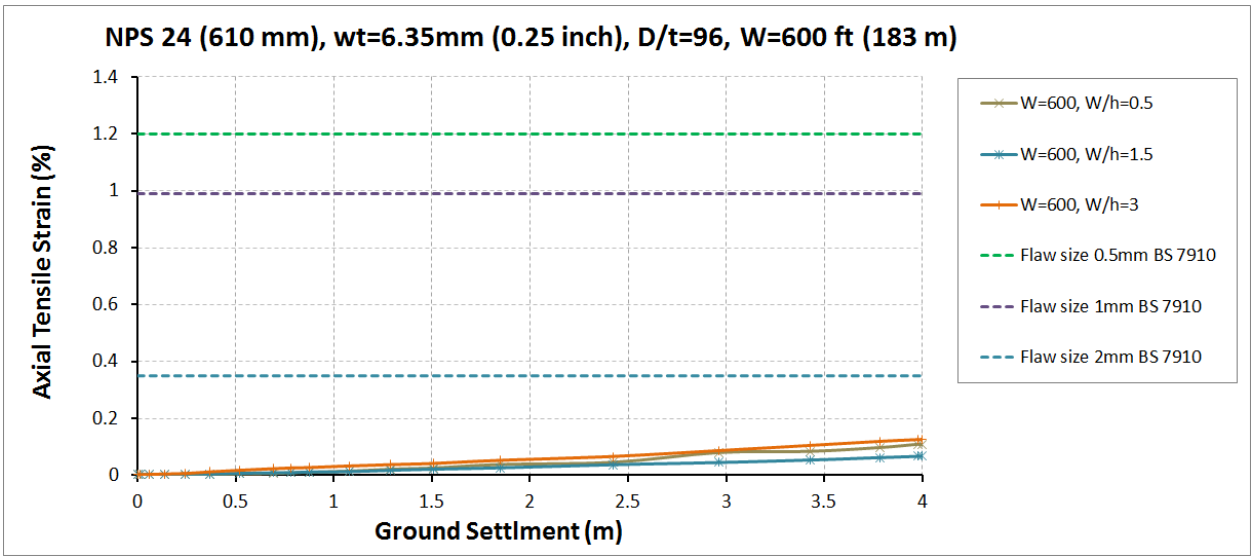

Figure 5.19: NPS 24 (D/t=96) - Maximum Tensile in the Pipe vs. Ground Subsidence W = 183 m (600 ft); W/h Ratio 0.5, 1.5 and 3

The information contained herein is the copyright of and proprietary to BMT Fleet Technology Limited. Use of this information is governed by the legend on the cover page of this document."

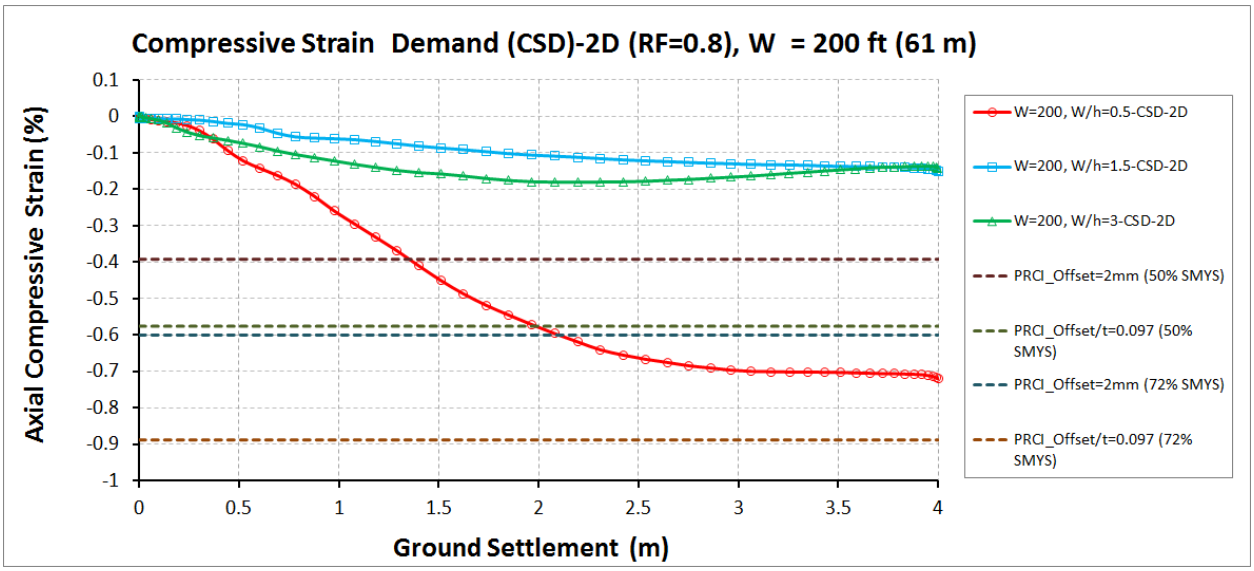

Figure 5.20: NPS 24 (D/t=96) - Maximum Nominal Compressive Strains in the Pipe vs. Ground Subsidence W = 61 m (200 ft); W/h Ratio 0.5, 1.5 and 3

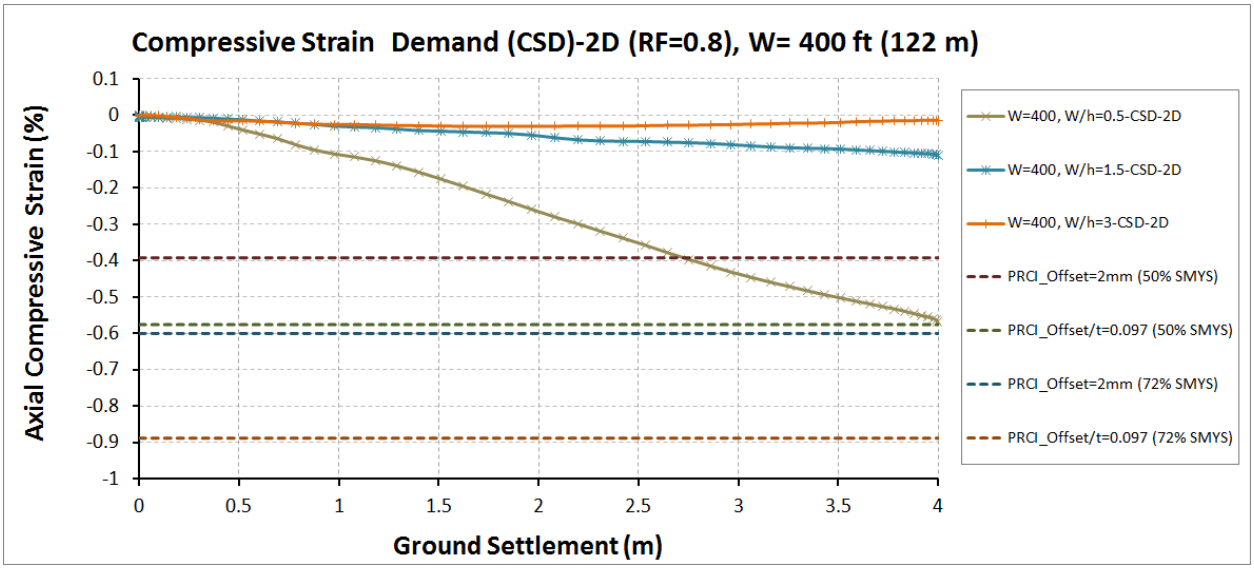

Figure 5.21: NPS 24 (D/t=96) - Maximum Nominal Compressive Strains in the Pipe vs. Ground Subsidence W = 122 m (400 ft); W/h Ratio 0.5, 1.5 and 3

The information contained herein is the copyright of and proprietary to BMT Fleet Technology Limited. Use of this information is governed by the legend on the cover page of this document."

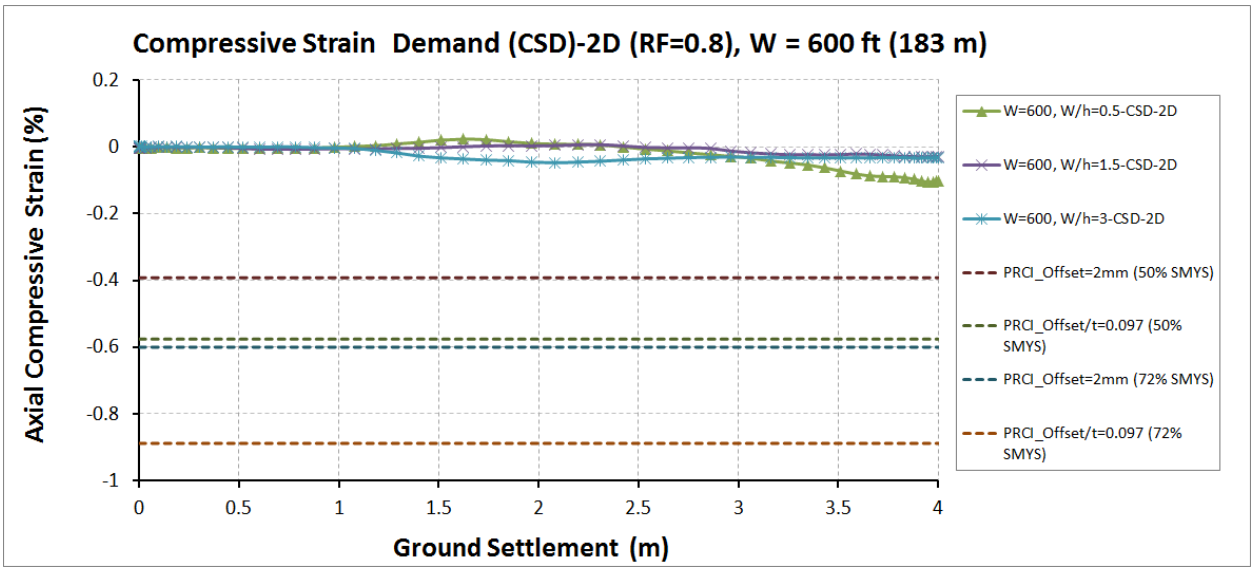

Figure 5.22: NPS 24 (D/t=96) - Maximum Nominal Compressive Strains in the Pipe vs. Ground Subsidence W = 183 m (600 ft); W/h Ratio 0.5, 1.5 and 3

5.3.4.1.1 Tensile Strain Capacity Envelopes (TSCE)

Figure 5.23, Figure 5.24 and Figure 5.25 present the maximum tensile strains in pipe versus the three (3) ground subsidence widths considered for given ground subsidence of 0.5, 1.0, 1.5, 2.5, 3.0, 3.0 and 4.0. In these figures, the BS-7910 tensile strain capacity is presented with a dashed horizontal line. Any tensile strain above the horizontal line is strain-related failure limit.

In these figures, the strain demands from the analysis were used to relate the geotechnical event (subsidence), soil, pipe and pipeline operating conditions to tensile and compressive strains produced ground settlement.

The results indicate that for this pipe and operating condition combination, panel width to depth ratio of 0.5 can be considered critical. The tensile strain-related failure limit for the critical width is reached for ground displacement from 1.5 to 3 m considering a flaw size of 2, 1 and 0.5 mm, respectively.

The information contained herein is the copyright of and proprietary to BMT Fleet Technology Limited. Use of this information is governed by the legend on the cover page of this document."

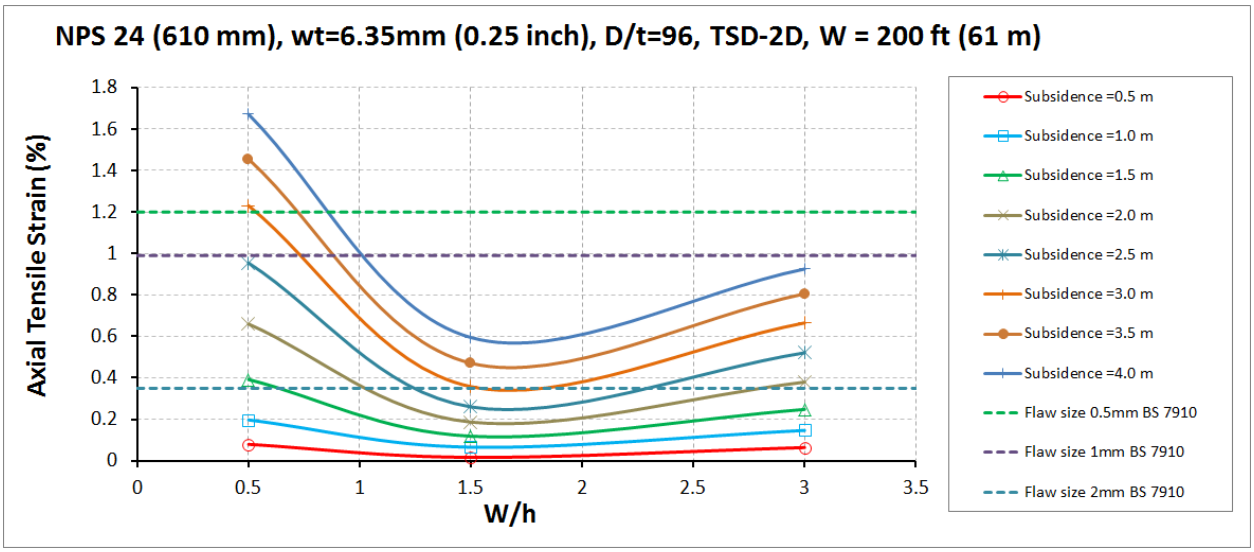

Figure 5.23: Pipe Axial Tensile Strains Envelopes versus Width to Depth Ratio (W = 61 m, 200 ft) for Ground Settlement of 0.5, 1, 1.5, 2.0, 2.5, 3.0, 3.5 and 4.0 m

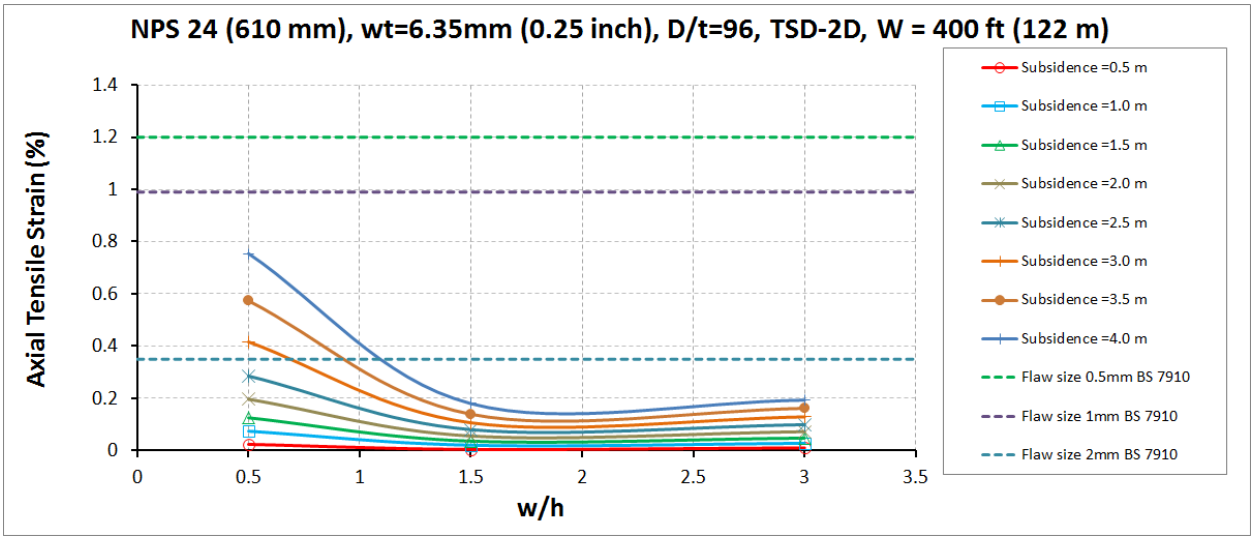

Figure 5.24: Pipe Axial Tensile Strains Envelopes versus Width to Depth Ratio (W = 122 m, 400 ft) for Ground Settlement of 0.5, 1, 1.5, 2.0, 2.5, 3.0, 3.5 and 4.0 m

The information contained herein is the copyright of and proprietary to BMT Fleet Technology Limited. Use of this information is governed by the legend on the cover page of this document."

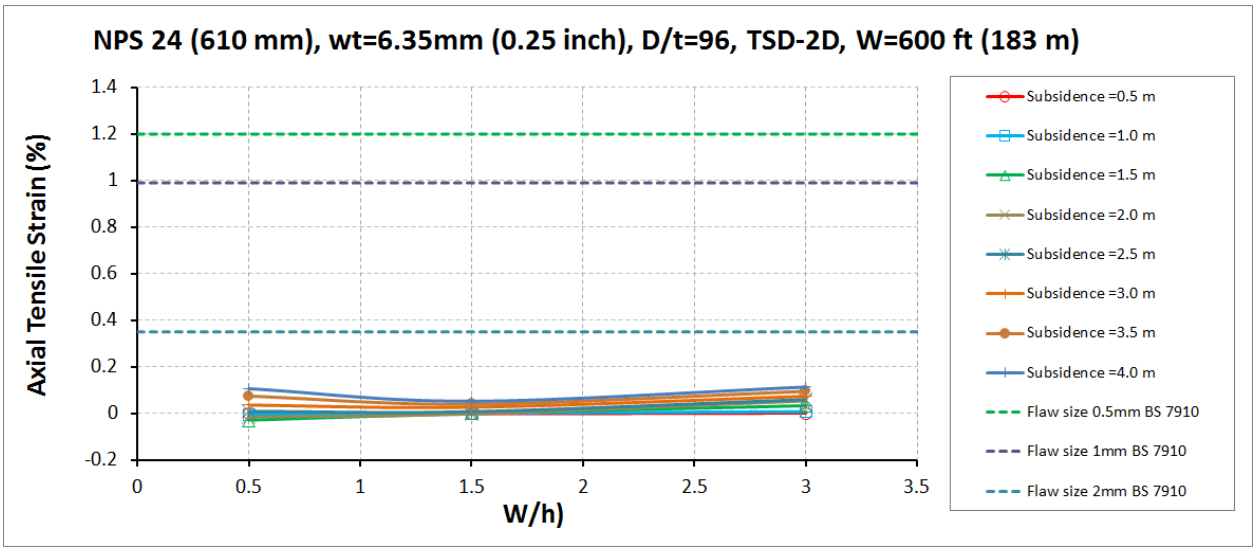

Figure 5.25: Pipe Axial Tensile Strains Envelopes versus Width to Depth Ratio (W = 183 m, 600 ft) for Ground Settlement of 0.5, 1, 1.5, 2.0, 2.5, 3.0, 3.5 and 4.0 m

5.3.4.1.2 Compressive Strain Capacity Envelopes (CSCE)

Figure 5.26, Figure 5.27 and Figure 5.28 present the maximum nominal compressive strain in the pipe versus the panel width to depth ratio (W/h) for given ground settlement of 0.5, 1.0, 1.5, 2.0, 2.5, 3.0, 3.5 and 4.0. The nominal compressive strain is defined as the average compressive strain measured over a gauge length of 2D (D is the pipe outside diameter). In this figure, the CSA and PRCI compressive strain capacity is presented with a dashed horizontal line.

The results indicate that for this pipe and operating condition combination, panel width to depth ratio of 0.5 can be considered critical. The tensile strain-related failure limit for the critical width is reached for ground subsidence from 1.5 to 3.5 m considering CSA and PRCI compressive strain limit criteria.

The information contained herein is the copyright of and proprietary to BMT Fleet Technology Limited. Use of this information is governed by the legend on the cover page of this document."

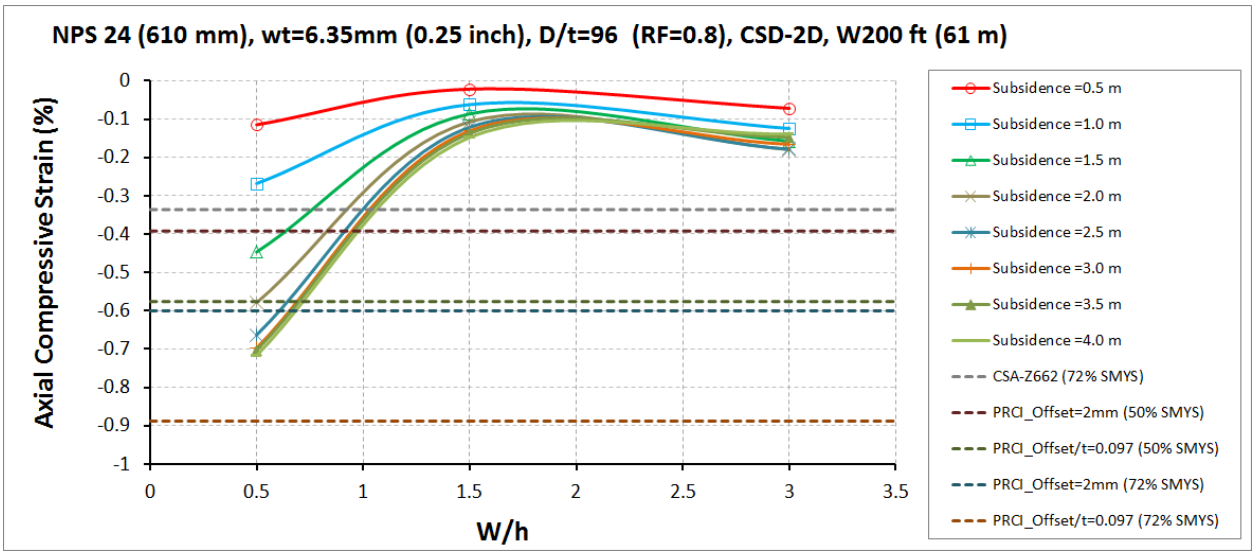

Figure 5.26: Pipe Axial Compressive Strains Envelopes versus Width to Depth Ratio (W =61 m, 200 ft) for Ground Settlement of 0.5, 1, 1.5, 2.0, 2.5, 3.0, 3.5 and 4.0 m

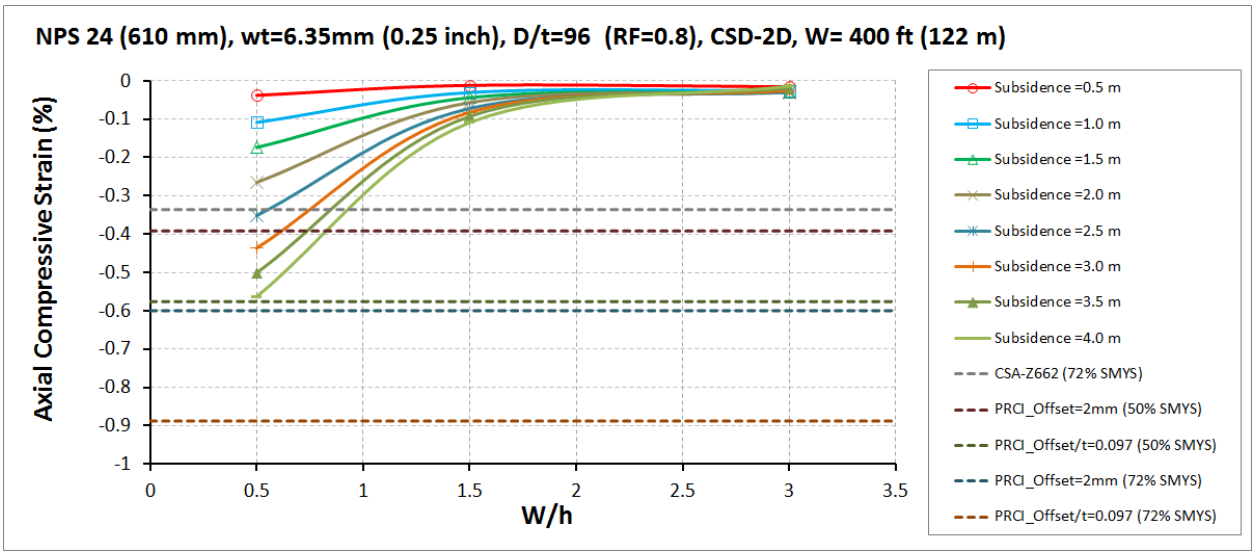

Figure 5.27: Pipe Axial Compressive Strains Envelopes versus Width to Depth Ratio (W = 122 m, 400 ft) for Ground Settlement of 0.5, 1, 1.5, 2.0, 2.5, 3.0, 3.5 and 4.0 m

The information contained herein is the copyright of and proprietary to BMT Fleet Technology Limited. Use of this information is governed by the legend on the cover page of this document."

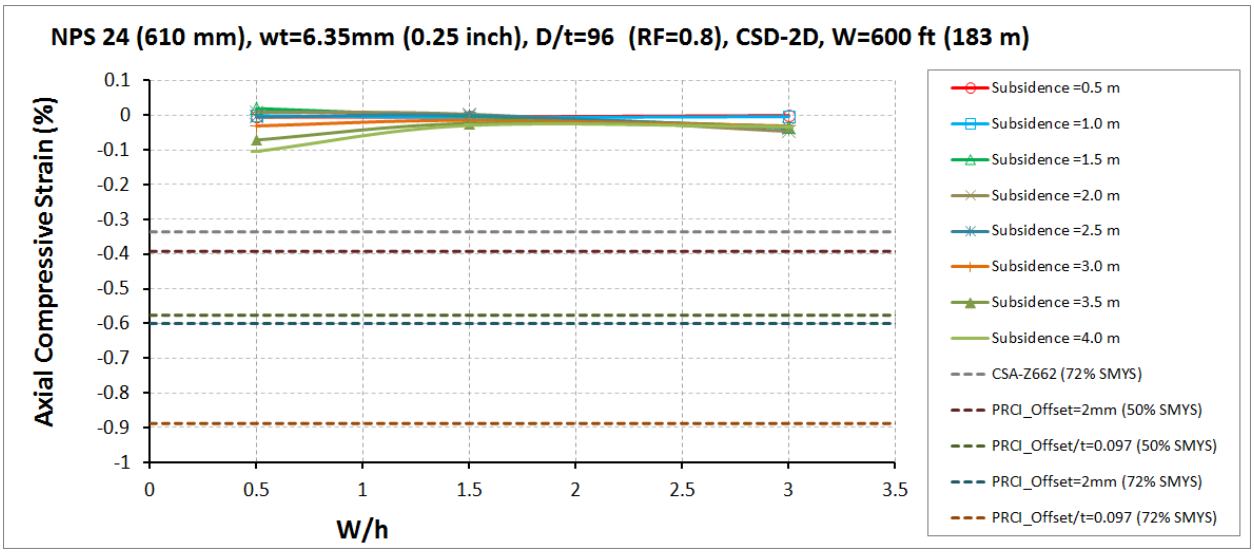

Figure 5.28: Pipe Axial Compressive Strains Envelopes versus Width to Depth Ratio (W = 183 m, 600 ft) for Ground Settlement of 0.5, 1, 1.5, 2.0, 2.5, 3.0, 3.5 and 4.0 m

5.4 Effect of Pipe Wall Thickness and D/t

The structural performance of the NPS 24-inch pipeline subjected to settlement was evaluated using a combination of three pipe wall thicknesses, for demonstration purposes.

The three wall thicknesses include the base case 9.52 mm (0.375), 6.35 mm (0.25 inch) and 12.7 mm (0.5 inch); corresponding to D/t ratios of 64, 96 and 48, respectively. The same pipe and soil materials assumptions used for the base case are used in the sensitivity:

- 72% SMYS internal pressure, corresponding to 5.4 MPa, 8 MPa and 10 MPa for D/t ratio of 96, 64 and 48, respectively;
- Grade 359 (X-52), a generic stress strain curves for Grade X-52 (359) pipe according to the CSA Z245.1;
- 45°C thermal differential (installation -20°C, max operating temperature 25°C);
- Burial depth H=1.2 m (5ft), corresponding to 1.5 m (5ft) depth to pipe center line, overburden ratio (H/D) of 2.46;
- Soil: sand/clay till with (ϕ'=30° and C'=5 kPa);
- Panel widths: three panel widths of 61 m (200 ft), 122 m (400 ft) and 183 m (600 ft)
- Mining depths: three different mining depth for each panel width;
- Panel extraction areas defined based on panel width to mining depth ratio (W/H): three W/H ratio of 0.5, 1.5 and 3.0 for each panel width; and
- Shape of ground displacement: three ground subsidence patterns.

The information contained herein is the copyright of and proprietary to BMT Fleet Technology Limited. Use of this information is governed by the legend on the cover page of this document."

A comparison of the results of the three wall thicknesses analyzed for ground subsidence considering ground subsidence of 61 m (200 ft) and three panel width to depth ratio (W/h 0.5, 1.5 and 3) is provided in Figure 5.29, Figure 5.30 and Figure 5.31.

Figure 5.32 and Figure 5.33 plot axial strains distribution at different clock positions 6 and 12 o'clock along the length of the pipeline. The results presented in these figures are ground subsidence width of 200 ft (61 m) and three W/h ratios of 0.5, 1.5 and 3. These results illustrate that for narrow subsidence events the pipe strains are maximized at the center of the ground movement. This indicates that the pipeline is following the soil displacement relatively closely. This trend would not necessarily be the case for lower strength soils.

The results in Figure 5.29 through Figure 5.33 and Table 5.2 indicated that pipeline with higher D/t ratio (lower pipe wall thickness) results in higher computed tensile and compressive strains with higher tensile strain than compressive strain. For example, for panel width to depth ratio of 0.5 the strain ranged from +1.68% and –0.79% for 6.35 mm (0.25 inch) wall thickness to +1.37% and –0.55% for 9.53 mm (0.375 inch) wall thickness while for 12.7 mm (0.5 inch) the corresponding strain range is +0.77% and -0.33%. The reported maximum strains in Table 6.2 are for ground settlement of 4.0 m.

Table 5.2: Maximum Tensile and Compressive Strain [%] for NPS 24, W =200 ft (61 m) – Effect of D/t (Settlement of 4m)

D/t	D/t= 96		D/t=64		D/t=48	
Strains	Tensile	Compressive	Tensile	Compressive	Tensile	Compressive
W/h = 0.5	1.68	-0.79	1.37	-0.55	0.77	-0.33
W/h = 1.5	0.6	-0.36	0.39	-0.08	0.46	-0.2
W/h = 3	0.92	-0.14	0.86	-0.2	0.75	-0.26

The information contained herein is the copyright of and proprietary to BMT Fleet Technology Limited. Use of this information is governed by the legend on the cover page of this document."

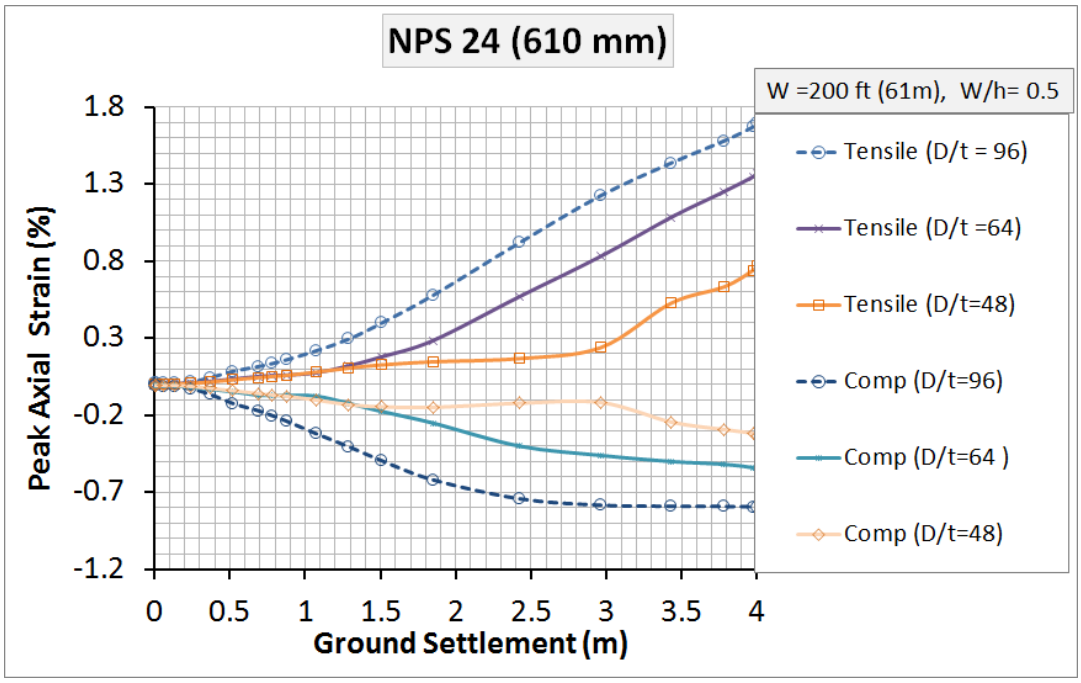

Figure 5.29: NPS 24 – Maximum Axial Strain versus Ground Settlement for Ground Subsidence Width of 200 ft (61 m) and W/h= 0.5

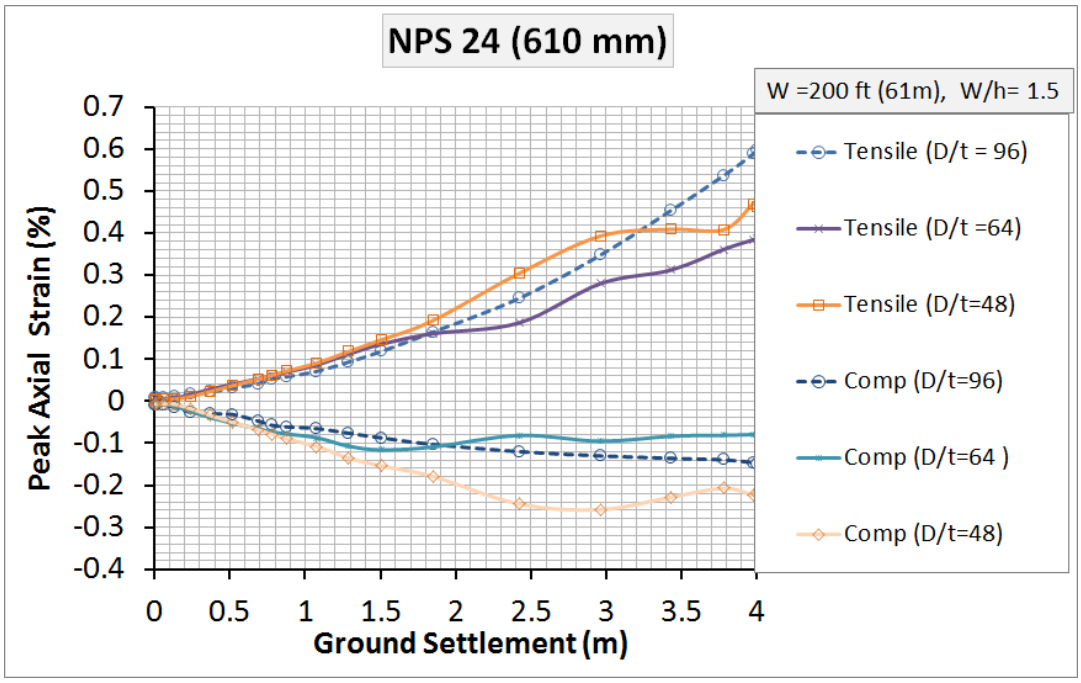

Figure 5.30: NPS 24 – Maximum Axial Strain versus Ground Settlement for Ground Subsidence Width of 200 ft (61 m) and W/h= 1.5

The information contained herein is the copyright of and proprietary to BMT Fleet Technology Limited. Use of this information is governed by the legend on the cover page of this document."

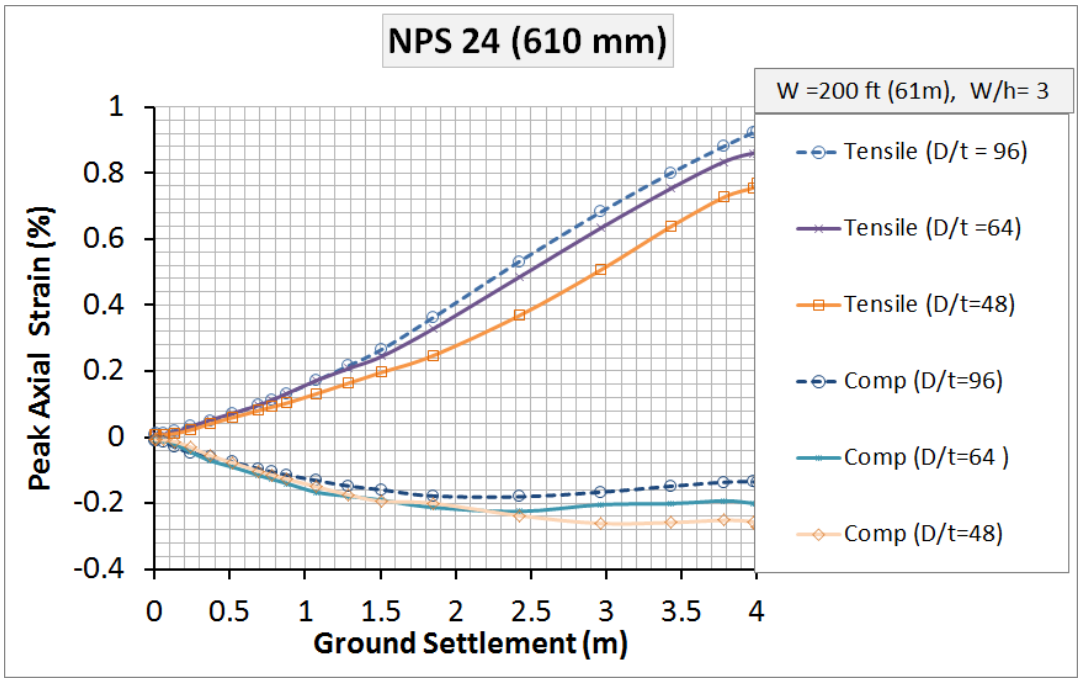

Figure 5.31: NPS 24 – Maximum Axial Strain versus Ground Settlement for Ground Subsidence Width of 200 ft (61 m) and W/h= 3

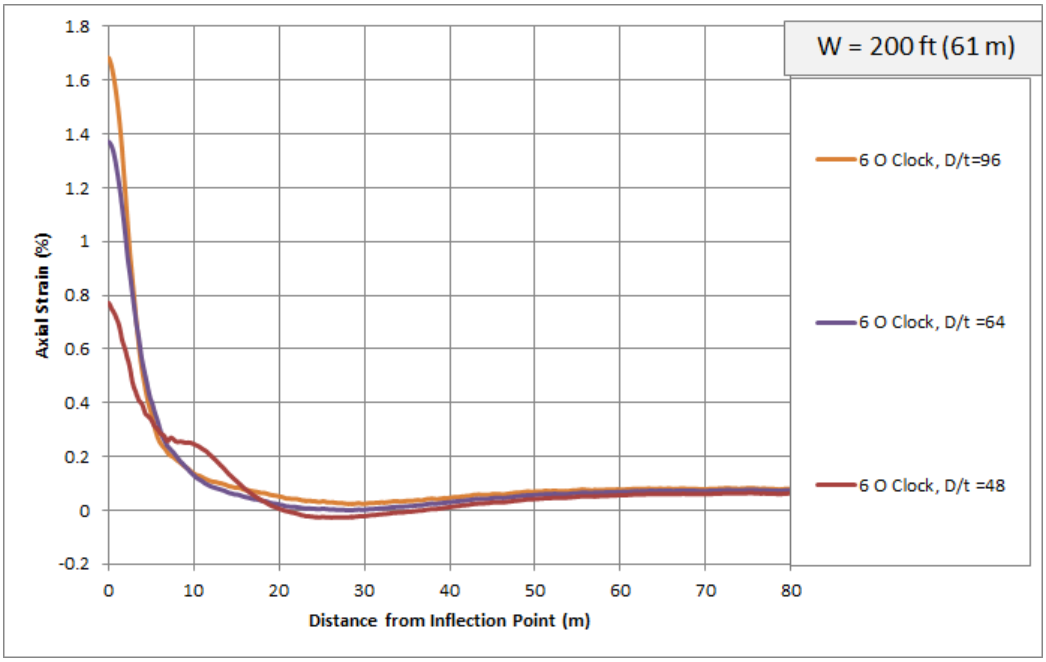

Figure 5.32: Total Axial Strains in NPS 24 at 6 o'clock Position for W = 200 ft (61 m), W/H = 0.5 and Soil Settlement of 4 m

The information contained herein is the copyright of and proprietary to BMT Fleet Technology Limited. Use of this information is governed by the legend on the cover page of this document."

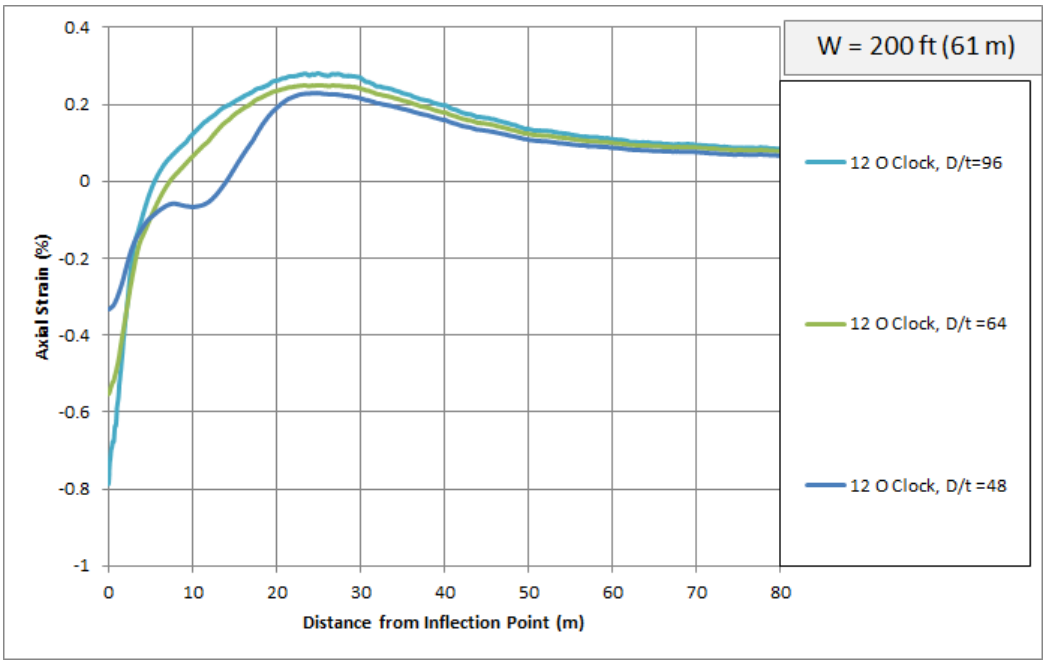

Figure 5.33: Total Axial Strains in NPS 24 at 12 o'clock Position for W = 200 ft (61 m), W/H = 0.5 and Soil Settlement of 4 m

5.4.1 Effect of the Width of Ground Movement

Figure 5.34 through Figure 5.39 present the maximum tensile and compressive strains in the pipe versus the maximum ground settlement for three (3) panel width analyzed; 200 ft (61m), 400 ft (122 m) and 600 ft (183m) considering panel width to depth ratio of 0.5, 1.5 and 3.0 for the two wall thicknesses includes 9.52 mm (0.375) and 12.7 mm (0.5 inch); corresponding to D/t ratios of 65 and 48, respectively. The same pipe and soil materials assumptions used for the base case are used in the sensitivity for each case (d/t). The results indicate that for the three (3) widths considered the width of 200 ft (61m) results in the largest tensile and compressive strain in the pipe for any given value of ground settlement. Also, the panel width to depth ratio of 0.5 results in the largest tensile and compressive strain in the pipe for the three (3) analyzed widths.

Figure 5.40 through Figure 5.45 present the sum of tensile (positive) and compressive (negative) strains in the pipe for the two wall thicknesses includes 9.52 mm (0.375) and 12.7 mm (0.5 inch); corresponding to D/t ratios of 64 and 48, respectively. The results indicated the sum of tensile (positive) and compressive (negative) strains in the pipe are negligible at ground settlement less than 1.5 m that indicate that the pipe is subjected to pure bending. At large ground displacement, tensile strains are higher than compressive strain. This differential in peak tensile and compressive strains indicates that there is a significant uniform axial strain in the pipe due to a large catenary effect.

The information contained herein is the copyright of and proprietary to BMT Fleet Technology Limited. Use of this information is governed by the legend on the cover page of this document."

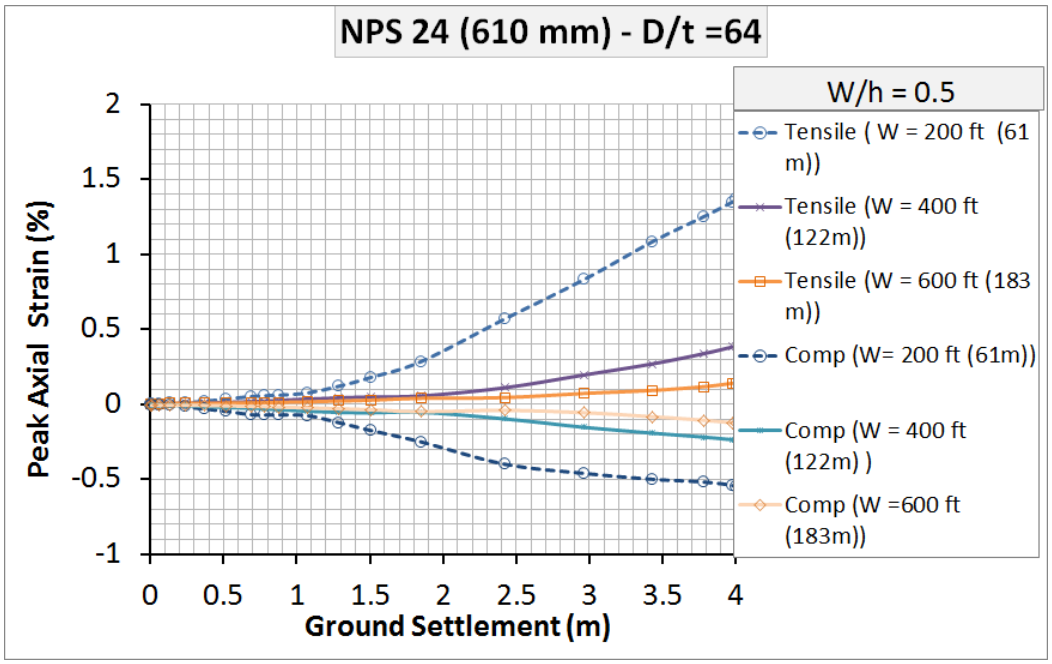

Figure 5.34: NPS 24 (D/t=64) - Maximum Tensile and Local Compressive Strains in the Pipe vs. Ground Settlement: [W/h= 0.5]

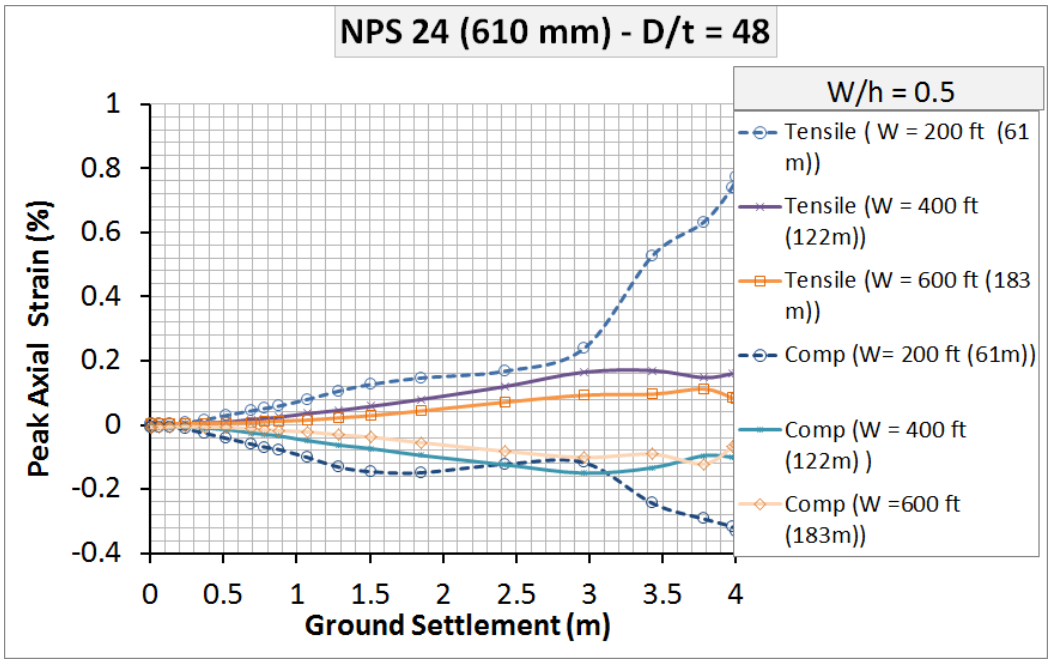

Figure 5.35: NPS 24 (D/t=48) - Maximum Tensile and Local Compressive Strains in the Pipe vs. Ground Settlement: [W/h= 0.5]

The information contained herein is the copyright of and proprietary to BMT Fleet Technology Limited. Use of this information is governed by the legend on the cover page of this document."

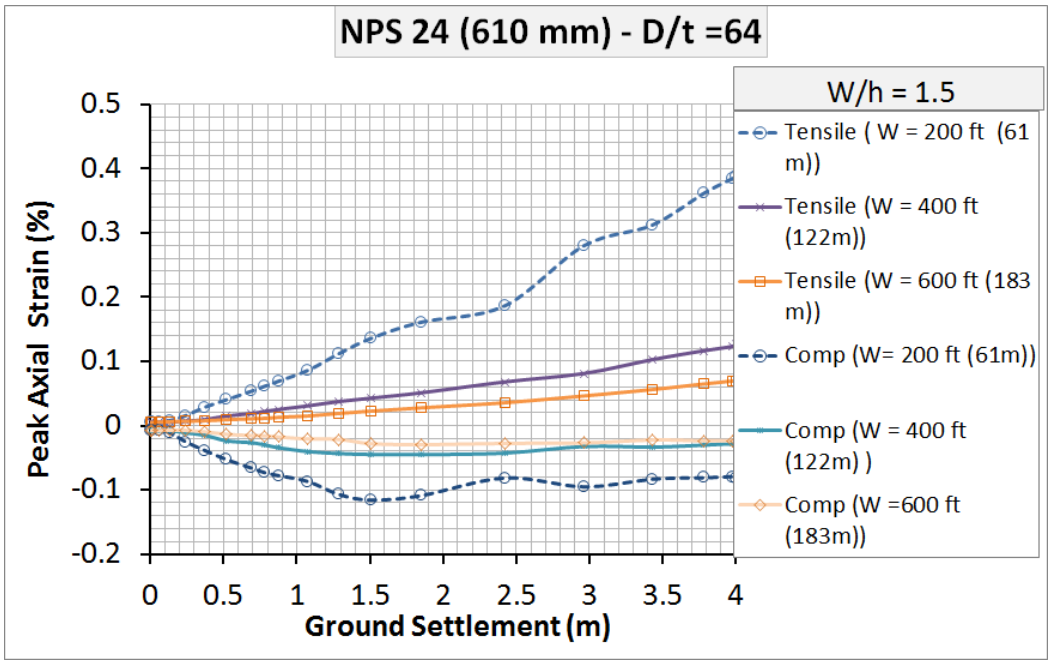

Figure 5.36: NPS 24 (D/t=64) - Maximum Tensile and Local Compressive Strains in the Pipe vs. Ground Settlement: [W/h= 1.5]

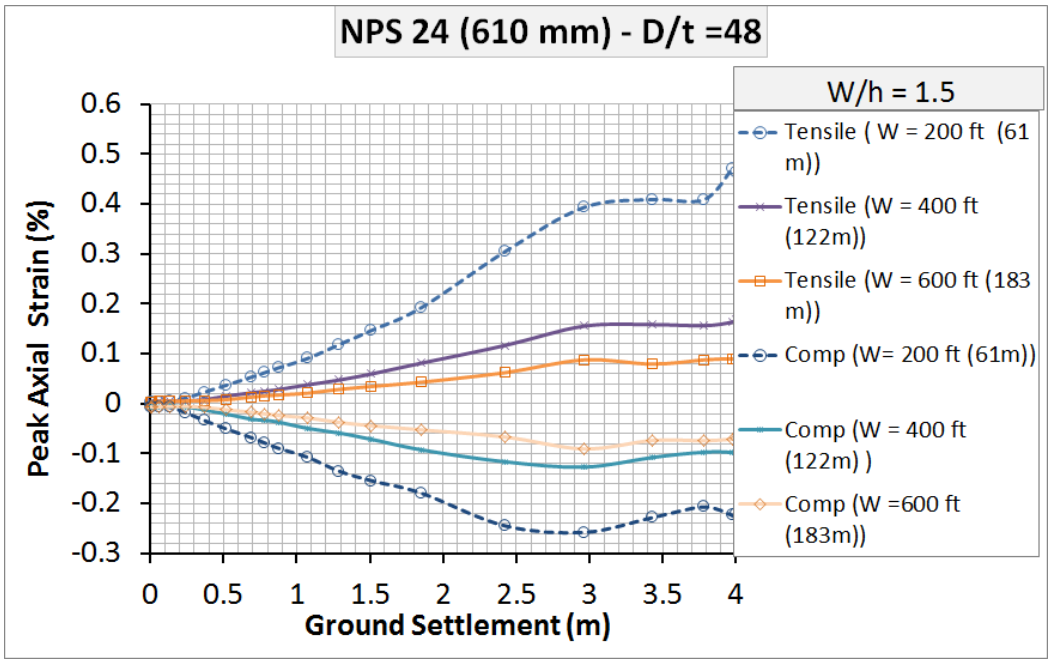

Figure 5.37: NPS 24 (D/t=48) - Maximum Tensile and Local Compressive Strains in the Pipe vs. Ground Settlement: [W/h= 1.5]

The information contained herein is the copyright of and proprietary to BMT Fleet Technology Limited. Use of this information is governed by the legend on the cover page of this document."

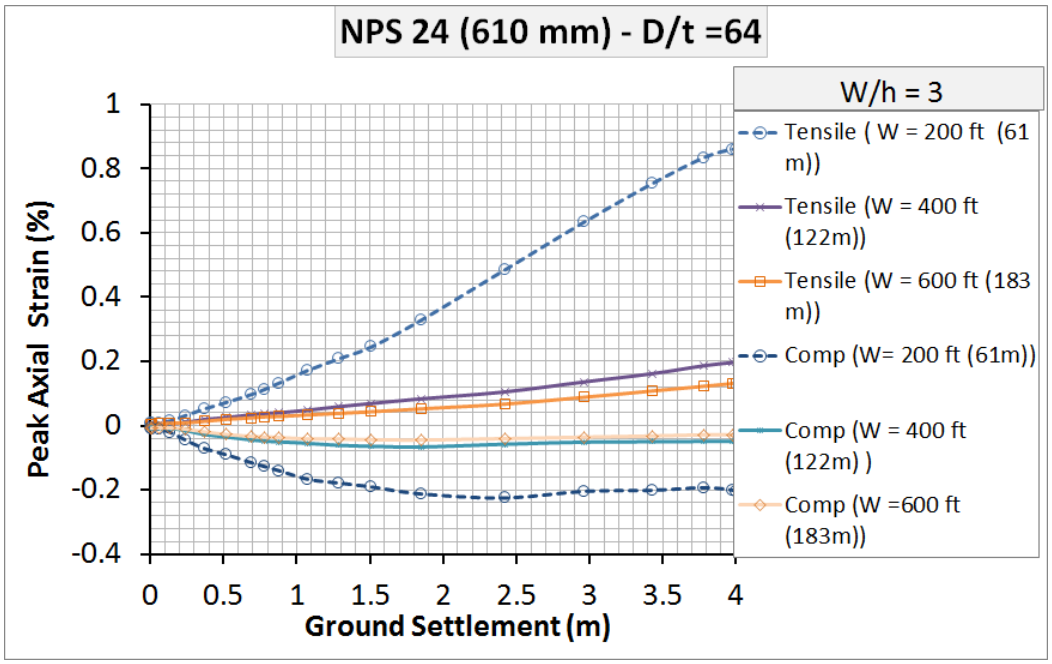

Figure 5.38: NPS 24 (D/t=64) - Maximum Tensile and Local Compressive Strains in the Pipe vs. Ground Settlement: [W/h= 3]

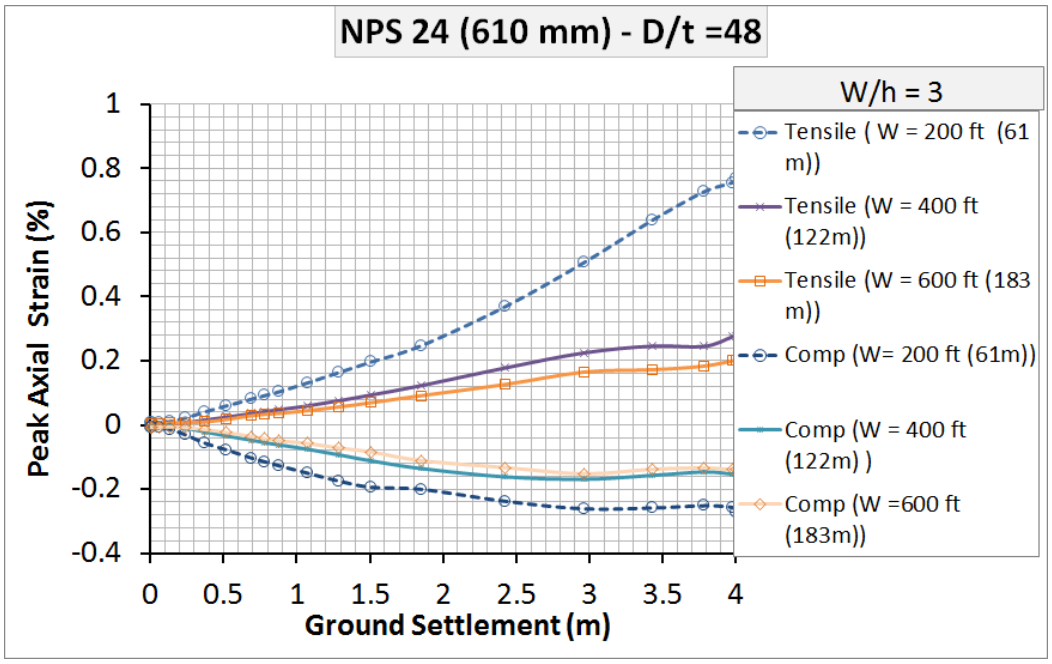

Figure 5.39: NPS 24 (D/t=48) – Sum of Maximum Tensile (Positive) and Local Compressive Strains (negative) vs. Ground Settlement: [W/h= 3]

The information contained herein is the copyright of and proprietary to BMT Fleet Technology Limited. Use of this information is governed by the legend on the cover page of this document."

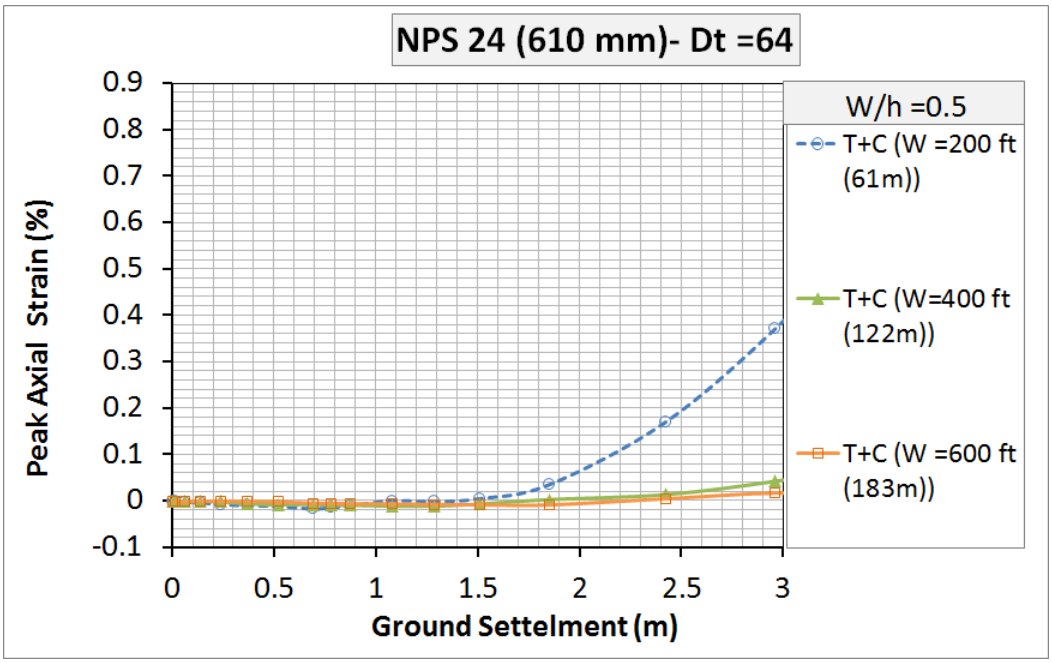

Figure 5.40: NPS 24 (D/t=64) – Sum of Maximum Tensile (Positive) and Local Compressive Strains (negative) vs. Ground Settlement: [W/h= 0.5]

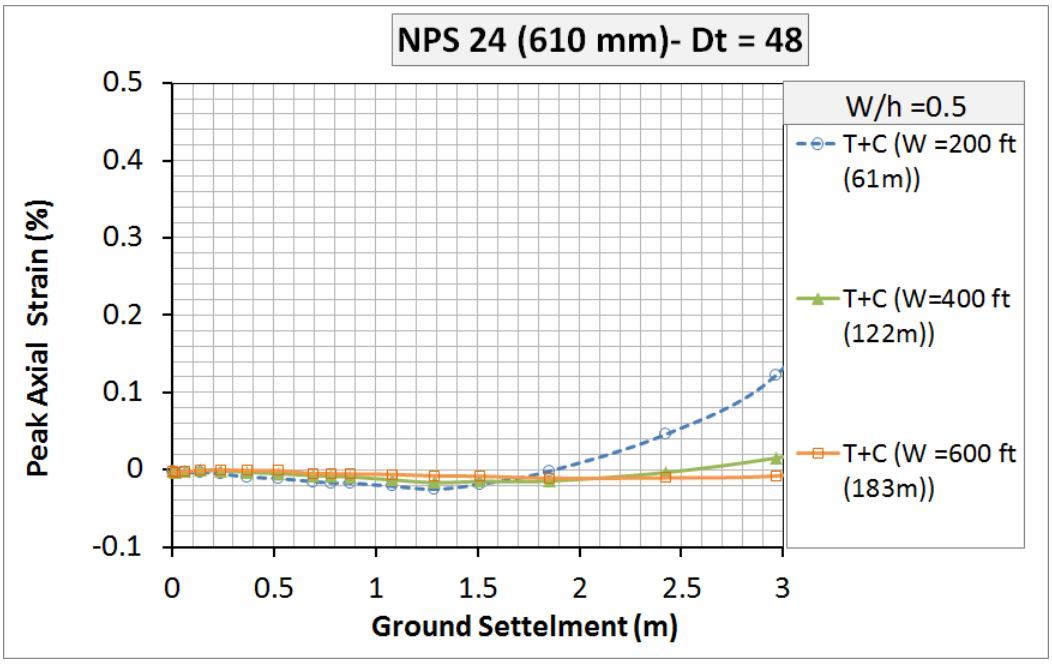

Figure 5.41: NPS 24 (D/t=48) – Sum of Maximum Tensile (Positive) and Local Compressive Strains (negative) vs. Ground Settlement: [W/h= 0.5]

The information contained herein is the copyright of and proprietary to BMT Fleet Technology Limited. Use of this information is governed by the legend on the cover page of this document."

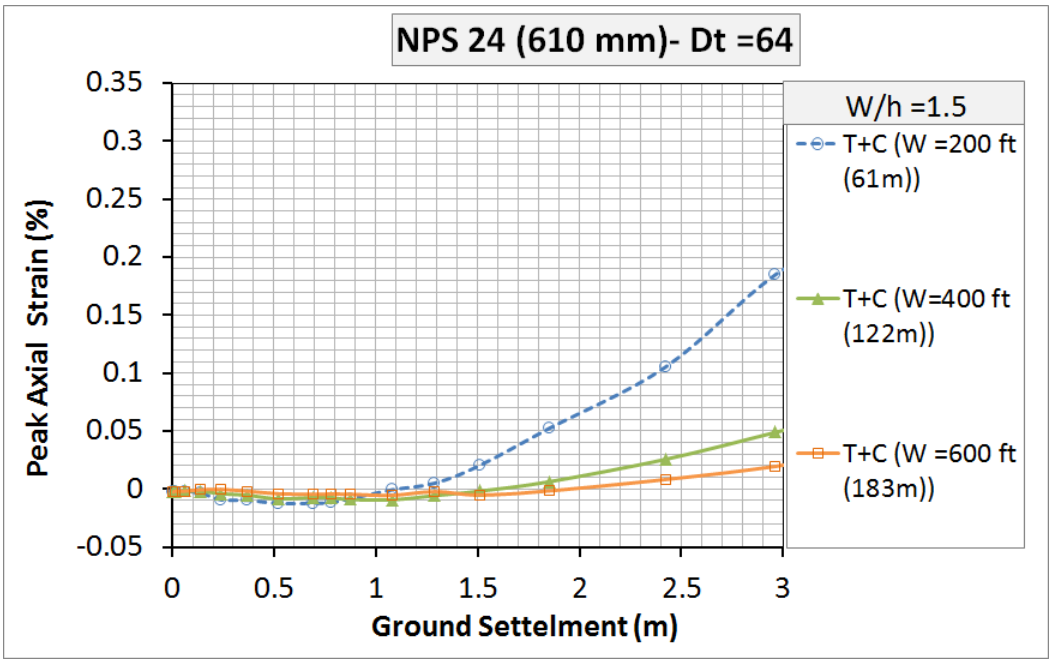

Figure 5.42: NPS 24 (D/t=64) – Sum of Maximum Tensile (Positive) and Local Compressive Strains (negative) vs. Ground Settlement: [W/h= 1.5]

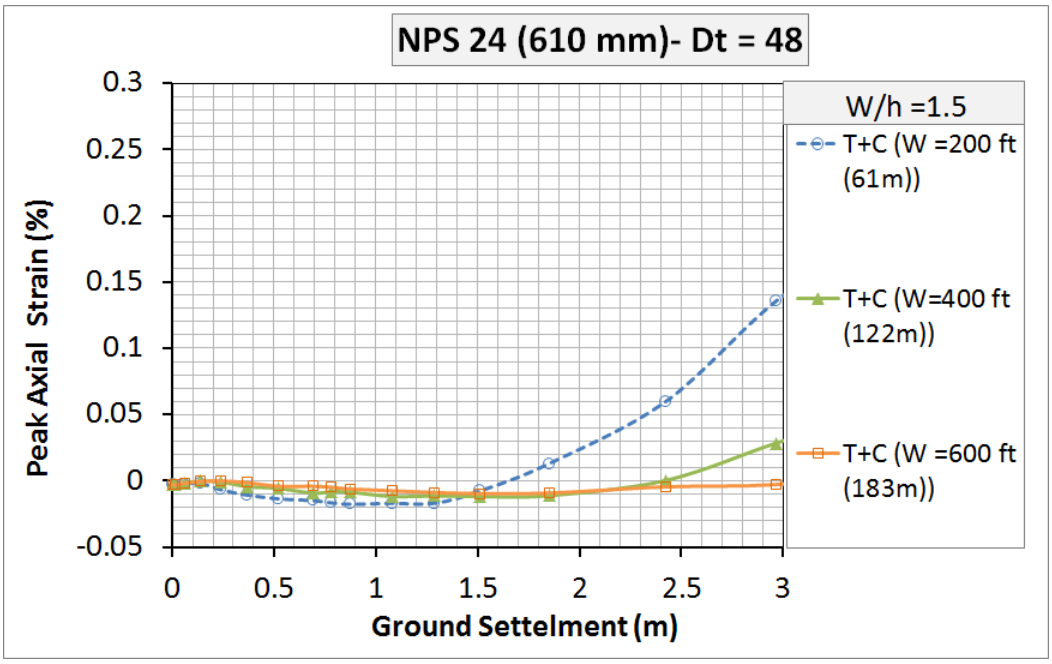

Figure 5.43: NPS 24 (D/t=48) – Sum of Maximum Tensile (Positive) and Local Compressive Strains (negative) vs. Ground Settlement: [W/h= 1.5]

The information contained herein is the copyright of and proprietary to BMT Fleet Technology Limited. Use of this information is governed by the legend on the cover page of this document."

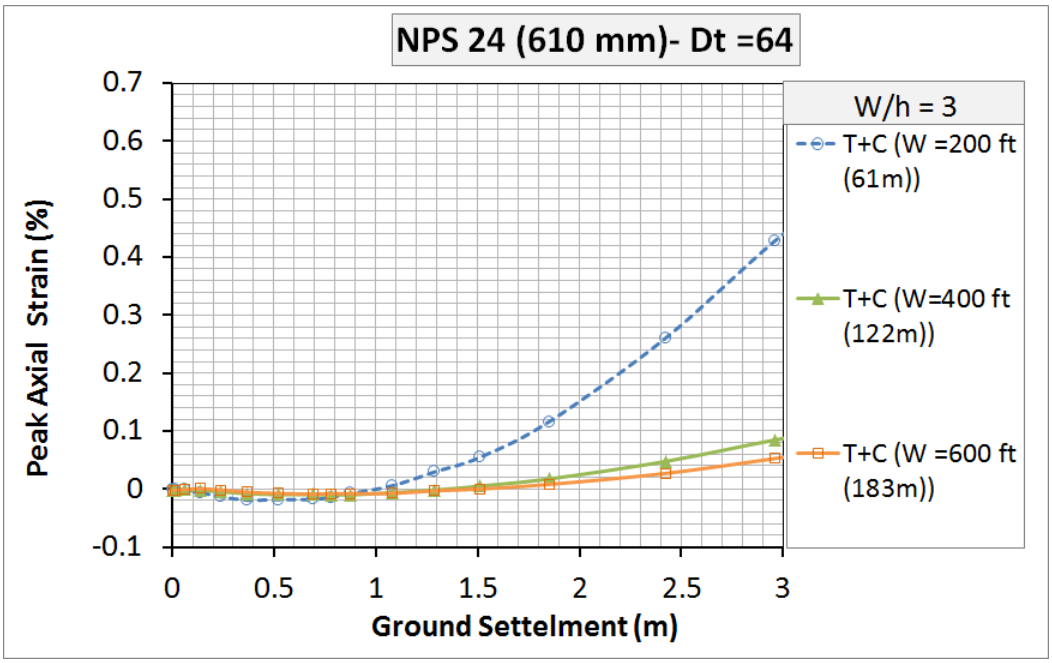

Figure 5.44: NPS 24 (D/t=64) – Sum of Maximum Tensile (Positive) and Local Compressive Strains (negative) vs. Ground Settlement: [W/h= 3]

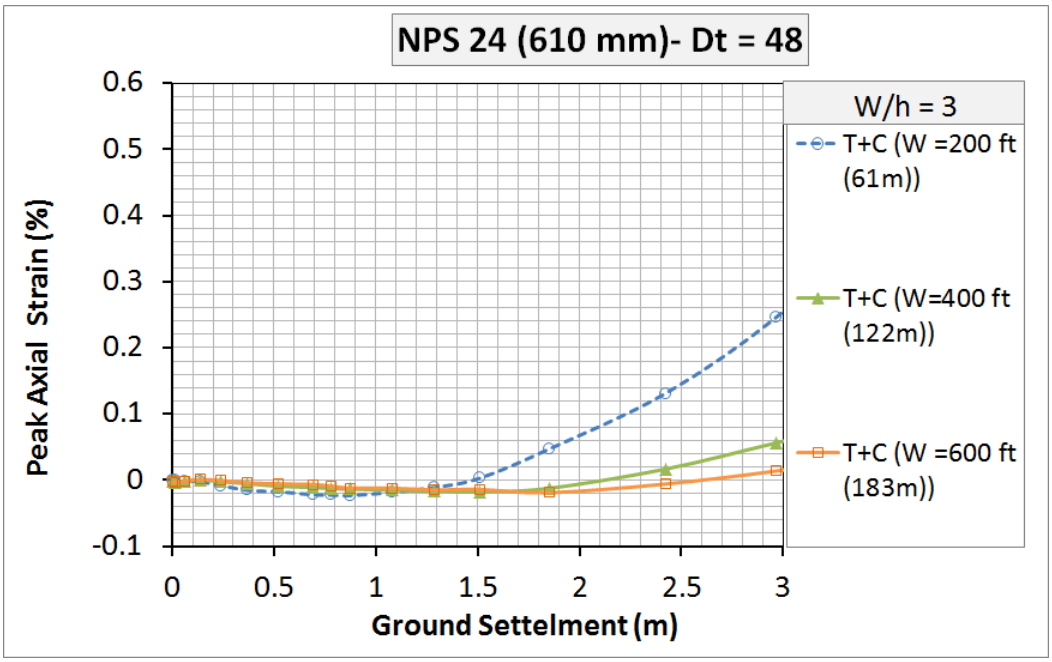

Figure 5.45: NPS 24 (D/t=48) – Sum of Maximum Tensile (Positive) and Local Compressive Strains (negative) vs. Ground Settlement: [W/h= 3]

The information contained herein is the copyright of and proprietary to BMT Fleet Technology Limited. Use of this information is governed by the legend on the cover page of this document."

5.4.2 Comparison with Strain Criteria and Safety Envelopes

The strain demand determined from the analysis was compared with the calculated strain limits defined from the guidance; BS 7910 for tensile strain, and CSA Z662 and PRCI 2004 for compressive strain. These strain limits are provided in Table 5.3 and Table 5.4 and presented with a dashed horizontal line in Figure 5.26 and Figure 5.27. The tensile strain limit considers the presence of several 50-mm long surface-breaking, semi-elliptical girth weld flaws and all of the strain limits consider the pipeline to be operating at an internal pressure that induces a pipe wall stress of 72% of its SMYS.

Table 5.3: Maximum Allowable Tensile and Compressive Strain for NPS 24, Wt=12.7 mm, D/t=48, Grade X52

Tensile Strain Limit (%)			Compressive Strain (%) –Resistance Factor =0.8		
BS 7910 Flaw Depth (mm)			CSA Z662	PRCI	
0.5	1	2	(72% SMYS)	(50% SMYS)	(72% SMYS)

Table 5.4: Maximum Allowable Tensile/Compressive Strain for NPS 24, Wt=9.52 mm, D/t=64, Grade X52

Tensile Strain Limit (%)			Compressive Strain (%) – Resistance Factor =0.8		
BS 7910 Flaw Depth (mm)			CSA Z662	PRCI (2 mm offset)	
0.5	1	2	(72% SMYS)	(50% SMYS)	(72% SMYS)
1.23	1.06	0.47	-0.54	-0.91	-1.41

Figure 5.46 through Figure 5.51 present the maximum tensile strains in the longitudinal direction of the pipeline versus the maximum ground settlement for various ground subsidence widths and width to depth ratio considered in the analyses. The results presented in this section are for the two wall thicknesses includes 9.52 mm (0.375) and 12.7 mm (0.5 inch); corresponding to D/t ratios of 96 and 48, respectively. In this figure, the BS-7910 tensile strain capacity is presented with dash horizontal line. Any tensile strain above the horizontal line is strain-related failure limit. The results indicated that subsidence width of 61 m (200 ft) with width to depth ratio of 0.5 results in the largest tensile and compressive strain. Lower subsidence widths and higher pipe D/t result in higher strain levels for a give subsidence magnitude.

Figure 5.52 through Figure 5.57 present the maximum nominal compressive strains in the longitudinal direction of the pipeline versus the maximum ground subsidence for various ground subsidence widths considered in the analyses. The nominal compressive strain is defined as the average compressive strain measured over a gauge length of 2D (D is the pipe outside diameter). This large stain gauge length is used to permit the analyses to be compared directly to codified permissible strain formulations which are reported over this gauge length. In this figure, the PRCI compressive strain capacity is presented with a dashed horizontal line. Any compressive

The information contained herein is the copyright of and proprietary to BMT Fleet Technology Limited. Use of this information is governed by the legend on the cover page of this document."

strain above the horizontal line is strain-related failure limit. Lower subsidence widths and higher pipe D/t result in higher strain levels for a give subsidence magnitude.

The results indicate that for the three (3) widths considered, the width of 61 m (200 ft) results in the largest tensile and compressive strain in the pipe for any given value of ground displacement.

The results indicated that subsidence width of 61 m (200 ft) with width to depth ratio of 0.5 results in the largest tensile and compressive strain. For large widths of 183 m (600 ft) the strain demand do not exceed the tensile and compressive strain limit for ground subsidence up to 4 m (13 ft).

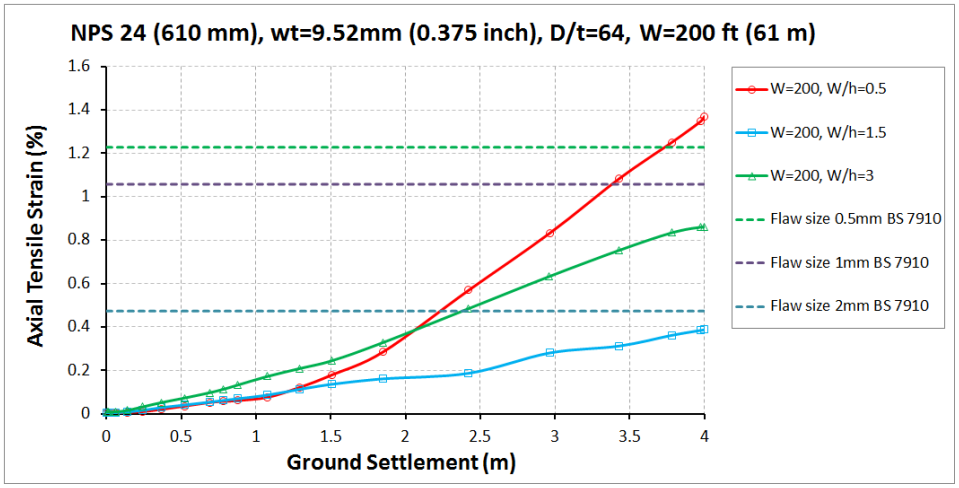

Figure 5.46: NPS 24 (D/t=64) - Maximum Tensile Strain in the Pipe vs. Ground Subsidence W =61 m (200 ft); W/h Ratio 0.5, 1.5 and 3

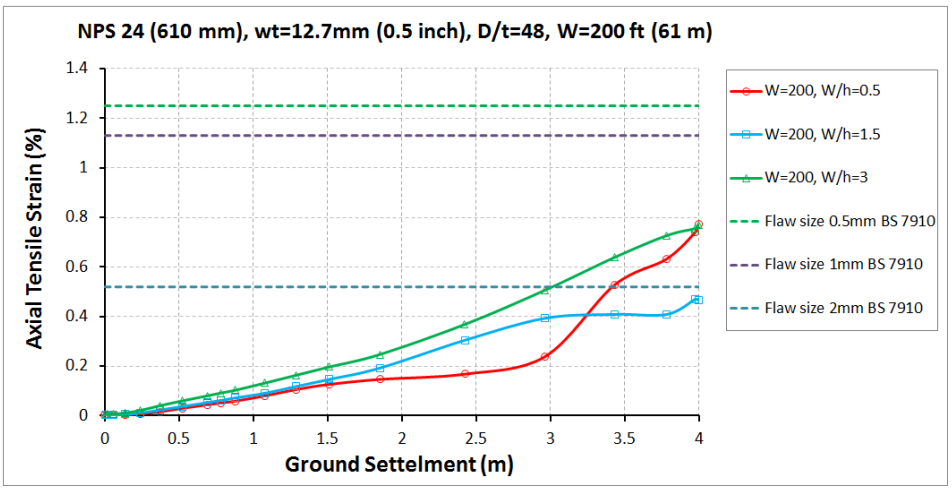

Figure 5.47: NPS 24 (D/t=48) - Maximum Tensile Strain in the Pipe vs. Ground Subsidence W =61 m (200 ft); W/h Ratio 0.5, 1.5 and 3

The information contained herein is the copyright of and proprietary to BMT Fleet Technology Limited. Use of this information is governed by the legend on the cover page of this document."

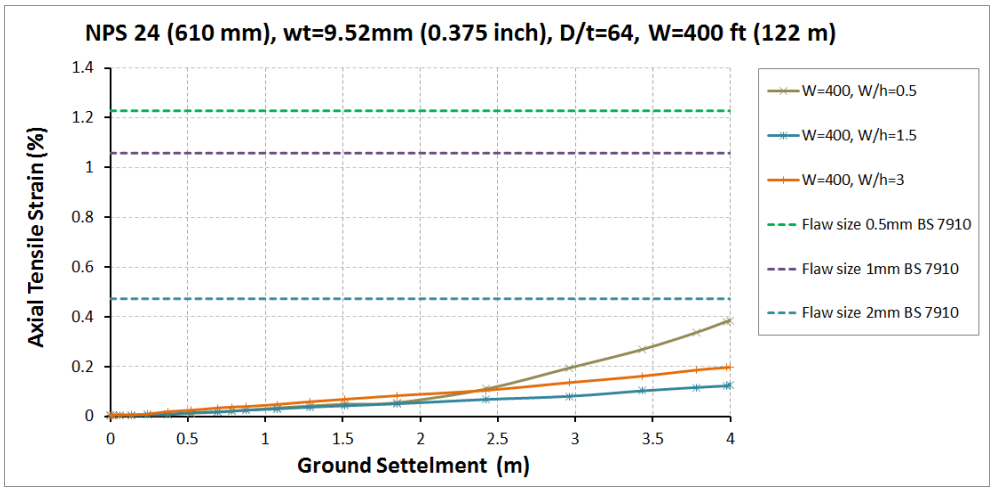

Figure 5.48: NPS 24 (D/t=64) - Maximum Tensile Strain in the Pipe vs. Ground Subsidence W =122 m (400 ft); W/h Ratio 0.5, 1.5 and 3

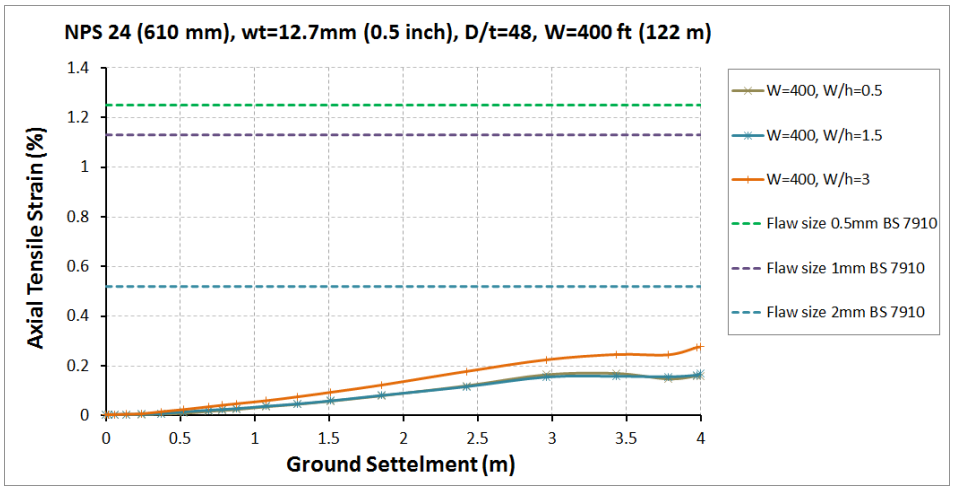

Figure 5.49: NPS 24 (D/t=48) - Maximum Tensile Strain in the Pipe vs. Ground Subsidence W =122 m (400 ft); W/h Ratio 0.5, 1.5 and 3

The information contained herein is the copyright of and proprietary to BMT Fleet Technology Limited. Use of this information is governed by the legend on the cover page of this document."

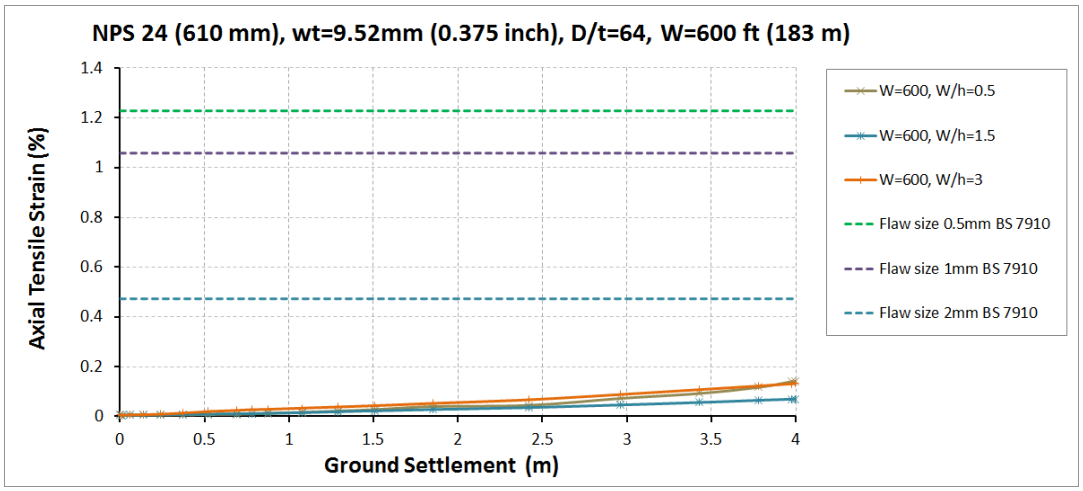

Figure 5.50: NPS 24 (D/t=64) - Maximum Tensile Strain in the Pipe vs. Ground Subsidence W =183 m (600 ft); W/h Ratio 0.5, 1.5 and 3

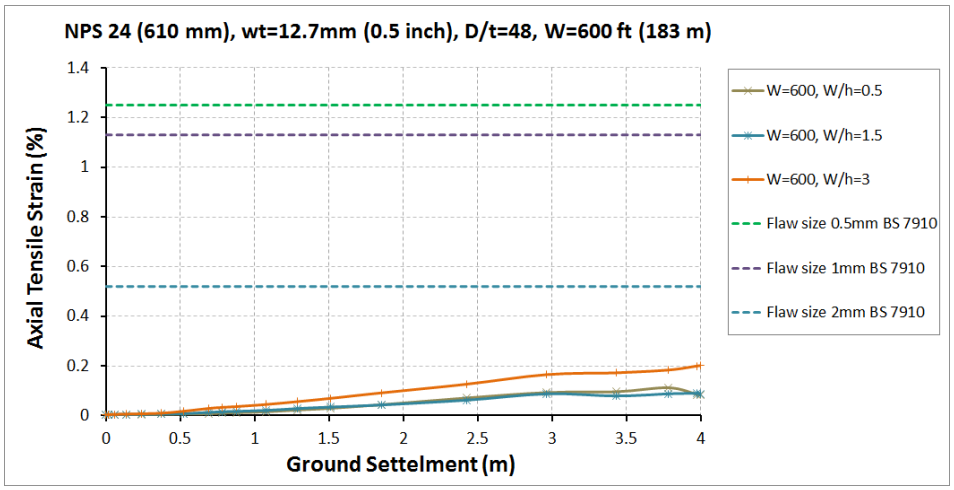

Figure 5.51: NPS 24 (D/t=48) - Maximum Tensile Strain in the Pipe vs. Ground Subsidence W =183 m (600 ft); W/h Ratio 0.5, 1.5 and 3

The information contained herein is the copyright of and proprietary to BMT Fleet Technology Limited. Use of this information is governed by the legend on the cover page of this document."

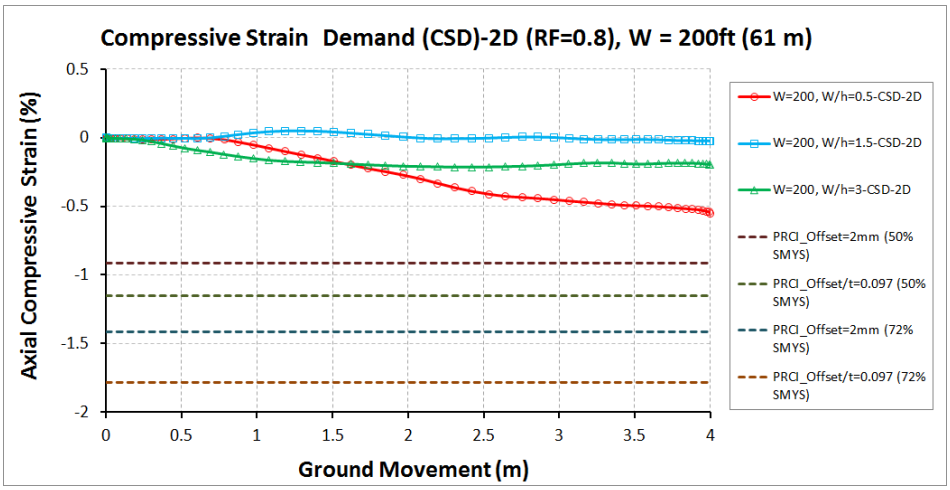

Figure 5.52: NPS 24 (D/t=64) - Maximum Nominal Compressive Strains in the Pipe vs. Ground Subsidence W =61 m (200 ft); W/h Ratio 0.5, 1.5 and 3

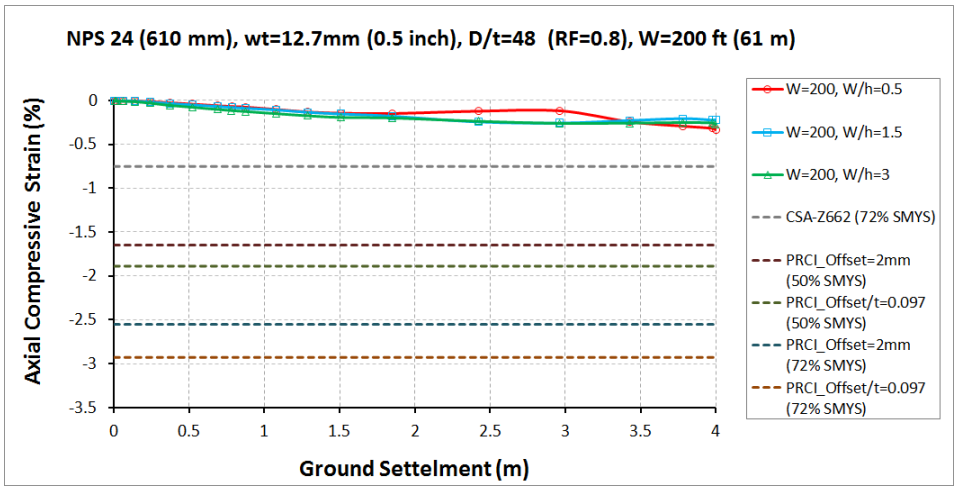

Figure 5.53: NPS 24 (D/t=48) - Maximum Nominal Compressive Strains in the Pipe vs. Ground Subsidence W =61 m (200 ft); W/h Ratio 0.5, 1.5 and 3

The information contained herein is the copyright of and proprietary to BMT Fleet Technology Limited. Use of this information is governed by the legend on the cover page of this document."

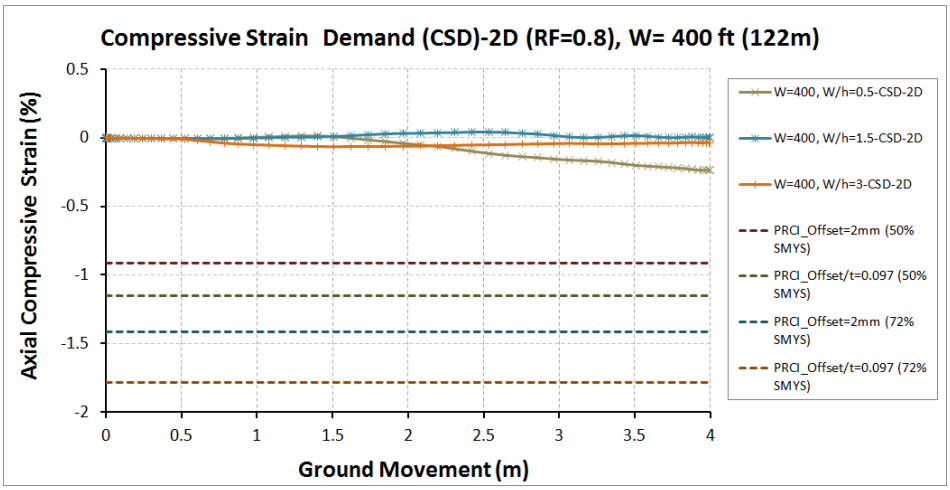

Figure 5.54: NPS 24 (D/t=64) - Maximum Nominal Compressive Strains in the Pipe vs. Ground Subsidence W =122 m (400 ft); W/h Ratio 0.5, 1.5 and 3

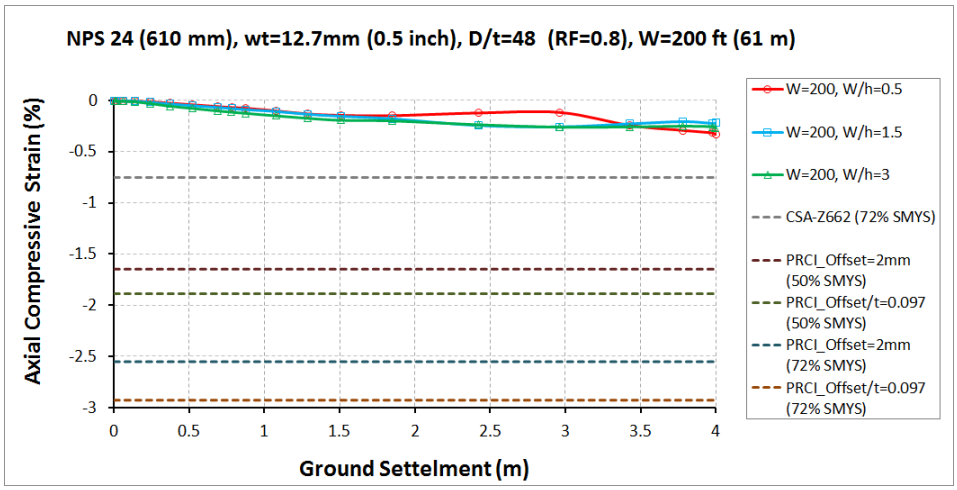

Figure 5.55: NPS 24 (D/t=48) - Maximum Nominal Compressive Strains in the Pipe vs. Ground Subsidence W =122 m (400 ft); W/h Ratio 0.5, 1.5 and 3

The information contained herein is the copyright of and proprietary to BMT Fleet Technology Limited. Use of this information is governed by the legend on the cover page of this document."

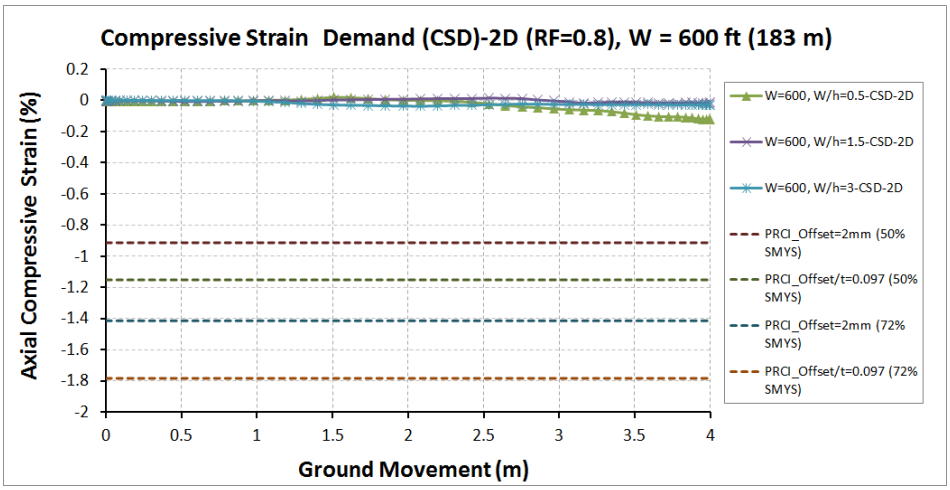

Figure 5.56: NPS 24 (D/t=64) - Maximum Nominal Compressive Strains in the Pipe vs. Ground Subsidence W =183 m (600 ft); W/h Ratio 0.5, 1.5 and 3

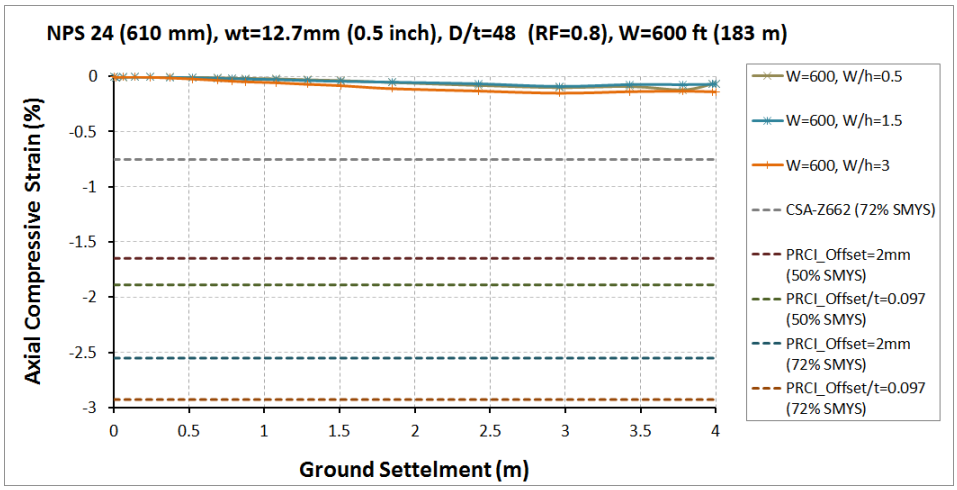

Figure 5.57: NPS 24 (D/t=48) - Maximum Nominal Compressive Strains in the Pipe vs. Ground Subsidence W =183 m (600 ft); W/h Ratio 0.5, 1.5 and 3

5.4.2.1.1 Tensile Strain Capacity Envelopes (TSCE)

Figures 5.67 through 5.72 present the maximum tensile strains in pipe versus the three (3) ground subsidence widths considered for given ground subsidence of 0.5, 1.0, 1.5, 2.5, 3.0, 3.0 and 4.0. In these figures, the BS-7910 tensile strain capacity is presented with a dashed horizontal line. Any tensile strain above the horizontal line is strain-related failure limit.

In these figures, the strain demands from the analysis were used to relate the geotechnical event (subsidence), soil, pipe and pipeline operating conditions to tensile and compressive strains produced ground settlement.

The information contained herein is the copyright of and proprietary to BMT Fleet Technology Limited. Use of this information is governed by the legend on the cover page of this document."

The results indicate that this pipe with:

- D/t equal to 64 and operating condition combination, panel width to depth ratio of 0.5. The tensile strain-related failure limit for the critical width is reached for ground settlement from 1.5 to 3 m considering a flaw size of 2, 1 and 0.5 mm, respectively.
- D/t equal to 48 and operating condition combination, panel width to depth ratio of 0.5 to 3. The tensile strain-related failure limit not exceeds the strain limit for ground settlement up to 4.0 m considering a flaw size of 2, 1 mm, respectively.

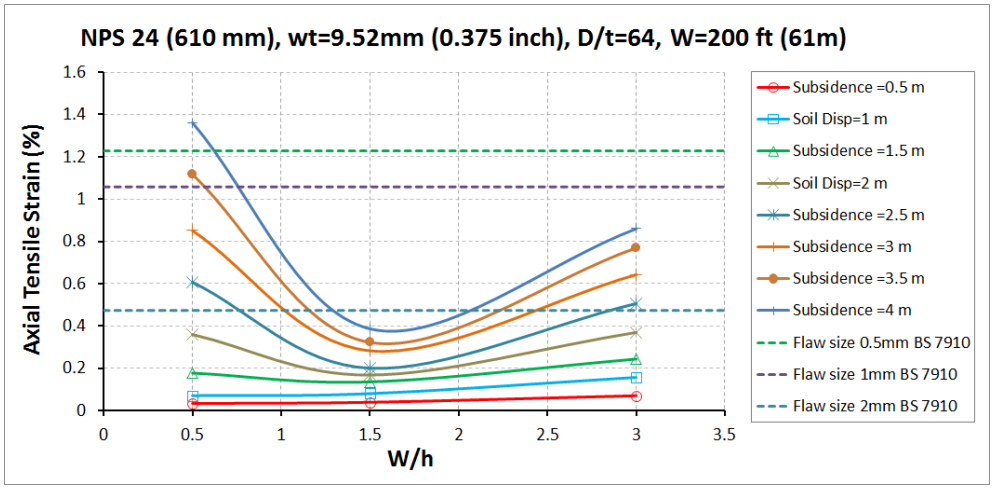

Figure 5.58: NPS 24 (D/t=64) - Pipe Axial Tensile Strains Envelopes versus Width to Depth Ratio (W =61 m, 200 ft) for Ground Settlement of 0.5, 1, 1.5, 2.0, 2.5, 3.0, 3.5 and 4.0

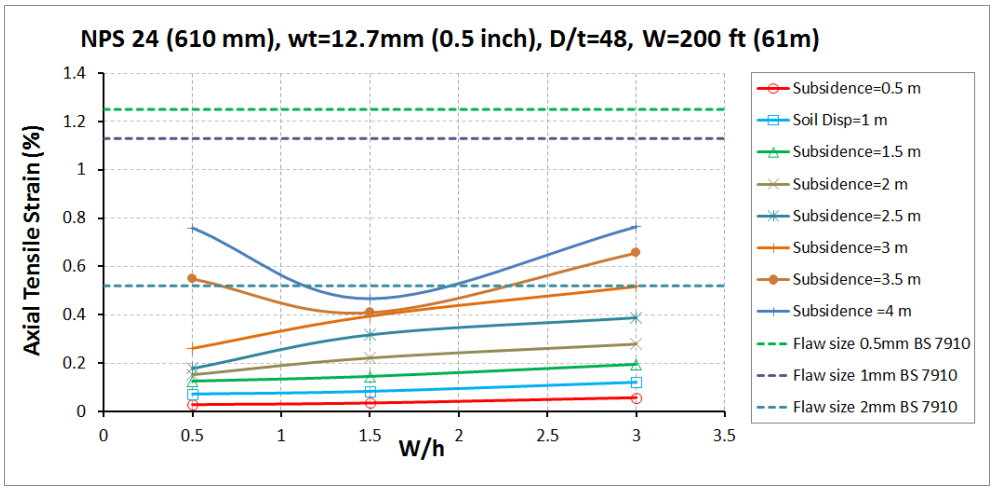

Figure 5.59: NPS 24 (D/t=48) - Pipe Axial Tensile Strains Envelopes versus Width to Depth Ratio (W =61 m, 200 ft) for Ground Settlement of 0.5, 1, 1.5, 2.0, 2.5, 3.0, 3.5 and 4.0 m

The information contained herein is the copyright of and proprietary to BMT Fleet Technology Limited. Use of this information is governed by the legend on the cover page of this document."

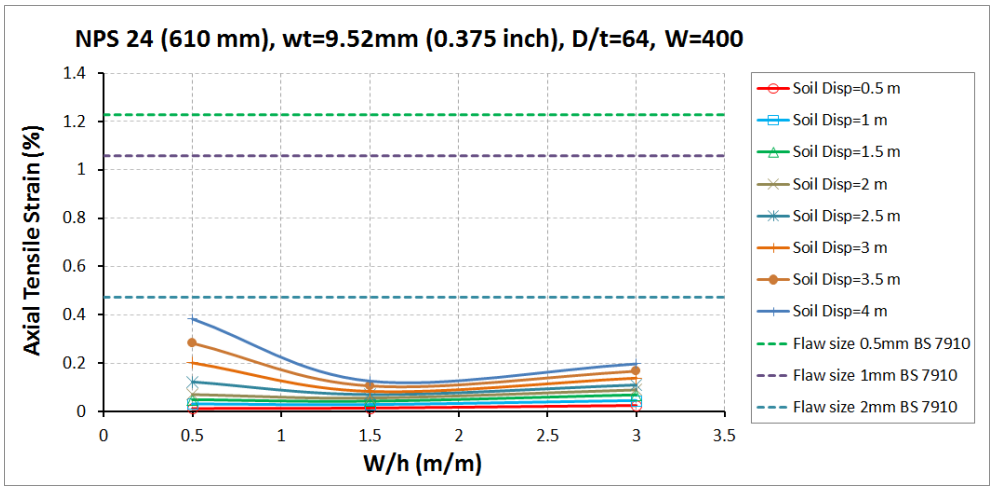

Figure 5.60: NPS 24 (D/t=64) - Pipe Axial Tensile Strains Envelopes versus Width to Depth Ratio (W =122 m, 400 ft) for Ground Settlement of 0.5, 1, 1.5, 2.0, 2.5, 3.0, 3.5 and 4.0 m

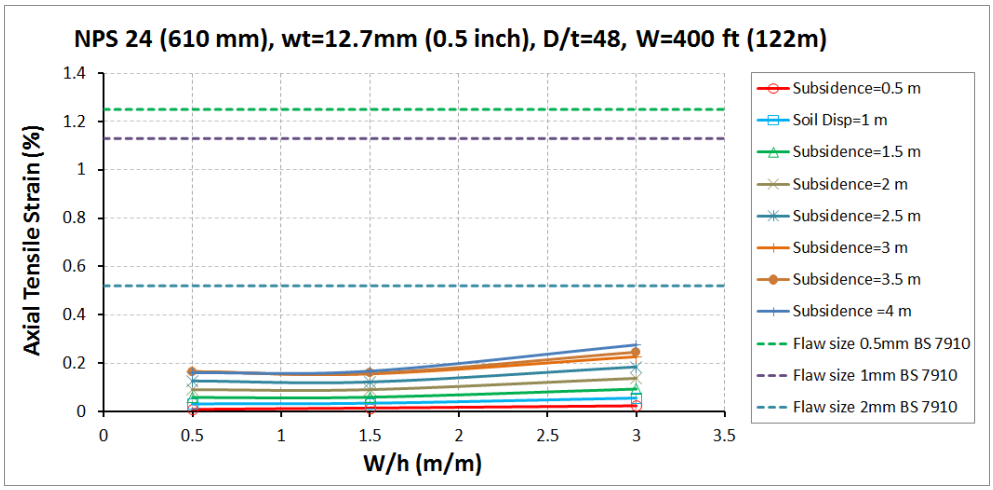

Figure 5.61: NPS 24 (D/t=48) - Pipe Axial Tensile Strains Envelopes versus Width to Depth Ratio (W =122 m, 400 ft) for Ground Settlement of 0.5, 1, 1.5, 2.0, 2.5, 3.0, 3.5 and 4.0 m

The information contained herein is the copyright of and proprietary to BMT Fleet Technology Limited. Use of this information is governed by the legend on the cover page of this document."

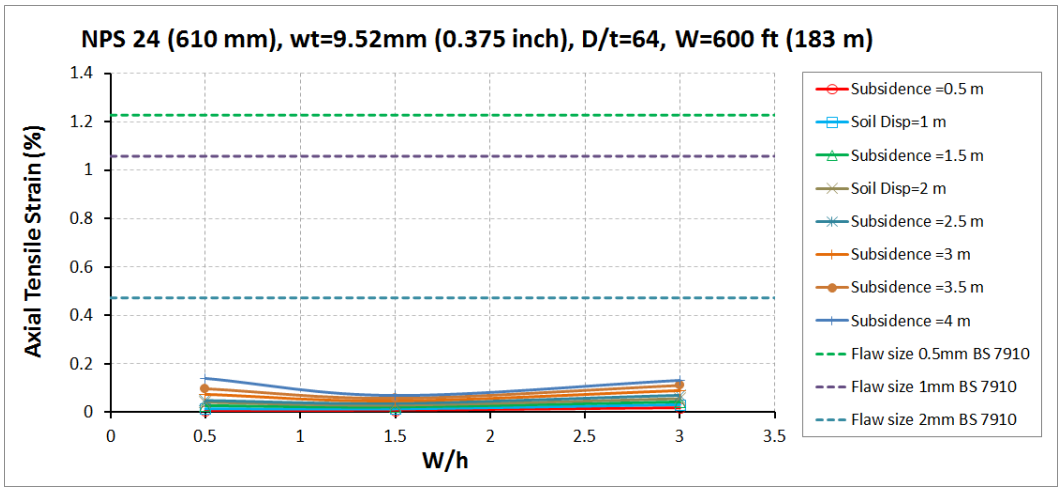

Figure 5.62: NPS 24 (D/t=64) - Pipe Axial Tensile Strains Envelopes versus Width to Depth Ratio (W =183 m, 600 ft) for Ground Settlement of 0.5, 1, 1.5, 2.0, 2.5, 3.0, 3.5 and 4.0 m

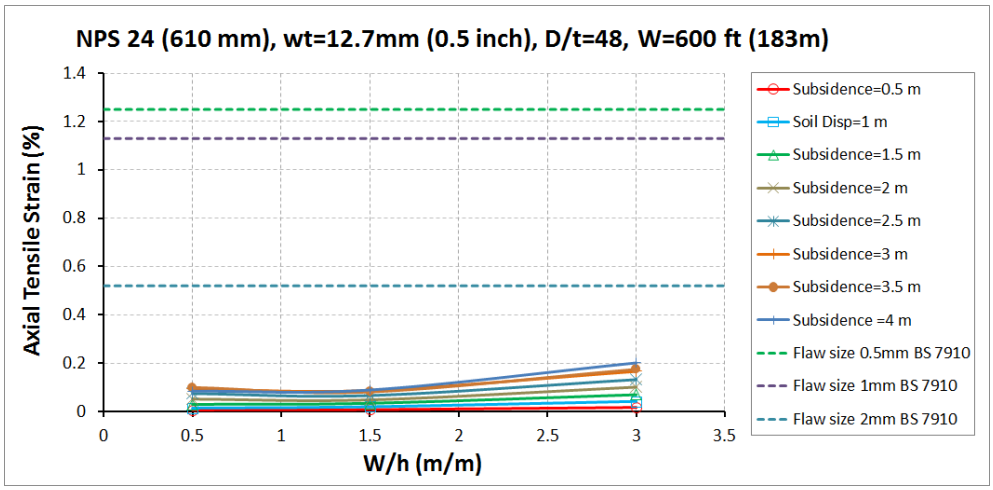

Figure 5.63: NPS 24 (D/t=48) - Pipe Axial Tensile Strains Envelopes versus Width to Depth Ratio (W =183 m, 600 ft) for Ground Settlement of 0.5, 1, 1.5, 2.0, 2.5, 3.0, 3.5 and 4.0 m

5.4.2.1.2 Compressive Strain Capacity Envelopes (CSCE)

Figures 5.73 through 5.78 present the maximum nominal compressive strain in the pipe versus the panel width to depth ratio (W/h) for given ground settlements of 0.5, 1.0, 1.5, 2.0, 2.5, 3.0, 3.5 and 4.0. The nominal compressive strain is defined as the average compressive strain measured over a gauge length of 2D (D is the pipe outside diameter). In this figure, the CSA and PRCI compressive strain capacity is presented with a dashed horizontal line.

The results indicate that for this pipe with low D/t ratio less than 64 and operating condition combination, panel width to depth ratio of 0.5 to 3. The compressive strain limit does not exceed the strain limit for ground settlement up to 4.0 m considering CSA and PRCI compressive strain limit criteria.

The information contained herein is the copyright of and proprietary to BMT Fleet Technology Limited. Use of this information is governed by the legend on the cover page of this document."

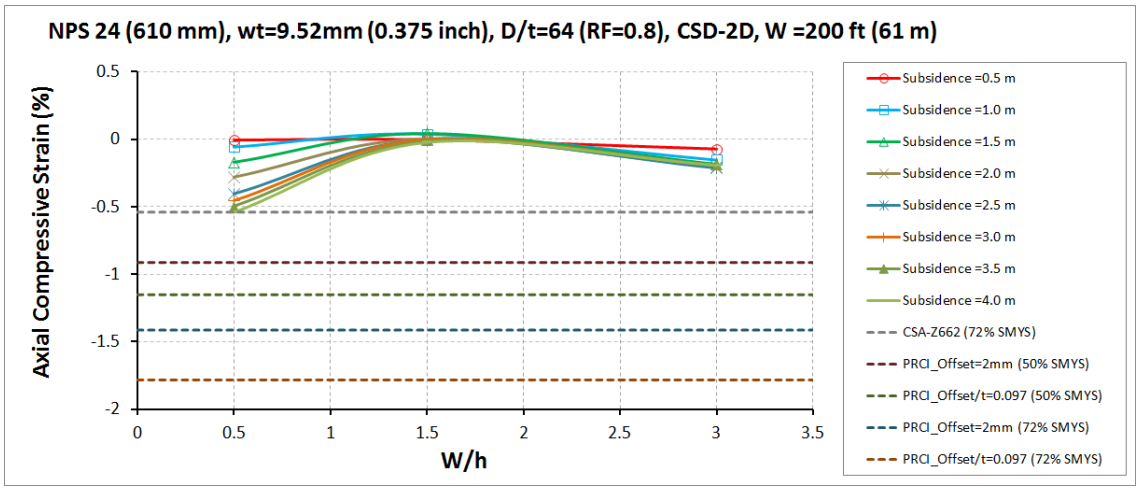

Figure 5.64: NPS 24 (D/t=64) - Pipe Axial Compressive Strains Envelopes versus Width to Depth Ratio (W =61 m, 200 ft) for Ground Settlement of 0.5, 1, 1.5, 2.0, 2.5, 3.0, 3.5 and 4.0 m

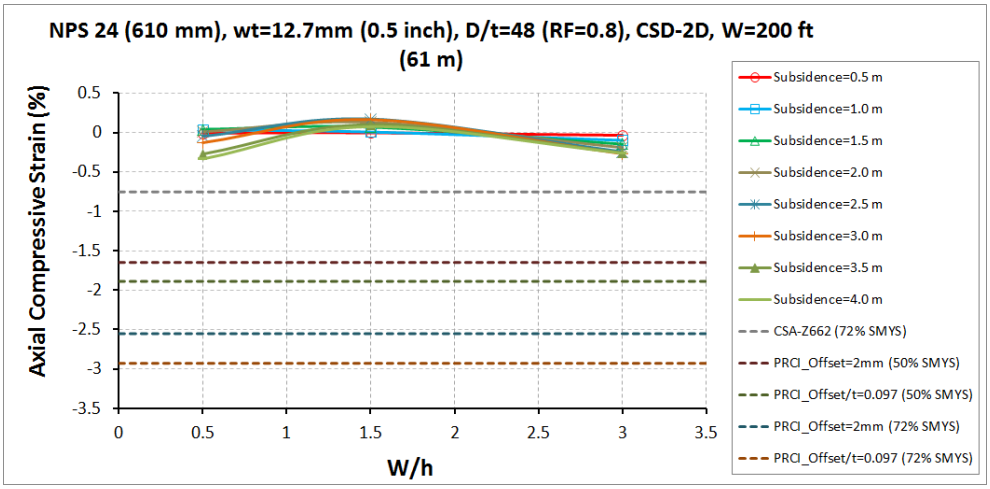

Figure 5.65: NPS 24 (D/t=48) - Pipe Axial Compressive Strains Envelopes versus Width to Depth Ratio (W =61 m, 200 ft) for Ground settlement of 0.5, 1, 1.5, 2.0, 2.5, 3.0, 3.5 and 4.0 m

The information contained herein is the copyright of and proprietary to BMT Fleet Technology Limited. Use of this information is governed by the legend on the cover page of this document."

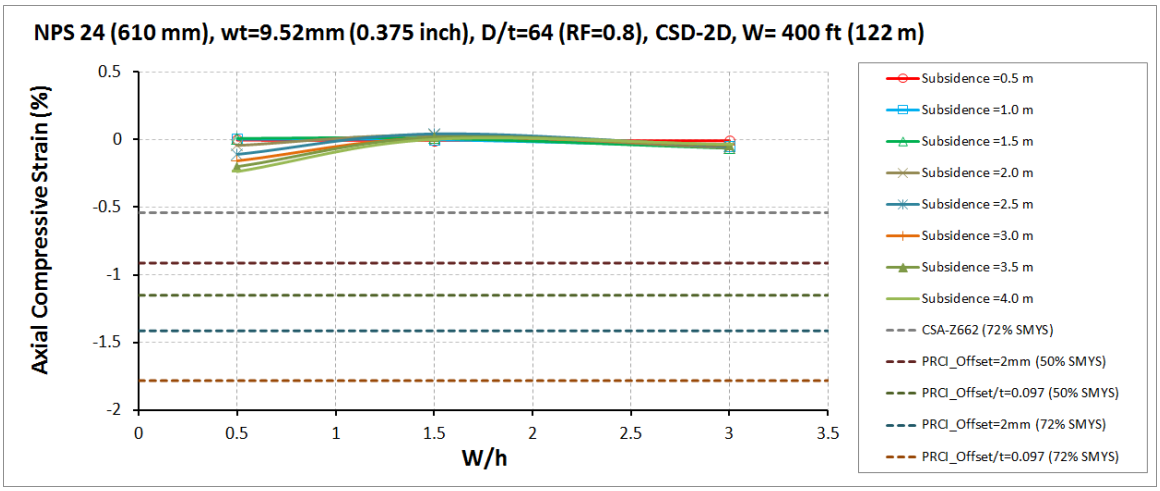

Figure 5.66: NPS 24 (D/t=64) - Pipe Axial Compressive Strains Envelopes versus Width to Depth Ratio (W =122 m, 400 ft) for Ground Settlement of 0.5, 1, 1.5, 2.0, 2.5, 3.0, 3.5 and 4.0 m

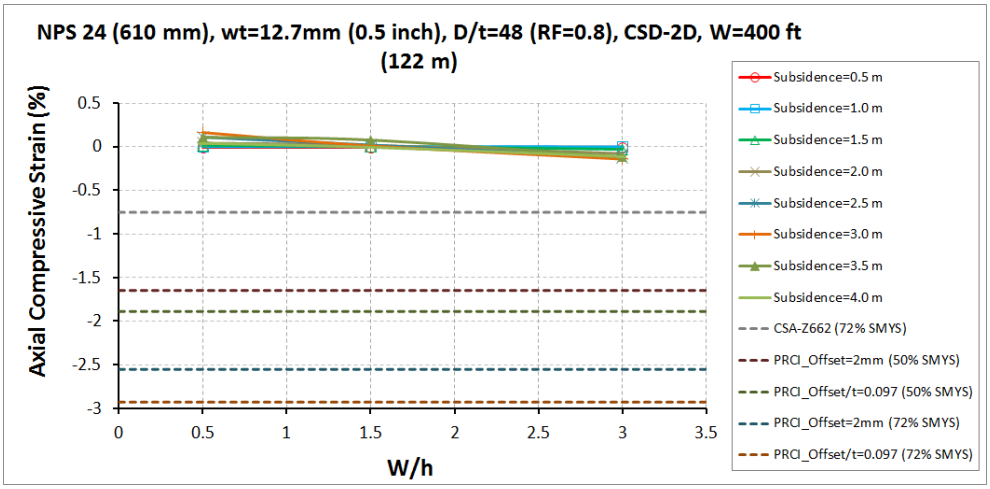

Figure 5.67: NPS 24 (D/t=48) - Pipe Axial Compressive Strains Envelopes versus Width to Depth Ratio (W =61 m, 200 ft) for Ground settlement of 0.5, 1, 1.5, 2.0, 2.5, 3.0, 3.5 and 4.0 m

The information contained herein is the copyright of and proprietary to BMT Fleet Technology Limited. Use of this information is governed by the legend on the cover page of this document."

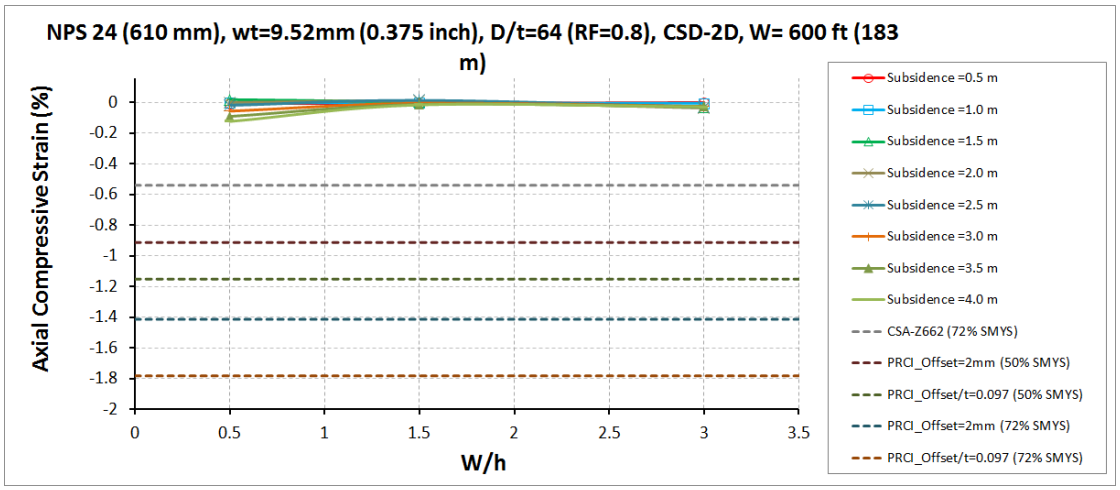

Figure 5.68: NPS 24 (D/t=64) - Pipe Axial Compressive Strains Envelopes versus Width to Depth Ratio (W = 183 m, 600 ft) for Ground Settlement of 0.5, 1, 1.5, 2.0, 2.5, 3.0, 3.5 and 4.0 m

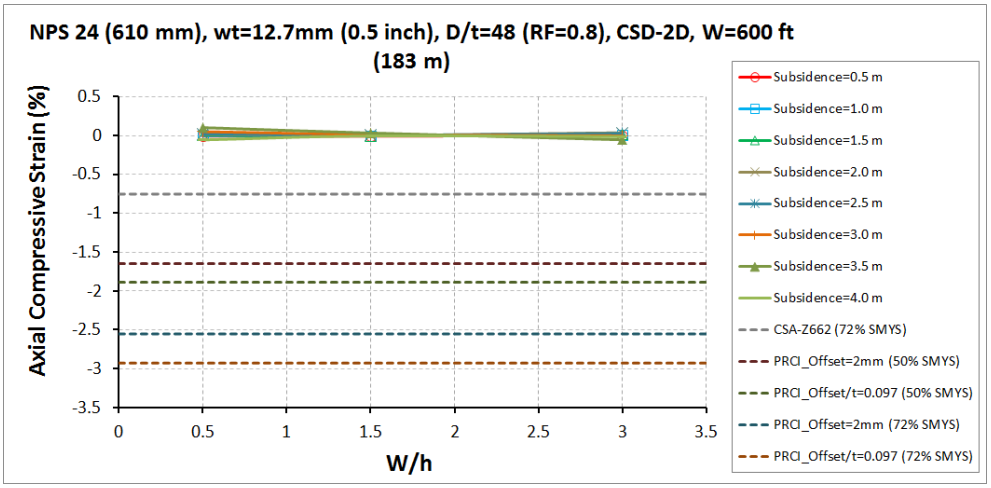

Figure 5.69: NPS 24 (D/t=48) - Pipe Axial Compressive Strains Envelopes versus Width to Depth Ratio (W =183 m, 600 ft) for Ground Settlement of 0.5, 1, 1.5, 2.0, 2.5, 3.0, 3.5 and 4.0 m

5.5 Effect of Temperature

Comparison between the results of three temperature differentials from construction to operation (0, 45 and 65°C) analyzed for subsidence width of 61 m (200 ft) (base case) is provided in Figure 5.70 and Figure 5.71. Both of these figures are for X-52 grade NPS 24 (610 mm) pipe with t =6.35 mm (0.25 in) [D/t=96]. Reduction in the differential temperature results in reduction in the maximum computed compressive strains. The maximum computed tensile strain is not significantly affected by the temperature differential. The computed compressive strain for case with the maximum temperature differential is more than twice the computed compressive strain for case with no temperature effect.

The information contained herein is the copyright of and proprietary to BMT Fleet Technology Limited. Use of this information is governed by the legend on the cover page of this document."

Figure 5.70 presents the maximum tensile and compressive strains in the pipe versus the maximum ground settlement for ground subsidence width of 61 m (200 ft) considering panel width to depth ratio of 0.5. Figure 5.71 presents the sum of tensile (positive) and compressive (negative) strains in the pipe. The results indicated that the calculated compressive strains are slightly higher at ground settlement less than 1.75 m for cases with a temperature differential; this is mainly due to compressive strain induced by thermal loading. At large ground displacement, tensile strains are higher than compressive strain. This differential in peak tensile and compressive strains indicates that there is a significant uniform axial strain in the pipe due to a large catenary effect. The compressive strains induced by the temperature differential attenuate the maximum tensile strains which are primarily promoted by uniform pipe extension.

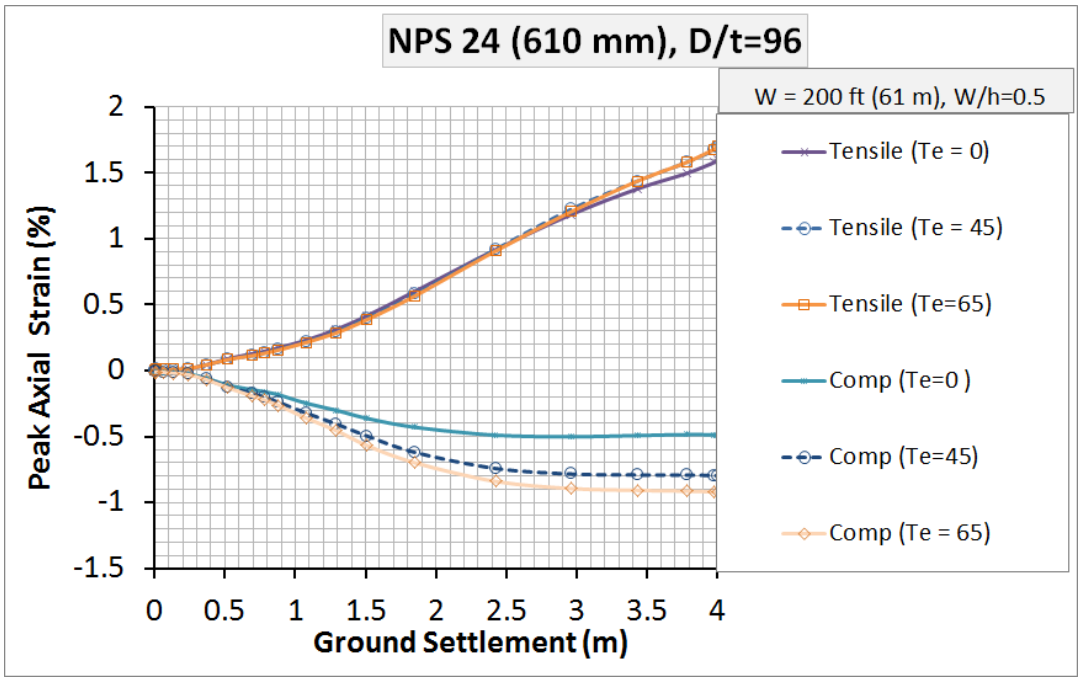

Figure 5.70: NPS 24 (D/t=96) – Maximum Axial Strain Versus Ground Settlement for Ground Subsidence Width of 61 m (200 ft) –Temperature Effect

The information contained herein is the copyright of and proprietary to BMT Fleet Technology Limited. Use of this information is governed by the legend on the cover page of this document."

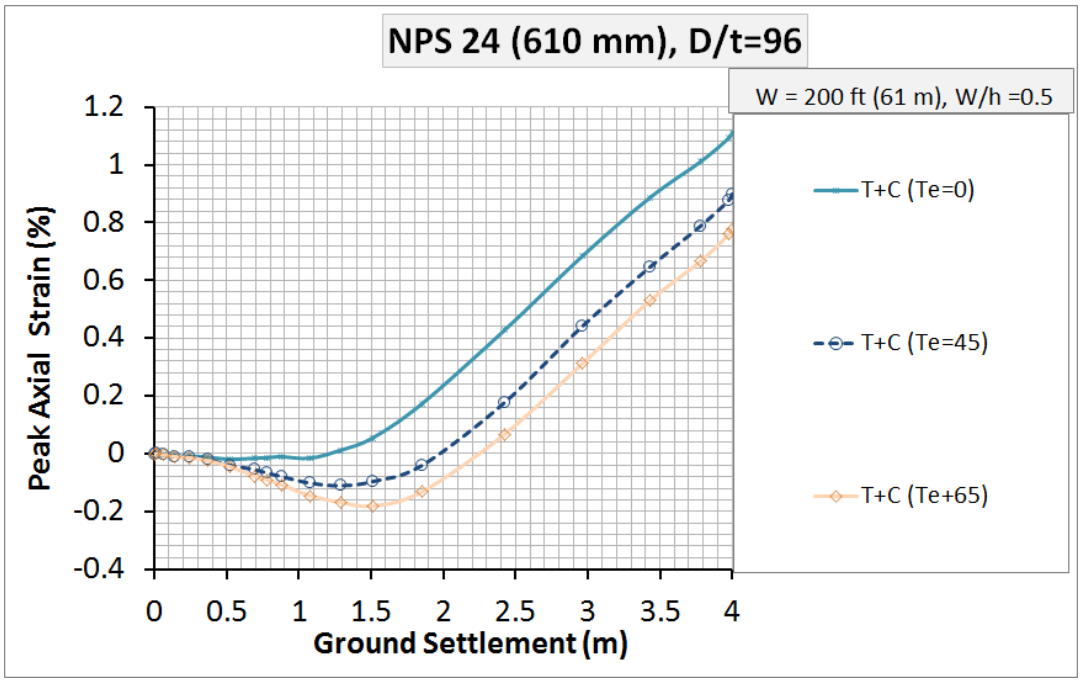

Figure 5.71: NPS 24 (D/t=96) – Sum of the Maximum Tensile and Compressive Strain versus Ground Settlement for Ground Subsidence Width of 61 m (200 ft) – Pressure Effect

5.6 Effect of Operating Pressure

Comparison between the results of three operating pressure of 2.7 MPa, 3.7 MPa and 5.4 MPa considering that the pipeline to be operating at an internal pressure that includes a pipe wall stress of 36%, 50% and 72% of its SMYS. The results of the analyses for subsidence width of 61 m (200 ft) are provided in Figures 5.81 and 5.82. These figures are for X-52 grade NPS 24 (610 mm) pipe with t =6.35 mm (0.25 in) and D/t=96. Figure 5.72 presents the maximum tensile and compressive strains in the pipe versus the maximum ground settlement for subsidence width of 61m (200 ft) considering panel width to depth ratio of 0.5. Reduction in the operating pressure results in an increase in the maximum computed compressive strains. The maximum computed tensile strain is not significantly affected.

Figure 5.73 presents the sum of tensile (positive) and compressive (negative) strains in the pipe. The results indicated that the calculated compressive strains are slightly higher at ground settlement less than 2.0 m for cases with a lower operating pressure. At large ground displacement, tensile strains are higher than compressive strain. This differential in peak tensile and compressive strains indicates that there is a significant uniform axial strain in the pipe due to larger catenary effect.

The information contained herein is the copyright of and proprietary to BMT Fleet Technology Limited. Use of this information is governed by the legend on the cover page of this document."

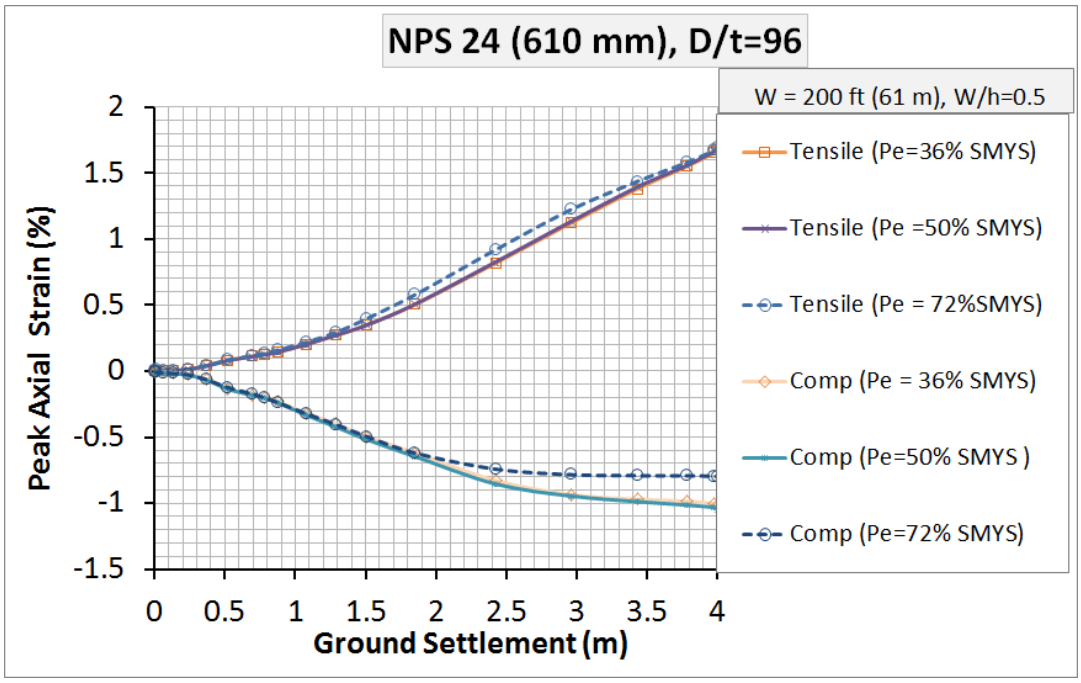

Figure 5.72: NPS 24 (D/t=64) – Maximum Pipe Axial Strain Due to Ground Settlement for Ground Subsidence Width of 61 m (200 ft) – Pressure Effect

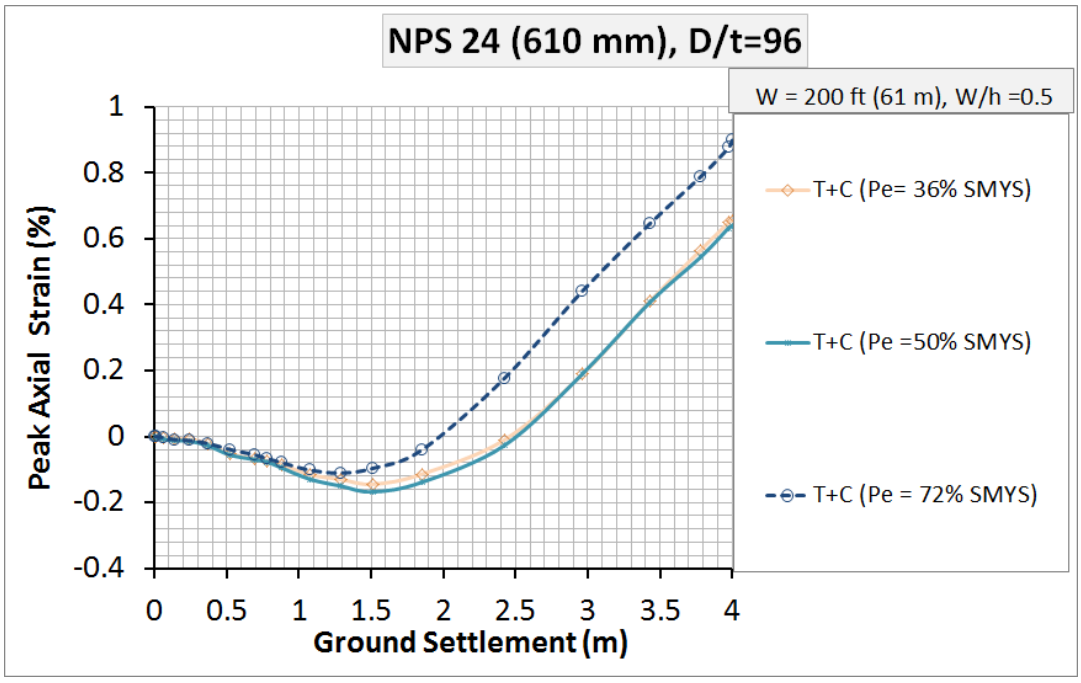

Figure 5.73: NPS 24 (D/t=64) – Sum of the Maximum Tensile and Compressive Strain versus Ground Settlement for Ground Subsidence Width of 61 m (200 ft) – Pressure Effect

The information contained herein is the copyright of and proprietary to BMT Fleet Technology Limited. Use of this information is governed by the legend on the cover page of this document."

5.7 Structural Analyses for the 12-inch Pipeline

Analyses were completed for the NPS 12 (324 mm outside diameter) pipeline to assess its response to ground subsidence and to determine the structural integrity significance of ground movement induced strain demands. A sensitivity analysis was conducted to evaluate the effect of D/t ratio and the width of then ground subsidence. The analyses considered 18 subsidence scenarios. The scenarios included the following:

- Pipe wall thickness: three wall thicknesses: 4.57 mm (0.18 inch), 6.35 mm and 9.52 mm (0.375 in); corresponding to D/t ratio of 71 and 34 respectively;
- Ground displacement direction: Perpendicular (lateral) to the pipeline axis;
- Panel widths: three panel widths of 61 m (200 ft), 122 m (400 ft) and 183 m (600 ft);
- Mining depths: three different mining depth for each panel width;
- Panel extraction areas defined based on panel width to mining depth ratio (W/H): three W/H ratio of 0.5, 1.5 and 3.0 for each panel width;
- Shape of ground displacement: three ground subsidence patterns;
- One soil conditions with soil properties consistent with sand/clay till;
- Pipeline burial depth: One burial depth of 1.2m (4 ft) to top pipe, corresponding to 1.5 m (5 ft) depth to pipe center line.

Assumptions for the pipeline were as follows:

- 72% SMYS internal pressure;
- 45°C thermal differential (installation -20°C, max operating temperature 25°C); and
- A generic stress strain curves for Grade X-52 (359) pipe according to the API 5L

5.7.1 12 Inch Pipeline Results

The results presented in in Appendix B illustrate the importance of the width of the ground subsidence and the panel width to depth ratio. The results demonstrate that the pipe deformation and strains in the pipe are significantly affected by the by the subsidence width and the panel width to mining depth ratio (W/H). A comparison of the results of the three wall thicknesses analyzed for ground subsidence considering ground subsidence of 61 m (200 ft) and three panel width to depth ratio (W/h 0.5, 1.5 and 3) is provided in Figure 5.83 through Figure 5.88.

Figure 5.83, Figure 5.84 and Figure 5.85 show the maximum tensile and compressive strains in the NPS 12 (609 mm) pipe along the longitudinal direction as function of the centerline (maximum) ground settlement subsidence width of 200 ft (61 m) and W/h of 0.5, 1.5 and 3. The results are for X52 grade, and D/t's (71 and 31).

Figure 5.86, Figure 5.87 and Figure 5.88 plot axial strains distribution at different clock positions, 6 and 12 o'clock along the length of the pipeline. The results presented in these figures are for ground subsidence width of 200 ft (61 m) and three W/h ratios of 0.5, 1.5 and 3. The

The information contained herein is the copyright of and proprietary to BMT Fleet Technology Limited. Use of this information is governed by the legend on the cover page of this document."

results in Figure 5.86 through Figure 5.87 and Table 5.5 indicated that pipeline with higher D/t ratio (lower pipe wall thickness) results in higher computed tensile with higher tensile strain than compressive strain. For example, for panel width to depth ratio of 0.5 the strain ranged from +1.0% and -0.36% for 6.35 mm (0.25 inch) wall thickness to +0.62% and –0.37% for 9.53 mm (0.375 inch) wall. The reported maximum strains in Table 5.5 are for ground settlement of 4.0 m.

Table 5.5: Maximum Tensile and Compressive Strain [%] for NPS 12, W =200 ft (61 m) – Effect of D/t

D/t	D/t= 71		D/t=34	
Strains	Tensile	Compressive	Tensile	Compressive
W/h = 0.5	1.0	-0.36	0.62	-0.37
W/h = 1.5	0.32	-0.05	0.53	-0.03
W/h = 3	0.53	-0.03	0.4	-0.13

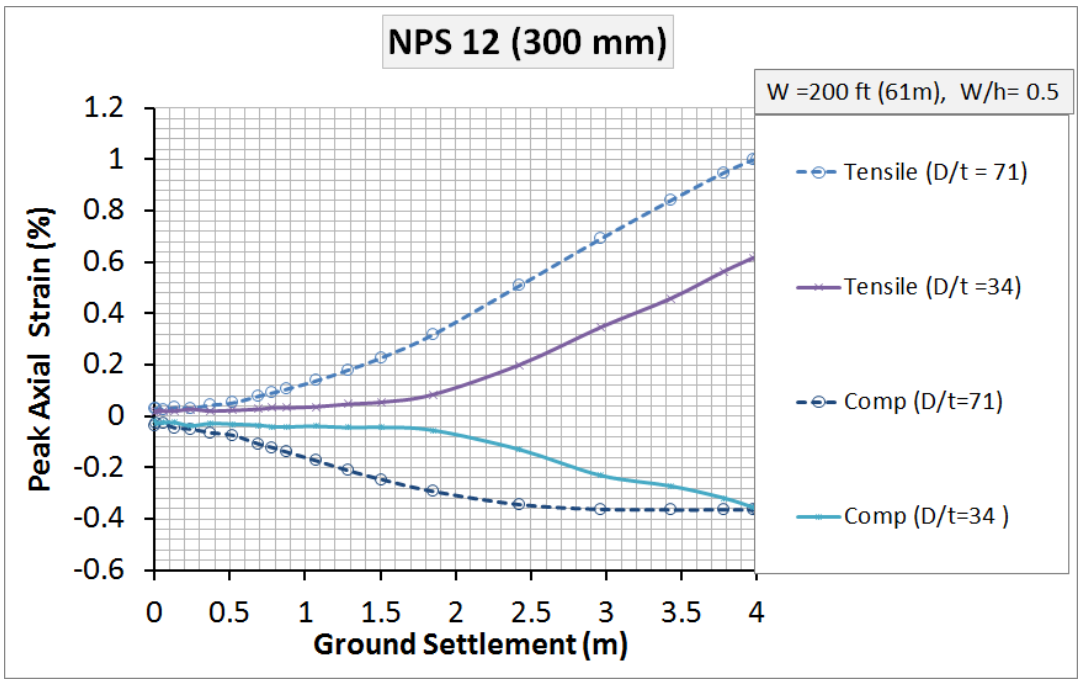

Figure 5.83: NPS 12 – Maximum Axial Strain Versus Ground Settlement for Ground Subsidence Width of 200 ft (61 m) and W/h = 0.5

The information contained herein is the copyright of and proprietary to BMT Fleet Technology Limited. Use of this information is governed by the legend on the cover page of this document."

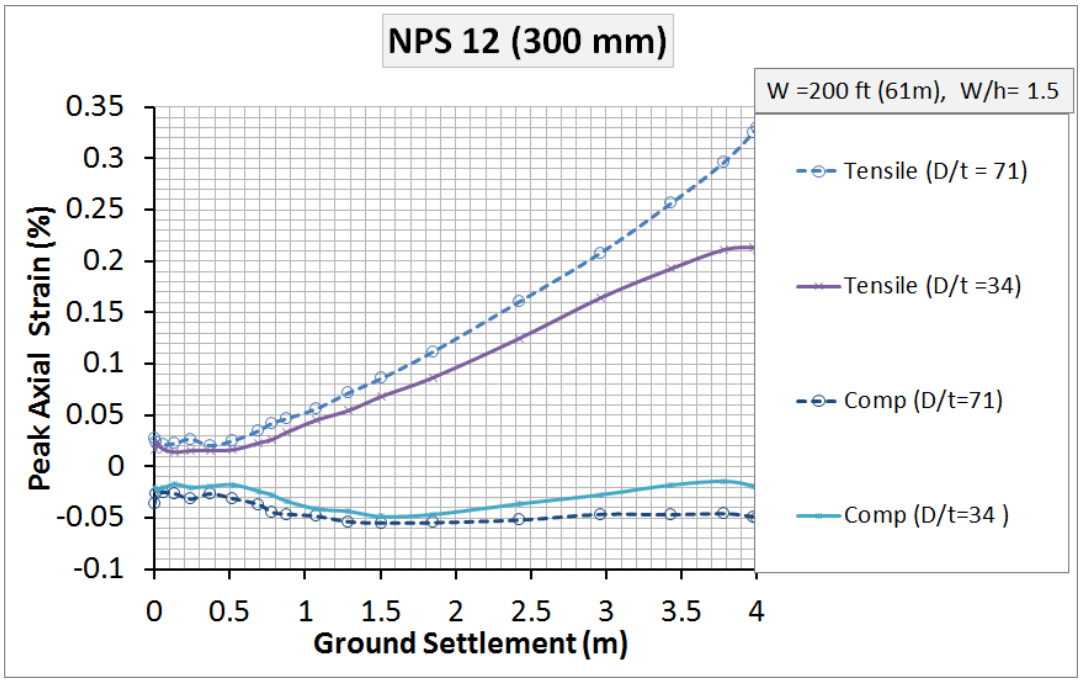

Figure 5.84: NPS 12 – Maximum Axial Strain Versus Ground Settlement for Ground Subsidence Width of 200 ft (61 m) and W/h = 1.5

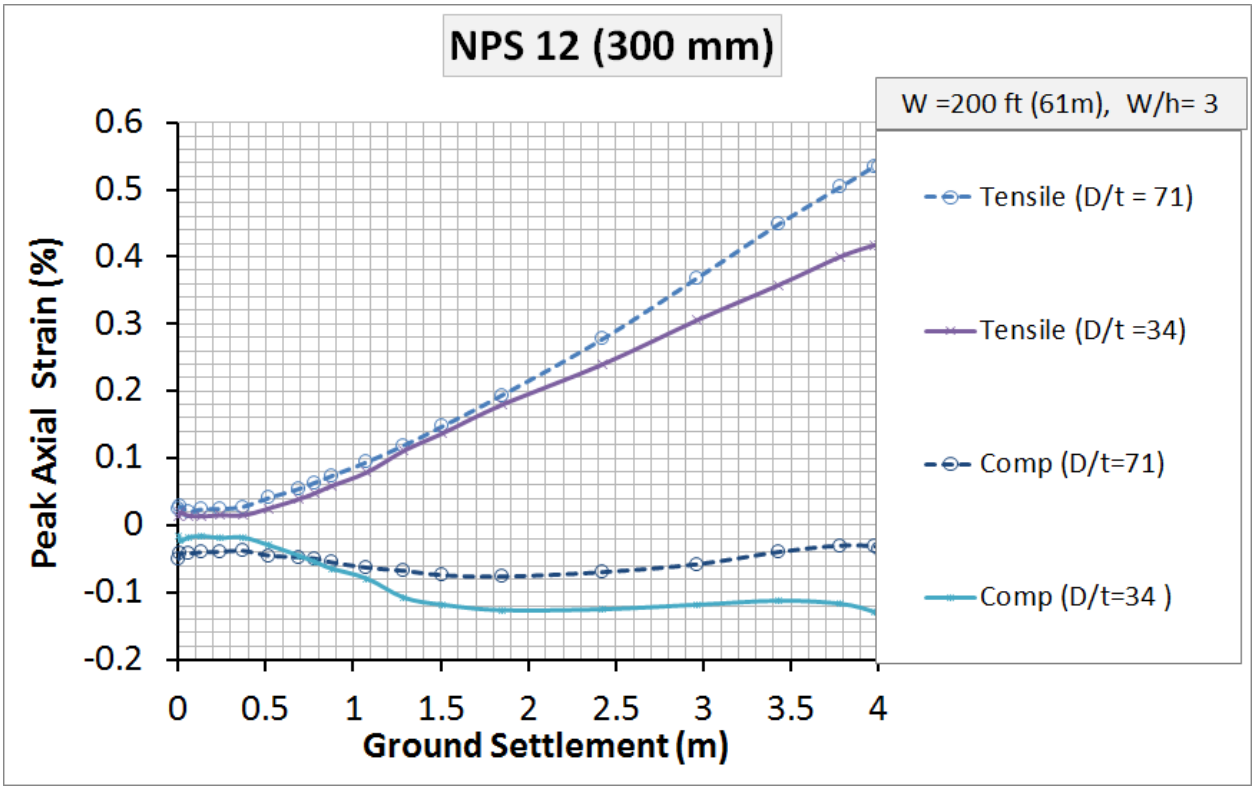

Figure 5.85: NPS 12 – Maximum Axial Strain versus Ground Settlement for Ground subsidence Width of 200 ft (61 m) and W/h = 3

The information contained herein is the copyright of and proprietary to BMT Fleet Technology Limited. Use of this information is governed by the legend on the cover page of this document."

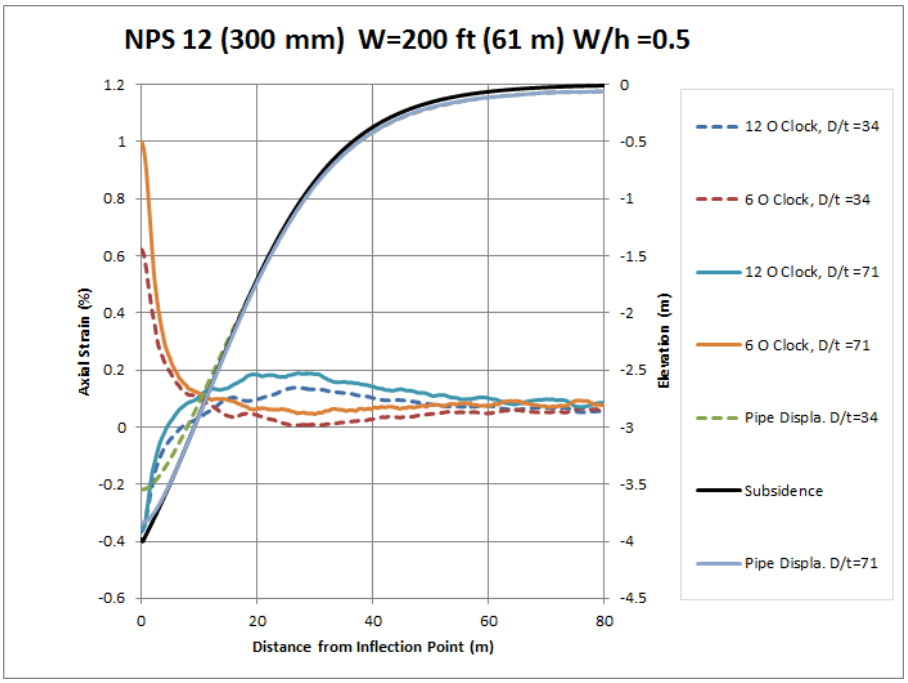

Figure 5.86: Total Axial Strains in NPS 12 at 6 o'clock position for W = 200 ft (61m), W/H = 0.5 and Soil Settlement of 4 m

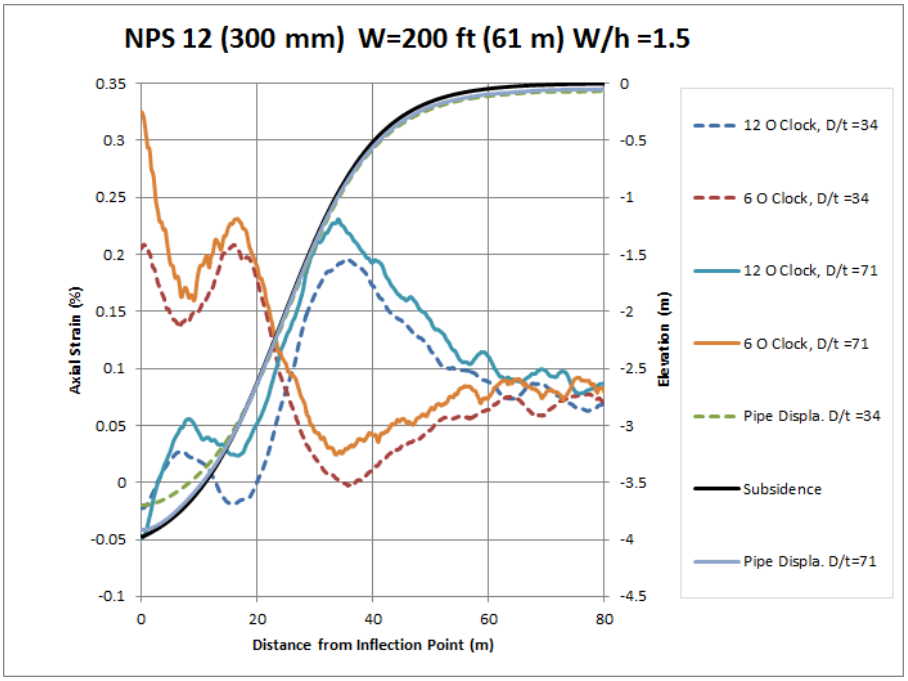

Figure 5.87: Total Axial Strains in NPS 12 at 12 o'clock Position for W = 200 ft (61m), W/H = 0.5 and Soil Settlement of 4 m

The information contained herein is the copyright of and proprietary to BMT Fleet Technology Limited. Use of this information is governed by the legend on the cover page of this document."

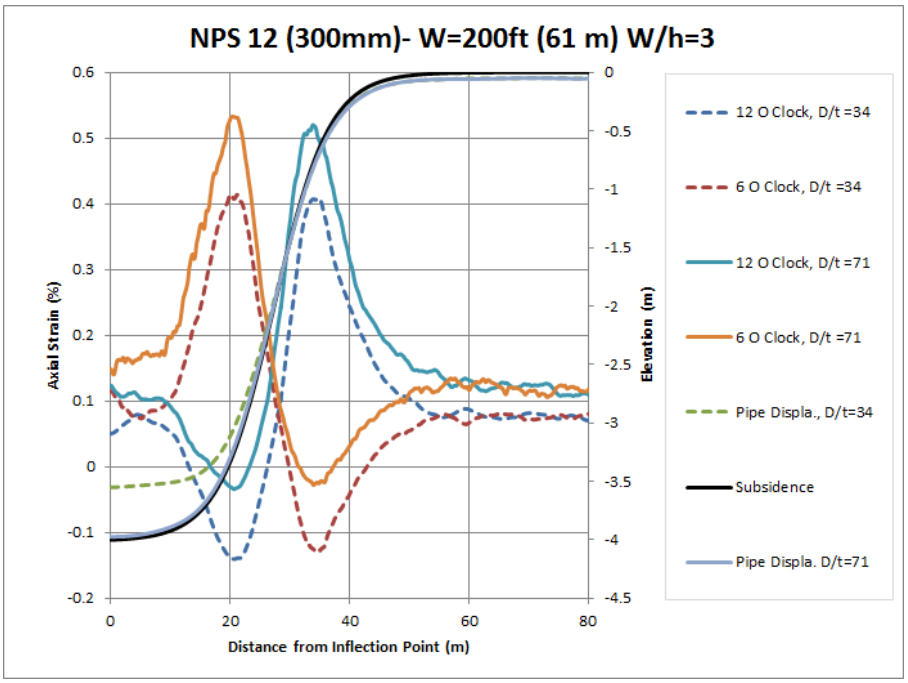

Figure 5.88: Total Axial Strains in NPS 12 at 12 o'clock Position for W = 200 ft (61m), W/H = 0.5 and Soil Settlement of 4 m

The strain demands determined from the analysis was compared with the calculated strain capacity defined from the guidance; BS 7910 for tensile strain, and CSA Z662 and PRCI 2004 for compressive strain. While there are many existing models for calculating the compressive and tensile strain capacity in codes and standards, it was decided to develop a simple a strain-based design methodology that can be easily adapted to any code and standards. These tensile and compressive strain demand 'envelopes' for a given ground subsidence, 0.5 m, 1.0 m, 1.5 m, 2.0 m , 2.5 m, 3.0 m, 3.5 m and 4.0 m will be presented in the final report. The safe pipeline operating goal of pipeline subjected to surface subsidence is to stay within the normal operating strain range defined by codes and standards.

5.8 Structural Analyses for an 18-inch Pipeline

Analyses were completed for the NPS 18 (450 mm outside diameter) pipeline to assess its response to ground subsidence and to determine the structural integrity significance of ground movement induced strain demands. A sensitivity analysis was conducted to evaluate the effect of D/t ratio and the width of then ground subsidence. The analyses considered 18 settlement scenarios. The scenarios included the following:

- Pipe wall thickness: three wall thicknesses: 4.57 mm (0.18 inch) and 9.52 mm (0.375 in); corresponding to D/t ratio of 96 and 48 respectively;
- Ground displacement direction: Perpendicular (lateral) to the pipeline axis;
- Panel widths: three panel widths of 61 m (200 ft), 122 m (400 ft) and 183 m (600 ft);
- Mining depths: three different mining depth for each panel width;

The information contained herein is the copyright of and proprietary to BMT Fleet Technology Limited. Use of this information is governed by the legend on the cover page of this document."

- Panel extraction areas defined based on panel width to mining depth ratio (W/H): three W/H ratio of 0.5, 1.5 and 3.0 for each panel width;
- Shape of ground displacement: three ground subsidence patterns;
- One soil conditions with soil properties consistent with sand/clay till;
- Pipeline burial depth: One burial depth of 1.2 m (4 ft) to top pipe, corresponding to 1.5 m (5 ft) depth to pipe center line.

Assumptions for the pipeline were as follows:

- 72% SMYS internal pressure;
- 45°C thermal differential (installation -20°C, max operating temperature 25°C); and
- A generic stress strain curves for Grade X-52 (359) pipe according to the API 5L.

5.8.1 Results

The results presented in in Appendix C, illustrate the importance of the width of the ground subsidence and the panel width to depth ratio. The results demonstrate that the pipe deformation and strains in the pipe are significantly affected by the by the subsidence width and the panel width to mining depth ratio (W/H).

A comparison of the results of the three wall thicknesses analyzed for ground subsidence considering ground subsidence of 61 m (200 ft) and three panel width to depth ratio (W/h 0.5, 1.5 and 3) is provided in Figure 5.89 through Figure 5.94. The results demonstrate that the pipe deformation and strains in the pipe are significantly affected by the subsidence width and the panel width to mining depth ratio (W/H).

Figure 5.89, Figure 5.90 and Figure 5.91 show the maximum tensile and compressive strains in the NPS 12 (609 mm) pipe along the longitudinal direction as function of the centerline (maximum) ground settlement subsidence width of 200 ft (61 m) and W/h of 0.5, 1.5 and 3. The results are for X52 grade, and D/t's (96, 48).

Figure 5.92 through 5.94 presents the sum of tensile (positive) and compressive (negative) strains in the pipe. The results indicated that for subsidence width of 200 ft (61 m) and W/h ratio of 0.5, 1.5 and 3 the calculated tensile strains are higher than compressive strains for pipe with higher D/t ratio (D/t=96). This differential in peak tensile and compressive strains indicates that there is a significant uniform axial strain in the pipe due to larger catenary effect in the pipe with higher D/t ratio.

Figure 5.95, Figure 5.96 and Figure 5.97 plot axial strains distribution at different clock positions, 6 and 12 o'clock along the length of the pipeline. The results presented in these figures are for ground subsidence width of 200 ft (61 m) and three W/h ratios of 0.5, 1.5 and 3. The results in Figure 5.92 through Figure 5.94 and Table 5.6 indicated that pipeline with higher D/t ratio (lower pipe wall thickness) results in higher computed tensile with higher tensile strain than compressive strain. For example, for panel width to depth ratio of 0.5 the strain ranged from

The information contained herein is the copyright of and proprietary to BMT Fleet Technology Limited. Use of this information is governed by the legend on the cover page of this document."

+1.41% and -0.80% for 6.35mm (0.25 inch) wall thickness to +0.74% and –0.57% for 9.53mm (0.375 inch) wall. The reported maximum strains in Table 5.6 are for ground settlement of 4.0 m

Table 5.6: Maximum Tensile/Compressive Strain [%] for NPS 18, W =200 ft (61 m) – Effect of D/t

D/t	D/t= 96		D/t= 48	
Strains	Tensile	Compressive	Tensile	Compressive
W/h = 0.5	1.41	-0.80	0.74	-0.57
W/h = 1.5	0.4	-0.13	0.24	-0.12
W/h = 3	0.65	-0.15	0.62	-0.31

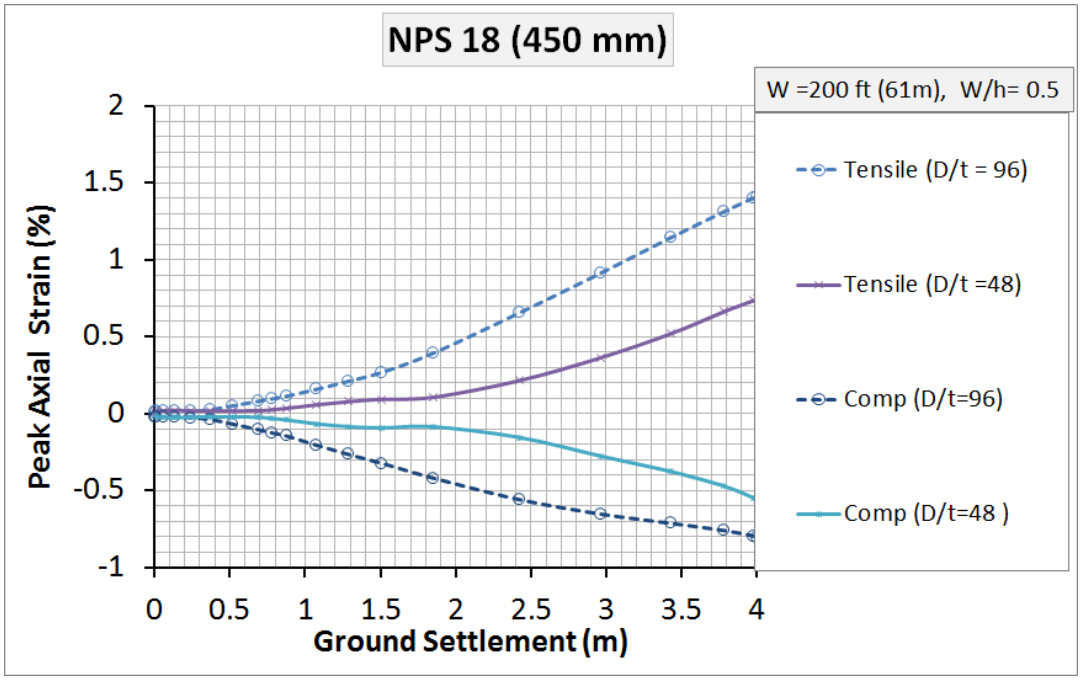

Figure 5.89: NPS 18 – Maximum Axial Strain versus Ground Settlement for Ground Subsidence Width of 200 ft (61 m) and W/h = 0.5

The information contained herein is the copyright of and proprietary to BMT Fleet Technology Limited. Use of this information is governed by the legend on the cover page of this document."

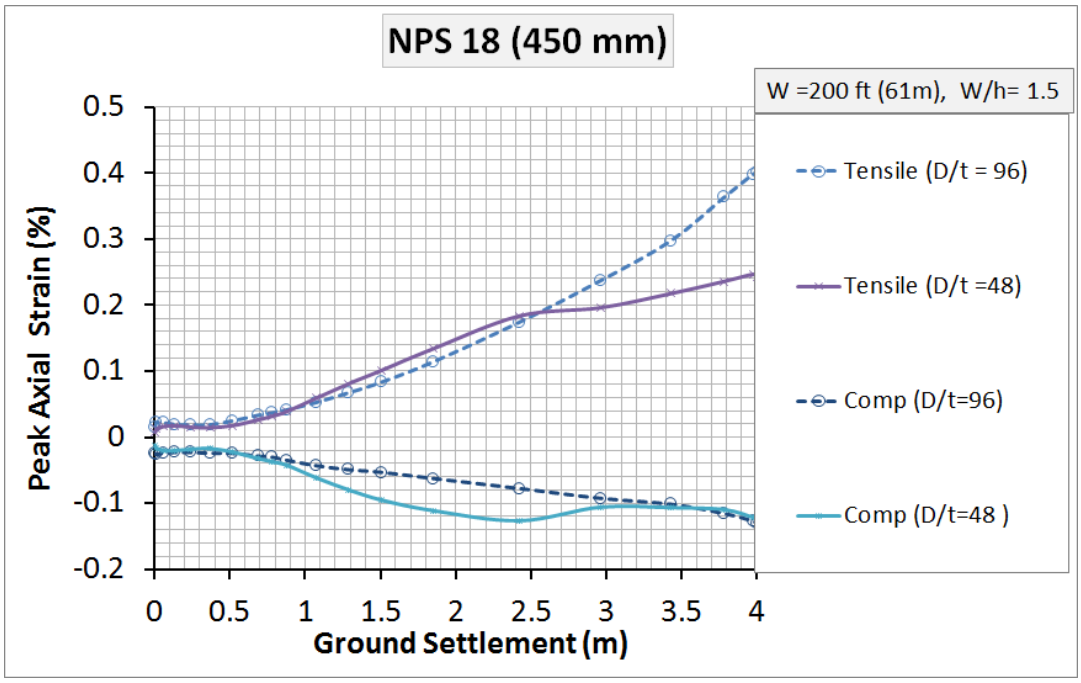

Figure 5.90: NPS 18 – Maximum Axial Strain versus Ground Settlement for Ground Subsidence Width of 200 ft (61 m) and W/h = 1.5

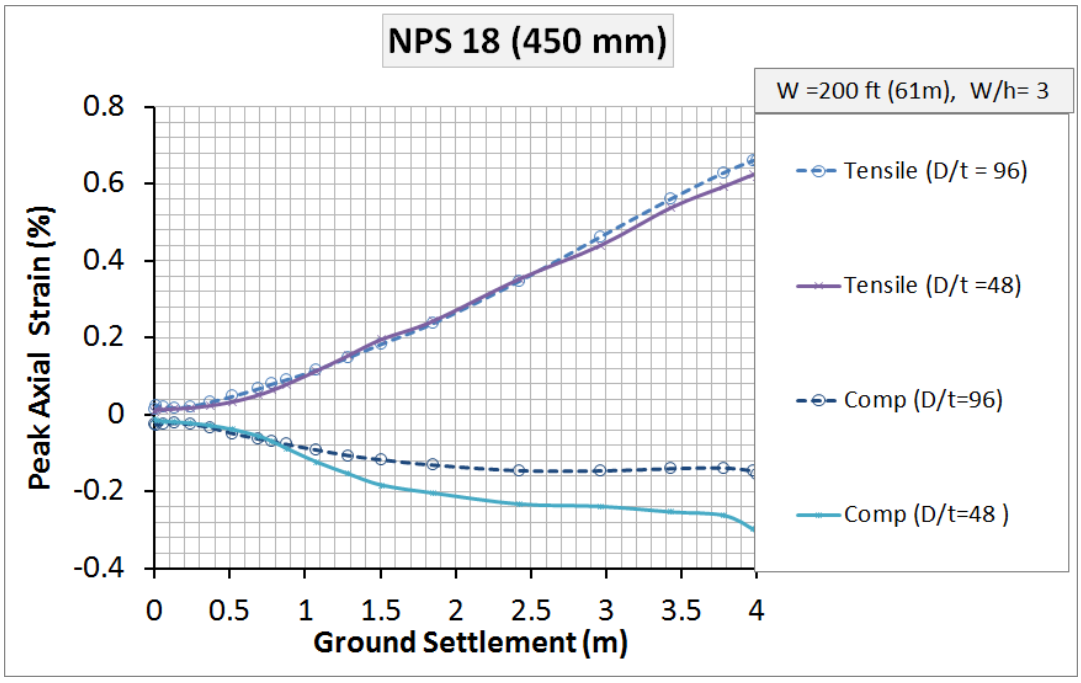

Figure 5.91: NPS 18 – Maximum Axial Strain versus Ground Settlement for Ground Subsidence Width of 200 ft (61 m) and W/h = 3

The information contained herein is the copyright of and proprietary to BMT Fleet Technology Limited. Use of this information is governed by the legend on the cover page of this document."

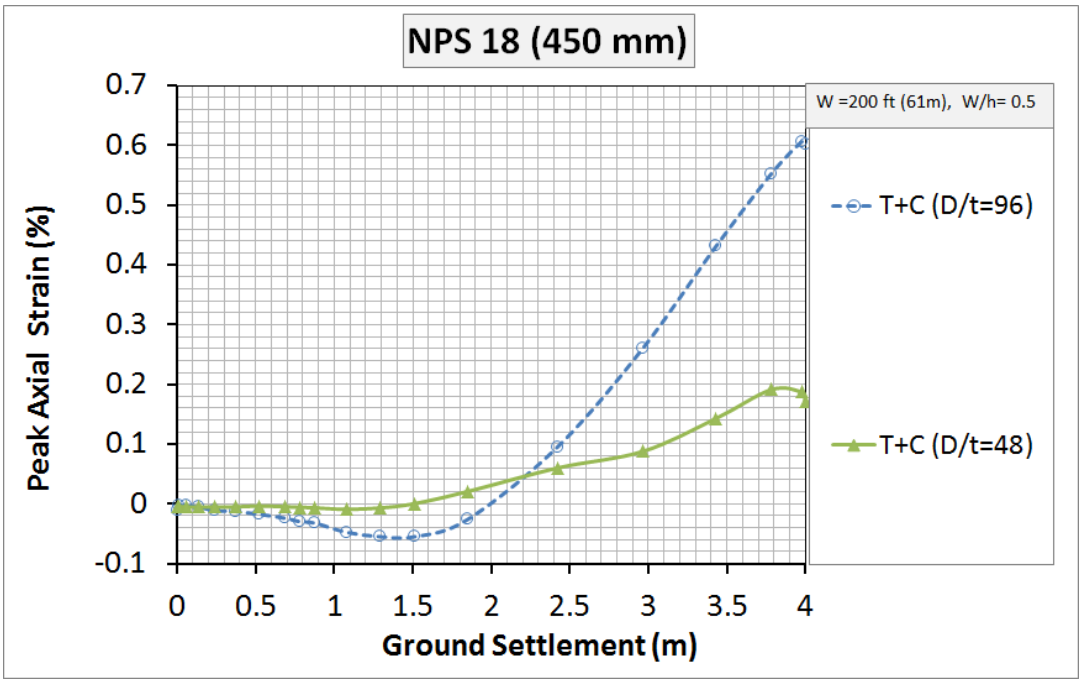

Figure 5.92: NPS 18 – Sum of Tensile and Compressive Axial Strain versus Ground Settlement for Ground Subsidence Width of 200 ft (61 m) and W/h = 0.5

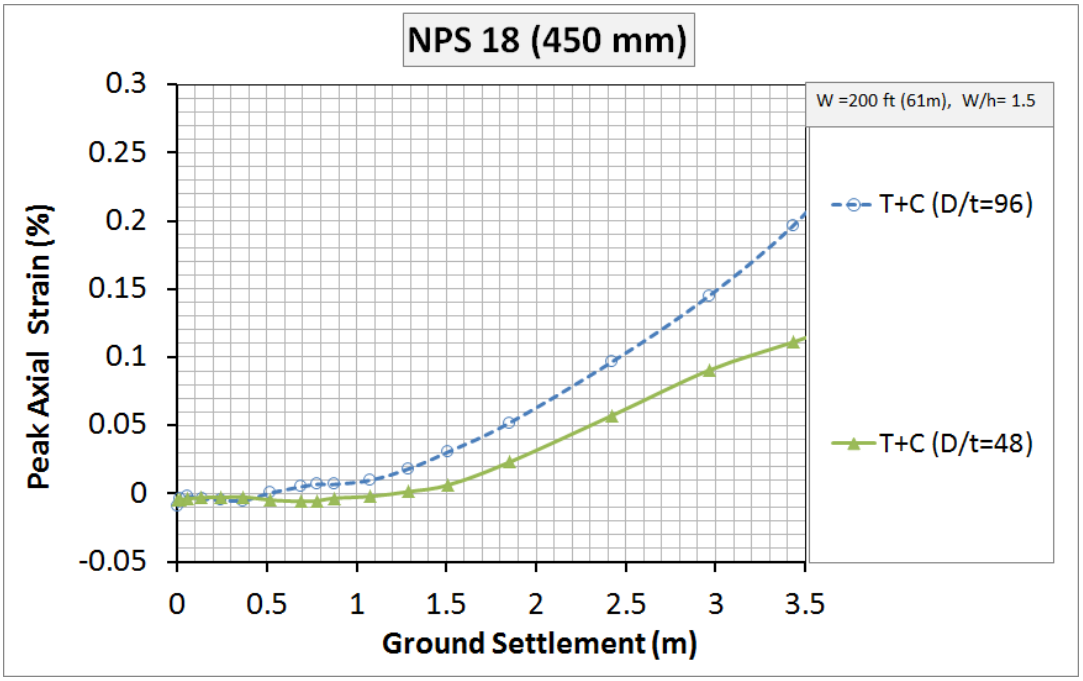

Figure 5.93: NPS 18 – Sum of Tensile and Compressive Axial Strain versus Ground Settlement for Ground Subsidence Width of 200 ft (61 m) and W/h = 1.5

The information contained herein is the copyright of and proprietary to BMT Fleet Technology Limited. Use of this information is governed by the legend on the cover page of this document."

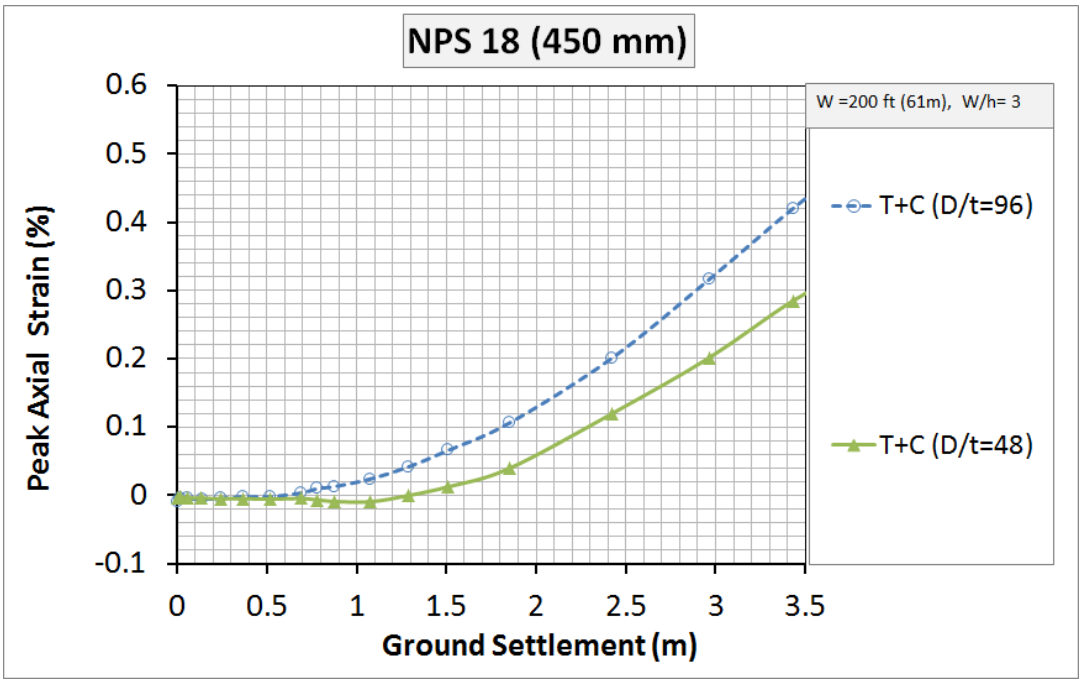

Figure 5.94: NPS 18 – Sum of Tensile and Compressive Axial Strain versus Ground Settlement for Ground Subsidence Width of 200 ft (61 m) and W/h = 3

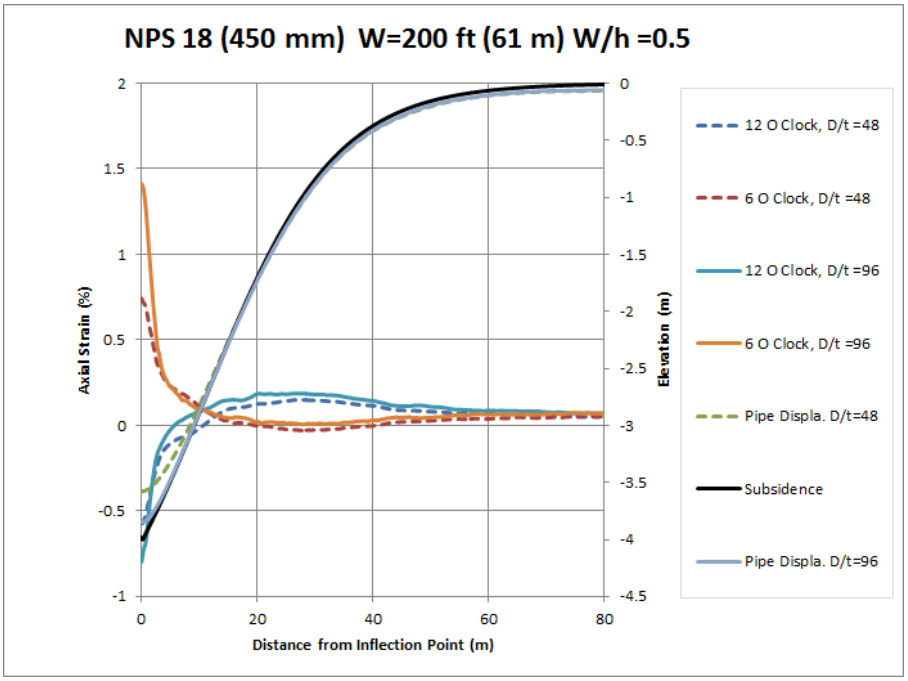

Figure 5.95: Total Axial Strains in NPS 18 at 6 o'clock Position for W = 200 ft (61 m), W/H = 0.5 and Soil Settlement of 4m

The information contained herein is the copyright of and proprietary to BMT Fleet Technology Limited. Use of this information is governed by the legend on the cover page of this document."

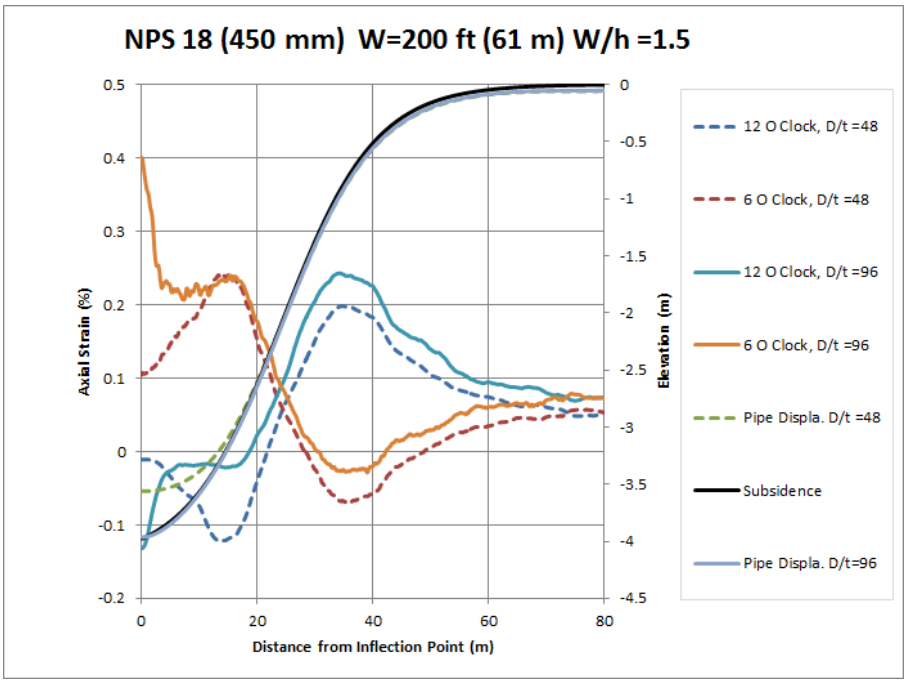

Figure 5.96: Total Axial Strains in NPS 18 at 12 o'clock Position for W = 200 ft (61 m), W/H = 0.5 and Soil Settlement of 4 m

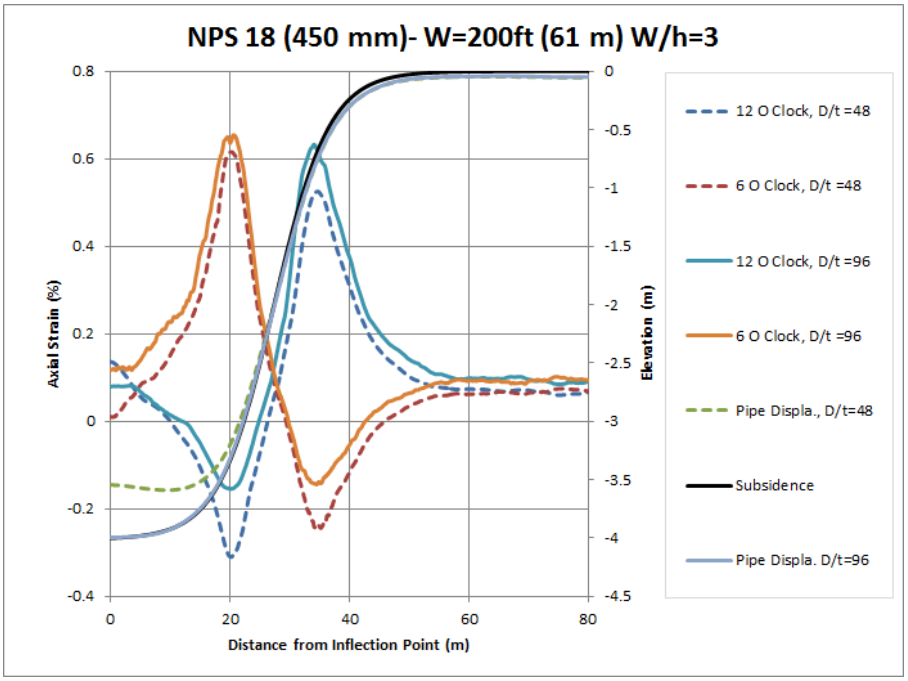

Figure 5.97: Total Axial Strains in NPS 18 at 12 o'clock Position for W = 200 ft (61 m), W/H = 0.5 and Soil Settlement of 4 m

The information contained herein is the copyright of and proprietary to BMT Fleet Technology Limited. Use of this information is governed by the legend on the cover page of this document."

The strain demands determined from the analysis was compared with the calculated strain capacity defined from the guidance; BS 7910 for tensile strain, and CSA Z662 and PRCI 2004 for compressive strain. While there are many existing models for calculating the compressive and tensile strain capacity in codes and standards, it was decided to develop a simple a strain-based design methodology that can be easily adapted to any code and standards. These tensile and compressive strain demand 'envelopes' for a given ground subsidence 0.5 m, 1.0 m, 1.5 m, 2.0 m, 2.5 m, 3.0 m, 3.5 m and 4.0 m will be presented in the final report. The safe pipeline operating goal of pipeline subjected to surface subsidence is to stay within the normal operating strain range defined by codes and standards.

5.9 Pipeline Subsidence Modelling Observations

The sample application of the DEM pipe-soil interaction geotechnical hazard assessment method was employed to investigate the strains developed in a pipeline subjected to mine subsidence. The primary focus was an NPS 24 (610 mm) pipe system, however, the analysis also considered 12 (305 mm) and 18 inch (457 mm) diameter pipes. The use of the simulated pipe responses to soil movement to consider the onset of tensile and compressive limit states in a strain-based assessment was demonstrated and the sensitivity of the pipe response to a number or geotechnical hazard scenario factors were presented. For the pipe-soil interaction in which across mining subsidence panel, it was shown that:

- The response of the pipeline and soil movement pattern is affected by the ground subsidence magnitude, width and patterns;
- The vertical soil movement-induced pipe displacements will produce both pipe bending and axial extension;
- The strains in the pipe are affected by the width of the surface subsidence and there is a critical surface subsidence width that promotes a peak strain. The critical width is a function of the pipe geometry, pipeline operating conditions and locked-in pipeline axial loads (i.e. those caused by thermal differential between operating and construction conditions) and as well as the subsidence parameters.

The use of the results presented in this report to consider subsidence at the edge of rock or similarly undeformable shelf should be treated with care.

The effect of the parameters considered in these sensitivity studies indicate that the parameters can be ranked based upon their impact on strain demand as follows:

Higher Importance	Medium Importance	Lower Importance
- Magnitude of ground subsidence - Ground subsidence pattern - Width of ground subsidence - Burial depth	- Pipe geometry (D/t) - Operating pressure - Temperature differential - Soil stiffness	- Soil to pipe friction - Material grade

The information contained herein is the copyright of and proprietary to BMT Fleet Technology Limited. Use of this information is governed by the legend on the cover page of this document."

Comparisons were made with limit state equations defined from the guidance; BS 7910 for tensile strain, and CSA Z662 and PRCI 2004 for compressive strain to demonstrate the application of the analysis results in an assessment process. While there are many existing models for calculating the compressive and tensile strain capacity in codes and standards, it was decided to develop a simple a strain-based design methodology that can be easily adapted to any code and standards, which is the purpose of this section.

The tensile and compressive strain demand envelopes along the longitudinal direction of the pipeline were developed. The maximum soil settlement versus ground width subsidence as a series of 'envelopes' was developed for a given pipe tensile and compressive strain demands. The safe pipeline operating goal of pipeline subjected to lateral ground displacement is to stay within the normal operating strain range defined by codes and standards.

The strain for critical width subsidence events (strain demand or applied strain) may be used conservatively to evaluate the response of pipeline system with similar geotechnical hazards. The allowable strain (strain capacity or resistance) should be evaluated for each pipe geometry, material and operating condition.

The information contained herein is the copyright of and proprietary to BMT Fleet Technology Limited. Use of this information is governed by the legend on the cover page of this document."

6 MODELING OF LANDSLIDE HAZARD

6.1 Introduction

- The objective of this section is to complete a sensitivity study to define the problem parameters and the pipe strains developed in lateral soil movement events and identify trends. The analyses considered 90 lateral ground movement scenarios. This work was focussed on ground movements involving deformable soils. Care should be taken in applying these results to ground movement across a pipeline surrounded by rock or very stiff soils that will not deform and will cause extremely localized pipe deformations. The scenarios included the following:Pipe geometry: four pipe diameter NPS 12 (324 mm OD) , NPS 18 (457 mm OD), NPS 24 (610 mm OD) and NPS 30 (762 mm OD);
- Pipe wall thickness: three wall thicknesses for each pipe diameter;
- Ground displacement direction: Perpendicular (lateral) to the pipeline axis;
- Width of ground displacement (W): Six potential ground movement scenarios with a total estimated width of movement perpendicular to the pipeline varying from 10 to 100 m (10, 20, 30, 40 50 and 100 m);
- Shape of ground displacement: two ground displacement patterns;
- Two soil conditions with soil properties consistent with sand and sand/clay till;
- Slopes: two slopes, 0 and 16 deg. The slope of 16 was considered to be the base case, and 0 degree was only investigated as a sensitivity check; and
- Pipeline burial depth: Three burial depths of 1.2 m (4 ft), 1.5 m (5 ft) and 1.8 m (6 ft) to top pipe. The burial depth of 1.2 m (4 ft) was considered to be the base case, and the 1.5 m (5 ft) and 1.8 m (6 ft) were only investigated as a sensitivity check.

The assumptions for the analyses included in the sensitivity study considering pipeline response to soil displacement pattern were as follows:

- 72%, 50% and 36 % SMYS internal pressure were considered;
- 45°C thermal differential (installation -20°C, max operating temperature 25°C) for the base case. Temperature differentials between construction and operation (ΔT) of 0 °C and 65°C were considered for the sensitivity analysis to evaluate the effect of the temperature differential; and
- Generic stress strain curves for Grade X-52 (359) and X-70 (483) pipe according to the API 5L.

6.2 Finite Element Model Description

LS-DYNA 971 was used to undertake 3D pipe-soil interaction modeling using a Discrete Element Method (DEM). In the DEM model considered in this report the soil is represented by discrete particles and the pipe is modeled using shell element with five (5) integration points through the thickness. The LS-DYNA MAT24 isotropic hardening material model incorporating

The information contained herein is the copyright of and proprietary to BMT Fleet Technology Limited. Use of this information is governed by the legend on the cover page of this document."

a Von Mises yield response was calibrated based upon a full true stress strain curve for the pipe material allowing the non-linear bi-axial stress state in the pipe to be considered.

The interaction between the pipeline and the surrounding soil is modeled by a robust penalty-based contact in which slip and separation are allowed between soil particles and the pipe. The DEM has been applied because it offers the ability to represent the soil as a continuous volume that appropriately permits large displacements while respecting the soil constitutive response and has proven to be a computationally efficient modeling technique. The background of this method is described in Section 5.1.1.

The soil mass in the simulation is taken to be stress free prior to the simulation and the simulation loading is imposed in three steps. In the first step, the gravitational acceleration is applied and sufficient time is allowed to ensure that the soil stress reaches a stationary state. In the second load step, an operating pressure equal to the MOP (72% SMYS) and a temperature differential of 45^0C were applied. In the third load step, the moving (unstable) soil mass was moved at a desired crossing angle.

The full stress-strain curves of the X70 and X52 pipe materials were incorporated in the finite element modeling and are described in Section 5.1.3.

6.3 Structural Analyses for the 24-inch Pipeline

Analyses were completed for the NPS 24 (609 mm outside diameter) pipeline to assess its response to lateral ground movement and to determine the structural integrity significance of ground movement induced strain demands. The analyses considered 50 lateral ground movement scenarios. The scenarios included the following

- Pipe wall thickness: three wall thicknesses: 6.35 mm (0.25 inch), 9.52 mm (0.375) and 12.7 mm (0.5 in); corresponding to D/t ratio of 96, 64 and 48, respectively;
- Ground displacement direction: Perpendicular (lateral) to the pipeline axis;
- Width of ground displacement (W): Six potential ground movement scenarios with a total estimated width of movement perpendicular to the pipeline varying from 10 to 100 m (10, 20, 30, 40 50 and 100 m);
- Shape of ground displacement: two ground displacement patterns;
- Two soil conditions with soil properties consistent with sand and sand/clay till;
- Slopes: two slopes, 0 and 16 deg. The slope of 16 was considered to be the base case, and 0 was only investigated as a sensitivity check;
- Pipeline burial depth: Three burial depths of 1.2 m (4 ft), 1.5 m (5 ft) and 1.8 m (6 ft) to top pipe, corresponding to 1.5 m (5 ft), 1.8 m (6 ft) and 2.1 m (7 ft) depth to pipe center line. The burial depth of 1.2 m (4 ft) was considered to be the base case, and the 1.5 m (5 ft) and 1.8 m (6 ft) were only investigated as a sensitivity check; and
- The lateral ground deformation was initiated using a cosine function raised to the power “n” similar to Suzuki et al. [48] and M. O’Rourke [47] function:

The information contained herein is the copyright of and proprietary to BMT Fleet Technology Limited. Use of this information is governed by the legend on the cover page of this document."

$$y(x) = \delta\left(\cos\frac{\pi x}{W}\right)^n$$

When considering this ground deformation function, a sensitivity analysis was conducted to evaluate the effect of patterns of ground deformation considering exponent "n" values varying from 0.2 to 2. Sample results of ground deformation with n = 2 and 0.2 are presented in Figures 6.1 and 6.2 shows the assumed patterns for a different widths (W) with n = 2.

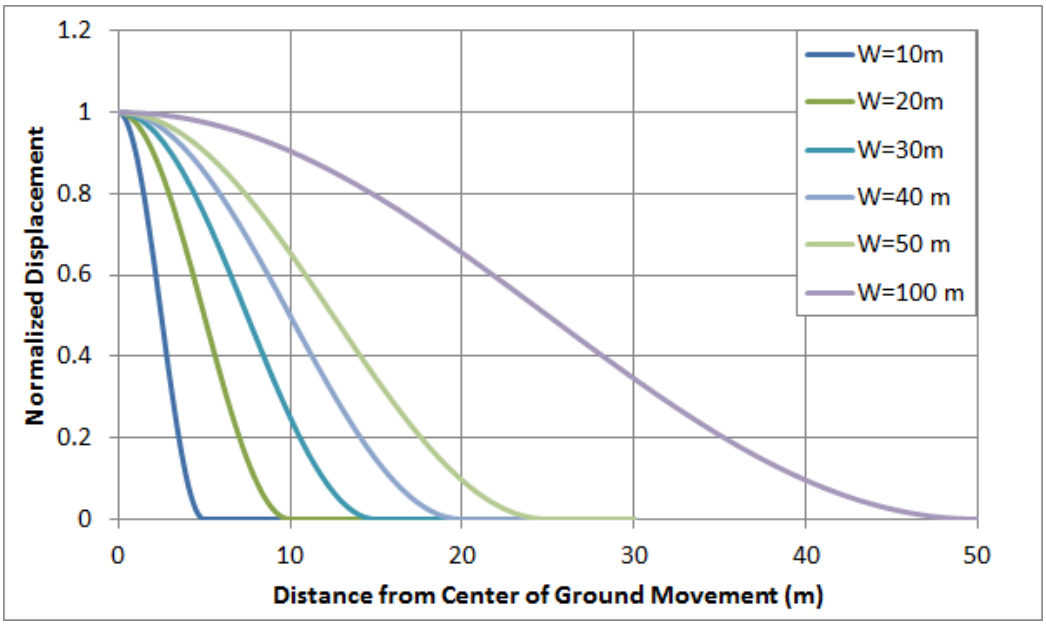

Figure 6.1: Ground Movement Pattern n=2

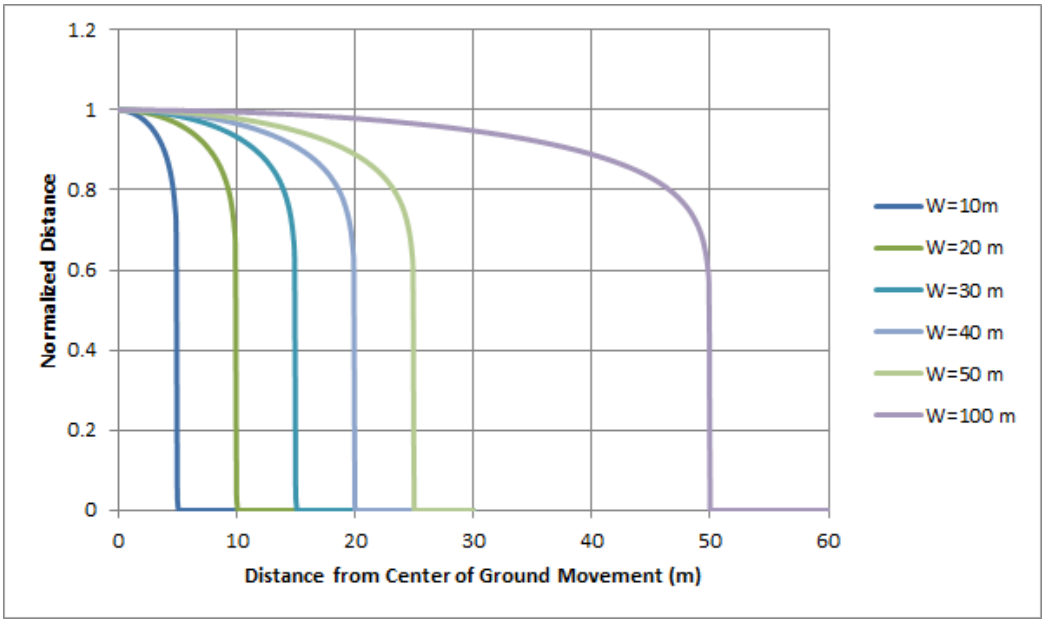

Figure 6.2: Ground Movement Pattern n=0.1

The information contained herein is the copyright of and proprietary to BMT Fleet Technology Limited. Use of this information is governed by the legend on the cover page of this document."

The assumptions for the analyses included in the sensitivity study considering pipeline response to soil displacement pattern were as follows:

- 72%, 50% and 36 % SMYS internal pressure were considered;
- 45°C thermal differential (installation -20°C, max operating temperature 25°C) for the base case. Temperature differentials between construction and operation (ΔT) of 0°C and 65°C were considered for the sensitivity analysis to evaluate the effect of the temperature differential;
- Generic stress strain curves for Grade X-52 (359) and X-70 (483) pipe according to the API 5L.

6.4 Results Base Case

The following section represents the summary results for the NPS 24 (609 mm outside diameter) for the base case with:

- 9.52 mm (0.375 inch) wall thickness (D/t =64);
- Grade 359 (X-52) pipes;
- 72% SMYS internal pressure, 5.4 MPa;
- 45°C thermal differential (installation -20°C, max operating temperature 25°C);
- Burial depth H=1.2 m (5 ft), corresponding to 1.5 m (5 ft) depth to pipe center line, overburden ratio (H/D) of 2.46;
- Soil: sand/clay till with (ϕ'=300 and C'=5 kPa);
- Slope angle of 16 degrees; and
- Lateral ground deformation was simulated using cosine function (described in section) raised to power n=2.

Typical graphical output from finite element model is illustrated in Figure 6.3. This figure illustrates the response of the pressurized NPS 24 pipeline subjected to ground movement for W=20 m. The figure also shows the axial strain distribution (blue color is compressive and red is tensile strain). In this figure, the soil above the pipe is hidden so the pipe deformation can be visualized.

Figure 6.4 shows the pipeline's longitudinal strains at the 3 o'clock and 9 o'clock positions for peak soil displacement of 3 m. The peak tensile strain is about 2.72% and is higher than the compressive strain which is approximately 1.79%. This differential in peak tensile and compressive strains indicates that there is a significant uniform axial strain in the pipe due to larger catenary effect.

The information contained herein is the copyright of and proprietary to BMT Fleet Technology Limited. Use of this information is governed by the legend on the cover page of this document."

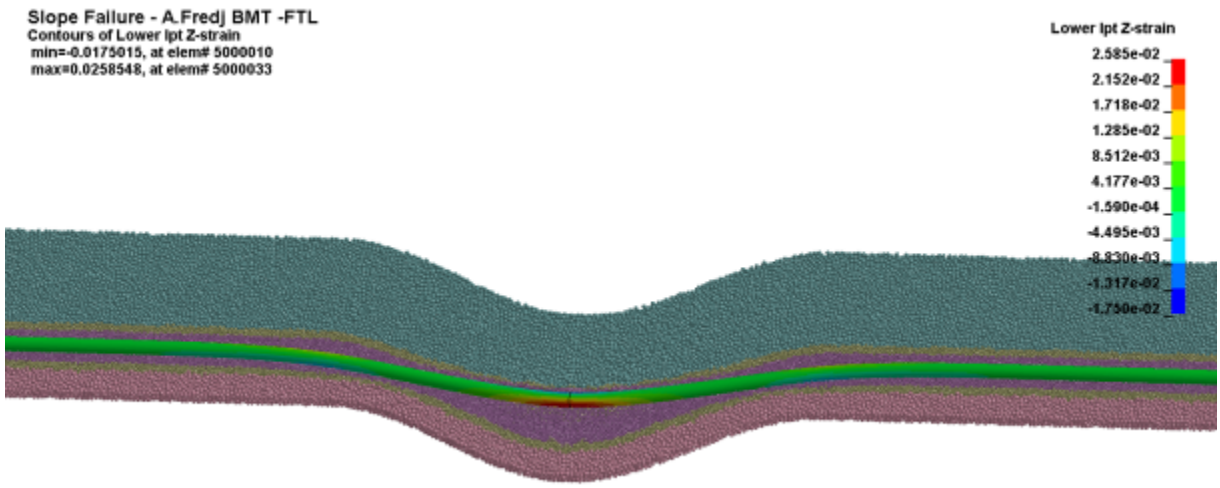

Figure 6.3: Pipe Deformation and Axial Strains for W= 20 m and Soil Movement of 3 m (Top View – Soil above the pipe is hidden)

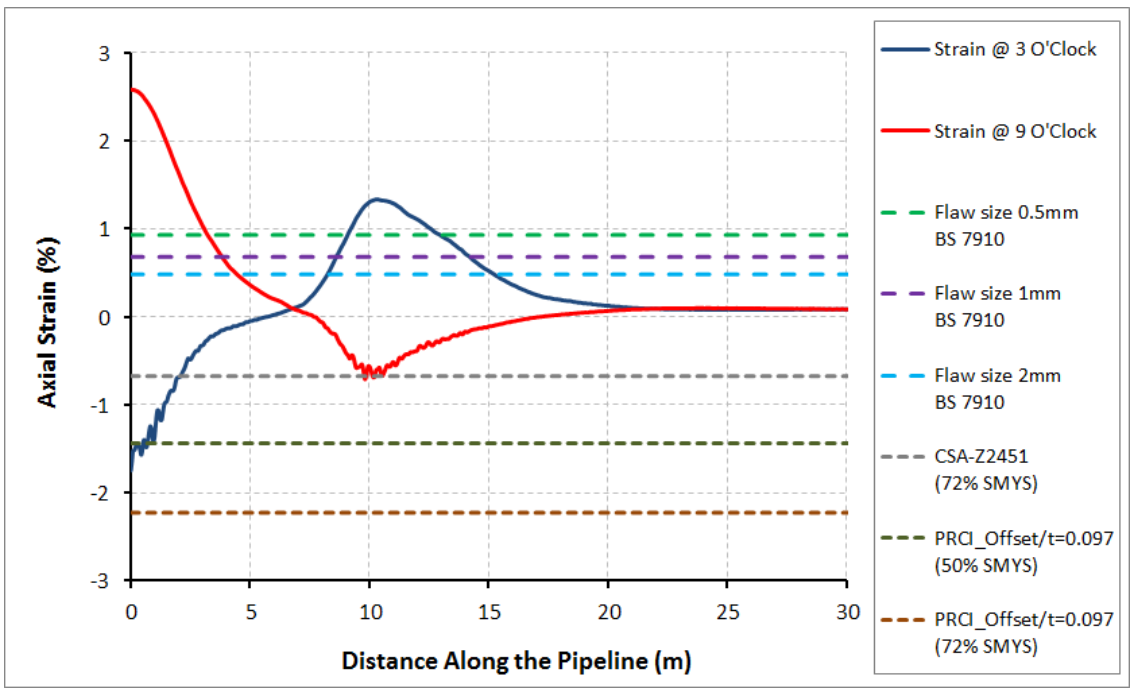

Figure 6.4: Total Axial Strains in NPS 24 (D/t=96) for W= 20 m and Soil Movement of 3 m

6.4.1 Effect of the Width of Ground Movement

A sensitivity study has been completed to understand the effect of ground movement width on pipe deformations or strains. Figure 6.5 presents the maximum tensile strains in the longitudinal direction of the pipeline versus the maximum ground displacement for various ground displacement widths considered in the analyses.

The information contained herein is the copyright of and proprietary to BMT Fleet Technology Limited. Use of this information is governed by the legend on the cover page of this document."

Figures 6.6 and 6.8 present the maximum local and nominal compressive strains in the longitudinal direction of the pipeline versus the maximum ground displacement for various ground displacement widths considered in the analyses. The nominal compressive strain is defined as the average compressive strain measured over a gauge length of 2D (D is the pipe outside diameter). This large stain gauge length is used to permit the analyses to be compared directly to codified permissible strain formulations which are reported over this gauge length.

The results indicate that for the six (6) widths considered, the width of 20 m (66 ft) results in the largest tensile and compressive strain in the pipe for any given value of ground displacement.

This work was focussed on ground movements involving deformable soils. Care should be taken in applying these results to ground movement across a pipeline surrounded by rock or very stiff soils that will not deform and will cause extremely localized pipe deformations where this critical width concept may not apply. It would be conservative to consider the maximum strain for all ground movement widths greater than the critical width of 20m (66 ft).

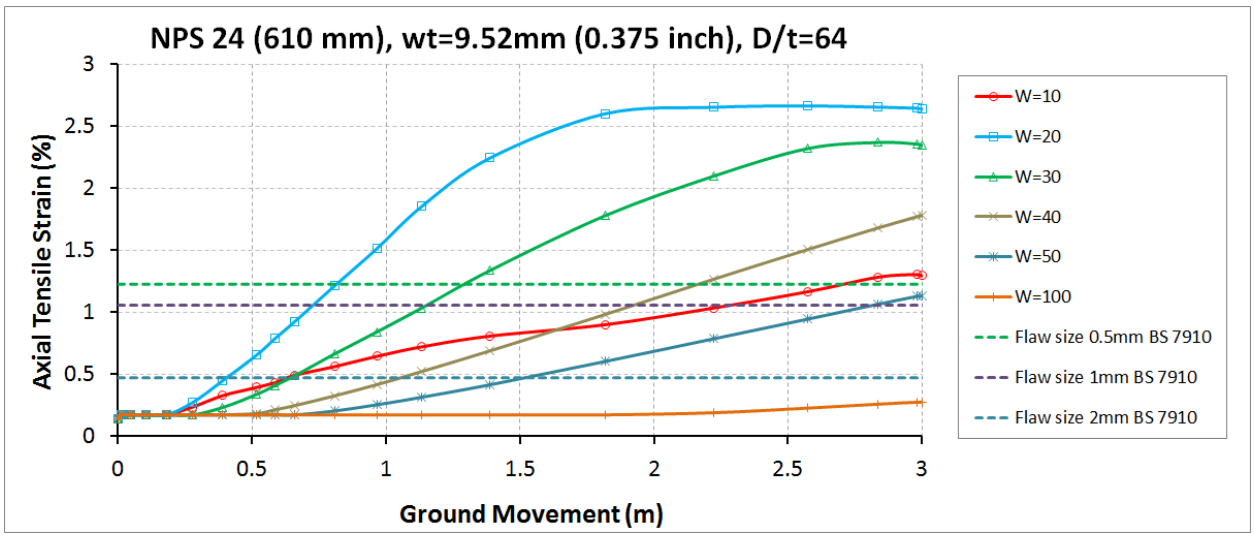

Figure 6.5: NPS 24 (D/t=64) - Maximum Tensile in the Pipe vs. Ground Movement Widths: [10-100 m]

The information contained herein is the copyright of and proprietary to BMT Fleet Technology Limited. Use of this information is governed by the legend on the cover page of this document."

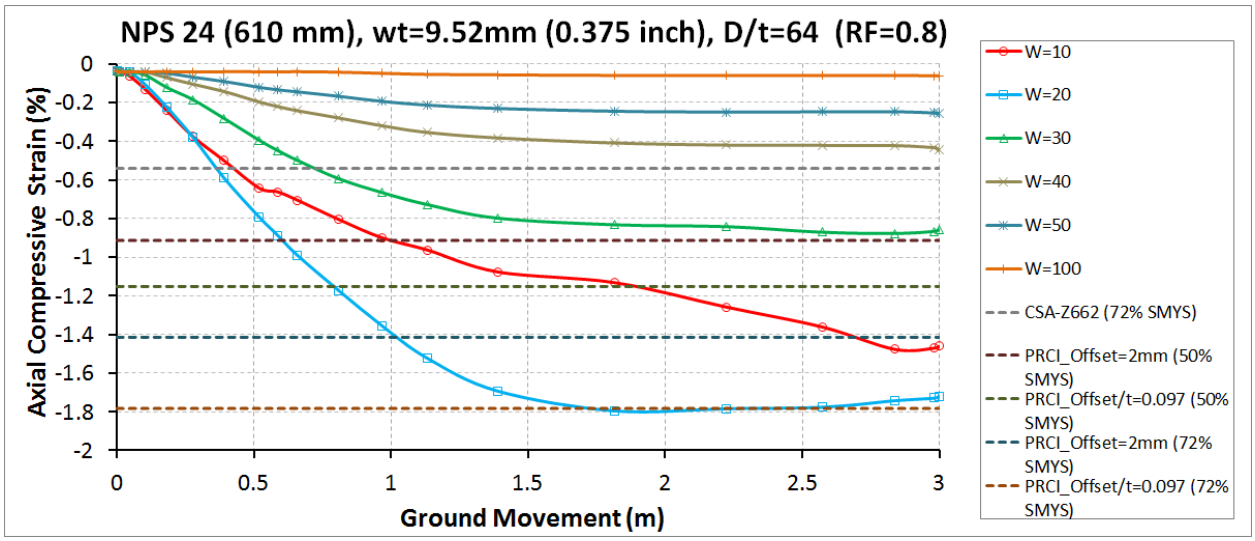

Figure 6.6: NPS 24 (D/t=64) - Maximum local Compressive Strain vs. Ground Movement Widths: [10-100 m]

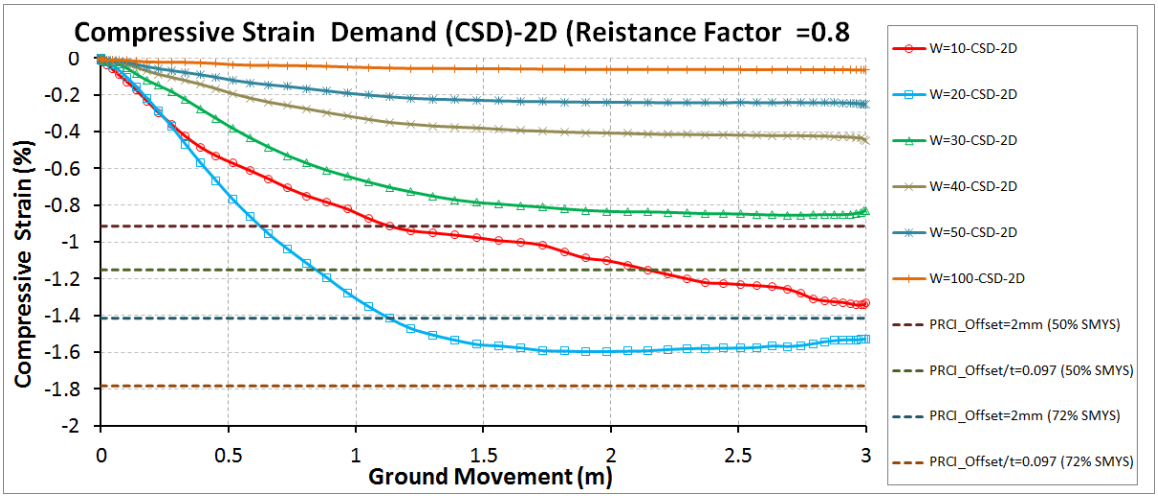

Figure 6.7: NPS 24 (D/t=64) - Maximum Nominal Compressive Strain vs. Ground Movement Widths: [10-100 m]

Figure 6.9 shows maximum pipe displacement versus the maximum ground displacement. The maximum pipe displacement follows the ground displacement up to certain ground displacement, then the pipe displacement increases more slowly with ground displacement, which results in a lower rate of increase in pipe strains per unit soil displacement.

The information contained herein is the copyright of and proprietary to BMT Fleet Technology Limited. Use of this information is governed by the legend on the cover page of this document."

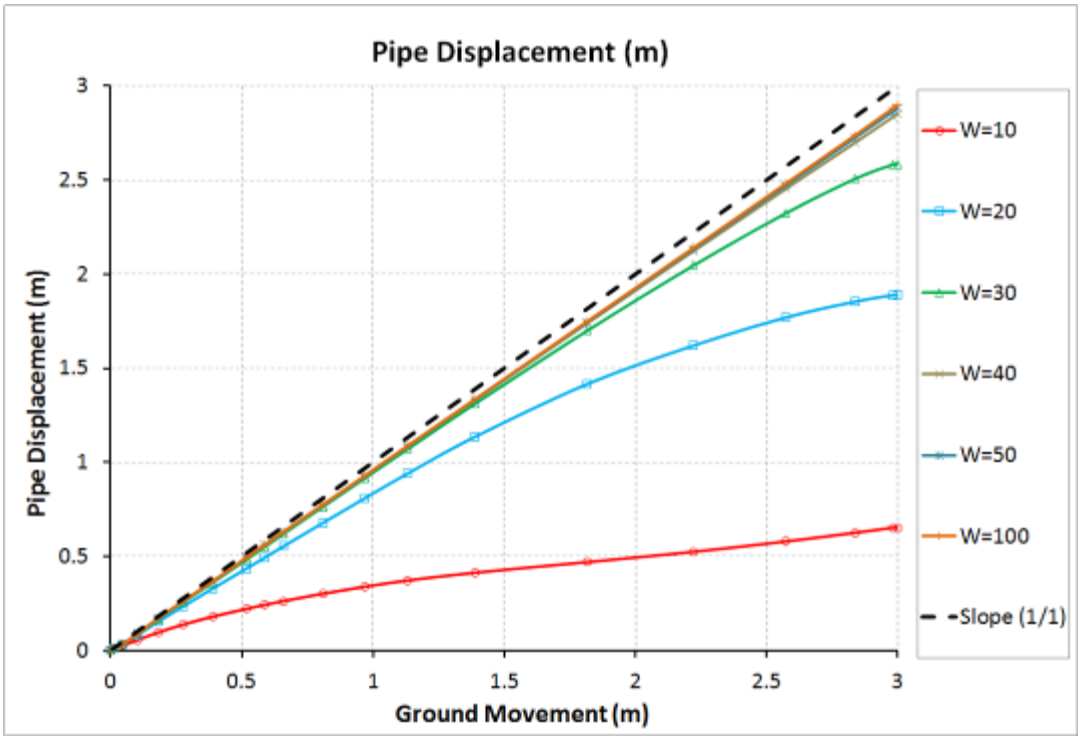

Figure 6.8: NPS 24 (D/t=64) – Pipe Displacement versus Ground Displacement

Figure 6.9 presents the maximum tensile and compressive strains in the pipe versus the maximum ground displacement for critical ground displacement widths of 20 m (66 ft). Also, Figure 6.9 presents the sum of tensile (positive) and compressive (negative) strains in the pipe. The results indicated that the calculated compressive strains are slightly higher at ground displacement less than 0.75 m; this is mainly due to compressive strain induced by thermal loading. At large ground displacement, tensile strains are higher than compressive strain. This differential in peak tensile and compressive strains indicates that there is a significant uniform axial strain in the pipe due to larger catenary effect.

As shown in Figure 6.9, the peak tensile strain is about 2.72% is higher than compressive strain which is approximately 1.79%. The results show that the peak strains increase with the soil displacement and remain constant beyond ground displacement of 2.0 m. This suggests the pipe resistance to movement at this point is sufficient to force the soil to flow around the pipe. Figure 6.10 illustrates the simulated displaced position of the pipe and the soil pattern for 1m, 2m and 3m ground displacement. In this figure, the soil above the pipe centerline is hidden so the pipe and soil deformation can be visualized. The results clearly show that at a given soil displacement less than 2m certain amount of the soil flows around the pipe.

The results presented in this section suggested that a width of 20 m (66 ft) results in the largest tensile and compressive strain in the pipe for any given value of ground displacement. Liu and O'Rourke (1997) [47], conducted a similar analysis using Winkler beam-soil model (soil springs). The Winkler model predicted a critical width of 30 m with a peak tensile strain less than 1.5% and a compressive strain about 0.5%, both of which remain constant beyond a ground

The information contained herein is the copyright of and proprietary to BMT Fleet Technology Limited. Use of this information is governed by the legend on the cover page of this document."

displacement of 1.3 m. This difference, we believe, is due to the ability of the 3D modeling approach to capture the three-dimensional behavior of the problem or condition and the more advanced soil constitutive model to better reflect the large soil displacement behavior.

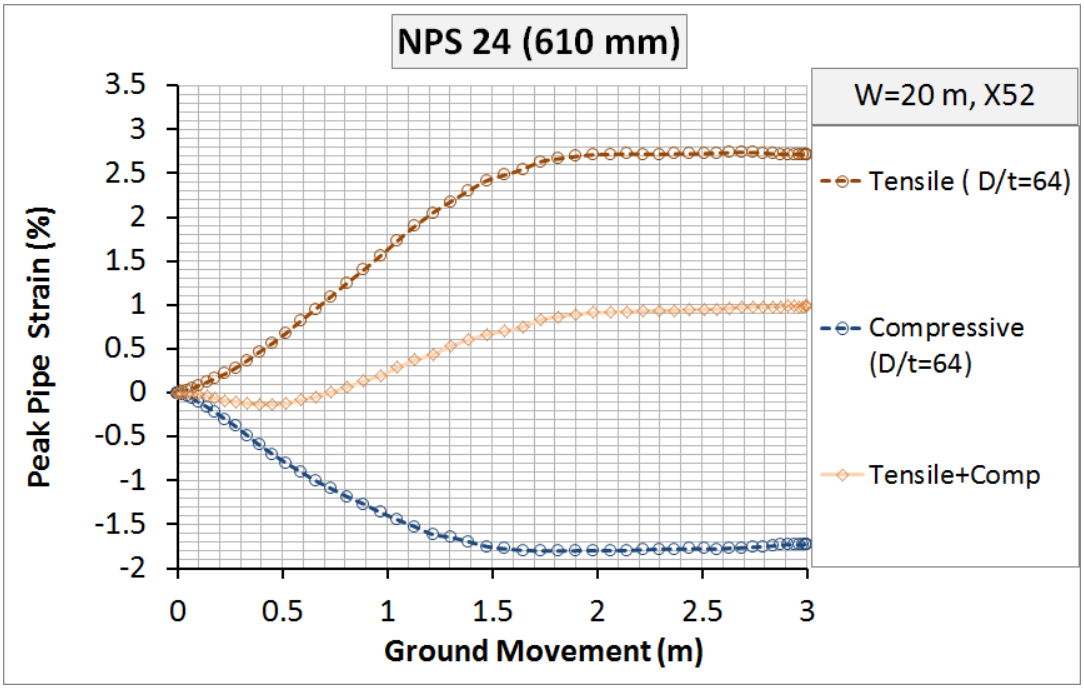

Figure 6.9: NPS 24(D/t=64) – Maximum Axial Strain vs. Ground Movement for the Critical Widths of 20 m (66 ft)

The information contained herein is the copyright of and proprietary to BMT Fleet Technology Limited. Use of this information is governed by the legend on the cover page of this document."

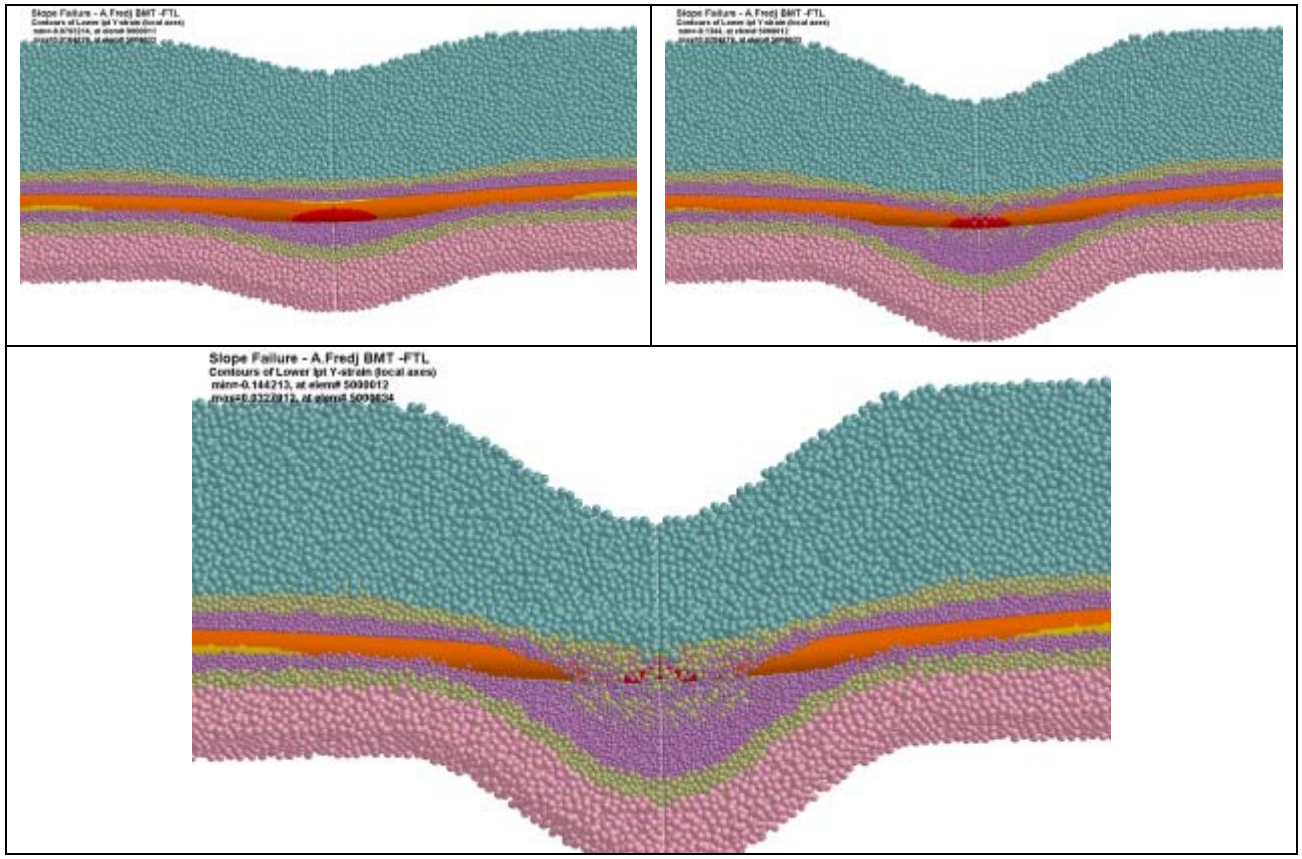

Figure 6.10: Pipe Deformation and Axial Strains for given Soil Movement of 1m, 2 m and 3 m (Top View)

6.4.2 Comparison with Strain Capacity and Strain Demand Envelopes

6.4.2.1 Comparison with Strain Capacity of the 24 inch pipeline(D/t=64)

The strain demand determined from the analysis was compared with the calculated strain capacity defined from the guidance; BS 7910 for tensile strain, and CSA Z662 and PRCI 2004 for compressive strain. In the final report other strain capacity formulations will be considered. These strain capacities calculated in this example and described in Sections 3.0 and 4.0 are provided in Table 6.1 and presented with dash horizontal line in Figure 6.11 and Figure 6.13. The compressive strain capacity (CSC) given in Table 6.1 is the value after applying a resistance factor (RF) of 0.8 to the computed CSC directly from CSA and PRCI equations. The tensile strain limit considers the presence of several 50-mm long surface-breaking, semi-elliptical girth weld flaws and all of the strain limits consider the pipeline to be operating at an internal pressure that induces a pipe wall stress of 72% of its SMYS.

The information contained herein is the copyright of and proprietary to BMT Fleet Technology Limited. Use of this information is governed by the legend on the cover page of this document."

Table 6.1: Maximum Allowable Tensile/Compressive Strain for NPS 24, Wt=9.52 mm, D/t=64, Grade X52

Tensile Strain Limit (%)			Compressive Strain (%) – Resistance Factor =0.8		
BS 7910 Flaw Depth (mm)			CSA Z662	PRCI (2 mm offset)	
0.5	1	2	(72% SMYS)	(50% SMYS)	(72% SMYS)
1.23	1.06	0.47	-0.54	-0.91	-1.41

6.4.2.1.1 Tensile Strain Capacity Envelopes (TSCE)

Figure 6.10 presents the maximum tensile strains in pipe versus the ground displacement width (W) for given ground displacement of 0.5, 1.0, 1.5, 2.0 and 2.5. In this figure, the BS-7910 tensile strain capacity is presented with dash horizontal line. Any tensile strain above the horizontal line is strain-related failure limit.

In Figure 6.5, Figure 6.6 and Figure 6.11 the strain demands from the analysis were used to relate the geotechnical event (lateral soil displacement), soil, pipe and pipeline operating conditions to tensile and compressive strains produced for soil movements along the axis of the pipe. Another way to present the results is to develop tensile strain capacity (TSC) envelopes based on BS 7910 guidance. These TSC envelopes are presented in Figure 6.112. The envelopes describe the maximum soil displacement and ground displacement width breakout the TSC envelopes, which represents the tensile strain-related failure limit, according to BS 7910.

The results indicate that for this pipe and operating condition combination, the ground movement width of 20 m (66 ft) can be considered critical. The tensile strain-related failure limit for the critical width is reached for ground displacement from 0.4 to 0.81 m considering a flaw size of 2, 1 and 0.5 mm, respectively.

The information contained herein is the copyright of and proprietary to BMT Fleet Technology Limited. Use of this information is governed by the legend on the cover page of this document."

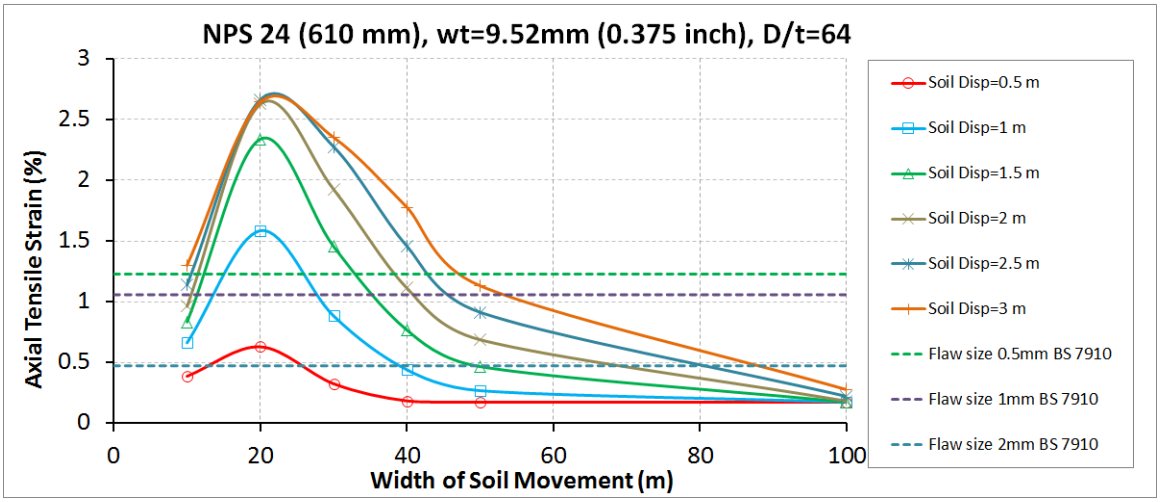

Figure 6.11: Pipe Axial Tensile Strains Envelopes versus Width (W) for Soil Movements of 0.5, 1, 1.5, 2.0 and 2.5 m

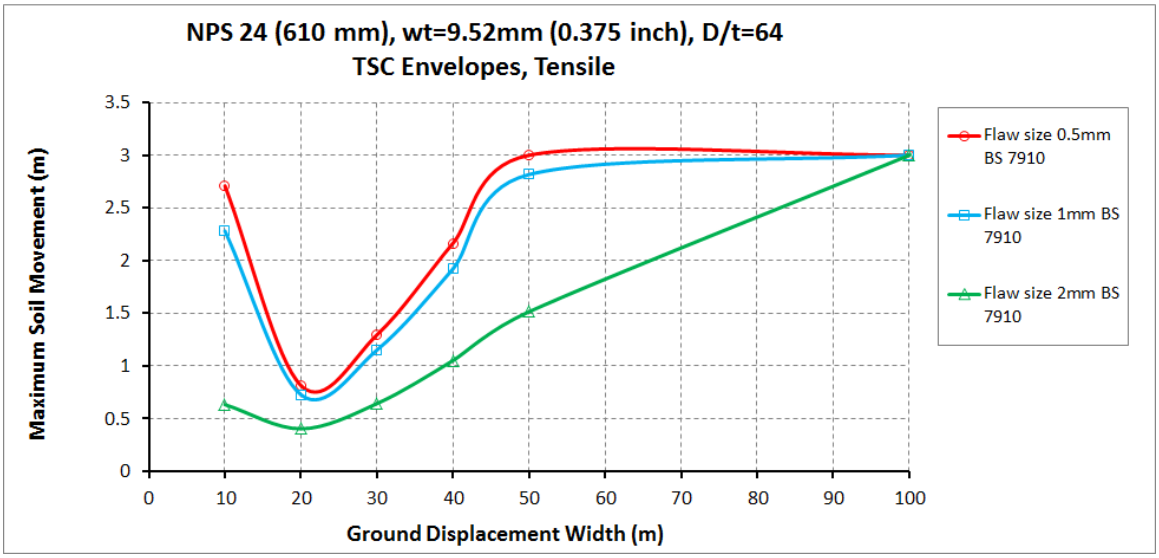

Figure 6.12: Tensile Strain Capacity Envelopes versus Ground Width (W) Movements

6.4.2.1.2 Compressive Strain Capacity Envelopes (CSCE)

Figure 6.13 presents the maximum nominal compressive strain in the pipe versus the ground displacement width (W) for given ground displacement of 0.5, 1.0, 1.5, 2.0 and 2.5. The nominal compressive strain is defined as the average compressive strain measured over a gauge length of 2D (D is the pipe outside diameter). In this figure, the CSA and PRCI compressive strain capacity is presented with dash horizontal line.

The envelopes presented in Figure 6.13 describe the pipe compressive strain demands in the pipe for a given ground displacement and ground width. In this figure, the CSA and PRCI compressive strain capacity is presented with dash horizontal line. Any compressive strain above the horizontal line is strain-related failure limit.

The information contained herein is the copyright of and proprietary to BMT Fleet Technology Limited. Use of this information is governed by the legend on the cover page of this document."

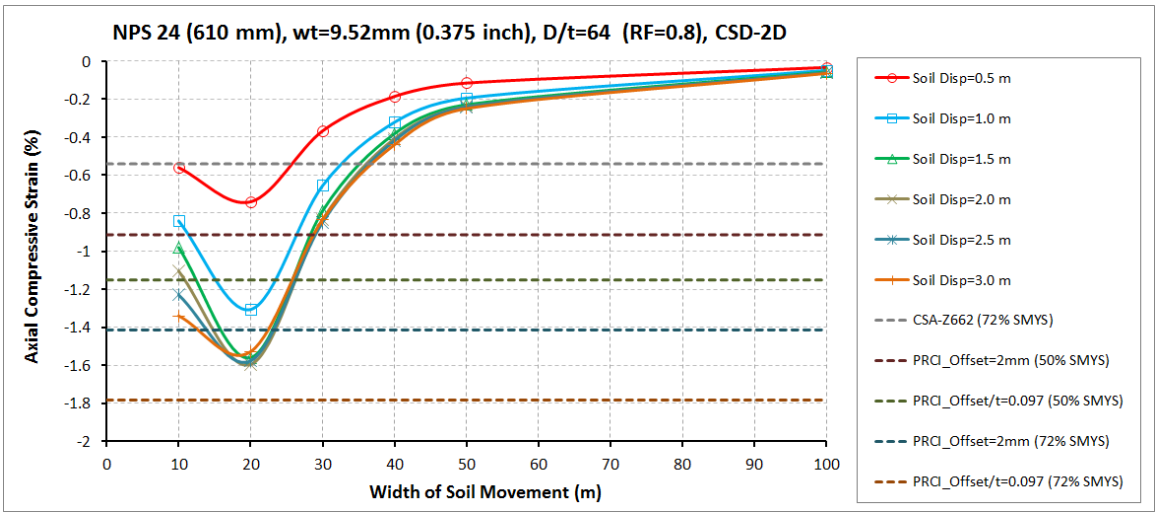

Figure 6.13: Pipe Axial Compressive Strains Envelopes versus Width (W) (for Soil Movement of 0.5, 1, 1.5, 2.0 and 2.5 m).

Similar to the tensile strain capacity (TSC) envelopes, the results were used to generate compressive strain capacity (CSC) envelopes based on PRCI Guidance. These envelopes can be used by used (operator) to estimate the allowable soil movement for a given ground width at the strain-related failure limit.

These CSC envelopes are presented in Figure 6.14. The envelopes describe the maximum soil displacement and ground displacement width breakout the CSC envelopes, which represents the tensile strain-related failure limit, according to CSA and PRCI Guidance.

For example, as shown in Figure 6.14 the compressive strain-related failure limit for the critical width of 20 m (66 ft) is reached for ground displacements from 0.5 to 1.13 m considering a girth weld misalignment (offset) of 2 mm and the pipeline to be operating at an internal pressure that induces a pipe wall stress of 50% and 72% of its SMYS, respectively.

The information contained herein is the copyright of and proprietary to BMT Fleet Technology Limited. Use of this information is governed by the legend on the cover page of this document."

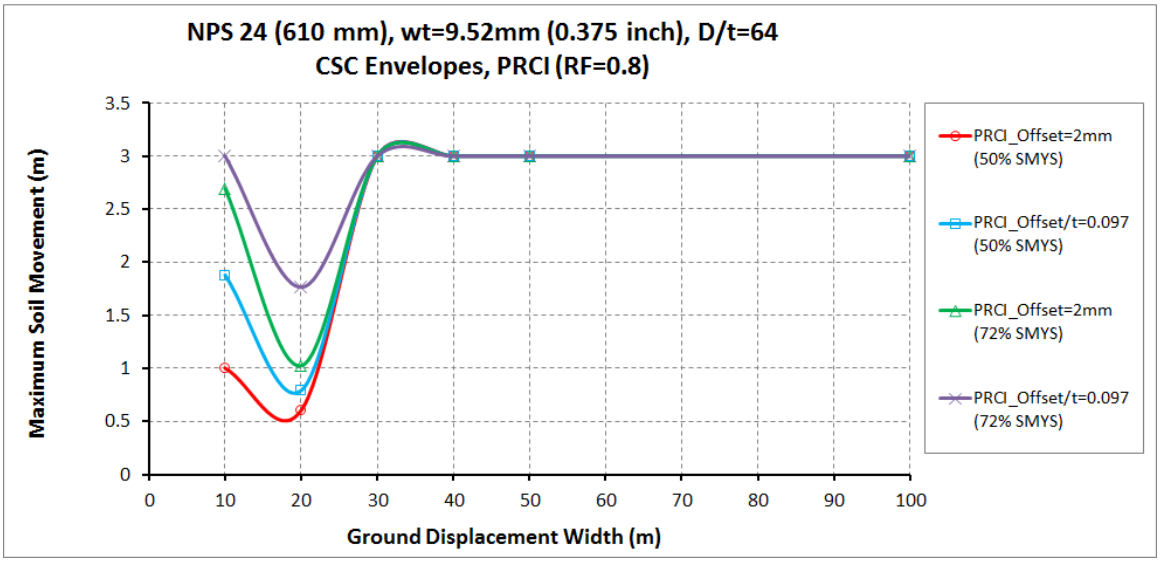

Figure 6.14: Compressive Strain Capacity Envelopes versus Ground Width (W) Movements

6.4.2.1.3 Strain Demand Envelopes (SDE)

In the previous section, the strain demands determined from the analysis was compared with the calculated strain capacity defined from the guidance; BS 7910 for tensile strain, and CSA Z662 and PRCI for compressive strain. While, there are many existing models for calculating the compressive and tensile strain capacity in codes and standards, it was decided to develop a simple a strain-based design methodology that can be easily adapted to any code and standards, which is the purpose of this section.

The tensile and compressive strain demand envelopes along the longitudinal direction of the pipeline are presented in Figure 6.15 and Figure 6.16. Figure 6.15 shows the maximum soil displacement versus ground width displacement as a series of 'envelopes' for a given pipe tensile and compressive strain demands of 0.25%, 0.5%, 0.75%, 1%, 1.25%, 1.5%, 1.75% and 2%. The safe pipeline operating goal of pipeline subjected to lateral ground displacement is to stay within the normal operating strain range defined by codes and standards.

The information contained herein is the copyright of and proprietary to BMT Fleet Technology Limited. Use of this information is governed by the legend on the cover page of this document."

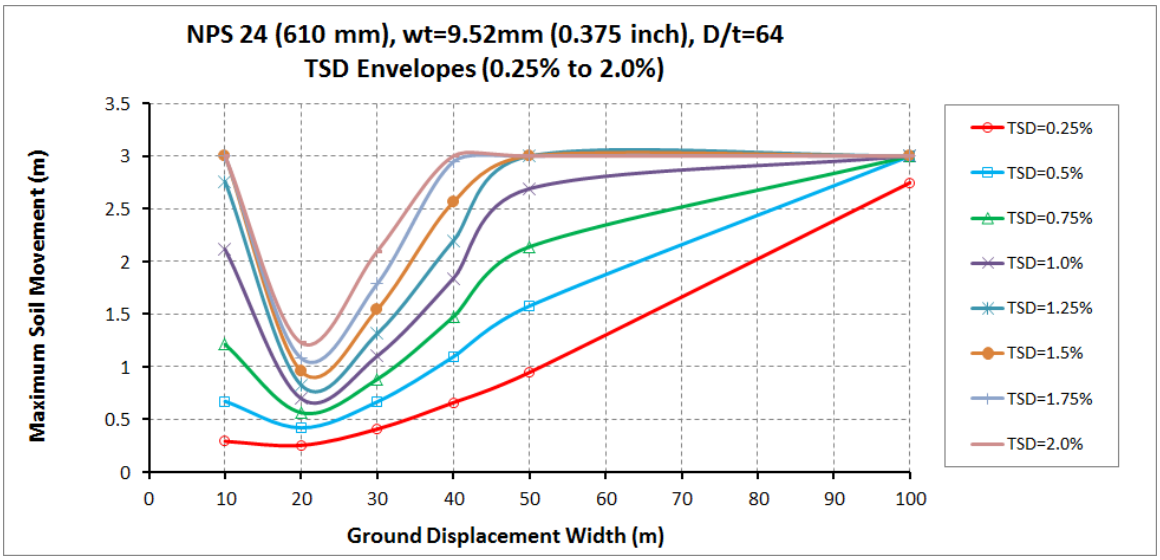

Figure 6.15: Tensile Strain Demand versus Width (W)

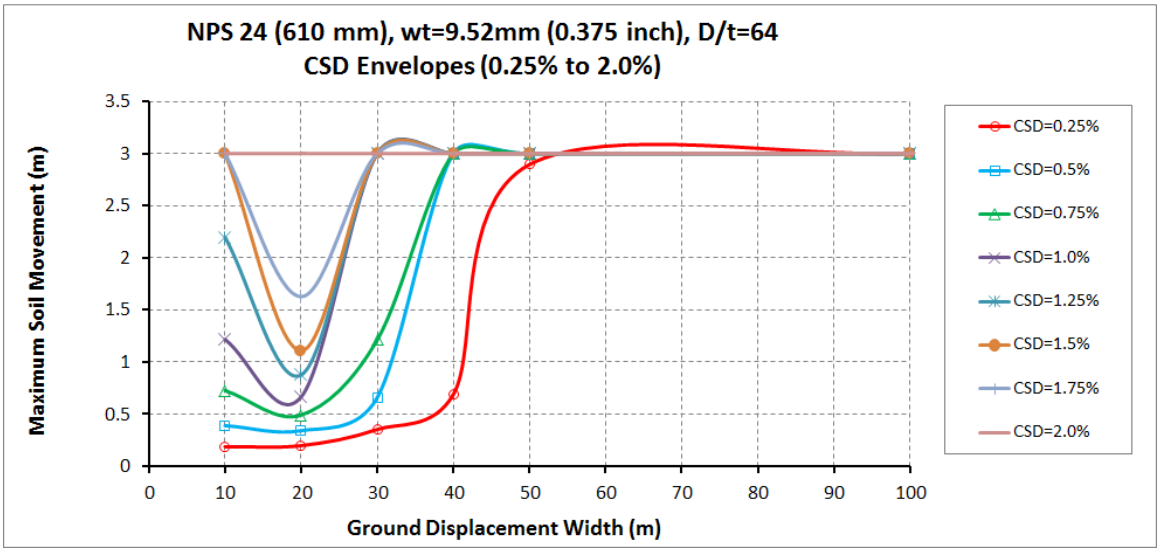

Figure 6.16: Compressive Strain Demand Envelopes versus Width (W)

6.5 Effect of Pipe Wall Thickness and D/t

The structural performance of the NPS 24-inch pipeline subjected to landslide was evaluated using combination of three pipe wall thicknesses, for demonstration purpose.

The three wall thicknesses includes the base case 9.52 mm (0.375), 6.35 mm (0.25 inch) and 12.7 mm (0.5 inch); corresponding to D/t ratios of 64, 96 and 48, respectively. The same pipe and soil materials assumptions used for the base case are used in the sensitivity:

The information contained herein is the copyright of and proprietary to BMT Fleet Technology Limited. Use of this information is governed by the legend on the cover page of this document."

- 72% SMYS internal pressure, 5.4, 8 MPa, corresponding to 5 MPa, 8 MPa and 10 MPa for D/t ratio of 96, 64 and 48, respectively;
- Grade 359 (X-52), a generic stress strain curves for Grade X-52 (359) pipe according to the CSA Z245.1;
- 45°C thermal differential (installation -20°C, max operating temperature 25°C);
- Burial depth H=1.2 m (5 ft), corresponding to 1.5 m (5 ft) depth to pipe center line, overburden ratio (H/D) of 2.46;
- Soil: sand/clay till with (ϕ'=30° and C'=5 kPa);
- Slope angle of 16 degrees; and
- Six (6) width of ground displacement varying from 10 to 100 m (10, 20, 30, 40 50 and 100 m).

A comparison of the results of the three wall thicknesses analyzed for ground displacement perpendicular to pipeline axis considering the critical ground displacement width of 20m is provided in Figure 6.17. The results indicated that pipeline with higher D/t ratio (lower pipe wall thickness) results in higher computed tensile and compressive strains with higher tensile strain than compressive strain. The strain ranged from +3.25% and -2.77% for 6.35 mm (0.25 inch) wall thickness to +2.7% and -1.72% for 9.53 mm (0.375 inch) wall thickness while for 12.7 mm (0.5 inch) the corresponding strain range is +2.38% and -1.58%. There is very little difference between the computed compressive strain for pipes with a D/t ratio of 64 and 48. The difference is about 0.14%; however, the maximum difference in compressive strain is higher than 1% for D/t equal to 64 and 96.

The information contained herein is the copyright of and proprietary to BMT Fleet Technology Limited. Use of this information is governed by the legend on the cover page of this document."

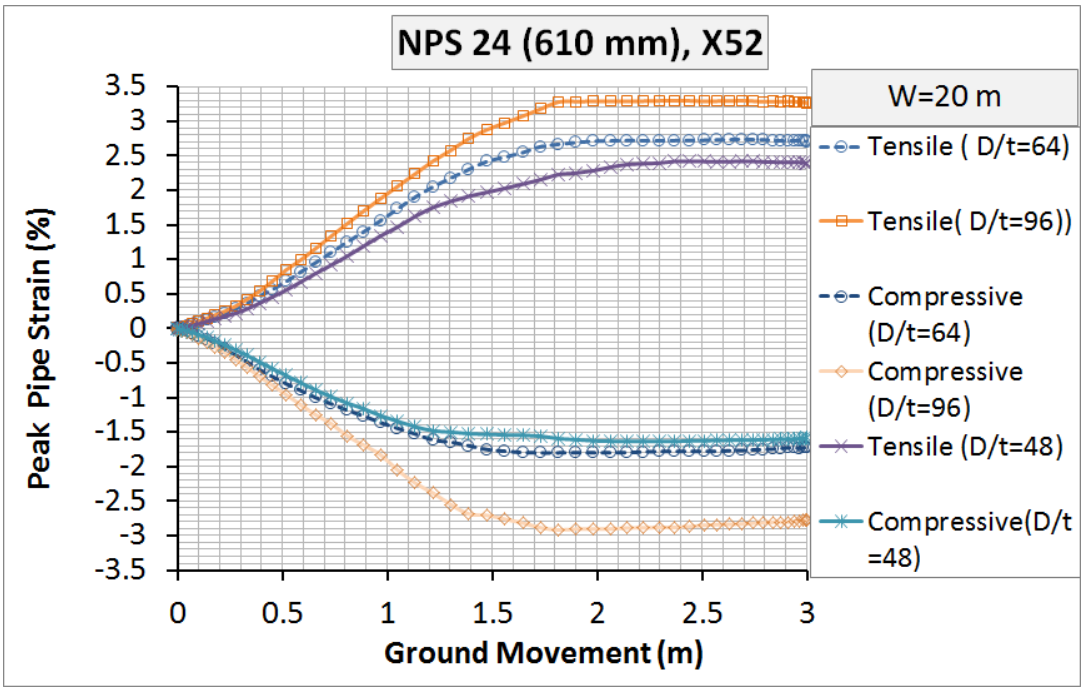

Figure 6.17: NPS 24 – Maximum Axial Strain versus Ground Movement for the Critical Widths of 20 m (66 ft)

6.5.1 Effect of the Width of Ground Movement

Figure 6.18 shows the maximum axial strains in the NPS 24 (609 mm) as function of the centerline (maximum) soil displacement for various ground displacement widths.

Figures 6.19 and 6.20 present the maximum local and nominal compressive strains in the longitudinal direction of the pipeline versus the maximum ground displacement for various ground displacement widths considered in the analyses. The nominal compressive strain is defined as the average compressive strain measured over a gauge length of 2D (where D is the pipe outside diameter).

The results Figures 6.20 and 6.21 are for NPS 24 (609 mm) with a wall thickness of 6.35 mm (0.25 inch) and D/t ratio of 96. The results illustrate the importance of the width of ground movement and how the critical width is a function of pipe stiffness (D/t ratio). The critical width is between 10 and 20 m. The width of 20 m (66 ft) results in the largest tensile strain in the pipe for any given value of ground displacement similar to the 9.52 mm (0.375) wall (Base Case discussed in Section 6.5). However, the width of 10 m (33 ft) results in the largest compressive strain in the pipe for any given value of ground displacement. A comparison of the strain results of the two wall thicknesses 6.35 mm (0.25 inch) and 9.52 (0.375 inch) is provided in Figure 6.23 for W=10 m. The pipe with 6.35 mm (0.25 inch) wall exceeds the compressive strain limit and a buckle/wrinkle forms at 1.5% local compressive strain or 1.12% nominal compressive strain for soil displacement of 0.7 m.

The information contained herein is the copyright of and proprietary to BMT Fleet Technology Limited. Use of this information is governed by the legend on the cover page of this document."

Figure 6.22 shows the soil and pipe deformation (wrinkle formation) for soil displacement of 2 m. The Figure 6.22 shows also the axial strain distribution (blue color is compressive and red is tensile strain). In Figure 6.24 the soil above the pipe is hidden so the pipe deformation can be visualized.

Figure 6.23 shows maximum pipe displacement versus the maximum ground displacement. The maximum pipe displacement follows the ground displacement up to certain ground displacement then the pipe displacement increases more slowly with increasing ground displacement. This reduction in pipe displacement rate results in a reduction rate of pipe strain increase per unit soil displacement.

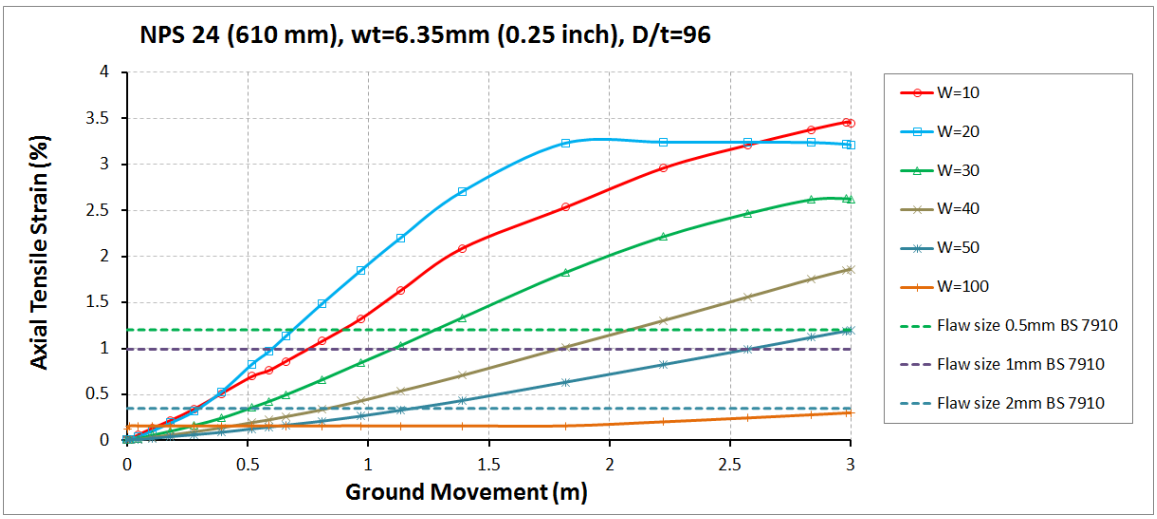

Figure 6.18: NPS 24 (D/t=64) - Maximum Tensile in the Pipe Versus Ground Movement Widths: [10-100 m]

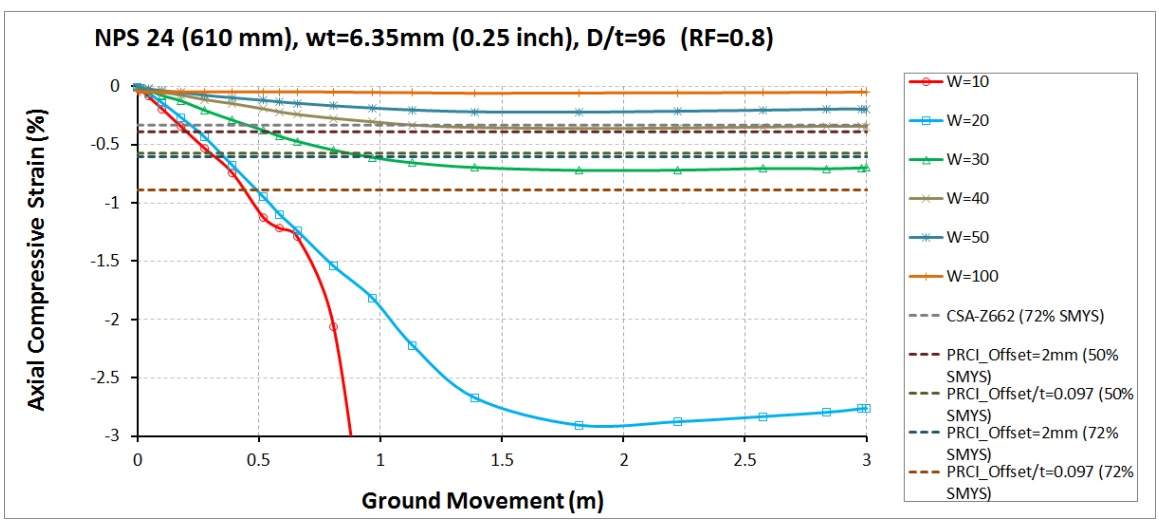

Figure 6.19: NPS 24 (D/t=64) - Maximum Local Compressive Strains in the Pipe versus Ground Movement Widths: [10-100 m]

The information contained herein is the copyright of and proprietary to BMT Fleet Technology Limited. Use of this information is governed by the legend on the cover page of this document."

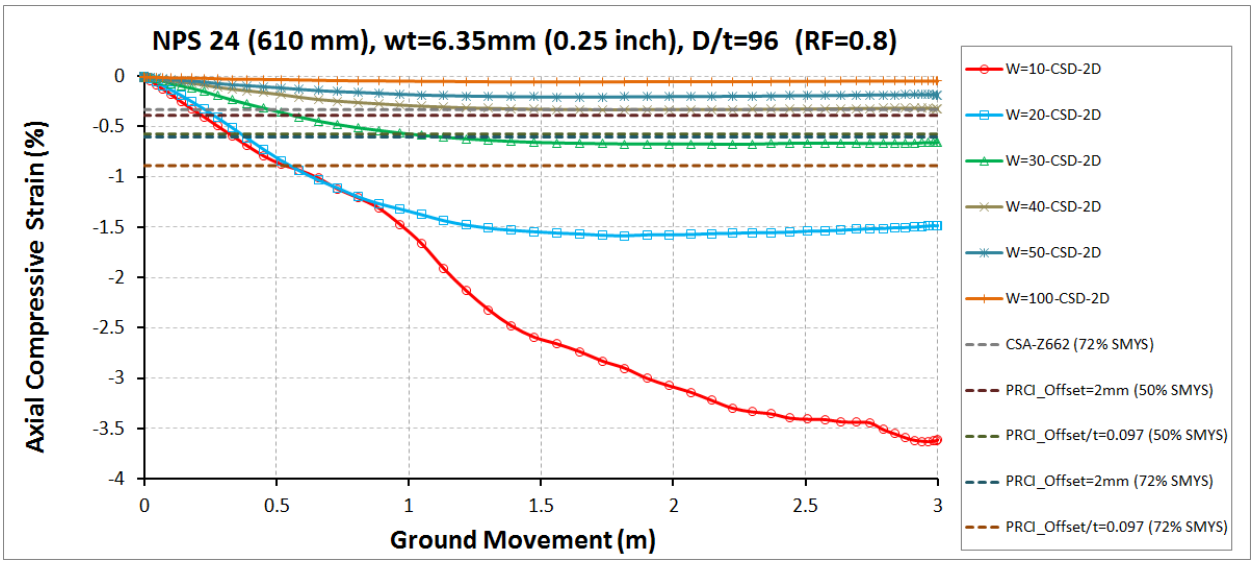

Figure 6.20: NPS 24 (D/t=64) - Maximum Nominal Compressive Strains in the Pipe versus Ground Movement Widths: [10-100 m]

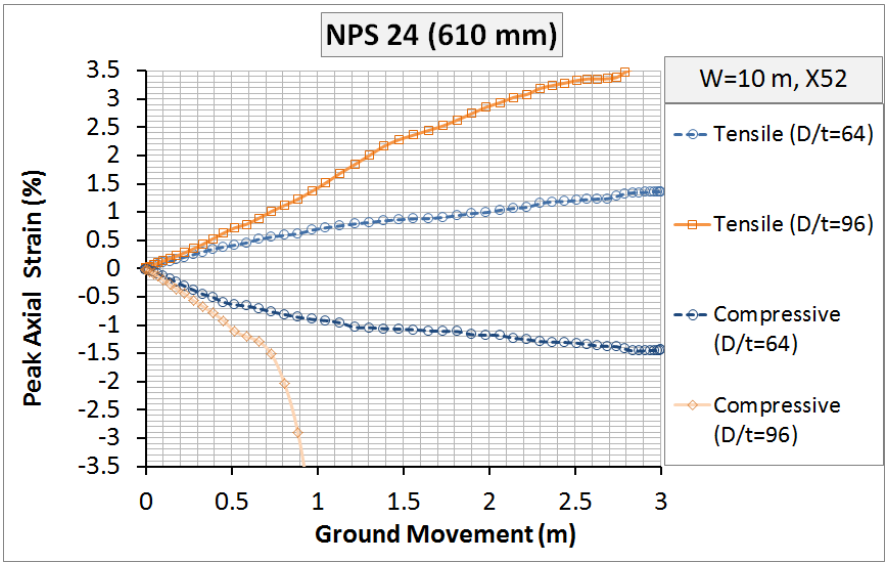

Figure 6.21: NPS 24 – Maximum Axial Strain versus Ground Movement for the Critical Widths of 20 m (33 ft)

The information contained herein is the copyright of and proprietary to BMT Fleet Technology Limited. Use of this information is governed by the legend on the cover page of this document."

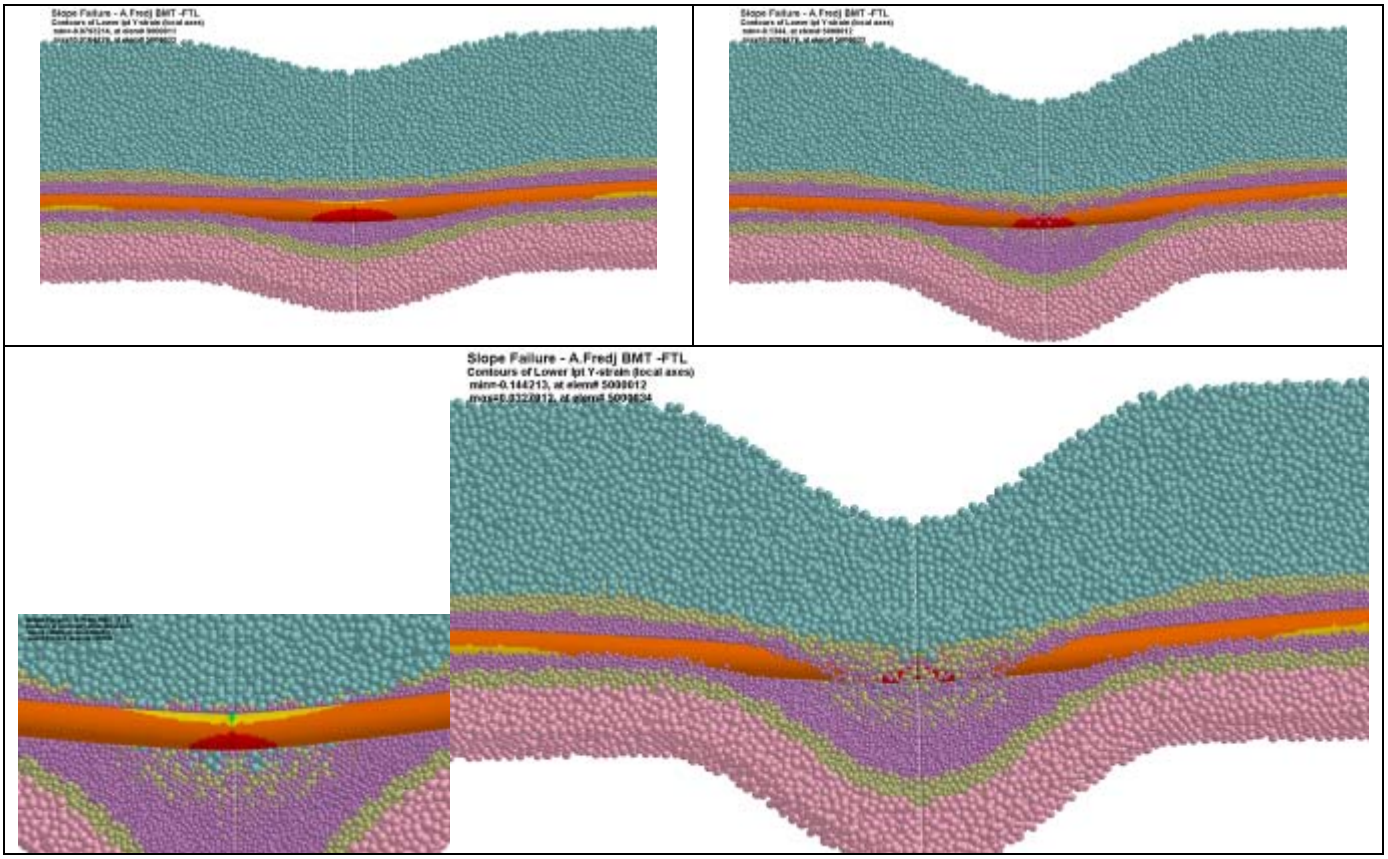

Figure 6.22: Pipe Deformation and Axial Strains for given Soil Movement of 1 m, 2 m and 3 m (Top View)

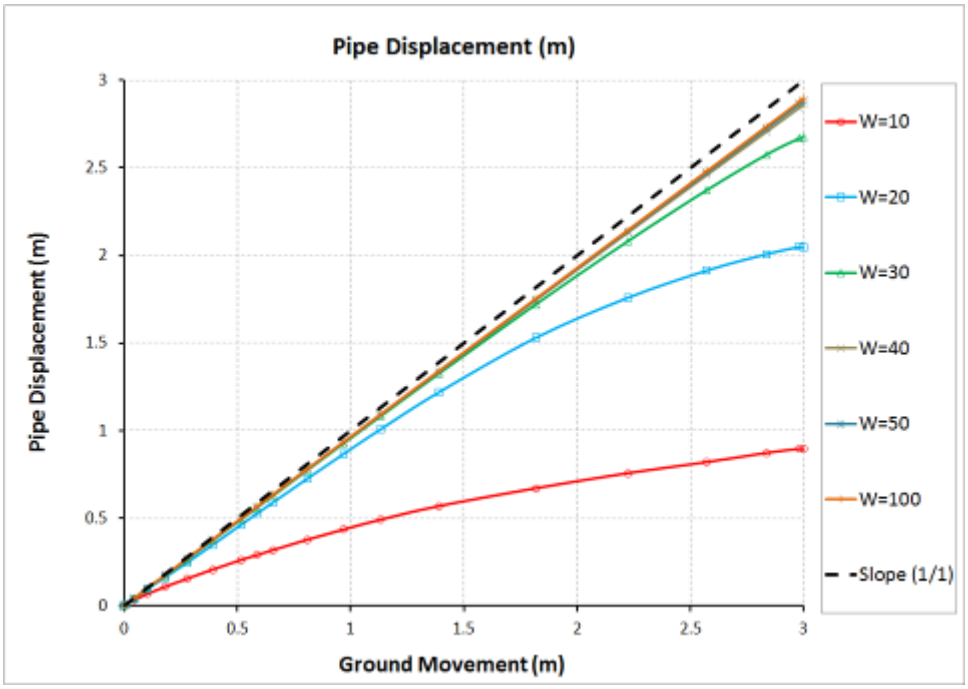

The information contained herein is the copyright of and proprietary to BMT Fleet Technology Limited. Use of this information is governed by the legend on the cover page of this document."

Figure 6.23: NPS 24 (D/t=64) - Maximum Pipe Displacement versus Ground Displacement

6.5.2 Comparison with Strain Criteria and Safety Envelopes

The strain demand determined from the analysis was compared with the calculated strain limits defined from the guidance; BS 7910 for tensile strain, and CSA Z662 and PRCI for compressive strain. These strain limits are provided in Table 6.2 and presented with dash horizontal line in Figure 6.24 and Figure 6.25. The tensile strain limit considers the presence of several 50-mm long surface-breaking, semi-elliptical girth weld flaws and all of the strain limits consider the pipeline to be operating at an internal pressure that induces a pipe wall stress of 72% of its SMYS.

Table 6.2: Maximum Allowable Tensile/Compressive Strain for NPS 24, Wt=6.35mm, D/t=96, Grade X52

Tensile Strain Limit (%)			Compressive Strain (%) –Resistance Factor =0.8		
BS 7910 Flaw Depth (mm)			CSA Z662	PRCI	
0.5	1	2	(72% SMYS)	(50% SMYS)	(72% SMYS)
1.2	0.99	0.35	-0.34	-0.39	-0.6

6.5.2.1.1 Tensile Strain Capacity Envelopes (TSCE)

Figures 6.24 present the maximum tensile strains in pipe versus the ground displacement width (W) for given ground displacement of 0.5, 1.0, 1.5, 2.0 and 2.5. In this figure, the BS-7910 tensile strain capacity is presented with dash horizontal line. Any tensile strain above the horizontal line is strain-related failure limit.

In Figure 6.19, Figure 6.20 and Figure 6.21 the strain demands from the analysis were used to relate the geotechnical event (lateral soil displacement), soil, pipe and pipeline operating conditions to tensile and compressive strains produced for soil movements along the axis of the pipe. Another way to present the results is to develop tensile strain capacity (TSC) envelopes based on BS 7910 guidance. These TSC envelopes are presented in Figure 6.25. The envelopes describe the maximum soil displacement and ground displacement width breakout the TSC envelopes, which represents the tensile strain-related failure limit, according to BS 7910.

The results indicate that for this pipe and operating condition combination, the ground movement width of 20 m (66 ft) can be considered critical. The tensile strain-related failure limit for the critical width is reached for ground displacement from 0.29 to 0.69 m considering a flaw size of 2, 1 and 0.5 mm, respectively.

The information contained herein is the copyright of and proprietary to BMT Fleet Technology Limited. Use of this information is governed by the legend on the cover page of this document."

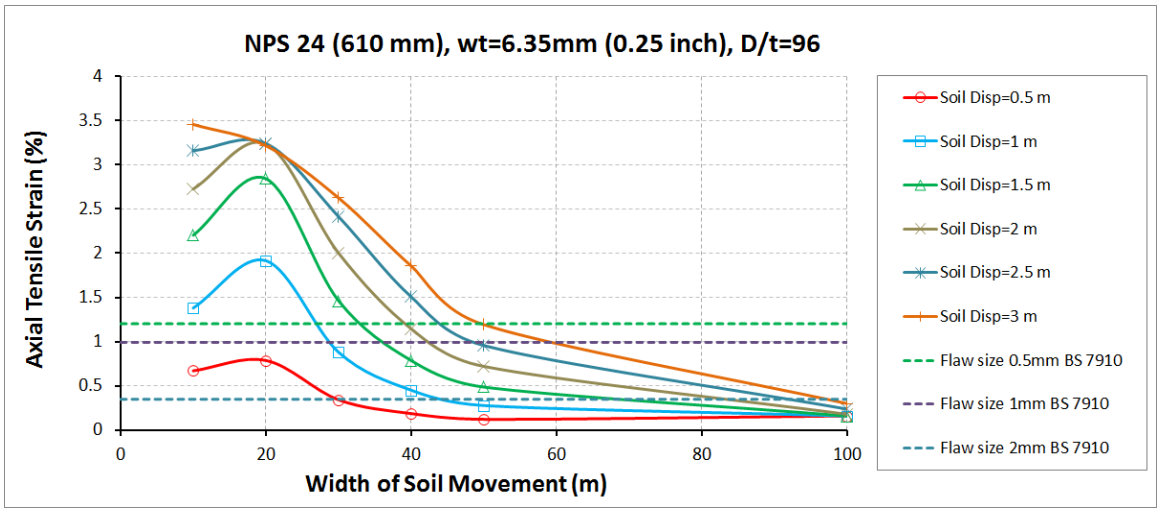

Figure 6.24: Pipe Axial Tensile Strains Envelopes versus Width (W) for Soil Movements of 0.5, 1, 1.5, 2.0 and 2.5 m.

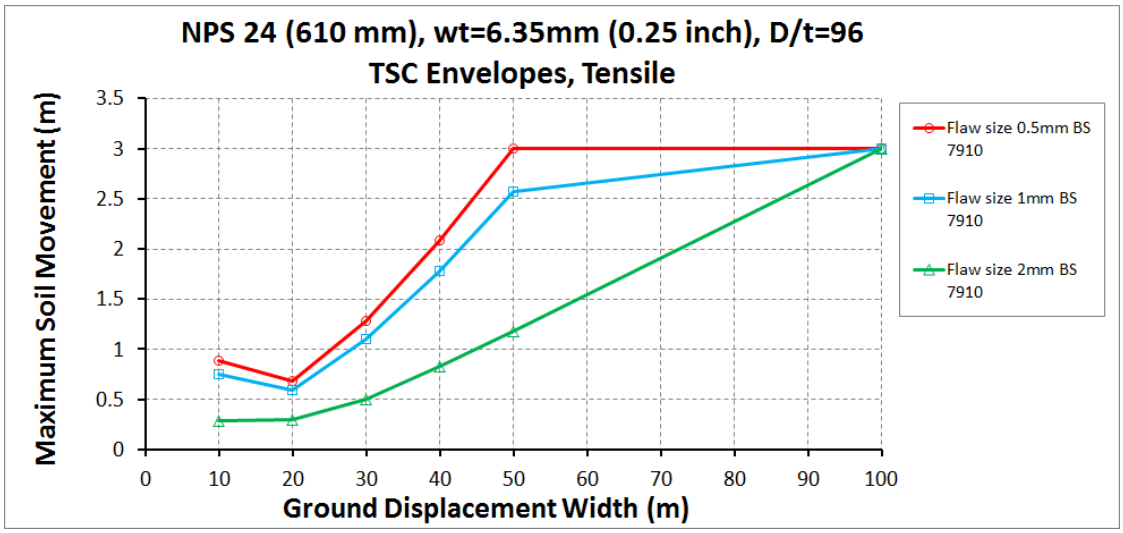

Figure 6.25: Tensile Strain Capacity Envelopes versus Ground Width (W) Movements

6.5.2.1.2 Compressive Strain Capacity Envelopes (CSCE)

Figure 6.26 presents the maximum nominal compressive strain in the pipe versus the ground displacement width (W) for given ground displacement of 0.5, 1.0, 1.5, 2.0 and 2.5. The nominal compressive strain is defined as the average compressive strain measured over a gauge length of 2D (D is the pipe outside diameter). In this figure, the CSA and PRCI compressive strain capacity is presented with dash horizontal line.

The envelopes presented in Figure 6.26 describe the pipe compressive strain demands in the pipe for a given ground displacement and ground width. In this figure, the CSA and PRCI compressive strain capacity is presented with dash horizontal line. Any compressive strain above the horizontal line is strain-related failure limit.

The information contained herein is the copyright of and proprietary to BMT Fleet Technology Limited. Use of this information is governed by the legend on the cover page of this document."

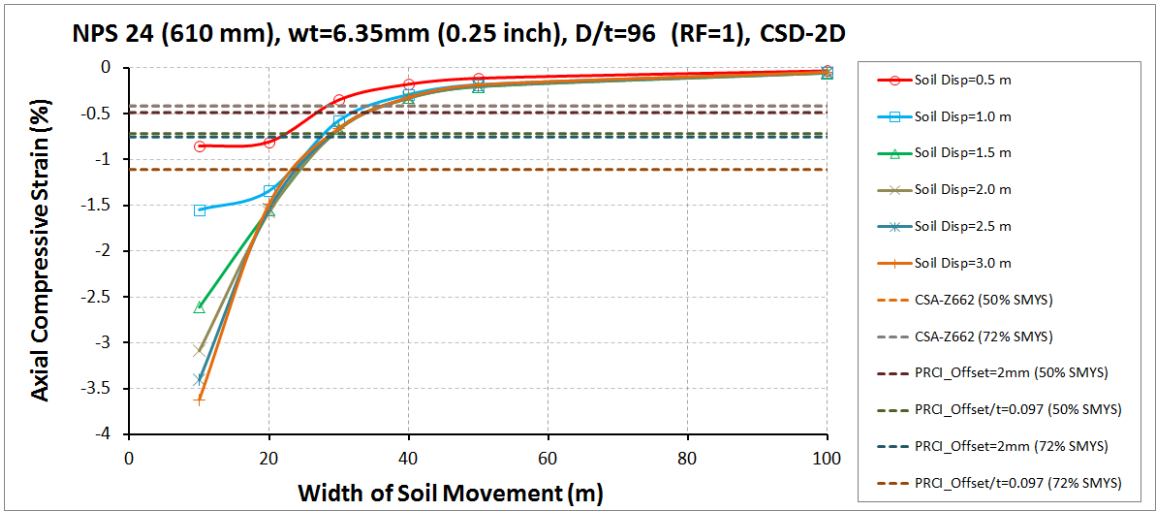

Figure 6.26: Pipe Axial Compressive Strains Envelopes versus Width (W) (for Soil Movement of 0.5, 1, 1.5, 2.0 and 2.5 m)

Similar to the tensile strain capacity (TSC) envelopes, the results were used to generate compressive strain capacity (CSC) envelopes based on PRCI Guidance. These envelopes can be used by used (operator) to estimate the allowable soil movement for a given ground width at the strain-related failure limit.

These CSC envelopes are presented in Figure 6.27. The envelopes describe the maximum soil displacement and ground displacement width. The CSC envelopes, which represents the compressive strain-related failure limit, according to CSA and PRCI Guidance.

For example, as shown in Figure 6.29 the compressive strain-related failure limit for the critical width of 10 m (33 ft) and 20 m (66 ft) is reached for ground displacement from 0.22 to 0.53 m considering girth weld misalignment (offset) of 2 mm and the pipeline to be operating at an internal pressure that induces a pipe wall stress of 50% and 72% of its SMYS, respectively.

The information contained herein is the copyright of and proprietary to BMT Fleet Technology Limited. Use of this information is governed by the legend on the cover page of this document."

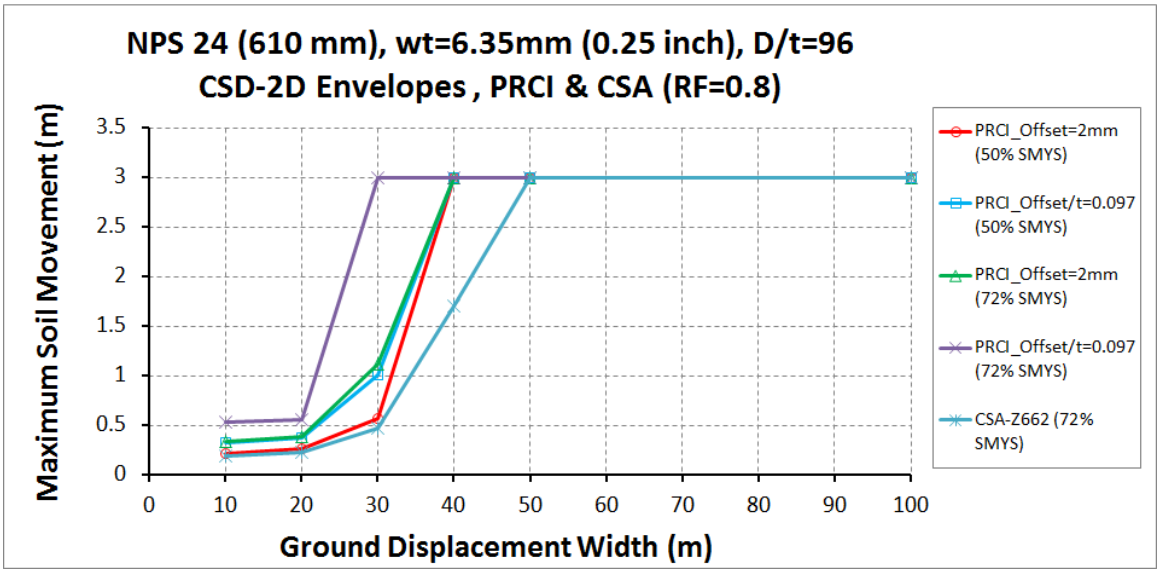

Figure 6.27: Compressive Strain Capacity Envelopes versus Ground Width (W) Movements

6.5.2.1.3 Strain Demand Envelopes (SDE)

In the previous section, the strain demands determined from the analysis was compared with the calculated strain capacity defined from the guidance; BS 7910 for tensile strain, and CSA Z662 and PRCI 2004 for compressive strain. While there are many existing models for calculating the compressive and tensile strain capacity in codes and standards, it was decided to develop a simple a strain-based design methodology that can be easily adapted to any code and standards, which is the purpose of this section.

The tensile and compressive strain demand envelopes along the longitudinal direction of the pipeline are presented in Figure 6.28 and Figure 6.29. These figures shows the maximum soil displacement versus ground width displacement as a series of 'envelopes' for a given pipe tensile and compressive strain demands of 0.25%, 0.5%, 0.75%, 1%, 1.25%, 1.5%, 1.75% and 2%. The safe pipeline operating goal of pipeline subjected to lateral ground displacement is to stay within the normal operating strain range defined by codes and standards.

The information contained herein is the copyright of and proprietary to BMT Fleet Technology Limited. Use of this information is governed by the legend on the cover page of this document."

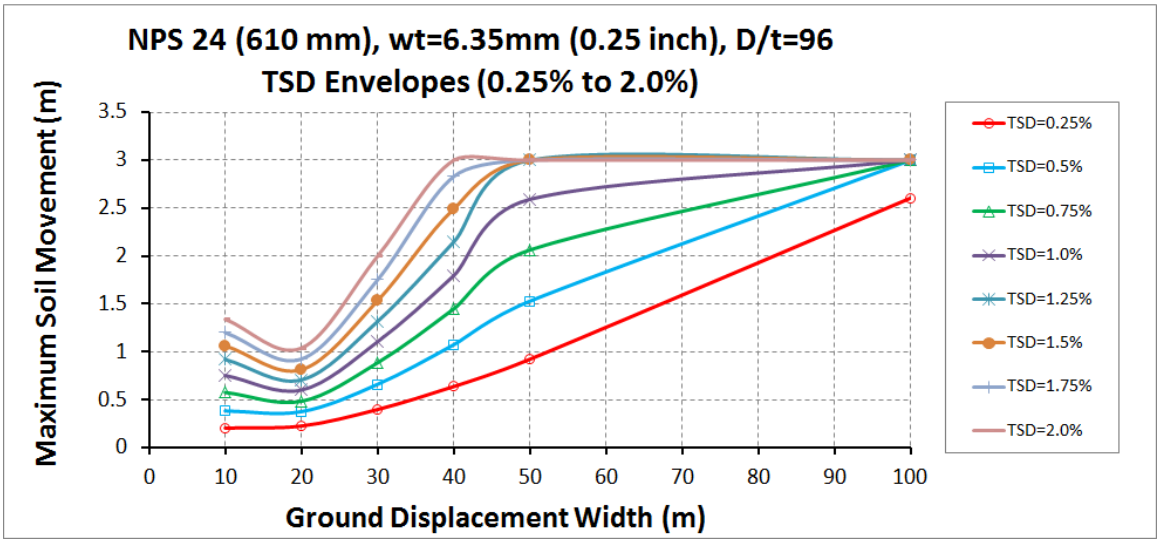

Figure 6.28: Tensile Strain Demand versus Width (W)

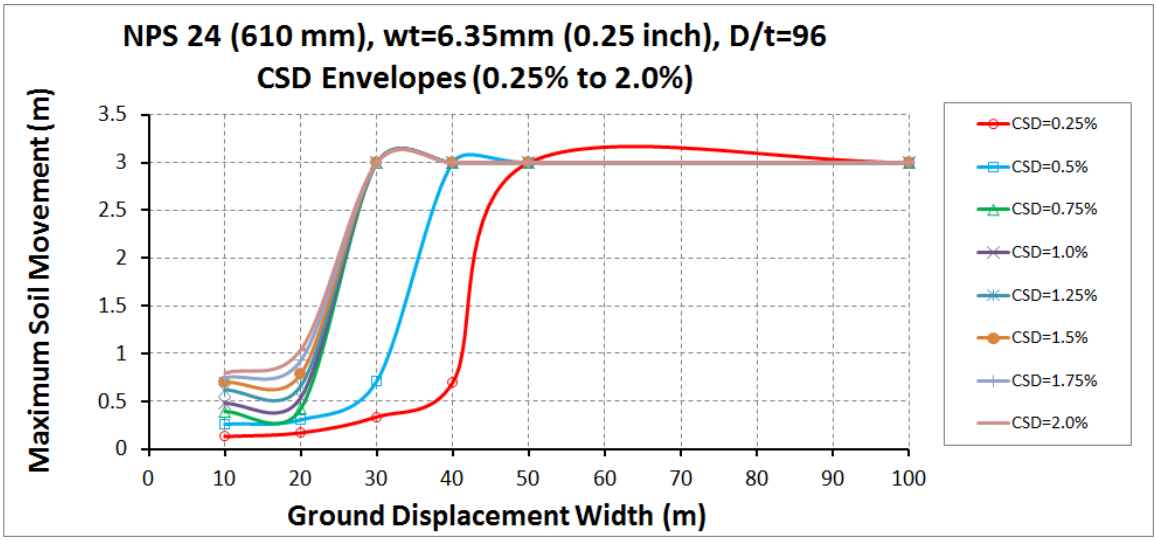

Figure 6.29: Compressive Strain Demand Envelopes versus Width (W)

6.6 Effect of Material Grade:

In order to evaluate the effect of material grade, the analyzed base case considering a pipeline material Grade X52 was repeated considering material grade of X70.

Figure 6.30 compares the maximum tensile and compressive strains in the pipe versus the maximum ground displacement for critical ground displacement widths of 20 m (66 ft) for a pipe material X52 and X70. The results indicate that lower material grade X52 results in largest tensile strain, and lower compressive strain for soil displacement larger than 0.75 m. Also, Figure 6.30 presents the sum of tensile (positive) and compressive (negative) strains in the pipe. These results indicated that the calculated compressive strains are slightly higher at ground

The information contained herein is the copyright of and proprietary to BMT Fleet Technology Limited. Use of this information is governed by the legend on the cover page of this document."

displacement less than 0.75 m and 1.25 for Material Grade X52 and X70, respectively. This is mainly due to compressive strain induced by thermal loading. At large ground displacement, tensile strains are higher than compressive strain for X52. This differential in peak tensile and compressive strains indicates that there is a significant uniform axial strain in the pipe due to larger catenary effect. While for X70, there is a little difference between the calculated compressive and tensile strain, this suggest that the pipe deforms mainly in bending.

Figure 6.31 shows maximum pipe displacement versus the maximum ground displacement. The maximum pipe displacement follows the ground displacement up to certain ground displacement then the pipe displacement increase slowly with ground displacement. The reduced pipe displacement results in a lower pipe strain increase per unit ground displacement. The results indicated that lower grade X52 results in larger pipe displacements for the same ground displacement. This behavior is due to the formation of a larger plastic zone which reduces the pipe resistance to movement.

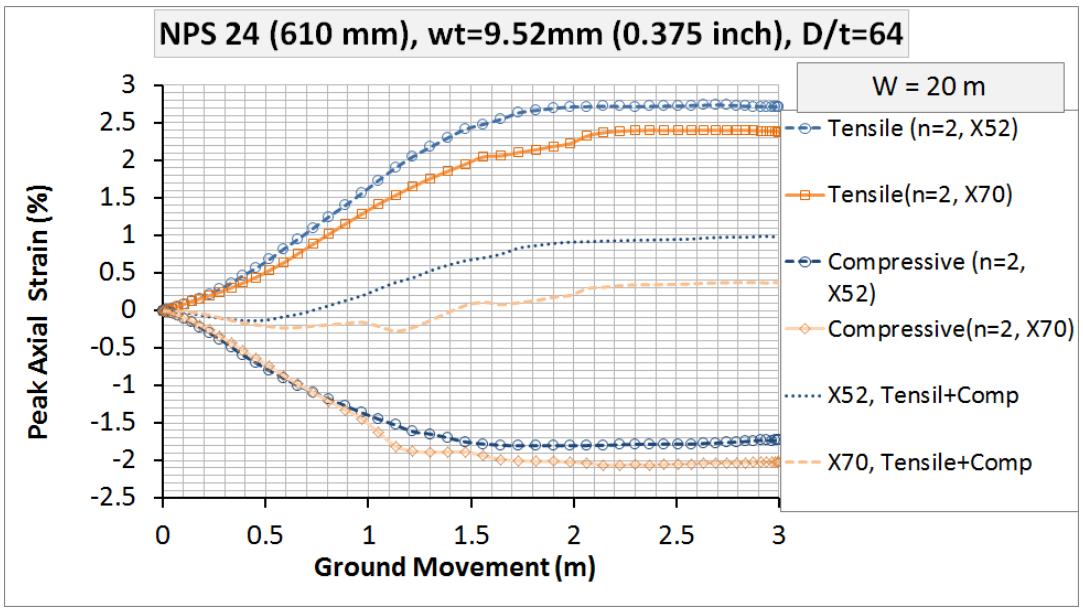

Figure 6.30: NPS 24 (D/t=64) – Maximum Axial Strain versus Ground Movement for the Critical Widths of 20 m (66 ft)

The information contained herein is the copyright of and proprietary to BMT Fleet Technology Limited. Use of this information is governed by the legend on the cover page of this document."

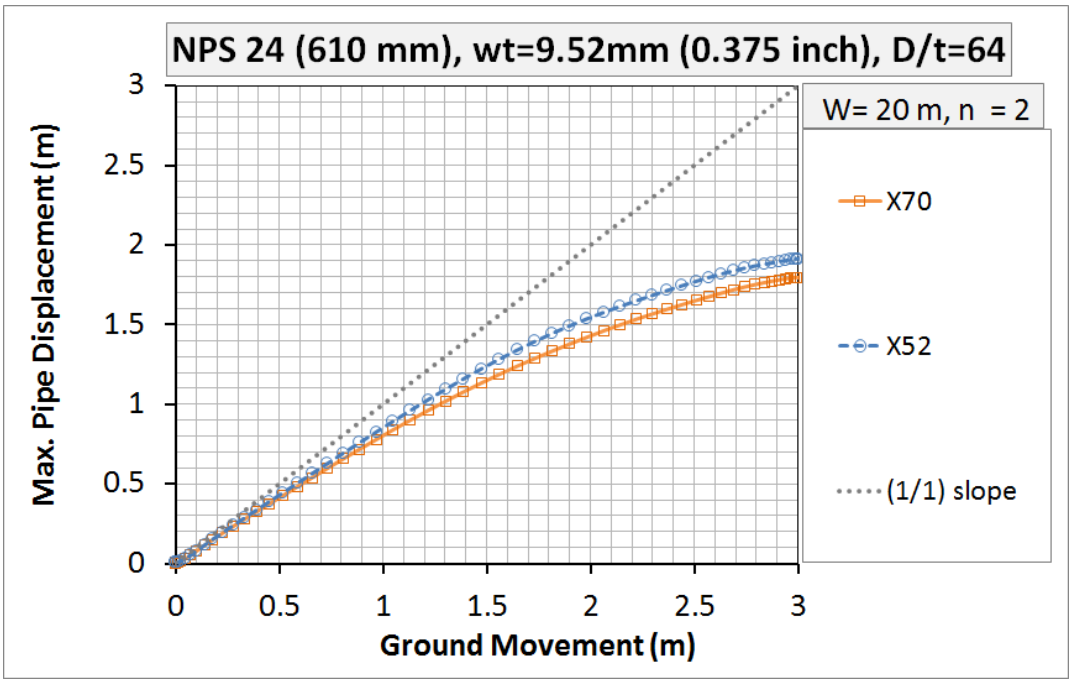

Figure 6.31: NPS 24 (D/t=64) – Maximum Pipe Displacement versus Ground Movement for the Critical Widths of 20 m (66 ft)

6.6.1 Effect of the Width of Ground Movement

Figure 6.32 presents the maximum tensile strains in the longitudinal direction of the pipeline versus the maximum ground displacement for various ground displacement widths considered in the analyses.

Figures 6.33 and 6.34 present the maximum local and nominal compressive strains in the longitudinal direction of the pipeline versus the maximum ground displacement for various ground displacement widths considered in the analyses. The nominal compressive strain is defined as the average compressive strain measured over a gauge length of 2D (where D is the pipe outside diameter).

The results indicate that for the six (6) widths considered, the width of 20 m (66 ft) results in the largest tensile and compressive strain in the pipe for any given value of ground displacement.

Figure 6.35 shows maximum pipe displacement versus the maximum ground displacement. The maximum pipe displacement follows the ground displacement up to certain ground displacement than the pipe displacement increase slowly with ground displacement, which results in slowly increase in pipe strains.

The information contained herein is the copyright of and proprietary to BMT Fleet Technology Limited. Use of this information is governed by the legend on the cover page of this document."

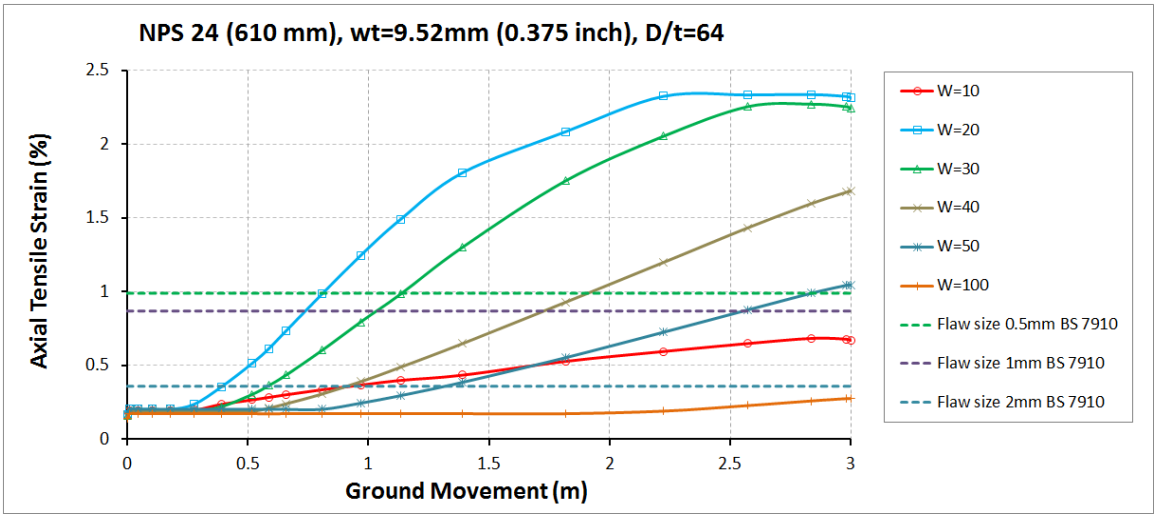

Figure 6.32: NPS 24 (D/t=64, X70) - Maximum Tensile in the Pipe vs. Ground Movement Widths: [10-100 m]

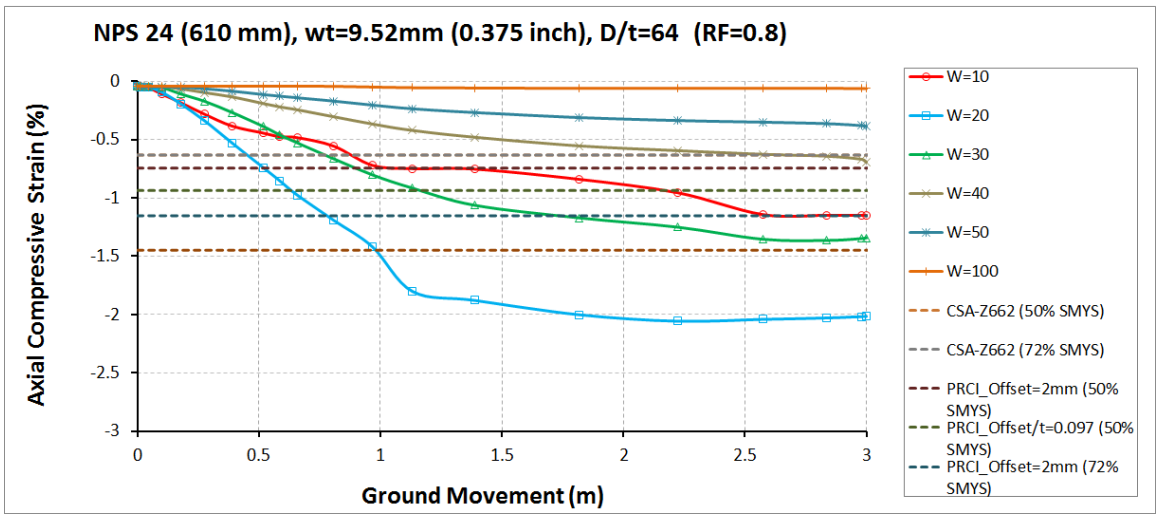

Figure 6.33: NPS 24 (D/t=64, X70) - Maximum local Compressive Strain vs. Ground Movement Widths: [10-100 m]

The information contained herein is the copyright of and proprietary to BMT Fleet Technology Limited. Use of this information is governed by the legend on the cover page of this document."

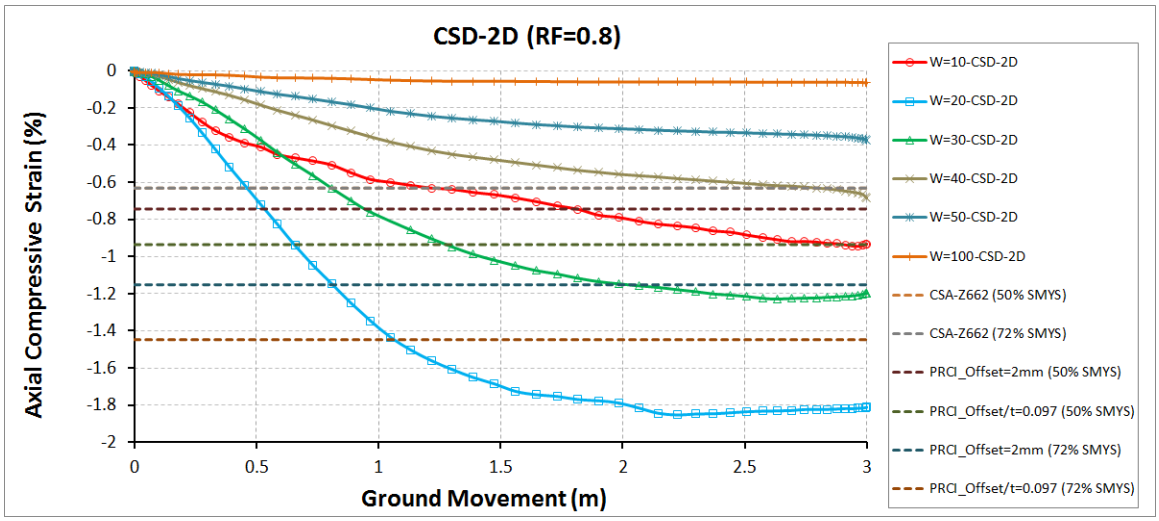

Figure 6.34: NPS 24 (D/t=64, X70) - Maximum Nominal Compressive Strain vs. Ground Movement Widths: [10-100 m]

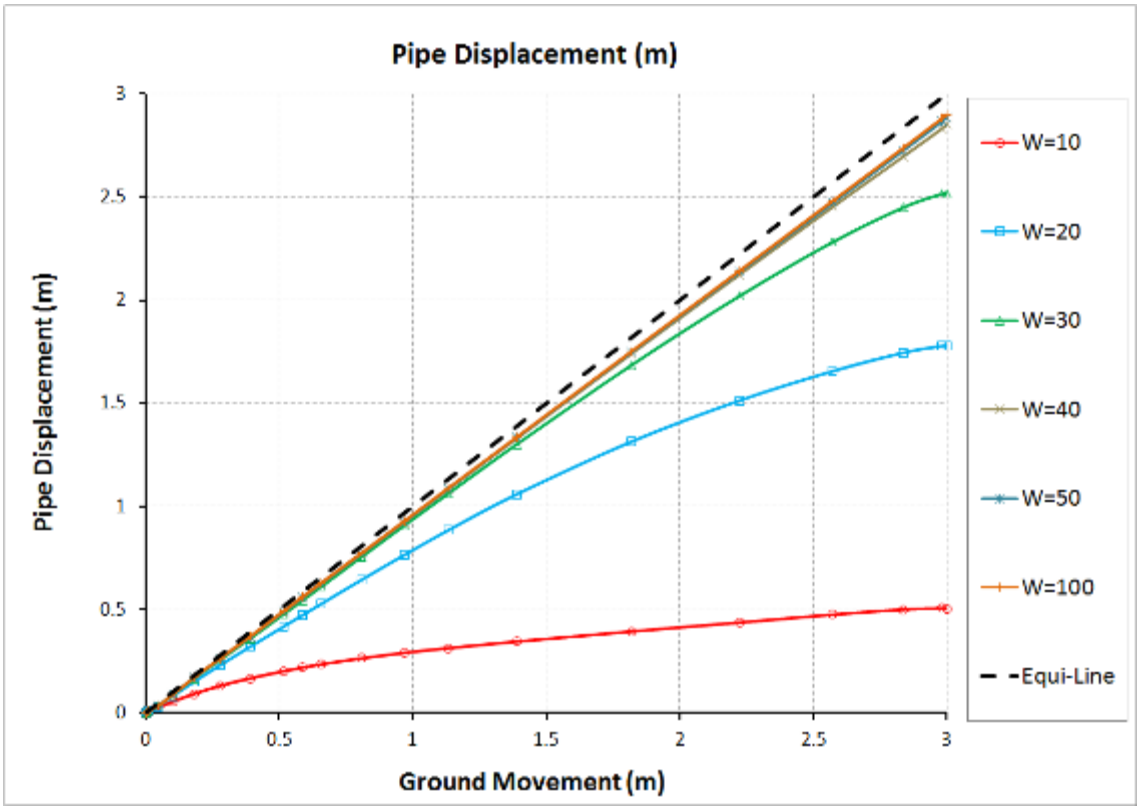

Figure 6.35: NPS 24 (D/t=64, X70) – Pipe Displacement versus Ground Displacement

The information contained herein is the copyright of and proprietary to BMT Fleet Technology Limited. Use of this information is governed by the legend on the cover page of this document."

6.6.2 Comparison with Strain Capacity and Strain Demand Envelopes

6.6.2.1 Comparison with Strain Capacity of the 24 inch Pipeline (D/t=64, X70)

The strain demand determined from the analysis was compared with the calculated strain capacity defined from the guidance; BS 7910 for tensile strain, and CSA Z662 and PRCI for compressive strain. These strain capacity are provided in Table 6.3 and presented with dash horizontal line in Figure 6.36 and Figure 6.37. The compressive strain capacity (CSC) given in Table 6.3 is the value after applying a resistance factor (RF) of 0.8 to the computed CSC directly from CSA and PRCI equations. The tensile strain limit considers the presence of several 50-mm long surface-breaking, semi-elliptical girth weld flaws and all of the strain limits consider the pipeline to be operating at an internal pressure that induces a pipe wall stress of 72% of its SMYS.

Table 6.3: Maximum Allowable Tensile/Compressive Strain for NPS 24, Wt=9.52mm, D/t=64, Grade X70

Tensile Strain Limit (%)			Compressive Strain (%) –Resistance Factor =0.8		
BS 7910 Flaw Depth (mm)			CSA Z662	PRCI (2 mm offset)	
0.5	1	2	(72% SMYS)	(50% SMYS)	(72% SMYS)
0.99	0.87	0.36	-0.63	-0.74	-1.15

6.6.2.1.1 Tensile Strain Capacity Envelopes (TSCE)

Figure 6.36 presents the maximum tensile strains in pipe versus the ground displacement width (W) for given ground displacement of 0.5, 1.0, 1.5, 2.0 and 2.5. In this figure, the BS-7910 tensile strain capacity is presented with dash horizontal line. Any tensile strain above the horizontal line is strain-related failure limit.

The TSC envelopes based on BS7910 guidance are presented in Figure 6.37. The envelopes describe the maximum soil displacement and ground displacement width breakout the TSC envelopes, which represents the tensile strain-related failure limit, according to BS 7910.

The results indicate that for this pipe and operating condition combination, the ground movement width of 20 m (66 ft) can be considered critical. The tensile strain-related failure limit for the critical width is reached for ground displacement from 0.39 to 0.81 m considering a flaw size of 2, 1 and 0.5 mm, respectively.

The information contained herein is the copyright of and proprietary to BMT Fleet Technology Limited. Use of this information is governed by the legend on the cover page of this document."

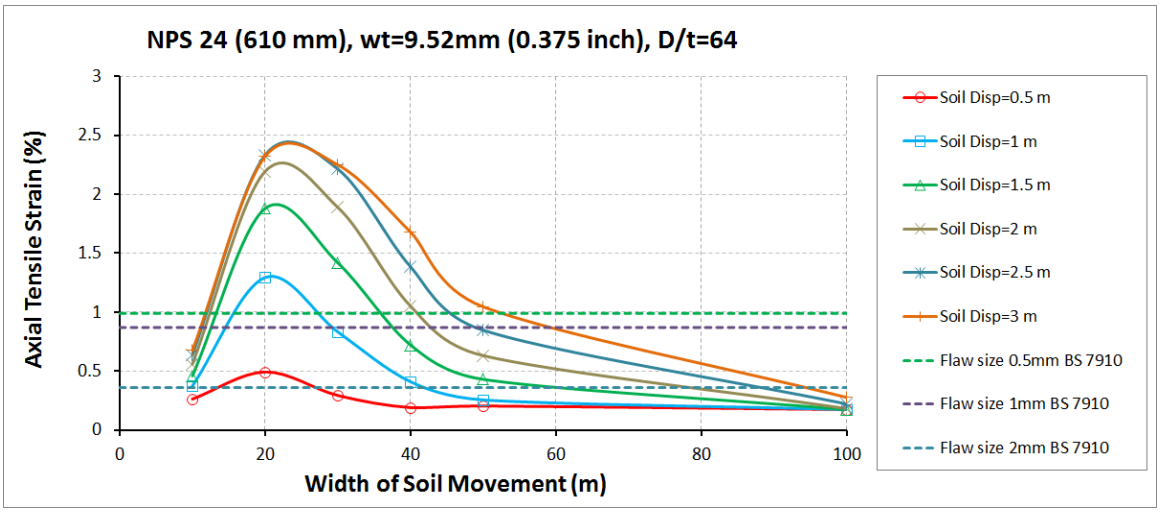

Figure 6.36: Pipe Axial Tensile Strains Envelopes versus Width (W) for Soil Movements of 0.5, 1, 1.5, 2.0 and 2.5 m, Material Grade X70

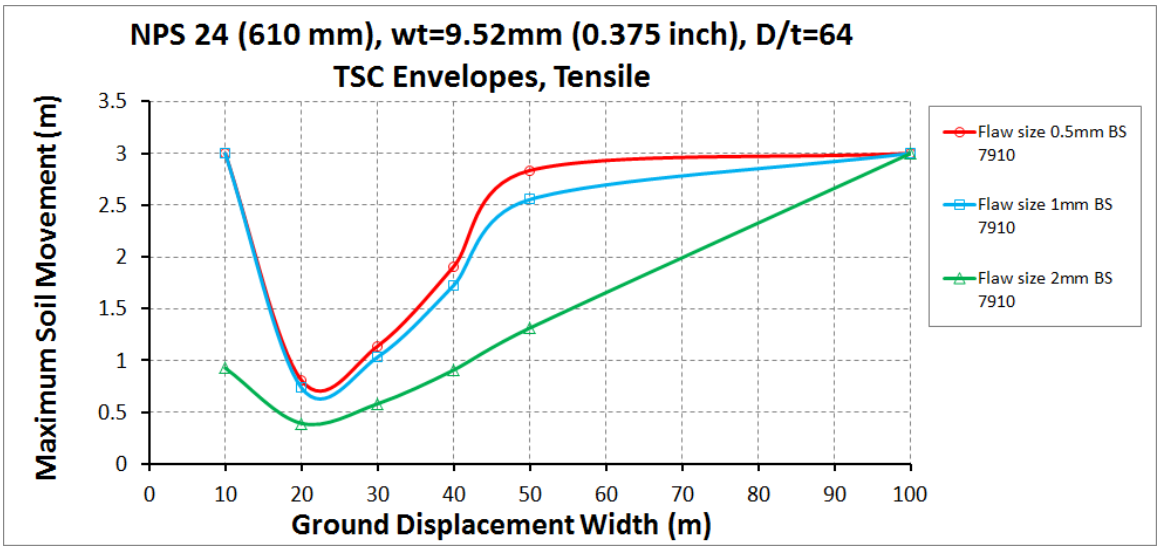

Figure 6.37: Tensile Strain Capacity Envelopes versus Ground Width (W) Movements Material Grade X70

6.6.2.1.2 Compressive Strain Capacity Envelopes (CSCE)

Figure 6.38 presents the maximum nominal compressive strain in the pipe versus the ground displacement width (W) for given ground displacement of 0.5, 1.0, 1.5, 2.0 and 2.5. The nominal compressive strain is defined as the average compressive strain measured over a gauge length of 2D (D is the pipe outside diameter). In this figure, the CSA and PRCI compressive strain capacity is presented with dash horizontal line.

The envelopes presented in Figure 6.38 describe the pipe compressive strain demands in the pipe for a given ground displacement and ground width. In this figure, the CSA and PRCI

The information contained herein is the copyright of and proprietary to BMT Fleet Technology Limited. Use of this information is governed by the legend on the cover page of this document."

compressive strain capacity is presented with dash horizontal line. Any compressive strain above the horizontal line is strain-related failure limit.

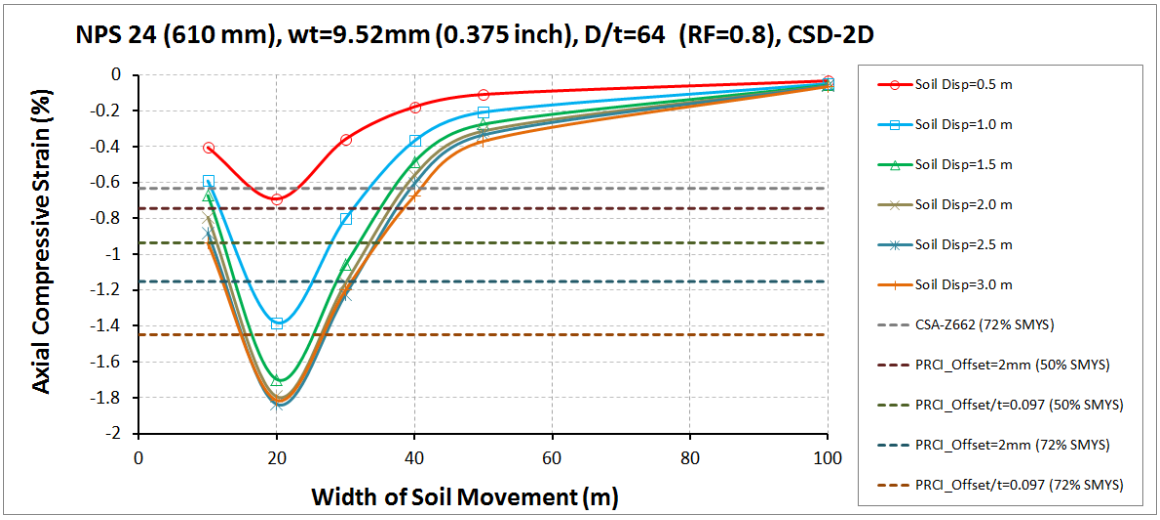

Figure 6.38: Pipe Axial Compressive Strains Envelopes (X70) versus Width (W) (for Soil Movement of 0.5, 1, 1.5, 2.0 and 2.5 m), Grade X70

Similar to the tensile strain capacity (TSC) envelopes, the results were used to generate compressive strain capacity (CSC) envelopes based on PRCI Guidance. These CSC envelopes are presented in Figure 6.39. The envelopes describe the maximum soil displacement and ground displacement width breakout the CSC envelopes, which represents the tensile strain-related failure limit, according to CSA and PRCI Guidance.

For example, as shown in Figure 6.39 the compressive strain-related failure limit for the critical width of 20 m (66 ft) is reached for ground displacement from 0.53 to 1.07 m considering girth weld misalignment (offset) of 2 mm and the pipeline to be operating at an internal pressure that induces a pipe wall stress of 50% and 72% of its SMYS, respectively.

The information contained herein is the copyright of and proprietary to BMT Fleet Technology Limited. Use of this information is governed by the legend on the cover page of this document."

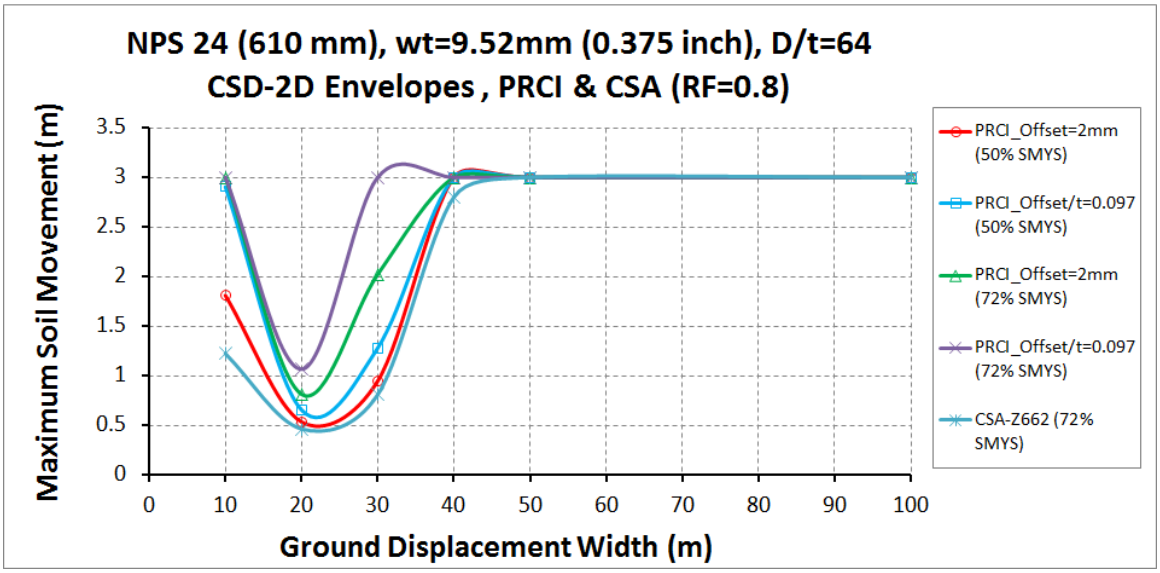

Figure 6.39: Compressive Strain Capacity Envelopes versus Ground Width (W) Movements. Grade X70

6.6.2.1.3 Strain Demand Envelopes (SDE)

In the previous section, the strain demands determined from the analysis was compared with the calculated strain capacity defined from the guidance; BS 7910 for tensile strain, and CSA Z662 and PRCI for compressive strain. While there are many existing models for calculating the compressive and tensile strain capacity in codes and standards, it was decided to develop a simple a strain-based design methodology that can be easily adapted to any code and standards, which is the purpose of this section.

The tensile and compressive strain demand envelops along the longitudinal direction of the pipeline are presented in Figure 6.40 and Figure 6.41. These figures show the maximum soil displacement versus ground width displacement as a series of 'envelopes' for a given pipe tensile and compressive strain demands of 0.25%, 0.5%, 0.75%, 1%, 1.25%, 1.5%, 1.75% and 2%. The safe pipeline operating goal of pipeline subjected to lateral ground displacement is to stay within the normal operating strain range defined by codes and standards.

The information contained herein is the copyright of and proprietary to BMT Fleet Technology Limited. Use of this information is governed by the legend on the cover page of this document."

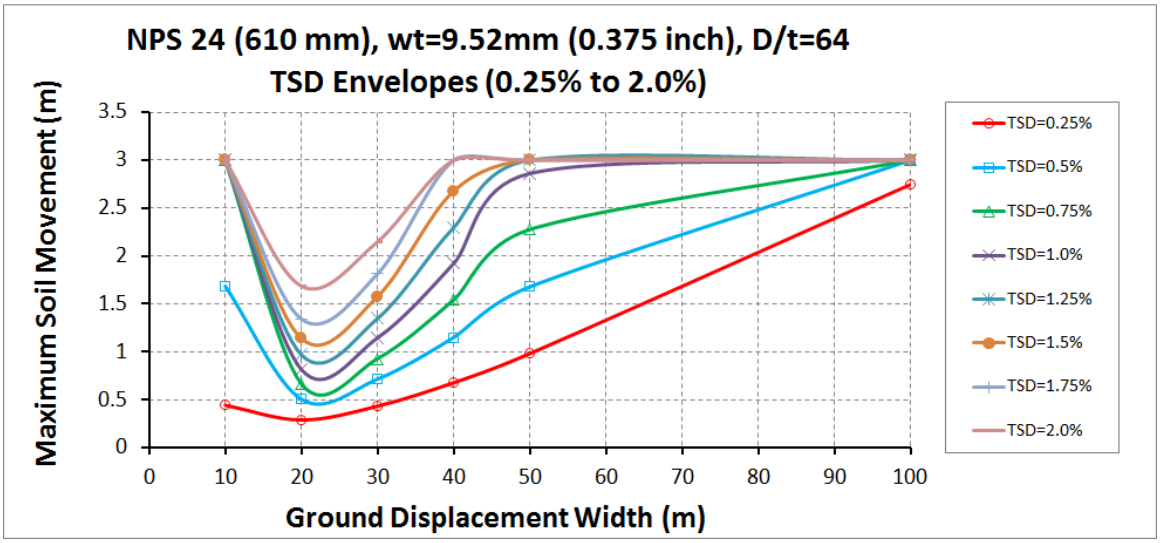

Figure 6.40: Tensile Strain Demand versus Width (W), Grade X70

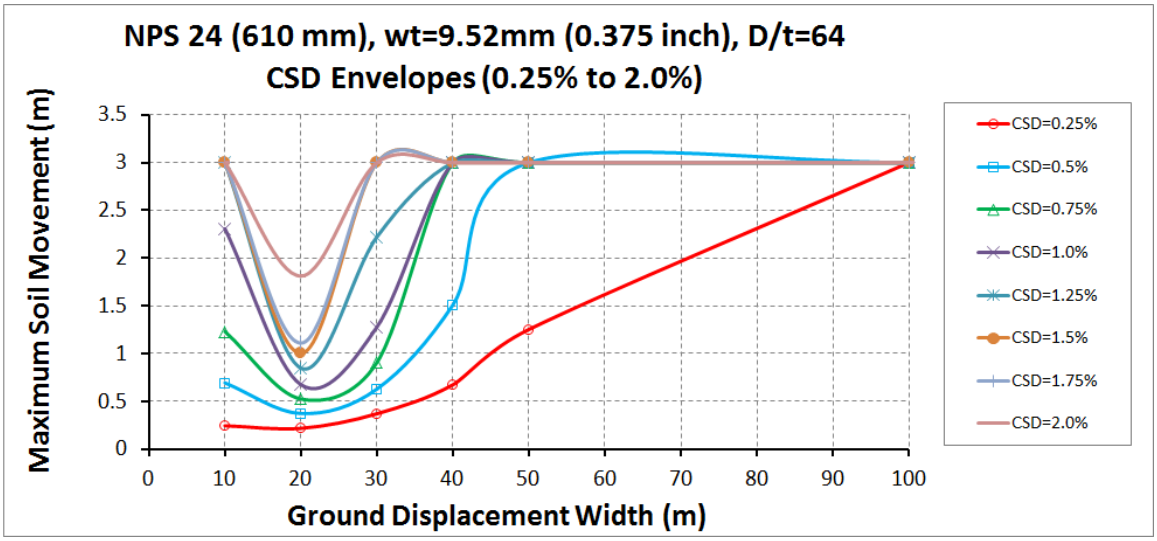

Figure 6.41: Compressive Strain Demand Envelopes versus Width (W), Grade X70

6.7 Effect of Temperature

Comparison between the results of three temperature differentials (0, 45 and 65 °C) analyzed for critical width of 20 m (base case) is provided in Figure 6.42 and Figure 6.43. Both of these figures are for X-52 grade NPS 24 (610 mm) pipe with t =9.5 mm (3/8 in) [D/t=64]. Reduction in the differential temperature results in reduction in the maximum computed compressive strains. The maximum computed tensile strain is not significantly affected. The computed tensile strain for case with no temperature is more than twice the computed compressive strain.

Figure 6.42 presents the maximum tensile and compressive strains in the pipe versus the maximum ground displacement for critical ground displacement widths of 20 m (66 ft). Figure 6.42 also presents the sum of tensile (positive) and compressive (negative) strains in the pipe.

The information contained herein is the copyright of and proprietary to BMT Fleet Technology Limited. Use of this information is governed by the legend on the cover page of this document."

The results indicated that the calculated compressive strains are slightly higher at ground displacement less than 0.75 m for cases with a temperature differential; this is mainly due to compressive strain induced by thermal loading. At large ground displacement, tensile strains are higher than compressive strain. This differential in peak tensile and compressive strains indicates that there is a significant uniform axial strain in the pipe due to larger catenary effect.

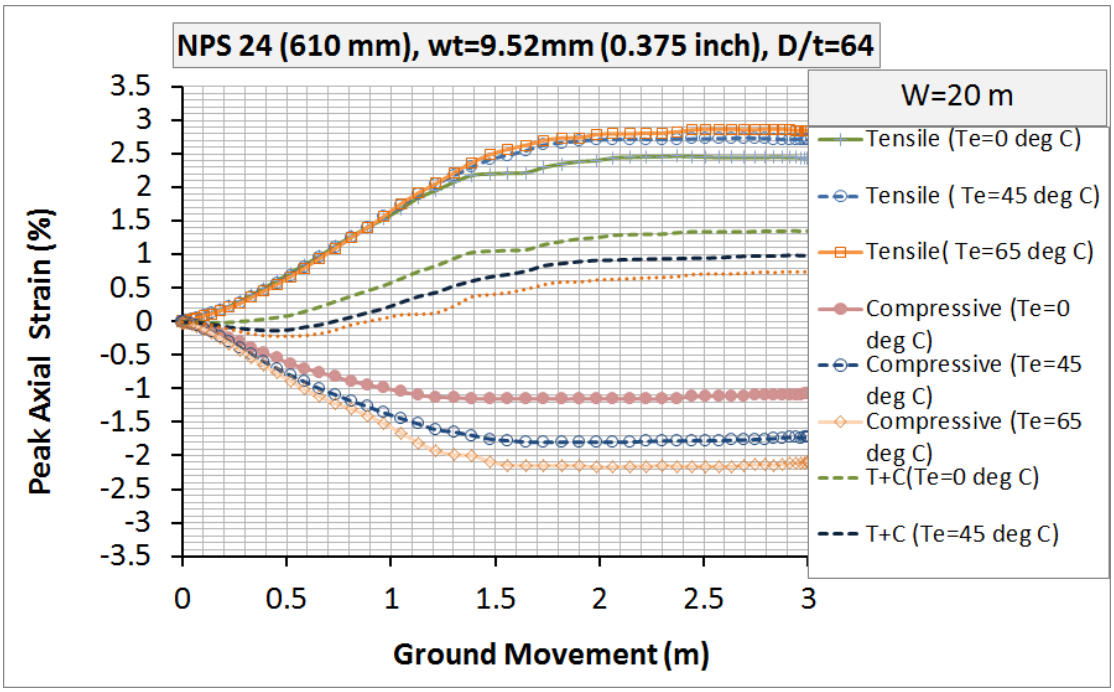

Figure 6.42: NPS 24 (D/t=64) – Maximum Axial Strain versus Ground Movement for the Critical Widths of 20 m (66 ft) –Temperature Effect

Figure 6.43 shows maximum pipe displacement versus the maximum ground displacement. The maximum pipe displacement follows the ground displacement up to certain ground displacement than the pipe displacement increase slowly with ground displacement, which results in slowly increase in pipe strains. The results indicated that higher operating temperature differential results in larger pipe displacement.

The information contained herein is the copyright of and proprietary to BMT Fleet Technology Limited. Use of this information is governed by the legend on the cover page of this document."

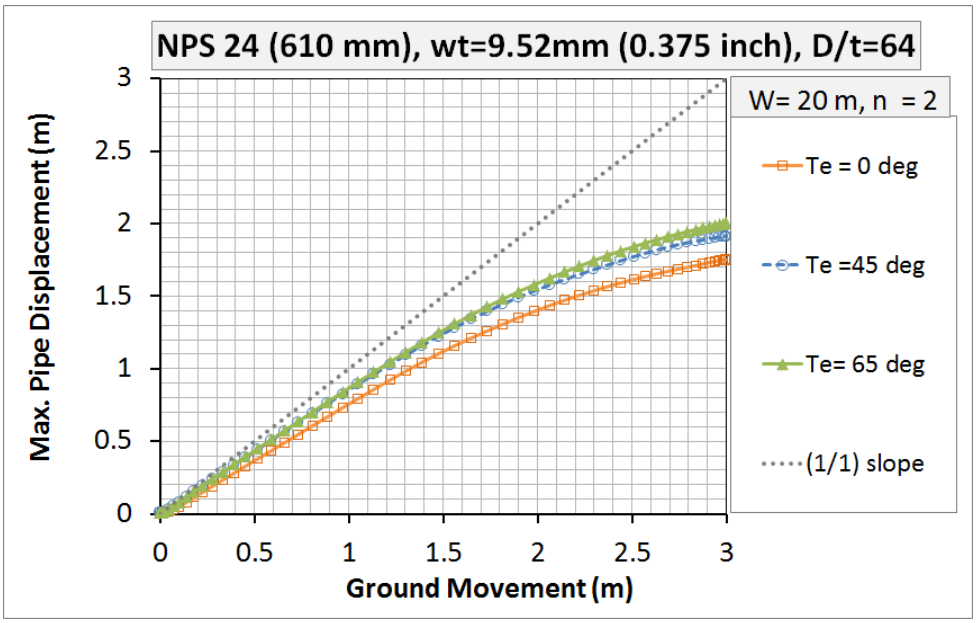

Figure 6.43: NPS 24 (D/t=64) – Maximum Pipe Displacement vs. Ground Movement for the Critical Widths of 20 m (66 ft) –Temperature Effect, Grade X52

6.8 Effect of Operating Pressure

The results presented in Section 6.6.1, illustrates the importance of the width of the ground displacement. The critical width which results in the largest axial strain in the pipe for any given value of ground is about 20 m (66 ft) for the analyzed case. It is possible that for very stiff soils the critical width concept does not apply because the pipe bending transition across an abrupt slip plane promotes the highest strains regardless of slip plane width.

Comparison between the results of three operating pressure of 4 MPa, 5.6 MPa and 8.1 MPa considering that the pipeline to be operating at an internal pressure that includes a pipe wall stress of 36%, 50% and 72% of its SMYS. The results of the analyses for critical width of 20m are provided in Figure 6.44 through Figure 6.45. These figures are for X-52 grade NPS 24 (610mm) pipe with t =9.5 mm (3/8 in) and D/t=64. Figure 6.44 presents the maximum tensile and compressive strains in the pipe versus the maximum ground displacement for critical ground displacement widths of 20 m (66 ft). Figure 6.45 also presents the sum of tensile (positive) and compressive (negative) strains in the pipe. The results indicated that reduction in the operating pressure results in and increase in the maximum computed compressive and tensile strains. The results also indicate that

- Pipe operating at 72% SMYS do not exceed compressive strain limit for the applied ground movement of 3.0 m. Figure 6.47 shows the pipe soil deformation for the analyzed case.
- Pipe operating at 50% SMYS exceeds the compressive strain limit and buckle/wrinkle at 0.65% compressive strain for soil displacement of 1.4 m. The

The information contained herein is the copyright of and proprietary to BMT Fleet Technology Limited. Use of this information is governed by the legend on the cover page of this document."

wrinkle amplitude grows up to 8 mm for soil movement of 2.25 m. Figure 6.48 shows the pipe soil deformation for the analyzed case.

- Pipe operating at 36% SMYS exceeds the compressive strain limit and buckle/wrinkle at 0.55 % compressive strain for soil displacement of 1.0 m. The wrinkle amplitude grows up to 28 mm for soil movement of 2.25 m. Figure 6.49 shows the pipe soil deformation for the analyzed case.

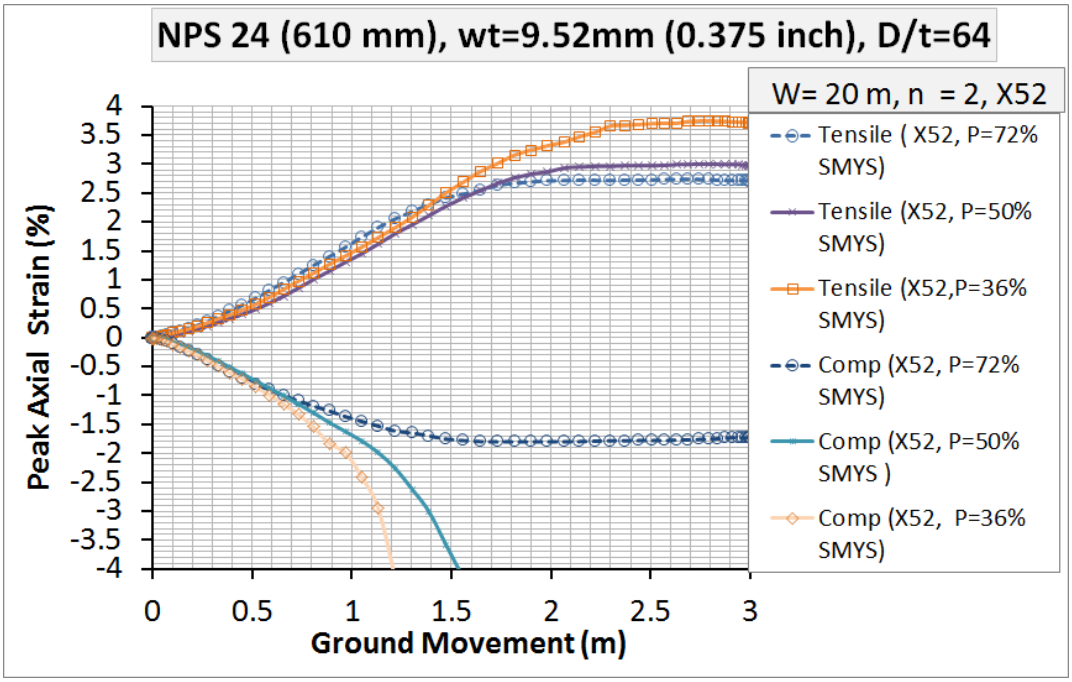

Figure 6.44: NPS 24 (D/t=64) – Maximum Axial Strain versus Ground Movement for the Critical Widths of 20 m (66 ft) –Pressure Effect

The information contained herein is the copyright of and proprietary to BMT Fleet Technology Limited. Use of this information is governed by the legend on the cover page of this document."

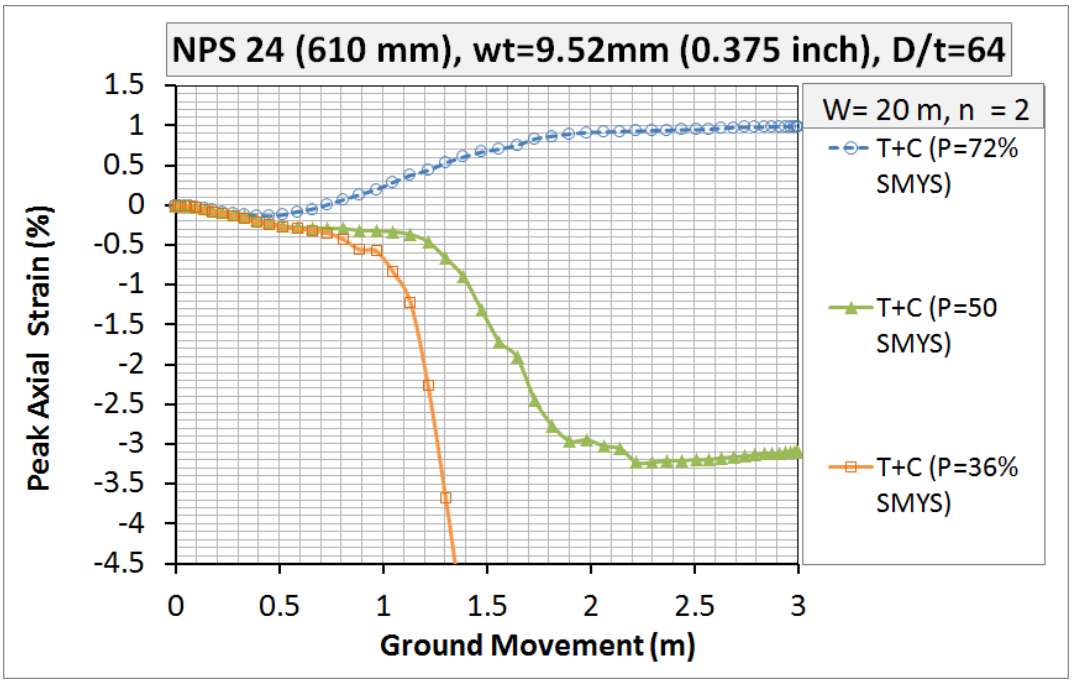

Figure 6.45: NPS 24 (D/t=64) – Sum of the Maximum Tensile and Compressive Strain versus Ground Movement for the Critical Widths of 20 m (66 ft) – Pressure Effect

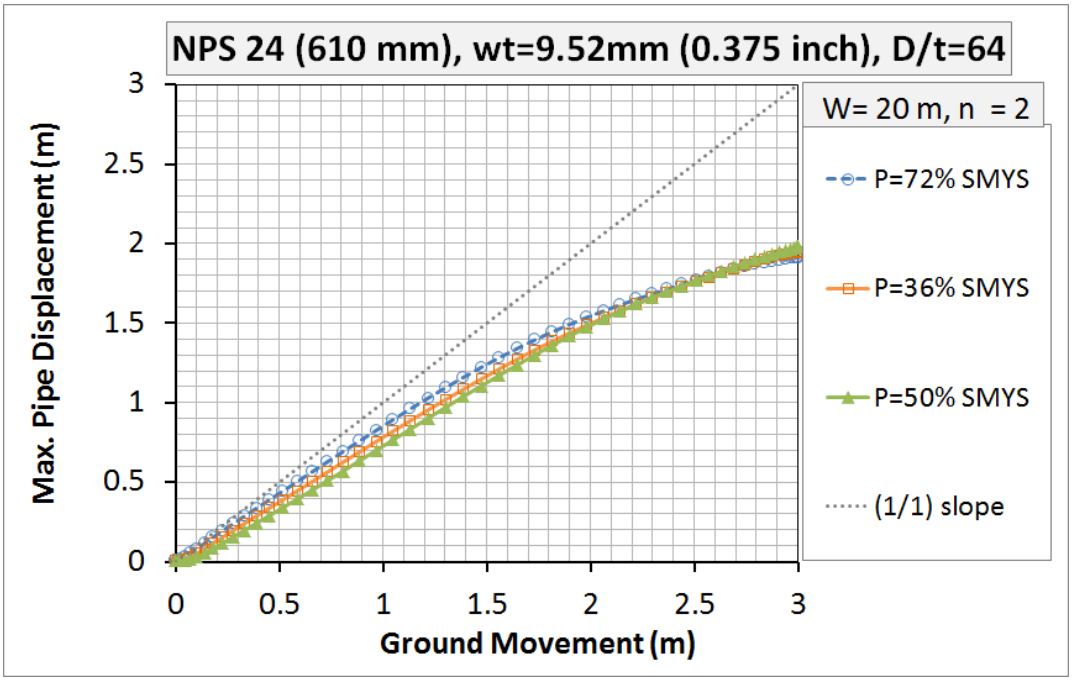

Figure 6.46: NPS 24 (D/t=64) – Maximum Pipe Displacement vs. Ground Movement for the Critical Widths of 20 m (66 ft) – Temperature Effect, Grade X52

The information contained herein is the copyright of and proprietary to BMT Fleet Technology Limited. Use of this information is governed by the legend on the cover page of this document."

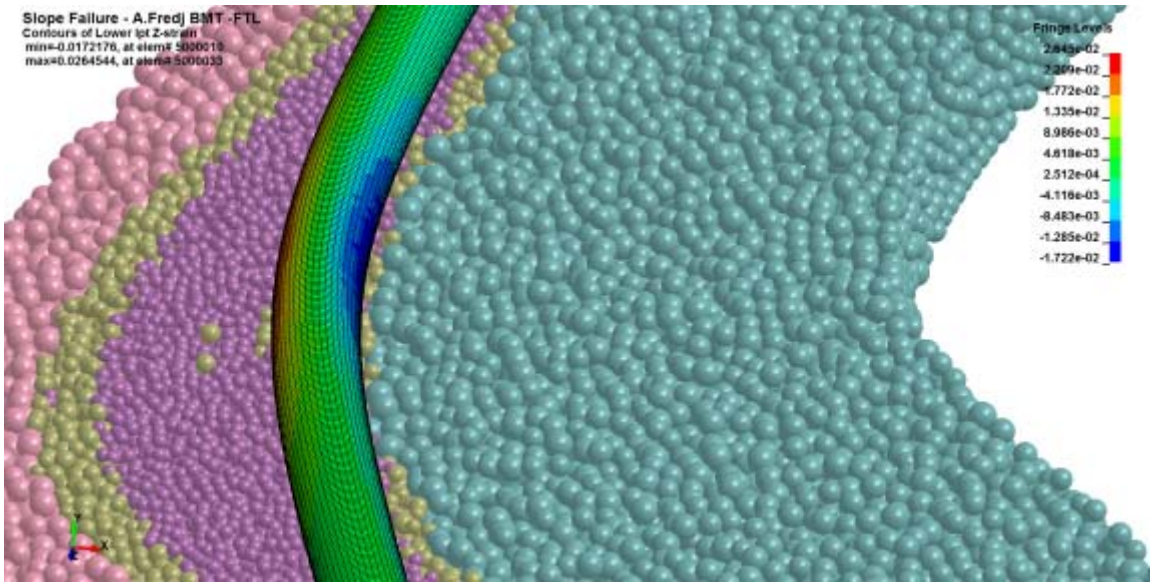

Figure 6.47: Pipe Deformation and Axial Strains for given Soil Movement of 2.5 m (Top View) – 0.72 SMYS Pressure (No Wrinkle observed)

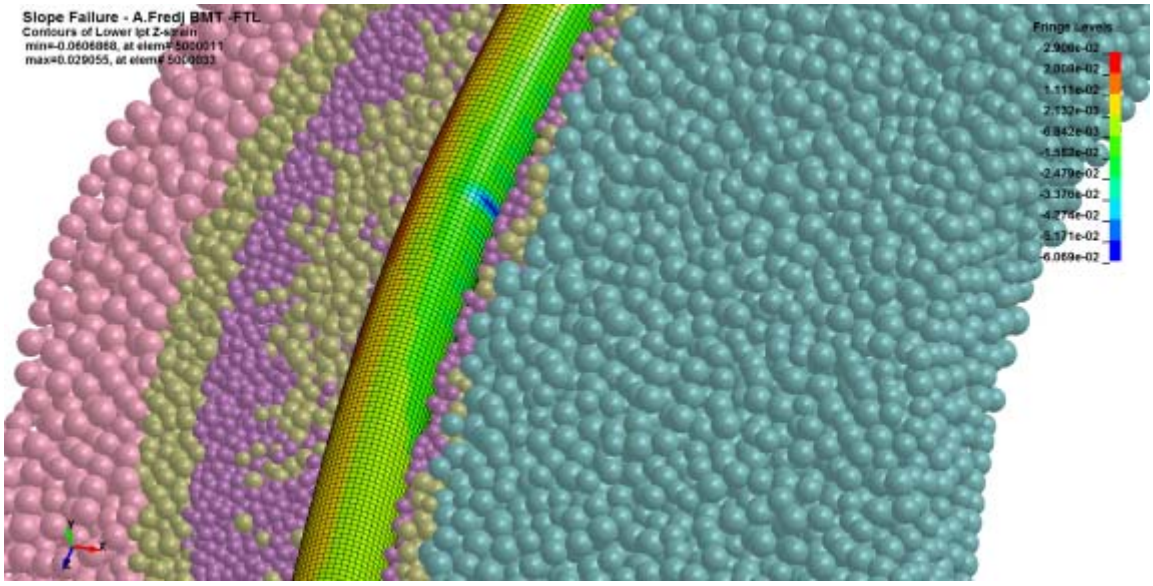

Figure 6.48: Pipe Deformation and Axial Strains for given Soil Movement of 2.5 m (Top View) – 0.50 SMYS Pressure (Wrinkle observed, Amplitude = 8 mm)

The information contained herein is the copyright of and proprietary to BMT Fleet Technology Limited. Use of this information is governed by the legend on the cover page of this document."

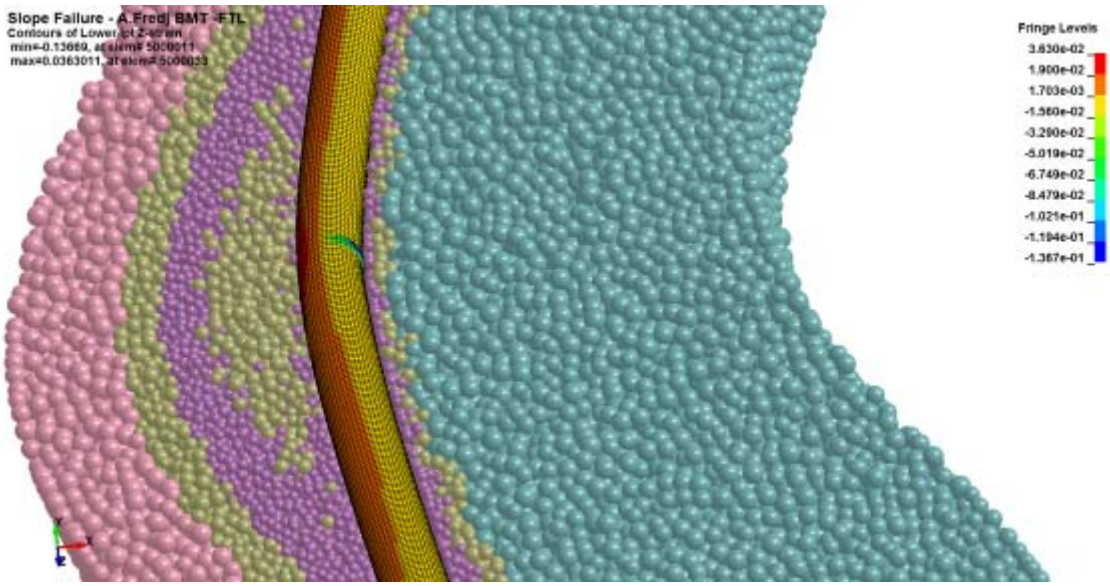

Figure 6.49: Pipe Deformation and Axial Strains for given Soil Movement of 2.5 m (Top View) –0.36 SMYS Pressure (Wrinkle observed, Amplitude = 28 mm)

6.8.1 Comparison with Strain Capacity and Strain Demand Envelopes

The following section represents the summary results for NPS 24 (609 mm outside diameter) considering that the pipeline to be operating at an internal pressure of 36% of its SMYS (4 MPa).

Detailed results are presented as follow:

- Figures 6.50 presents the maximum tensile strains in the longitudinal direction of the pipeline versus the maximum ground displacement for various ground displacement widths considered in the analyses. Figures 6.51 and 6.52 present the maximum local and nominal compressive strains in the longitudinal direction of the pipeline versus the maximum ground displacement for various ground displacement widths considered in the analyses. The nominal compressive strain is defined as the average compressive strain measured over a gauge length of 2D (where D is the pipe outside diameter). The results indicate that for the six (6) widths considered, the width of 20 m (66 ft) results in the largest tensile and compressive strain in the pipe for any given value of ground displacement.
- Figure 6.53 presents the maximum compressive strains in pipe versus the ground displacement width (W) for given ground displacement of 0.5, 1.0, 1.5, 2.0 and 2.5. In this figure the BS-7910 tensile strain capacity is presented with dash horizontal line. Any tensile strain above the horizontal line is strain-related failure limit. The TSC envelopes based on BS7910 guidance are presented in Figure 6.54. The envelopes describe the maximum soil displacement and ground displacement width breakout the TSC envelopes, which represents the tensile strain-related failure limit, according to BS 7910. The results indicate that for this pipe and operating condition combination, the ground movement width of 20 m (66 ft) can be considered critical.

The information contained herein is the copyright of and proprietary to BMT Fleet Technology Limited. Use of this information is governed by the legend on the cover page of this document."

- Figure 6.55 presents the maximum compressive strains in pipe versus the ground displacement width (W) for given ground displacement of 0.5, 1.0, 1.5, 2.0 and 2.5. In this figure the PRCI compressive strain capacity is presented with dash horizontal line. Any compressive strain below the horizontal line is strain-related failure limit. The CSC envelopes based on PRCI guidance are presented in Figure 6.56. The envelopes describe the maximum soil displacement and ground displacement width breakout the CSC envelopes, which represents the compressive strain-related failure limit, according to PRCI. The results indicate that for this pipe and operating condition combination, the ground movement width of 20 m (66 ft) can be considered critical.
- Figure 6.57 and Figure 6.58 present the tensile and compressive strain demand 'envelopes' for a given pipe tensile and compressive strain demands of 0.25%, 0.5%, 0.75%, 1%, 1.25%, 1.5%, 1.75% and 2% along the longitudinal direction of the pipeline. The safe pipeline operating goal of pipeline subjected to lateral ground displacement is to stay within the normal operating strain range defined by codes and standards.

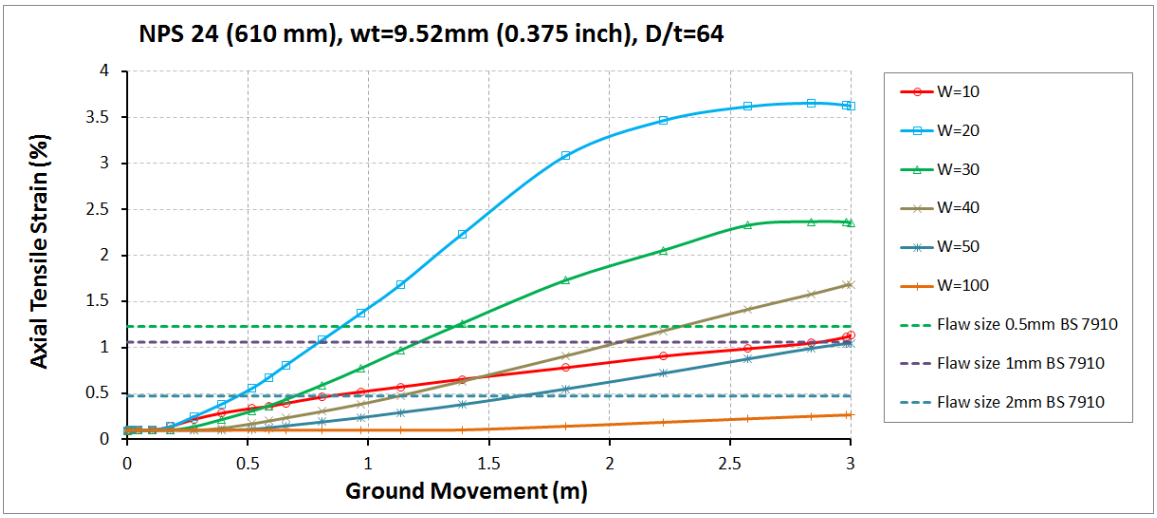

Figure 6.50: NPS 24 (D/t=64, X52) - Maximum Tensile in the Pipe vs. Ground Movement Widths: [10-100m]

The information contained herein is the copyright of and proprietary to BMT Fleet Technology Limited. Use of this information is governed by the legend on the cover page of this document."

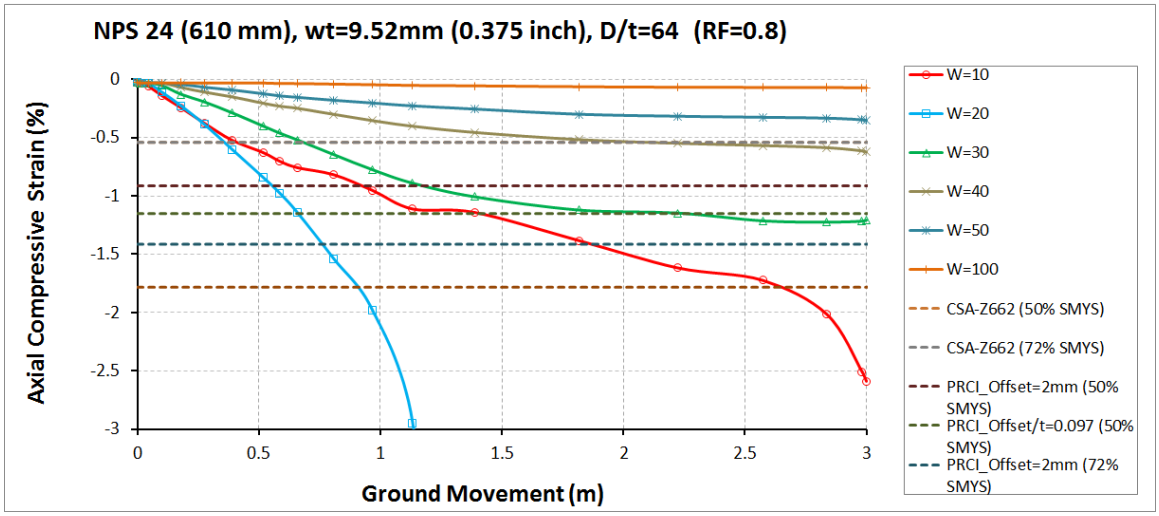

Figure 6.51: NPS 24 (D/t=64, X52) - Maximum Local Compressive Strain in the Pipe vs. Ground Movement Widths: [10-100 m]

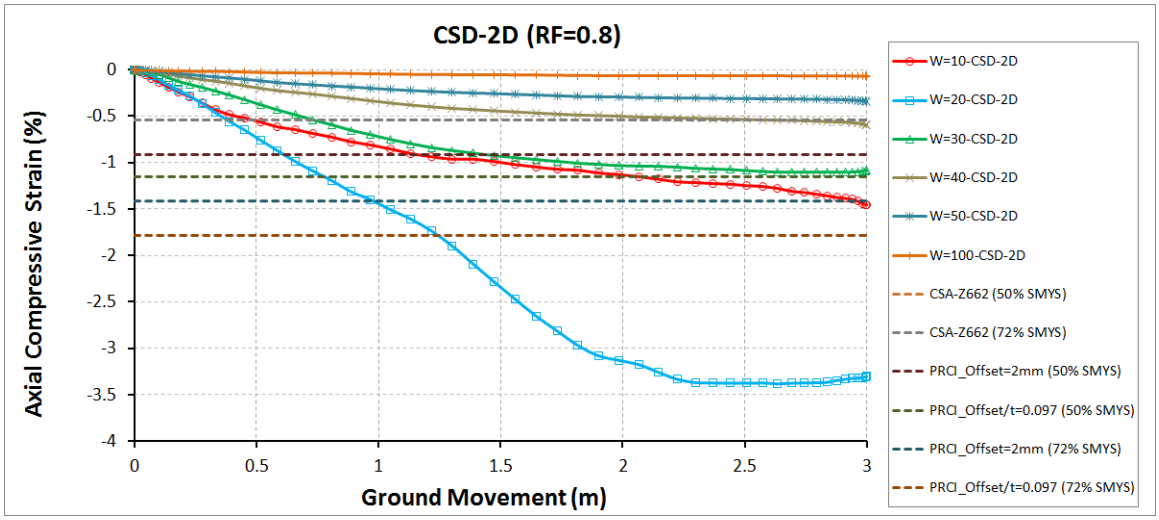

Figure 6.52: NPS 24 (D/t=64, X52) - Maximum Nominal Compressive Strain in the Pipe vs. Ground Movement Widths: [10-100 m]

The information contained herein is the copyright of and proprietary to BMT Fleet Technology Limited. Use of this information is governed by the legend on the cover page of this document."

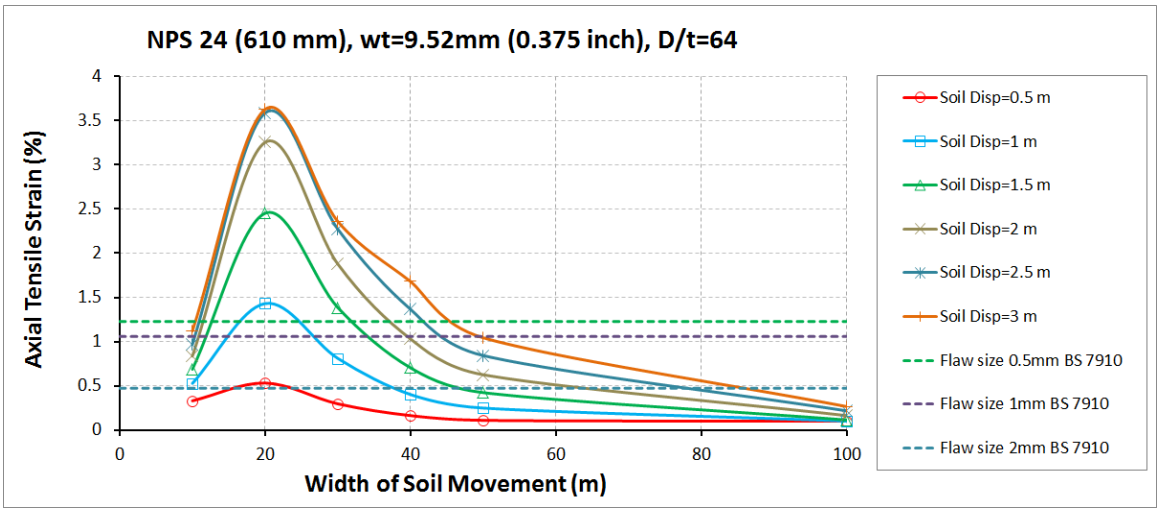

Figure 6.53: Pipe Axial Tensile Strains Envelopes versus Width (W) for Soil Movements of 0.5, 1, 1.5, 2.0 and 2.5 m Operating Pressure 36% SMYS

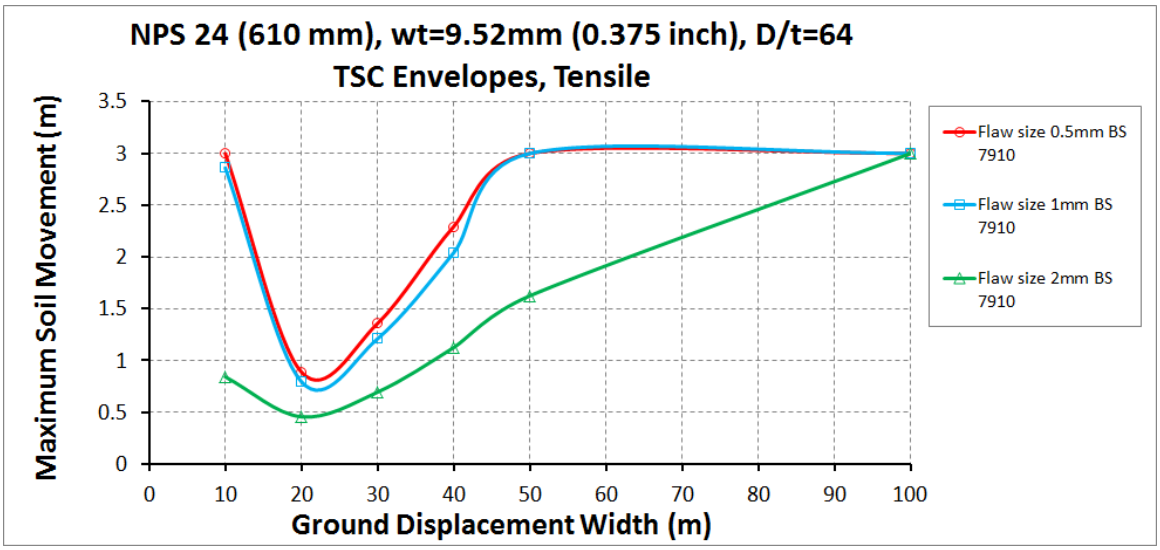

Figure 6.54: Tensile Strain Capacity Envelopes versus Ground Width (W) Movements

The information contained herein is the copyright of and proprietary to BMT Fleet Technology Limited. Use of this information is governed by the legend on the cover page of this document."

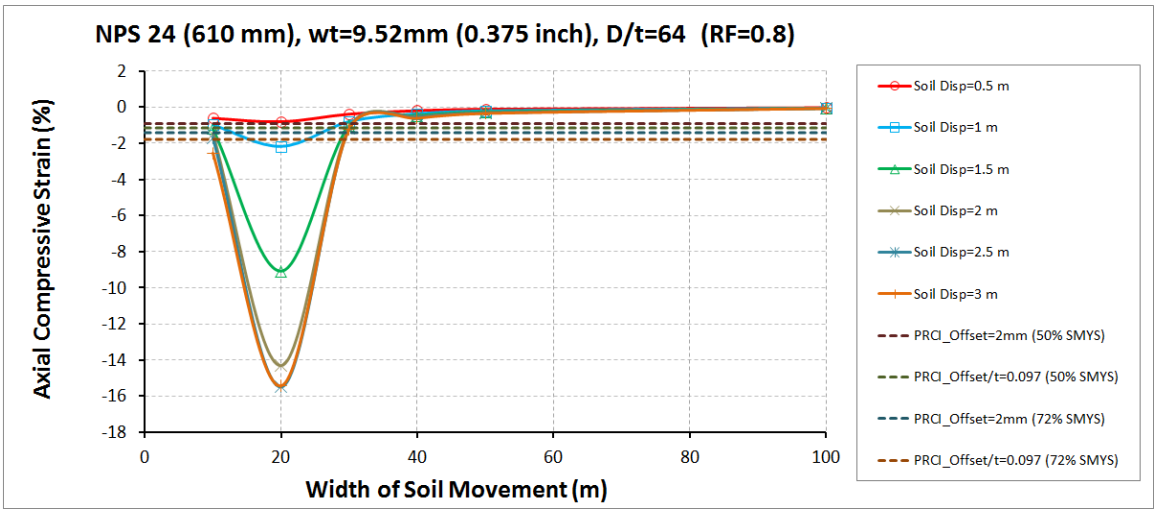

Figure 6.55: Pipe Axial Compressive Strains Envelopes versus Width (W) for Soil Movements of 0.5, 1, 1.5, 2.0 and 2.5 m Operating Pressure 36% SMYS

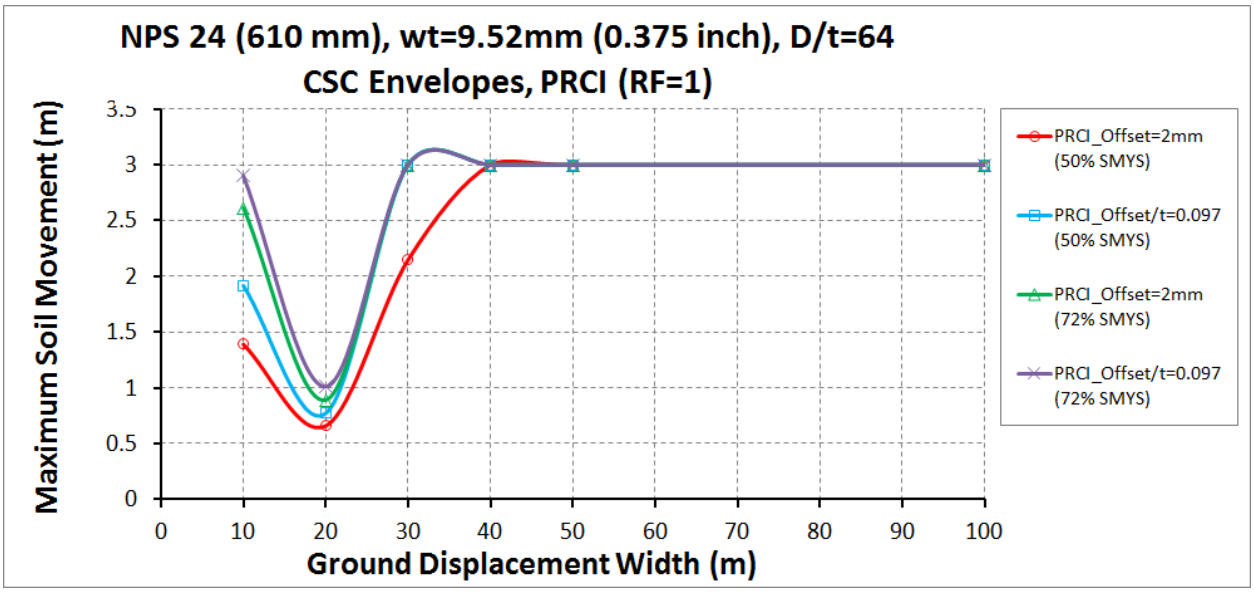

Figure 6.56: Compressive Strain Capacity Envelopes versus Ground Width (W) Movements

The information contained herein is the copyright of and proprietary to BMT Fleet Technology Limited. Use of this information is governed by the legend on the cover page of this document."

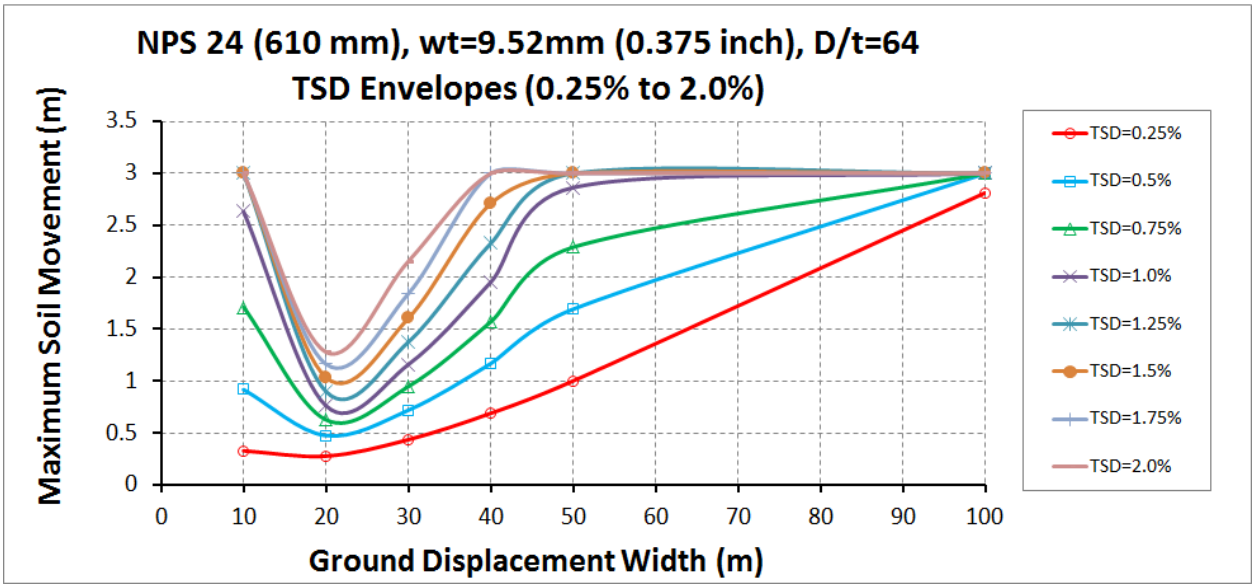

Figure 6.57: Tensile Strain Demand versus Width (W), (Pressure is 36% SMYS)

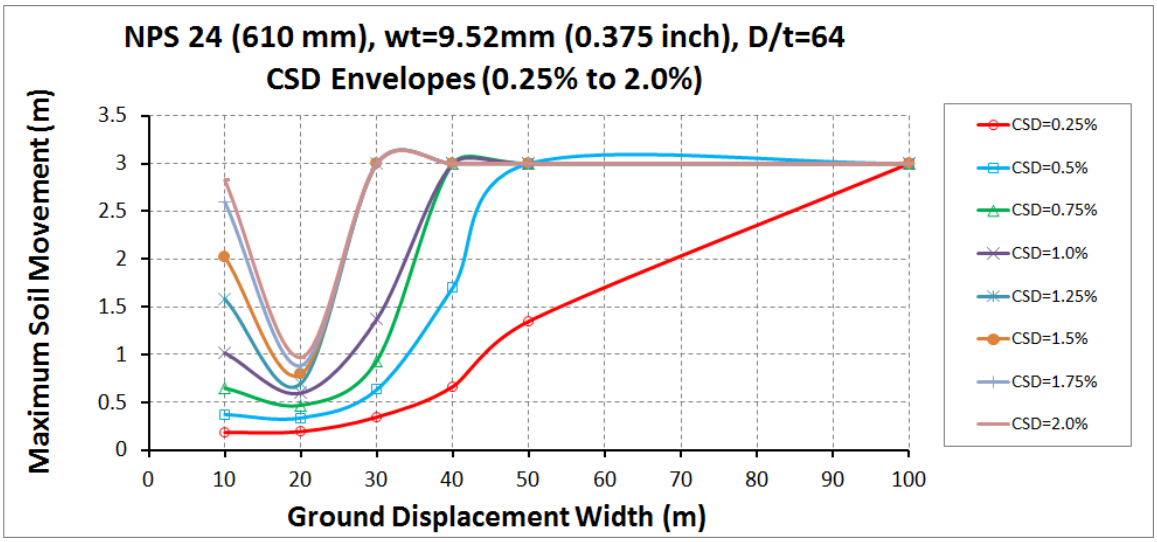

Figure 6.58: Compressive Strain Demand versus Width (W), (Pressure is 36% SMYS)

6.9 Effect of Ground Movement Pattern

In order to evaluate the effect soil movement pattern, the base case simulated using cosine function raised to power 2 was repeated using cosine function raised to power 0.1. Figure 6.59 presents the alternative soil movement patterns that will be simulated.

The information contained herein is the copyright of and proprietary to BMT Fleet Technology Limited. Use of this information is governed by the legend on the cover page of this document."

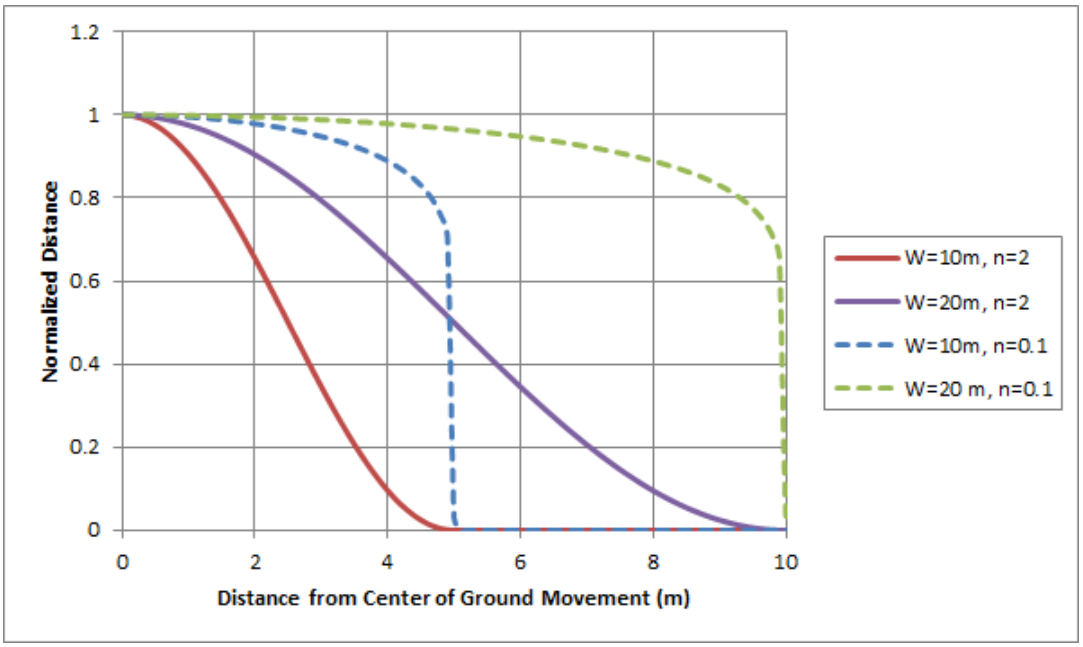

Figure 6.59: Soil Movement Patterns, Width W=10m, and 20 m

Figures 6.60 and 6.61 illustrate the simulated displaced position of the pipe and the soil patterns for both loading scenario considering ground movement width of 20 m.

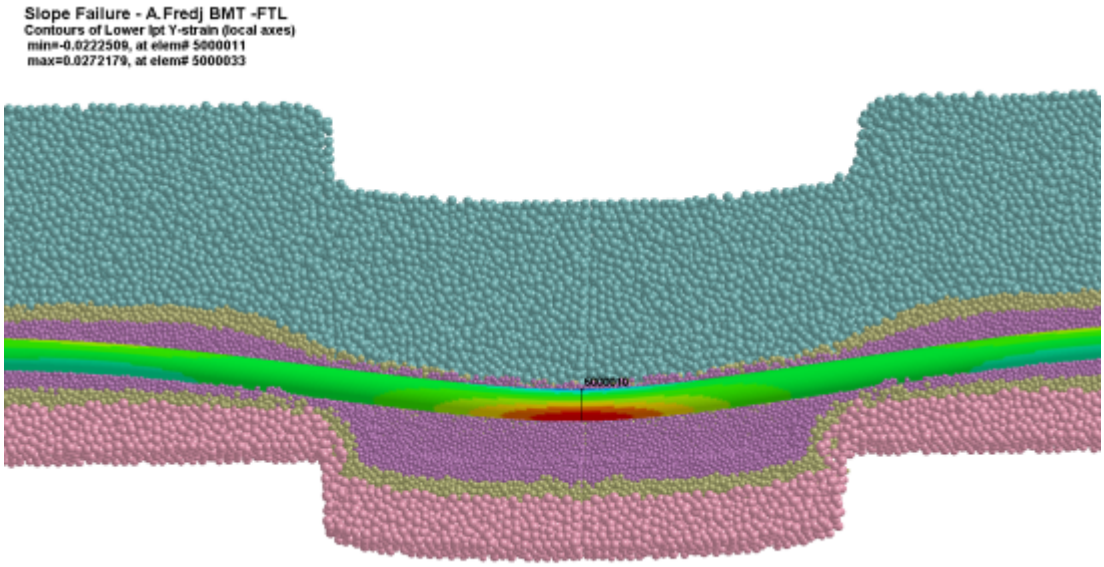

Figure 6.60: Pipe Deformation and Axial Strains for given Soil Movement of 2 m and W=20 m (Top View), n=2

The information contained herein is the copyright of and proprietary to BMT Fleet Technology Limited. Use of this information is governed by the legend on the cover page of this document."

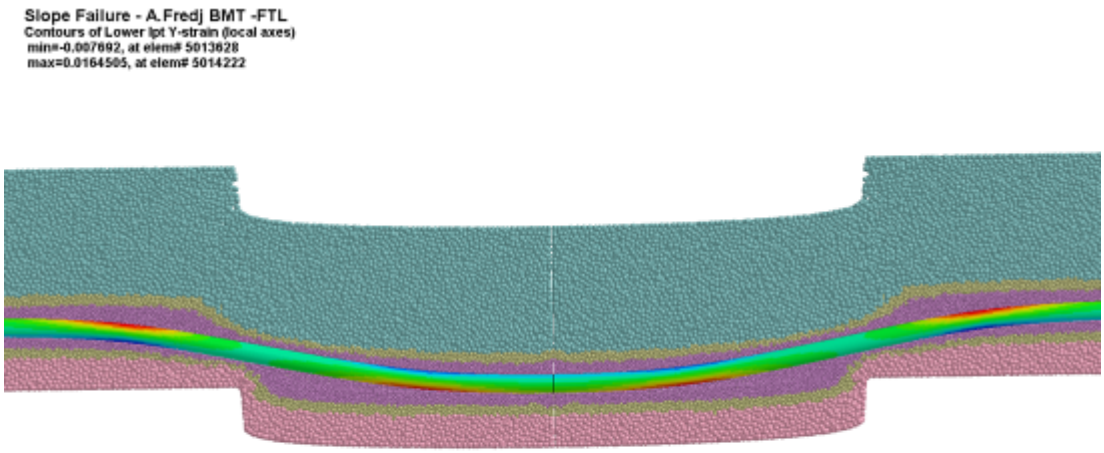

Figure 6.61: Pipe Deformation and Axial Strains for given Soil Movement of 2 m and W=20 m (Top View), n=0.1

Figures 6.62 and 6.63 present the maximum tensile and compressive strains in the pipe versus the maximum ground displacement for ground displacement widths of W=10 m and W=20 m. The results clearly show that the critical ground movement depends on the soil movement function (pattern). From these results it is noted that:

- The width of 20 m (66 ft) results in the largest tensile and compressive strain in the pipe for any given value of ground displacement considering soil parameter n equal to 2.
- The width of 10 m (33 ft) results in the largest tensile and compressive strain in the pipe for any given value of ground displacement considering soil parameter n equal to 0.1.

The information contained herein is the copyright of and proprietary to BMT Fleet Technology Limited. Use of this information is governed by the legend on the cover page of this document."

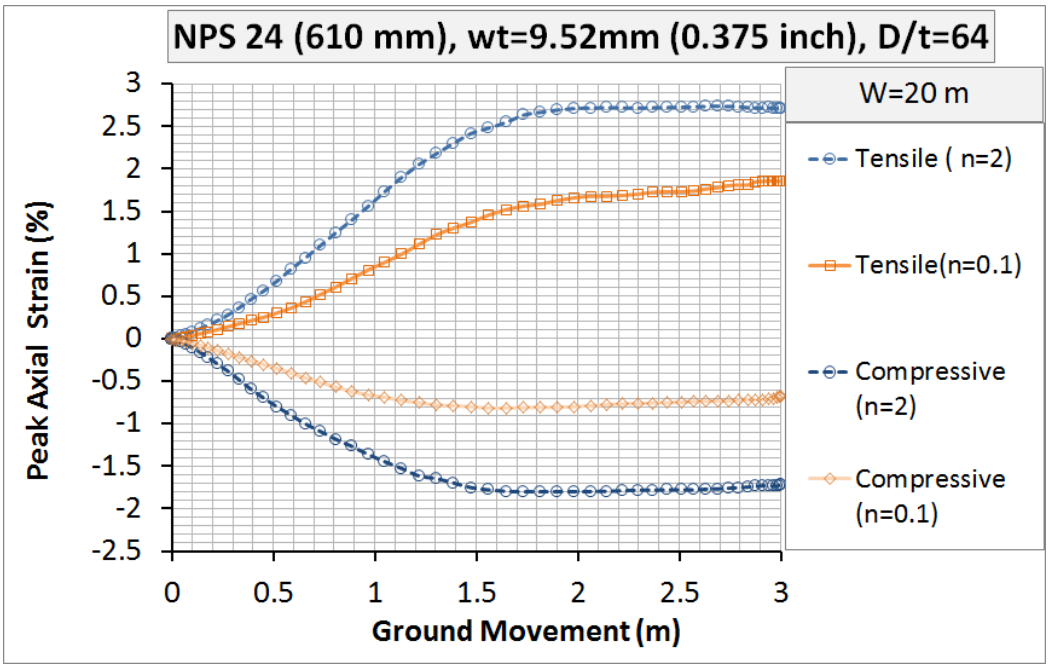

Figure 6.62: NPS 24 (D/t=64) – Maximum Axial Strain vs. Ground Movement for the Critical Widths of 20 m (66 ft)

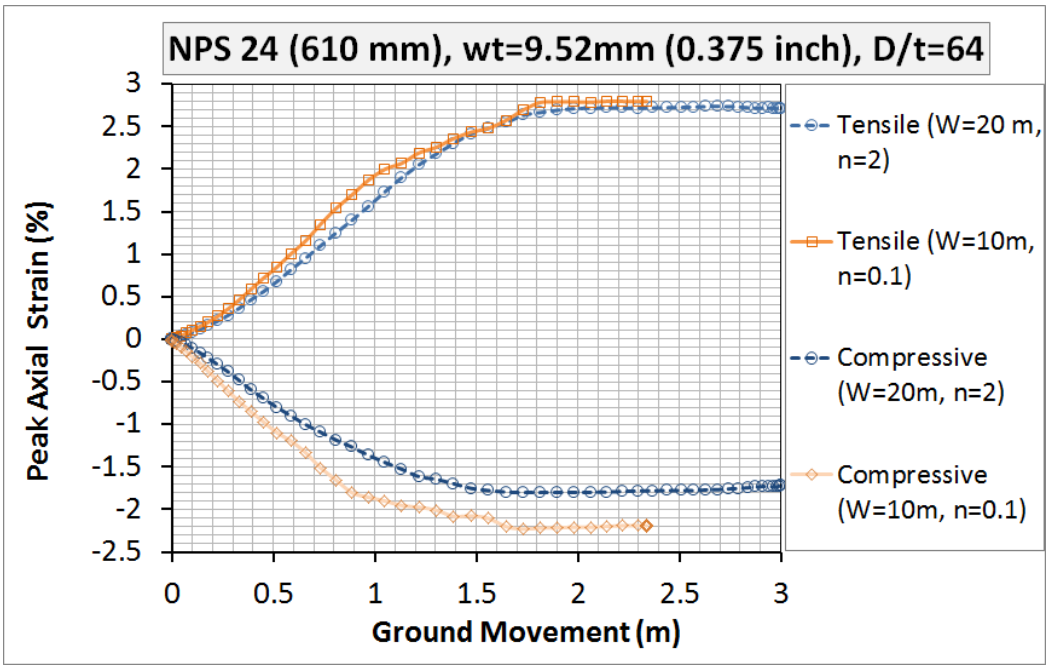

Figure 6.63: NPS 24 (D/t=64) –Maximum Axial Strain vs. Ground Movement for the Critical Widths of 20 m (66 ft) and 10 m (33ft)

The information contained herein is the copyright of and proprietary to BMT Fleet Technology Limited. Use of this information is governed by the legend on the cover page of this document."

6.9.1 Comparison with Strain Capacity and Strain Demand Envelopes

The following section represents the summary results for NPS 24 (609 mm outside diameter) considering soil movement pattern using cosine function raised to power 0.1.

Detailed results are presented as follow:

- Figures 6.64 presents the maximum tensile strains in the longitudinal direction of the pipeline versus the maximum ground displacement for various ground displacement widths considered in the analyses. Figures 6.65 and 6.66 present the maximum local and nominal compressive strains in the longitudinal direction of the pipeline versus the maximum ground displacement for various ground displacement widths considered in the analyses. The nominal compressive strain is defined as the average compressive strain measured over a gauge length of 2D (where D is the pipe outside diameter). The results indicate that for the six (6) widths considered, the width of 10 m (33 ft) results in the largest tensile and compressive strain in the pipe for any given value of ground displacement.
- Figure 6.67 presents the maximum compressive strains in pipe versus the ground displacement width (W) for given ground displacement of 0.5, 1.0, 1.5, 2.0 and 2.5. In this figure, the BS-7910 tensile strain capacity is presented with dash horizontal line. Any tensile strain above the horizontal line is strain-related failure limit. The TSC envelopes based on BS7910 guidance are presented in Figure 6.68. The envelopes describe the maximum soil displacement and ground displacement width breakout the TSC envelopes, which represents the tensile strain-related failure limit, according to BS 7910. The results indicate that for this pipe and operating condition combination, the ground movement width of 10 m (33 ft) can be considered critical.
- Figure 6.69 presents the maximum compressive strains in pipe versus the ground displacement width (W) for given ground displacement of 0.5, 1.0, 1.5, 2.0 and 2.5. In this figure, the PRCI compressive strain capacity is presented with dash horizontal line. Any compressive strain below the horizontal line is strain-related failure limit. The CSC envelopes based on PRCI guidance are presented in Figure 6.70. The envelopes describe the maximum soil displacement and ground displacement width breakout the CSC envelopes, which represents the compressive strain-related failure limit, according to PRCI. The results indicate that for this pipe and operating condition combination, the ground movement width of 10 m (33 ft) can be considered critical.
- Figure 6.71 and Figure 6.72 present the tensile and compressive strain demand 'envelopes' for a given pipe tensile and compressive strain demands of 0.25%, 0.5%, 0.75%, 1%, 1.25%, 1.5%, 1.75% and 2% along the longitudinal direction of the pipeline. The safe pipeline operating goal of pipeline subjected to lateral ground displacement is to stay within the normal operating strain range defined by codes and standards.

The information contained herein is the copyright of and proprietary to BMT Fleet Technology Limited. Use of this information is governed by the legend on the cover page of this document."

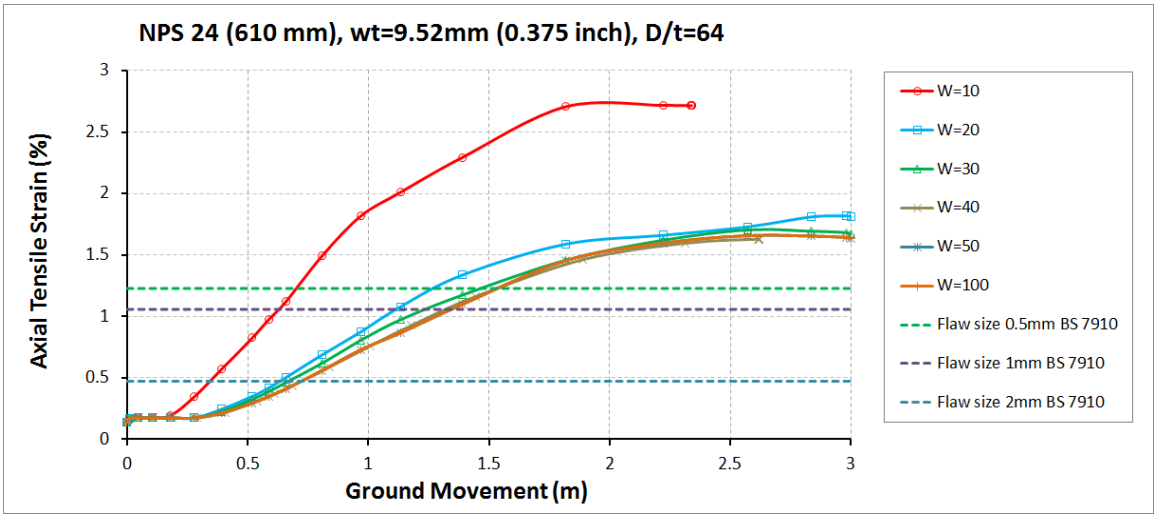

Figure 6.64: NPS 24 (D/t=64, X52) - Maximum Tensile in the Pipe vs. Ground Movement Widths: [10-100 m], n = 0.1

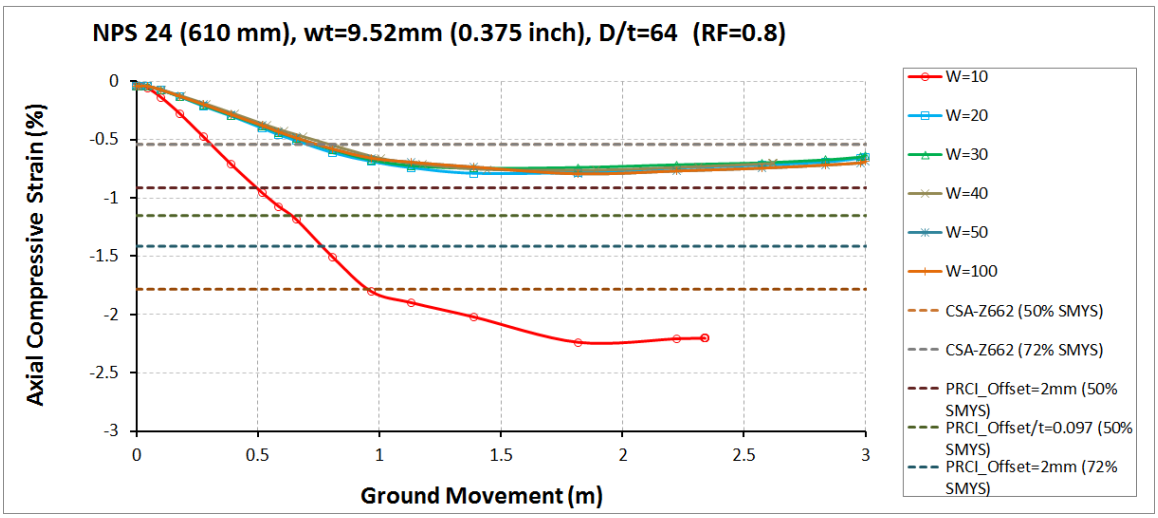

Figure 6.65: NPS 24 (D/t=64, X52) - Maximum Local Compressive Strain in the Pipe vs. Ground Movement Widths: [10-100 m], n = 0.1

The information contained herein is the copyright of and proprietary to BMT Fleet Technology Limited. Use of this information is governed by the legend on the cover page of this document."

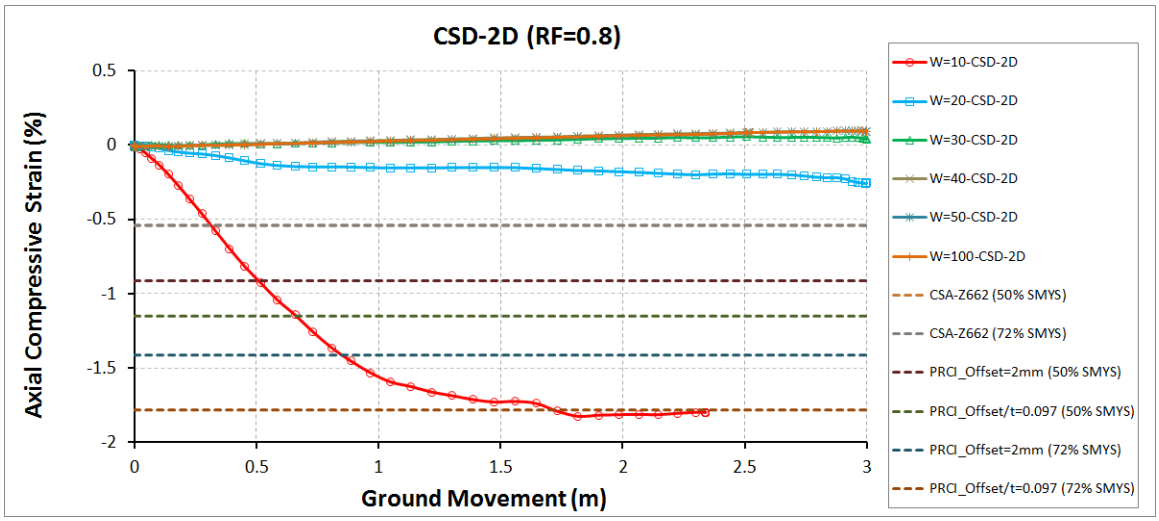

Figure 6.66: NPS 24 (D/t=64, X52) - Maximum Nominal Compressive Strain in the Pipe vs. Ground Movement Widths: [10-100 m], n = 0.1

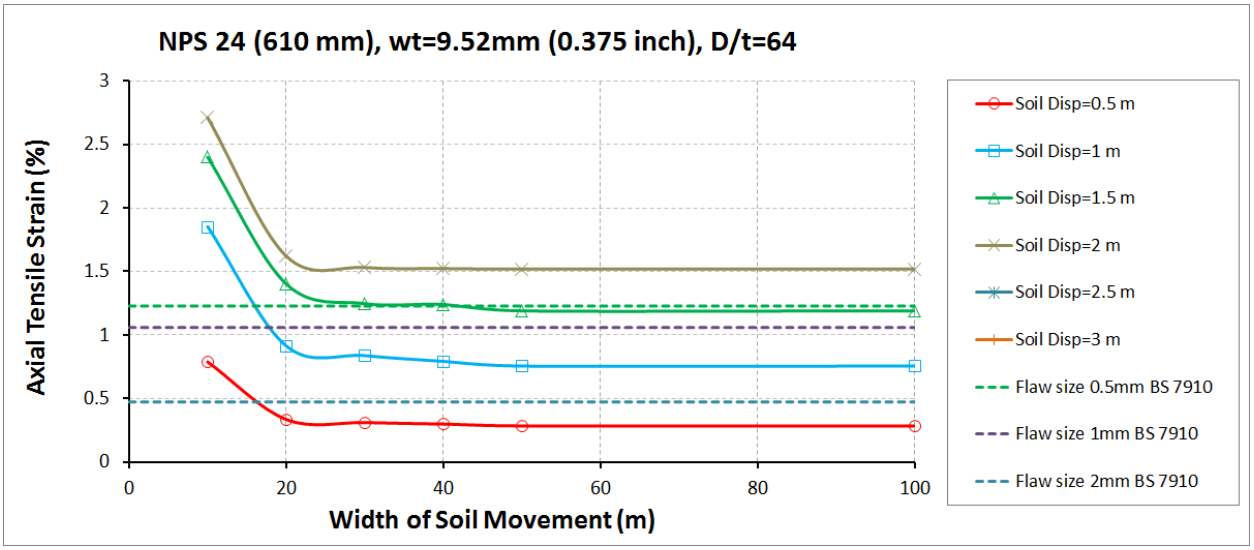

Figure 6.67: Pipe Axial Tensile Strains Envelopes versus Width (W) for Soil Movements of 0.5, 1, 1.5, 2.0 and 2.5 m, n = 0.1

The information contained herein is the copyright of and proprietary to BMT Fleet Technology Limited. Use of this information is governed by the legend on the cover page of this document."

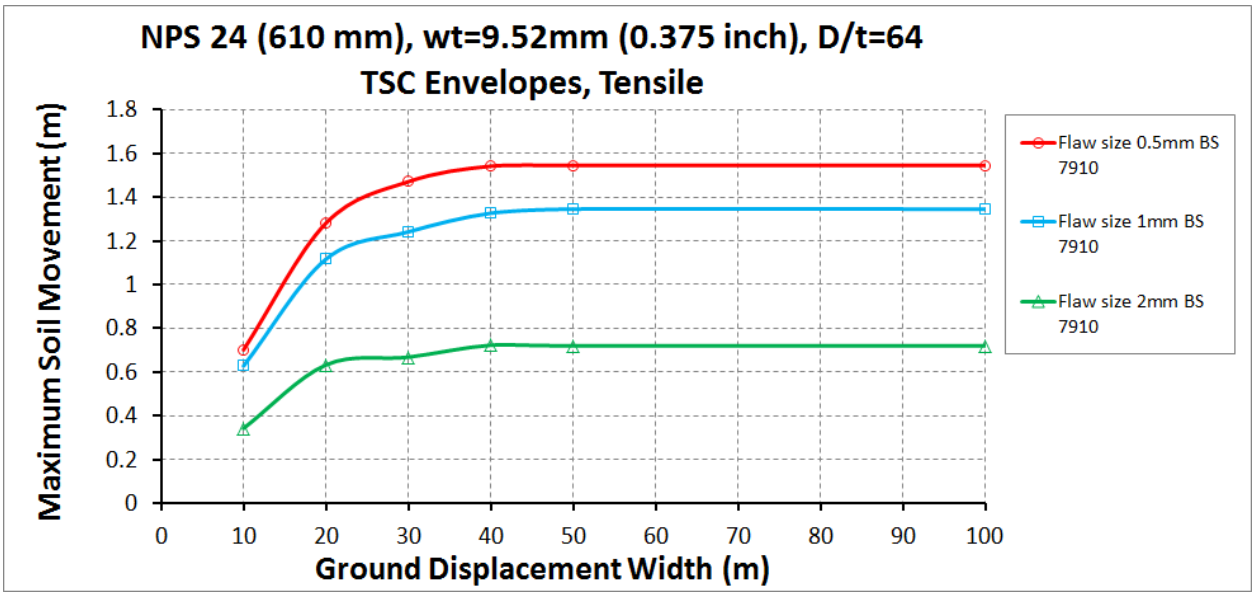

Figure 6.68: Tensile Strain Capacity Envelopes versus Ground Width (W) Movements, n = 0.1

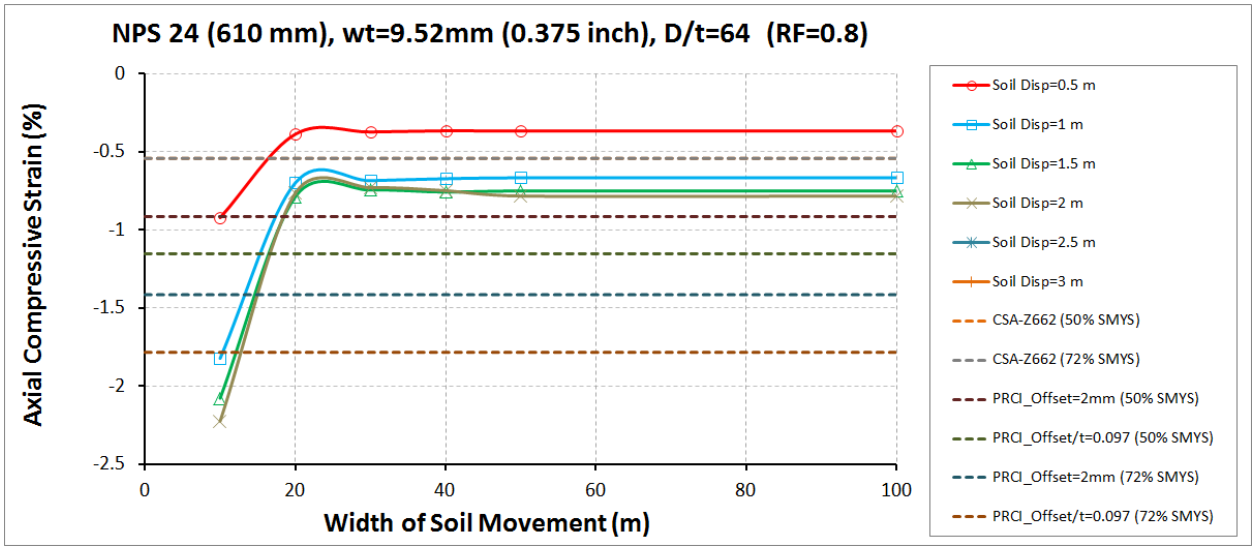

Figure 6.69: Pipe Axial Compressive Strains Envelopes versus Width (W) for Soil Movements of 0.5, 1, 1.5, 2.0 and 2.5 m, n = 0.1

The information contained herein is the copyright of and proprietary to BMT Fleet Technology Limited. Use of this information is governed by the legend on the cover page of this document."

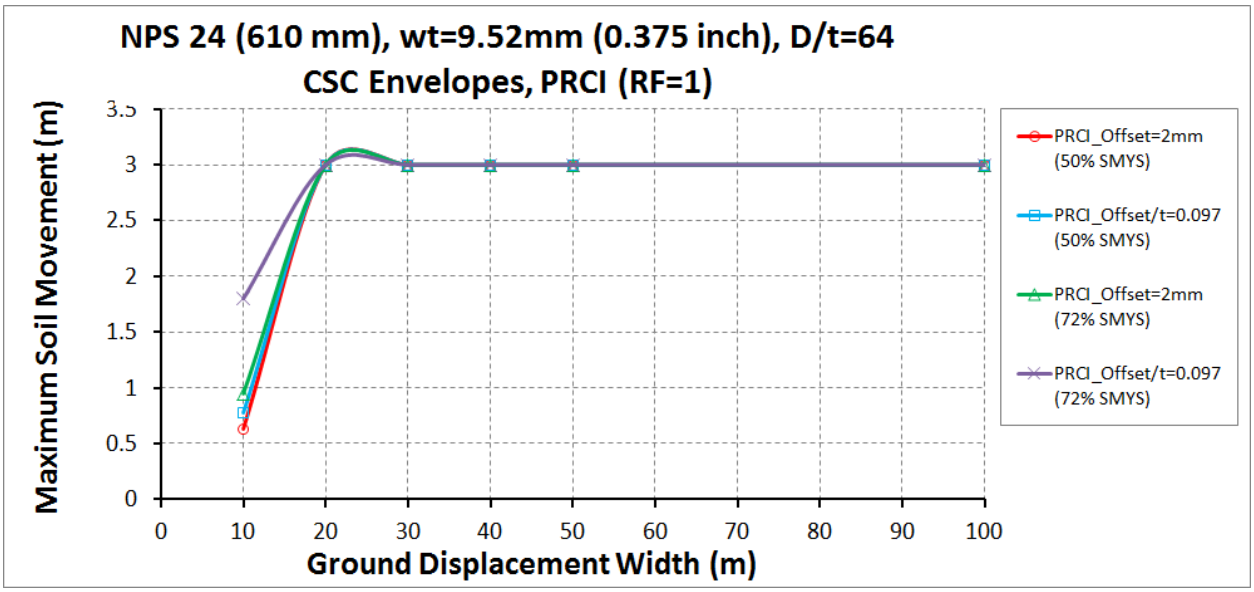

Figure 6.70: Compressive Strain Capacity Envelopes versus Ground Width (W) Movements, n = 0.1

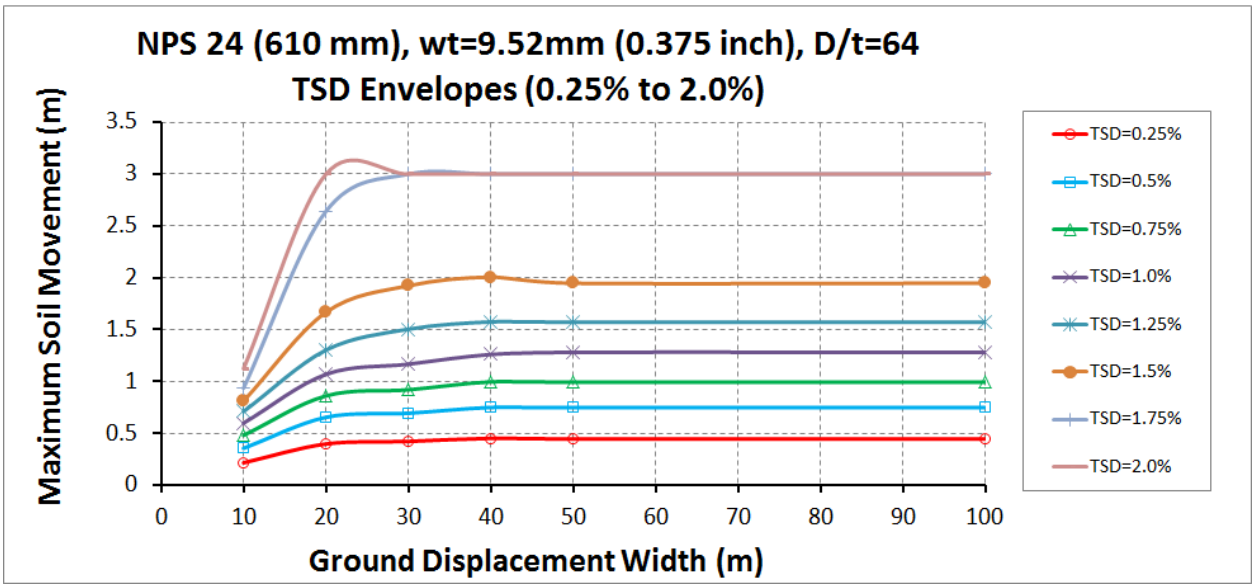

Figure 6.71: Tensile Strain Demand versus Width (W), n = 0.1

The information contained herein is the copyright of and proprietary to BMT Fleet Technology Limited. Use of this information is governed by the legend on the cover page of this document."

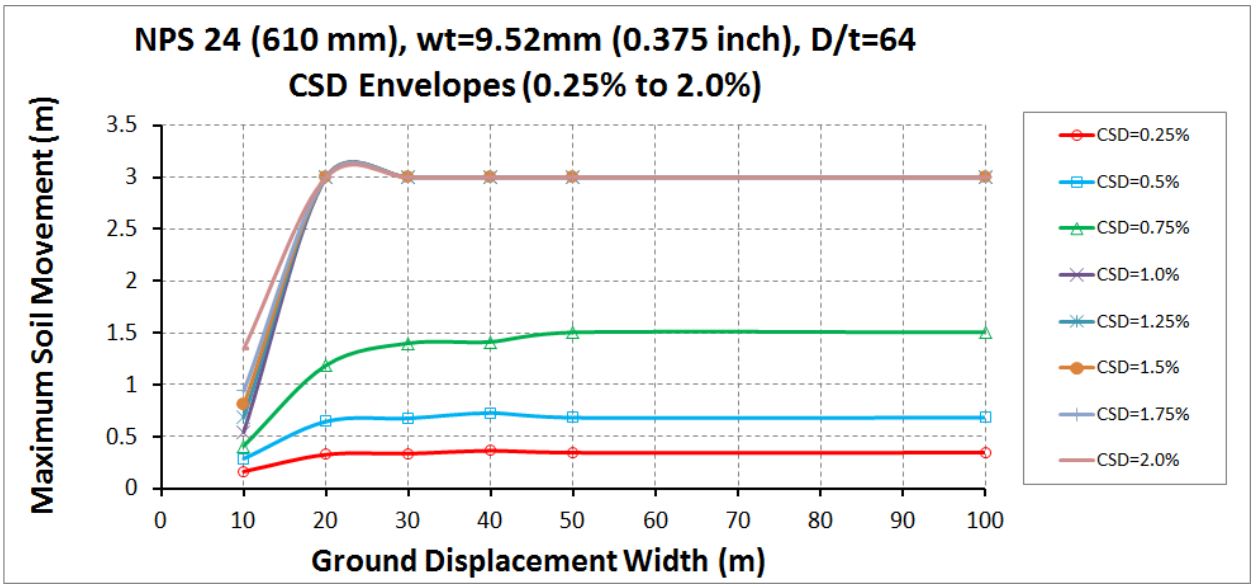

Figure 6.72: Compressive Strain Demand versus Width (W), (n = 0.1)

6.10 Effect of Burial Depth

Comparison between the results of three pipe burial depths of 1.5 m, 1.8 m and 2.1 m considering that the pipeline to be operating at an internal pressure that includes a pipe wall stress of 72% of its SMYS. The results of the analyses for critical width of 20 m (base case) are provided in Figure 6.73 through Figure 6.75. These figures are for X-52 grade NPS 24 (610 mm) pipe with t=9.5 mm (3/8 in) and D/t=64. Figure 6.73 presents the maximum tensile and compressive strains in the pipe versus the maximum ground displacement for critical ground displacement widths of 20 m (66 ft). Figure 6.74 presents the sum of tensile (positive) and compressive (negative) strains in the pipe. The results indicated that increase of the burial depth results in and increase in the maximum computed tensile strains and little effects on the computed compressive strains. The results suggest that axial effects are important in that the tensile strains are larger than compressive strains with burial depth increase.

The information contained herein is the copyright of and proprietary to BMT Fleet Technology Limited. Use of this information is governed by the legend on the cover page of this document."

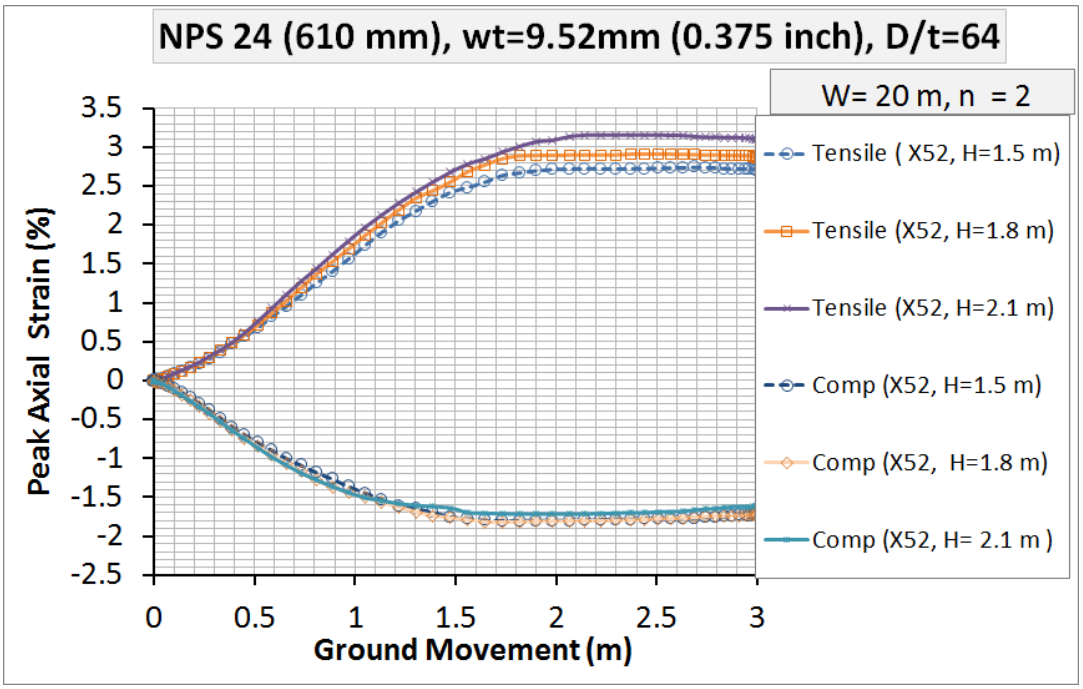

Figure 6.73: NPS 24 (D/t=64) – Maximum Axial Strain vs. Ground Movement for the Critical Widths of 20 m (66 ft)

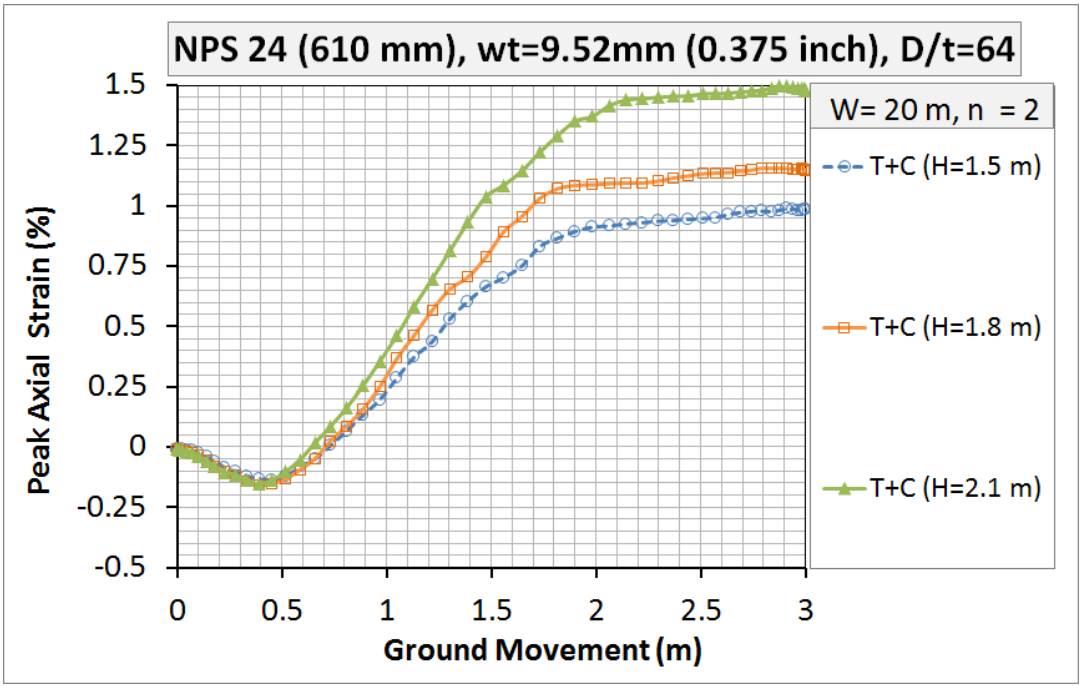

Figure 6.74: NPS 24 (D/t=64) – Sum of the Maximum Tensile and Compressive Strain versus Ground Movement for the Critical Widths of 20 m (66 ft) –Burial Depth Effect

The information contained herein is the copyright of and proprietary to BMT Fleet Technology Limited. Use of this information is governed by the legend on the cover page of this document."

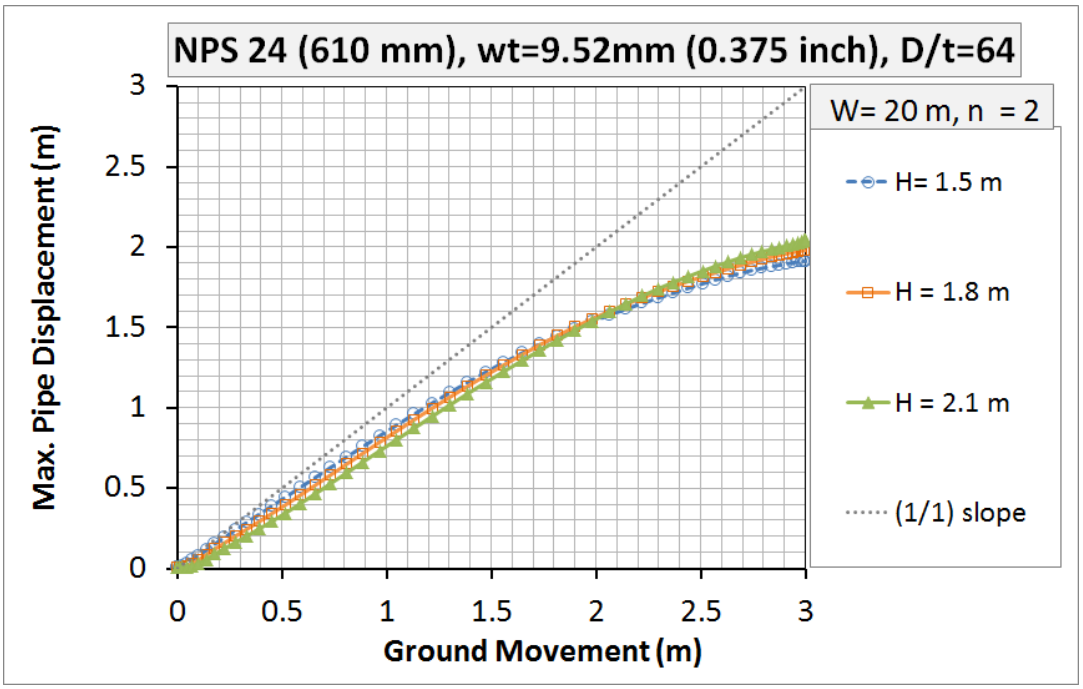

Figure 6.75: NPS 24 (D/t=64) – Maximum Pipe Displacement vs. Ground Movement for the Critical Widths of 20 m (66 ft) – Temperature Effect, Grade X52

6.11 Effect of Slope

In order, to evaluate the effect of slope inclination, the analyzed base case considering a pipeline crossing a slope with an inclination angle of 16 degrees was repeated considering a flat surface.

Figures 6.76 and 6.78 illustrate the simulated displaced position of the pipe and the soil patterns for a pipeline embedded in a flat surface and a pipeline crossing a slope with an inclination angle of 16 degrees, respectively. In the flat surface (Figure 6.53) simulation, the soil surface heave and settlement can be seen on the upstream and downstream sides of the soil flow passing the pipe, respectively. In contrast, for the sloped soil movement crossing a pipeline, the soil surface heaving and subsiding is less pronounced. This reduction in vertical soil displacement is due to the soil tending to move as a more coherent mass due to gravity and the applied soil displacement in the lateral and vertical directions.

The information contained herein is the copyright of and proprietary to BMT Fleet Technology Limited. Use of this information is governed by the legend on the cover page of this document."

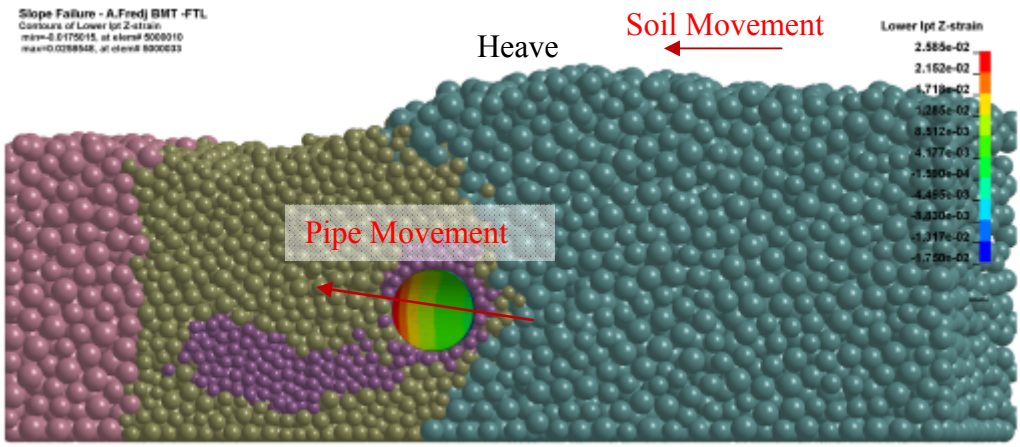

Figure 6.76: Pipe and Soil Deformation for Maximum Soil Movement of 3 m

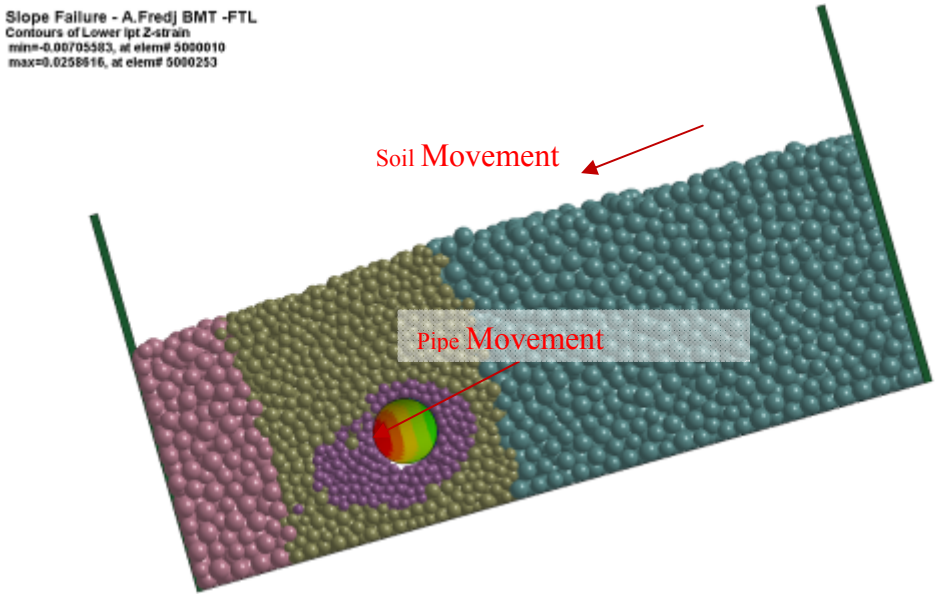

Figure 6.77 Pipe and Soil Deformation for Maximum Soil Movement of 3 m Considering Slope of 16 Deg.

Figures 6.79 and 6.80 present the maximum tensile and compressive strains in the pipe versus the maximum ground displacement for various ground displacement widths considered in the analyses. The width of 20 m (66 ft) results in the largest tensile and compressive strain for pipeline crossing slope with an inclination angle of 16 degrees similar to pipeline embedded in flat surface.

Figure 6.80 compares the maximum tensile and compressive strains in the pipe versus the maximum ground displacement for critical ground displacement widths of 20 m (66 ft) for a pipeline embedded in a flat surface (base case) and a pipeline crossing a slope with an inclination angle of 16 degrees. The results indicate that slope inclination of 16 degrees has almost no effect on compressive axial strain with slightly higher tensile strain.

The information contained herein is the copyright of and proprietary to BMT Fleet Technology Limited. Use of this information is governed by the legend on the cover page of this document."

Figure 6.81 shows maximum pipe displacement versus the maximum ground displacement. The maximum pipe displacement follows the ground displacement up to certain ground displacement than the pipe displacement increase slowly with ground displacement, which results in slowly increase in pipe strains. The results indicated that higher slope inclination results in larger pipe displacement.

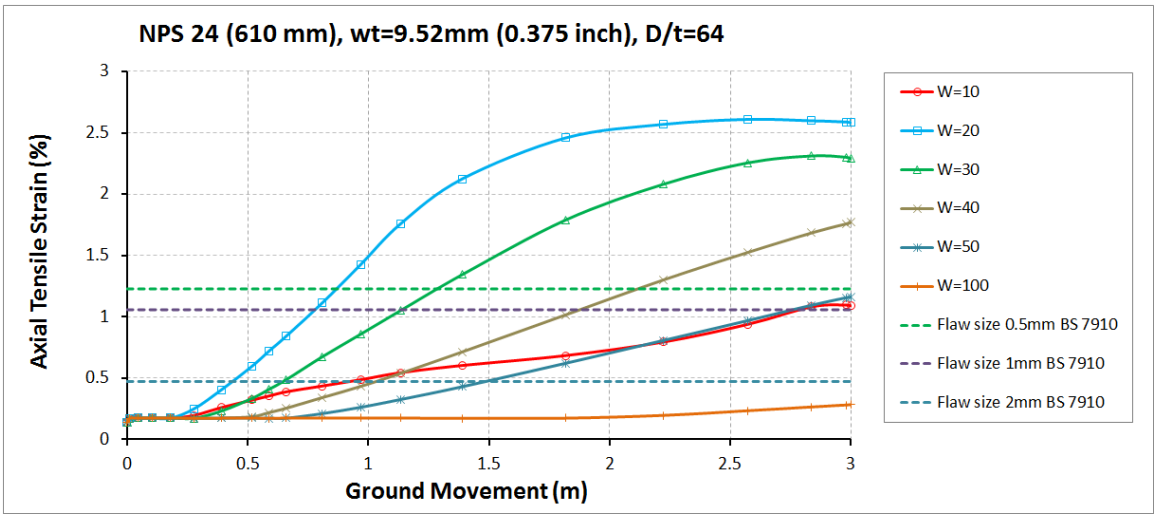

Figure 6.78: NPS 24 (D/t=64) - Maximum Tensile in the Pipe versus Ground Movement Widths: [10-100 m]

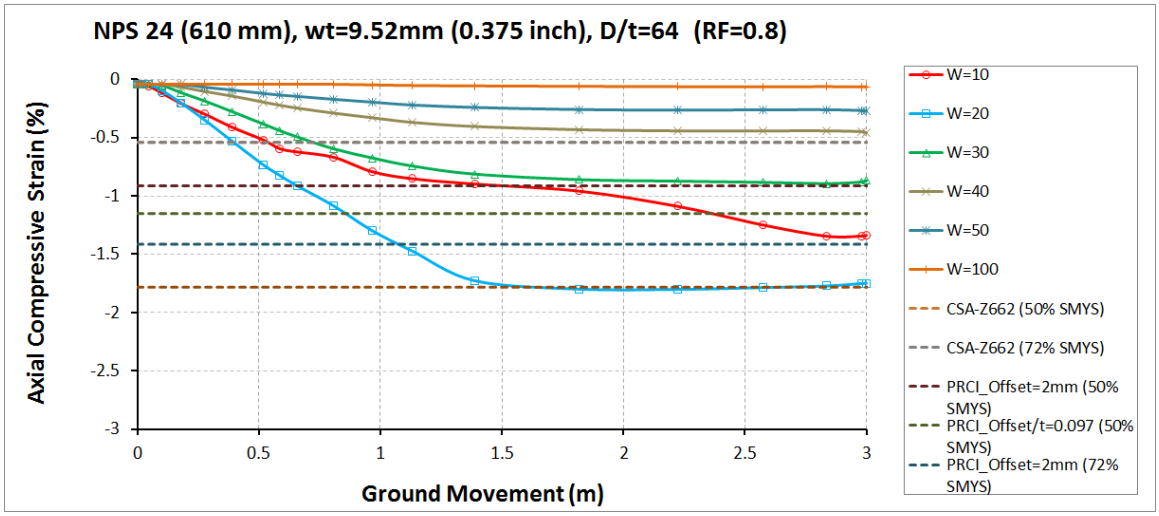

Figure 6.79: NPS 24 (D/t=64) - Maximum Tensile in the Pipe versus Ground Movement Widths: [10-100 m]

The information contained herein is the copyright of and proprietary to BMT Fleet Technology Limited. Use of this information is governed by the legend on the cover page of this document."

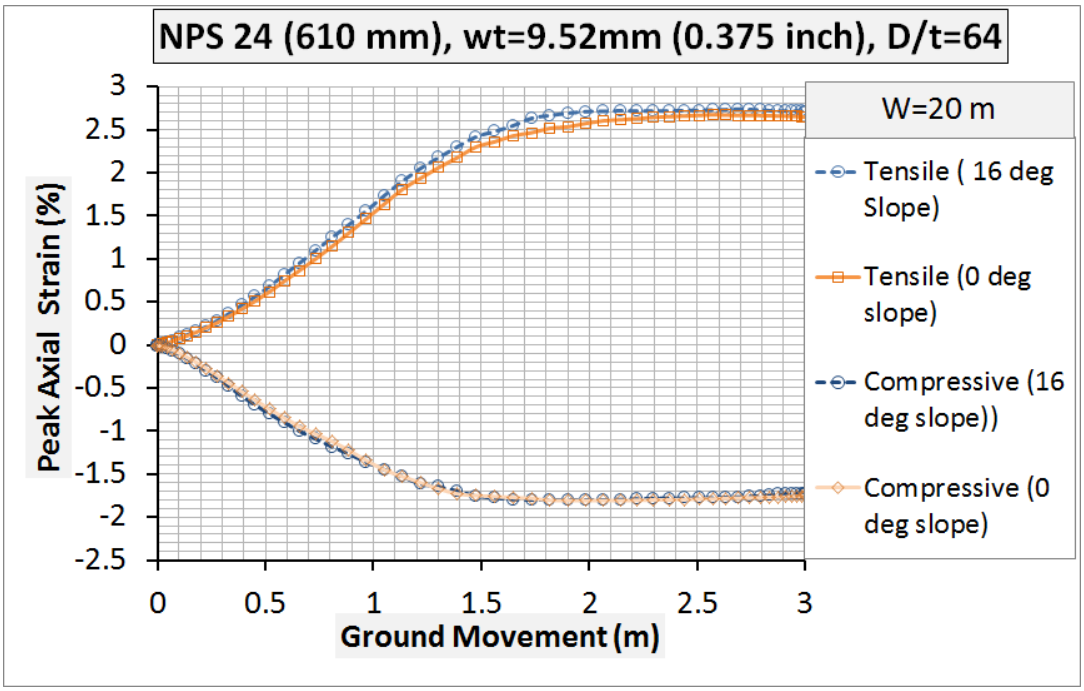

Figure 6.80: NPS 24 (D/t=64) – Maximum Axial Strain versus Ground Movement for the Critical Widths of 20 m (66 ft)

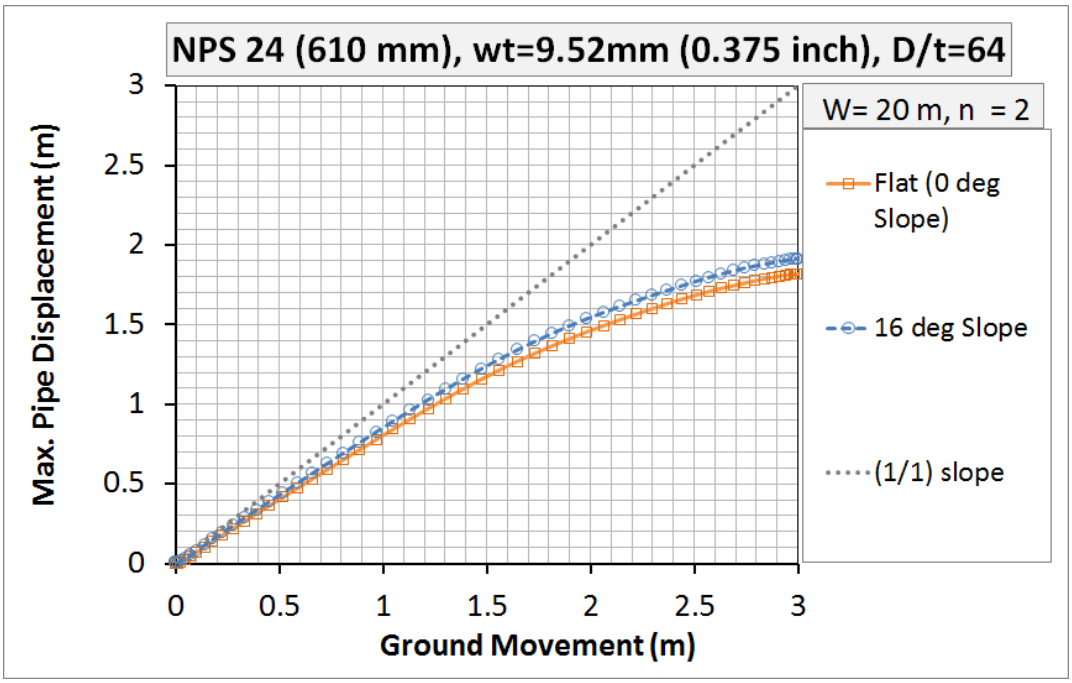

Figure 6.81: NPS 24 (D/t=64) –Maximum Pipe Displacement versus Ground Movement for the Critical Widths of 20 m (66 ft)

The information contained herein is the copyright of and proprietary to BMT Fleet Technology Limited. Use of this information is governed by the legend on the cover page of this document."

6.11.1 Comparison with Strain Capacity and Strain Demand Envelopes

6.11.1.1 Tensile Strain Capacity Envelopes (TSCE)

Figure 6.82 present the maximum tensile strains in pipe versus the ground displacement width (W) for given ground displacement of 0.5, 1.0, 1.5, 2.0 and 2.5. In this figure, the BS-7910 tensile strain capacity is presented with dash horizontal line. Any tensile strain above the horizontal line is strain-related failure limit.

The TSC envelopes based on BS7910 guidance are presented in Figure 6.83. The envelopes describe the maximum soil displacement and ground displacement width breakout the TSC envelopes, which represents the tensile strain-related failure limit, according to BS 7910.

The results indicate that for this pipe and operating condition combination, the ground movement width of 20 m (66 ft) can be considered critical. The tensile strain-related failure limit for the critical width is reached for ground displacement from 0.44 to 0.87 m considering a flaw size of 2, 1 and 0.5 mm, respectively.

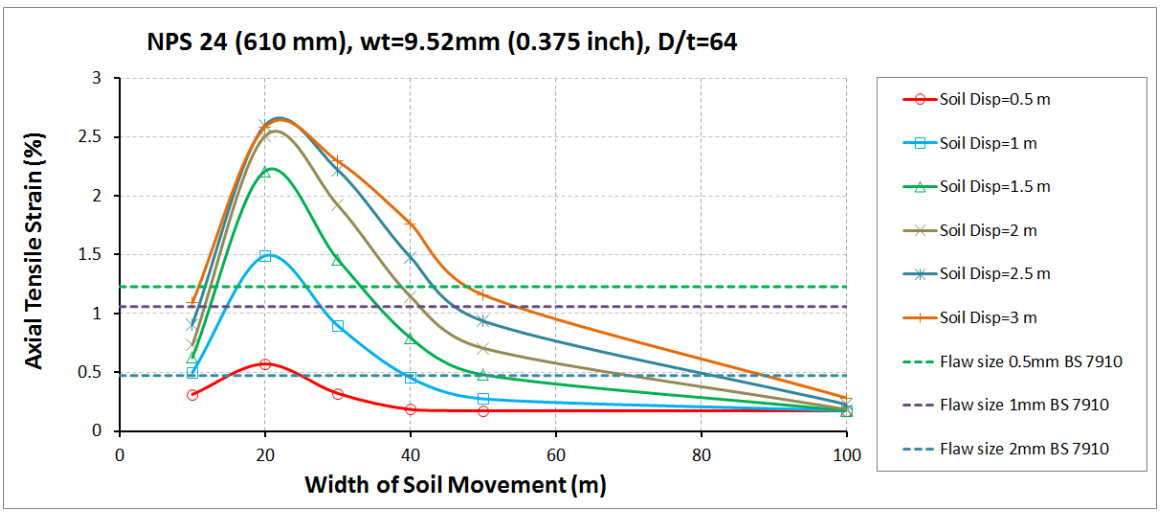

Figure 6.82: Pipe Axial Tensile Strains Envelopes versus Width (W) for Soil Movements of 0.5, 1, 1.5, 2.0 and 2.5 m, Material Grade X70

The information contained herein is the copyright of and proprietary to BMT Fleet Technology Limited. Use of this information is governed by the legend on the cover page of this document."

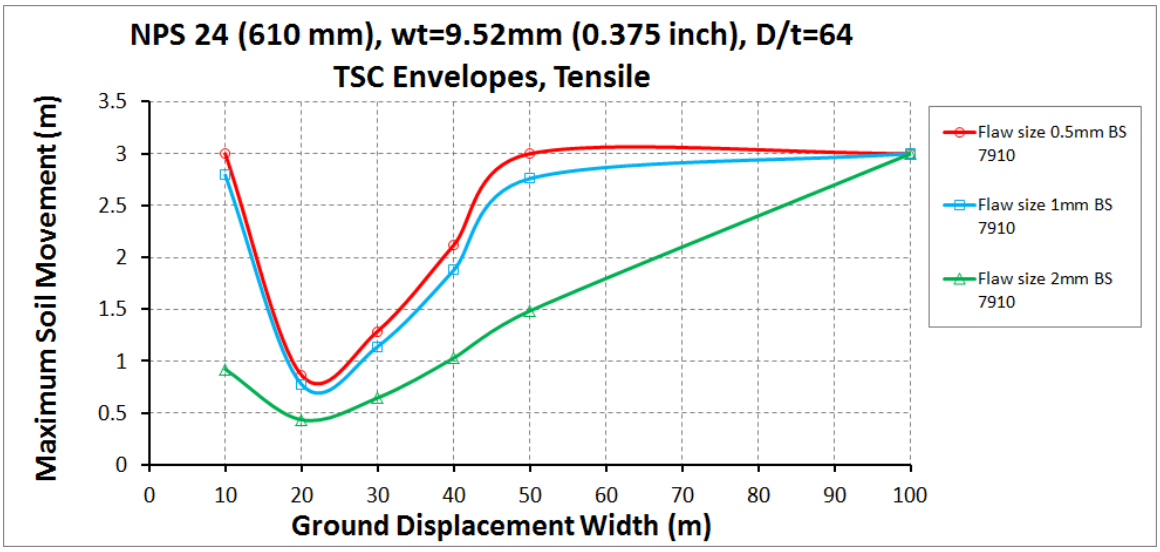

Figure 6.83: Tensile Strain Capacity Envelopes versus Ground Width (W) Movements, Grade X52

6.11.1.1.1 Compressive Strain Capacity Envelopes (CSCE)

Figure 6.84 presents the maximum nominal compressive strain in the pipe versus the ground displacement width (W) for given ground displacement of 0.5, 1.0, 1.5, 2.0 and 2.5. The nominal compressive strain is defined as the average compressive strain measured over a gauge length of 2D (D is the pipe outside diameter). In this figure, the CSA and PRCI compressive strain capacity is presented with dash horizontal line.

The envelopes presented in Figure 6.84 describe the pipe compressive strain demands in the pipe for a given ground displacement and ground width. In this figure, the CSA and PRCI compressive strain capacity is presented with dash horizontal line. Any compressive strain above the horizontal line is strain-related failure limit.

The information contained herein is the copyright of and proprietary to BMT Fleet Technology Limited. Use of this information is governed by the legend on the cover page of this document."

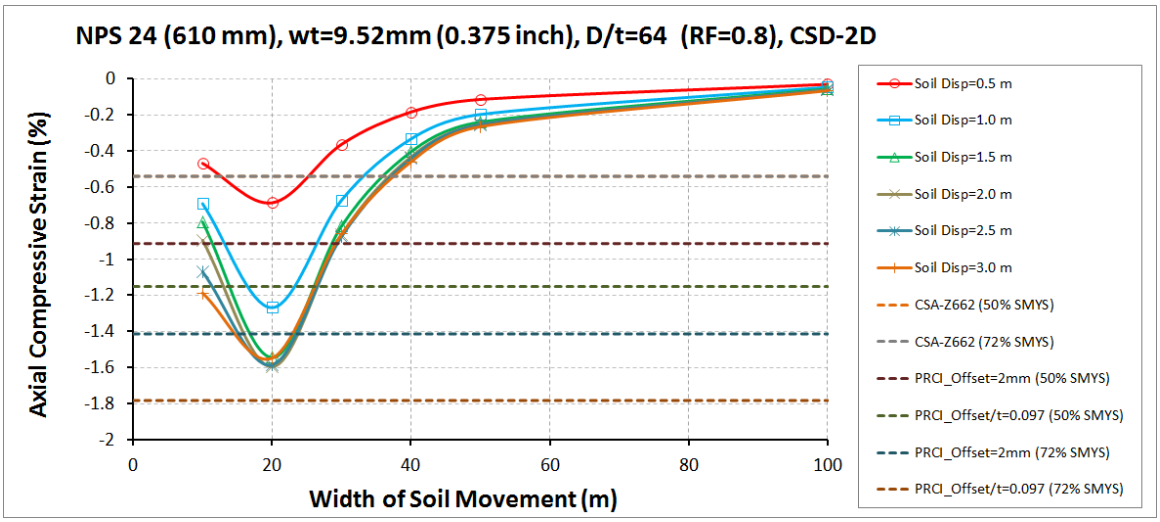

Figure 6.84: Pipe Axial Compressive Strains Envelopes (X70) versus Width (W) (for Soil Movement of 0.5, 1, 1.5, 2.0 and 2.5 m), Grade X70

Similar to the tensile strain capacity (TSC) envelopes, the results were used to generate compressive strain capacity (CSC) envelopes based on PRCI Guidance. These CSC envelopes are presented in Figure 6.85. The envelopes describe the maximum soil displacement and ground displacement width breakout the CSC envelopes, which represents the tensile strain-related failure limit, according to CSA and PRCI Guidance.

For example, as shown in Figure 6.86, the compressive strain-related failure limit for the critical width of 20 m (66 ft) is reached for ground displacement from 0.68 to 1.16 m considering girth weld misalignment (offset) of 2 mm and the pipeline to be operating at an internal pressure that induces a pipe wall stress of 50% and 72% of its SMYS, respectively.

The information contained herein is the copyright of and proprietary to BMT Fleet Technology Limited. Use of this information is governed by the legend on the cover page of this document."

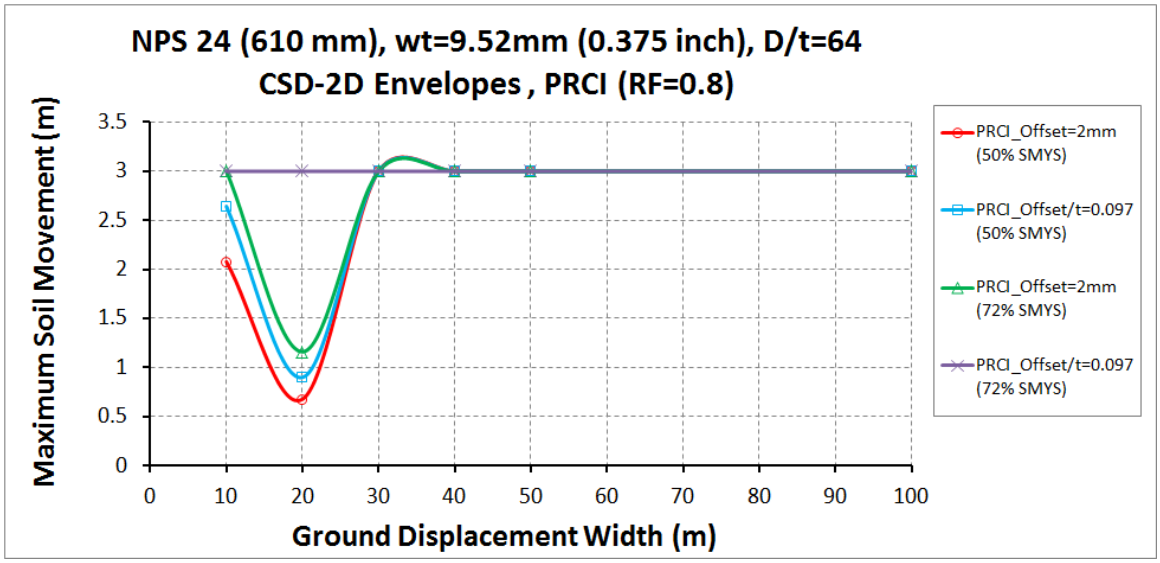

Figure 6.85: Compressive Strain Capacity Envelopes versus Ground Width (W) Movements, Grade X52

6.11.1.1.2 Strain Demand Envelopes (SDE)

In the previous section, the strain demands determined from the analysis was compared with the calculated strain capacity defined from the guidance; BS 7910 for tensile strain, and CSA Z662 and PRCI for compressive strain. While there are many existing models for calculating the compressive and tensile strain capacity in codes and standards, it was decided to develop a simple a strain-based design methodology that can be easily adapted to any code and standards, which is the purpose of this section.

The tensile and compressive strain demand envelopes along the longitudinal direction of the pipeline are presented in Figure 6.86 and Figure 6.87. These figures show the maximum soil displacement versus ground width displacement as a series of 'envelopes' for a given pipe tensile and compressive strain demands of 0.25%, 0.5%, 0.75%, 1%, 1.25%, 1.5%, 1.75% and 2%. The safe pipeline operating goal of pipeline subjected to lateral ground displacement is to stay within the normal operating strain range defined by codes and standards.

The information contained herein is the copyright of and proprietary to BMT Fleet Technology Limited. Use of this information is governed by the legend on the cover page of this document."

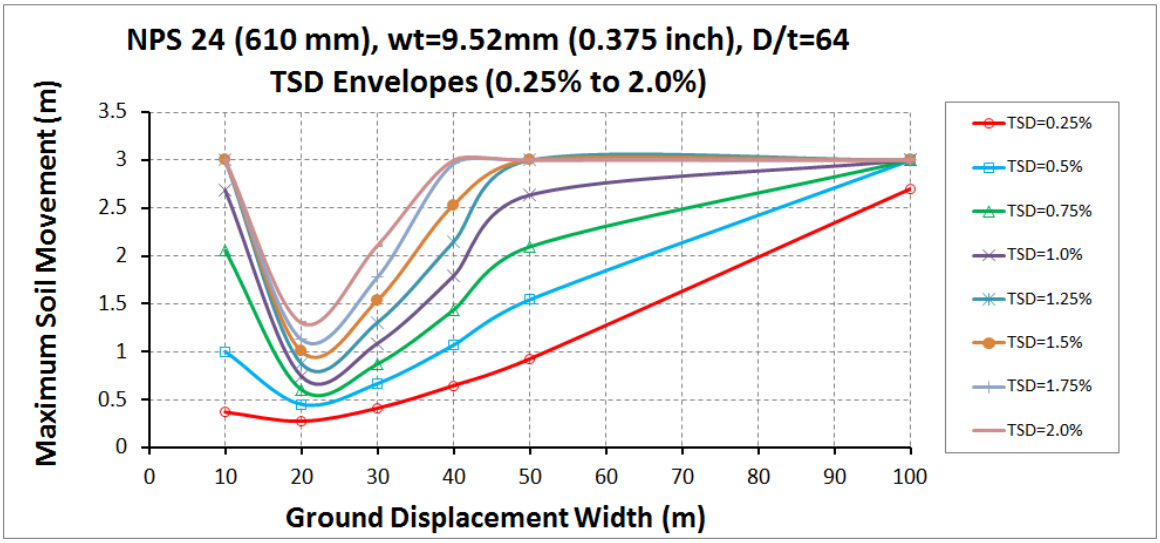

Figure 6.86: Tensile Strain Demand versus Width (W), Grade X52

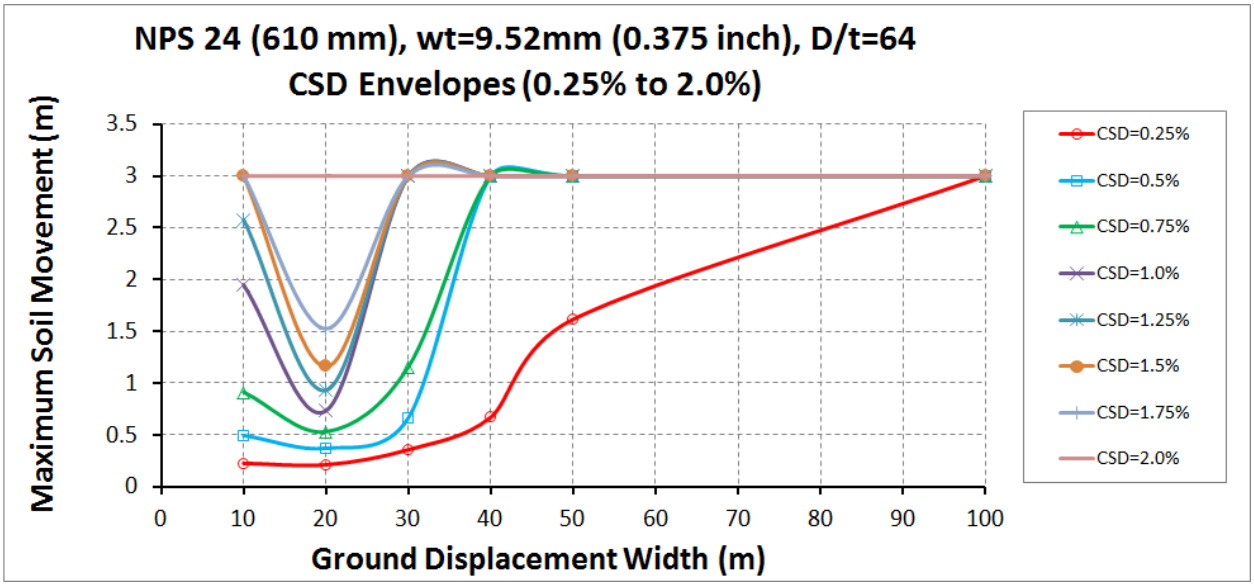

Figure 6.87: Compressive Strain Demand Envelopes versus Width (W), Grade X52

6.12 Effect of Soil Properties

In order to evaluate the effect of soil properties, the base case was simulated considering to alternate soils as follows:

- Soil 1: Properties consistent with a Sand ($\phi'=30^o$ and C'=5 kPa)
- Soil 2: Properties consistent with a Clay ($\phi'=20^o$ and C'=20 kPa)

The information contained herein is the copyright of and proprietary to BMT Fleet Technology Limited. Use of this information is governed by the legend on the cover page of this document."

Figure 6.88 presents the maximum tensile and compressive strains in the pipe versus the maximum ground displacement for the two alternate soil types. The results clearly show that the strains are not significantly affected by the change in soil properties.

Figure 6.89 also presents the sum of tensile (positive) and compressive (negative) strains in the pipe. The results suggest that axial effects are important in that the tensile strains are larger than compressive strains with stiffer soil.

The soil displacement patterns of the two soil types are illustrated in Figure 6.90. The clay tends to hold its shape and forms a cavity behind the pipe and this higher stiffness clay results in greater vertical pipe movement.

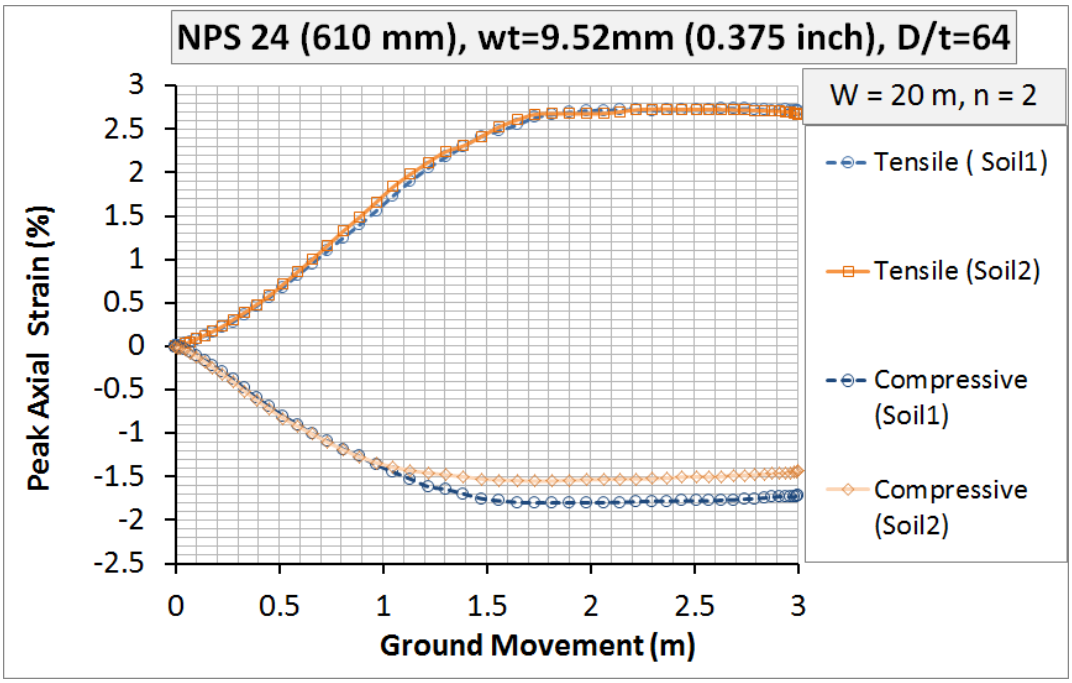

Figure 6.88: NPS 24 (D/t=64) – Maximum Axial Strain versus Ground Movement for the Critical Widths of 20 m (66 ft) – Soil 1 and 2

The information contained herein is the copyright of and proprietary to BMT Fleet Technology Limited. Use of this information is governed by the legend on the cover page of this document."

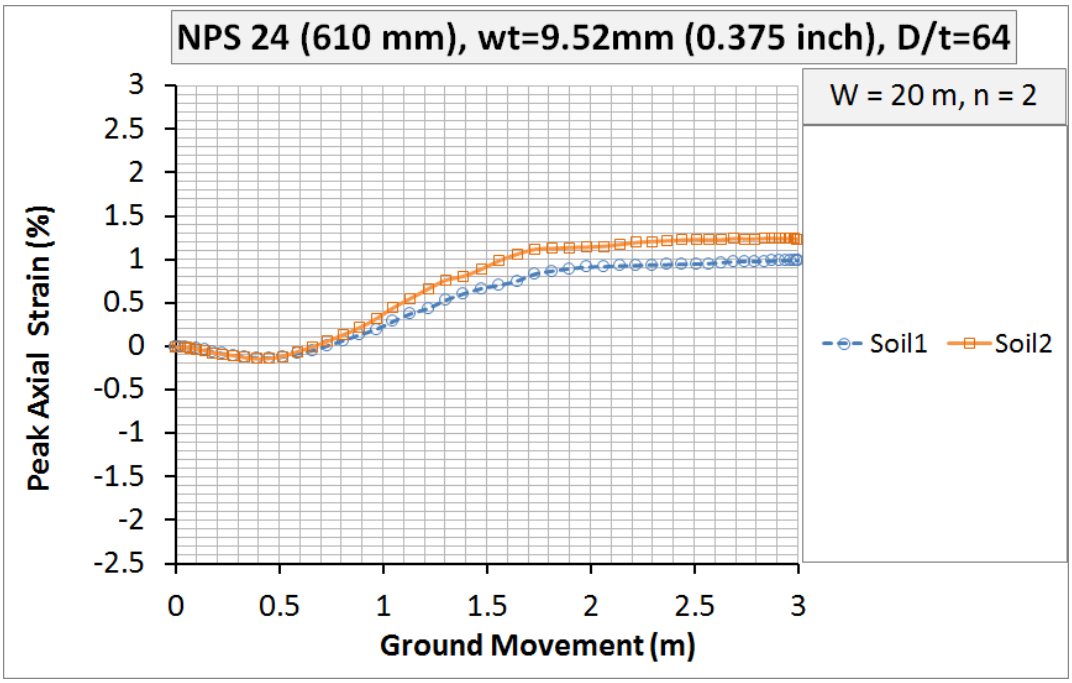

Figure 6.89: NPS 24 (D/t=64) – Sum of Maximum Axial Compressive and Tensile Strains versus Ground Movement for the Critical Widths of 20 m (66 ft) – Soil 1 and 2

The information contained herein is the copyright of and proprietary to BMT Fleet Technology Limited. Use of this information is governed by the legend on the cover page of this document."

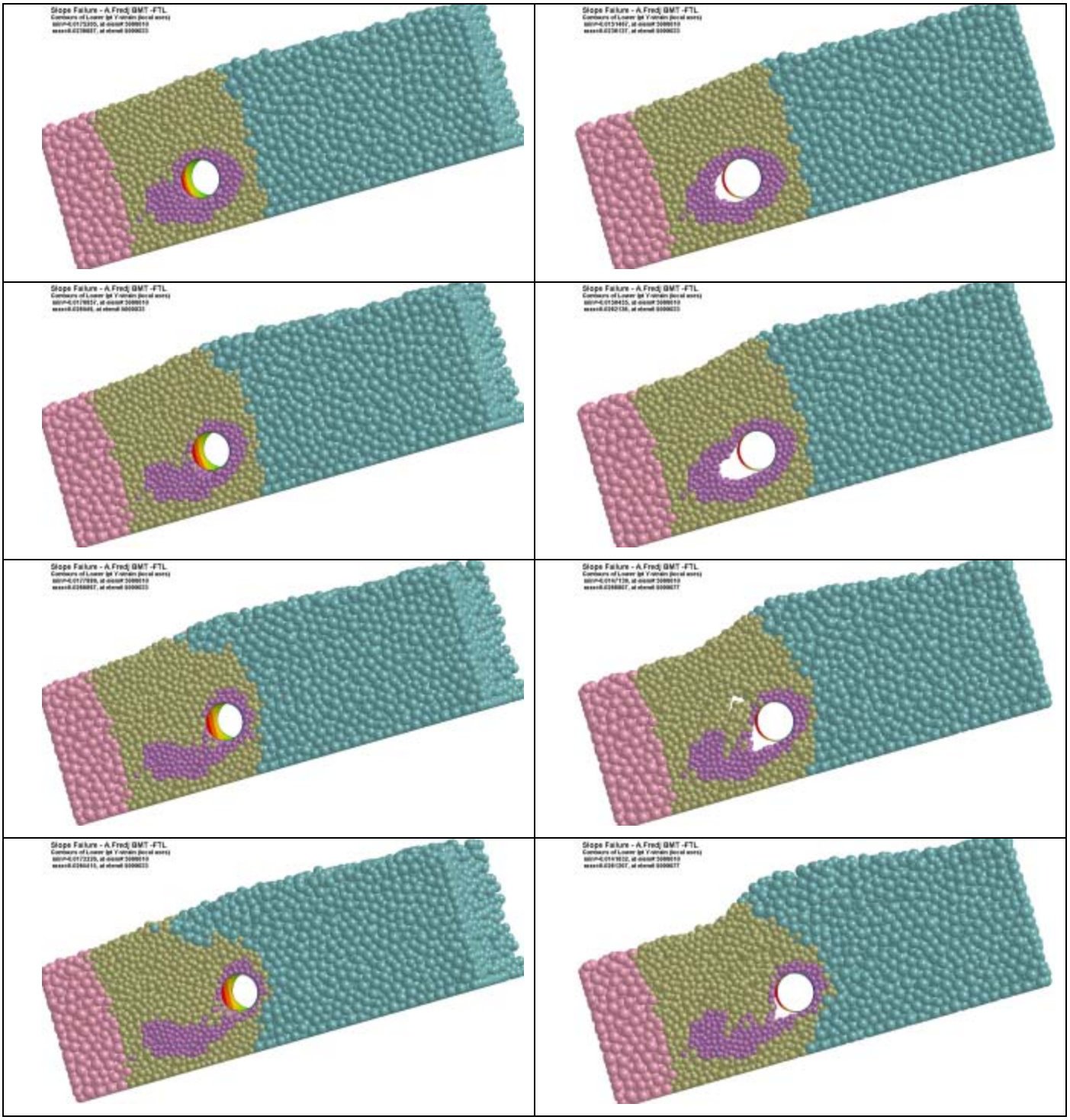

Figure 6.90: Pipe Soil Deformation Left (sand), Right clay (soil displacement 1.5, 2, 2.5 and 3 m)

The information contained herein is the copyright of and proprietary to BMT Fleet Technology Limited. Use of this information is governed by the legend on the cover page of this document."

6.13 Effect of Soil to Pipe Friction

The pipe-soil force-displacement responses are sensitive to pipe-soil interaction and there is much uncertainty associated with interface friction between the pipe material and soil. Ligon et al.,[49] conducted static friction tests to determine the coefficient of friction between coal tar felt and thin film epoxy pipe coating and eight representative backfill soil samples along pipeline. Ligon et al., reported that the friction coefficients are significantly higher than those extrapolated from literature. For coal tar felt coating, the coefficient varied from 0.59 to 0.91 (corresponding to a friction angle of 30° to 42°) depending on the soil and moisture content. The thin film epoxy coating friction coefficient varies from 0.51 to 0.71 (corresponding to friction angle of 27° to 35°) under the same conditions.

The effects of the coefficient of friction for pipe coating materials were investigated by considering three different friction values, 0.32, 0.56 and 0.72 corresponding to friction angles of 20°, 30° and 36°.

The results of the analyses for critical width of 20 m (base case) are provided in Figure 6.91 and Figure 6.92. These figures are for X-52 grade NPS 24 (610mm) pipe with t = 9.5 mm (3/8 in) and D/t=64. Figure 6.91 presents the maximum tensile and compressive strains in the pipe versus the maximum ground displacement for critical ground displacement widths of 20 m (66 ft). Figure 6.92 presents the sum of tensile (positive) and compressive (negative) strains in the pipe. The results indicated that increase in the coefficient of friction for pipe coating materials results in decrease in the maximum computed compressive strains. The results also indicate that the tensile strains are higher than compressive strains. This differential in peak tensile strains and compressive strains increase with increasing the friction coefficient. This suggests that a significant uniform strain in the pipe along the longitudinal direction of the pipe due to friction and catenary effect.

The information contained herein is the copyright of and proprietary to BMT Fleet Technology Limited. Use of this information is governed by the legend on the cover page of this document."

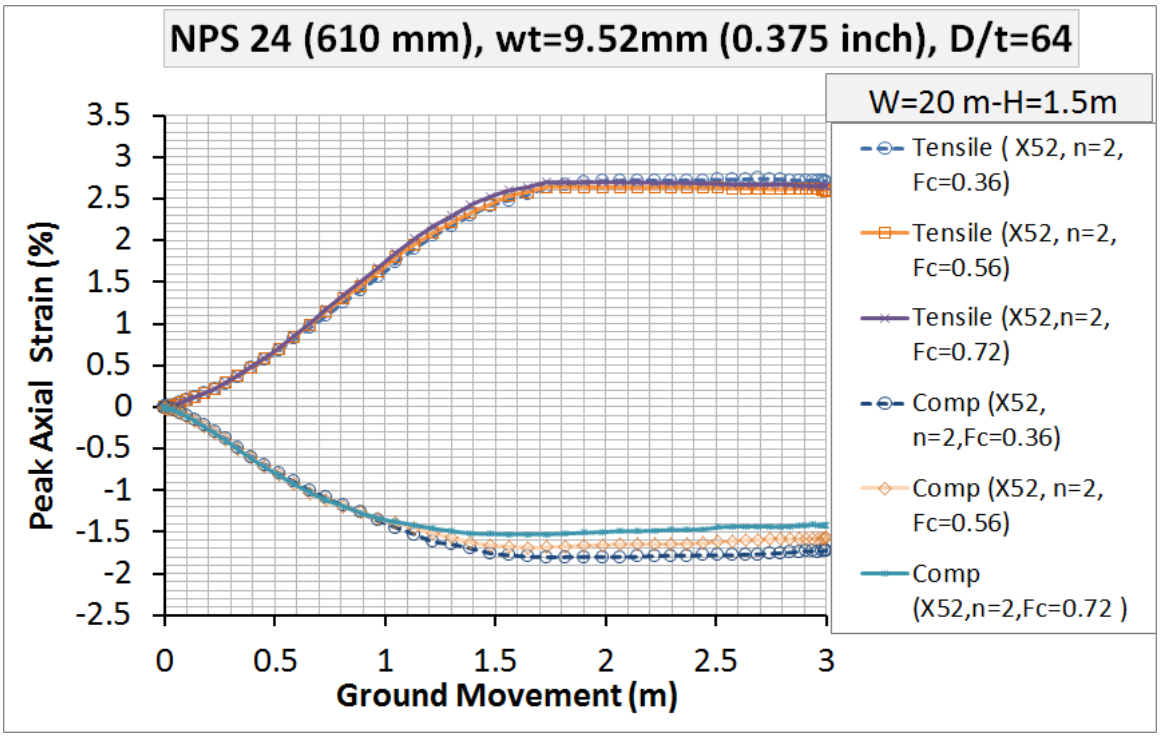

Figure 6.91: NPS 24 (D/t=64) – Maximum Axial Strain versus Ground Movement for the Critical Widths of 20 m (66 ft) – Friction 0.32, 0.56 and 0.72

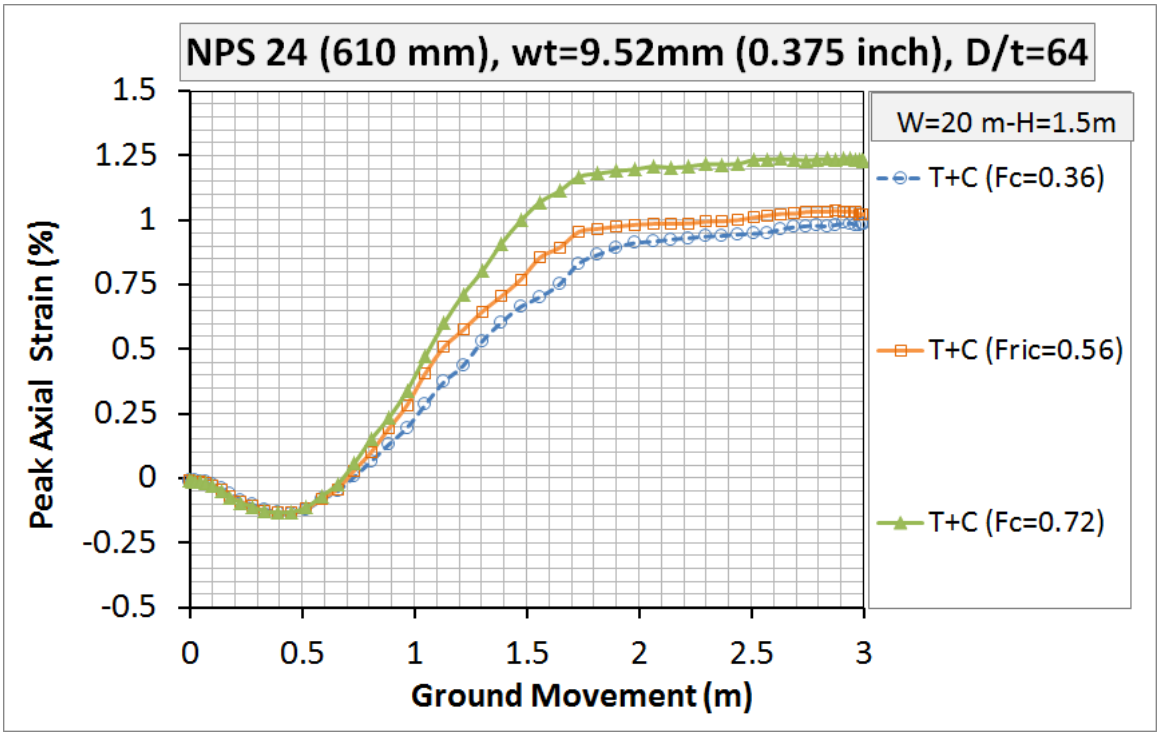

Figure 6.92: NPS 24 (D/t=64) – Sum of the Maximum Axial Tensile and Compressive Strains versus Ground Movement for the Critical Widths of 20 m (66 ft) – Friction 0.32, 0.56 and 0.72

The information contained herein is the copyright of and proprietary to BMT Fleet Technology Limited. Use of this information is governed by the legend on the cover page of this document."

6.14 Structural Analyses for a 12-Inch Pipeline

Analyses were completed for the NPS 12 (324 mm outside diameter) pipeline to assess its response to lateral ground movement and to determine the structural integrity significance of ground movement induced strain demands. A sensitivity analysis was conducted to evaluate the of D/t ratio and ground width displacement. The analyses considered 18 lateral ground movement scenarios. The scenarios included the following:

- Pipe wall thickness: three wall thicknesses: 4.57 mm (0.18 in), 6.35 mm (0.25 in) and 9.52 mm (0.375 in); corresponding to D/t ratio of 71, 51 and 34 respectively;
- Ground displacement direction: Perpendicular (lateral) to the pipeline axis;
- Width of ground displacement (W): Six potential ground movement failures with a total estimated width of failure perpendicular to the pipeline varying from 10 to 100m (10, 20, 30, 40 50 and 100 m);
- Shape of ground displacement: one ground displacement pattern initiated using a cosine function raised to the power "n=2";
- One soil conditions sand/clay till;
- Pipe slope: one slopes, 16 deg.;
- Pipeline burial depth: one depth of 1.2m (4 ft) to top pipe, corresponding to 1.36 m (4.5 ft), depth to pipe center line; and
- The lateral ground deformation was initiated using a cosine function raised to the power "n" similar to Suzuki et al. (1988) and M. O'Rourke (1989) function.

Assumptions for the pipeline were as follows:

- 72% SMYS internal pressure;
- 45°C thermal differential (installation -20°C, max operating temperature 25°C); and
- A generic stress strain curves for Grade X-52 (359) pipe according to the API 5L

6.14.1 12-Inch Pipeline Results

The results presented in Appendix D, illustrate the importance of the width of the ground displacement. The critical width which results in the largest tensile strain in the pipe for any given value of ground is about 10 m (33 ft) for the three analyzed D/t's (71, 51 and 31).

Figure 6.93 shows the maximum tensile and compressive strains in the NPS 12 (609 mm) pipe along the longitudinal direction as function of the centerline (maximum) soil displacement for the critical width of 10 m (33 ft). Figure 6.94 presents the sum of the tensile and compressive strains. The results are for X52 grade, and D/t's (71, 51 and 31).

The results indicated that pipeline with higher D/t ratio (lower pipe wall thickness) results in higher computed tensile and compressive strains with higher compressive strain than tensile

The information contained herein is the copyright of and proprietary to BMT Fleet Technology Limited. Use of this information is governed by the legend on the cover page of this document."

strain. The strains ranged from +3.6% and -4.32% for 4.57 mm (0.18 inch) wall thickness to +3.17% and -2.6% for 6.35 mm (0.25 inch) wall thickness while for 9.52 mm (0.375 inch) the corresponding strain range is +2.65% and -2.50%. The pipe with 4.57 mm (0.18 inch) wall exceeds the compressive strain limit and buckle/wrinkle at 3.5% local compressive strain or 2.12% nominal compressive strain for soil displacement of 1.1 m.

Figure 6.95 presents the maximum pipe displacement versus ground displacement. The results show that pipeline with higher D/t ratio (lower pipe wall thickness) results in higher pipe displacement.

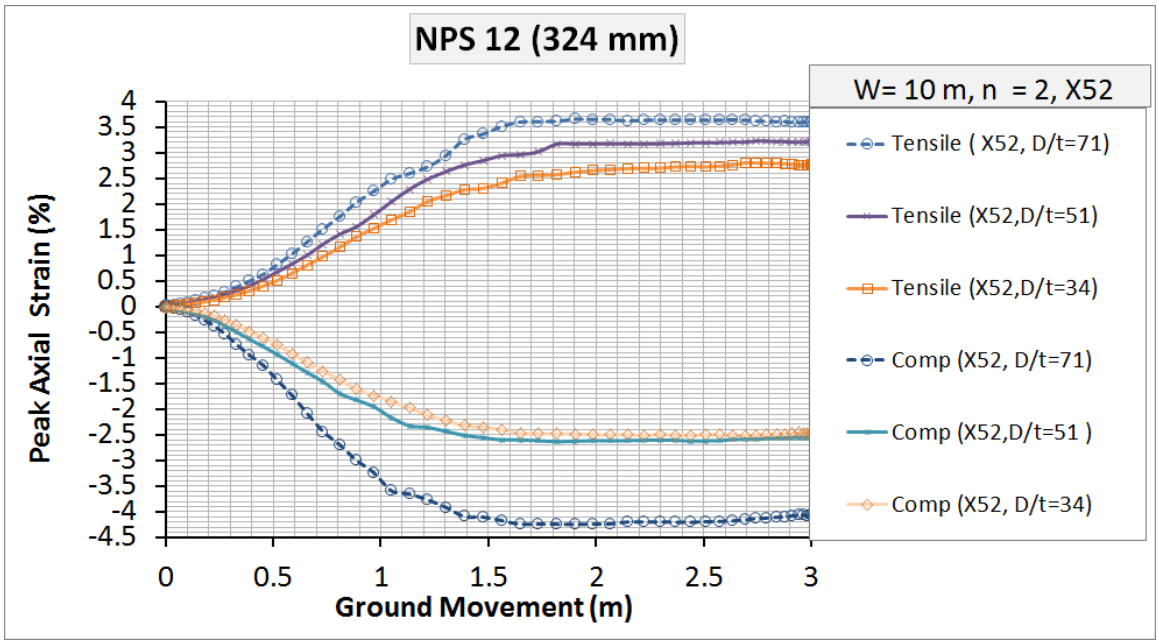

Figure 6.93: NPS 12 (D/t =71, 51 and 34) – Maximum Axial Strain versus Ground Movement for the Critical Widths of 10 m (33 ft)

The information contained herein is the copyright of and proprietary to BMT Fleet Technology Limited. Use of this information is governed by the legend on the cover page of this document."

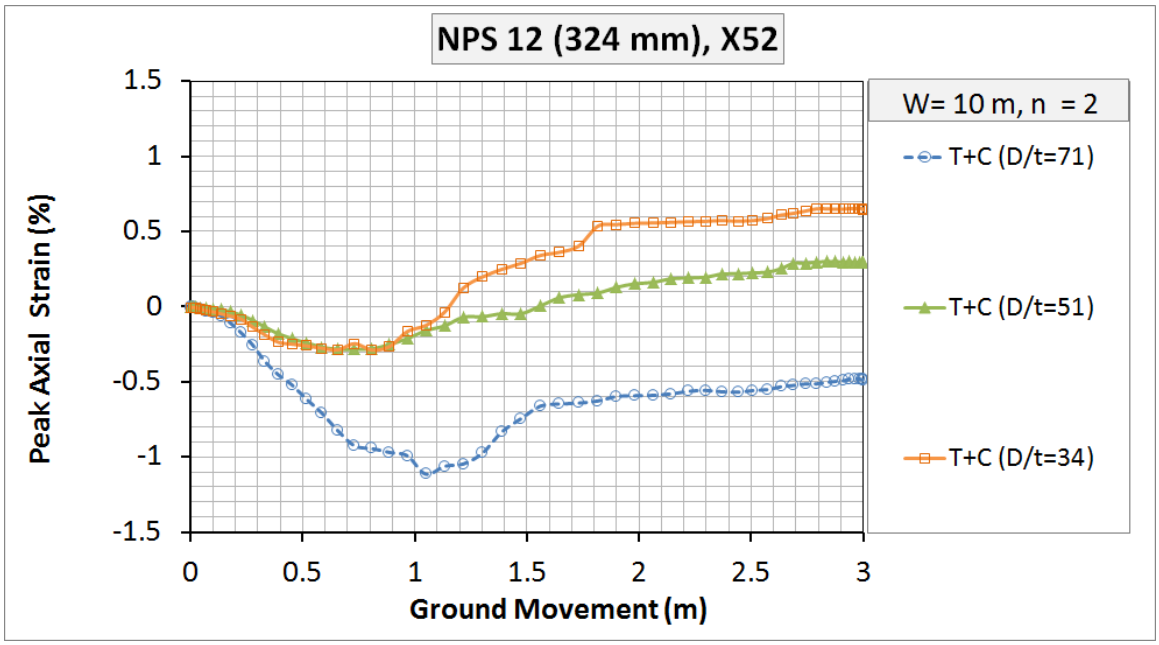

Figure 6.94: NPS 12 (D/t =71, 51 and 34) – Sum of Maximum Axial Tensile and Compressive Strain versus Ground Movement for the Critical Widths of 10 m (33 ft)

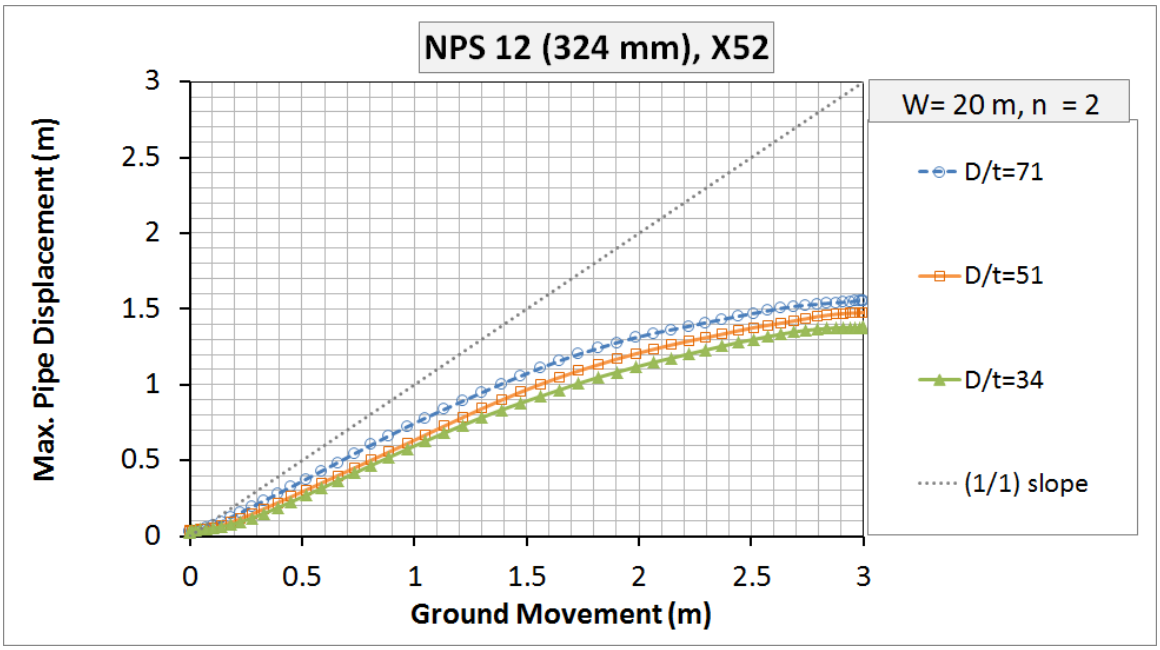

Figure 6.95: NPS 12 (D/t =71, 51 and 34) – Maximum Pipe Displacement versus Ground Movement for the Critical Widths of 10 m (33 ft)

The strain demands determined from the analysis was compared with the calculated strain capacity defined from the guidance; BS 7910 for tensile strain, and CSA Z662 and for compressive strain. While there are many existing models for calculating the compressive and tensile strain capacity in codes and standards, it was decided to develop a simple a strain-based

The information contained herein is the copyright of and proprietary to BMT Fleet Technology Limited. Use of this information is governed by the legend on the cover page of this document."

design methodology that can be easily adapted to any code and standards. These tensile and compressive strain demand 'envelopes' for a given pipe tensile and compressive strain demands of 0.25%, 0.5%, 0.75%, 1%, 1.25%, 1.5%, 1.75% and 2% along the longitudinal direction of the pipeline are presented in Appendix D. The safe pipeline operating goal of pipeline subjected to lateral ground displacement is to stay within the normal operating strain range defined by codes and standards.

6.15 Structural Analyses for an 18-Inch Pipeline

Analyses were completed for the NPS 18 (457 mm outside diameter) pipeline to assess its response to lateral ground movement and to determine the structural integrity significance of ground movement induced strain demands. A sensitivity analysis was conducted to evaluate the of D/t ratio and ground width displacement. The analyses considered 6 lateral ground movement scenarios. The scenarios included the following:

- Pipe wall thickness: one wall thicknesses: 6.35 mm (0.25); corresponding to D/t ratio of 72;
- Ground displacement direction: Perpendicular (lateral) to the pipeline axis;
- Width of ground displacement (W): Six potential ground movement failures with a total estimated width of failure perpendicular to the pipeline varying from 10 to 100 m (10, 20, 30, 40 50 and 100 m);
- Shape of ground displacement: one ground displacement pattern initiated using a cosine function raised to the power "n=2";
- One soil conditions sand/clay till;
- Pipe slope: one slopes, 16 deg.; and
- Pipeline burial depth: one depth of 1.2m (4 ft) to top pipe, corresponding to 1.43 m (4.7 ft), depth to pipe center line.

Assumptions for the pipeline were as follows:

- 72% SMYS internal pressure;
- 45°C thermal differential (installation -20°C, max operating temperature 25°C);
- A generic stress strain curves for Grade X-52 (359) pipe according to the API 5L.

6.15.1 18 Inch Pipeline Results

The results presented in Appendix E, illustrates the importance of the width of the ground displacement. The critical width which results in the largest tensile strain in the pipe for any given value of ground is about 10 m (33 ft) for the analyzed case. The pipe exceeds the compressive strain limit for the critical width of 10 m (33 ft) and buckle/wrinkle at 2.4% local compressive strain or 1.76% nominal compressive strain for soil displacement of 0.8 m. Figure 6.96 shows the soil and pipe deformation and also shows pipe wrinkle and the axial strain distribution (blue color is compressive and red is tensile strain); in this figure the soil above the pipe is hidden so the pipe deformation can be visualized.

The information contained herein is the copyright of and proprietary to BMT Fleet Technology Limited. Use of this information is governed by the legend on the cover page of this document."

The strain demands determined from the analysis was compared with the calculated strain capacity defined from the guidance; BS 7910 for tensile strain, and CSA Z662 and for compressive strain. While there are many existing models for calculating the compressive and tensile strain capacity in codes and standards, it was decided to develop a simple a strain-based design methodology that can be easily adapted to any code and standards. These tensile and compressive strain demand 'envelopes' for a given pipe tensile and compressive strain demands of 0.25%, 0.5%, 0.75%, 1%, 1.25%, 1.5%, 1.75% and 2% along the longitudinal direction of the pipeline are presented in Appendix (E). The safe pipeline operating goal of pipeline subjected to lateral ground displacement is to stay within the normal operating strain range defined by codes and standards.

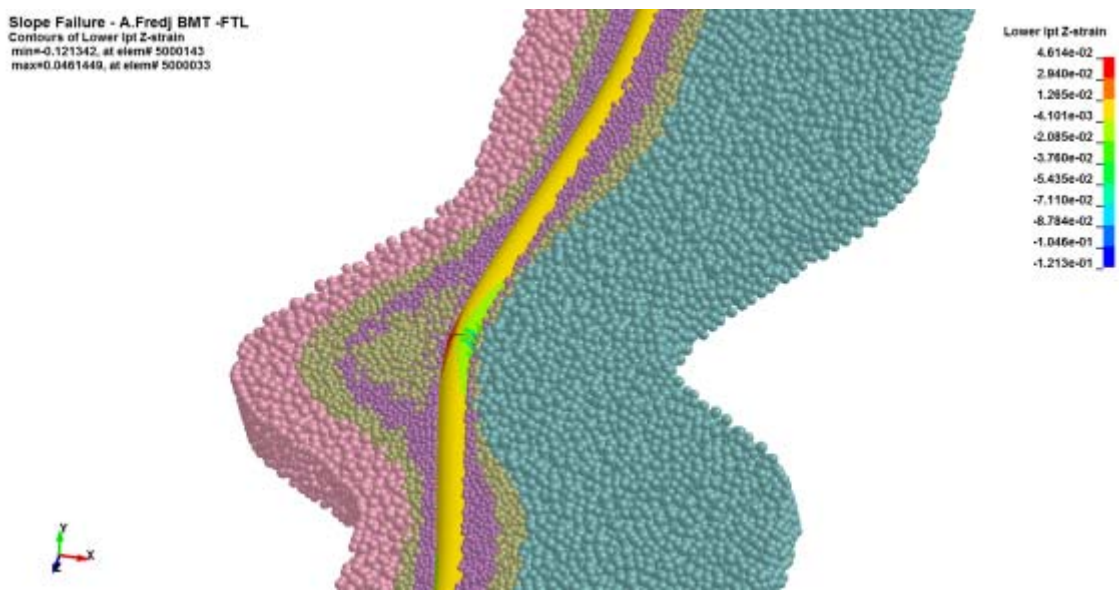

Figure 6.96: Pipe Deformation and Axial Strains for given Soil Movement of 3 m and W=10 m (Top View)

6.16 Structural Analyses for a 30-Inch Pipeline

Analyses were completed for the NPS 30 (762 mm outside diameter) pipeline to assess its response to lateral ground movement and to determine the structural integrity significance of ground movement induced strain demands. A sensitivity analysis was conducted to evaluate the effect of D/t ratio, burial depth and ground width displacement. The analyses considered 18 lateral ground movement scenarios. The scenarios included the following:

- Pipe wall thickness: three wall thicknesses: 7.92 mm (0.312 inch), 9.525 mm (0.375) and; corresponding to D/t ratio of 96 and 80 respectively;
- Ground displacement direction: Perpendicular (lateral) to the pipeline axis;

The information contained herein is the copyright of and proprietary to BMT Fleet Technology Limited. Use of this information is governed by the legend on the cover page of this document."

- Width of ground displacement (W): Six potential ground movement failures with a total estimated width of failure perpendicular to the pipeline varying from 10 to 100 m (10, 20, 30, 40 50 and 100 m);
- Shape of ground displacement: one ground displacement pattern initiated using a cosine function raised to the power "n=2";
- One soil conditions sand/clay till;
- Pipe slope: one slopes, 16 deg.; and
- Pipeline burial depth: two depths of 1.2 m (4 ft) to top pipe and 1.5 m (5 ft), corresponding to 1.6 m (5 ft) and 1.9 m (6 ft), depth to pipe center line.

Assumptions for the pipeline were as follows:

- 72% SMYS internal pressure;
- 45°C thermal differential (installation -20°C, max operating temperature 25°C);
- A generic stress strain curves for Grade X-70 (483) pipe according to the API 5L.

6.16.1 30 Inch Pipeline Results

Detailed results are presented in Appendix F. Figures 6.97 and 6.98 present the maximum tensile and compressive strains in the pipe versus the maximum ground displacement for various ground displacement widths considered in the analyses. The results are for X70, grade and wall thickness of 7.92 mm (0.312 inch) (D/t=96). Both these figures indicate that a Width of 20 m (66 ft) and 30 m (99 ft) results in the largest tensile and compressive strain. The results also indicate that:

- For W= 20 m, pipe with 7.92 mm (0.312 inch) [D/t=96] operating at 72% SMYS exceeds the compressive strain limit and buckle/wrinkle at 0.9% local compressive strain or 0.78% nominal compressive strain for soil displacement of 0.58 m.

For W= 30 m, Pipe with 7.92 mm (0.312 inch) [D/t=96] operating at 72% SMYS exceeds the compressive strain limit and buckle/wrinkle at 1.42% local compressive strain or 1.1% nominal compressive strain for soil displacement of 1.13 m.

Figures 6.99 and 6.100 present the maximum tensile and compressive strains in the pipe versus the maximum ground displacement for various ground displacement widths considered in the analyses. The results are for X70, grade and wall thickness of 9.52 mm (0.375 inch) (D/t=80). Both these figures indicate that a width of 20 m (66 ft) results in the largest tensile and compressive strain. The results also indicate that for W= 20 m the pipe exceeds the compressive strain limit and buckle/wrinkle at 1.9% local compressive strain or 1.64% nominal compressive strain for soil displacement of 1.13 m.

The strain demands determined from the analysis was compared with the calculated strain capacity defined from the guidance; BS 7910 for tensile strain, and CSA Z662 and PRCI for compressive strain. While there are many existing models for calculating the compressive and

The information contained herein is the copyright of and proprietary to BMT Fleet Technology Limited. Use of this information is governed by the legend on the cover page of this document."

tensile strain capacity in codes and standards, it was decided to develop a simple a strain-based design methodology that can be easily adapted to any code and standards. These tensile and compressive strain demand 'envelopes' for a given pipe tensile and compressive strain demands of 0.25%, 0.5%, 0.75%, 1%, 1.25%, 1.5%, 1.75% and 2% along the longitudinal direction of the pipeline are presented in Appendix F. The safe pipeline operating goal of pipeline subjected to lateral ground displacement is to stay within the normal operating strain range defined by codes and standards.

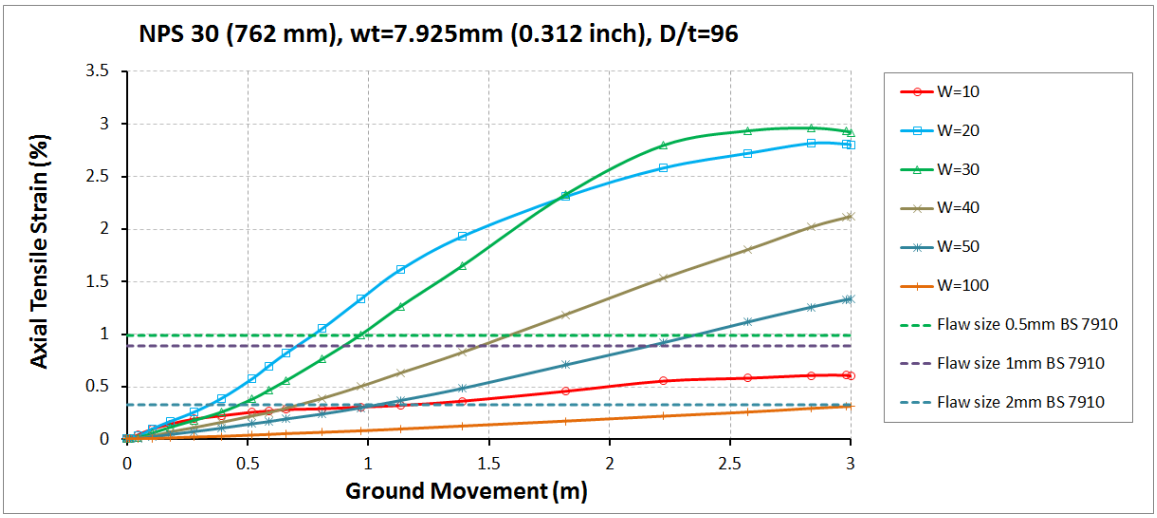

Figure 6.97: NPS 30 (D/t = 96) - Maximum Tensile Strains in the Pipe versus Ground Movement Widths: [10-100 m]

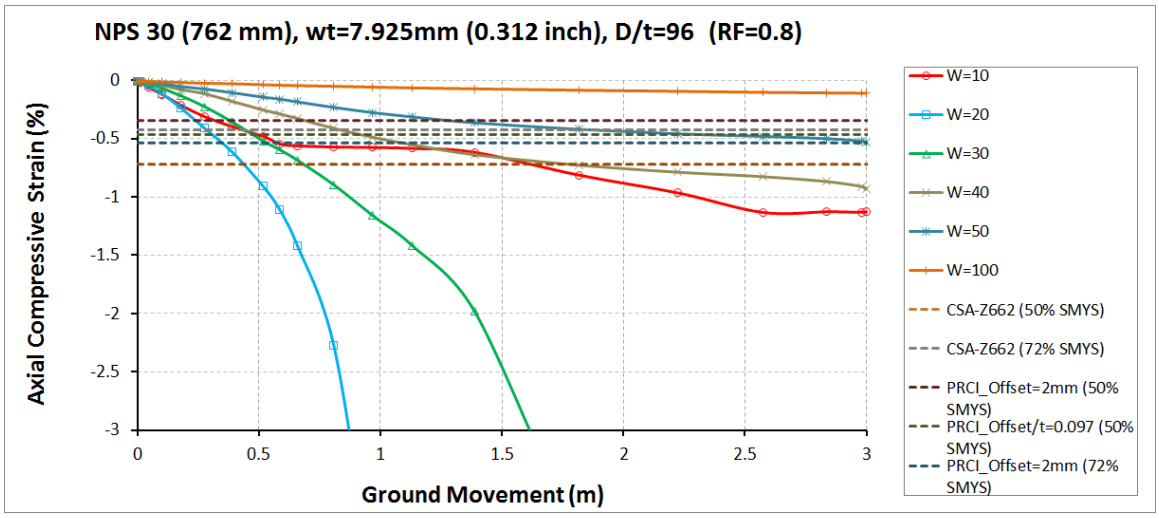

Figure 6.98: NPS 30 (D/t = 96) - Maximum Compressive Strains in the Pipe versus Ground Movement Widths: [10-100 m]

The information contained herein is the copyright of and proprietary to BMT Fleet Technology Limited. Use of this information is governed by the legend on the cover page of this document."

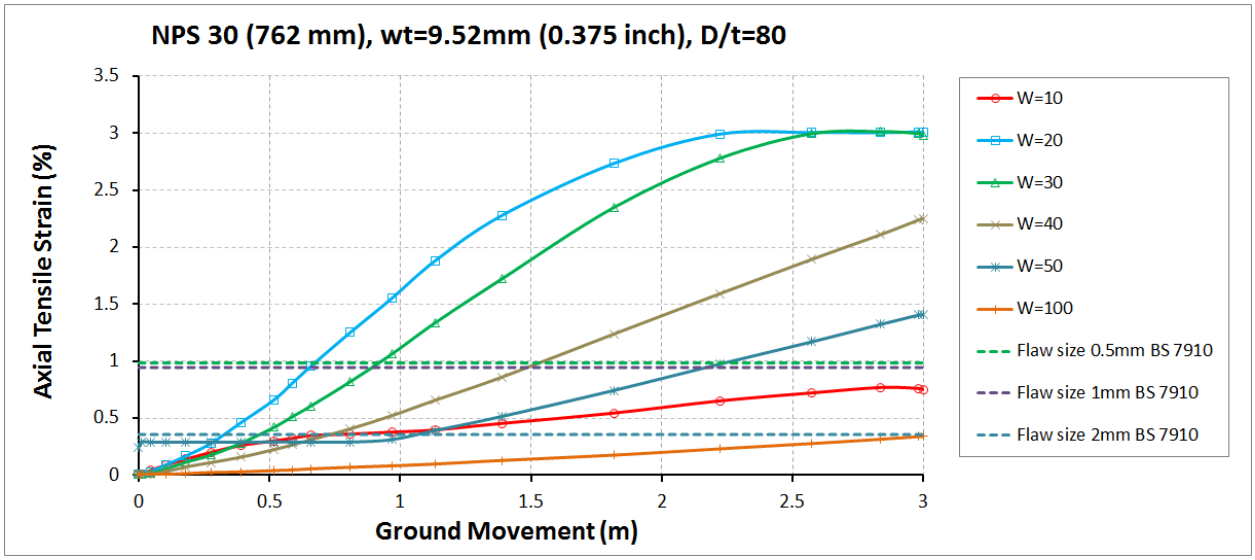

Figure 6.99: NPS 30 (D/t = 80) - Maximum Tensile Strains in the Pipe versus Ground Movement Widths: [10-100m]

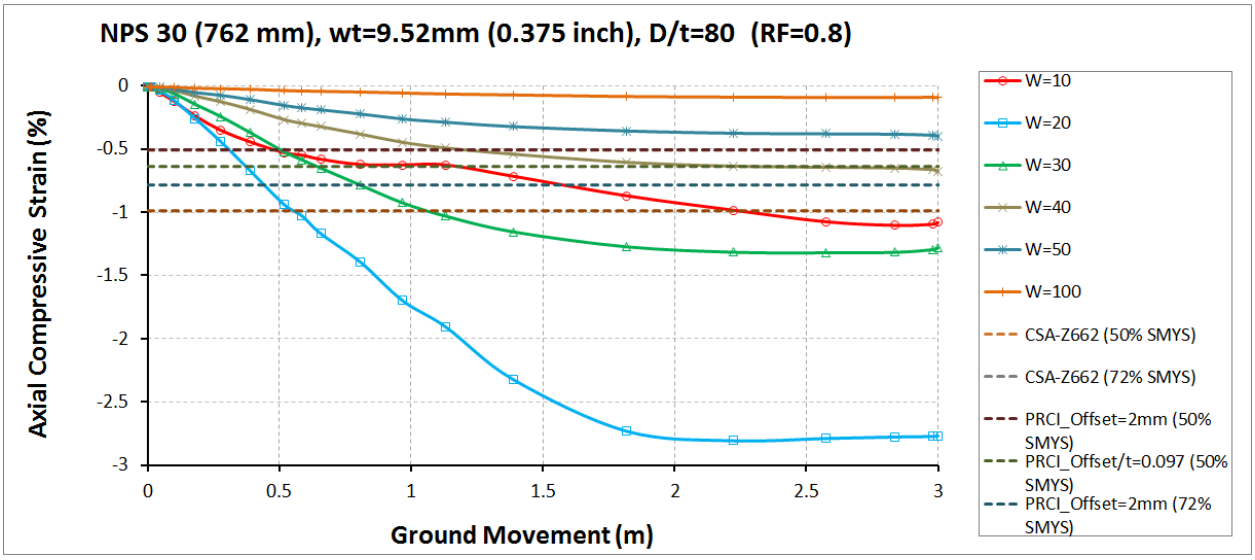

Figure 6.100: NPS 30 (D/t = 80) - Maximum Compressive Strains in the Pipe versus Ground Movement Widths: [10-100 m]

6.17 Pipeline Lateral Ground Movement Modelling Observations

The sample applications of the DEM pipe-soil interaction geotechnical hazard assessment method was employed to investigate the strains developed in pipelines subjected to lateral soil movement. The primary focus was an NPS 24 (610 mm) pipe system, however, the analysis also considered 12 (305 mm) and 18 inch (457 mm) diameter pipes. The use of the simulated pipe responses to soil movement to consider the onset of tensile and compressive limit states in a strain-based assessment was demonstrated and the sensitivity of the pipe response to a number or

The information contained herein is the copyright of and proprietary to BMT Fleet Technology Limited. Use of this information is governed by the legend on the cover page of this document."

geotechnical hazard scenario factors were presented. For the pipe-soil interaction in which the ground movement is across the longitudinal axis of the pipe, it was shown that:

- The response of the pipeline and soil movement pattern is affected by the ground slope. More specifically, the orientation of the ground movement is relative to direction of the gravitation acceleration. This effect gives rise to differences in the ground surface appearance (heave and subsidence) ahead of and after the pipe. The pipe accumulated strains for a given ground displacement are not significantly affected by the slope.
- The lateral soil movement-induced pipe displacements will produce both pipe bending and axial extension.
- The strains in the pipe are affected by the width of the soil movement and there is a critical movement width that promotes a peak strain. The critical width is a function of the pipe geometry, pipeline operating conditions and locked-in pipeline axial loads (i.e. those caused by thermal differential between operating and construction conditions).

The observations made in this report are related to ground movements involving deformable soils. Care should be taken in applying these results to ground movement across a pipeline surrounded by rock or very stiff soils that will not deform and will cause extremely localized pipe deformations.

The effect of the parameters considered in these sensitivity studies indicate that the parameters can be ranked based upon their impact on strain demand as follows:

Higher Importance	Medium Importance	Lower Importance
- Magnitude of soil movement - Width of soil movement - Soil stiffness	- Pipe geometry (D/t) - Operating pressure - Temperature differential	- Soil to pipe friction - Material grade

Comparisons were made with limit state equations defined from the guidance; BS 7910 for tensile strain, and CSA Z662 and PRCI for compressive strain to demonstrate the application of the analysis results in an assessment process. While there are many existing models for calculating the compressive and tensile strain capacity in codes and standards, it was decided to develop a simple a strain-based design methodology that can be easily adapted to any code and standards, which is the purpose of this section.

The tensile and compressive strain demand envelopes along the longitudinal direction of the pipeline were developed. The maximum soil displacement versus ground width displacement as a series of 'envelopes' was developed for a given pipe tensile and compressive strain demands of 0.25%, 0.5%, 0.75%, 1%, 1.25%, 1.5%, 1.75% and 2%. The safe pipeline operating goal of pipeline subjected to lateral ground displacement is to stay within the normal operating strain range defined by codes and standards.

The information contained herein is the copyright of and proprietary to BMT Fleet Technology Limited. Use of this information is governed by the legend on the cover page of this document."

The strain for critical width lateral movement ground movement events (strain demand or applied strain) may be used conservatively to evaluate the response of pipeline system with similar geotechnical hazards. The allowable strain (strain capacity or resistance) should be evaluated for each pipe geometry, material and operating condition.

The information contained herein is the copyright of and proprietary to BMT Fleet Technology Limited. Use of this information is governed by the legend on the cover page of this document."

7 CONCLUDING REMARKS

The objective of this project was to develop an engineering tool to define the effects of operational and geotechnical loads on liquid and gas pipeline systems to support decision making regarding threat severity or repair scheduling. This tool could be incorporated in strain based design and assessment to facilitate the consideration of complex loading scenarios inducing significant flexural loads, including pipeline subsidence or lowering, and ground movements inducing lateral pipeline movements. The results of this project define the local nominal strain state that can be used to assess localized anomalies/defects (e.g., corrosion, cracks, dents, weld faults, gouges, etc.) or the potential for the formation of a wrinkle or buckle.

The report provided examples of the numerical model validation studies that have been completed to demonstrate the ability of the modelling tools to simulate physical trials. These sample applications demonstrate the ability of the numerical modelling tools to reproduce the behaviors of the pipe and soil in the full-scale experimental trials.

The observations made in this report are related to ground movements involving deformable soils. Care should be taken in applying these results to ground movement across a pipeline surrounded by rock or very stiff soils that will not deform and will cause extremely localized pipe deformations.

The objective of the numerical simulation work completed in this project was to explore the sensitivity of the pipeline strains to changes in the geotechnical hazard and pipeline parameters. This report provided examples of the peak tensile and compressive strains generated in subsidence and slope movements transverse to the pipe axis considering the effects of:

- Pipe geometry
- Soil types
- Operating Pressure
- Ground movement pattern
- Material Grade
- Widths of soil movement
- Slope
- Temperature (axial load)

The analysis results illustrate that not all parameters investigated had the same magnitude of impact. The effect of the parameters considered in these sensitivity studies indicate that the parameters can be ranked based upon their impact on strain demand as follows:

Subsidence Events

Higher Importance	Medium Importance	Lower Importance
- Magnitude of ground subsidence - Ground subsidence pattern - Width of ground subsidence - Burial depth	- Pipe geometry (D/t) - Operating pressure - Temperature differential - Soil stiffness	- Soil to pipe friction - Material grade

Lateral Ground Movement Events

Higher Importance	Medium Importance	Lower Importance
- Magnitude of soil movement - Width of soil movement - Soil stiffness	- Pipe geometry (D/t) - Operating pressure - Temperature differential	- Soil to pipe friction - Material grade

The information contained herein is the copyright of and proprietary to BMT Fleet Technology Limited. Use of this information is governed by the legend on the cover page of this document."

The sample application of the DEM pipe-soil interaction geotechnical hazard assessment method was employed to investigate the strains developed in a range of pipe sizes however the NPS 24 (610 mm) pipeline was used as the baseline case. Lower diameter pipelines have lower moments of inertia and would be expected to be more flexible when subjected to lateral loading.

The results developed in this work may be used to estimate the effects of geotechnical hazards to consider the onset of tensile and compressive limit states in a strain-based assessment. Several limit state formulations were used to demonstrate this comparison and sample tensile and compressive strain demand envelopes were developed.

The use of the simulated pipe responses to soil movement to evaluate train demand (applied strains) in the pipeline for strain-based assessment was demonstrated and the sensitivity of the pipe response to a number or geotechnical hazard scenario factors were presented. For the pipe-soil interaction involving mining subsidence, it was shown that:

- The response of the pipeline and soil movement pattern is affected by the ground subsidence magnitude, width and patterns;
- The vertical soil movement-induced pipe displacements will produce both pipe bending and axial extension;
- The strains in the pipe are affected by the width of the surface subsidence and there is a critical surface subsidence width that promotes a peak strain. The critical width is a function of the pipe geometry, pipeline operating conditions and locked-in pipeline axial loads (i.e. those caused by thermal differential between operating and construction conditions) and as well as the subsidence parameters.

The use of the results presented in this report to consider subsidence at the edge of rock or similarly undeformable shelf should be treated with care.

For the pipe-soil interaction in which the ground movement is across the longitudinal axis of the pipe, it was shown that:

- The response of the pipeline and soil movement pattern is affected by the ground slope. More specifically, the orientation of the ground movement is relative to direction of the gravitation acceleration. This effect gives rise to differences in the ground surface appearance (heave and subsidence) ahead of and after the pipe. The pipe accumulated strains for a given ground displacement are not significantly affected by the slope.
- The lateral soil movement-induced pipe displacements will produce both pipe bending and axial extension.
- The strains in the pipe are affected by the width of the soil movement and there is a critical movement width that promotes a peak strain. The critical width is a function of the pipe geometry, pipeline operating conditions and locked-in pipeline axial loads (i.e. those caused by thermal differential between operating and construction conditions).

The information contained herein is the copyright of and proprietary to BMT Fleet Technology Limited. Use of this information is governed by the legend on the cover page of this document."

- The strains in the pipe are affected by the operating pressure. Lower operating pressures effectively reduce the stiffness of the pipeline permitting greater strain accumulations.

The observations made in this report are related to lateral ground movements involving deformable soils. Care should be taken in applying these results to ground movement across a pipeline surrounded by rock or very stiff soils that will not deform and will cause extremely localized pipe deformations.

The results presented in this report provide reference data that may be used as a tool to evaluate the strain accumulation in a pipeline. It was demonstrated that a critical width can be defined for a pipeline and applying the strain derived from this critical width may be conservatively considered for all widths of the geotechnical hazard.

Allowable strains (strain capacity or resistance) should be evaluated for each pipe geometry, material and operating condition. The focus of this research was to demonstrate the strain demand and it is recommended in the application of this information the allowable strains be defied by the user to suit their needs and incorporate a factor of safety suitable to their requirements.

In future, it would be desirable to consider ground movement along the pipe axis or other geotechnical hazard scenarios to provide a more complete reference data set for the geotechnical hazard assessment. The results developed in this project could be extended to consider any arbitrary direction of soil movement relative to the pipeline.

The subsidence modelling results could be extended to consider both vertical and lateral movement in the soil and the response of the pipeline beyond the bounds of the subsidence and post buckling behaviour could also be explored.

The ability of ILI tools to detect and characterize pipe displacements could be correlated with the results presented in this report to support fitness for purpose assessment of geotechnical hazards.

The information contained herein is the copyright of and proprietary to BMT Fleet Technology Limited. Use of this information is governed by the legend on the cover page of this document."

8 REFERENCES

[1] LS-DYNA *"Keywords user's Manual", version 971*, Livermore Software and Technology Corporation, Livermore, CA, April 2007.

[2] Souli, M, A. Ouahsine, L. Lewin, "Arbitrary Lagrangian Eulerian Formulation for Fluid-Structure Interaction Problems", Computer Methods in Applied Mechanics and Engineering, Volume 190, Pages 659-675, (2000).

[3] Schwer, L.E., "LS-DYNA Geomaterial Modeling Short Course Notes", February, 2002.

[4] Karimian, H., and Wijewickreme, D. Full−Scale Laboratory Testing to Assess Methods for Reduction of Soil Loads on Buried Pipes Subject to Transverse Ground Movement. Proceedings of IPC2006 6th International Pipeline Conference September 25-29, 2006, Calgary, Alberta, Canada.

[5] Cappelletto, A., Tagliaferri, R., Giurlani, G., Andrei, G., Furlani, G., and Scarpelli, G. (1998). Field Full Scale Tests on Longitudinal Pipeline-Soil Interaction. Proceedings of International Pipeline Conference 1998, Calgary, vol. 2, pp.771-778.

[6] Scarpelli,G, Sakellariadi, S and Furlani, G: Evaluation of soil-Pipeline Longitudinal Interaction Forces Rivisata Italiana Di Geotecnica 4/2003.

[7] O'Rourke, T.D, Jezerski, J.M, Olson, N.A, Boneau, A.L, Palmer, M.C, Stewart, H.E., O'Rourke, M.J., Abdoun, T., 2008; Geotechnicas of Pipeline System Response to earthquakes. Proceedings Geotechnical Earthquake Engineering and Soil Dynamics IV, Sacramento, Ca, May 2008.

[8] Karimian, H., and Wijewickreme, D. and Honegger D. Response of Buried Pipelines Subjected to Relative Axial Soil Movement. Can. Geotech. J. 46: 735-752, 2009.

[9] C-Core, "Full Scale Pipe/Soil Interaction" Prepared for Minerals Management Service.N0 99 –C12, April 1999.

[10] Paulin, M.J., Phillips, R., Clark, J.I., Trigg, A., and Konuk, I. (1998). "A Full-Scale Investigation into Pipeline/Soil Interaction." *Proc., 1998 Int. Pipeline Conf.*, ASME, Calgary, AB, Canada, Vol. 2, 779–787.

[11] Popescu, R., Phillips, R., Konuk, I., Guo, P., and Nobahar, A. (2002)."Pipe–Soil Interaction: Large-Scale Tests and Numerical Modeling." *Proc., Int. Conf. on Physical Modelling in Geotechnique, ICPMG'02*, St. John's, Newfoundland, Canada, 917–922.

[12] Popescu, R. and Nobahar, A., 2003, "3D Finite Element Analysis of Pipe-Soil Interaction- Effects of Ground Water", C-CORE Report R-02-029-076.v2.pdf.

[13] Yimsiri, S., Soga, K., Yoshisaki, K., Dasari, G.R., and O'Rouke, T.D., 2004 " Lateral and Upward Soil-Pipeline Interactions in Sand for Deep Embedment conditions.

[14] Yusima, Y. and Kishida, T. (1981). "A Ring Torsion Apparatus for Evaluating Friction between Soil and Metal Surfaces." Geotech. Test. J., ASTM, 4(4), 145-152.

The information contained herein is the copyright of and proprietary to BMT Fleet Technology Limited. Use of this information is governed by the legend on the cover page of this document."

[15] Shoop, S., Affleck R., Janno, V., Haehlen, R., and Barrett, B., 2005, "Constitutive Model for Thawing Frost-Susceptible Sand.", ERDC/CRREL TR-05-3.

[16] Yoshisaki, K., O'Rourke, T.D. and Hamada, M., (2001). Large Deformation Behavior of Buried Pipelines with Low-Angle Elbows Subjected to Permanent Ground Deformation. Journal of Structural Mechanics and Earthquake Engineering, JSME, No. 50, Vol. 4, April 2001, pp. 215-228.

[17] Yoshisaki, K., O'Rourke, T.D. and Hamada, M., (2004). Study Probes Pipelines With Elbows Subjected To Permanent Ground Deformation. Pipeline & Gas Journal/January 2004/ www.pipelineandgasjournal.com.

[18] Yoshisaki, K., O'Rourke, T.D. and Hamada, M., Large Scale Experiments of Permanent Ground Deformation Effects on Steel Pipelines http://mceer.buffalo.edu/publications/resaccom/01-SP01/ rpa_pdfs/03orourke_tkyogas.pdf

[19] Fredj, A., and Dinovitzer, A., 2014, Pipeline Response to Slope Movement and Evaluation of Pipeline Strain Demand, Proceedings of International Pipeline Conference, Alberta, IPC2014-33611.

[20] Dinovitzer, A., Fredj, A., and Sen , M, 2014, Pipeline Stress Relief and Evaluation of Strain Measurement Technology at a Moving Slope, Proceedings of International Pipeline Conference, Alberta, IPC2014-33497.

[21] Fredj, A., and Dinovitzer, A., 2012, Simulation of the Response of Buried Pipelines to Slope Movement Using 3D Continuum Modeling, Proceedings of International Pipeline Conference, Alberta, IPC2012-90437.

[22] Fredj, A, Comfort, G, Dinovitzer, A Case Study of High Pressure/High Temperature Pipeline for Ice Scour Design Using 3D Continuum Modeling Interaction, International Conference on Offshore Mechanics and Arctic Engineering (CD), Paper No: OMAE2008-57702, June 15 - 20 2008, Estoril, Portugal.

[23] Fredj, A., Dinovitzer, A., and Zhou, J., 2008a, A 3-Dimentional Continuum ALE Model for soil-Pipe Interaction, Proceedings of International Pipeline Conference, Alberta, IPC2008-64624.

[24] Fredj, A., and Dinovitzer, A., 2010a, Three-Dimensional Response of Buried Pipelines Subjected to Large Soil Deformation Effects- Part I: 3D Continuum Modeling Using ALE and SPH Formulations, Proceedings of International Pipeline Conference, Alberta, IPC2010-31516.

[25] Fredj, A., and Dinovitzer, A., 2010b, Three-Dimensional Response of Buried Pipelines Subjected to Large Soil Deformation Effects- Part II: Effects of the Soil Restraint on the Response of Pipe/Soil Systems, Proceedings of International Pipeline Conference, Alberta, IPC2010-31517.

[26] Fredj, A, Comfort, K, Been, The Forces Required to Produce Seabed Gouges. POAC 11-185: Proceedings of the 21st International Conference on Port and Ocean Engineering under Arctic Conditions. July 10-14, 2011, Montréal, Canada.

The information contained herein is the copyright of and proprietary to BMT Fleet Technology Limited. Use of this information is governed by the legend on the cover page of this document."

[27] CSA-Z662-11 Standards Oil and Gas Pipeline Systems, 2011.

[28] Honegger, D.G., and Nyman, D., (2004), "PRCI Guidelines for the Seismic Design and Assessment of Natural Gas and Liquid Hydrocarbon Pipelines," Pipeline Research Council International, published by Technical Toolboxes, Houston, Texas.

[29] Dory, A.B., Cheng, J.J.R., and Murray, D.W., (3001), "Critical Buckling Strains for Energy Pipelines", University of Alberta Department of Civil & Environmental Engineering. Structural Engineering Report N0.237.

[30] BS 7910:2005, Guide to methods for assessing the acceptability of flaws in metallic structures.

[31] USGS-2008 Landslide and Land Subsidence Hazards to Pipeline. Open File Report 2008 -1164

[32] Bauer, R.A., and Hunt, S.R., 1982, Profile, Strain and Time Characteristics of Subsidence from Coal Mining in Illinois, in Peng, S.S., and Harthill, M., eds., Proceedings, Workshop on Surface Subsidence due to Underground Mining: West Virginia University, Morgantown, W. Va., Nov. 1981, P.207 –219.

[33] BMT, "A 3-Dimentional Continuum ALE Model for Soil-Pipe Interaction", PRCI ENV-3 PR-214-05403

[34] Konuk, Fredj, "FEM for Pipeline Analysis of Ice Scour – A Critical Review", Paper 51477, OMAE 2004

[35] C.Cáceres and M. Ordoñez, "Pipeline Modeling and assessment in unstable Slopes", IPC20210

[36] F. Zhang, M. Liu, Y. Wang, Z. Yu and L. Tong, "Strain demand in Areas of Mine Subsidence", IPC2012

[37] C-Core, "Guidelines for constructing Natural Gas and Liquid Hydrocarbon Pipelines Through Areas Prone to Landslide and Subsidence Hazards", PRCI/US DOT project 2009.

[38] D.J. Varnes,"Landslide Hazard Zonation: A review of Principles and Practice", UNESCO, 1984.

[39] ASCE 1984: Guidelines for the Seismic Design of Oil and Gas Pipeline System. Published by the American Society of Civil Engineers, New York.

[40] Monroy M. Soil Restraints on Steel Buried Pipelines Crossing Active Seismic Faults. Ph.D. Thesis; Department of Civil Engineering University of British Columbia, Vancouver, Canada, 2013.

[41] D. Wijewickreme, M. Monroy, D. G. Honegger and D.J. Nyman: Response of Buried Pipelines Subjected to Ground Displacement under Different Trench Backfill Conditions. Tenth U.S. National Conference on Earthquake Engineering, July 21-25, 2014; Anchorage Alaska, USA.

[42] ALA 2001, American Lifelines Alliance (ALA): Guidelines for the Design of Buried Pipeline, July 2001.

The information contained herein is the copyright of and proprietary to BMT Fleet Technology Limited. Use of this information is governed by the legend on the cover page of this document."

[43] C.H. Trautmann and T.D. O'Rourke Lateral Force Displacement Response of Buried Pipe, ASCE Journal of Geotechnical Engineering 1985; 111 (9): 1077-1092.

[44] USGS-2008 Landslide and Land Subsidence Hazards to Pipeline. Open File Report 2008 -1164

[45] Cundall, P.A. and Strack, O.D.L.: A Discrete Element Models: Similarity Principles Engineering Computations: International Journal for Computer-Aided Engineering and Software 26 (2009) 599-609.

[46] Karajan, N.; Han, Z.; Ten, H. and Wang, J.: Interaction Possibilities of Bonded and Loose Particles in LS-DYNA, Proceedings of 9th European Conference, Manchester, 2013.

[47] M.J. O'Rourke (1989), "Approximate Analysis Procedures for Permanent Ground Deformation for Permanent Ground Deformation Effects on Buried Pipelines," Proceedings of the Second U.S.-Japan Workshop on Liquefaction, Large Ground Deformation and Their Effects on Lifelines, Buffalo, New York, Technical Report NCEER-89-0032, Multidisciplinary Center for Earthquake Engineering Research, Buffalo, New York, pp. 336-347.

[48] H. Suzuki (1988), "Damage to Buried Pipes Caused by Large Ground Displacement". Proceedings of the First Japan-U-S. Workshop on Liquefaction, Large Ground Deformation and Their Effects on Lifeline Facilities, Tokyo, Japan, pp.127-132.

[49] Ligon, J.B and Mayer G.R, Coefficient of friction for Pipe Coating Material, Pipe Line Rules of Thumb Handbook , Fourth Edition,1998.

The information contained herein is the copyright of and proprietary to BMT Fleet Technology Limited. Use of this information is governed by the legend on the cover page of this document."

APPENDIX A: STRAIN LIMIT CAPACITY

The information contained herein is the copyright of and proprietary to BMT Fleet Technology Limited. Use of this information is governed by the legend on the cover page of this document."

A.1 COMPRESSIVE STRAIN LIMIT:

The slope movement will result in axial strain in the pipe. These strains are generally compressive at the toe of the slope and tensile at the top of the slope. Compressive strains may result in local buckling/wrinkling of the pipe in the compressive zone. The tensile strains may result in girth weld failure in the tensile strain zone.

The onset of local buckling is considered a serviceability limit state and can be evaluated using a number of limit state equations including those found in CSA Z662 and PRCI 2004 or UOA. In these standards, the limit state is considered when the load is secondary, such as displacement controlled ground movement. Although local buckling or wrinkling does not immediately result in loss of the integrity of the pressure boundary (leakage), the buckles/wrinkles make the pipe line segment prone to subsequent fatigue damage.

Tables A.1 through A.11 show the allowable compressive strain limits calculated for the 12 inch, 18 inch, 24 inch and 30 inch pipes using CSA and the PRCI 2004 or University of Alberta equation.

Tensile Strain Limit:

The maximum allowable tensile strains are considered to be governed by the failure stress or strain state for a circumferential defect. This assessment was completed using a British Standard 7190 Level 2A failure assessment approach [4]. These strain limits were estimated by considering the axial pipe wall membrane strain that would cause a reference flaw to extend. The BS7910 failure assessment approach considering the potential for both ductile and brittle crack extension was used to define the membrane stress/strain state that would cause crack extension.

In developing the tensile strain limit, the following data and assumptions were considered:

- The pipe was assumed to have the minimum specified strength properties the welds were assumed to overmatch the base material. Conservatively, the weld metal properties were assumed to be the same as the base material;
- The design flaw that was adopted was 0.5 mm, 1 mm and 2 mm deep, 50 mm long semi-elliptical surface flaw;
- The design flaw was assumed to be located at the weld toe. The stress concentrating effects of the weld toe defined in BS 7910 were applied considering a maximum weld width of 25 mm; and
- The pipe CTOD fracture toughness was assumed to be 0.05 mm. Based upon experience this represents low toughness (brittle) behavior.

The FlawCheck software was used to apply the BS7910 Level 2A assessment procedure to each pipe geometry and material combination to define the pipe wall local membrane stress and strain state that would result in crack extension. The results of this assessment are listed in Table A.1 through A.11 below. The results presented below are consistent with the girth weld defect

The information contained herein is the copyright of and proprietary to BMT Fleet Technology Limited. Use of this information is governed by the legend on the cover page of this document."

acceptance techniques adopted by API 579 and CSA Z662, as both of these standards have incorporated the BS 7910 procedure.

Table A.1: Tensile (2c=50 mm & CTOD=0.05 mm) and Compressive (CSA & PRCI) Strain Limits; X52, OD=12 in, WT=0.18 in

Tensile Strain Limit				Compressive Strain Limit (Resistance Factor=0.8)					
BS-7910 Flaw size=				CSA-Z662		PRCI			
						50% SMYS		72% SMYS	
0.5mm	1mm	2mm		50% SMYS	72% SMYS	Offset=2mm	Offset/WT=0.097mm	Offset=2mm	Offset/WT=0.097mm
1.10	0.74	0.23		-0.48	-0.48	-0.56	-0.97	-0.87	-1.50

Table A.2: Tensile (2c=50 mm & CTOD=0.05 mm) and Compressive (CSA & PRCI) Strain Limits; X52, OD=12 in, WT=0.25 in

Tensile Strain Limit				Compressive Strain Limit (Resistance Factor=0.8)					
BS-7910 Flaw size=				CSA-Z662		PRCI			
						50% SMYS		72% SMYS	
0.5mm	1mm	2mm		50% SMYS	72% SMYS	Offset=2mm	Offset/WT=0.097mm	Offset=2mm	Offset/WT=0.097mm
1.15	0.85	0.32		-0.70	-0.70	-1.15	-1.70	-1.79	-2.63

Table A.3: Tensile (2c=50 mm & CTOD=0.05 mm) and Compressive (CSA & PRCI) Strain Limits; X52, OD=12 in, WT=0.375 in

Tensile Strain Limit				Compressive Strain Limit (Resistance Factor=0.8)					
BS-7910 Flaw size=				CSA-Z662		PRCI			
						50% SMYS		72% SMYS	
0.5mm	1mm	2mm		50% SMYS	72% SMYS	Offset=2mm	Offset/WT=0.097mm	Offset=2mm	Offset/WT=0.097mm
1.18	1.02	0.43		-1.09	-1.09	-2.71	-3.42	-4.20	-5.29

Table A.4: Tensile (2c=50 mm & CTOD=0.05 mm) and Compressive (CSA & PRCI) Strain Limits; X52, OD=24 in, WT=0.25 in

Tensile Strain Limit				Compressive Strain Limit (Resistance Factor=0.8)					
BS-7910 Flaw size=				CSA-Z662		PRCI			
						50% SMYS		72% SMYS	
0.5mm	1mm	2mm		50% SMYS	72% SMYS	Offset=2mm	Offset/WT=0.097mm	Offset=2mm	Offset/WT=0.097mm
1.20	0.99	0.35		-0.34	-0.34	-0.39	-0.58	-0.60	-0.89

The information contained herein is the copyright of and proprietary to BMT Fleet Technology Limited. Use of this information is governed by the legend on the cover page of this document."

Table A.5: Tensile (2c=50 mm & CTOD=0.05 mm) and Compressive (CSA & PRCI) Strain Limits; X52, OD=24 in, WT=0.375 in

Tensile Strain Limit				Compressive Strain Limit (Resistance Factor=0.8)					
BS-7910 Flaw size=				CSA-Z662		PRCI			
						50% SMYS		72% SMYS	
0.5mm	1mm	2mm		50% SMYS	72% SMYS	Offset=2mm	Offset/WT=0.097mm	Offset=2mm	Offset/WT=0.097mm
1.23	1.06	0.47		-0.54	-0.54	-0.91	-1.15	-1.41	-1.78

Table A.6: Tensile (2c=50 mm & CTOD=0.05 mm) and Compressive (CSA & PRCI) Strain Limits; X52, OD=24 in, WT=0.5 in

Tensile Strain Limit				Compressive Strain Limit (Resistance Factor=0.8)					
BS-7910 Flaw size=				CSA-Z662		PRCI			
						50% SMYS		72% SMYS	
0.5mm	1mm	2mm		50% SMYS	72% SMYS	Offset=2mm	Offset/WT=0.097mm	Offset=2mm	Offset/WT=0.097mm
1.25	1.13	0.52		-0.75	-0.75	-1.65	-1.89	-2.55	-2.93

Table A.7: Tensile (2c=50 mm & CTOD=0.05 mm) and Compressive (CSA & PRCI) Strain Limits; X70, OD=24 in, WT=0.375 in

Tensile Strain Limit				Compressive Strain Limit (Resistance Factor=0.8)					
BS-7910 Flaw size=				CSA-Z662		PRCI			
						50% SMYS		72% SMYS	
0.5mm	1mm	2mm		50% SMYS	72% SMYS	Offset=2mm	Offset/WT=0.097mm	Offset=2mm	Offset/WT=0.097mm
0.99	0.87	0.36		-0.63	-0.63	-0.74	-0.94	-1.15	-1.45

Table A.8: Tensile (2c=50 mm & CTOD=0.05 mm) and Compressive (CSA & PRCI) Strain Limits; X52, OD=18 in, WT=0.25 in

Tensile Strain Limit				Compressive Strain Limit (Resistance Factor=0.8)					
BS-7910 Flaw size=				CSA-Z662		PRCI			
						50% SMYS		72% SMYS	
0.5mm	1mm	2mm		50% SMYS	72% SMYS	Offset=2mm	Offset/WT=0.097mm	Offset=2mm	Offset/WT=0.097mm
1.20	0.93	0.34		-0.47	-0.47	-0.64	-0.94	-0.99	-1.46

Table A.9: Tensile (2c=50 mm & CTOD=0.05 mm) and Compressive (CSA & PRCI) Strain Limits; X70, OD=30 in, WT=0.312 in

Tensile Strain Limit				Compressive Strain Limit (Resistance Factor=0.8)					
BS-7910 Flaw size=				CSA-Z662		PRCI			
						50% SMYS		72% SMYS	
0.5mm	1mm	2mm		50% SMYS	72% SMYS	Offset=2mm	Offset/WT=0.097mm	Offset=2mm	Offset/WT=0.097mm
0.99	0.89	0.33		-0.42	-0.42	-0.34	-0.46	-0.54	-0.72

The information contained herein is the copyright of and proprietary to BMT Fleet Technology Limited. Use of this information is governed by the legend on the cover page of this document."

Table A.10: Tensile (2c=50 mm & CTOD=0.05 mm) and Compressive (CSA & PRCI) Strain Limits; X70, OD=30 in, WT=0.375 in

Tensile Strain Limit				Compressive Strain Limit (Resistance Factor=0.8)					
BS-7910 Flaw size=				CSA-Z662		PRCI			
						50% SMYS		72% SMYS	
0.5mm	1mm	2mm		50% SMYS	72% SMYS	Offset=2mm	Offset/WT=0.097mm	Offset=2mm	Offset/WT=0.097mm
0.99	0.95	0.36		-0.51	-0.51	-0.51	-0.64	-0.78	-0.99

Table A.11: Tensile (2c=50 mm & CTOD=0.05 mm) and Compressive (CSA & PRCI) Strain Limits; X70, OD=30 in, WT=0.5 in

Tensile Strain Limit				Compressive Strain Limit (Resistance Factor=0.8)					
BS-7910 Flaw size=				CSA-Z662		PRCI			
						50% SMYS		72% SMYS	
0.5mm	1mm	2mm		50% SMYS	72% SMYS	Offset=2mm	Offset/WT=0.097mm	Offset=2mm	Offset/WT=0.097mm
1.01	0.97	0.40		-0.67	-0.67	-0.91	-1.05	-1.42	-1.62

The information contained herein is the copyright of and proprietary to BMT Fleet Technology Limited. Use of this information is governed by the legend on the cover page of this document."

APPENDIX B: MODELING OF LANDSLIDE HAZARD –SUMMARY RESULTS 12-INCH PIPELINE

The information contained herein is the copyright of and proprietary to BMT Fleet Technology Limited. Use of this information is governed by the legend on the cover page of this document."

B.1 MODELING OF LANDSLIDE HAZARD – SUMMARY RESULTS 12-INCH PIPELINE

Analyses were completed for the NPS 12 (323 mm outside diameter) pipeline to assess its response to ground subsidence and to determine the structural integrity significance of ground settlement induced strain demands. A sensitivity analysis was conducted to evaluate the effect of D/t ratio, burial depth and ground subsidence width. The analyses considered 18 ground subsidence scenarios. The scenarios included the following:

- Pipe wall thickness: three wall thicknesses: 4.57 mm (0.18 inch), and 9.52 mm (0.375) ; corresponding to D/t ratio of 71, and 34;
- Ground displacement direction: Subsidence, vertical to the pipeline axis;
- Panel widths: three panel widths of 61 m (200 ft), 122 m (400 ft) and 183 m (600 ft)
- Mining depths: three different mining depth for each panel width
- Panel extraction areas defined based on panel width to mining depth ratio (W/H): three W/H ratio of 0.5, 1.5 and 3.0 for each panel width;
- Shape of ground displacement: three ground subsidence patterns;
- One soil conditions with soil properties consistent with sand/clay till; and
- Pipeline burial depth: One burial depth of 1.2 m (4 ft) to top pipe, corresponding to 1.36 m (4.5 ft) depth to pipe center line.

The surface subsidence profile was initiated using Appalachian method developed based upon Applachian mining experience in The USA.

Assumptions for the pipeline were as follows:

- 72% SMYS internal pressure;
- 45^0C thermal differential (installation -20^0C, max operating temperature 25^0C); and
- A generic stress strain curves for Grade X-52 (359) pipe according to the API 5L.

Detailed results for D/t=71 and burial depth of 1.2 m is presented as follows:

- Figure B1 presents the maximum tensile strains in the longitudinal direction of the pipeline versus the maximum ground subsidence for panel extraction width of 61 m, 122 m and 183 m (200 ft, 400ft and 600 ft) considering three (3) potential panel depth that influence surface subsidence, including:
  - sub-critical panel extraction width (W/h =0.5);
  - critical panel extraction width; and (W/h =1.5);
  - super-critical panel extraction width (W/h =3).

- Figure B2 and Figure B3 present the maximum local and nominal compressive strains in the longitudinal direction of the pipeline versus the maximum ground subsidence for

The information contained herein is the copyright of and proprietary to BMT Fleet Technology Limited. Use of this information is governed by the legend on the cover page of this document."

various ground subsidence widths to depth ratio considered in the analyses. The nominal compressive strain is defined as the average compressive strain measured over a gauge length of 2D (D is the pipe outside diameter). This large stain gauge length is used to permit the analyses to be compared directly to codified permissible strain formulations which are reported over this gauge length.

- The results indicate that for the three (3) cases considered, the sub-critical panel extraction width (W/h =0.5) results in the largest tensile and compressive strain in the pipe for any given value of ground subsidence for analyzed cases.
- Figure B4 presents the maximum tensile strains in pipe versus the ground subsidence width (W) to panel depth for given ground displacement of 0.5, 1.0, 1.5, 2.5, 3.0, 3.0 and 4.0. In this figure, the BS-7910 tensile strain capacity is presented with dash horizontal line. Any tensile strain above the horizontal line is strain-related failure limit.
- The results indicate that for this pipe and operating condition combination, panel width to depth ratio of 0.5 can be considered critical. This result suggests that the pipeline is forced to follow the ground subsidence pattern and more sharp subsidence profiles promotes higher curvature along with pipe axial extension.
- Figure B5 presents the maximum nominal compressive strain in the pipe versus the panel width to depth ratio (W/h) for given ground settlement of 0.5, 1.0, 1.5, 2.0, 2.5, 3.0, 3.5 and 4.0. The nominal compressive strain is defined as the average compressive strain measured over a gauge length of 2D (D is the pipe outside diameter). In this figure, the CSA and PRCI compressive strain capacity is presented with dash horizontal line. The compressive strains are maximized for lower panel width ratios.

The information contained herein is the copyright of and proprietary to BMT Fleet Technology Limited. Use of this information is governed by the legend on the cover page of this document."

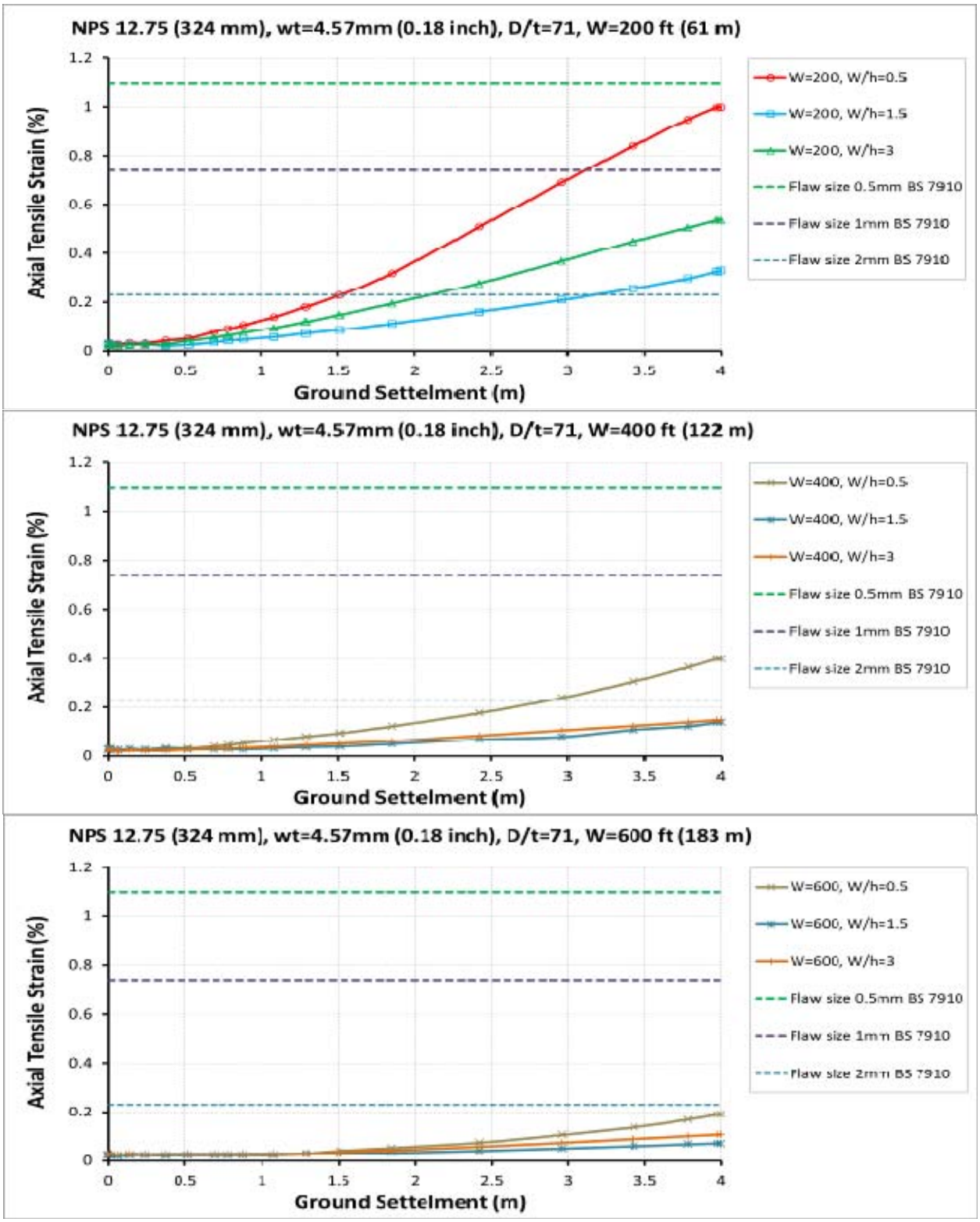

Figure B1: NPS 12.75 (D/t=71) - Maximum Tensile in the Pipe vs. Ground Subsidence W=61, 122 and 183 m (200, 400 and 600 ft); W/h Ratio 0.5, 1.5 and 3

The information contained herein is the copyright of and proprietary to BMT Fleet Technology Limited. Use of this information is governed by the legend on the cover page of this document."

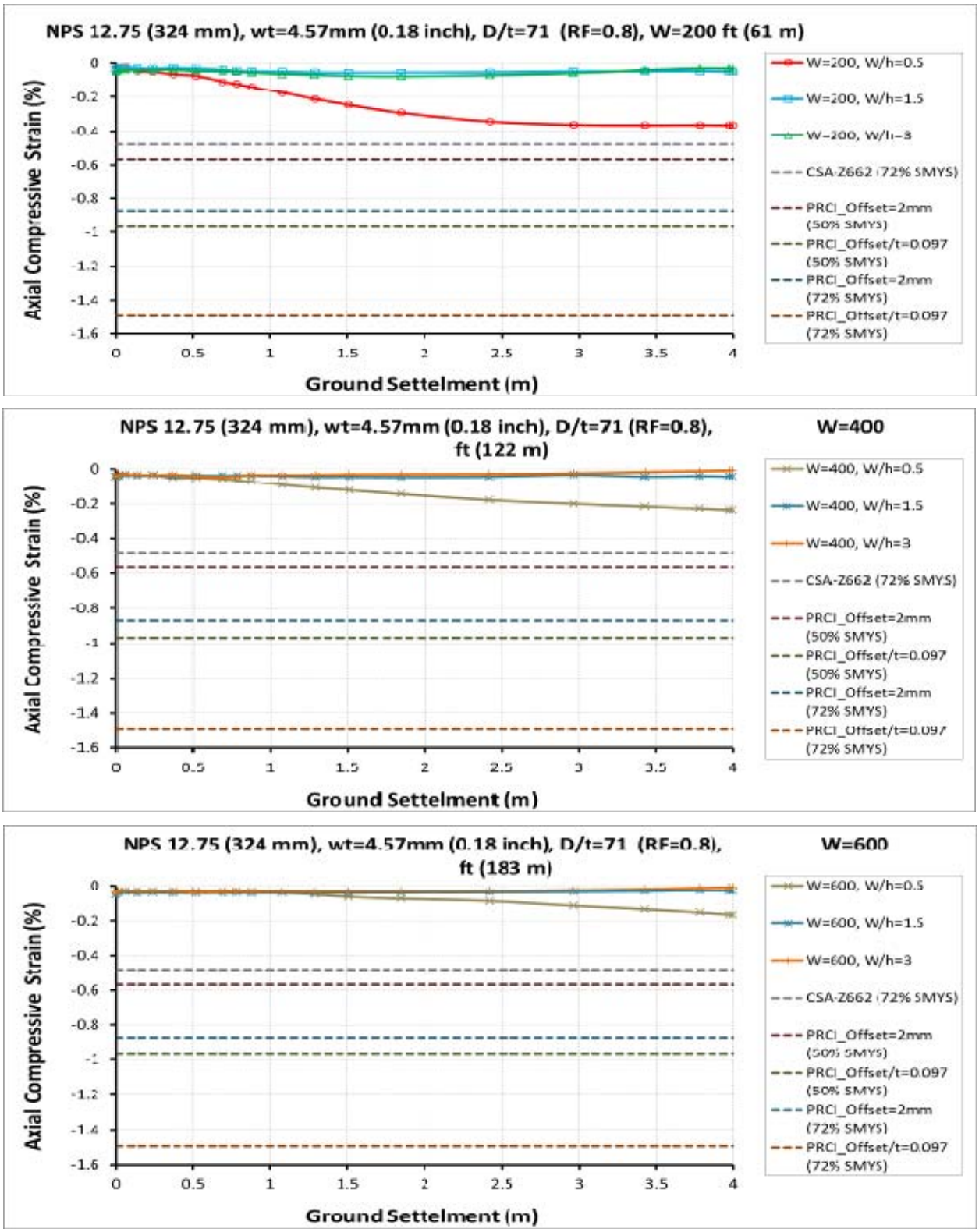

Figure B2: NPS 12.75 (D/t=71) - Maximum Local Compressive Strains in the Pipe vs. Ground Subsidence W=61, 122 and 183 m (200, 400 and 600 ft); W/h Ratio 0.5, 1.5 and 3

The information contained herein is the copyright of and proprietary to BMT Fleet Technology Limited. Use of this information is governed by the legend on the cover page of this document."

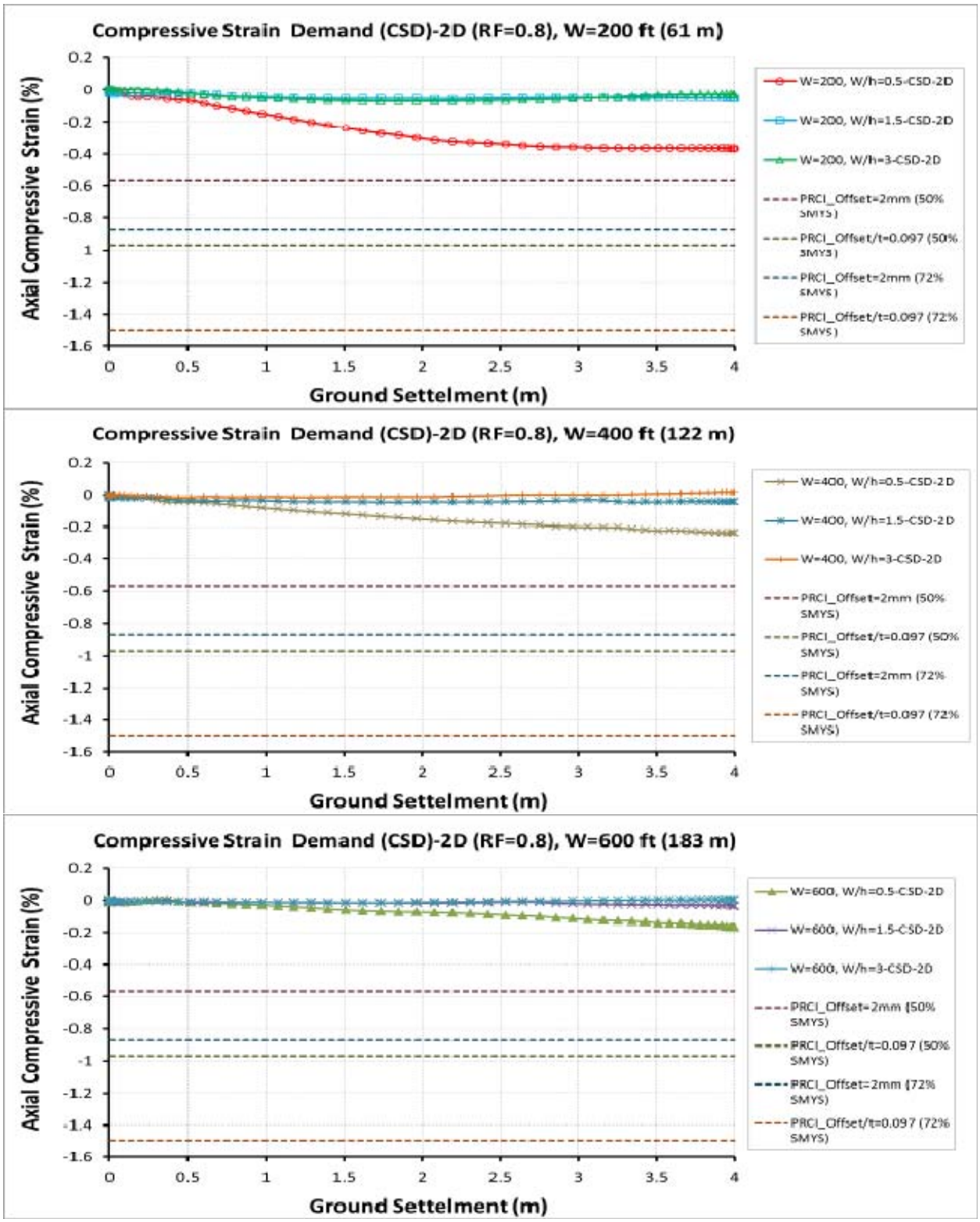

Figure B3: NPS 12.75 (D/t=71) - Maximum Nominal Compressive Strains in the Pipe vs. Ground Subsidence W=61, 122 and 183 m (200, 400 and 600 ft); W/h Ratio 0.5, 1.5 and 3

The information contained herein is the copyright of and proprietary to BMT Fleet Technology Limited. Use of this information is governed by the legend on the cover page of this document."

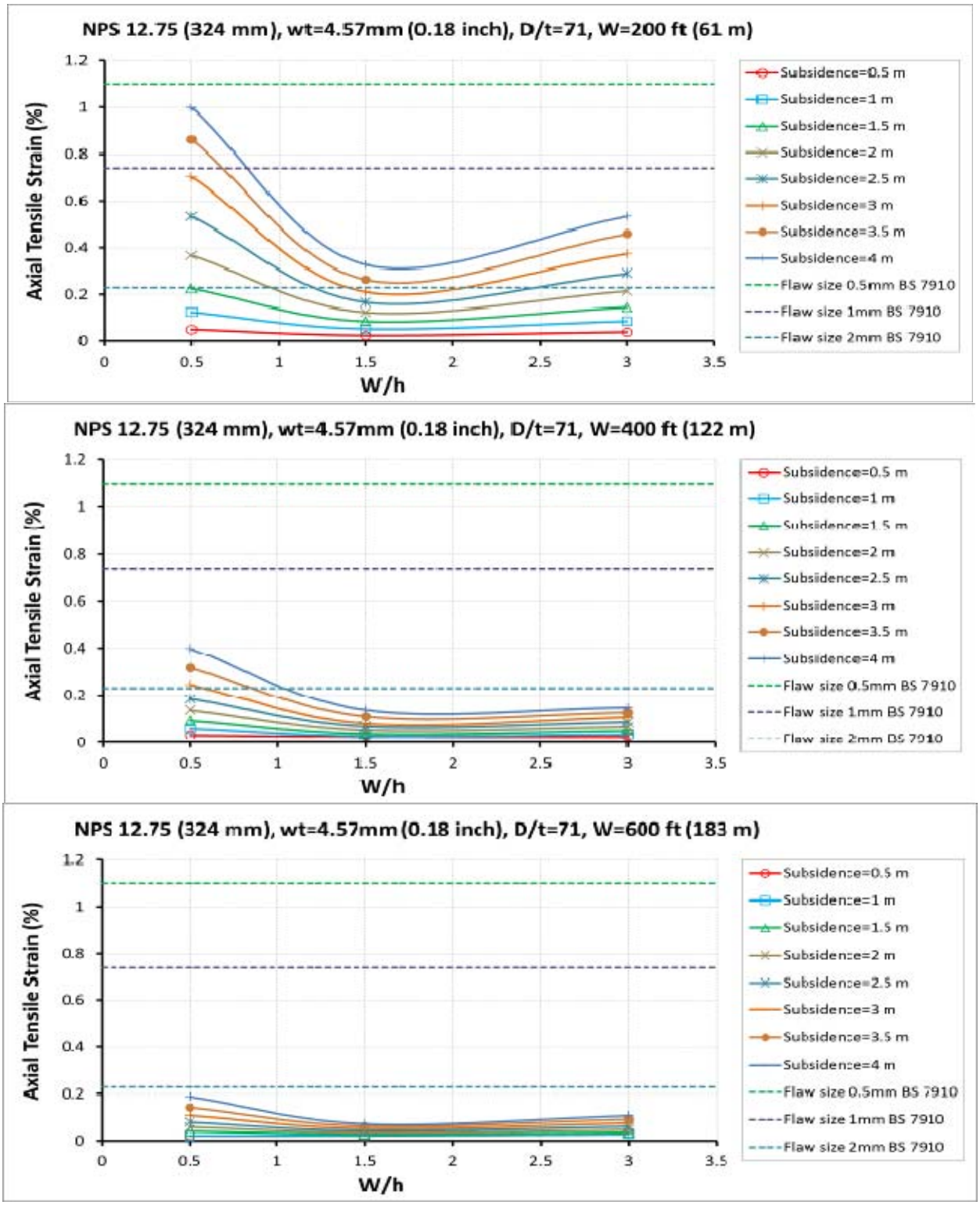

Figure B4: NPS 12.75 (D/t=71)- Pipe Axial Tensile Strains Envelopes versus Width to Depth Ratio [W=61, 122 and 183 m (200, 400 and 600 ft)] for Ground Settlement of 0.5, 1, 1.5, 2.0, 2.5, 3.0, 3.5 and 4.0 m

The information contained herein is the copyright of and proprietary to BMT Fleet Technology Limited. Use of this information is governed by the legend on the cover page of this document."

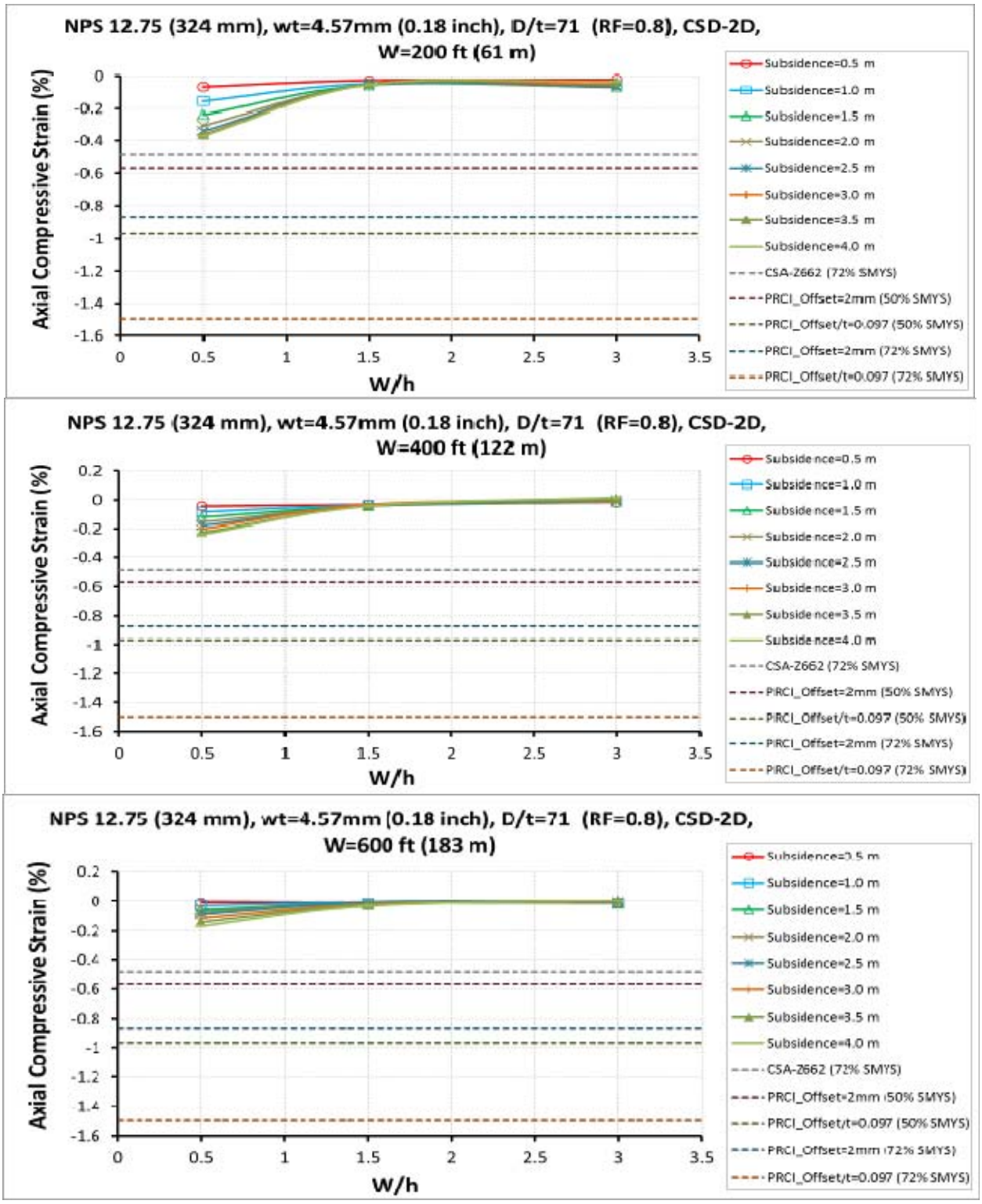

Figure B5: NPS 12.75 (D/t=71) -Pipe Axial Compressive Strains Envelopes versus Width to Depth Ratio [W=61, 122 and 183 m (200, 400 and 600 ft)] for Ground Settlement of 0.5, 1, 1.5, 2.0, 2.5, 3.0, 3.5 and 4.0 m

The information contained herein is the copyright of and proprietary to BMT Fleet Technology Limited. Use of this information is governed by the legend on the cover page of this document."

Detailed results for D/t=34 and burial depth of 1.2 m is presented as follows:

- Figure B6 presents the maximum tensile strains in the longitudinal direction of the pipeline versus the maximum ground subsidence for panel extraction width of 61 m, 122 m and 183 m (200 ft, 400 ft and 600 ft) considering three (3) potential panel depth that influence surface subsidence, including:

  - sub-critical panel extraction width (W/h =0.5);
  - critical panel extraction width; and (W/h =1.5);
  - super-critical panel extraction width (W/h =3).

- Figure B7 and Figure B8 present the maximum local and nominal compressive strains in the longitudinal direction of the pipeline versus the maximum ground subsidence for various ground subsidence widths to depth ratio considered in the analyses. The results indicate that for the three (3) cases considered, the sub-critical panel extraction width (W/h=0.5) results in the largest tensile and compressive strain in the pipe for any given value of ground subsidence for analyzed cases.
- Figure B9 presents the maximum tensile strains in pipe versus the ground subsidence width (W) to panel depth for given ground displacement of 0.5, 1.0, 1.5, 2.5, 3.0, 3.0 and 4.0. In this figure, the BS-7910 tensile strain capacity is presented with dash horizontal line. Any tensile strain above the horizontal line is strain-related failure limit.
- Figure B10 presents the maximum nominal compressive strain in the pipe versus the panel width to depth ratio (W/h) for given ground settlement of 0.5, 1.0, 1.5, 2.0, 2.5, 3.0, 3.5 and 4.0. The nominal compressive strain is defined as the average compressive strain measured over a gauge length of 2D (D is the pipe outside diameter). In this figure, the CSA and PRCI compressive strain capacity is presented with dash horizontal line. The compressive strains are maximized for lower panel width ratios.

The information contained herein is the copyright of and proprietary to BMT Fleet Technology Limited. Use of this information is governed by the legend on the cover page of this document."

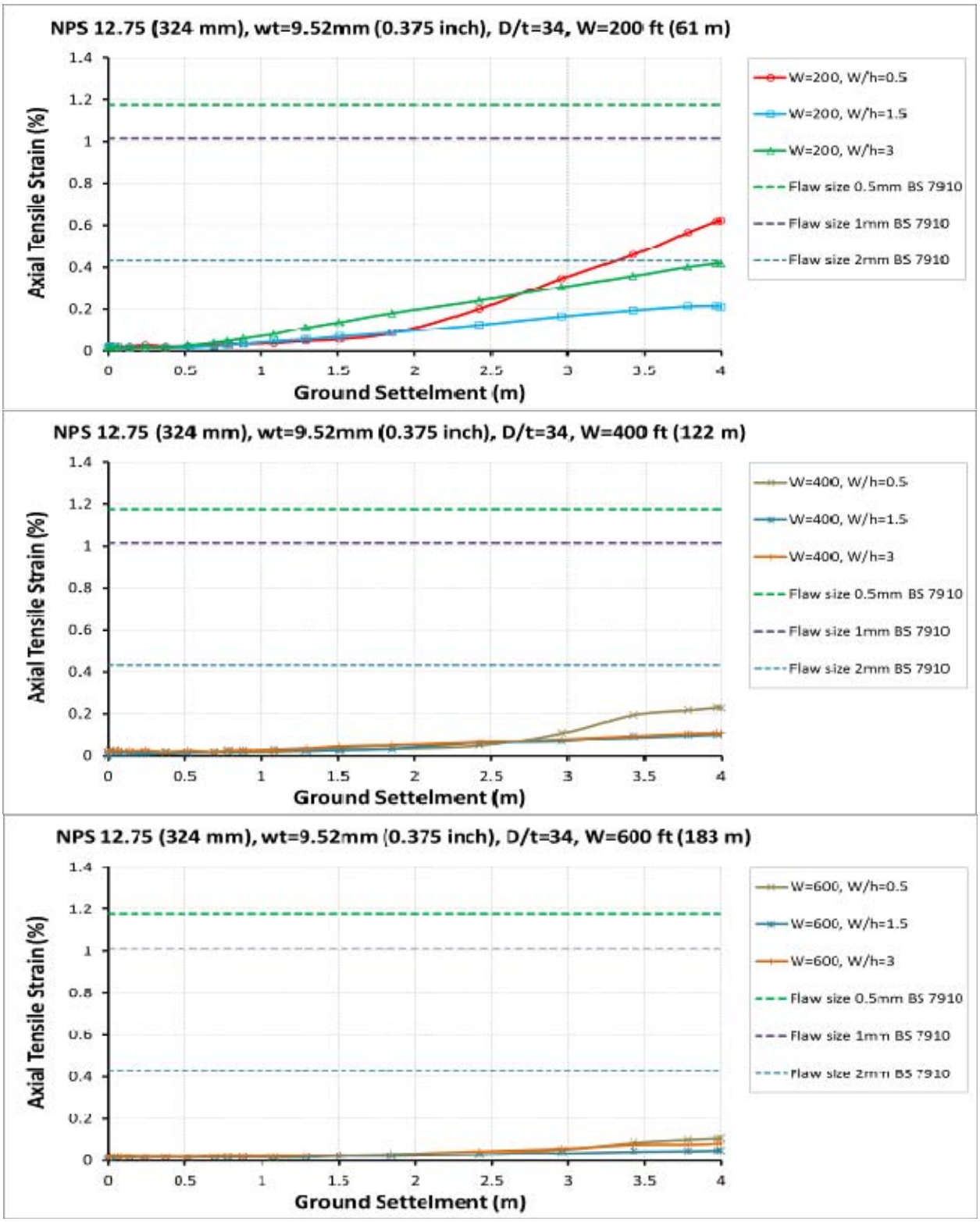

Figure B6: NPS 12.75 (D/t=34) - Maximum Tensile in the Pipe vs. Ground Subsidence W=61, 122 and 183 m (200, 400 and 600 ft); W/h Ratio 0.5, 1.5 and 3

The information contained herein is the copyright of and proprietary to BMT Fleet Technology Limited. Use of this information is governed by the legend on the cover page of this document."

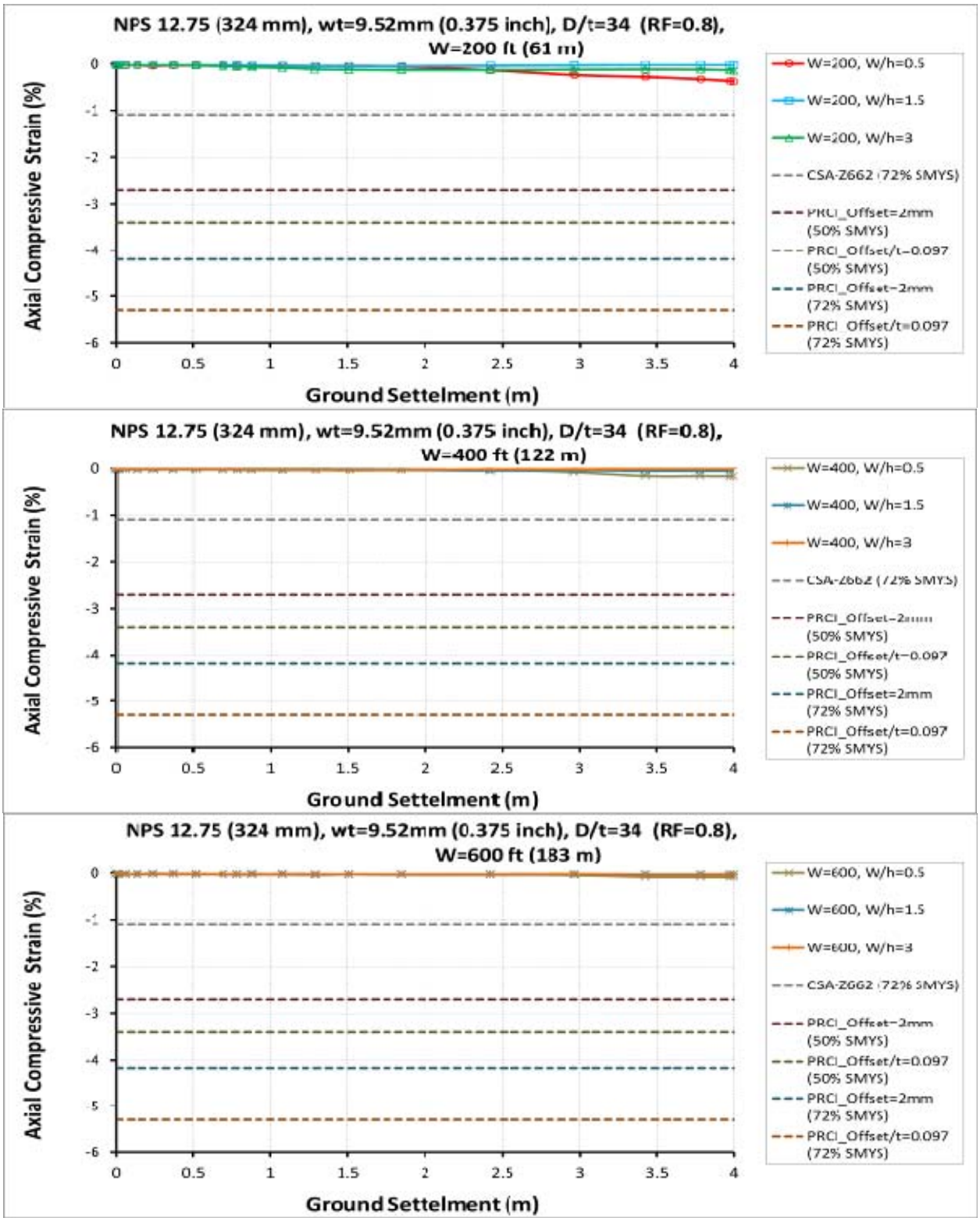

Figure B7: NPS 12.75 (D/t=34) - Maximum Local Compressive Strains in the Pipe vs. Ground Subsidence W=61, 122 and 183 m (200, 400 and 600 ft); W/h Ratio 0.5, 1.5 and 3

The information contained herein is the copyright of and proprietary to BMT Fleet Technology Limited. Use of this information is governed by the legend on the cover page of this document."

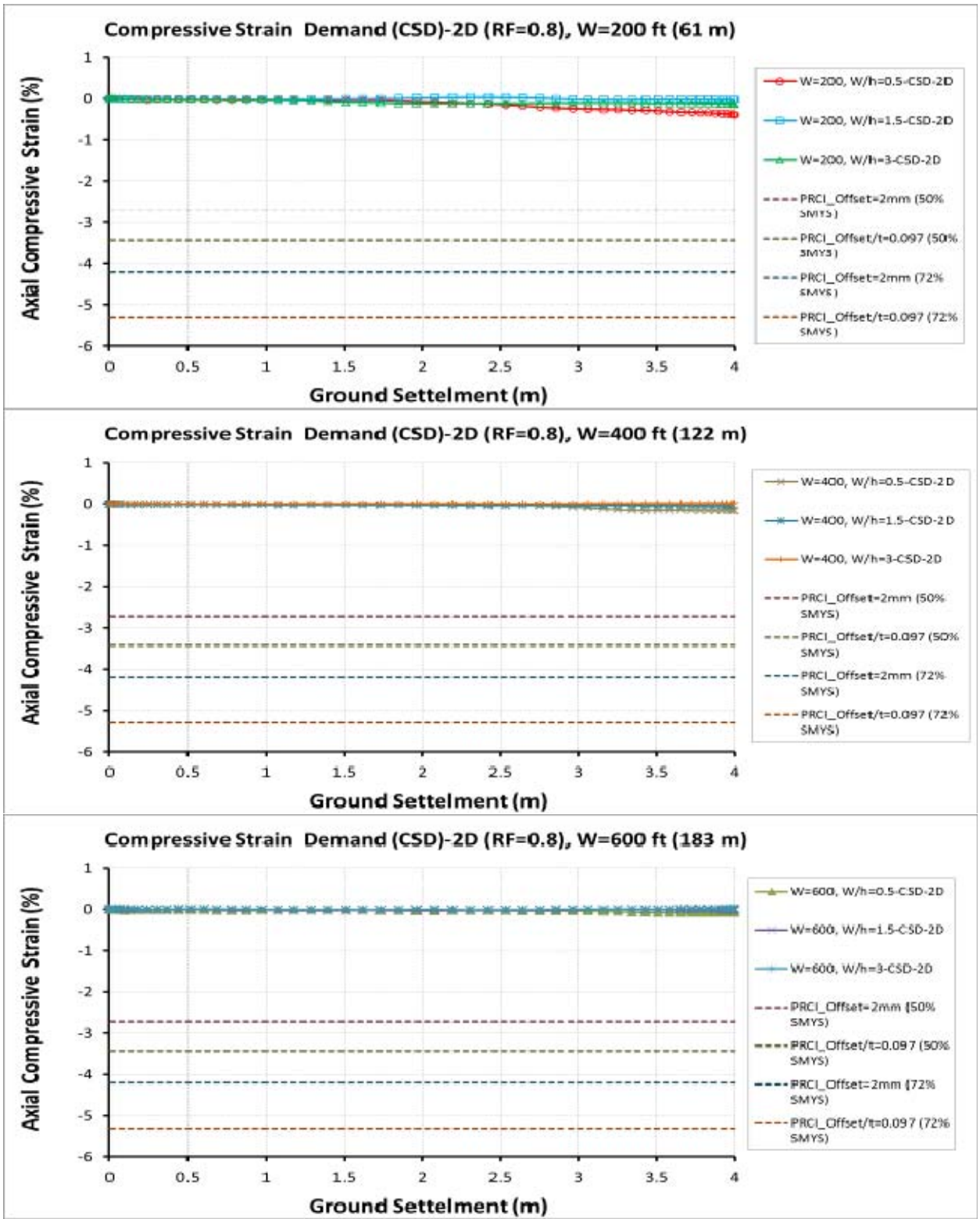

Figure B8: NPS 12.75 (D/t=34) - Maximum Nominal Compressive Strains in the Pipe vs. Ground Subsidence W=61, 122 and 183 m (200, 400 and 600 ft); W/h Ratio 0.5, 1.5 and 3

The information contained herein is the copyright of and proprietary to BMT Fleet Technology Limited. Use of this information is governed by the legend on the cover page of this document."

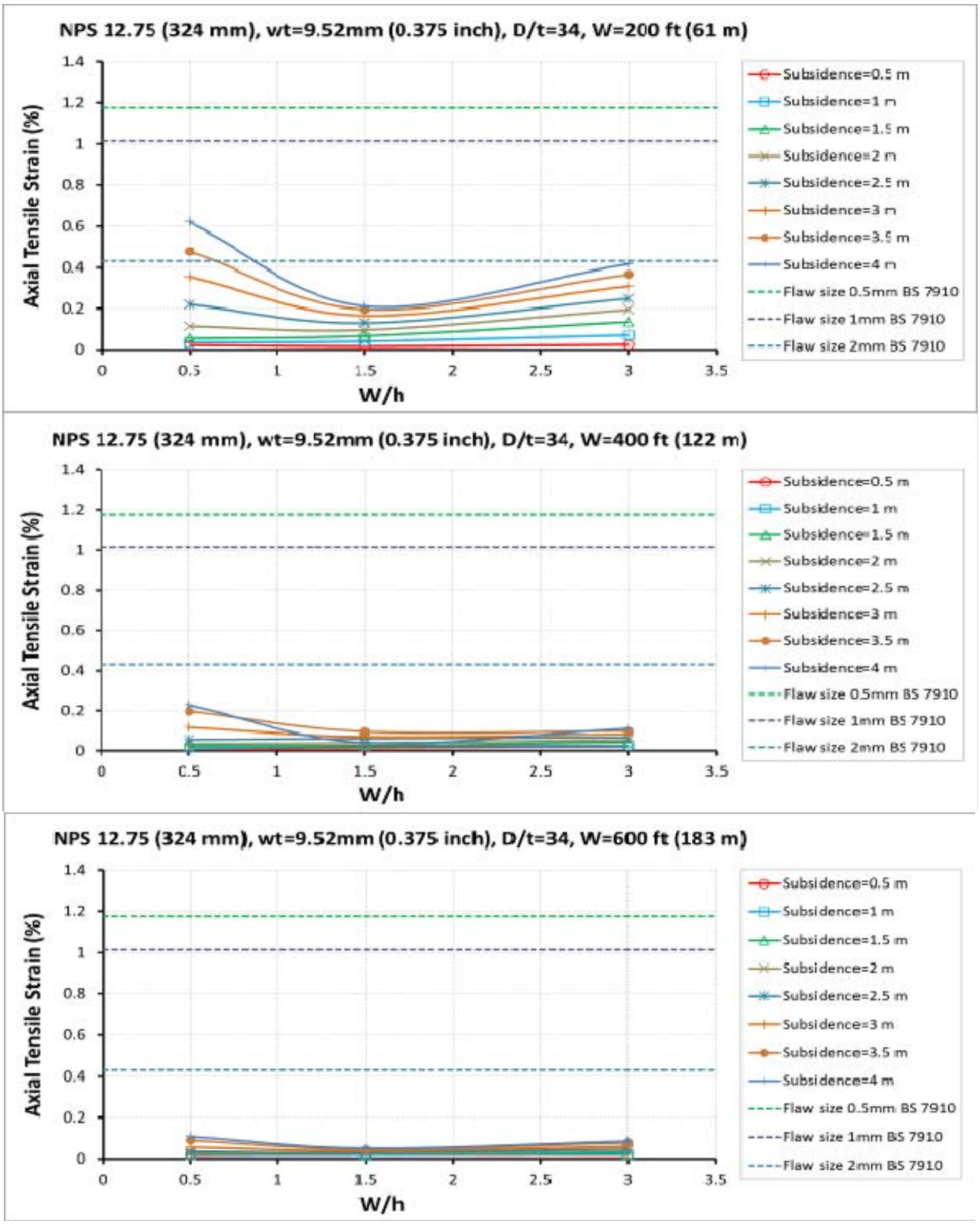

Figure B9: NPS 12.75 (D/t=34) - Pipe Axial Tensile Strains Envelopes versus Width to Depth Ratio [W=61, 122 and 183 m (200, 400 and 600 ft)] for Ground Settlement of 0.5, 1, 1.5, 2.0, 2.5, 3.0, 3.5 and 4.0 m

The information contained herein is the copyright of and proprietary to BMT Fleet Technology Limited. Use of this information is governed by the legend on the cover page of this document."

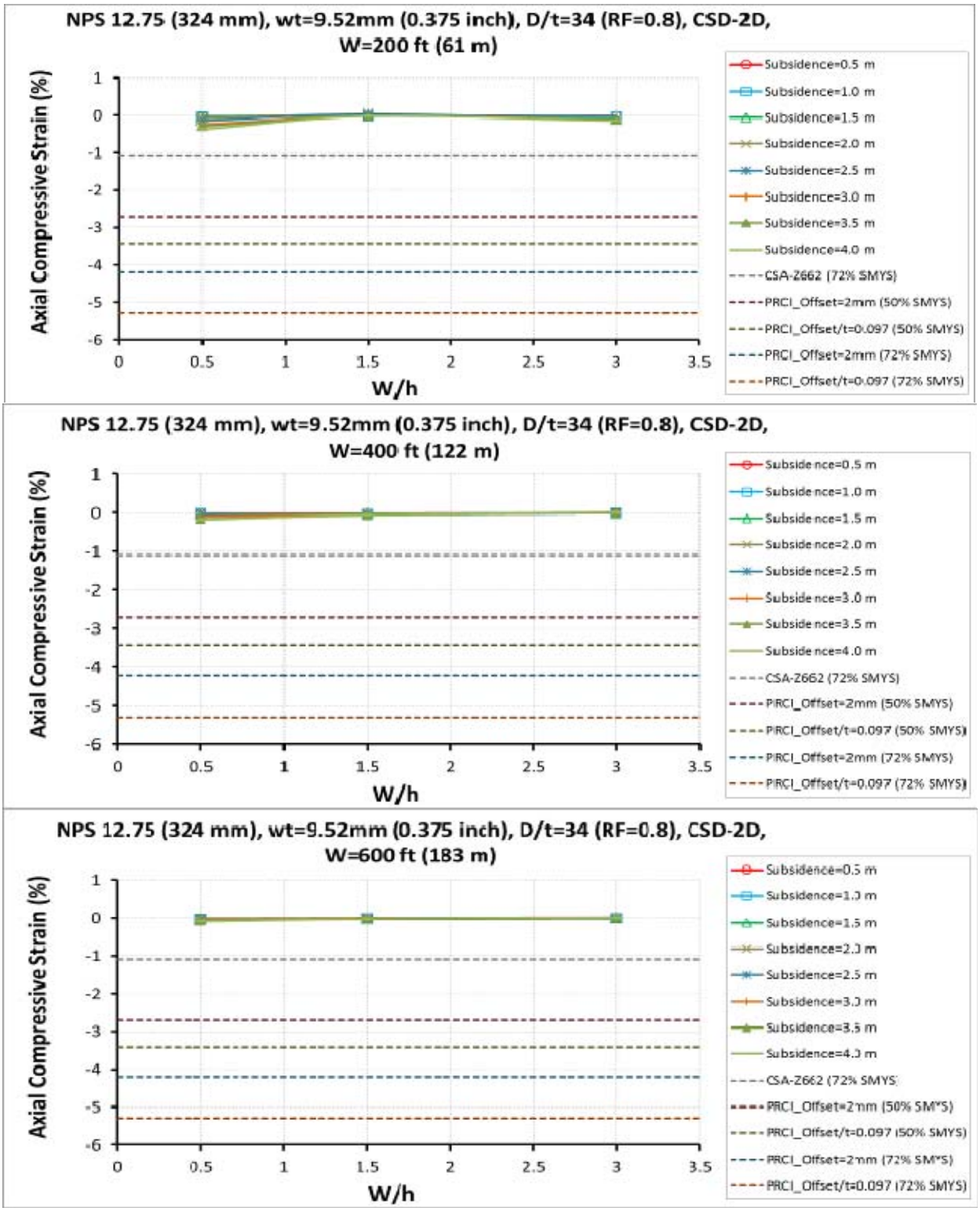

Figure B10: NPS 12.75 (D/t=34) - Pipe Axial Compressive Strains Envelopes versus Width to Depth Ratio [W=61, 122 and 183 m (200, 400 and 600 ft)] for Ground Settlement of 0.5, 1, 1.5, 2.0, 2.5, 3.0, 3.5 and 4.0 m

The information contained herein is the copyright of and proprietary to BMT Fleet Technology Limited. Use of this information is governed by the legend on the cover page of this document."

APPENDIX C - MODELING OF LANDSLIDE HAZARD – SUMMARY RESULTS 18-INCH PIPELINE

The information contained herein is the copyright of and proprietary to BMT Fleet Technology Limited. Use of this information is governed by the legend on the cover page of this document."

C.1 MODELING OF LANDSLIDE HAZARD – SUMMARY RESULTS 18-INCH PIPELINE

Analyses were completed for the NPS 18 (456 mm outside diameter) pipeline to assess its response to ground subsidence and to determine the structural integrity significance of ground settlement induced strain demands. A sensitivity analysis was conducted to evaluate the effect of D/t ratio, burial depth and ground subsidence width. The analyses considered 18 ground subsidence scenarios. The scenarios included the following:

- Pipe wall thickness: three wall thicknesses: 4.57 mm (0.18 inch), and 9.52 mm (0.375), corresponding to D/t ratio of 96, and 48;
- Ground displacement direction: Subsidence, vertical to the pipeline axis;
- Panel widths: three panel widths of 61 m (200 ft), 122 m (400 ft) and 183 m (600 ft)
- Mining depths: three different mining depth for each panel width
- Panel extraction areas defined based on panel width to mining depth ratio (W/H): three W/H ratio of 0.5, 1.5 and 3.0 for each panel width;
- Shape of ground displacement: three ground subsidence patterns;
- One soil conditions with soil properties consistent with sand/clay; and
- Pipeline burial depth: One burial depth of 1.2 m (4 ft) to top pipe, corresponding to 1.42 m (4.7 ft) depth to pipe center line.

The surface subsidence profile was initiated using Appalachian method developed based upon Applachian mining experience in The USA.

Assumptions for the pipeline were as follows:

- 72% SMYS internal pressure;
- 45^0C thermal differential (installation -20^0C, max operating temperature 25^0C); and
- A generic stress strain curves for Grade X-52 (359) pipe according to the API 5L.

Detailed results for D/t=96 and burial depth of 1.2 m is presented as follow:

- Figure C1 presents the maximum tensile strains in the longitudinal direction of the pipeline versus the maximum ground subsidence for panel extraction width of 61 m, 122 m and 183 m (200 ft, 400 ft and 600 ft) considering three (3) potential panel depth that influence surface subsidence, including:
  - sub-critical panel extraction width (W/h =0.5);
  - critical panel extraction width; and (W/h =1.5);
  - super-critical panel extraction width (W/h =3).
- Figure C2 and Figure C3 present the maximum local and nominal compressive strains in the longitudinal direction of the pipeline versus the maximum ground subsidence for various ground subsidence widths to depth ratio considered in the analyses. The nominal compressive strain is defined as the average compressive strain measured over a gauge

The information contained herein is the copyright of and proprietary to BMT Fleet Technology Limited. Use of this information is governed by the legend on the cover page of this document."

length of 2D (D is the pipe outside diameter). This large stain gauge length is used to permit the analyses to be compared directly to codified permissible strain formulations which are reported over this gauge length.

- The results indicate that for the three (3) cases considered, the sub-critical panel extraction width (W/h=0.5) results in the largest tensile and compressive strain in the pipe for any given value of ground subsidence for analyzed cases.
- Figure C4 presents the maximum tensile strains in pipe versus the ground subsidence width (W) to panel depth for given ground displacement of 0.5, 1.0, 1.5, 2.5, 3.0, 3.0 and 4.0. In this figure, the BS-7910 tensile strain capacity is presented with dash horizontal line. Any tensile strain above the horizontal line is strain-related failure limit.
- The results indicate that for this pipe and operating condition combination, panel width to depth ratio of 0.5 can be considered critical. This result suggests that the pipeline is forced to follow the ground subsidence pattern and more sharp subsidence profiles promotes higher curvature along with pipe axial extension.
- Figure C5 presents the maximum nominal compressive strain in the pipe versus the panel width to depth ratio (W/h) for given ground settlement of 0.5, 1.0, 1.5, 2.0, 2.5, 3.0, 3.5 and 4.0. The nominal compressive strain is defined as the average compressive strain measured over a gauge length of 2D (D is the pipe outside diameter). In this figure, the CSA and PRCI compressive strain capacity is presented with dash horizontal line. The compressive strains are maximized for lower panel width ratios.

The information contained herein is the copyright of and proprietary to BMT Fleet Technology Limited. Use of this information is governed by the legend on the cover page of this document."

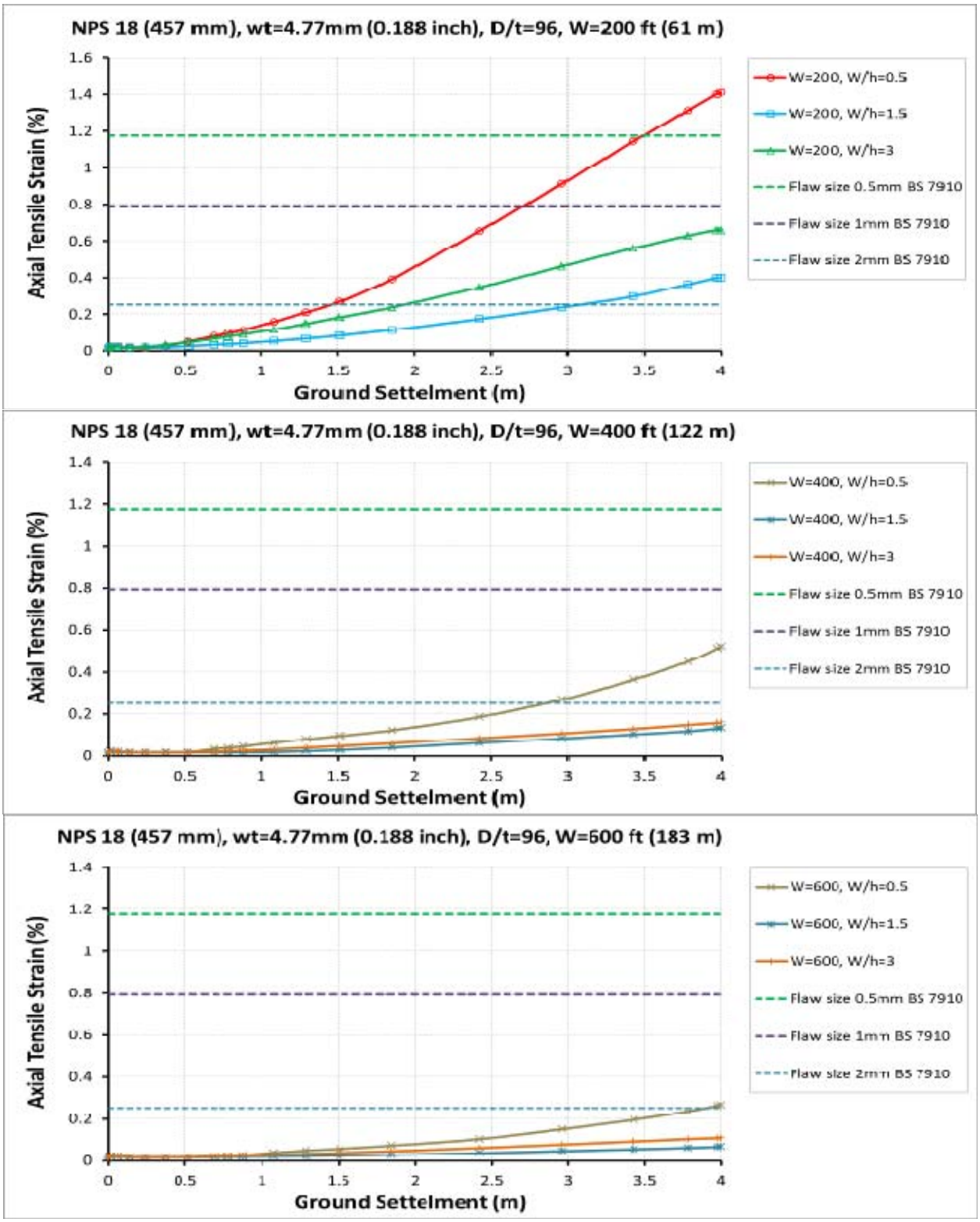

Figure C1: NPS 18 (D/t=96) - Maximum Tensile in the Pipe vs. Ground Subsidence W=61, 122 and 183 m (200, 400 and 600 ft); W/h Ratio 0.5, 1.5 and 3

The information contained herein is the copyright of and proprietary to BMT Fleet Technology Limited. Use of this information is governed by the legend on the cover page of this document."

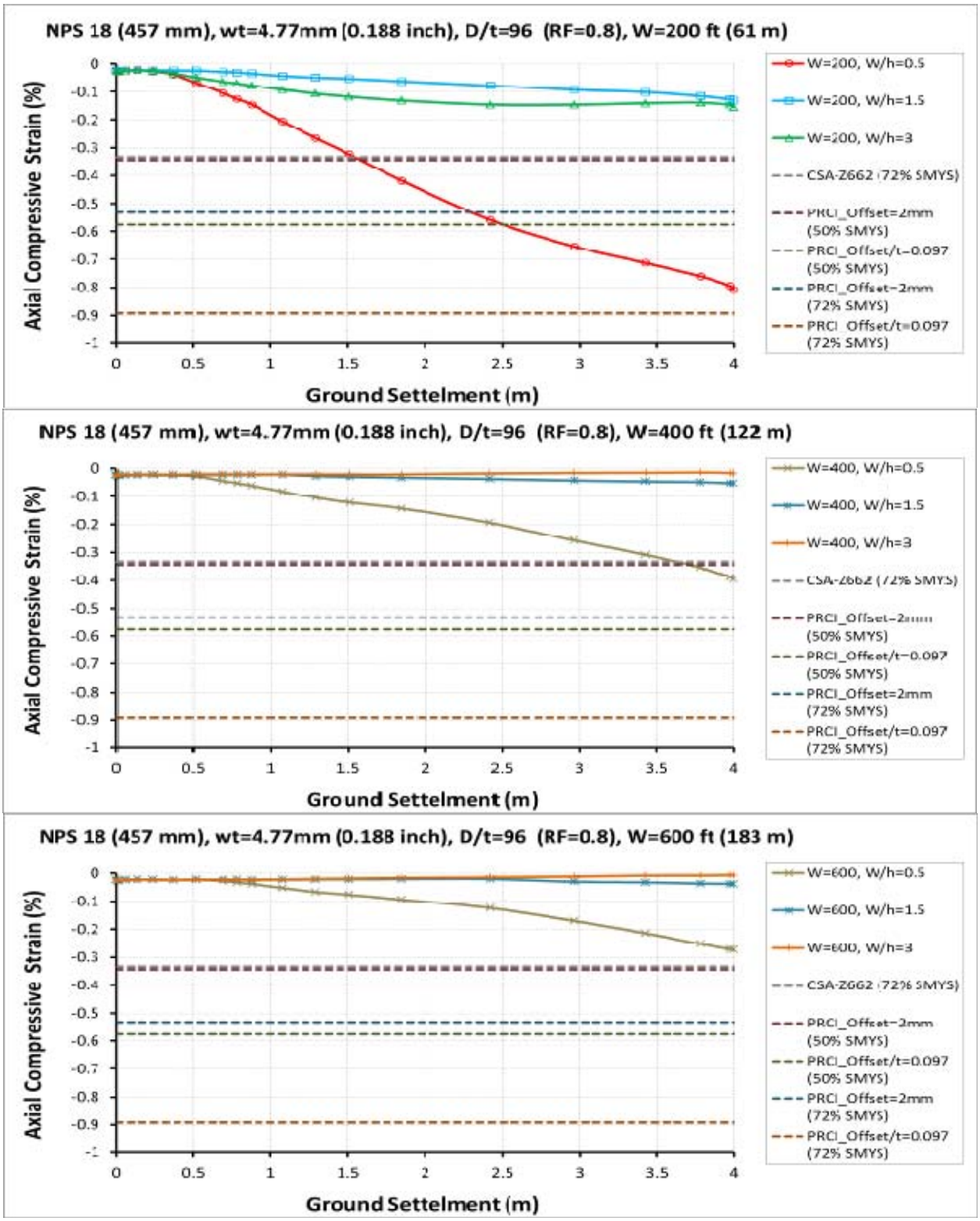

Figure C2: NPS 18 (D/t=96) - Maximum Local Compressive Strains in the Pipe vs. Ground Subsidence W=61, 122 and 183 m (200, 400 and 600 ft); W/h Ratio 0.5, 1.5 and 3

The information contained herein is the copyright of and proprietary to BMT Fleet Technology Limited. Use of this information is governed by the legend on the cover page of this document."

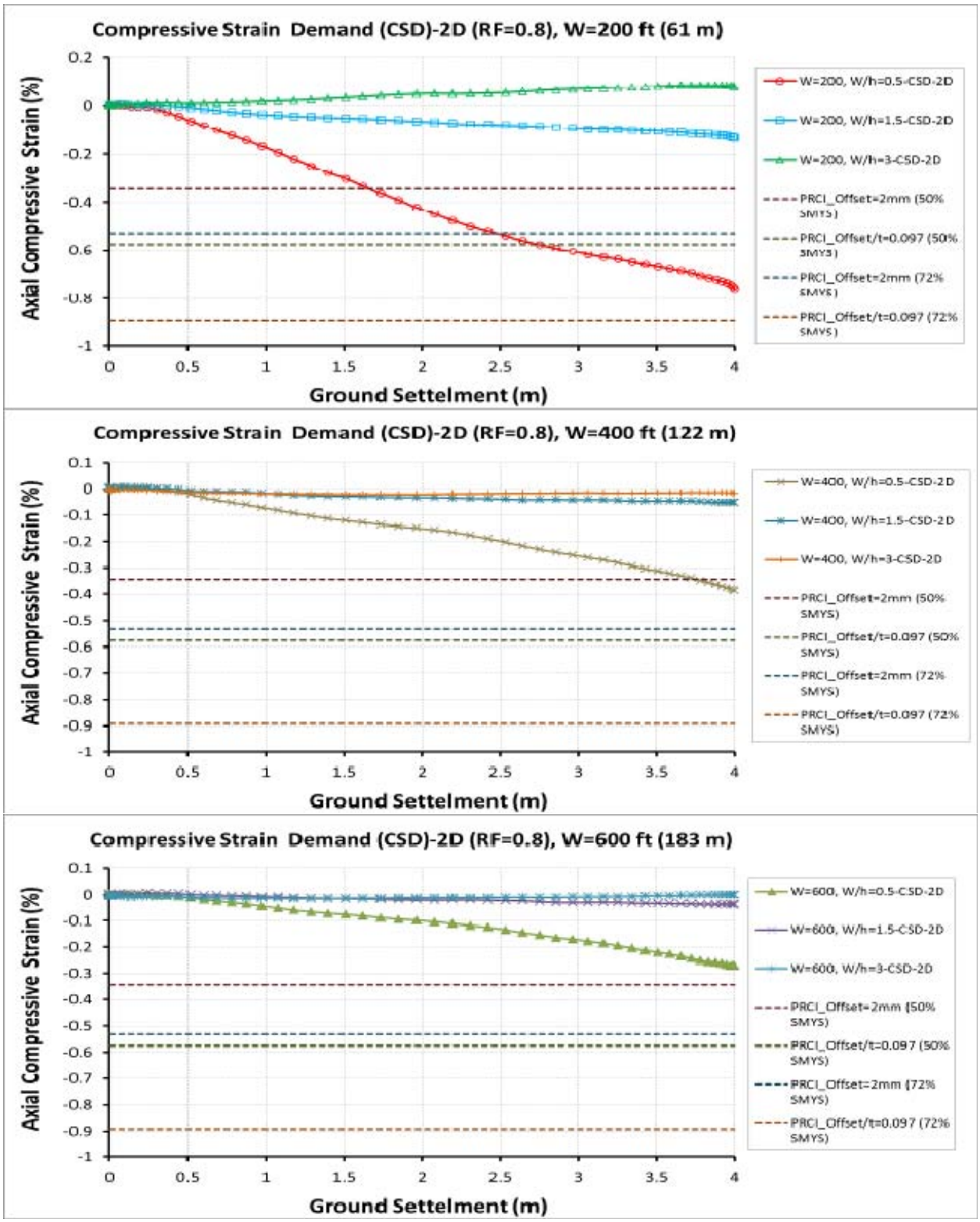

Figure C3: NPS 18 (D/t=96) - Maximum Nominal Compressive Strains in the Pipe vs. Ground Subsidence W=61, 122 and 183 m (200, 400 and 600 ft); W/h Ratio 0.5, 1.5 and 3

The information contained herein is the copyright of and proprietary to BMT Fleet Technology Limited. Use of this information is governed by the legend on the cover page of this document."

C.1.1 Tensile Strain Capacity Envelopes (TSCE), TSD-2D

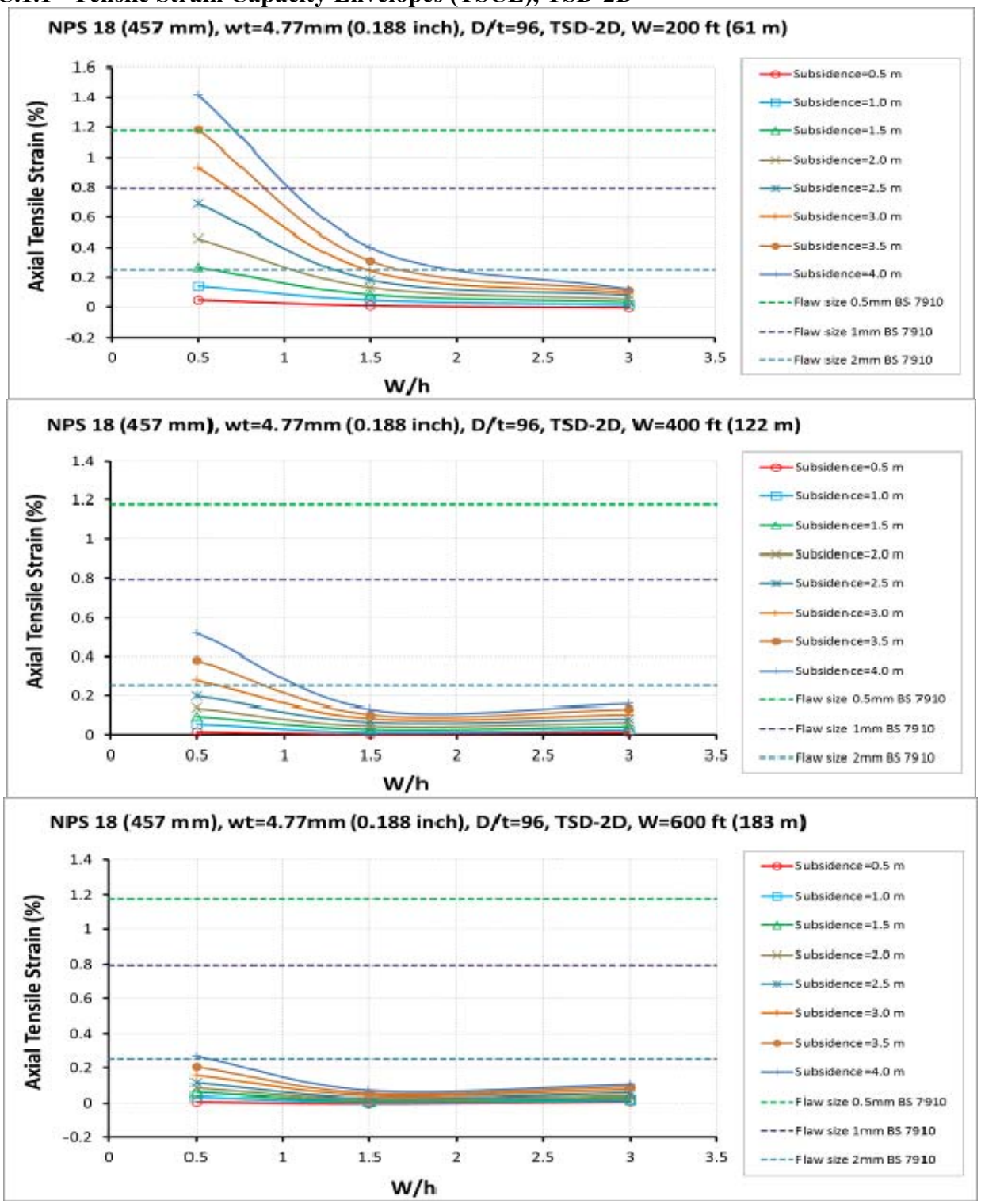

Figure C4 : NPS 18 (D/t=96) - Pipe Axial Tensile Strains Envelopes versus Width to Depth Ratio [W=61, 122 and 183 m (200, 400 and 600 ft)] for Ground Settlement of 0.5, 1, 1.5, 2.0, 2.5, 3.0, 3.5 and 4.0 m

The information contained herein is the copyright of and proprietary to BMT Fleet Technology Limited. Use of this information is governed by the legend on the cover page of this document."

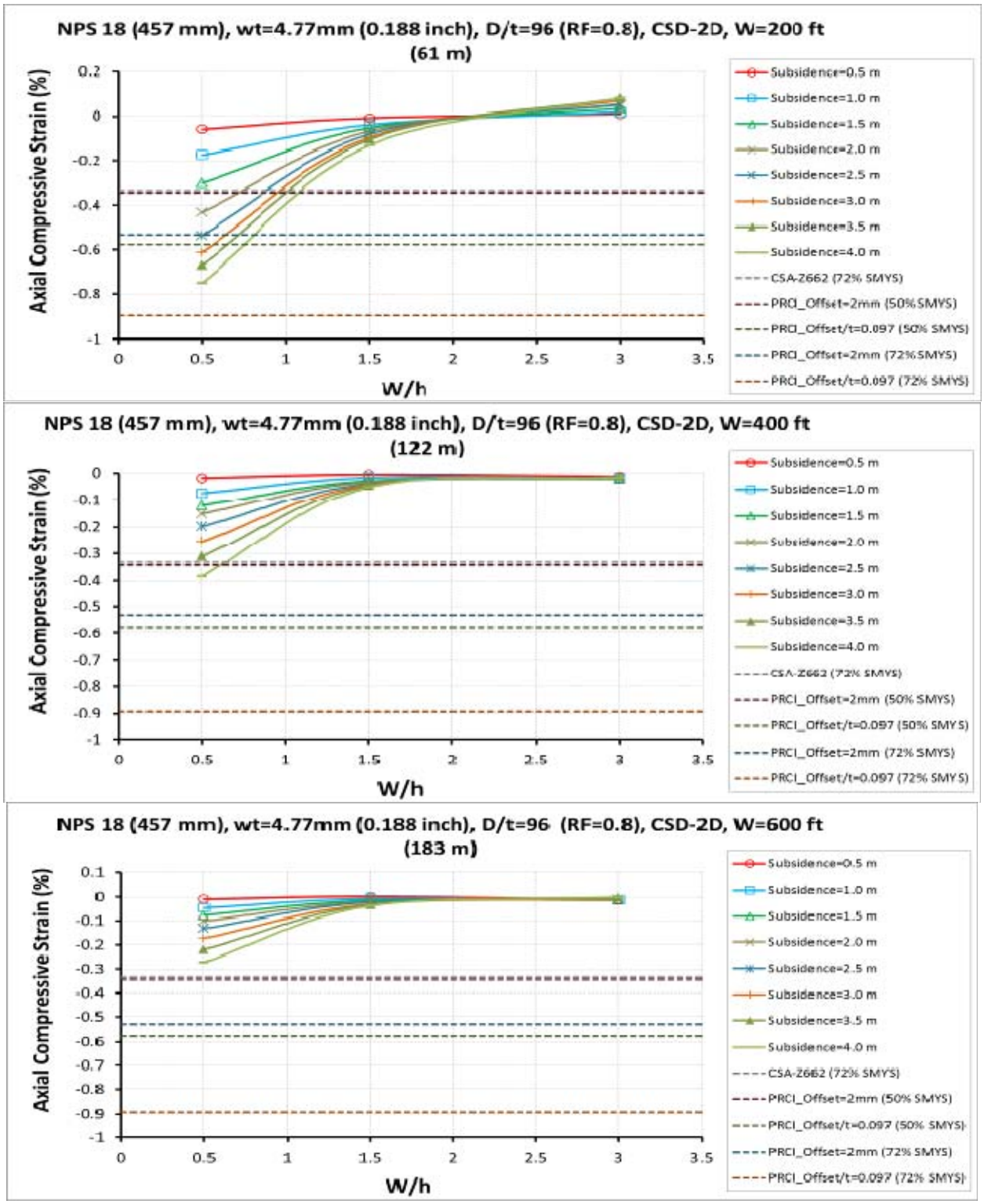

Figure C5: NPS 18 (D/t=96) - Pipe Axial Compressive Strains Envelopes versus Width to Depth Ratio [W=61, 122 and 183 m (200, 400 and 600 ft)] for Ground Settlement of 0.5, 1, 1.5, 2.0, 2.5, 3.0, 3.5 and 4.0 m

The information contained herein is the copyright of and proprietary to BMT Fleet Technology Limited. Use of this information is governed by the legend on the cover page of this document."

Detailed results for D/t=48 and burial depth of 1.2 m is presented as follow:

- Figure C6 presents the maximum tensile strains in the longitudinal direction of the pipeline versus the maximum ground subsidence for panel extraction width of 61 m, 122 m and 183 m (200 ft, 400ft and 600 ft) considering three (3) potential panel depth that influence surface subsidence, including:
  - sub-critical panel extraction width (W/h =0.5);
  - critical panel extraction width; and (W/h =1.5);
  - super-critical panel extraction width (W/h =3).
- Figure C7 and Figure C8 present the maximum local and nominal compressive strains in the longitudinal direction of the pipeline versus the maximum ground subsidence for various ground subsidence widths to depth ratio considered in the analyses. The results indicate that for the three (3) cases considered, the sub-critical panel extraction width (W/h =0.5) results in the largest tensile and compressive strain in the pipe for any given value of ground subsidence for analyzed cases.
- Figure C9 presents the maximum tensile strains in pipe versus the ground subsidence width (W) to panel depth for given ground displacement of 0.5, 1.0, 1.5, 2.5, 3.0, 3.0 and 4.0. In this figure, the BS-7910 tensile strain capacity is presented with dash horizontal line. Any tensile strain above the horizontal line is strain-related failure limit.
- Figure C10 presents the maximum nominal compressive strain in the pipe versus the panel width to depth ratio (W/h) for given ground settlement of 0.5, 1.0, 1.5, 2.0, 2.5, 3.0, 3.5 and 4.0. The nominal compressive strain is defined as the average compressive strain measured over a gauge length of 2D (D is the pipe outside diameter). In this figure, the CSA and PRCI compressive strain capacity is presented with dash horizontal line. The compressive strains are maximized for lower panel width ratios.

The information contained herein is the copyright of and proprietary to BMT Fleet Technology Limited. Use of this information is governed by the legend on the cover page of this document."

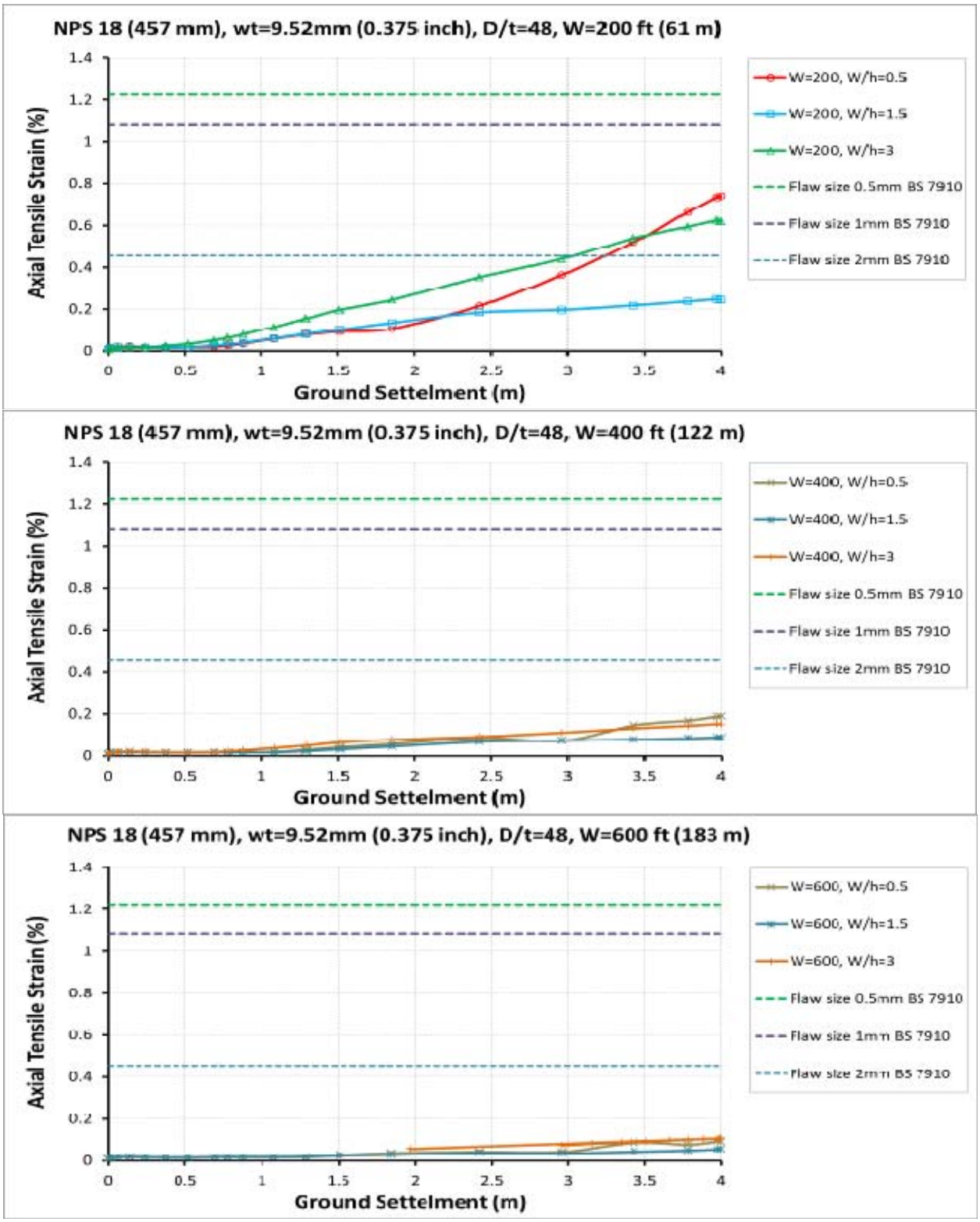

Figure C6: NPS 18 (D/t=48) - Maximum Tensile in the Pipe vs. Ground Subsidence W=61, 122 and 183 m (200, 400 and 600 ft); W/h Ratio 0.5, 1.5 and 3

The information contained herein is the copyright of and proprietary to BMT Fleet Technology Limited. Use of this information is governed by the legend on the cover page of this document."

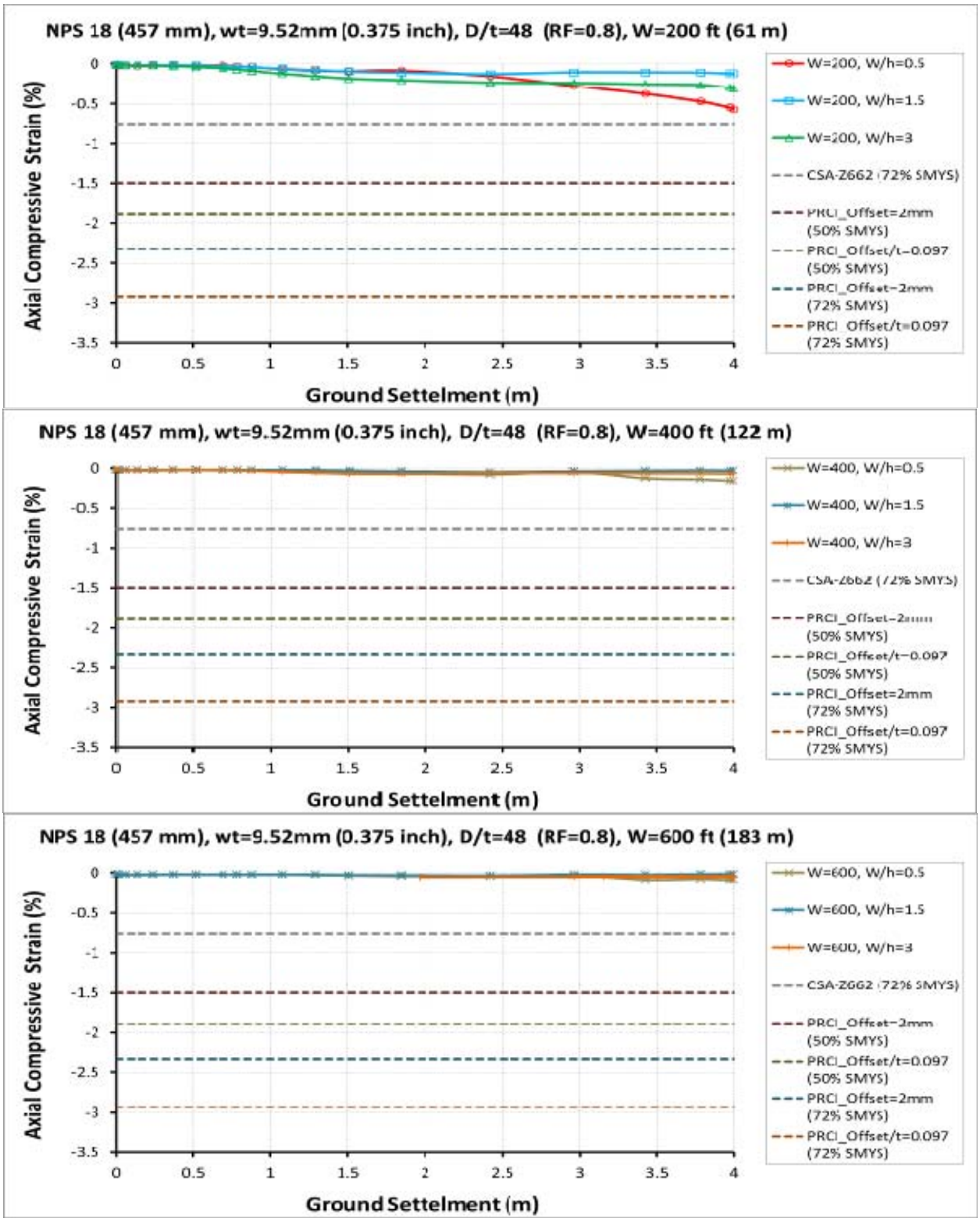

Figure C7: NPS 18 (D/t=48) - Maximum Local Compressive Strains in the Pipe vs. Ground Subsidence W=61, 122 and 183 m (200, 400 and 600 ft); W/h Ratio 0.5, 1.5 and 3

The information contained herein is the copyright of and proprietary to BMT Fleet Technology Limited. Use of this information is governed by the legend on the cover page of this document."

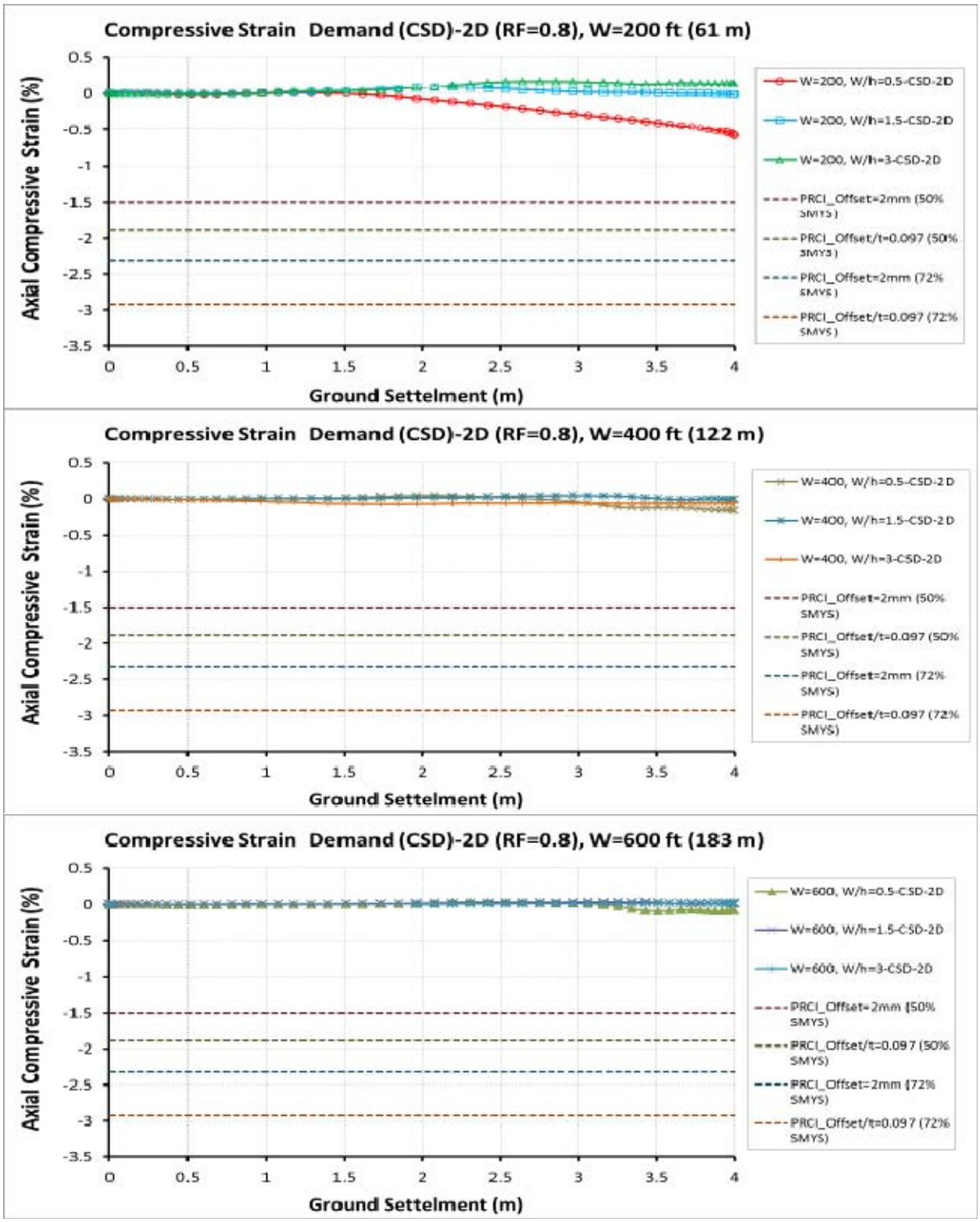

Figure C8: NPS 18 (D/t=48) - Maximum Nominal Compressive Strains in the Pipe vs. Ground Subsidence W=61, 122 and 183 m (200, 400 and 600 ft); W/h Ratio 0.5, 1.5 and 3

The information contained herein is the copyright of and proprietary to BMT Fleet Technology Limited. Use of this information is governed by the legend on the cover page of this document."

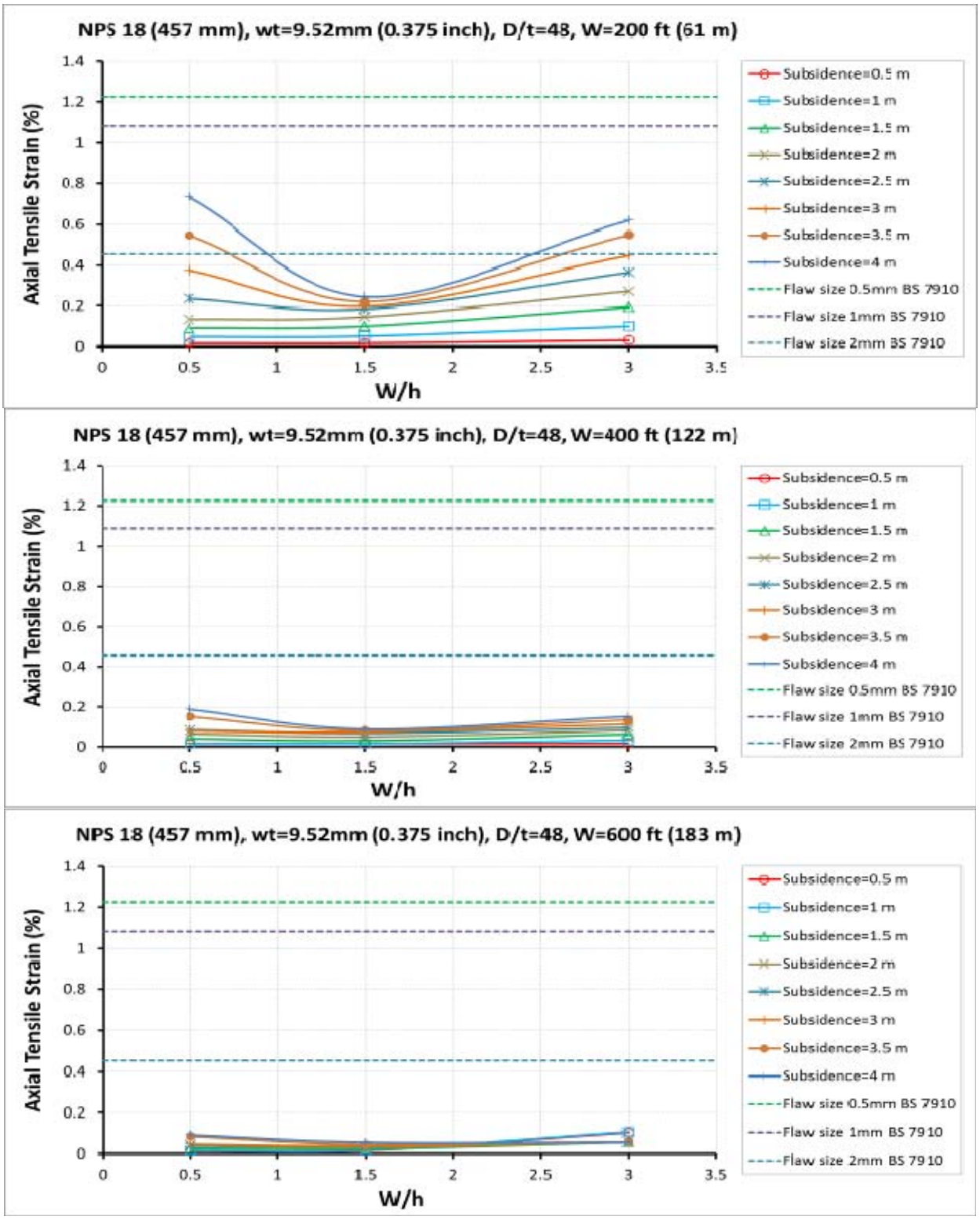

Figure C9: NPS 18 (D/t=48) - Pipe Axial Tensile Strains Envelopes versus Width to Depth Ratio [W=61, 122 and 183 m (200, 400 and 600 ft)] for Ground Settlement of 0.5, 1, 1.5, 2.0, 2.5, 3.0, 3.5 and 4.0 m

The information contained herein is the copyright of and proprietary to BMT Fleet Technology Limited. Use of this information is governed by the legend on the cover page of this document."

C.1.2 Compressive Strain Capacity Envelopes (CSCE), CSD-2D

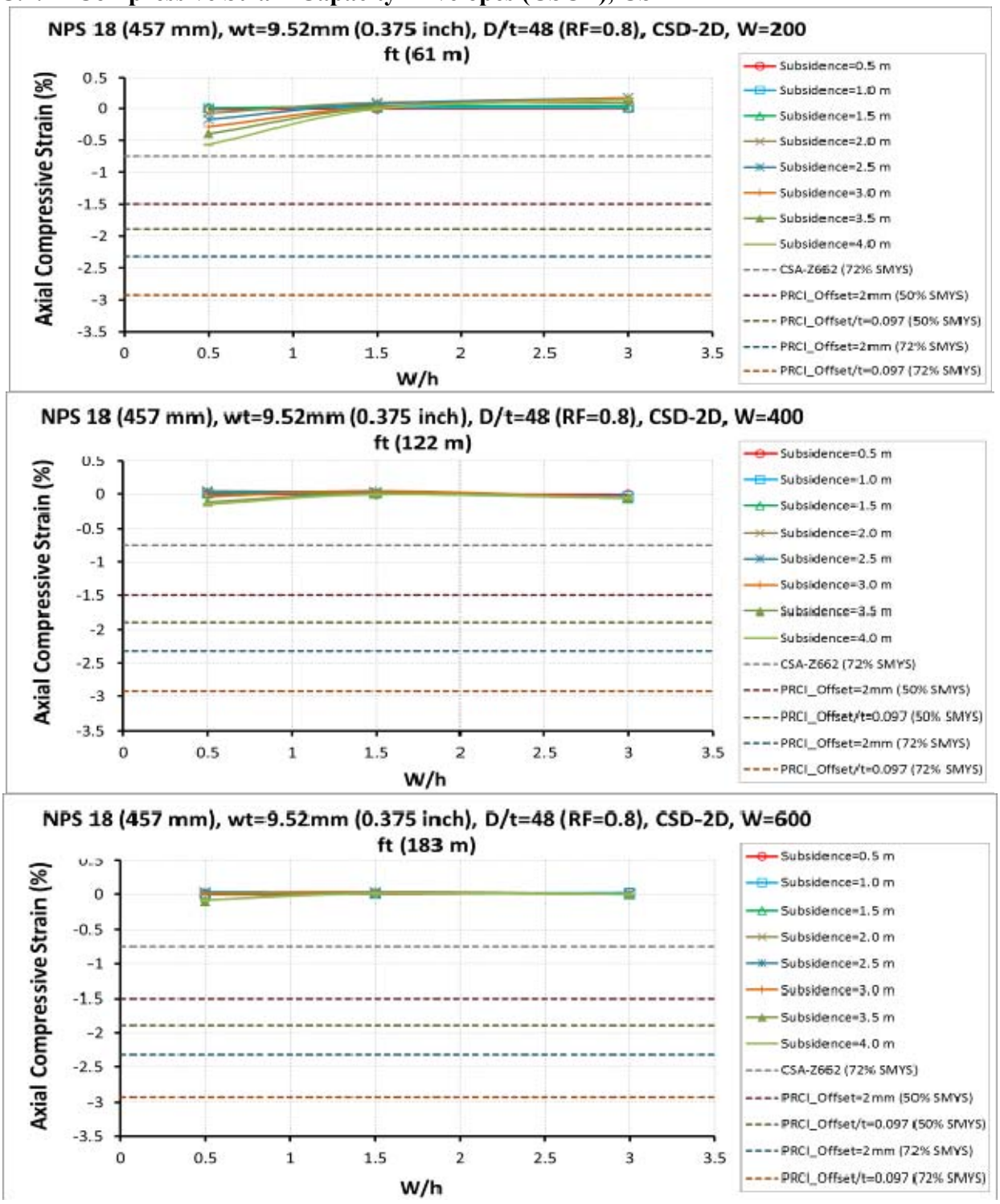

Figure C10 : NPS 18 (D/t=48) - Pipe Axial Compressive Strains Envelopes versus Width to Depth Ratio [W=61, 122 and 183 m (200, 400 and 600 ft)] for Ground Settlement of 0.5, 1, 1.5, 2.0, 2.5, 3.0, 3.5 and 4.0 m

The information contained herein is the copyright of and proprietary to BMT Fleet Technology Limited. Use of this information is governed by the legend on the cover page of this document."

APPENDIX D: MODELING OF LANDSLIDE HAZARD – SUMMARY RESULTS 12-INCH PIPELINE

The information contained herein is the copyright of and proprietary to BMT Fleet Technology Limited. Use of this information is governed by the legend on the cover page of this document."

D.1 MODELING OF LANDSLIDE HAZARD – SUMMARY RESULTS 12-INCH PIPELINE

The following section represents the summary results for the NPS 12 (324 mm outside diameter) for the base case with:

- Pipe wall thickness: three wall thicknesses: 4.57 mm (0.18 in), 6.35 mm (0.25 in) and 9.52 mm (0.375 in); corresponding to D/t ratio of 71, 51 and 34 respectively;
- Ground displacement direction: Perpendicular (lateral) to the pipeline axis;
- Width of ground displacement (W): Six potential ground movement failures with a total estimated width of failure perpendicular to the pipeline varying from 10 to 100 m (10, 20, 30, 40 50 and 100 m);
- Shape of ground displacement: one ground displacement pattern initiated using a cosine function raised to the power "n=2";
- One soil conditions sand/clay till;
- Pipe slope: one slopes, 16 deg.; and
- Pipeline burial depth: one depth of 1.2 m (4 ft) to top pipe, corresponding to 1.36 m (4.5 ft), depth to pipe center line.

Assumptions for the pipeline were as follows:

- 72% SMYS internal pressure;
- 45 ^{0}C thermal differential (installation -20^{0}C, max operating temperature 25^{0}C); and
- A generic stress strain curves for Grade X-52 (359) pipe according to the API 5L.

Detailed results for D/t=71 are presented as follow:

- Figures D.1 presents the maximum tensile strains in the longitudinal direction of the pipeline versus the maximum ground displacement for various ground displacement widths considered in the analyses. Figures D.2 and D.3 present the maximum local and nominal compressive strains in the longitudinal direction of the pipeline versus the maximum ground displacement for various ground displacement widths considered in the analyses. The nominal compressive strain is defined as the average compressive strain measured over a gauge length of 2D (where D is the pipe outside diameter). The results indicate that for the six (6) widths considered, the width of 10 m (33 ft) results in the largest tensile and compressive strain in the pipe for any given value of ground displacement.
- Figure D.5 presents the maximum compressive strains in pipe versus the ground displacement width (W) for given ground displacement of 0.5, 1.0, 1.5, 2.0 and 2.5. In this figure the BS-7910 tensile strain capacity is presented with dash horizontal line. Any tensile strain above the horizontal line is strain-related failure limit. The TSC envelopes based on BS7910 guidance are presented in Figure D.6. The envelopes describe the maximum soil displacement and ground displacement width breakout the TSC envelopes, which represents the tensile strain-related failure limit, according to BS 7910. The results

The information contained herein is the copyright of and proprietary to BMT Fleet Technology Limited. Use of this information is governed by the legend on the cover page of this document."

indicate that for this pipe and operating condition combination, the ground movement width of 10 m (33 ft) can be considered critical.

- Figure D.7 presents the maximum compressive strains in pipe versus the ground displacement width (W) for given ground displacement of 0.5, 1.0, 1.5, 2.0 and 2.5. In this figure the PRCI (UOA) compressive strain capacity is presented with dash horizontal line. Any compressive strain below the horizontal line is strain-related failure limit. The CSC envelopes based on PRCI guidance are presented in Figure D.8. The envelopes describe the maximum soil displacement and ground displacement width breakout the CSC envelopes, which represents the compressive strain-related failure limit, according to PRCI/UOA. The results indicate that for this pipe and operating condition combination, the ground movement width of 10 m (33 ft) can be considered critical
- Figure D.9 and Figure D.10 present the tensile and compressive strain demand 'envelops' for a given pipe tensile and compressive strain demands of 0.25%, 0.5%, 0.75%, 1%, 1.25%, 1.5%, 1.75% and 2% along the longitudinal direction of the pipeline. The safe pipeline operating goal of pipeline subjected to lateral ground displacement is to stay within the normal operating strain range defined by codes and standards.

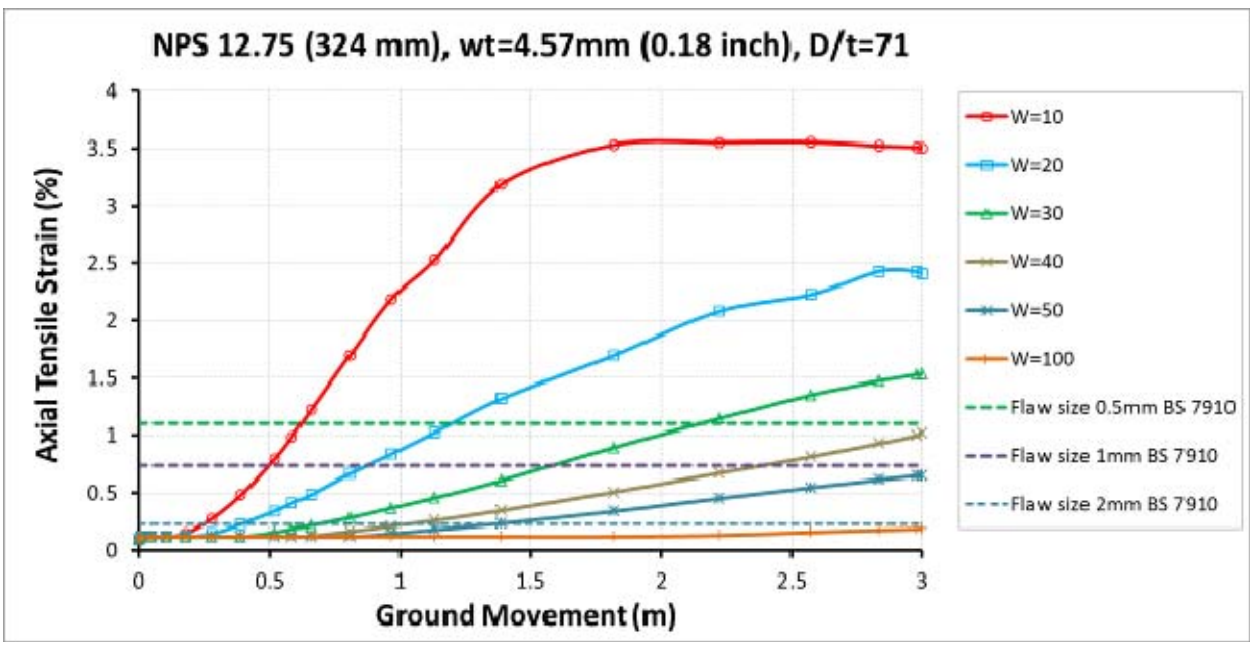

Figure D.1: NPS 12.75 (D/t=71) - Maximum Tensile in the Pipe vs. Ground Movement Widths: [10-100 m]

The information contained herein is the copyright of and proprietary to BMT Fleet Technology Limited. Use of this information is governed by the legend on the cover page of this document."

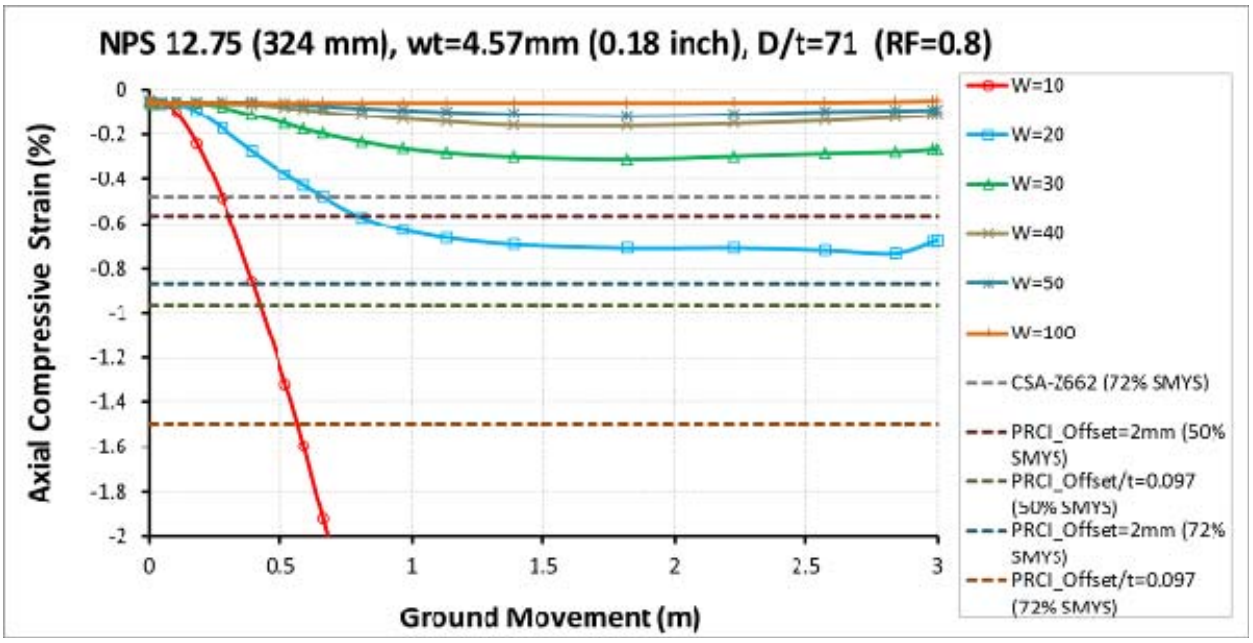

Figure D.2: NPS 12.75 (D/t=71) - Maximum local Compressive Strain vs. Ground Movement Widths: [10-100 m]

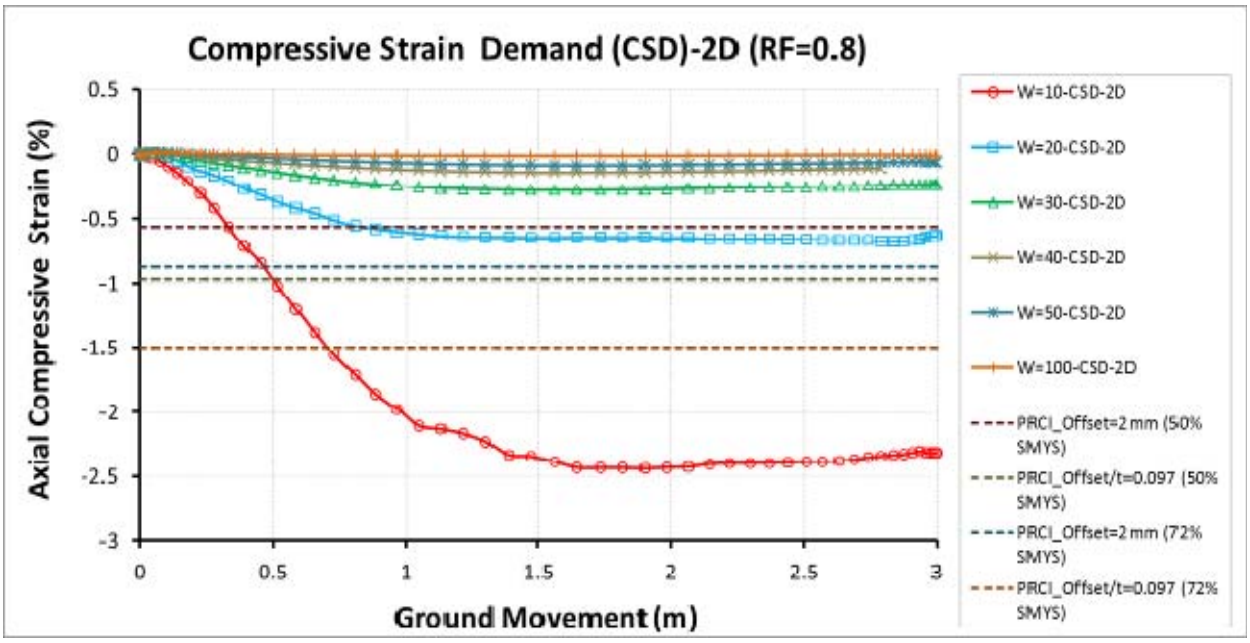

Figure D.3: NPS 12.75 (D/t=71) - Maximum Nominal Compressive Strain vs. Ground Movement Widths: [10-100 m]

The information contained herein is the copyright of and proprietary to BMT Fleet Technology Limited. Use of this information is governed by the legend on the cover page of this document."

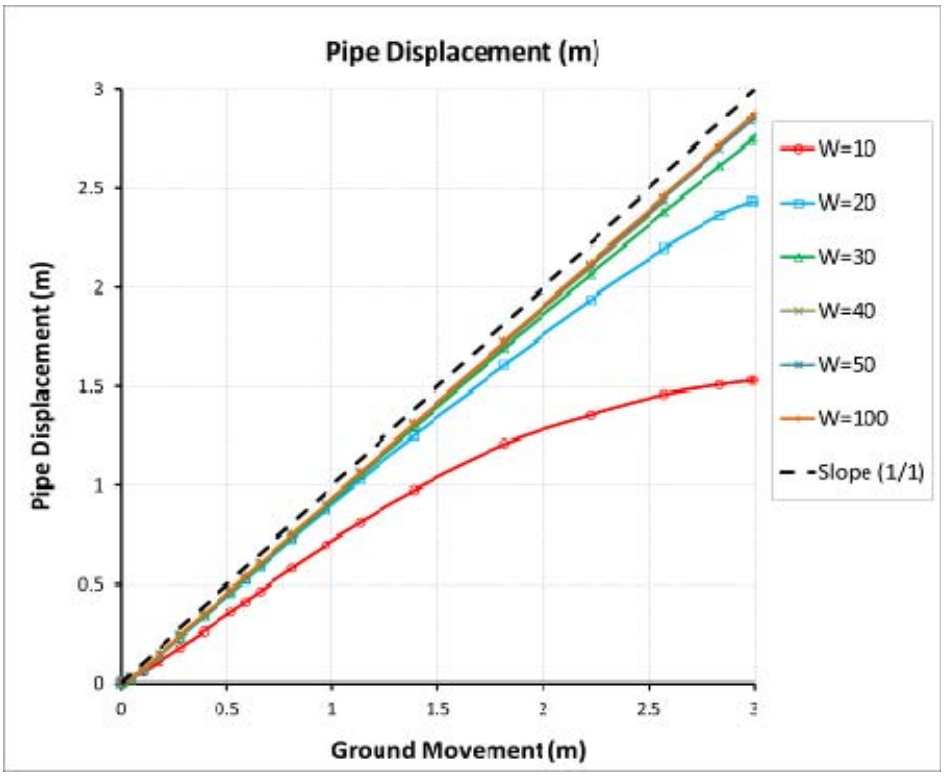

Figure D.4: NPS 12.75 (D/t=71) – Pipe Displacement versus Ground Displacement

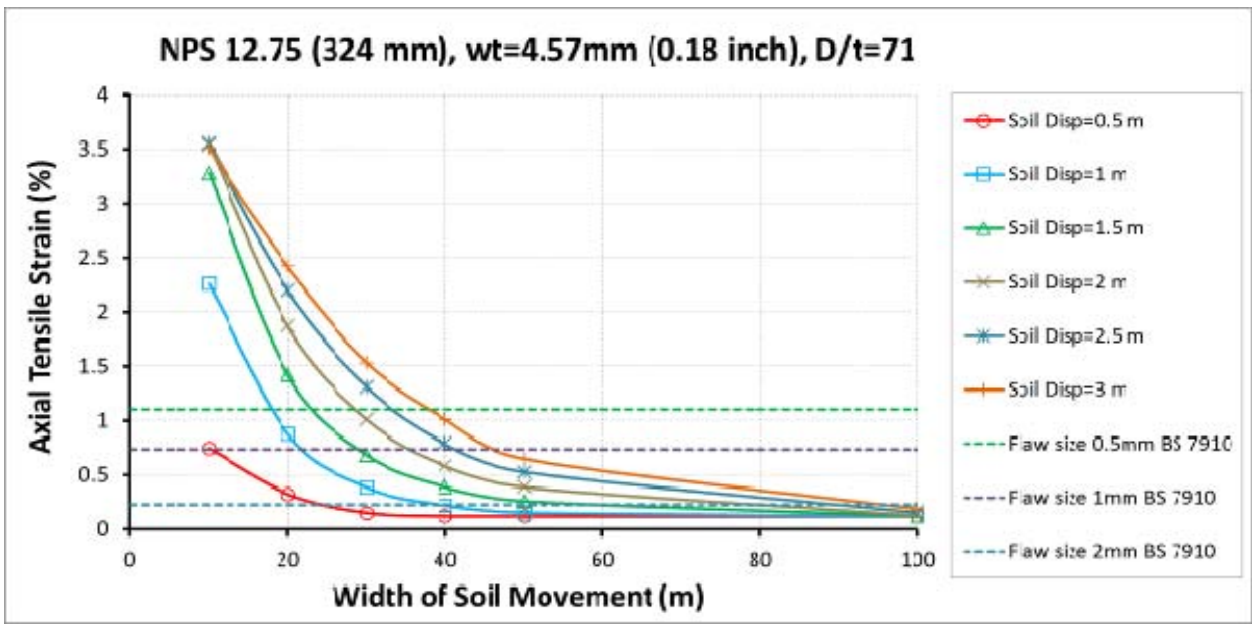

Figure D.5: Pipe Axial Tensile Strains Envelopes versus Width (W) for Soil Movements of 0.5, 1, 1.5, 2.0 and 2.5 m

The information contained herein is the copyright of and proprietary to BMT Fleet Technology Limited. Use of this information is governed by the legend on the cover page of this document."

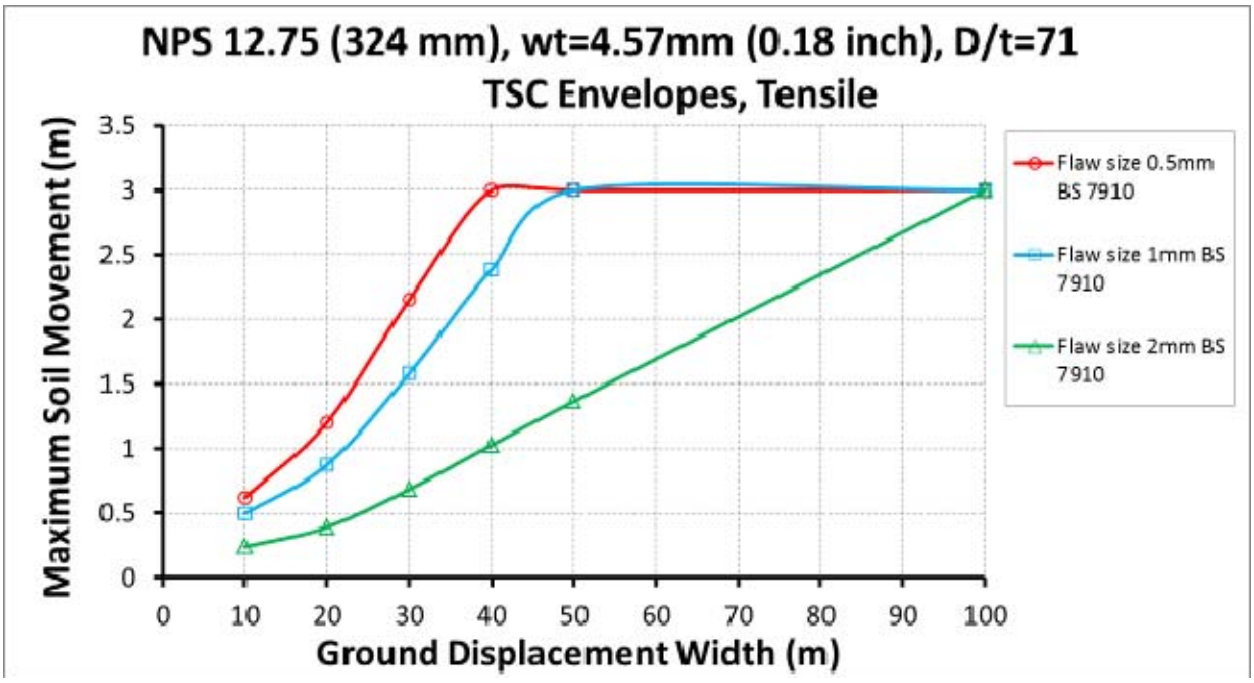

Figure D.6: Tensile Strain Capacity Envelopes versus Ground Width (W) Movements

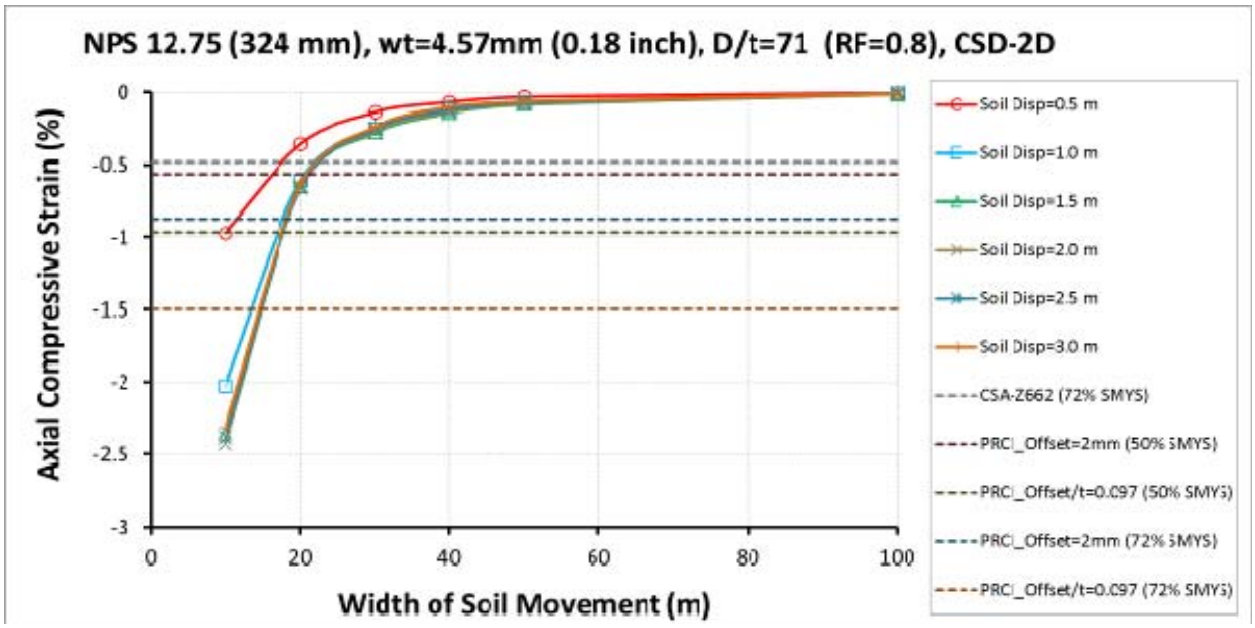

Figure D.7: Pipe Axial Compressive Strains Envelopes versus Width (W) (for Soil Movement of 0.5, 1, 1.5, 2.0 and 2.5 m)

The information contained herein is the copyright of and proprietary to BMT Fleet Technology Limited. Use of this information is governed by the legend on the cover page of this document."

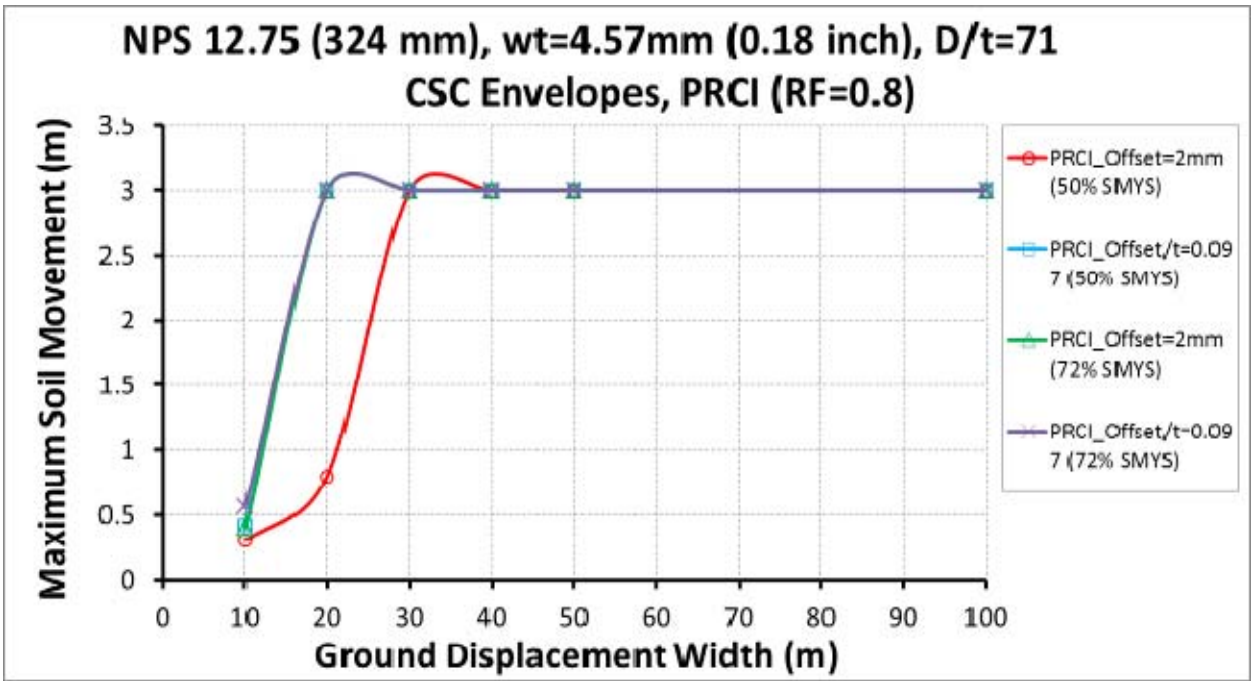

Figure D.8: Compressive Strain Capacity Envelopes versus Ground Width (W) Movements

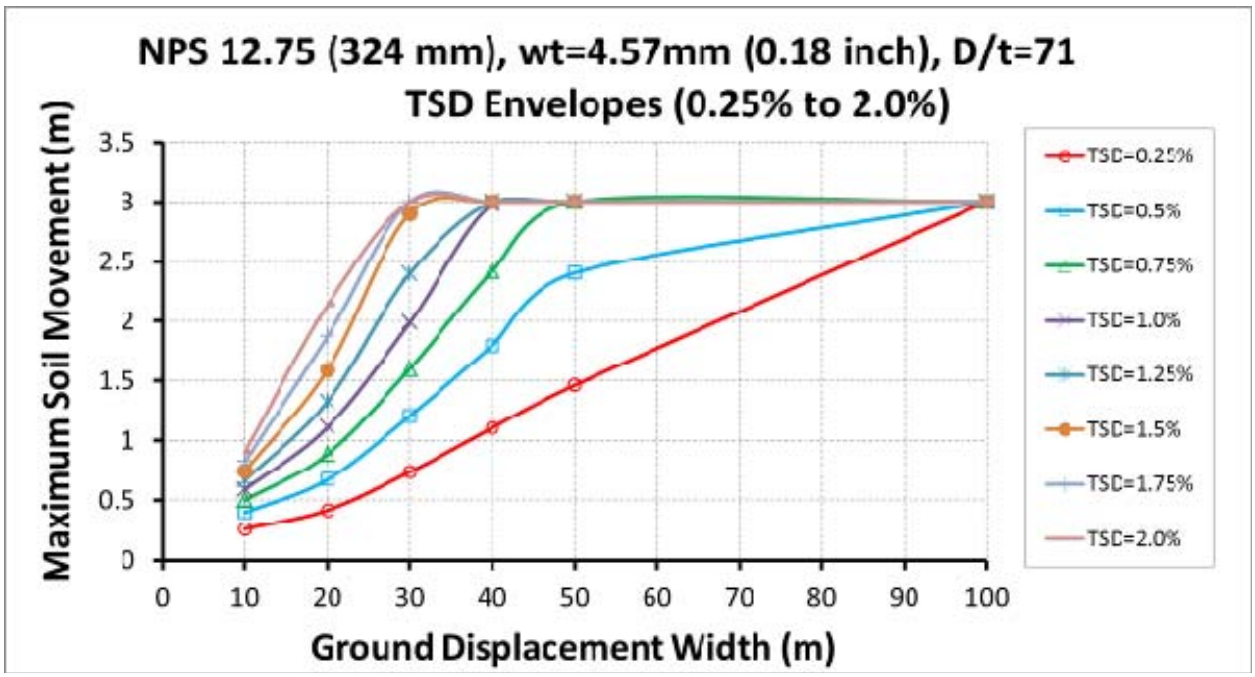

Figure D.9: Tensile Strain Demand Envelopes versus Width (W)

The information contained herein is the copyright of and proprietary to BMT Fleet Technology Limited. Use of this information is governed by the legend on the cover page of this document."

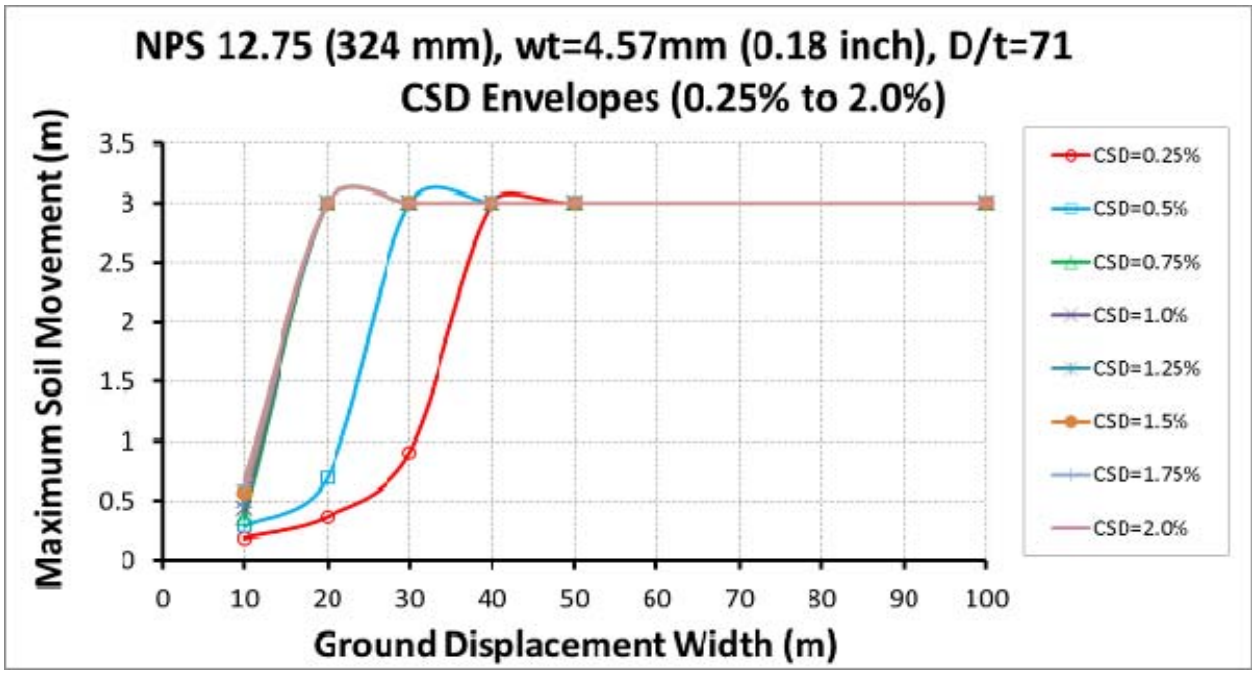

Figure D.10: Compressive Strain Demand Envelopes versus Width (W)

The information contained herein is the copyright of and proprietary to BMT Fleet Technology Limited. Use of this information is governed by the legend on the cover page of this document."

Detailed results for D/t=71 are presented as follow:

- Figures D.11 presents the maximum tensile strains in the longitudinal direction of the pipeline versus the maximum ground displacement for various ground displacement widths considered in the analyses. Figures D.12 and D.13 present the maximum local and nominal compressive strains in the longitudinal direction of the pipeline versus the maximum ground displacement for various ground displacement widths considered in the analyses. The nominal compressive strain is defined as the average compressive strain measured over a gauge length of 2D (where D is the pipe outside diameter). The results indicate that for the six (6) widths considered, the width of 10 m (33 ft) results in the largest tensile and compressive strain in the pipe for any given value of ground displacement.
- Figure D.15 presents the maximum compressive strains in pipe versus the ground displacement width (W) for given ground displacement of 0.5, 1.0, 1.5, 2.0 and 2.5. In this figure the BS-7910 tensile strain capacity is presented with dash horizontal line. Any tensile strain above the horizontal line is strain-related failure limit. The TSC envelopes based on BS7910 guidance are presented in Figure D.16. The envelopes describe the maximum soil displacement and ground displacement width breakout the TSC envelopes, which represents the tensile strain-related failure limit, according to BS 7910. The results indicate that for this pipe and operating condition combination, the ground movement width of 10 m (33 ft) can be considered critical.
- Figure D.17 presents the maximum compressive strains in pipe versus the ground displacement width (W) for given ground displacement of 0.5, 1.0, 1.5, 2.0 and 2.5. In this figure the PRCI (UOA) compressive strain capacity is presented with dash horizontal line. Any compressive strain below the horizontal line is strain-related failure limit. The CSC envelopes based on PRCI guidance are presented in Figure D.18. The envelopes describe the maximum soil displacement and ground displacement width breakout the CSC envelopes, which represents the compressive strain-related failure limit, according to PRCI/UOA. The results indicate that for this pipe and operating condition combination, the ground movement width of 10 m (33 ft) can be considered critical
- Figure D.19 and Figure D.20 present the tensile and compressive strain demand 'envelopes' for a given pipe tensile and compressive strain demands of 0.25%, 0.5%, 0.75%, 1%, 1.25%, 1.5%, 1.75% and 2% along the longitudinal direction of the pipeline. The safe pipeline operating goal of pipeline subjected to lateral ground displacement is to stay within the normal operating strain range defined by codes and standards.

The information contained herein is the copyright of and proprietary to BMT Fleet Technology Limited. Use of this information is governed by the legend on the cover page of this document."

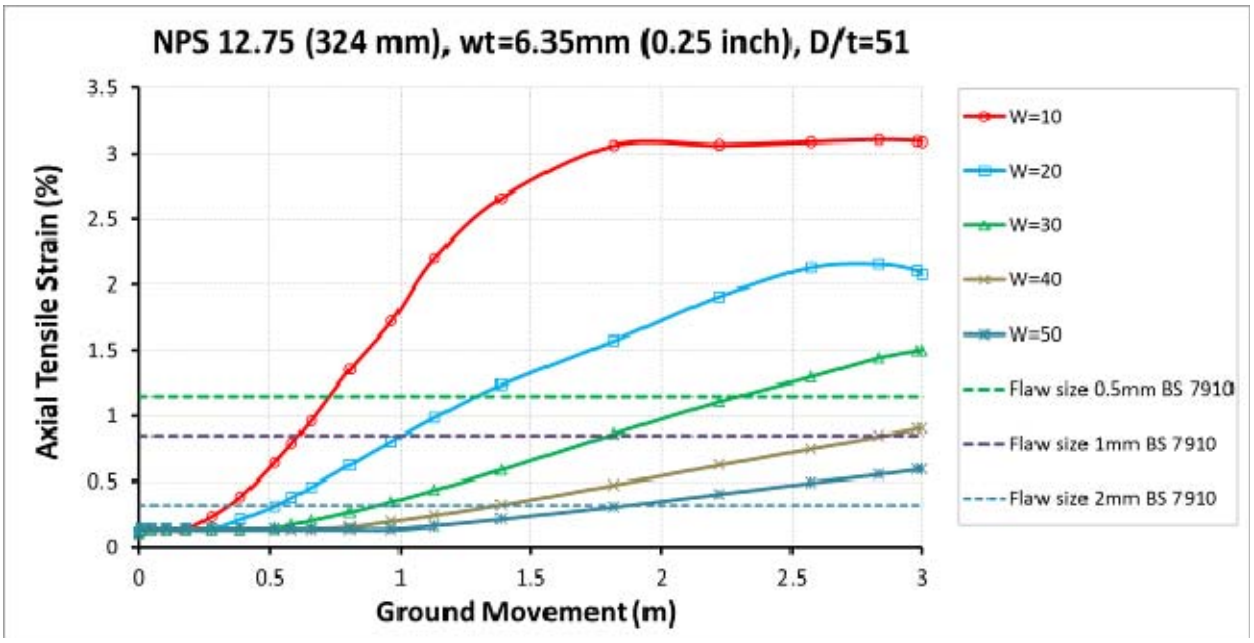

Figure D.11: NPS 12.75 (D/t=51) - Maximum Tensile in the Pipe vs. Ground Movement Widths: [10-100m]

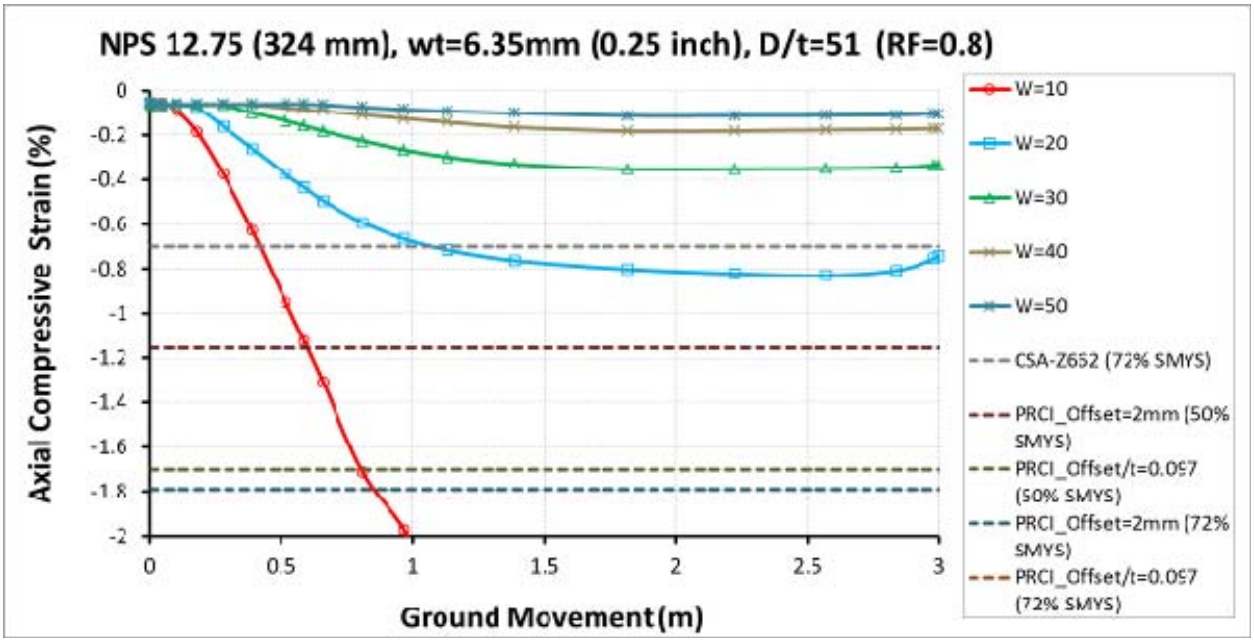

Figure D.12: NPS 12.75 (D/t=51) - Maximum local Compressive Strain vs. Ground Movement Widths: [10-100m]

The information contained herein is the copyright of and proprietary to BMT Fleet Technology Limited. Use of this information is governed by the legend on the cover page of this document."

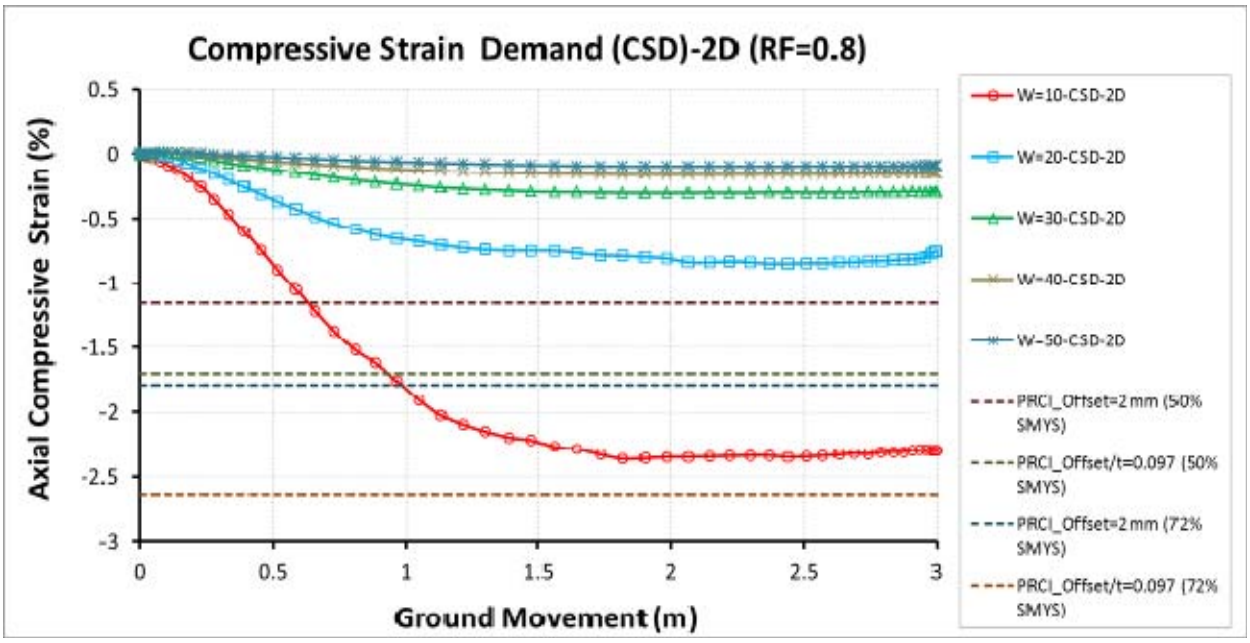

Figure D.13: NPS 12.75 (D/t=51) - Maximum Nominal Compressive Strain vs. Ground Movement Widths: [10-100m]

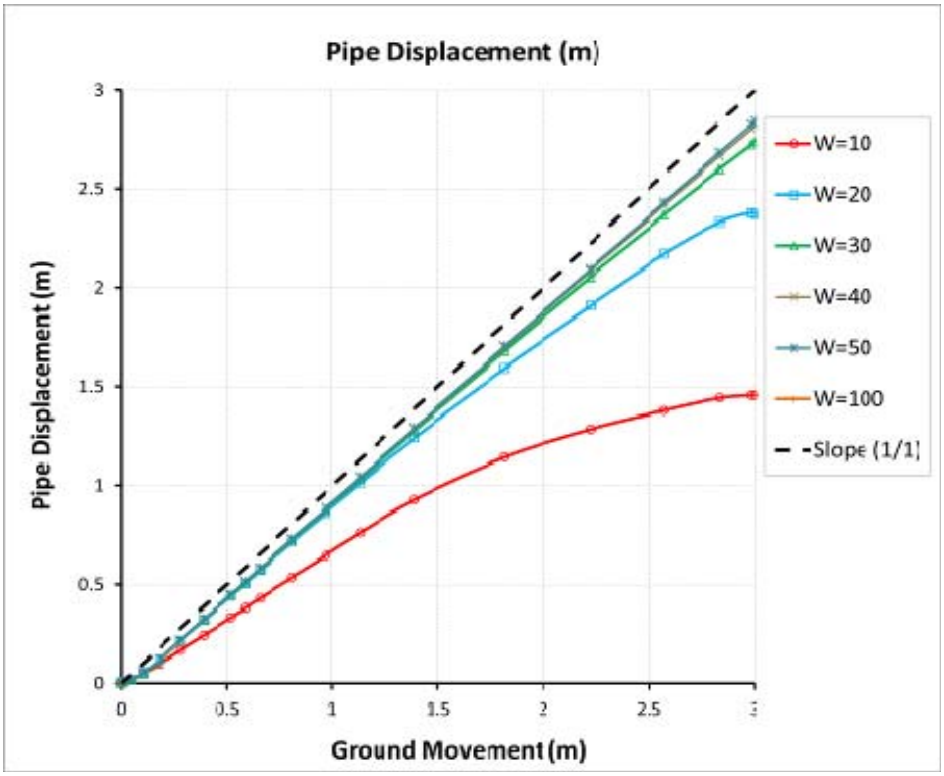

Figure D.14: NPS 12.75 (D/t=51) – Pipe Displacement versus Ground Displacement

The information contained herein is the copyright of and proprietary to BMT Fleet Technology Limited. Use of this information is governed by the legend on the cover page of this document."

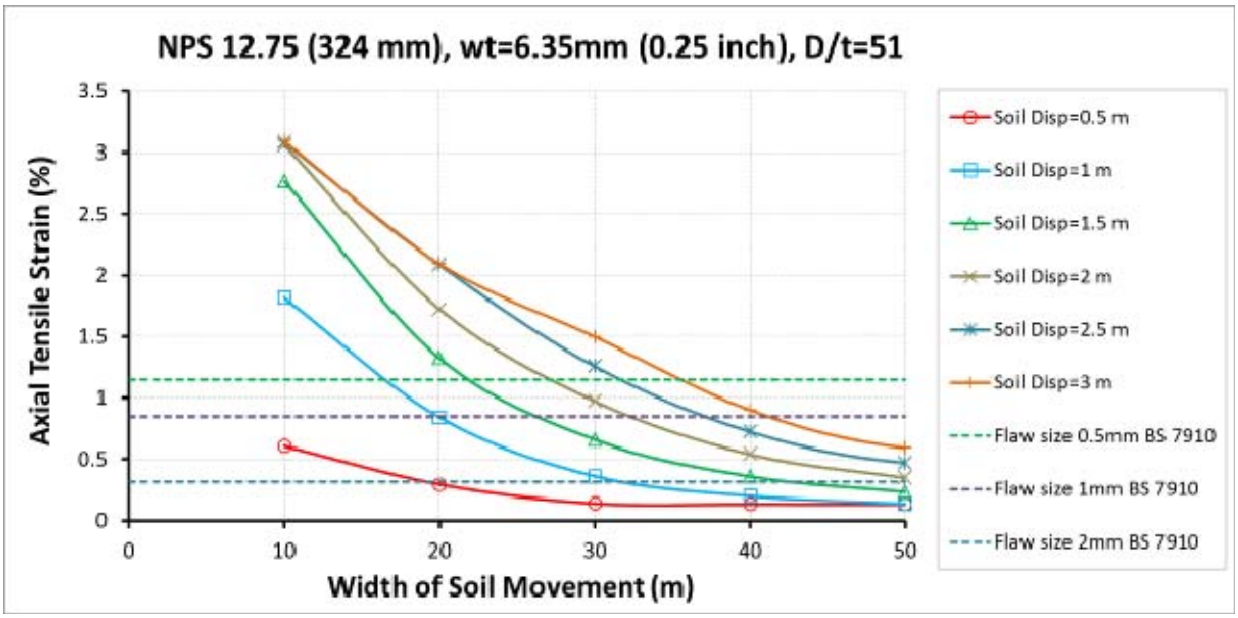

Figure D.15: Pipe Axial Tensile Strains Envelopes versus Width (W) for Soil Movements of 0.5, 1, 1.5, 2.0 and 2.5 m

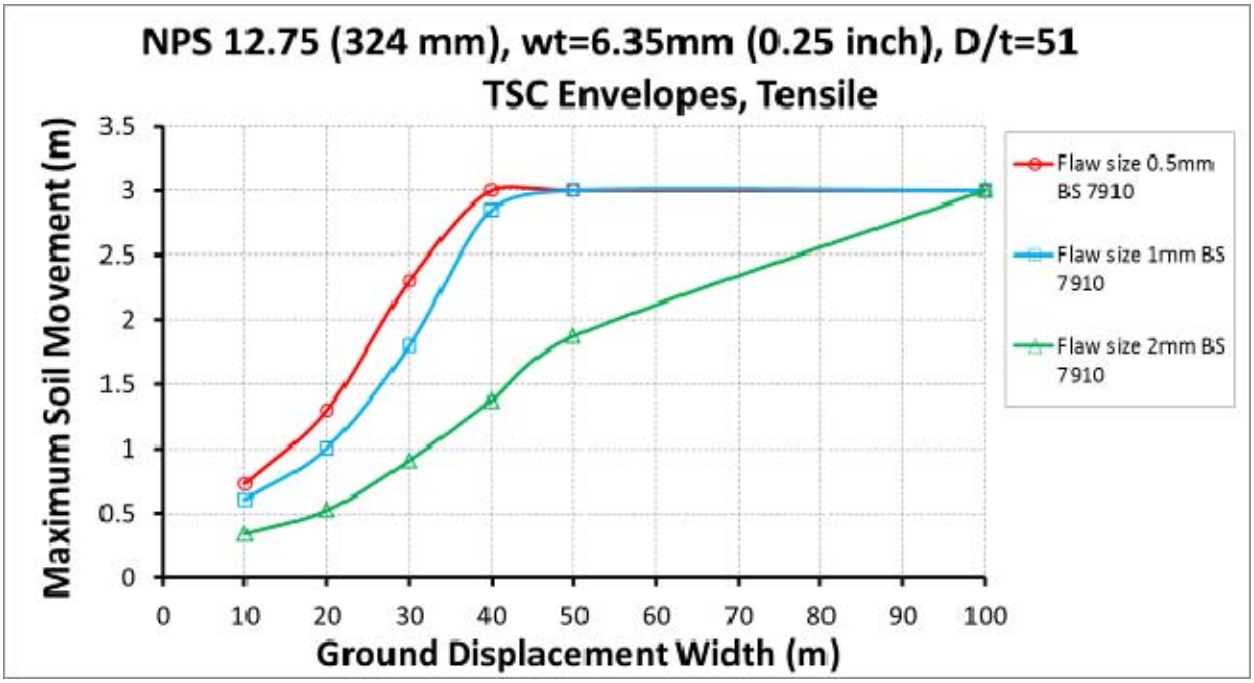

Figure D.16: Tensile Strain Capacity Envelopes versus Ground Width (W) Movements

The information contained herein is the copyright of and proprietary to BMT Fleet Technology Limited. Use of this information is governed by the legend on the cover page of this document."

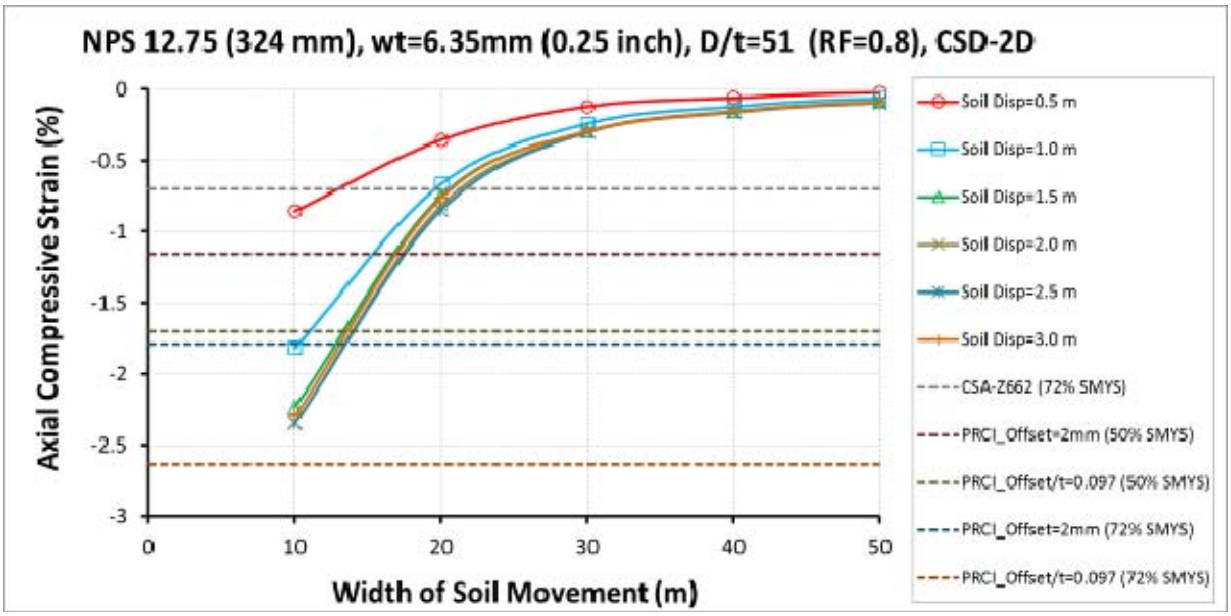

Figure D.17: Pipe Axial Compressive Strains Envelopes versus Width (W) (for Soil Movement of 0.5, 1, 1.5, 2.0 and 2.5 m)

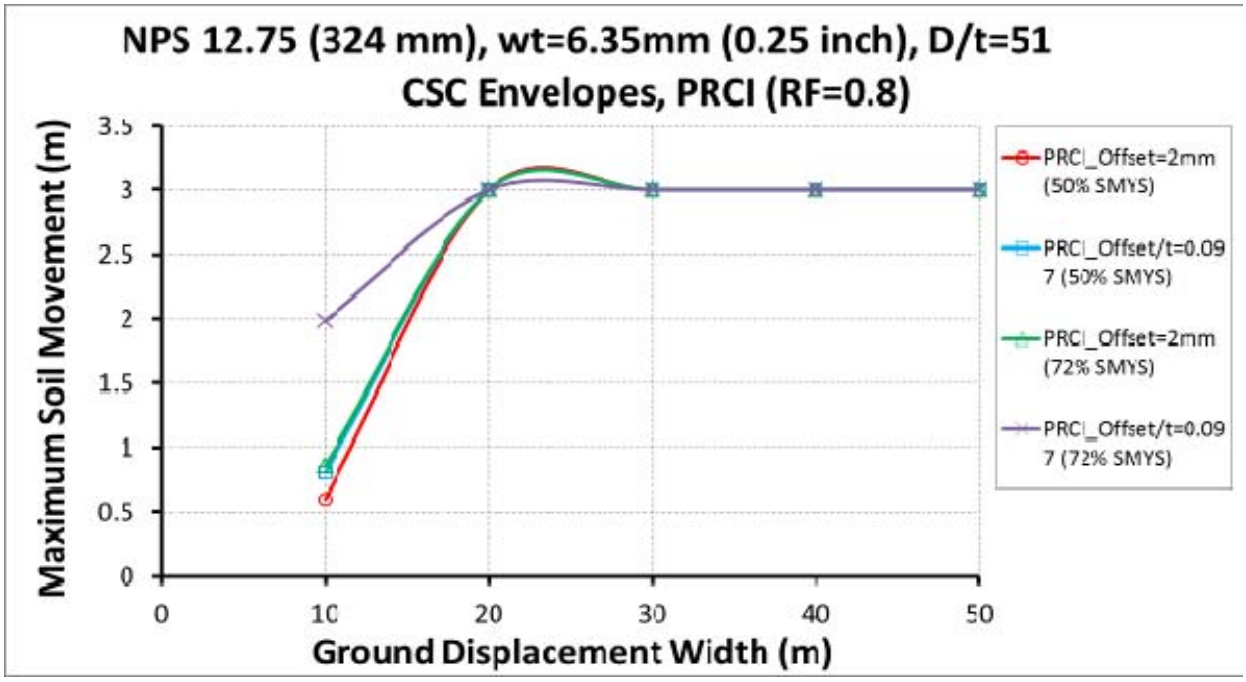

Figure D.18: Compressive Strain Capacity Envelopes versus Ground Width (W) Movements

The information contained herein is the copyright of and proprietary to BMT Fleet Technology Limited. Use of this information is governed by the legend on the cover page of this document."

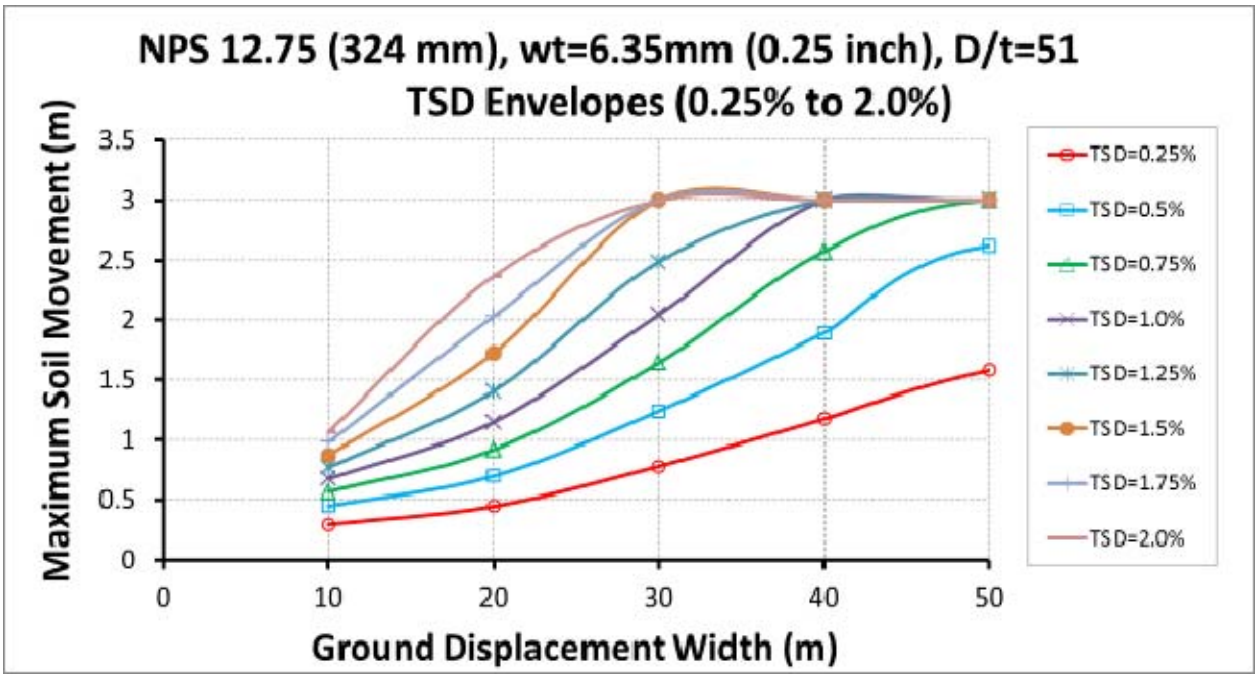

Figure D.19: Tensile Strain Demand Envelopes versus Width (W)

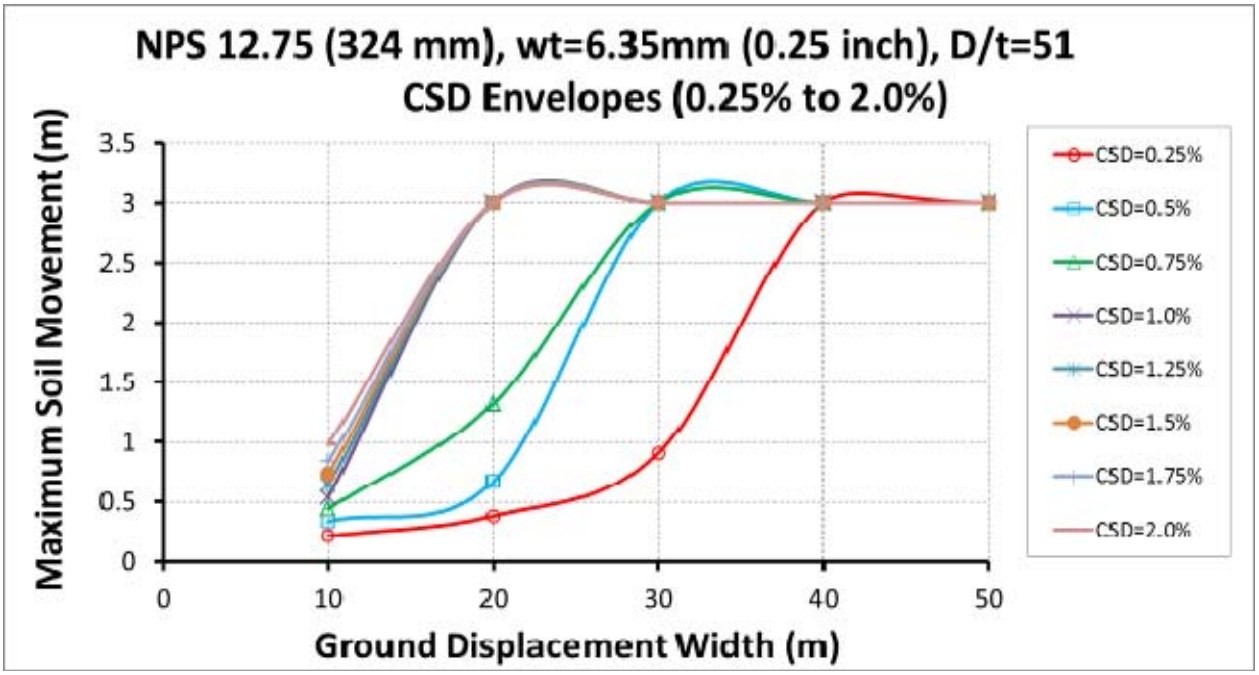

Figure D.20: Compressive Strain Demand Envelopes versus Width (W)

The information contained herein is the copyright of and proprietary to BMT Fleet Technology Limited. Use of this information is governed by the legend on the cover page of this document."

Detailed results for D/t=34 are presented as follow:

- Figures D.21 presents the maximum tensile strains in the longitudinal direction of the pipeline versus the maximum ground displacement for various ground displacement widths considered in the analyses. Figures D.22 and D.23 present the maximum local and nominal compressive strains in the longitudinal direction of the pipeline versus the maximum ground displacement for various ground displacement widths considered in the analyses. The nominal compressive strain is defined as the average compressive strain measured over a gauge length of 2D (where D is the pipe outside diameter). The results indicate that for the six (6) widths considered, the width of 10 m (33 ft) results in the largest tensile and compressive strain in the pipe for any given value of ground displacement.
- Figure D.25 presents the maximum compressive strains in pipe versus the ground displacement width (W) for given ground displacement of 0.5, 1.0, 1.5, 2.0 and 2.5. In this figure the BS7910 tensile strain capacity is presented with dash horizontal line. Any tensile strain above the horizontal line is strain-related failure limit. The TSC envelopes based on BS7910 guidance are presented in Figure D.26. The envelopes describe the maximum soil displacement and ground displacement width breakout the TSC envelopes, which represents the tensile strain-related failure limit, according to BS7910. The results indicate that for this pipe and operating condition combination, the ground movement width of 10 m (33 ft) can be considered critical.
- Figure D.27 presents the maximum compressive strains in pipe versus the ground displacement width (W) for given ground displacement of 0.5, 1.0, 1.5, 2.0 and 2.5. In this figure the PRCI (UOA) compressive strain capacity is presented with dash horizontal line. Any compressive strain below the horizontal line is strain-related failure limit. The CSC envelopes based on PRCI guidance are presented in Figure D.28. The envelopes describe the maximum soil displacement and ground displacement width breakout the CSC envelopes, which represents the compressive strain-related failure limit, according to PRCI/UOA. The results indicate that for this pipe and operating condition combination, the ground movement width of 10 m (33 ft) can be considered critical
- Figure D.29 and Figure D.30 present the tensile and compressive strain demand 'envelopes' for a given pipe tensile and compressive strain demands of 0.25%, 0.5%, 0.75%, 1%, 1.25%, 1.5%, 1.75% and 2% along the longitudinal direction of the pipeline. The safe pipeline operating goal of pipeline subjected to lateral ground displacement is to stay within the normal operating strain range defined by codes and standards.

The information contained herein is the copyright of and proprietary to BMT Fleet Technology Limited. Use of this information is governed by the legend on the cover page of this document."

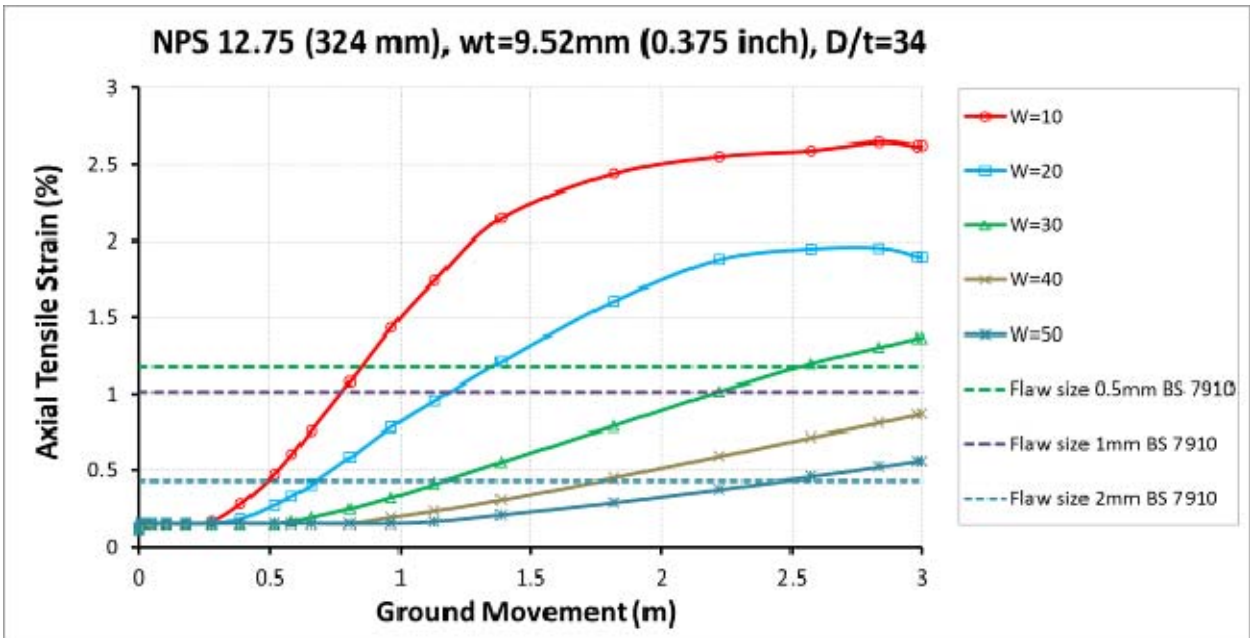

Figure D.21: NPS 12.75 (D/t=34) - Maximum Tensile in the Pipe vs. Ground Movement Widths: [10-100 m]

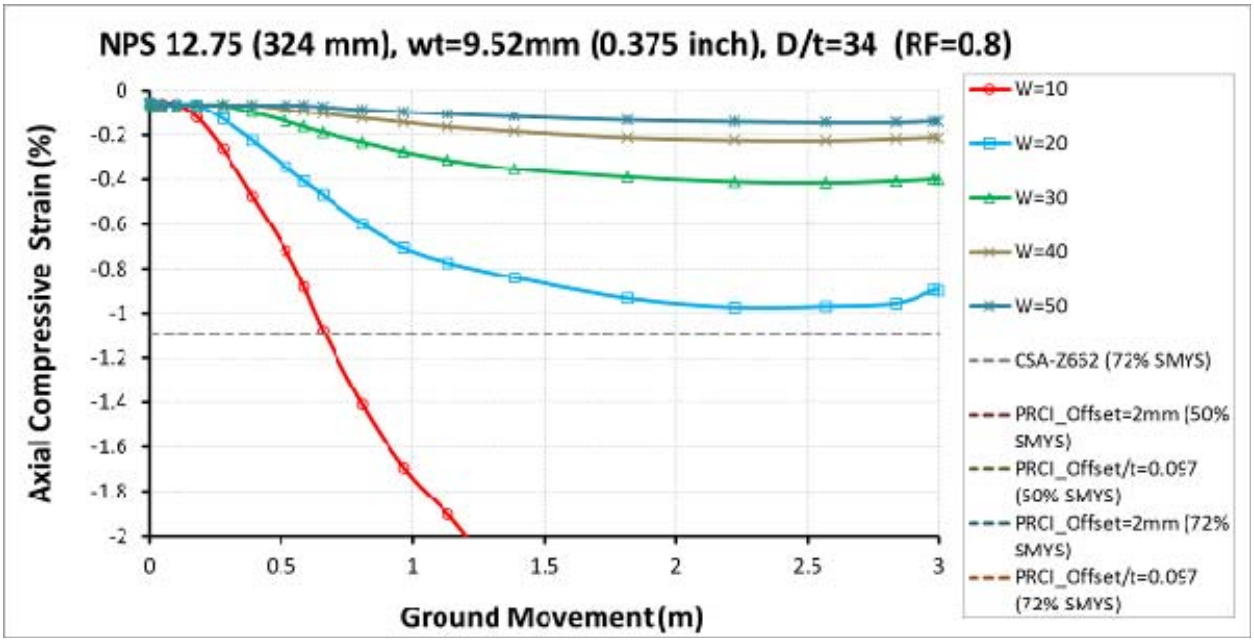

Figure D.22: NPS 12.75 (D/t=34) - Maximum local Compressive Strain vs. Ground Movement Widths: [10-100 m]

The information contained herein is the copyright of and proprietary to BMT Fleet Technology Limited. Use of this information is governed by the legend on the cover page of this document."

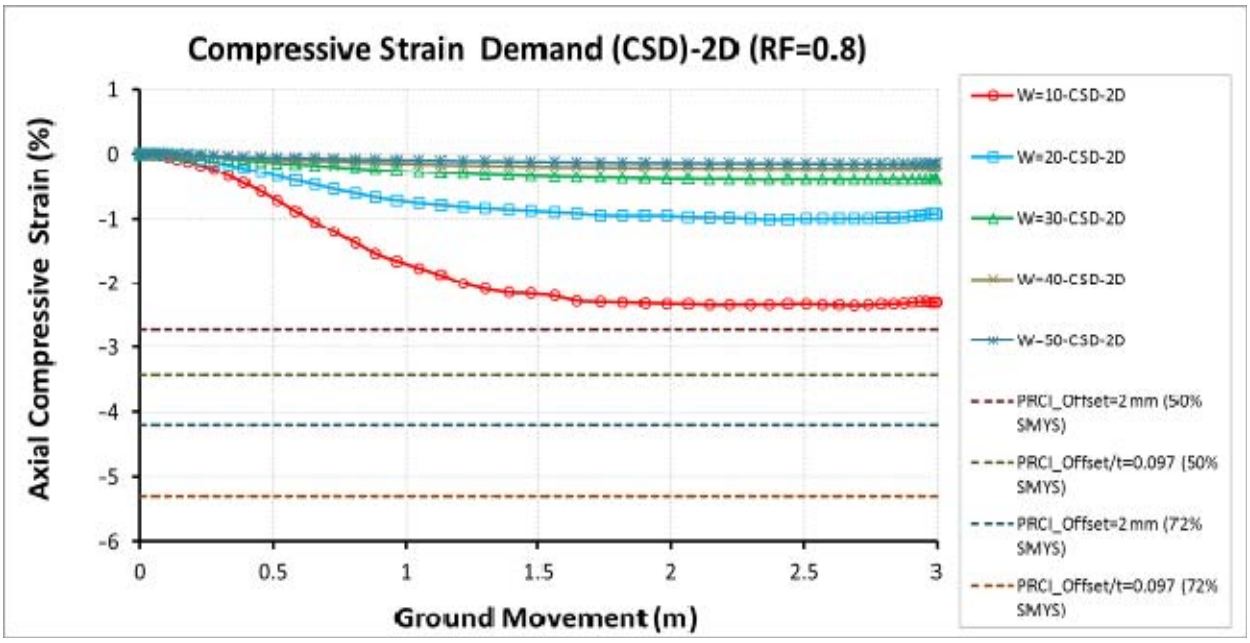

Figure D.23: NPS 12.75 (D/t=34) - Maximum Nominal Compressive Strain vs. Ground Movement Widths: [10-100 m]

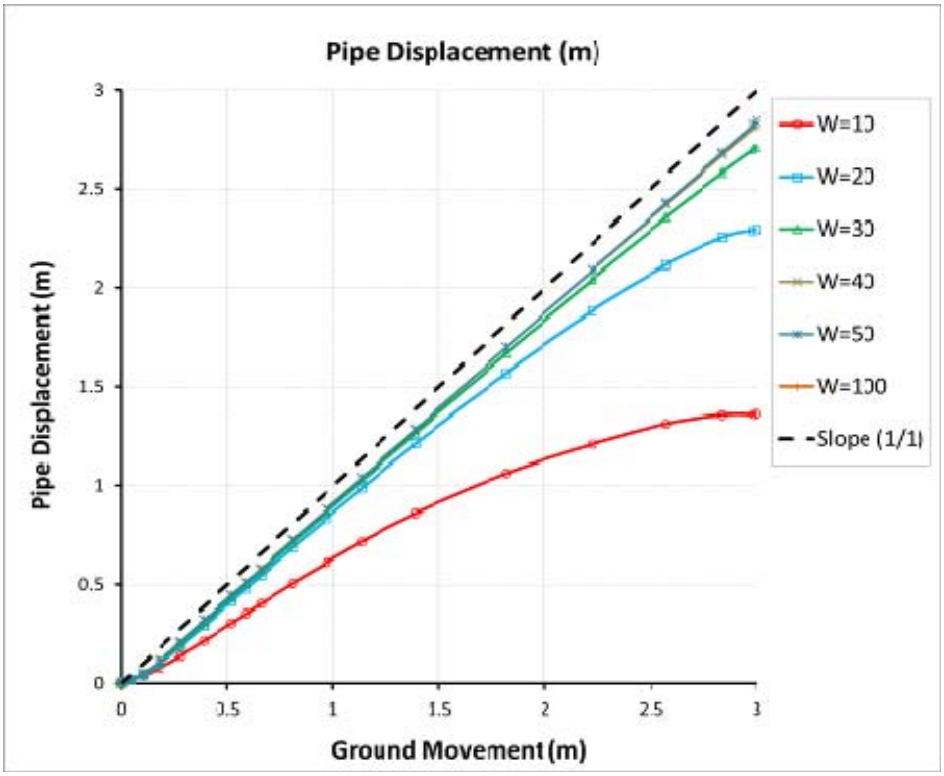

Figure D.24: NPS 12.75 (D/t=34) – Pipe Displacement versus Ground Displacement

The information contained herein is the copyright of and proprietary to BMT Fleet Technology Limited. Use of this information is governed by the legend on the cover page of this document."

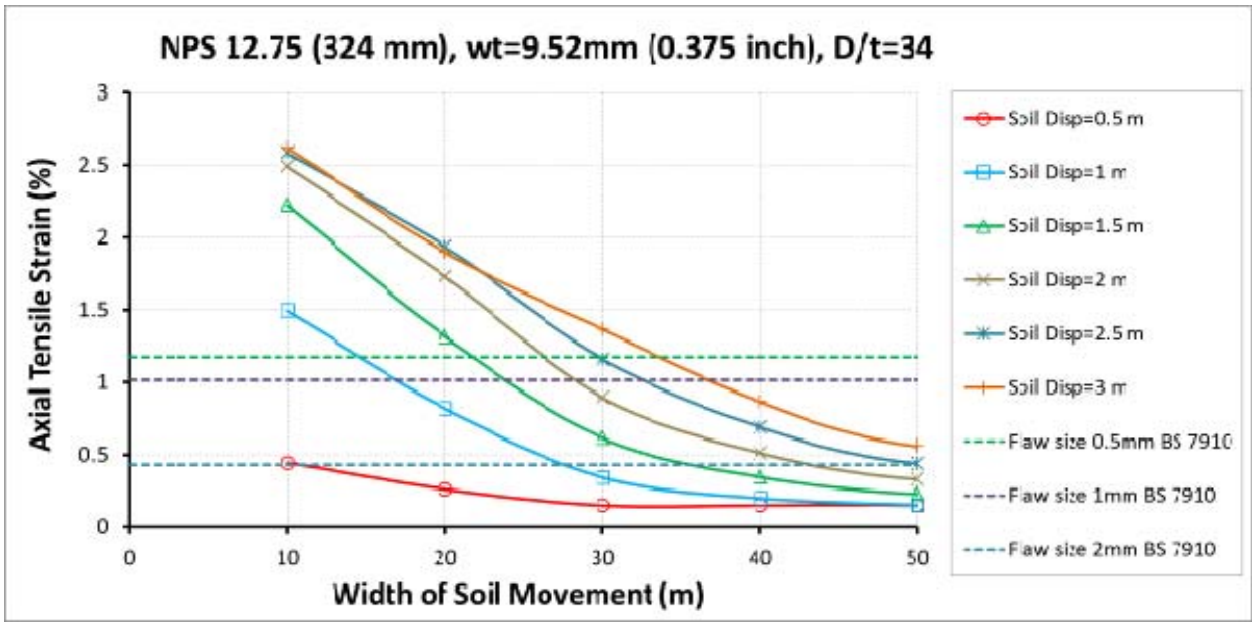

Figure D.25: Pipe Axial Tensile Strains Envelopes versus Width (W) for Soil Movements of 0.5, 1, 1.5, 2.0 and 2.5 m

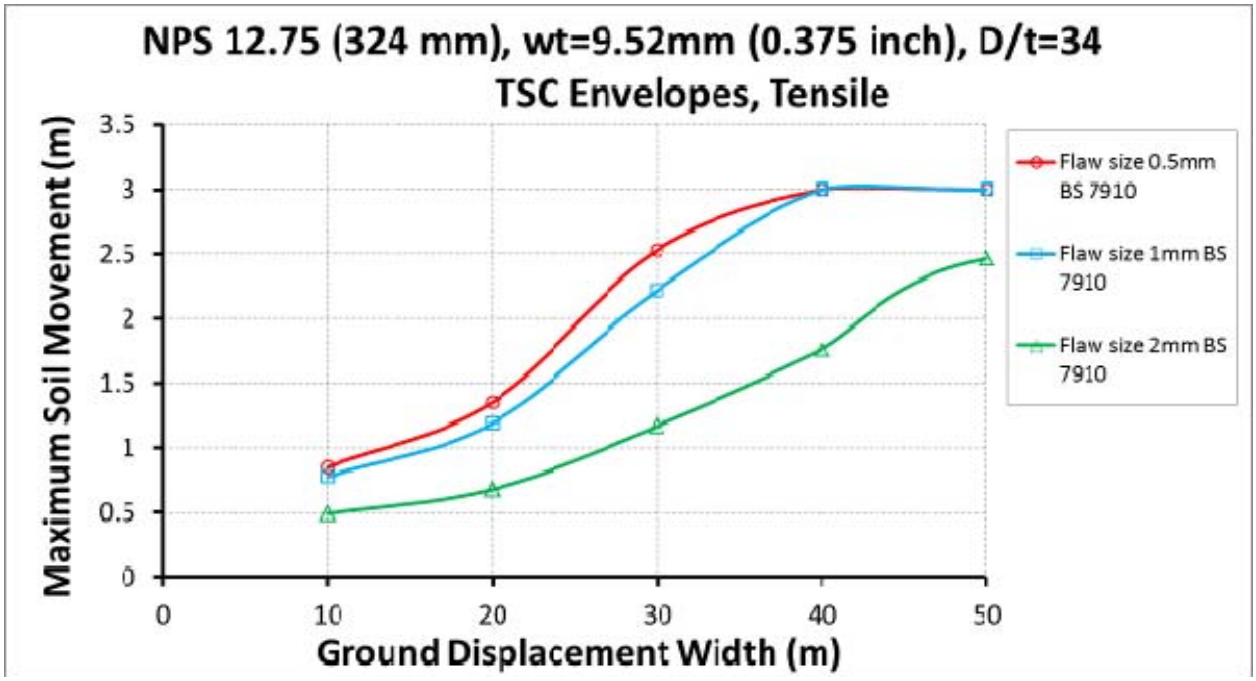

Figure D.26: Tensile Strain Capacity Envelopes versus Ground Width (W) Movements

The information contained herein is the copyright of and proprietary to BMT Fleet Technology Limited. Use of this information is governed by the legend on the cover page of this document."

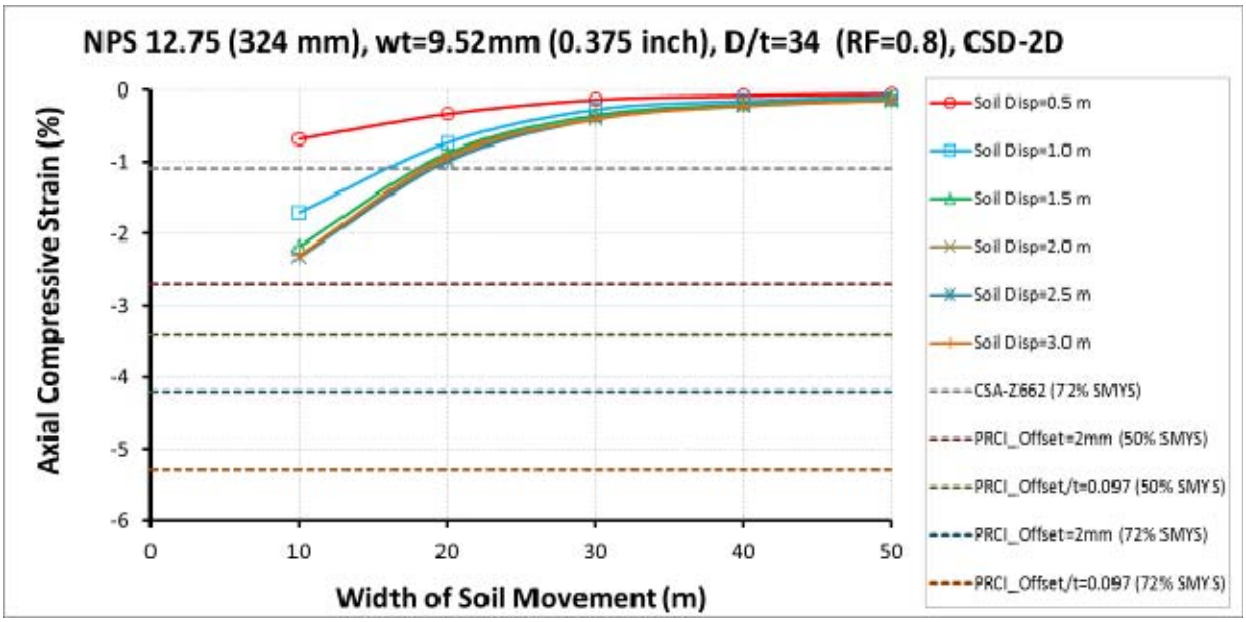

Figure D.27: Pipe Axial Compressive Strains Envelopes versus Width (W) (for Soil Movement of 0.5, 1, 1.5, 2.0 and 2.5 m)

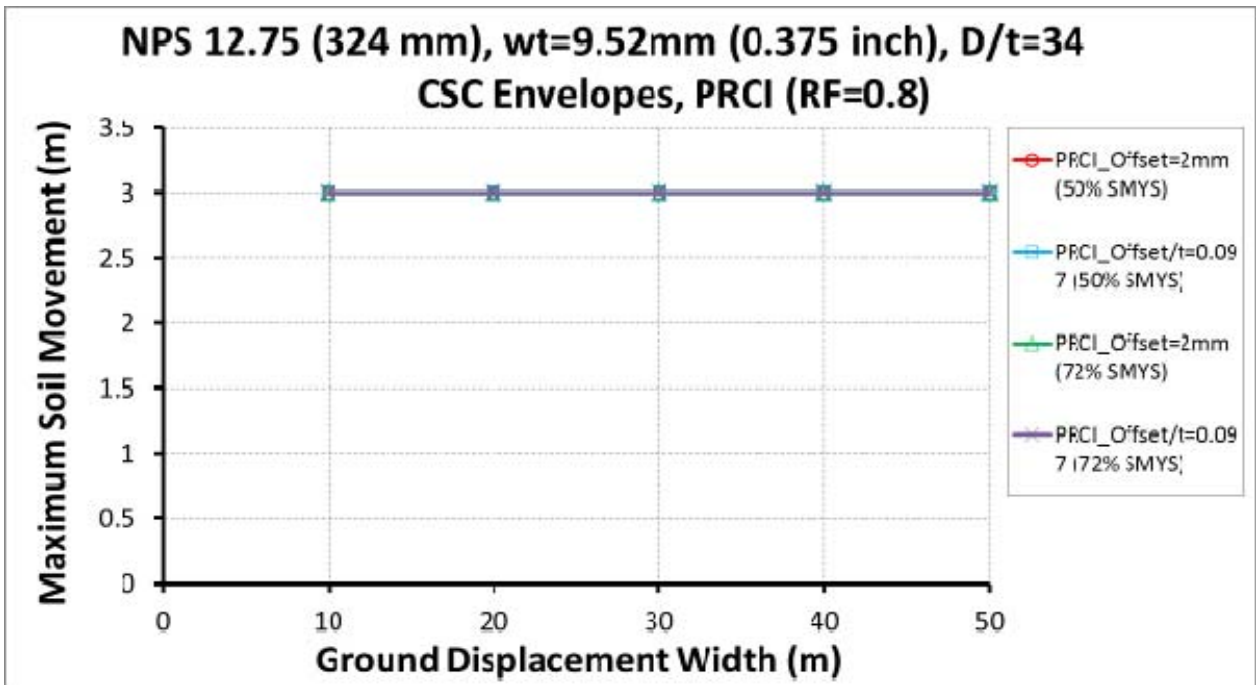

Figure D.28: Compressive Strain Capacity Envelopes versus Ground Width (W) Movements

The information contained herein is the copyright of and proprietary to BMT Fleet Technology Limited. Use of this information is governed by the legend on the cover page of this document."

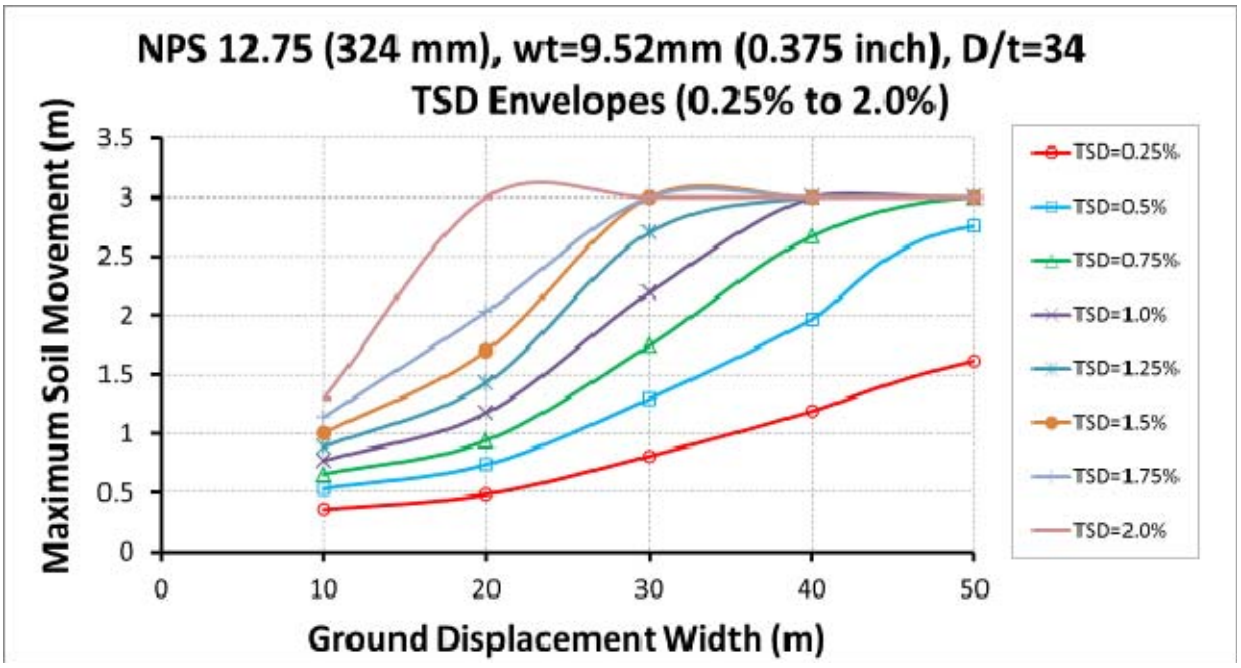

Figure D.29: Tensile Strain Demand Envelopes versus Width (W)

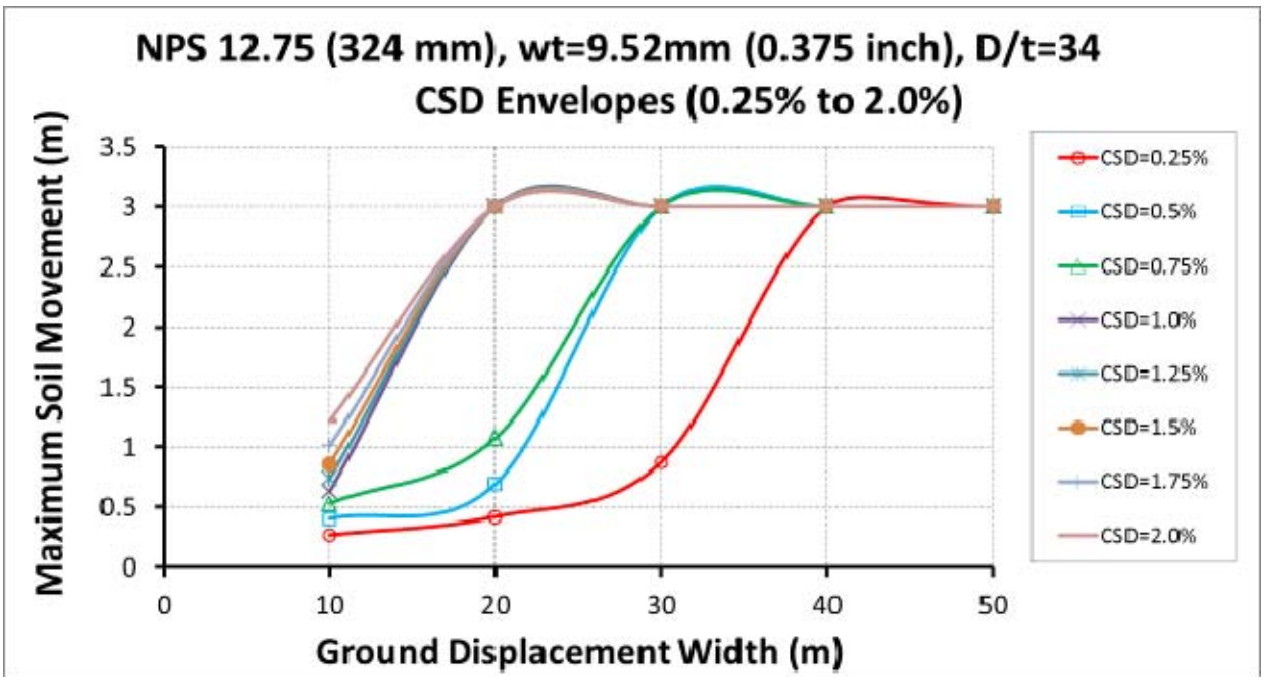

Figure D.30: Compressive Strain Demand Envelopes versus Width (W)

The information contained herein is the copyright of and proprietary to BMT Fleet Technology Limited. Use of this information is governed by the legend on the cover page of this document."

APPENDIX E: MODELING OF LANDSLIDE HAZARD – SUMMARY RESULTS 18-INCH PIPELINE

The information contained herein is the copyright of and proprietary to BMT Fleet Technology Limited. Use of this information is governed by the legend on the cover page of this document."

E.1 MODELING OF LANDSLIDE HAZARD – SUMMARY RESULTS 18-INCH PIPELINE

Analyses were completed for the NPS 18 (457 mm outside diameter) pipeline to assess its response to lateral ground movement and to determine the structural integrity significance of ground movement induced strain demands. A sensitivity analysis was conducted to evaluate the of D/t ratio and ground width displacement. The analyses considered 6 lateral ground movement scenarios. The scenarios included the following

- Pipe wall thickness: one wall thicknesses: 6.35 mm (0.25); corresponding to D/t ratio of 72;
- Ground displacement direction: Perpendicular (lateral) to the pipeline axis;
- Width of ground displacement (W): Six potential ground movement failures with a total estimated width of failure perpendicular to the pipeline varying from 10 to 100 m (10, 20, 30, 40 50 and 100 m);
- Shape of ground displacement: one ground displacement pattern initiated using a cosine function raised to the power "n=2";
- One soil conditions sand/clay till;
- Pipe slope: one slopes, 16 deg.; and
- Pipeline burial depth: one depth of 1.2m (4 ft) to top pipe, corresponding to 1.43 m (4.7 ft), depth to pipe center line.

Assumptions for the pipeline were as follows:

- 72% SMYS internal pressure
- 45^0C thermal differential (installation -20^0C, max operating temperature 25^0C)
- A generic stress strain curves for Grade X-52 (359) pipe according to the API 5L

Detailed results for D/t=72 are presented as follow:

- Figures E.1 presents the maximum tensile strains in the longitudinal direction of the pipeline versus the maximum ground displacement for various ground displacement widths considered in the analyses. Figures E.2 and E.3 present the maximum local and nominal compressive strains in the longitudinal direction of the pipeline versus the maximum ground displacement for various ground displacement widths considered in the analyses. The nominal compressive strain is defined as the average compressive strain measured over a gauge length of 2D (where D is the pipe outside diameter). The results indicate that for the six (6) widths considered, the width of 10 m (33 ft) results in the largest tensile and compressive strain in the pipe for any given value of ground displacement.
- Figure E.5 presents the maximum compressive strains in pipe versus the ground displacement width (W) for given ground displacement of 0.5, 1.0, 1.5, 2.0 and 2.5. In this figure the BS-7910 tensile strain capacity is presented with dash horizontal line. Any tensile strain above the horizontal line is strain-related failure limit. The TSC envelopes based on BS7910 guidance are presented in Figure E.6. The envelopes describe the

The information contained herein is the copyright of and proprietary to BMT Fleet Technology Limited. Use of this information is governed by the legend on the cover page of this document."

maximum soil displacement and ground displacement width breakout the TSC envelopes, which represents the tensile strain-related failure limit, according to BS 7910. The results indicate that for this pipe and operating condition combination, the ground movement width of 10 m (33 ft) can be considered critical.

- Figure E.7 presents the maximum compressive strains in pipe versus the ground displacement width (W) for given ground displacement of 0.5, 1.0, 1.5, 2.0 and 2.5. In this figure the PRCI (UOA) compressive strain capacity is presented with dash horizontal line. Any compressive strain below the horizontal line is strain-related failure limit. The CSC envelopes based on PRCI guidance are presented in Figure E.8. The envelopes describe the maximum soil displacement and ground displacement width breakout the CSC envelopes, which represents the compressive strain-related failure limit, according to PRCI/UOA. The results indicate that for this pipe and operating condition combination, the ground movement width of 10 m (33 ft) can be considered critical
- Figure E.9 and Figure E.10 present the tensile and compressive strain demand 'envelopes' for a given pipe tensile and compressive strain demands of 0.25%, 0.5%, 0.75%, 1%, 1.25%, 1.5%, 1.75% and 2% along the longitudinal direction of the pipeline. The safe pipeline operating goal of pipeline subjected to lateral ground displacement is to stay within the normal operating strain range defined by codes and standards.

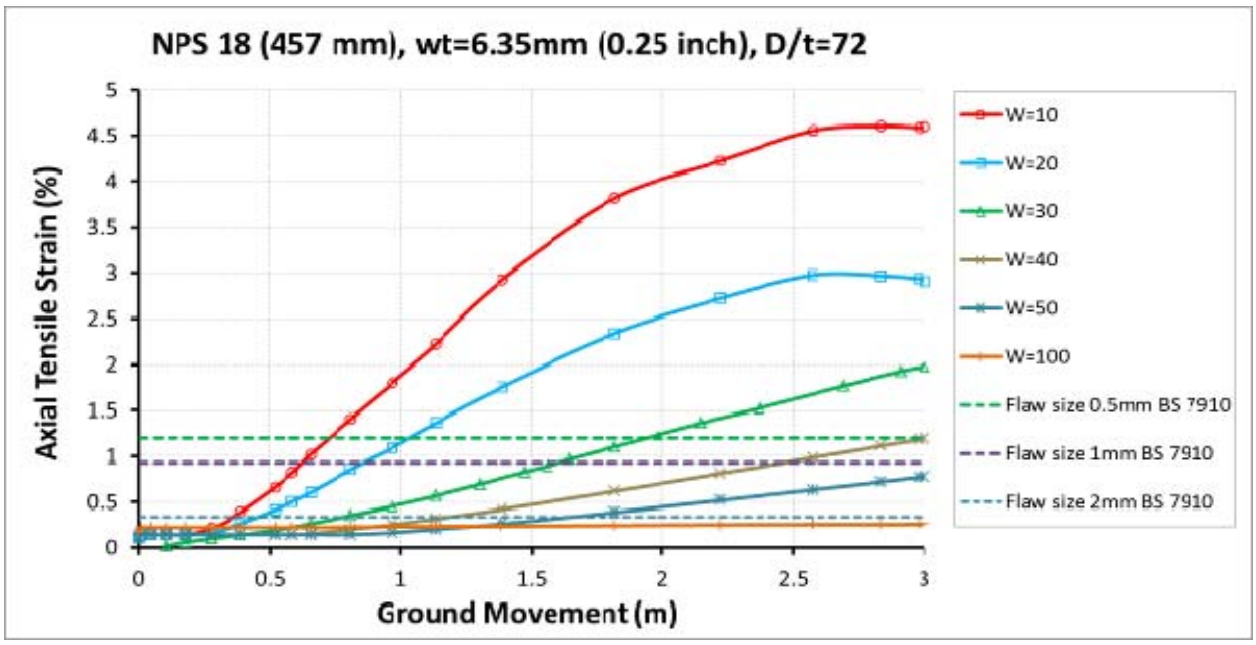

Figure C.1: NPS 18 (D/t=72) - Maximum Tensile in the Pipe vs. Ground Movement Widths: [10-100 m]

The information contained herein is the copyright of and proprietary to BMT Fleet Technology Limited. Use of this information is governed by the legend on the cover page of this document."

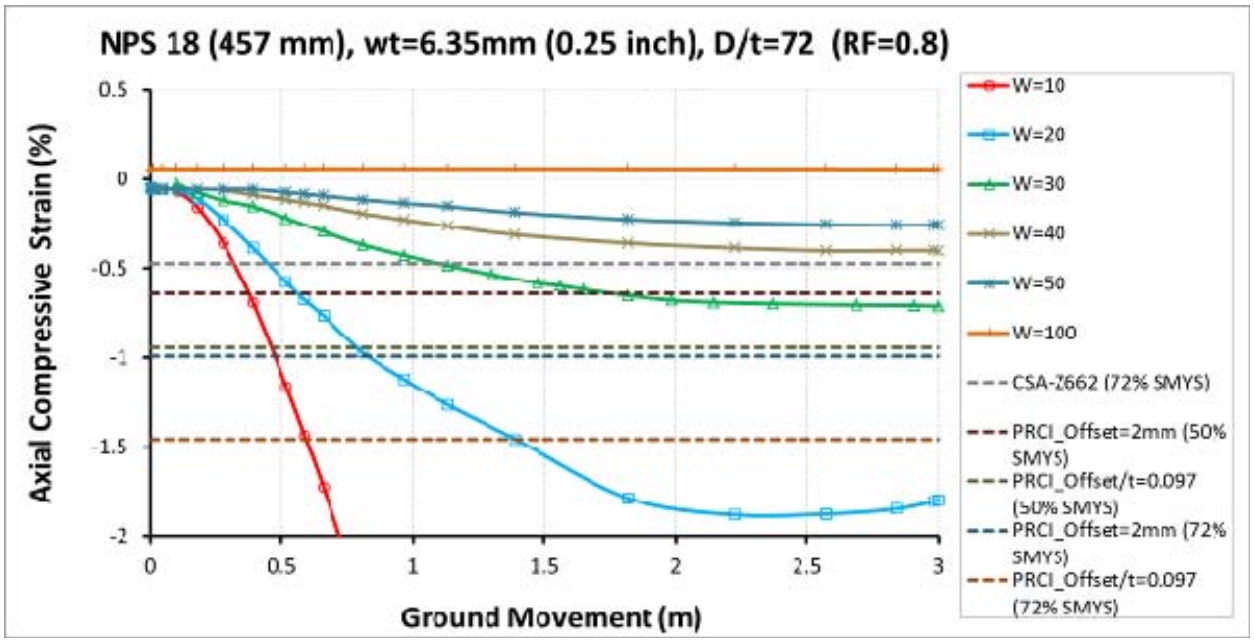

Figure E.2: NPS 18 (D/t=72) - Maximum local Compressive Strain vs. Ground Movement Widths: [10-100 m]

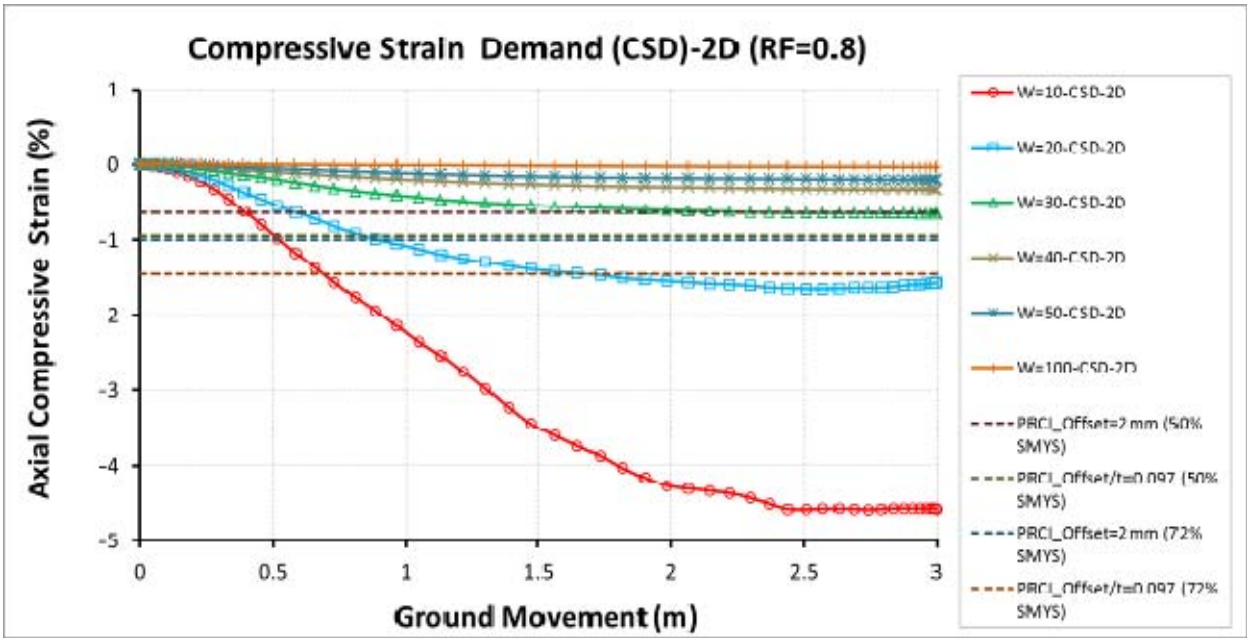

Figure E.3: NPS 18 (D/t=72) - Maximum Nominal Compressive Strain vs. Ground Movement Widths: [10-100 m]

The information contained herein is the copyright of and proprietary to BMT Fleet Technology Limited. Use of this information is governed by the legend on the cover page of this document."

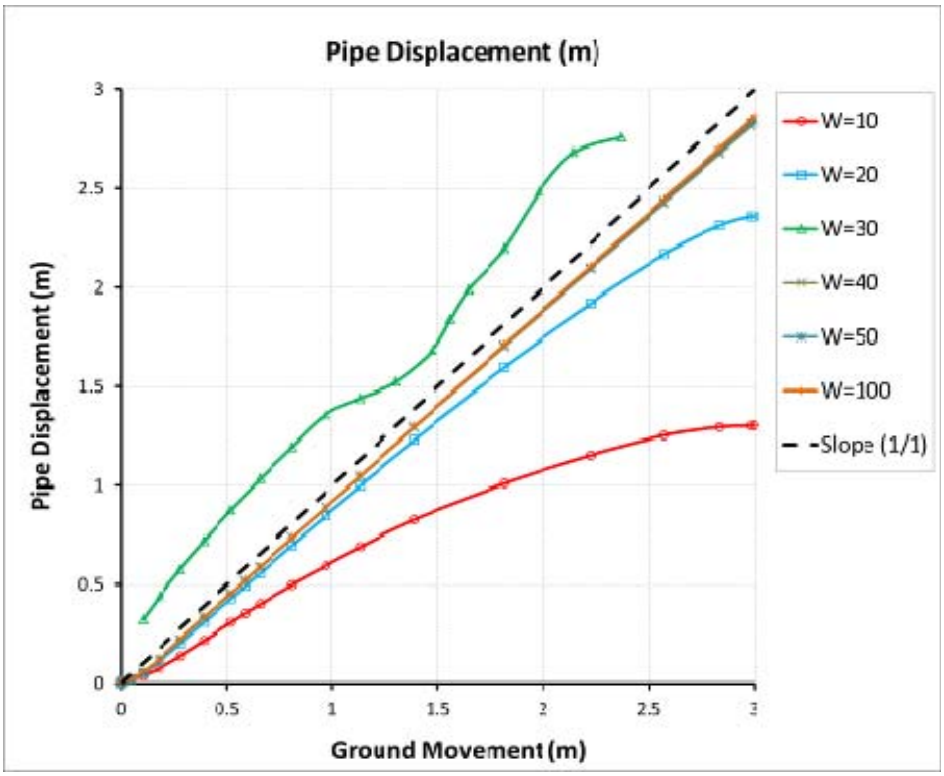

Figure E.4: NPS 18 (D/t=72) – Pipe Displacement versus Ground Displacement

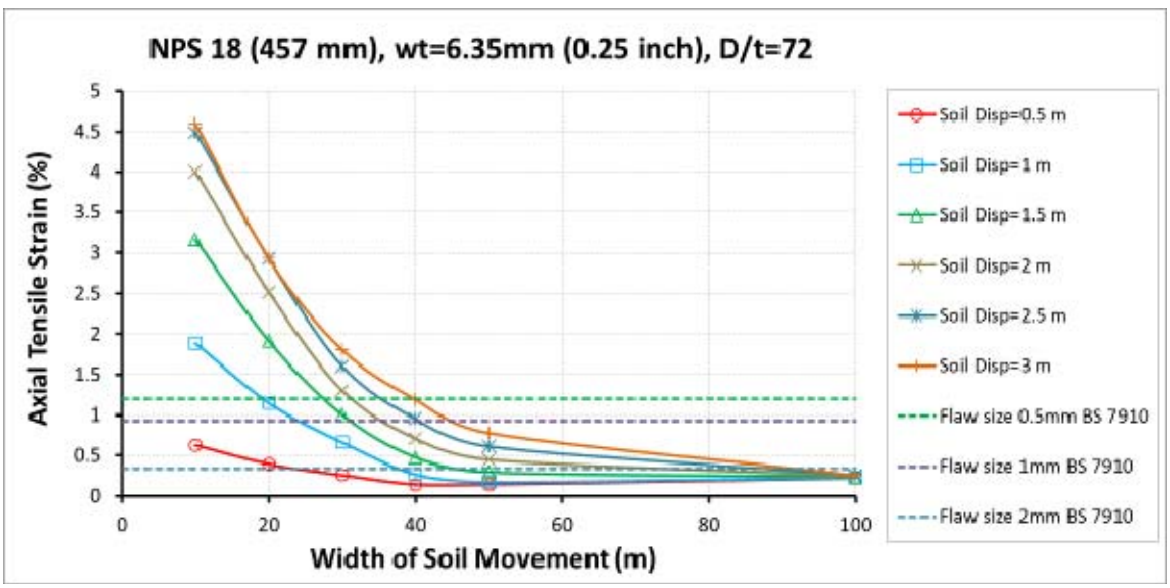

Figure E.5: Pipe Axial Tensile Strains Envelopes versus Width (W) for Soil Movements of 0.5, 1, 1.5, 2.0 and 2.5 m

The information contained herein is the copyright of and proprietary to BMT Fleet Technology Limited. Use of this information is governed by the legend on the cover page of this document."

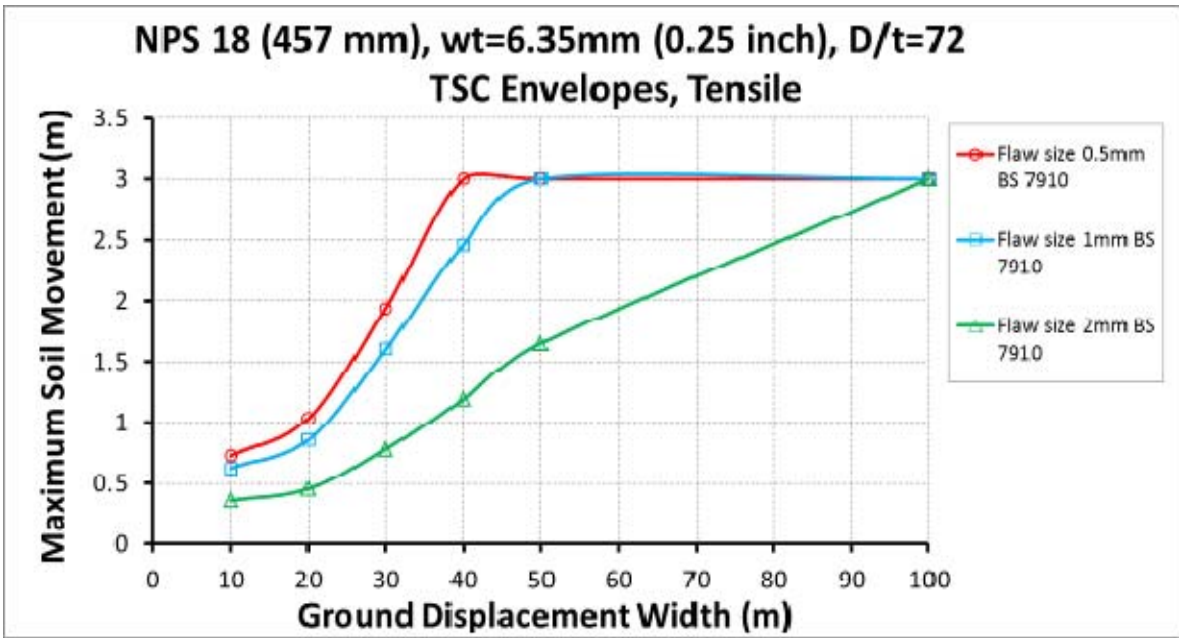

Figure E.6: Tensile Strain Capacity Envelopes versus Ground Width (W) Movements

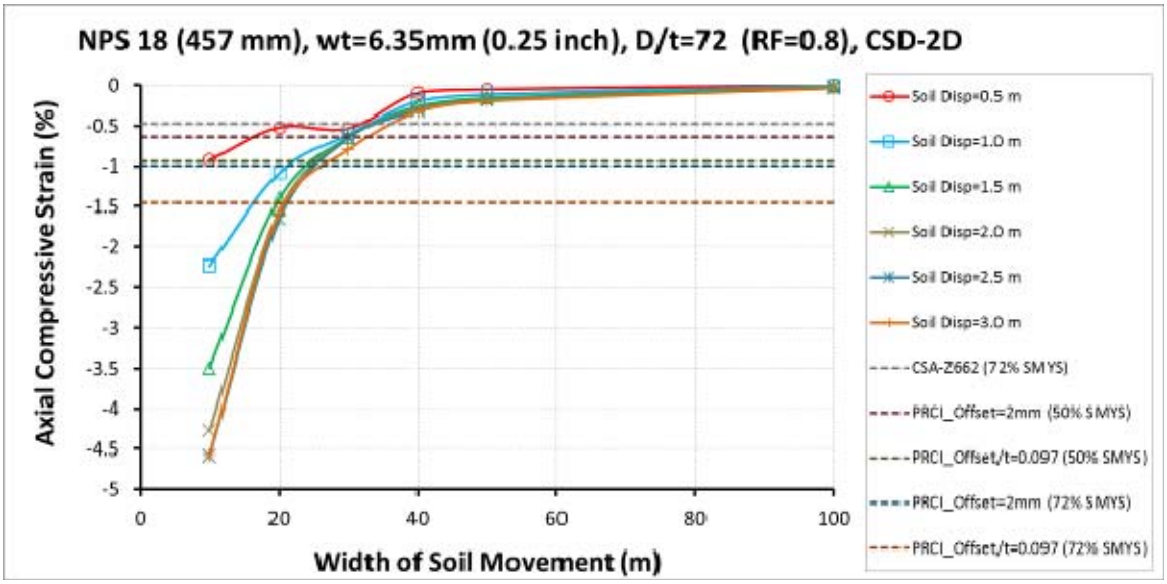

Figure E.7: Pipe Axial Compressive Strains Envelopes versus Width (W) (for Soil Movement of 0.5, 1, 1.5, 2.0 and 2.5 m)

The information contained herein is the copyright of and proprietary to BMT Fleet Technology Limited. Use of this information is governed by the legend on the cover page of this document."

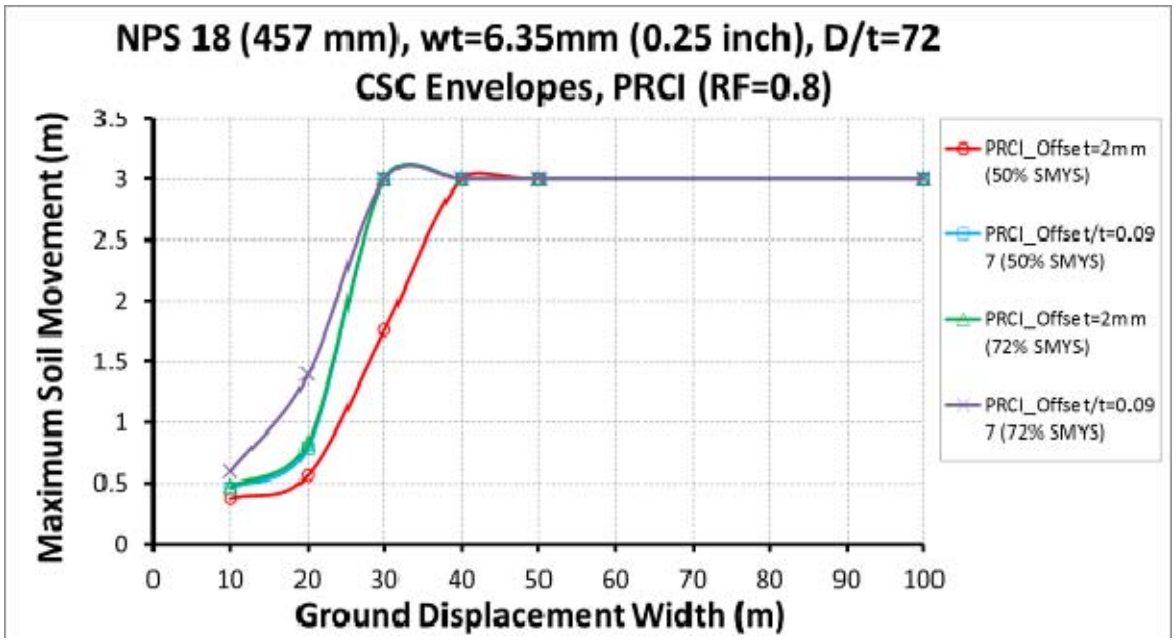

Figure E.8: Compressive Strain Capacity Envelopes versus Ground Width (W) Movements

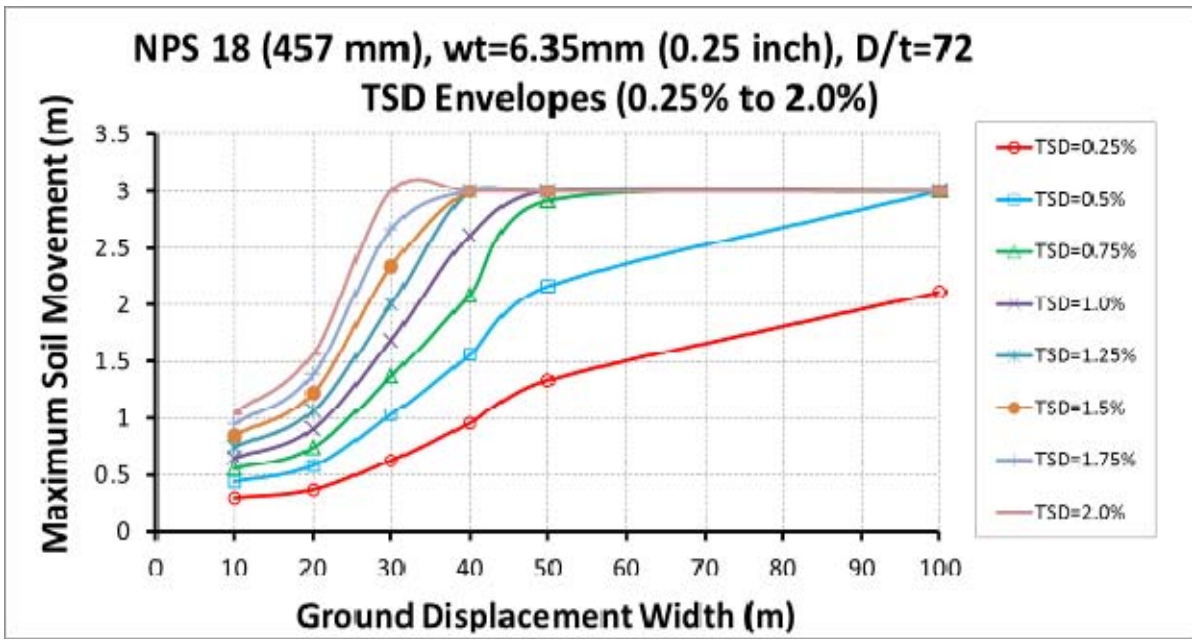

Figure E.9: Tensile Strain Demand Envelopes versus Width (W)

The information contained herein is the copyright of and proprietary to BMT Fleet Technology Limited. Use of this information is governed by the legend on the cover page of this document."

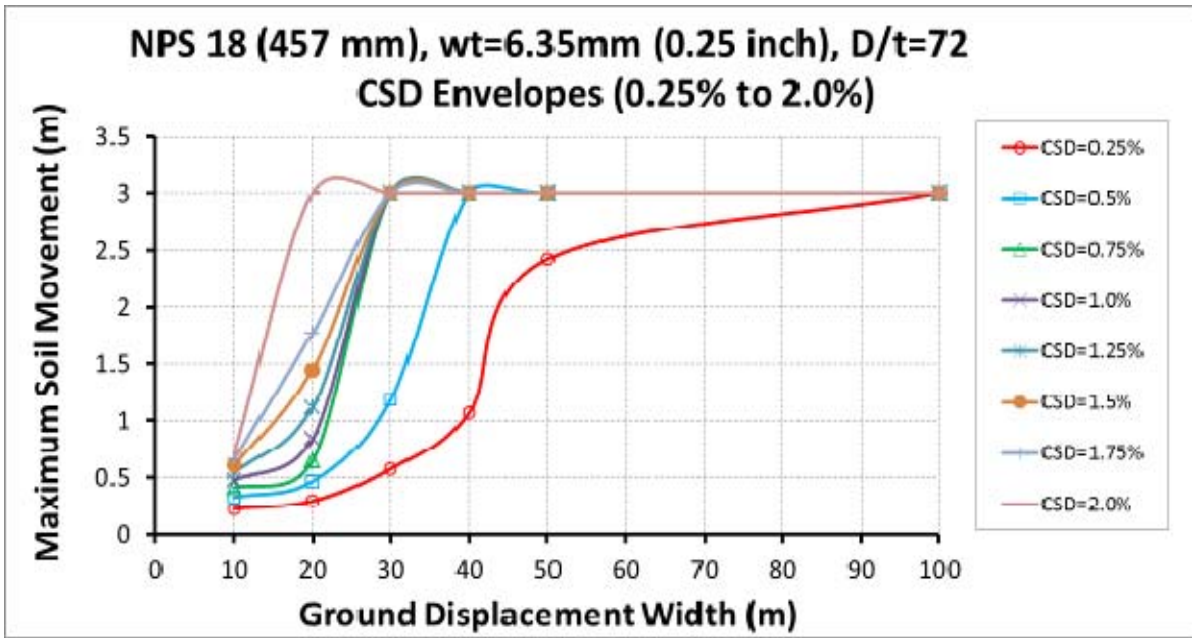

Figure E.10: Compressive Strain Demand Envelopes versus Width (W)

The information contained herein is the copyright of and proprietary to BMT Fleet Technology Limited. Use of this information is governed by the legend on the cover page of this document."

APPENDIX F: MODELING OF LANDSLIDE HAZARD – SUMMARY RESULTS 30-INCH PIPELINE

F.1 MODELING OF LANDSLIDE HAZARD – SUMMARY RESULTS 30-INCH PIPELINE

Analyses were completed for the NPS 30 (762 mm outside diameter) pipeline to assess its response to lateral ground movement and to determine the structural integrity significance of ground movement induced strain demands. A sensitivity analysis was conducted to evaluate the effect of D/t ratio, burial depth and ground width displacement. The analyses considered 18 lateral ground movement scenarios. The scenarios included the following:

- Pipe wall thickness: three wall thicknesses: 7.92 mm (0.312 in), 9.525 mm (0.375 in) and; corresponding to D/t ratio of 96 and 80 respectively;
- Ground displacement direction: Perpendicular (lateral) to the pipeline axis;
- Width of ground displacement (W): Six potential ground movement failures with a total estimated width of failure perpendicular to the pipeline varying from 10 to 100 m (10, 20, 30, 40 50 and 100 m);
- Shape of ground displacement: one ground displacement pattern initiated using a cosine function raised to the power "n=2";
- One soil conditions sand/clay till;
- Pipe slope: one slopes, 16 deg.;
- Pipeline burial depth: two depth of 1.2m (4 ft) and 1.5 m (5 ft) to top pipe and 1.5 m (5 ft), corresponding to 1.6 m (5 ft) and 1.9m (6 ft), depth to pipe center line.

Assumptions for the pipeline were as follows:

- 72% SMYS internal pressure;
- 45 ^{0}C thermal differential (installation -20 ^{0}C, max operating temperature 25 ^{0}C); and
- A generic stress strain curves for Grade X-70 (483) pipe according to the API 5L.

Detailed results for D/t=96 and burial depth of 1.2 m are presented as follow:

- Figures F.1 presents the maximum tensile strains in the longitudinal direction of the pipeline versus the maximum ground displacement for various ground displacement widths considered in the analyses. Figures F.2 and F.3 present the maximum local and nominal compressive strains in the longitudinal direction of the pipeline versus the maximum ground displacement for various ground displacement widths considered in the analyses. The nominal compressive strain is defined as the average compressive strain measured over a gauge length of 2D (where D is the pipe outside diameter). The results indicate that for the six (6) widths considered, the width of 10 m (33 ft) results in the largest tensile and compressive strain in the pipe for any given value of ground displacement.
- Figure F.5 presents the maximum compressive strains in pipe versus the ground displacement width (W) for given ground displacement of 0.5, 1.0, 1.5, 2.0 and 2.5. In this figure the BS-7910 tensile strain capacity is presented with dash horizontal line. Any tensile strain above the horizontal line is strain-related failure limit. The TSC envelopes based on BS7910 guidance are presented in Figure F.6. The envelopes describe the maximum soil displacement and ground displacement width breakout the TSC envelopes,

which represents the tensile strain-related failure limit, according to BS 7910. The results indicate that for this pipe and operating condition combination, the ground movement width of 10 m (33 ft) and 20 m (66 ft) can be considered critical.

- Figure F.7 presents the maximum compressive strains in pipe versus the ground displacement width (W) for given ground displacement of 0.5, 1.0, 1.5, 2.0 and 2.5. In this figure the PRCI (UOA) compressive strain capacity is presented with dash horizontal line. Any compressive strain below the horizontal line is strain-related failure limit. The CSC envelopes based on PRCI guidance are presented in Figure F.8. The envelopes describe the maximum soil displacement and ground displacement width breakout the CSC envelopes, which represents the compressive strain-related failure limit, according to PRCI/UOA. The results indicate that for this pipe and operating condition combination, the ground movement width of 10 m (33 ft) and 20 m (66 ft) can be considered critical
- Figure F.9 and Figure F.10 present the tensile and compressive strain demand 'envelopes' for a given pipe tensile and compressive strain demands of 0.25%, 0.5%, 0.75%, 1%, 1.25%, 1.5%, 1.75% and 2% along the longitudinal direction of the pipeline. The safe pipeline operating goal of pipeline subjected to lateral ground displacement is to stay within the normal operating strain range defined by codes and standards.

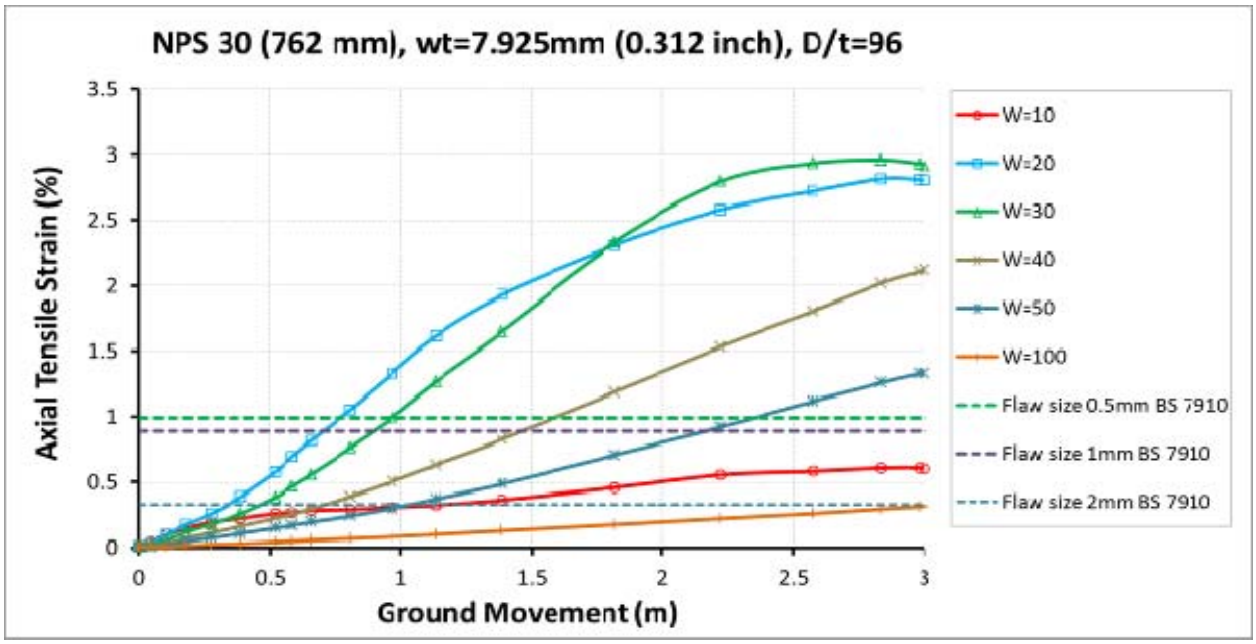

Figure F.1: NPS 30 (D/t=96) - Maximum Tensile in the Pipe vs. Ground Movement Widths: [10-100 m]

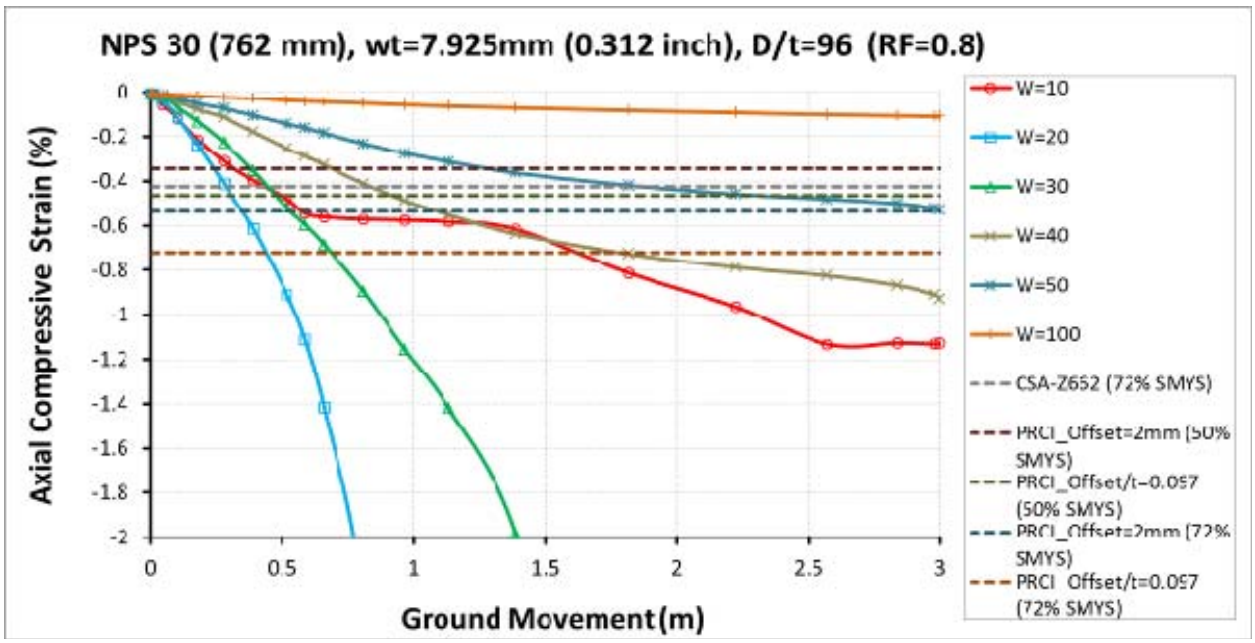

Figure F.2: NPS 30 (D/t=96) - Maximum local Compressive Strain vs. Ground Movement Widths: [10-100 m]

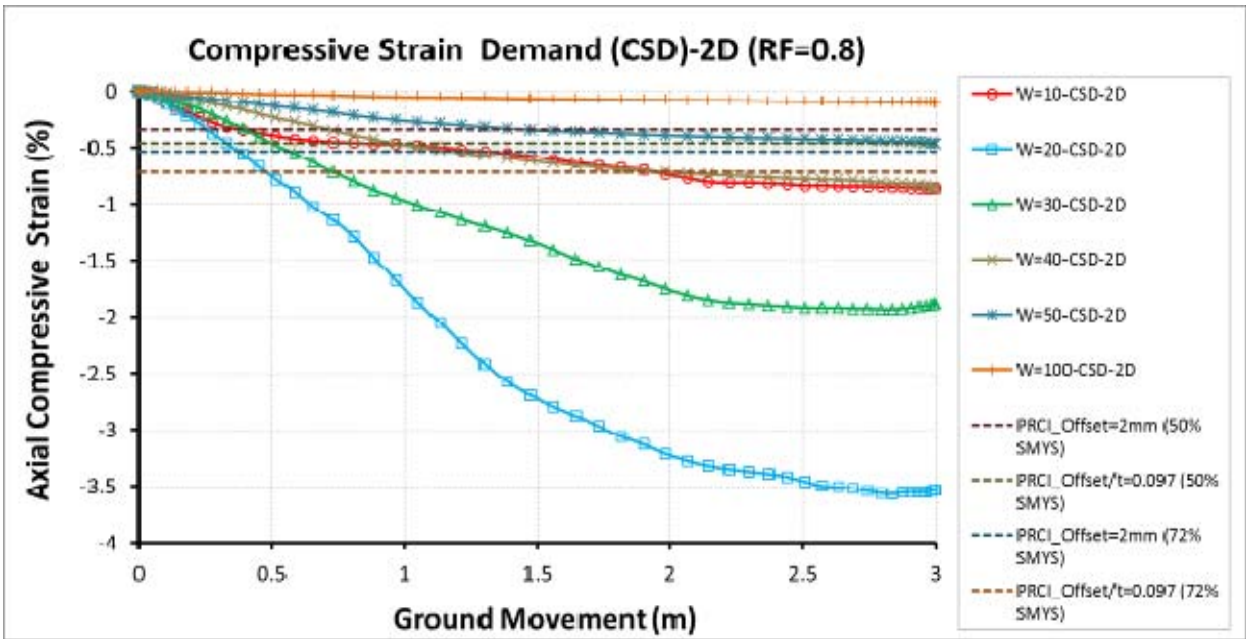

Figure F.3: NPS 30 (D/t=96) - Maximum Nominal Compressive Strain vs. Ground Movement Widths: [10-100 m]

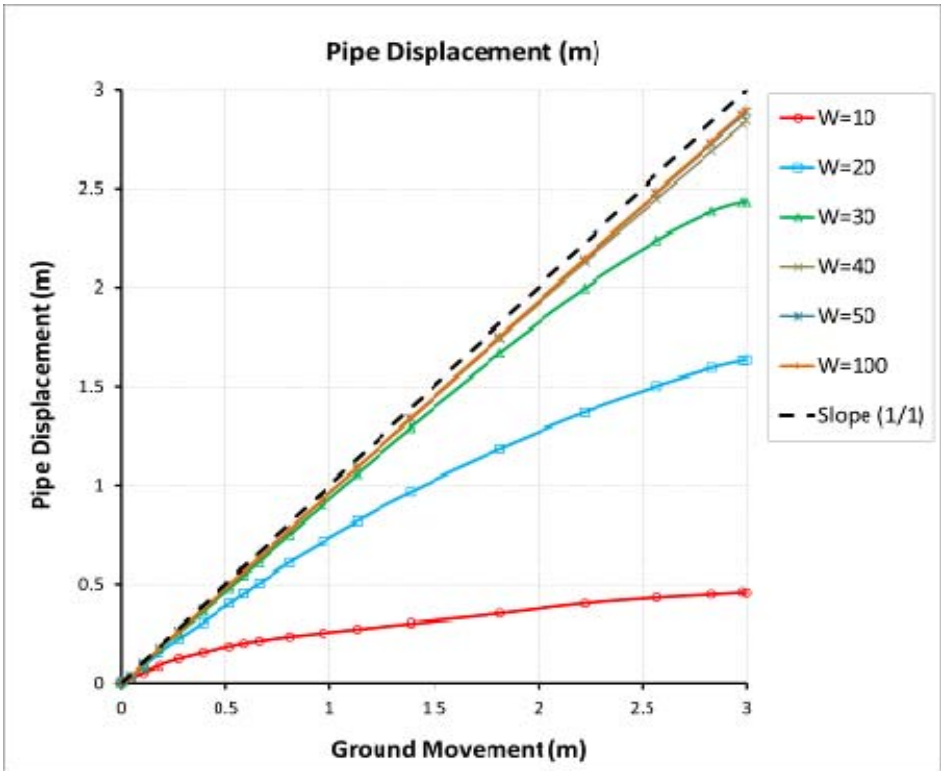

Figure F.4: NPS 30 (D/t=96) – Pipe Displacement versus Ground Displacement

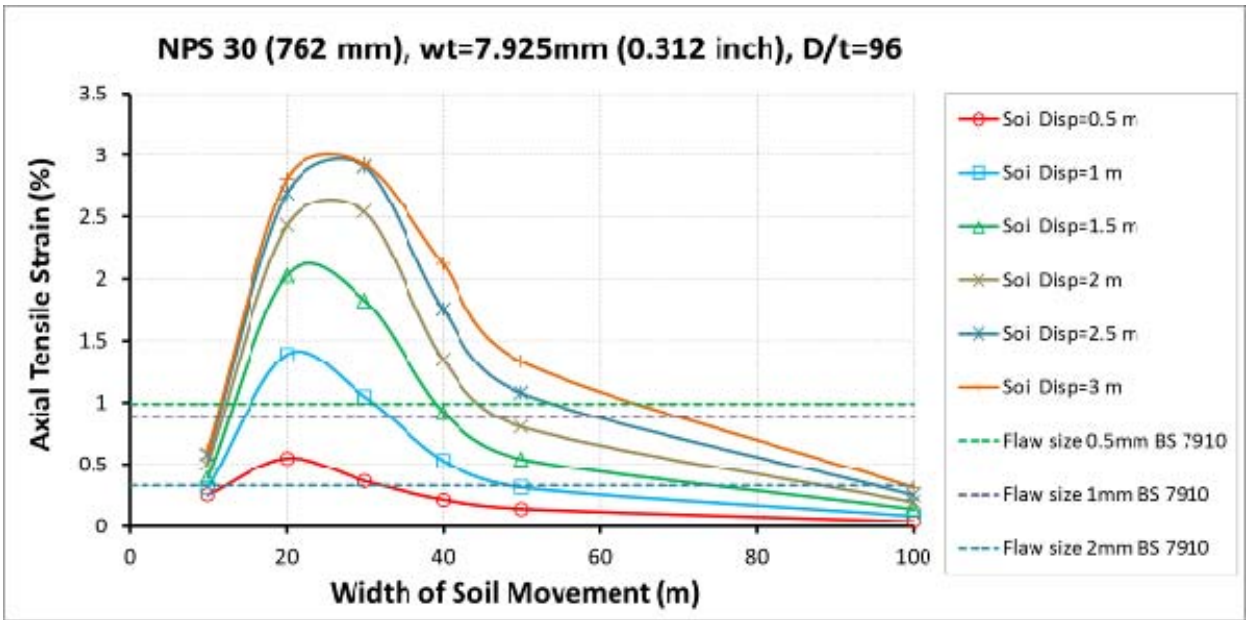

Figure F.5: Pipe Axial Tensile Strains Envelopes versus Width (W) for Soil Movements of 0.5, 1, 1.5, 2.0 and 2.5 m

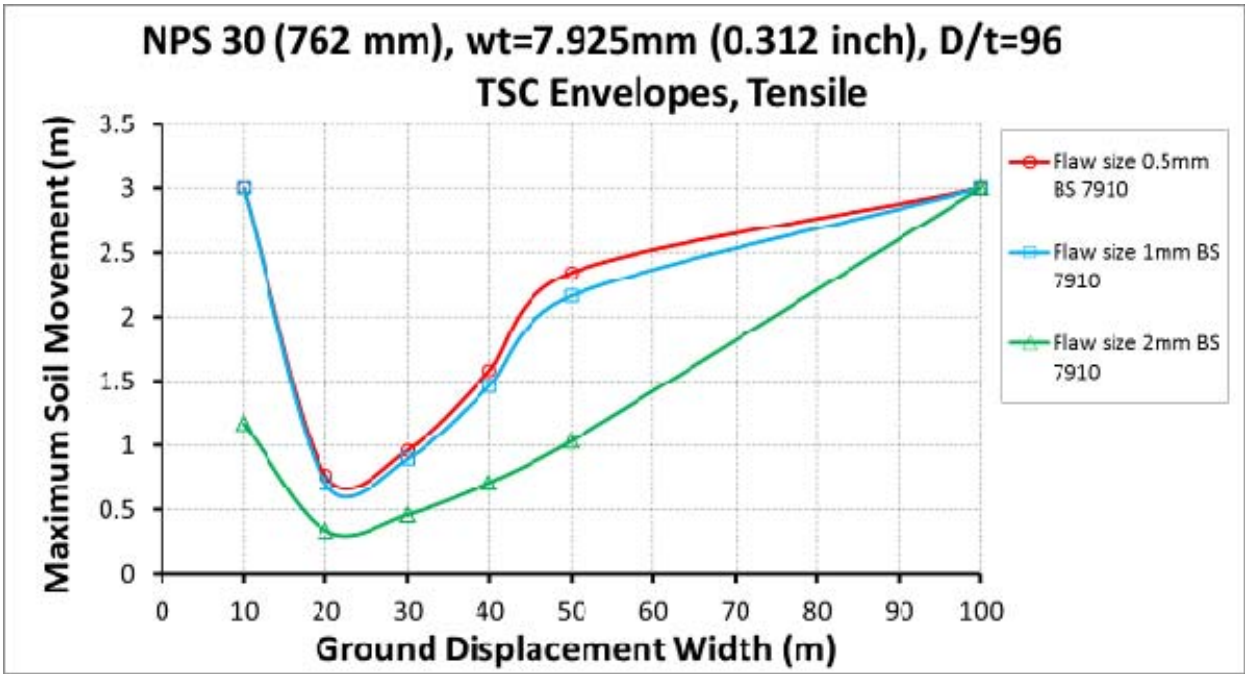

Figure F.6: Tensile Strain Capacity Envelopes versus Ground Width (W) Movements

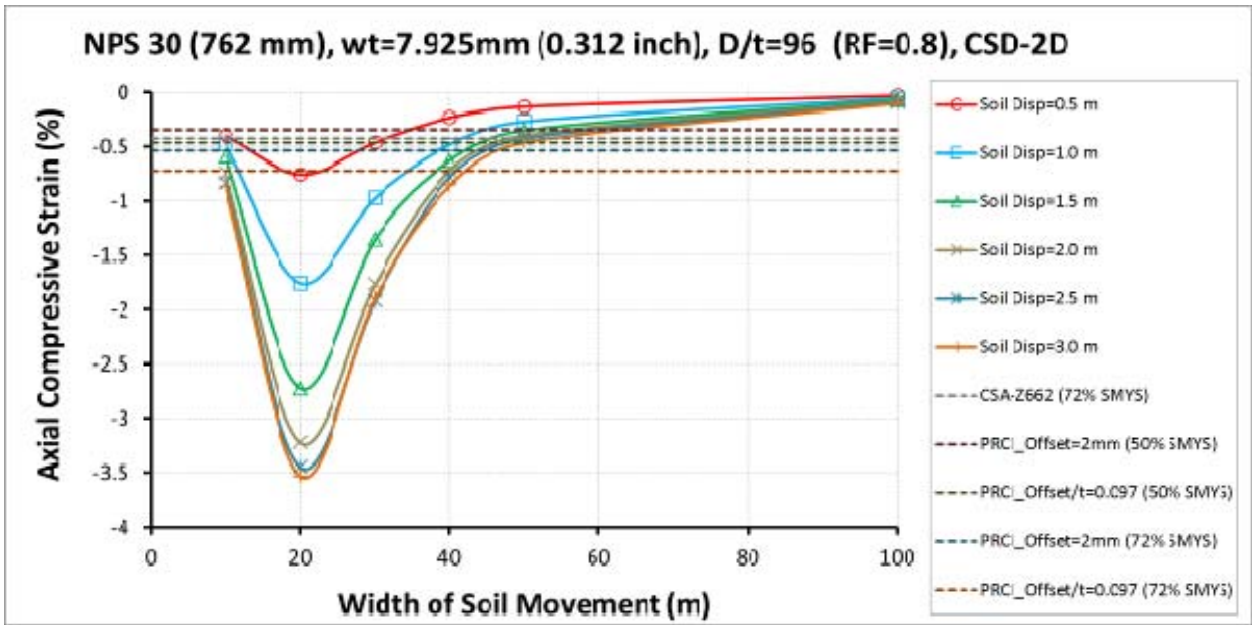

Figure F.7: Pipe Axial Compressive Strains Envelopes versus Width (W) (for Soil Movement of 0.5, 1, 1.5, 2.0 and 2.5 m)

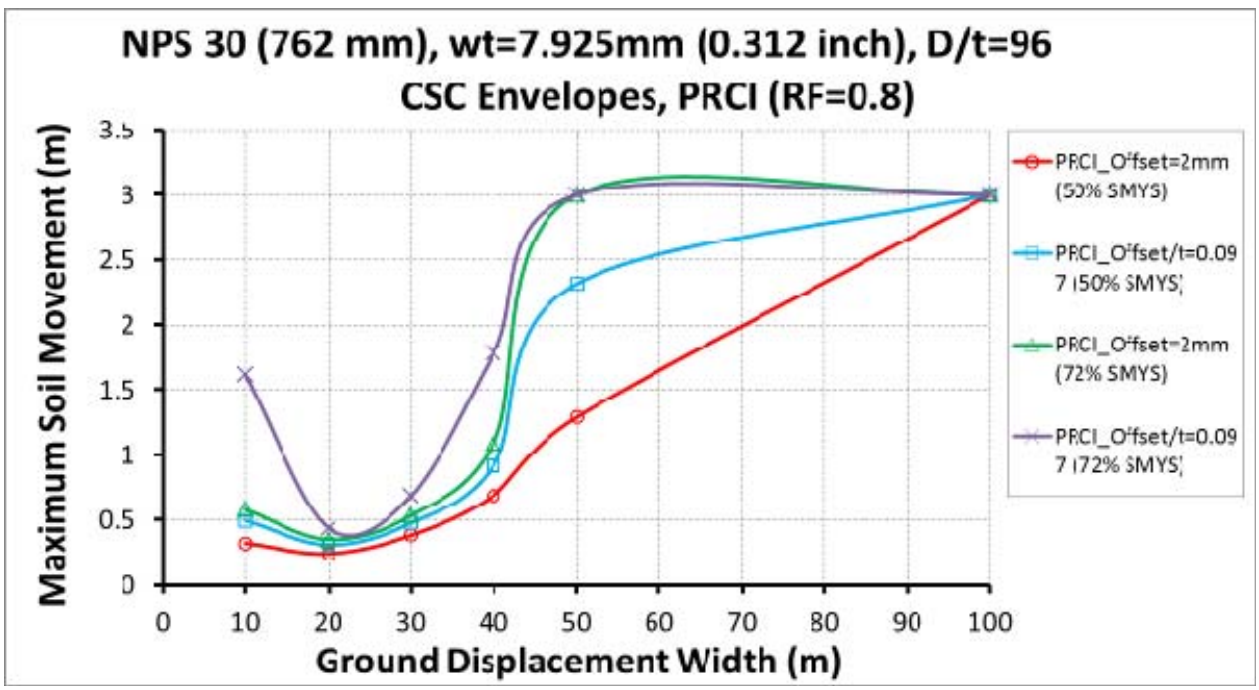

Figure F.8: Compressive Strain Capacity Envelopes versus Ground Width (W) Movements

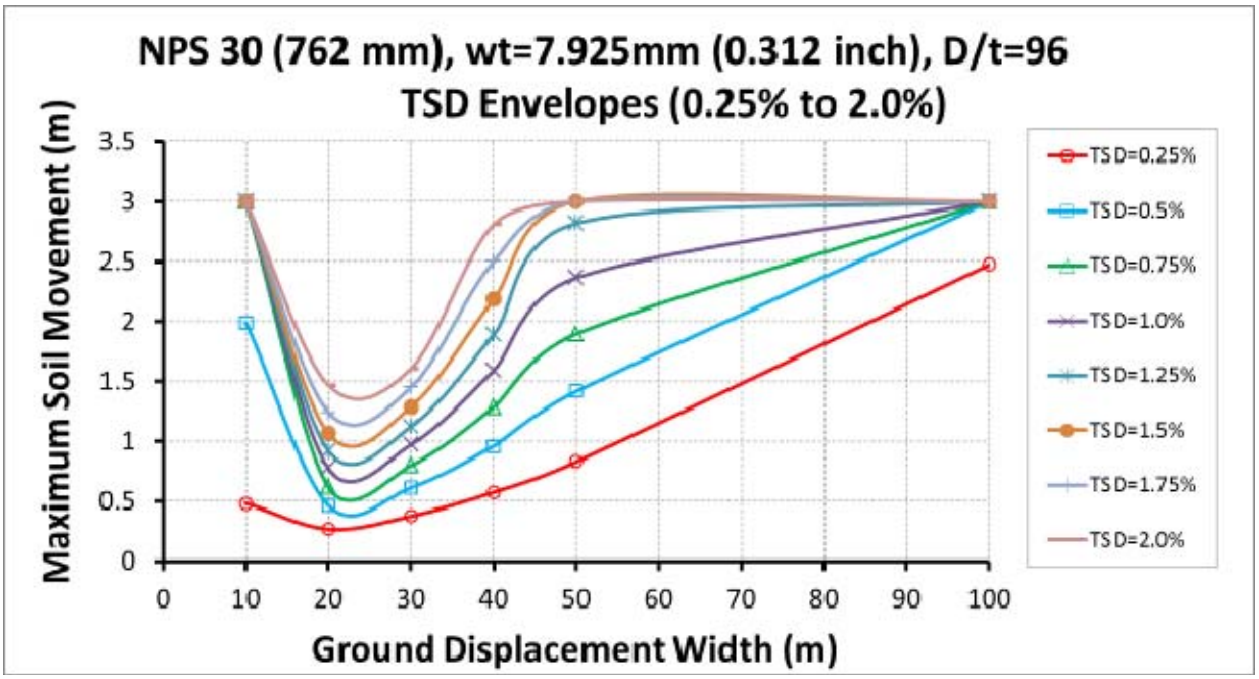

Figure F.9: Tensile Strain Demand Envelopes versus Width (W)

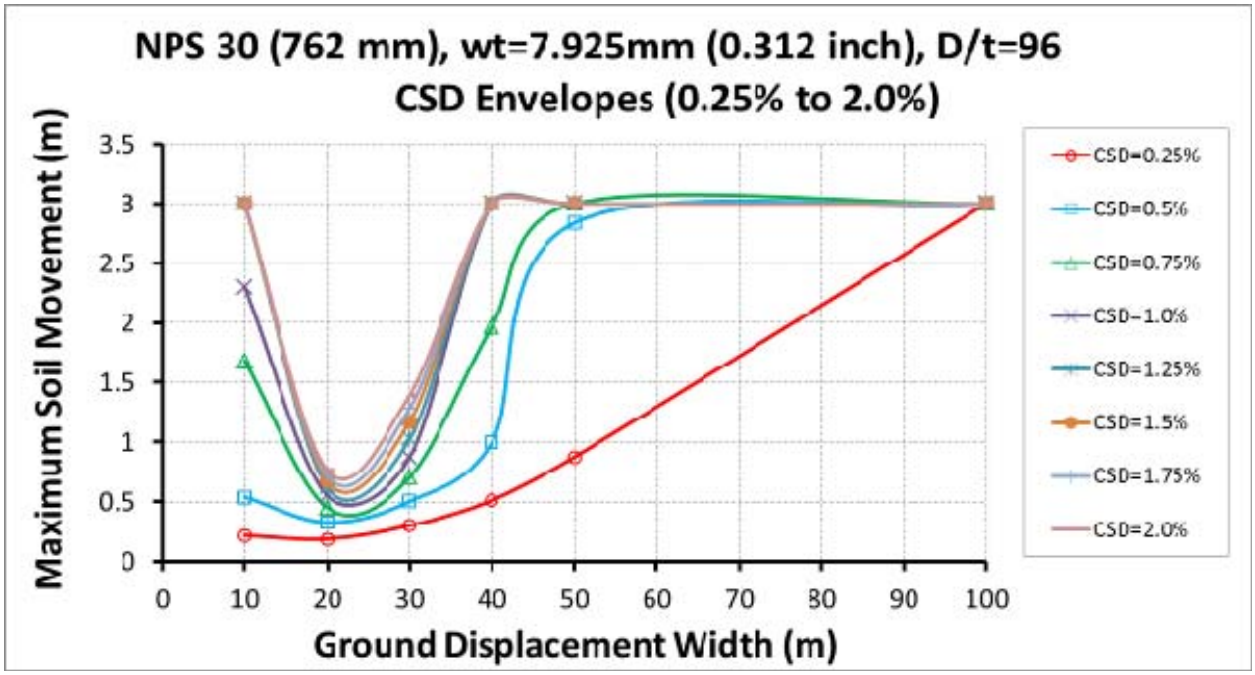

Figure F.10: Compressive Strain Demand Envelopes versus Width (W)

Detailed results for D/t=96 and burial depth of 1.5 m are presented as follows:

- Figures F.11 presents the maximum tensile strains in the longitudinal direction of the pipeline versus the maximum ground displacement for various ground displacement widths considered in the analyses. Figures F.12 and F.13 present the maximum local and nominal compressive strains in the longitudinal direction of the pipeline versus the maximum ground displacement for various ground displacement widths considered in the analyses. The nominal compressive strain is defined as the average compressive strain measured over a gauge length of 2D (where D is the pipe outside diameter). The results indicate that for the six (6) widths considered, the width of 10 m (33 ft) and 20 m 966 ft) results in the largest tensile and compressive strain in the pipe for any given value of ground displacement.
- Figure F.15 presents the maximum compressive strains in pipe versus the ground displacement width (W) for given ground displacement of 0.5, 1.0, 1.5, 2.0 and 2.5. In this figure the BS-7910 tensile strain capacity is presented with dash horizontal line. Any tensile strain above the horizontal line is strain-related failure limit. The TSC envelopes based on BS7910 guidance are presented in Figure D.16. The envelopes describe the maximum soil displacement and ground displacement width breakout the TSC envelopes, which represents the tensile strain-related failure limit, according to BS 7910. The results indicate that for this pipe and operating condition combination, the ground movement width of 10 m (33 ft) and 20 m (66 ft) can be considered critical.
- Figure F.17 presents the maximum compressive strains in pipe versus the ground displacement width (W) for given ground displacement of 0.5, 1.0, 1.5, 2.0 and 2.5. In this figure the PRCI (UOA) compressive strain capacity is presented with dash horizontal line. Any compressive strain below the horizontal line is strain-related failure limit. The CSC envelopes based on PRCI guidance are presented in Figure D.18. The envelopes describe the maximum soil displacement and ground displacement width breakout the CSC envelopes, which represents the compressive strain-related failure limit, according to PRCI/UOA. The results indicate that for this pipe and operating condition combination, the ground movement width of 10 m (33 ft) and 20 m (66 ft) can be considered critical
- Figure F.19 and Figure F.20 present the tensile and compressive strain demand 'envelopes' for a given pipe tensile and compressive strain demands of 0.25%, 0.5%, 0.75%, 1%, 1.25%, 1.5%, 1.75% and 2% along the longitudinal direction of the pipeline. The safe pipeline operating goal of pipeline subjected to lateral ground displacement is to stay within the normal operating strain range defined by codes and standards.

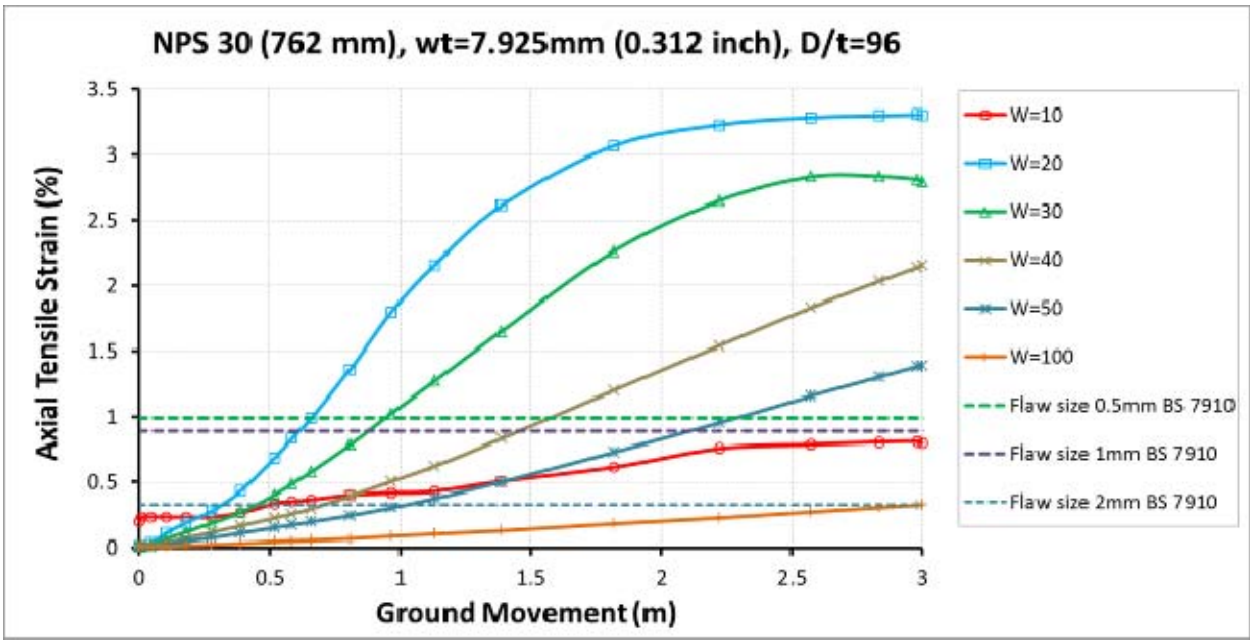

Figure F.11: NPS 30 (D/t=96) - Maximum Tensile in the Pipe vs. Ground Movement Widths: [10-100 m]

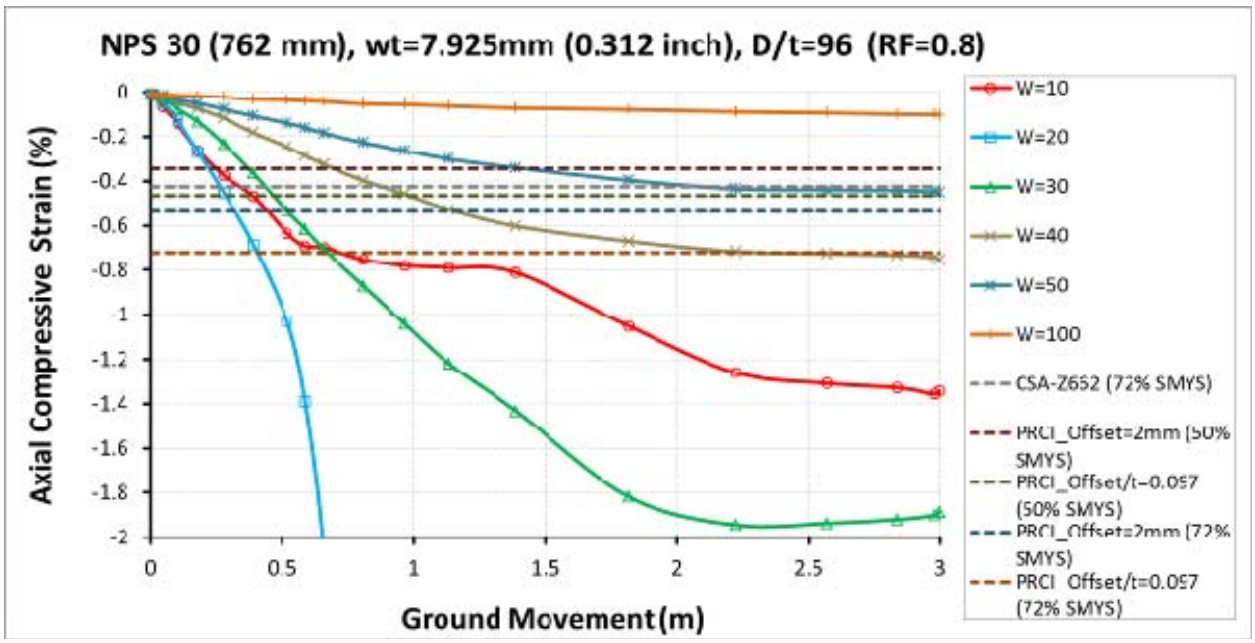

Figure F.12: NPS 30 (D/t=96) - Maximum local Compressive Strain vs. Ground Movement Widths: [10-100 m]

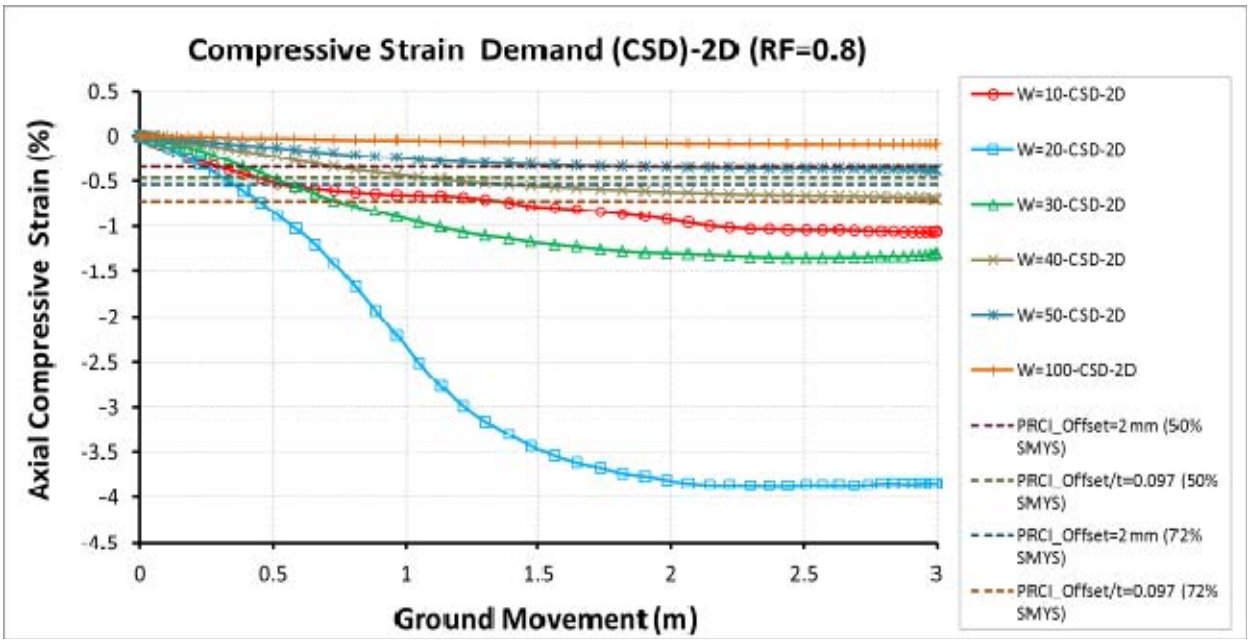

Figure F.13: NPS 30 (D/t=96) - Maximum Nominal Compressive Strain vs. Ground Movement Widths: [10-100 m]

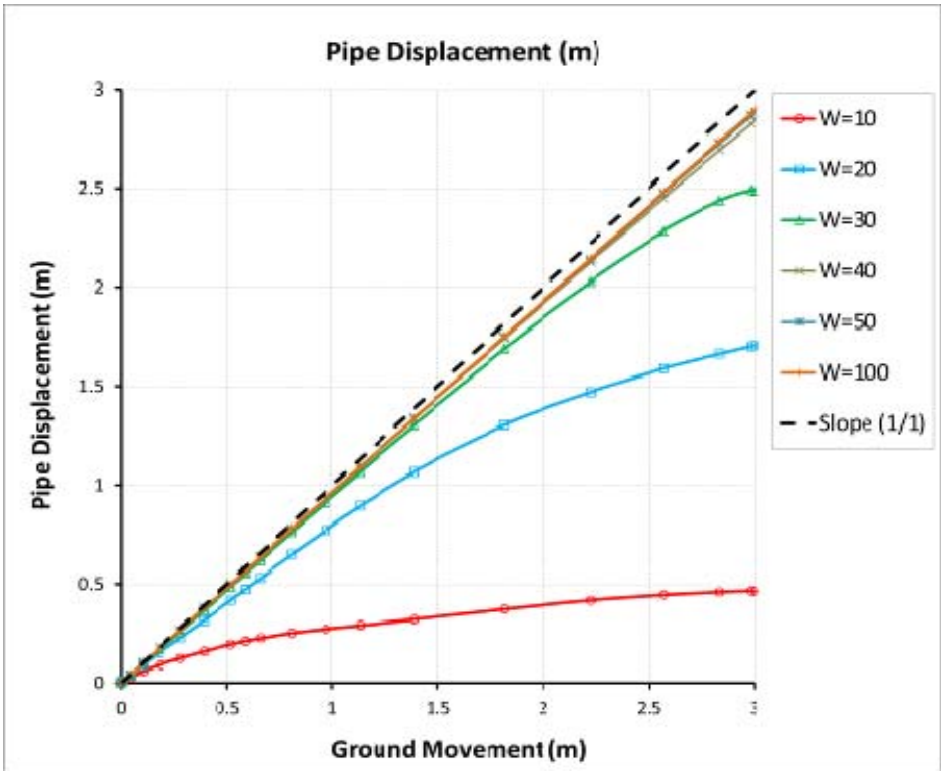

Figure F.14: NPS 30 (D/t=96) – Pipe Displacement versus Ground Displacement

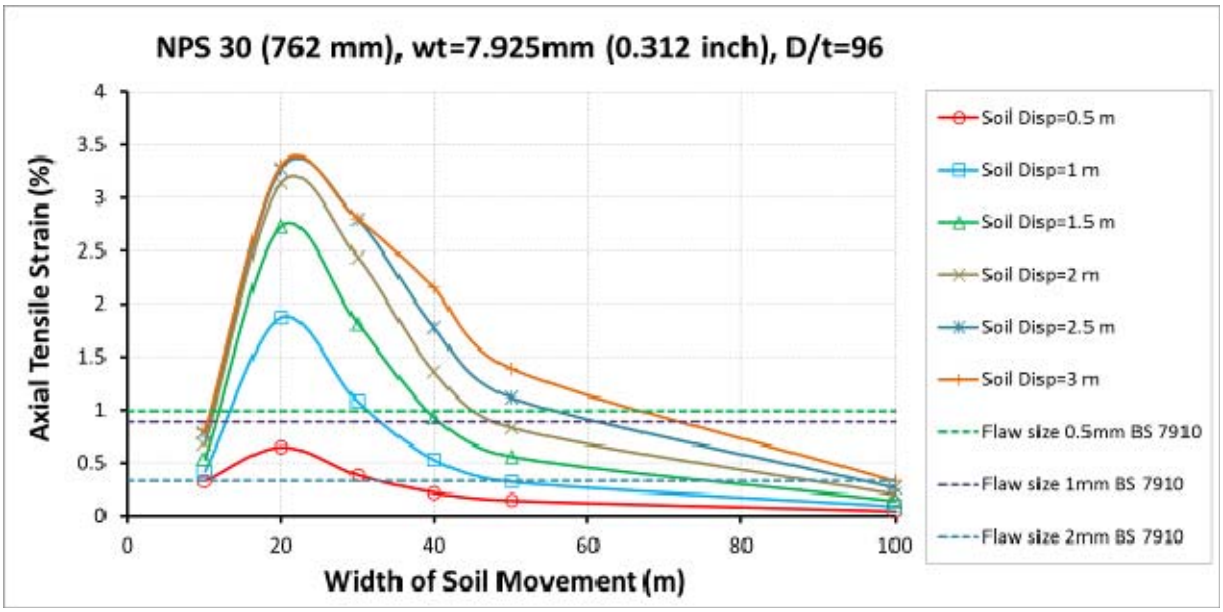

Figure F.15: Pipe Axial Tensile Strains Envelopes versus Width (W) for Soil Movements of 0.5, 1, 1.5, 2.0 and 2.5 m

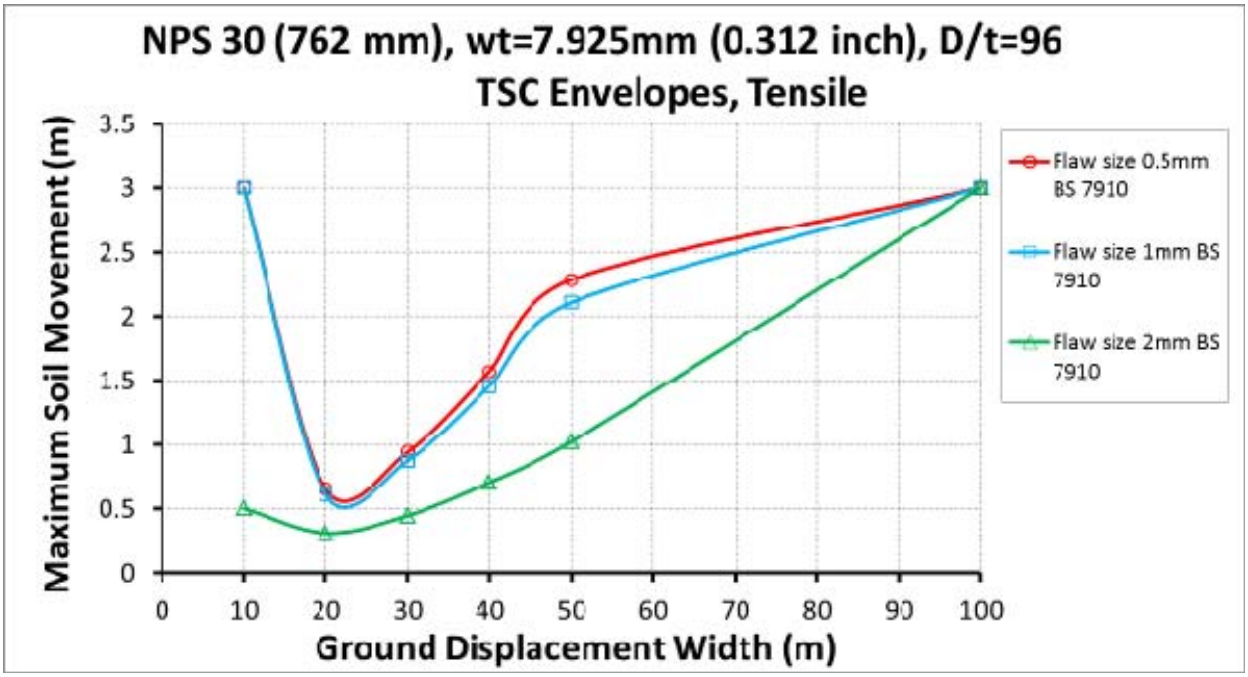

Figure F.16: Tensile Strain Capacity Envelopes versus Ground Width (W) Movements

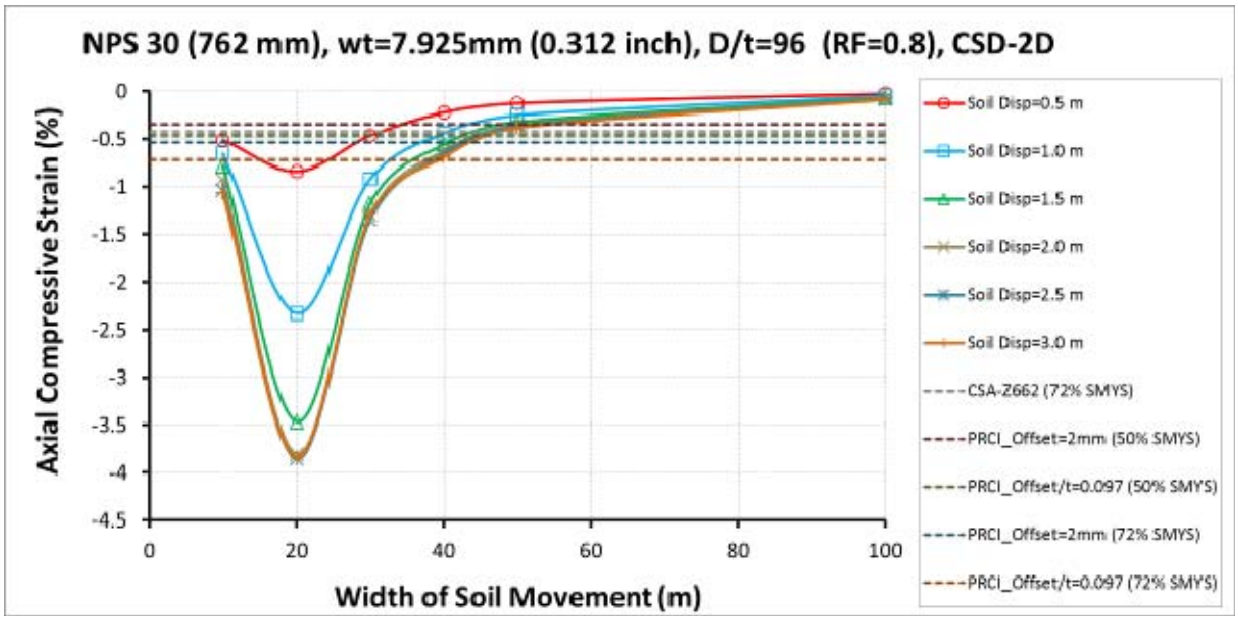

Figure F.17: Pipe Axial Compressive Strains Envelopes versus Width (W) (for Soil Movement of 0.5, 1, 1.5, 2.0 and 2.5 m)

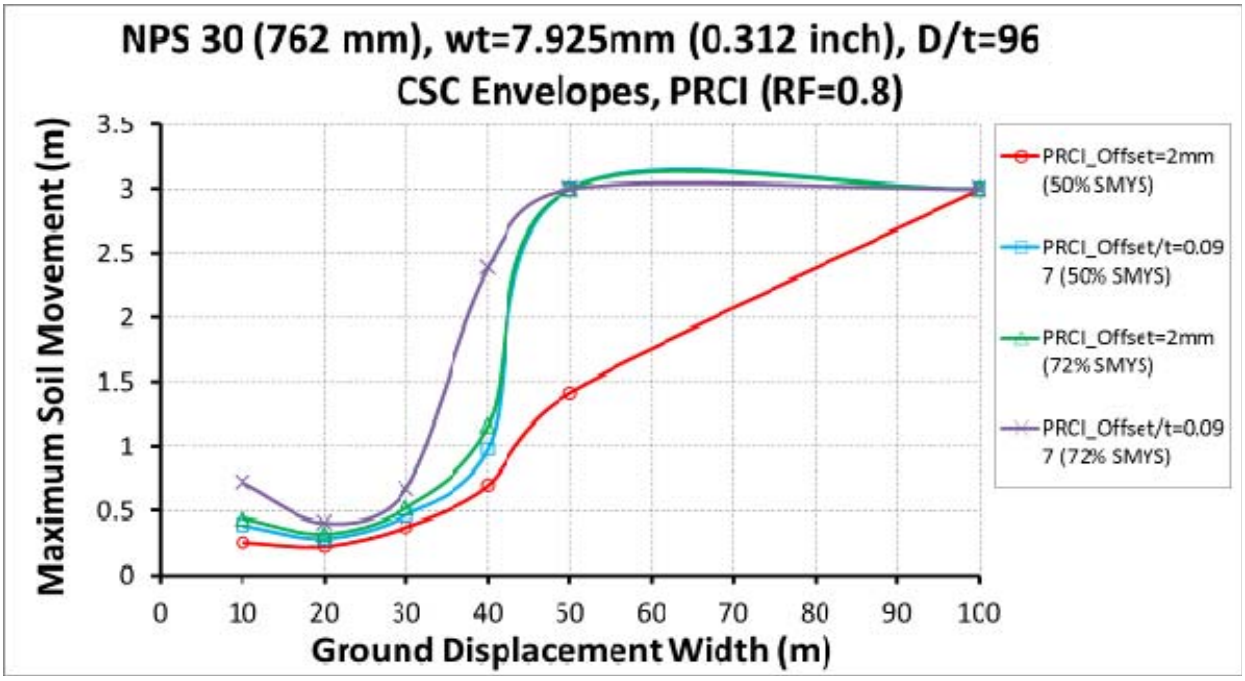

Figure F.18: Compressive Strain Capacity Envelopes versus Ground Width (W) Movements

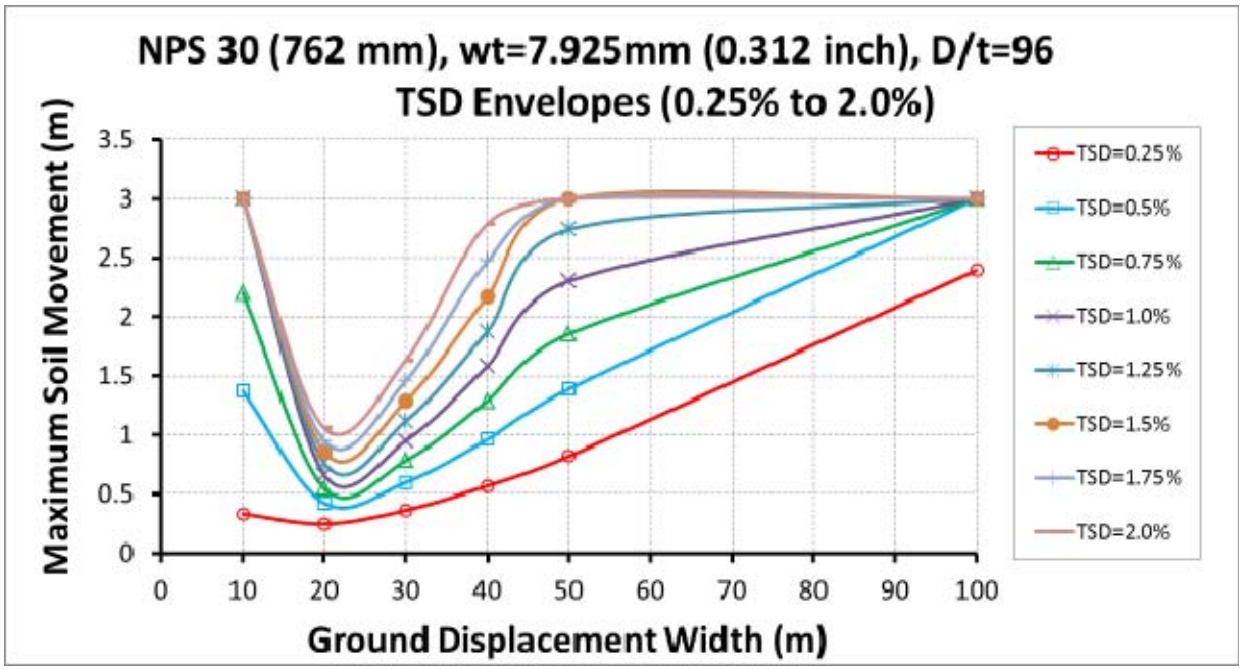

Figure F.19: Tensile Strain Demand Envelopes versus Width (W)

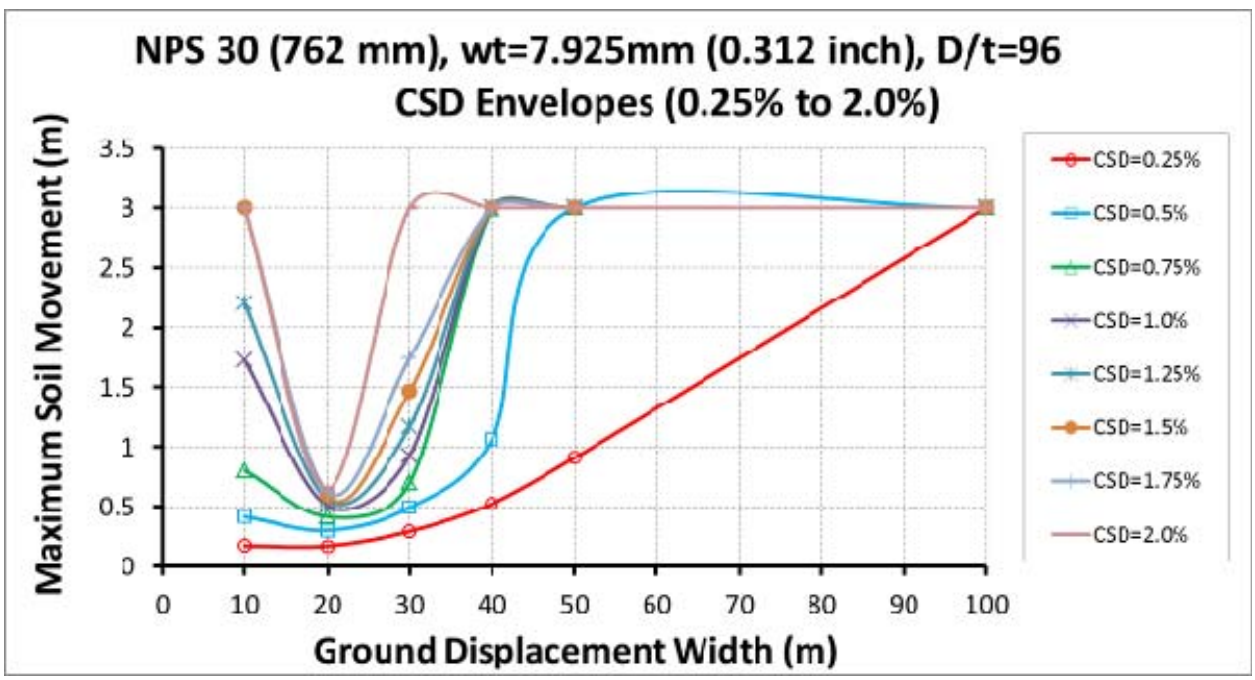

Figure F.20: Compressive Strain Demand Envelopes versus Width (W)

Detailed results for D/t = 80m and burial depth of 1.2 m are presented as follow:

- Figures F.21 presents the maximum tensile strains in the longitudinal direction of the pipeline versus the maximum ground displacement for various ground displacement widths considered in the analyses. Figures F.22 and F.23 present the maximum local and nominal compressive strains in the longitudinal direction of the pipeline versus the maximum ground displacement for various ground displacement widths considered in the analyses. The nominal compressive strain is defined as the average compressive strain measured over a gauge length of 2D (where D is the pipe outside diameter). The results indicate that for the six (6) widths considered, the width of 20 m (33 ft) results in the largest tensile and compressive strain in the pipe for any given value of ground displacement.
- Figure F.25 presents the maximum compressive strains in pipe versus the ground displacement width (W) for given ground displacement of 0.5, 1.0, 1.5, 2.0 and 2.5. In this figure the BS-7910 tensile strain capacity is presented with dash horizontal line. Any tensile strain above the horizontal line is strain-related failure limit. The TSC envelopes based on BS7910 guidance are presented in Figure F.26. The envelopes describe the maximum soil displacement and ground displacement width breakout the TSC envelopes, which represents the tensile strain-related failure limit, according to BS 7910. The results indicate that for this pipe and operating condition combination, the ground movement width of 20 m (66 ft) can be considered critical.
- Figure F.27 presents the maximum compressive strains in pipe versus the ground displacement width (W) for given ground displacement of 0.5, 1.0, 1.5, 2.0 and 2.5. In this figure the PRCI (UOA) compressive strain capacity is presented with dash horizontal line. Any compressive strain below the horizontal line is strain-related failure limit. The CSC envelopes based on PRCI guidance are presented in Figure F.28. The envelopes describe the maximum soil displacement and ground displacement width breakout the CSC envelopes, which represents the compressive strain-related failure limit, according to PRCI/UOA. The results indicate that for this pipe and operating condition combination, the ground movement width of 20 m (66 ft) can be considered critical
- Figure F.29 and Figure F.30 present the tensile and compressive strain demand 'envelopes' for a given pipe tensile and compressive strain demands of 0.25%, 0.5%, 0.75%, 1%, 1.25%, 1.5%, 1.75% and 2% along the longitudinal direction of the pipeline. The safe pipeline operating goal of pipeline subjected to lateral ground displacement is to stay within the normal operating strain range defined by codes and standards.

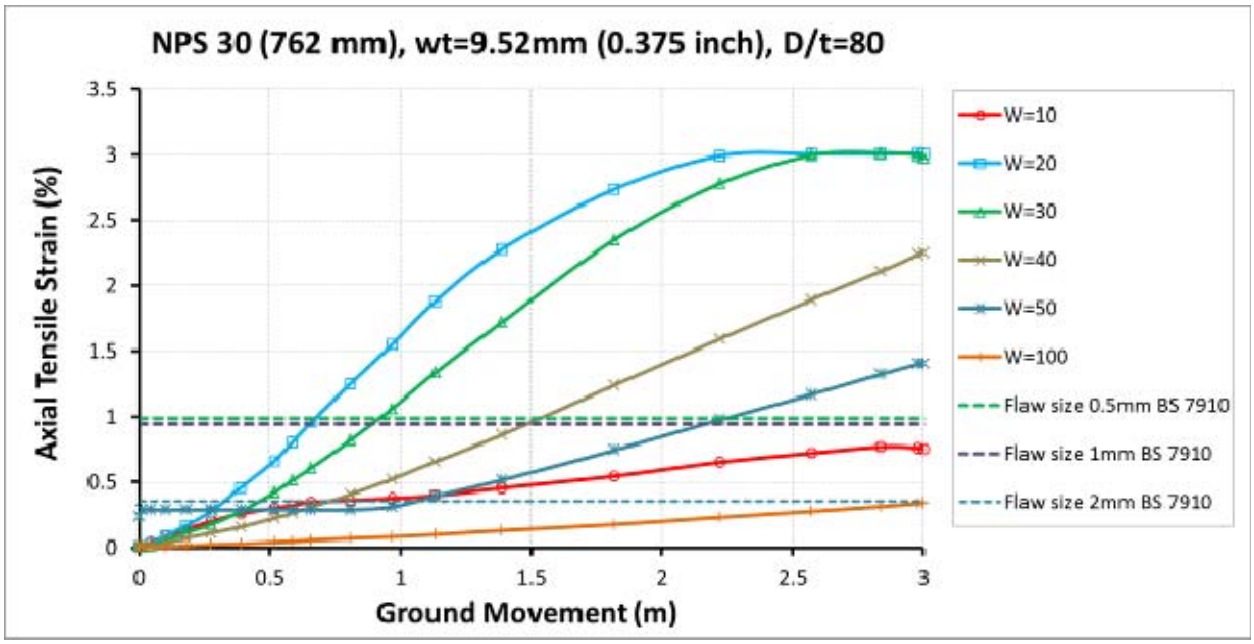

Figure F.21: NPS 30 (D/t=80) - Maximum Tensile in the Pipe vs. Ground Movement Widths: [10-100 m]

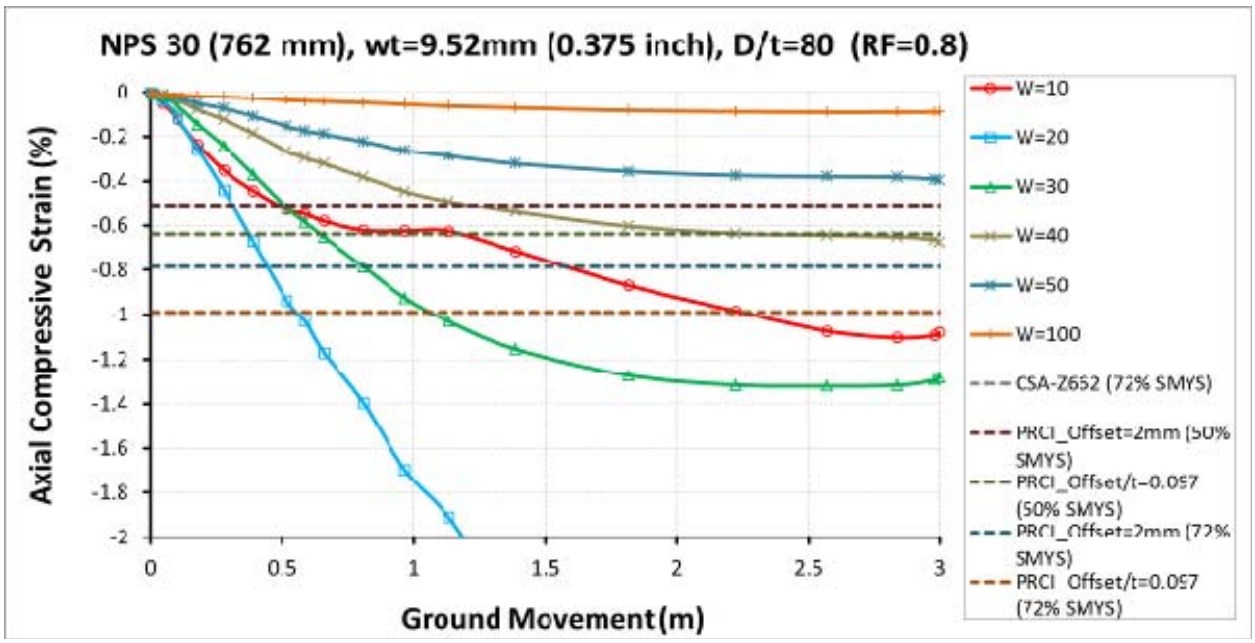

Figure F.22: NPS 30 (D/t=80) - Maximum local Compressive Strain vs. Ground Movement Widths: [10-100 m]

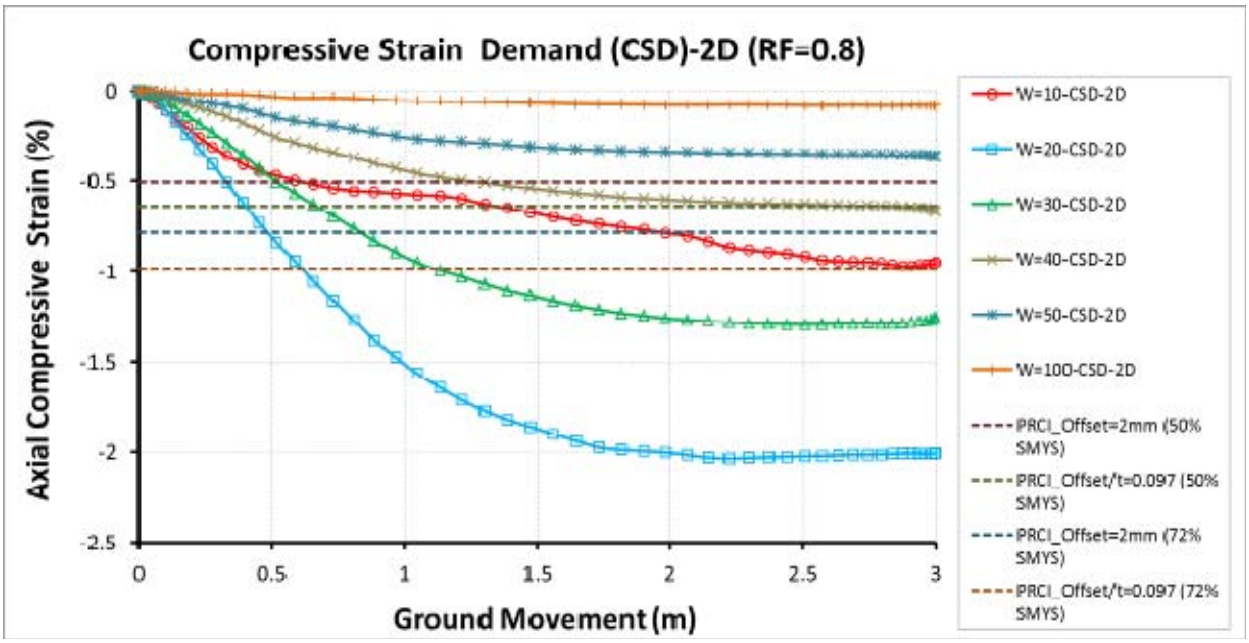

Figure F.23: NPS 30 (D/t=80) - Maximum Nominal Compressive Strain vs. Ground Movement Widths: [10-100 m]

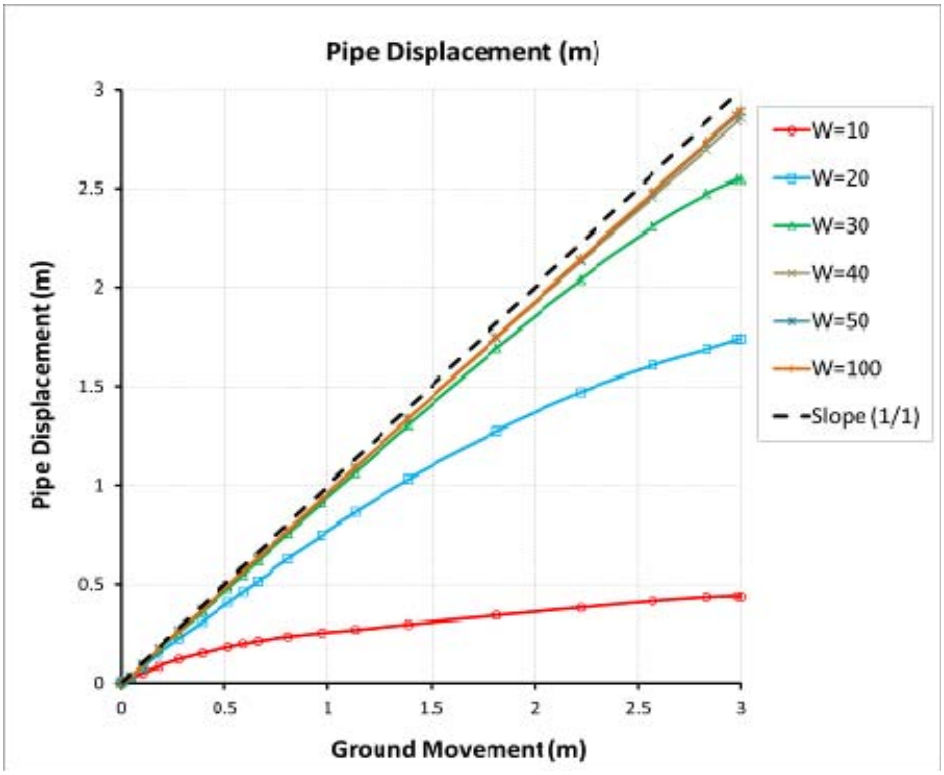

Figure F.24: NPS 30 (D/t=80) – Pipe Displacement versus Ground Displacement

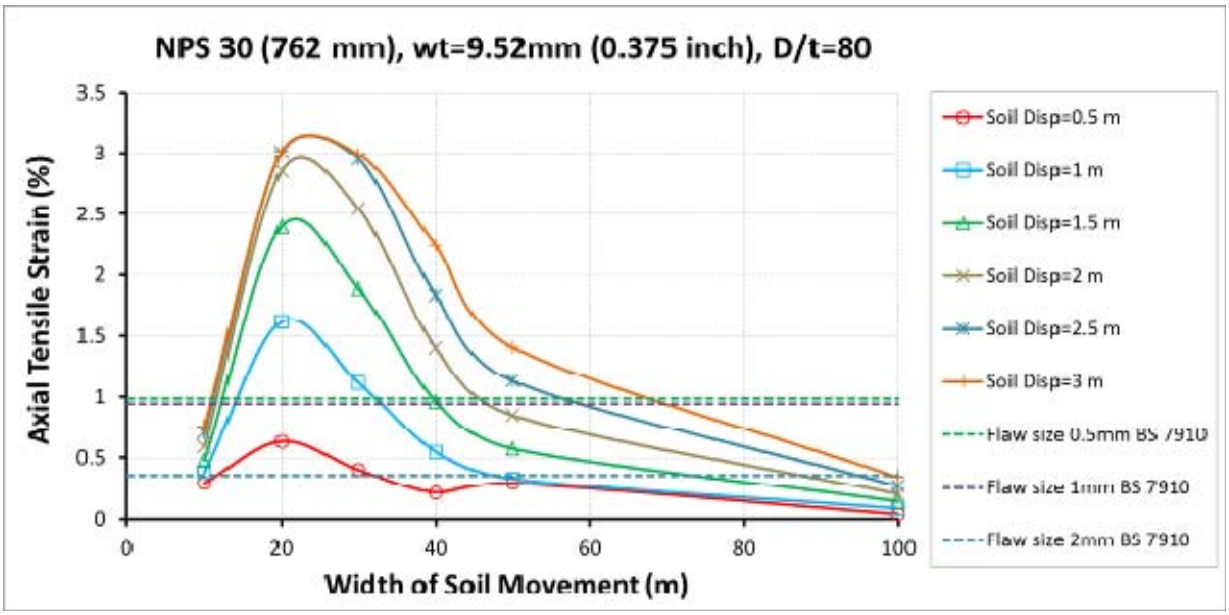

Figure F.25: Pipe Axial Tensile Strains Envelopes versus Width (W) for Soil Movements of 0.5, 1, 1.5, 2.0 and 2.5 m

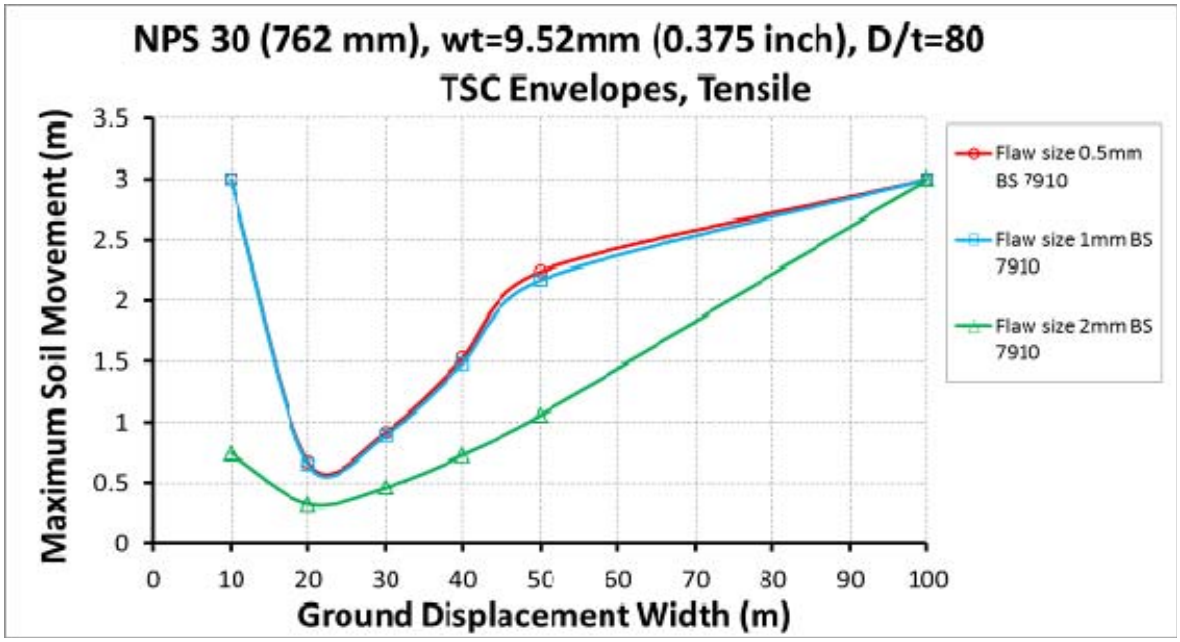

Figure F.26: Tensile Strain Capacity Envelopes versus Ground Width (W) Movements

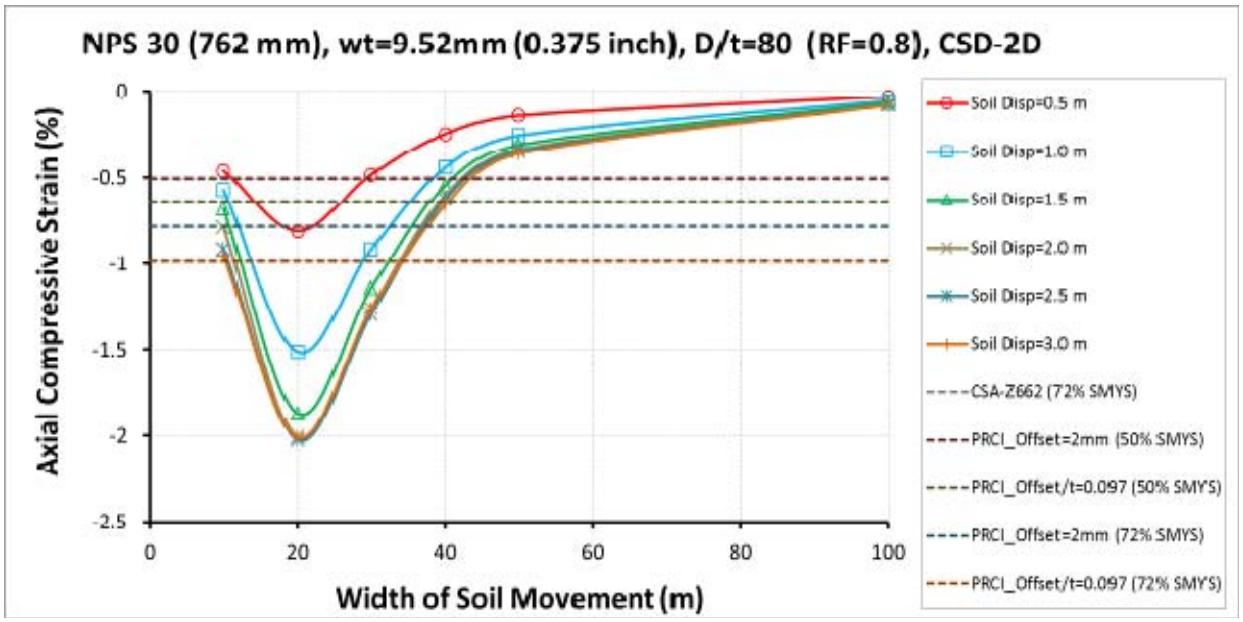

Figure F.27: Pipe Axial Compressive Strains Envelopes versus Width (W) (for Soil Movement of 0.5, 1, 1.5, 2.0 and 2.5 m)

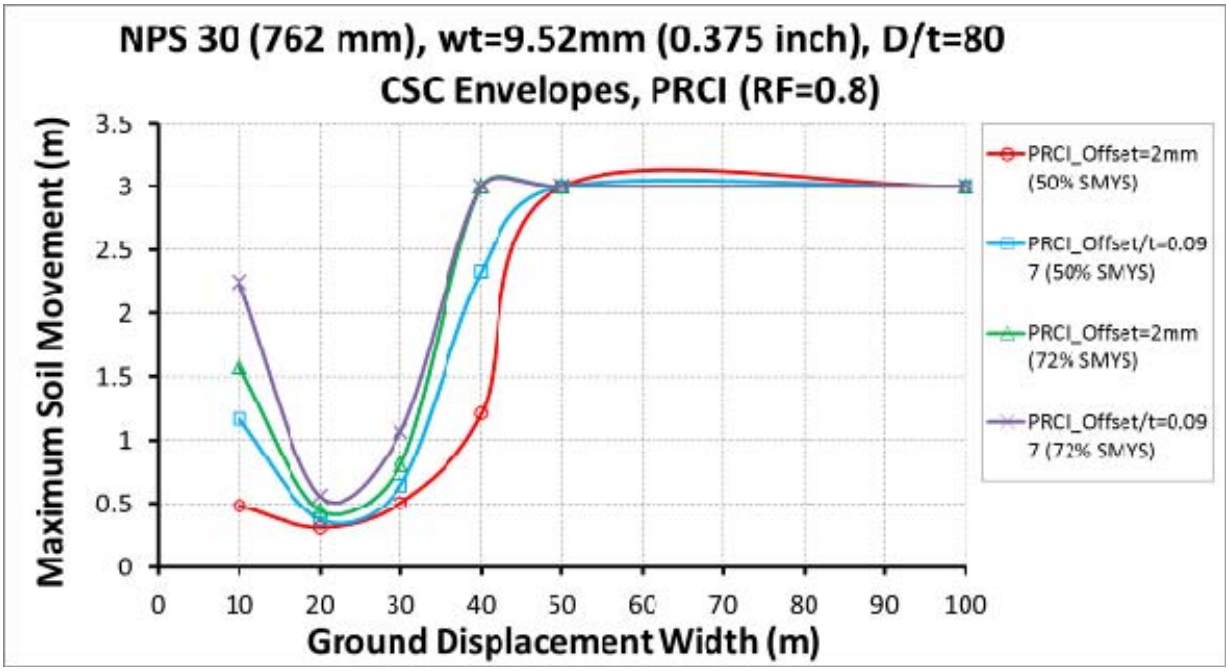

Figure F.28: Compressive Strain Capacity Envelopes versus Ground Width (W) Movements

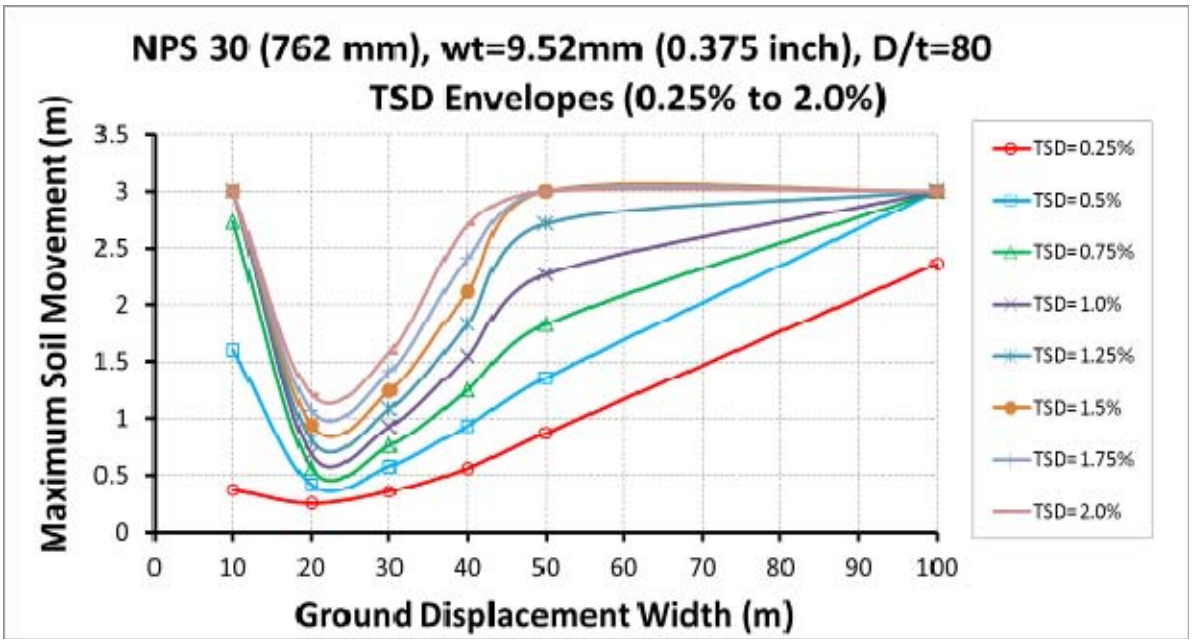

Figure F.29: Tensile Strain Demand Envelopes versus Width (W)

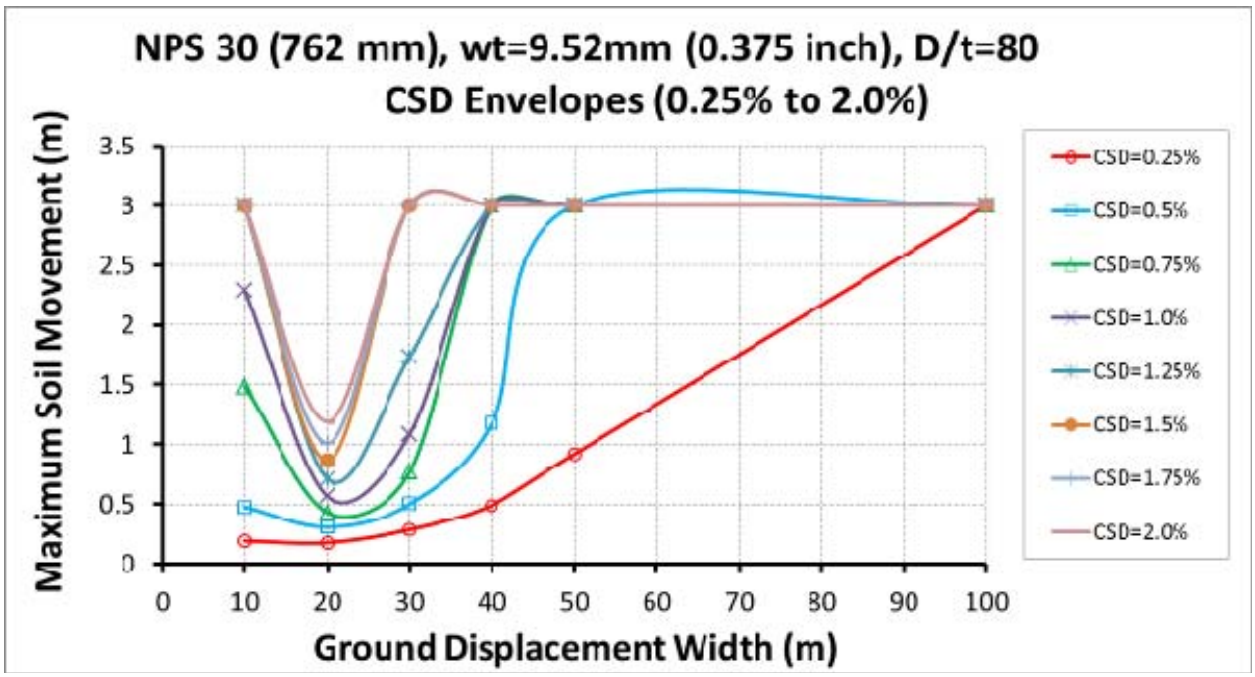

Figure F.30: Compressive Strain Demand Envelopes versus Width (W)

9 CONCLUDING REMARKS

The objective of the assessment of subsidence events was to develop an engineering basis to define the effects of operational and geotechnical loads on liquid and gas pipeline systems to support decision making regarding threat severity or repair scheduling. This tool could be incorporated in strain based design and assessment to facilitate the consideration of complex loading scenarios inducing significant flexural loads, including pipeline subsidence or lowering, and ground movements inducing lateral pipeline movements. The results of this project will define the local nominal strain state that can be used to assess localized anomalies/defects (e.g., corrosion, cracks, dents, weld faults, gouges, etc.) or the potential for the formation of a wrinkle or buckle.

The objective of the numerical simulation work completed in this task was to explore the sensitivity of the pipeline strains to changes in the geotechnical hazard and pipeline parameters. This report provides examples of the peak tensile and compressive strains generated in a slope movement transverse to the pipe axis considering the effects of:

- Pipe geometry
- Soil types
- Operating Pressure
- Ground subsidence pattern
- Material Grade
- Subsidence Widths
- Burial depth
- Temperature (axial load)

The analysis results illustrate that not all parameters investigated had the same magnitude of impact. The effect of the parameters considered in these sensitivity studies indicate that the parameters can be ranked based upon their impact on strain demand as follows:

High Importance	Medium Importance	Low Importance
- Magnitude of ground subsidence - Ground subsidence pattern - Width of ground subsidence - Burial depth	- Pipe geometry (D/t) - Operating pressure - Temperature differential - Soil stiffness	- Soil to pipe friction - Material grade

The sample application of the DEM pipe-soil interaction geotechnical hazard assessment method was employed to investigate the strains developed in NPS 24, 18 and 12 (610, 457, 305 mm) pipeline subjected to lateral soil movement. The use of the simulated pipe responses to soil movement to consider the onset of tensile and compressive limit states in a strain-based assessment was demonstrated and the sensitivity of the pipe response to a number or geotechnical hazard scenario factors were presented. For the pipe-soil interaction in which across mining subsidence panel, it was shown that:

- The response of the pipeline and soil movement pattern is affected by the ground subsidence magnitude, width and patterns;
- The vertical soil movement-induced pipe displacements will produce both pipe bending and axial extension;

- The strains in the pipe are affected by the width of the surface subsidence and there is a critical surface subsidence width that promotes a peak strain. The critical width is a function of the pipe geometry, pipeline operating conditions and locked-in pipeline axial loads (i.e. those caused by thermal differential between operating and construction conditions) and as well as the subsidence parameters.

The width, magnitude and pattern of ground subsidence were shown to be primary parameters in determining the maximum pipe compression and tension strains, followed by pipe geometry (diameter and wall thickness), operating pressure and temperature differential, soil properties and material grade.

Comparisons were made with limit state equations defined from the guidance; BS 7910 [4] for tensile strain, and CSA Z662 and UOA/PRCI 2004 [3, 2] for compressive strain to demonstrate the application of the analysis results in an assessment process. While there are many existing models for calculating the compressive and tensile strain capacity in codes and standards, it was decided to develop a simple a strain-based design methodology that can be easily adapted to any code and standards, which is the purpose of this section.

The tensile and compressive strain demand envelopes along the longitudinal direction of the pipeline were developed. The maximum soil settlement versus ground width subsidence as a series of 'envelopes' was developed for a given pipe tensile and compressive strain demands. The safe pipeline operating goal of pipeline subjected to lateral ground displacement is to stay within the normal operating strain range defined by codes and standards.

BMT Fleet Technology (BMT) is an independent Canadian consultant company specializing in engineering, science and management services in the defence, energy and transport sectors.

BMT supplies customers with unbiased solutions and trusted and experienced professionals who provide proven capability to a broad range of complex engineering and program challenges.

BMT Fleet Technology is an operating company of BMT Group.

Follow BMT Group

www.bmt.org/linkedin

www.bmt.org/youtube

www.bmt.org/twitter

www.bmt.org/facebook

Head Office - Ottawa
311 Legget Drive
Ottawa, ON, Canada, K2K 1Z8
Tel: +1 613 592 2830
Fax: +1 613 592 4950

fleet@fleetech.com
www.fleetech.com

Registered to ISO 9001:2008. We are dedicated to ongoing quality and management systems.